GENCORP
AEROJET

DEVELOPMENT OF LIFE PREDICTION CAPABILITIES FOR LIQUID PROPELLANT ROCKET ENGINES

Task 3

Sensor Data Validation And Reconstruction

Phase 1: System Architecture Study

Contract NAS 3-25883

CR-187124

Phase I Final Report

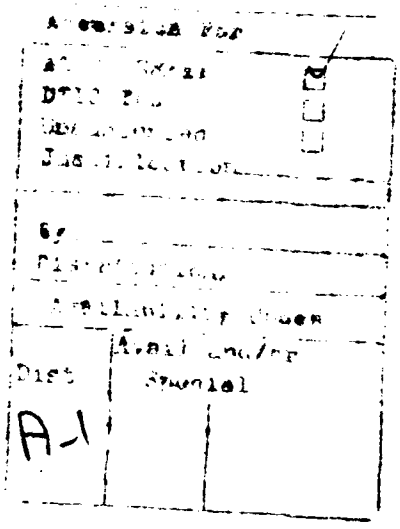

Prepared for: National Aeronautics and Space Administration
Lewis Research Center, MS 500-219
21000 Brookpark Road
Cleveland, OH 44135

Submitted by: Aerojet Propulsion Division
P.O. Box 13222
Sacramento, CA 95813-6000

June 1991

Propulsion Division

CONTENTS

FIGURES

Tables

1.0 INTRODUCTION

This report summarizes the System Architecture Study of the Sensor Data Validation and Reconstruction Task of the *Development of Life Prediction Capabilites For Liquid Propellant Rocket Engines Program*, NAS 3-25883. The effort to develop reusable rocket engine health monitoring systems has made apparent the need for life prediction techniques for various engine systems, components, and subcomponents. The design of reusable space propulsion systems is such that many critical components are subject to extreme fluctuations causing limited life, which is not adequately explained by current techniques. Therefore, the need exists to develop advanced life prediction techniques. In order to develop a reliable rocket engine condition monitoring system, erroneous transducer data must be identified and segregated from valid data. Erroneous sensor data may result from either (1) "hard" failures which are typically large in magnitude and occur rapidly or (2) "soft" failures which are typically small in magnitude and occur slowly with time. The underlying causes of such failures can include physical damage (e.g. wire or diaphragm breakage), calibration/software errors, or thermal drift. The objective of this task has been to develop a methodology for using proven analytical and numerical techniques to screen the SSME CADS and facility data sets for invalid sensor data and to provide signal reconstruction capability. This methodology is structured to be an element of an overall Engine Diagnostic System [1].

The approach taken to develop this methodology has been to evaluate sensor failure detection and isolation (FDI) and signal reconstruction techniques relative to the problem of SSME sensor data validation. From this evaluation, applicable techniques have been identified and an overall computational strategy has been developed to provide automated FDI and signal reconstruction capability. The overall computational strategy is based on the use of an advanced data synthesis technique which is capable of combining the results of several different test of sensor validity (such as limit checks, hardware redundancy, sensor reliability data, and predictive models). The output of this task is a software specification for this strategy and a software implementation plan.

2.0 EXECUTIVE SUMMARY

The current SSME data validation procedure at NASA MSFC is based on a manual review of test data by expert analysts. To date this system has worked well, but is an inefficient use of the valuable time of the expert, who must visually inspect each data plot looking for anomalous data. One of the key elements of the Engine Diagnostic System currently under development by NASA, is to exploit recent advances in computational and graphics performance of modern RISC type work stations and advanced computational techniques to automate, streamline, and improve the rocket engine diagnostic procedure. The System Achitecture Study described in this report has addressed this issue for the problem of sensor data validation. Verifying test data is essential prior to doing performance calculations or engine health assessments.

The System Architecture Study has consisted of (1) a review of the current SSME data validation process at MSFC, (2) selection of key SSME CADS and facility data set parameters for which automated data validation and reconstruction is desirable, (3) review and selection of potential techniques for parameter fault detection and reconstruction, and (4) development of a computational scheme incorporating the techniques. Based on the work conducted in this phase of the program a software specification of the Sensor Data Validation and Reconstruction System (SDV&RS) has been developed and is described in detail in Section 4.0. The recommended development plan for implementation of the software specification is described in Section 5.0.

A wide range of sensor failure modes exists for the SSME digital data sets. Table 1 lists some of the causes and effects of several known modes documented in the SSME Failure Modes and Effects Analysis [2] and documented in the UCR (Unsatisfactory Condition Report) database. The resultant transducer signals range from hard-open, shorted, noisy, intermittent, to slight drifts and shifts. In order detect, isolate, and reconstruct signals resulting from this wide range of failure modes several potential validation techniques have been reviewed and evaluated. Table 2 summarizes the techniques which have been examined for use in the SDV&SR system.

No single fault detection scheme appears solely capable of accurately detecting and reconstructing all of the important SSME sensor malfunctions. Each technique provides some evidence regarding sensor failure, and different techniques work best for different failure modes. The overall conclusion of this study is that the best approach for

Table 1. A Wide Range Of SSME Failure Modes Exist

Failure Mode	Typical Causes	Typical Occurrence and Detection
Open Circuit	• Broken Lead Wire or Pin • Recessed Pin Connector	• Any Time
Short Circuit	• Bridge Corrosion • Contamination • Bent Pin	• Any Time
Cross-Wired	• Installation Error	• Pretest – Condition May Not Be Seen Until Startup
Miscalibrated	• Calibration Error	• Pretest
Disconnected	• Installation Error	• Pretest – Pretest Value in Error
Shift	• Lead Wire/Connector Resistance	• Any Time
Drift	• Inadequate Thermal Isolation • Mechanical Failure – Diaphragm – Bearing	• Main Stage
Over/Under Shoot	• Transducer Response	• Entering and Leaving Transients
Spikes	• Faulty A/D Converter	• Any Time
Noise	• Poor Connections • Mechanical Failure	• Any Time

Source: SSME FMEA-RSS-8553-11, July 1988

M16/D31/SVC-2

Table 1. Cont.

Technique	Literature Reviewed	Known Application of Technique For Data Validation and Reconstruction	Aerojet Evaluated With SSME Data
Pattern Matching			
Pattern Overlap	Yes	SSME Flight Data Using SSA Code	No
K-Nearest Neighbor Rule	Yes	None	No
Neural Networks	Yes	Guo & Nurre, "Sensor Failure Detection and Recovery By Neural Networks"	No
Expert Systems			
Belief Networks	Yes	Time of Flight Detector Array (University of California, Berkeley)	No
Rule Based Heuristics	Yes	Hubble Space Telescope Thermal Monitoring System (Lockheed)	No

Table 2. SSME Data Validation Techniques Reviewed

Technique	Literature Reviewed	Known Application of Technique For Data Validation and Reconstruction	Aerojet Evaluated With SSME Data
Range Checking			
– Sigma Levels	Yes	Current SSME Data Validation Procedure	Yes
Signal Analysis			
– Moving Average	Yes	Titan IV Data Validation	Yes
– Standard Deviation	Yes	Titan IV Data Validation	Yes
– Time Series/ $\frac{\text{Average Signal}}{\text{Power}}$	Yes	Meyer & Zakrajsek, AIAA-90-1993	No
– Spike Detection	Yes	Current SSME Data Validation Procedure	No
Hardware Redundancy			
– Δ = A-B	Yes	Current SSME Data Validation Procedure	Yes
– Weighted Average	Yes	Voter Estimator Demonstrated for SSME MCC Pc NAS 3-25823	No
Analytical Redundancy			
– System Wide 1st Principle Models	Yes	Power/Chemical Plants	No
– Engine Characteristics Based on 1st Principle	Yes	Titan IV Data Validation	Yes
– Empirical Correlation Equations	Yes	Advanced Propulsion Monitoring Program AFWAL-TR-84-2057	Yes

robust and complete sensor data validation is to use several methods and fuse their individual results into a single pass/fail decision for every sensor at every time slice in the test.

Information fusion techniques provide explicit representation of and accounting for the uncertainties in the sensors and in the various fault detection schemes. Of the various techniques for performing information fusion, Belief Networks have been determined to be the most appropriate for the advanced liquid rocket engines such as the SSME.

The overall SDV&SR system as currently specified is illustrated in Figure 1. The system will run in two major stages; initial batch processing mode, followed by an interactive post processing mode. In the batch mode, the SSME test data (in engineering units) is thoroughly analyzed by the sensor validation system, with PID failure detection and PID value reconstruction performed automatically and stored in a separate data file. The batch mode process will be completed overnight following a test and the results will be available to the analyst at the start of the day. The purpose of the interactive mode is to allow analysts to quickly review and understand the results of the batch mode processing and either confirm or override the failure and reconstruction decisions made by the sensor validation system.

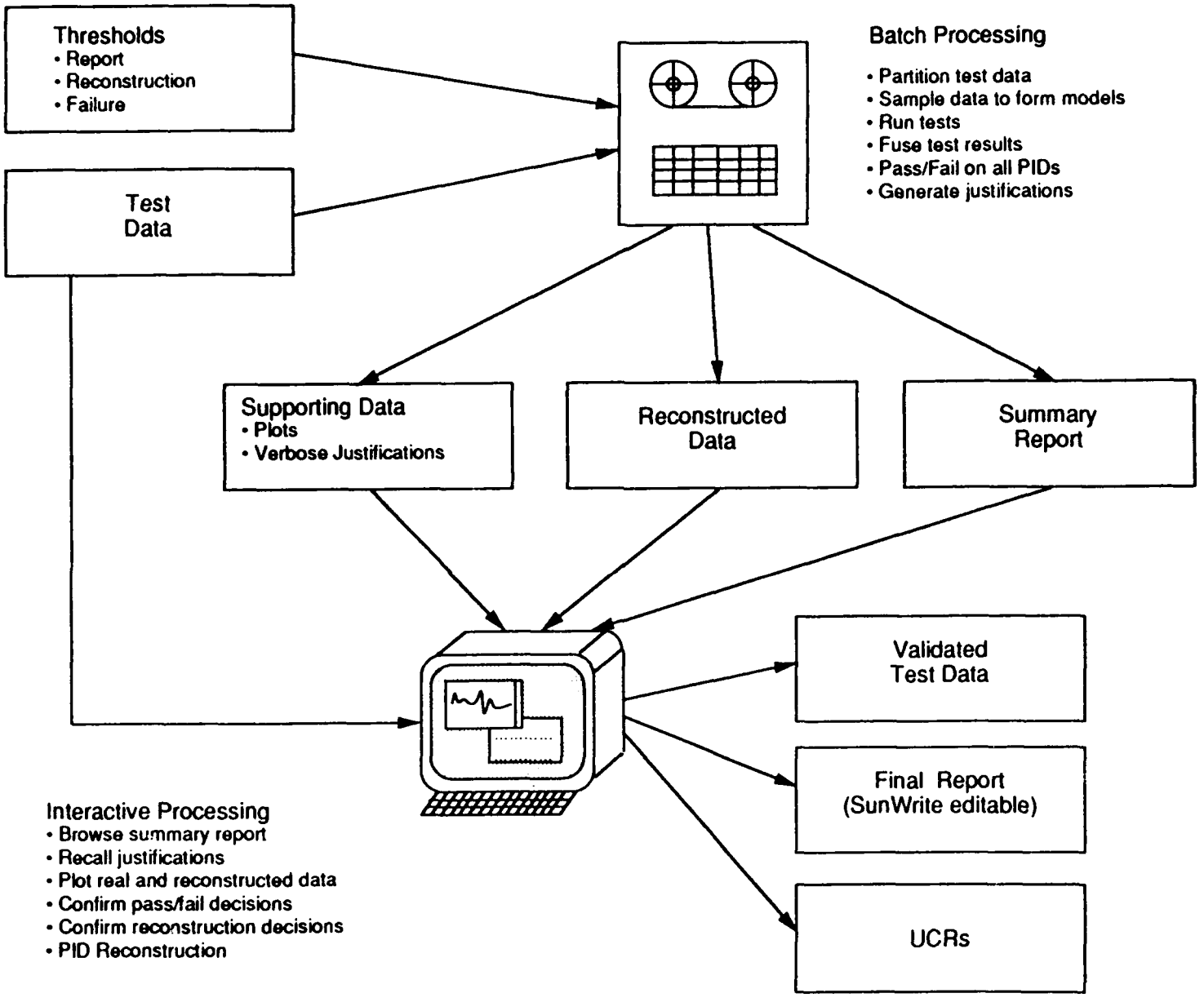

Figure 1. Elements the Sensor Data Validation and Signal Recontruction System

3.0 TECHNICAL DISCUSSION

The following section describes the technical progress accomplished during the Phase 1 of the task. The principle sections consist of (1) review of SSME test data and current validation procedure, (2) evaluation of fault detection and signal reconstruction techniques, and (3) review of information synthesis techniques for combining tests of sensor validity.

3.1 Review of SSME Test Data and Validation Procedure

3.1.1 SSME CADS and Facility Digital Data

The SSME CADS and facility data sets consist of approximately 130 and 280 individual parameters respectively. Each parameter is identified with a unique number code call a parameter identification number (PID). The various PIDs consist of transducer signals, calculated parameters, and controller signals. Of the approximately 410 PIDs, there are approximately 325 actual sensor signals. A complete PID list is provided in Appendix A.

A review of CADS and facility sensors for which automated data validation and reconstruction would be desirable has been conducted. The list sensors for which validation and signal reconstruction selected is given in Table 3. A total of 115 transducers have been selected. The criterion used to select a sensor for validation were, in order of importance:

(1) Is the sensor an engine control parameter?
(2) Is the sensor an engine redline parameter?
(3) Is the parameter plotted for pre or post-test reviews?
(4) Is the sensor used in the steady state engine power balance model?
(5) Additional sensors providing redundancy or correlation to sensors in (1) through (4).

Categories (1) and (2) comprise the most critical sensors in the engine. Sensors which fall under category (3) are assumed to be important for diagnosing engine health since they are routinely examined by the MSFC SSME data analysts. It is expected that engine diagnostics elements of the Engine Diagnostic System (EDS) would use the same set of inputs. The sensors falling under category (4) should be validated since they are used in the performance model calculate specific impulse of the engine.

Table 3. SSME Sensors Selected For Sensor Validation

MEASUREMENT	MEAS SET	PID	UNITS	DATA LOW	DATA HIGH	DISCRIPTION
MCC COOLANT DISCH PRESS CH A1	C	17	PSIA	0	7000	Pressure
MCC COOLANT DISCH TEMP CH B	C	18	DEG R	360	760	Temperature
MCC OXID INJ TEMP	C	21	DEG R	110	610	Temperature
MCC HOT GAS INJ PRESS CH A	C	24	PSIA	0	7000	Pressure
LPOP SPD CH B	C	30	RPM	180	6000	Rate
LPFP SPD CH A	C	32	RPM	600	20000	Rate
HEX DS PR (A49P9655H)	C	34	PSIA	0	7000	Pressure
HPFP COOLANT PRESS CH A	C	53	PSIA	0	4500	Pressure
HPFP COOLANT PRESS CH B	C	54	PSIA	0	4500	Pressure
HPOTP SEC SEAL CAV PRESS CH A	C	91	PSIA	0	300	Pressure
HPOTP SEC SEAL CAV PRESS CH B	C	92	PSIA	0	300	Pressure
PBP DISCH TEMP CH A	C	93	DEG R	160	210	Temperature
PBP DISCH TEMP CH B	C	94	DEG R	160	210	Temperature
MCC PRESSURE CH A2	C	129	PSIA	0	3500	Pressure
MCC PRESSURE CH A1	C	130	PSIA	0	3500	Pressure
FUEL FLOWRATE CH A1	C	133	GPM	1080	18000	Rate
MFV ACTUATOR POSITION CH A	C	136	PCT	-5	105	Position/Disp.
MFV ACTUATOR POSITION CH B	C	137	PCT	-5	105	Position/Disp.
MOV ACTUATOR POSITION CH A	C	138	PCT	-5	105	Position/Disp.
MOV ACTUATOR POSITION CH B	C	139	PCT	-5	105	Position/Disp.
OPOV ACTUATOR POSITION CH A	C	140	PCT	-5	105	Position/Disp.
OPOV ACTUATOR POSITION CH B	C	141	PCT	-5	105	Position/Disp.
FPOV ACTUATOR POSITION CH A	C	142	PCT	-5	105	Position/Disp.
FPOV ACTUATOR POSITION CH B	C	143	PCT	-5	105	Position/Disp.
CCV ACTUATOR POSITION CH A	C	145	PCT	-5	105	Position/Disp.
CCV ACTUATOR POSITION CH B	C	146	PCT	-5	105	Position/Disp.
HYDRAULIC SYS PRESSURE A	C	147	PSIA	0	4000	Pressure
FUEL PREBURN PGE PRESS CH A	C	148	PSIA	0	1500	Pressure
OXID PREBNR PGE PRESS B	C	149	PSIA	0	1500	Pressure
HPFP DISCH PRESS CH A	C	152	PSIA	0	9500	Pressure
FPB CHMBR PR A	C	158	PSIA	0	7000	Pressure
PBP DISCH PRESS CH B	C	159	PSIA	0	9500	Pressure
MCC PRESSURE B2	C	161	PSIA	0	3500	Pressure
MCC PRESSURE B1	C	162	PSIA	0	3500	Pressure
HPOP DISCH PRESS CH A	C	190	PSIA	0	7000	Pressure
LPFP DISCH PRESS CH A	C	203	PSIA	0	300	Pressure
LPFP DISCH PRESS CH B	C	204	PSIA	0	300	Pressure
LPOP DISCH PRESS CH A	C	209	PSIA	0	600	Pressure
LPOP DISCH PRESS CH B	C	210	PSIA	0	600	Pressure
HPOTP I-SEAL PGE PRESS CH A	C	211	PSIA	0	600	Pressure
HPOTP I-SEAL PGE PRESS CH B	C	212	PSIA	0	600	Pressure
HYDRAULIC SYS PRESSURE CH B	C	214	PSIA	0	4000	Pressure
FUEL SYS PGE PRESS CH A	C	219	PSIA	0	600	Pressure
FUEL SYS PGE PRESS CH B	C	220	PSIA	0	600	Pressure
POGO PRECHG PRESS CH A	C	221	PSIA	0	1500	Pressure
POGO PRECHG PRESS CH B	C	222	PSIA	0	1500	Pressure
EMERG SHT DN PRESS CH A	C	223	PSIA	0	1500	Pressure
EMERG SHT DN PRESS CH B	C	224	PSIA	0	1500	Pressure
LPFP DISCH TEMP CH A	C	225	DEG R	30	55	Temperature
LPFP DISCH TEMP CH B	C	226	DEG R	30	55	Temperature
HPFT DISCH TEMP CH A	C	231	DEG R	460	2760	Temperature
HPFT DISCH TEMP CH B	C	232	DEG R	460	2760	Temperature
HPOT DISCH TEMP CH A	C	233	DEG R	460	2760	Temperature
HPOT DISCH TEMP CH B	C	234	DEG R	460	2760	Temperature
MFV HYD TEMP CH A	C	237	DEG R	360	760	Temperature
MFV HYD TEMP CH B	C	238	DEG R	360	760	Temperature
MOV HYD TEMP CH A	C	239	DEG R	360	760	Temperature
MOV HYD TEMP CH B	C	240	DEG R	360	760	Temperature
FUEL FLOWRATE CH A2	C	251	GPM	1080	18000	Rate
FUEL FLOWRATE CH B2	C	253	GPM	1080	18000	Rate
FUEL FLOWRATE CH A1	C	258	GPM	1080	18000	Rate
HPFP SPD A	C	260	RPM	1350	45000	Rate
HPFP SPD B	C	261	RPM	1350	45000	Rate
ANTI-FLOOD VLV POS CH A	C	268	PCT	-5	105	Position/Disp.
ANTI-FLOOD VLV POS CH B	C	269	PCT	-5	105	Position/Disp.
FUEL FLOWRATE CH B1	C	301	GPM	1080	18000	Rate
LVL S BARO PR	F	316				Pressure
HPOP DS PR NFD	F	334	PSIA	0	7000	Pressure
PBP DS PR NFD	F	341	PSIG	0	9500	Pressure
MAIN INJECTOR LOX INJECTION PR N	F	395	PSIG	0	5000	Pressure
LPFT IN PR	F	436	PSIG	0	10000	Pressure
HPFTP DISCH PR NFD	F	459	PSIA	0	9500	Pressure
OPB PC	F	480	PSIS	0	10000	Pressure
MFV DIS SKIN T1	F	553	DEG R	35	560	Temperature

Table 3. Con't.

MEASUREMENT	MEAS SET	PID	UNITS	DATA LOW	DATA HIGH	DISCRIPTION
MFV DIS SKIN T2	F	554	DEG R	35	560	Temperature
MCC LOX DOME T NO 3 (NOT APPROV	F	595	DEG R	110	610	Temperature
HPFP CLNT LINER TEMP	F	650	DEG R	0	560	Temperature
HPFP DS TEMP	F	659	DEG R	30	1200	Temperature
ENGINE FUEL FLOW NFD (A49R8038A)	F	722	GPM	0	29000	Rate
LPOP SPD NFD (A49R8651A)	F	734	RPM	0	6400	Rate
LPFP SPD NFD (A49R8001A)	F	754	RPM	0	24000	Rate
HPFP SPD NFD (A49R8101A)	F	764	RPM	0	48000	Rate
ENG FL IN PR 2	F	819	PSIS	0	100	Rate
ENG FL IN PR 1	F	821	PSIS	0	100	Pressure
ENG FL IN PR 3	F	827	PSIS	0	100	Pressure
ENG OX IN PR 1	F	858	PSIS	0	250	Pressure
ENG OX IN PR 2	F	859	PSIS	0	250	Pressure
ENG OX IN PR 3	F	860	PSIS	0	250	Pressure
HEAT EXCHANGER INTERFACE PRESS	F	878	PSIS	0	5000	Pressure
HEAT EXCHANGER INTERFACE TEMP	F	879	DEG F	160	1900	Temperature
HPOP PR SL DR PR 1	F	951	PSIG	0	100	Pressure
HPOP PR SL DR P2	F	952	PSI	0	100	Pressure
HPOP PR SL DR P3	F	953	PSI	0	100	Pressure
ENGINE GN2 PURGE INTRF PRESS	F	957	PSIS	0	1000	Pressure
HPOT PR SL DR PR	F	990	PSIG	0	100	Pressure
FAC LH2 FLOWMETER OUTLET TEMP	F	1017	DEG R	-430	-380	Temperature
LPTOP INLET TEMP	F	1058	DEG R	160	180	Temperature
FAC FUEL FLOW 1	F	1205	GPM	0	22000	Rate
FAC FUEL FLOW 2	F	1206	GPM	0	22000	Rate
FAC OX FLOW 1	F	1212	GPM	0	8500	Rate
FAC OX FLOW 2	F	1213	GPM	0	8500	Rate
HORZ F1A	F	1345	KLB	0	100	Force
HORZ F2A	F	1350	KLB	0	100	Force
VERT F1A	F	1360	KLB	0	225	Force
VERT F1B	F	1361	KLB	0	225	Force
VERT F2A	F	1365	KLB	0	225	Force
VERT F3A	F	1370	KLB	0	225	Force
VERT F3B	F	1371	KLB	0	225	Force
AFV DIS SKIN TEMP NO 1	F	1420	DEG R	160	560	Temperature
AFV DIS SKIN TEMP NO 2	F	1421	DEG R	160	560	Temperature
GIM BR LNG 1 (A49D8607A)	F	1543	GRMS	0	30	Vibration
GIM BR LNG 2 (A49D8608A)	F	1544	GRMS	0	30	Vibration
GIM BR LNG 3 (A49D8609A)	F	1547	GRMS	0	30	Vibration
MCC LINER CAV P2	F	1956	PSI	0	200	Pressure
MCC LINER CAV P3	F	1957	PSI	0	200	Pressure

The specific breakdown of sensors for which data validation and reconstruction is recommended is:

Engine Control Parameters	13 PIDs
Flight Red Line Sensors	16 PIDs
Test Red Line Sensors	23 PIDs
Sensors Used For Engine Diagnostic	39 PIDs
Sensors Used In Power Balance Model	23 PIDs

3.1.2 Current SSME Data Validation Procedure

The current SSME data validation procedure at NASA MSFC was reviewed to (1) determine the performance requirements (turn-around time, accuracy, etc.) of an automated data validation and reconstruction system from a user stand point, (2) assess the techniques currently employed for data validation, and (3) obtain first-hand knowledge of the characteristics of the SSME data. Interviews were conducted with NASA and Martin Marietta personnel directly involved in day-to-day evaluation of test data. Summaries of the specific interviews are contained in Appendix A.

Sensor data validation is the responsibility of Martin Marietta data analysts employed at NASA MSFC. Data validation is performed as part of their overall responsibility for assessing the health of particular engines. The current MSFC data validation process is illustrated in Figure 3. The elements of the process described below. A detailed description of the process is contained in Reference [1].

1.0 Following an SSME test firing at NASA Stennis, the raw test data (voltages) are converted to engineering units using transducer calibration data. The data is transferred to NASA MSFC and down loaded to Perkin Elmer 4 computer system.

2.0 A standard set of plots is prepared and is available to the data analyst by 8:00 am following the day of a test. Included in these plot packages are data from previous test firings which have been requested by the data analysts. These previous data are chosen from the most recent tests which involved either the (1) the same engine, (2) the same power-head set, and (3) preferably the same test stand (A1, A2, or B2).

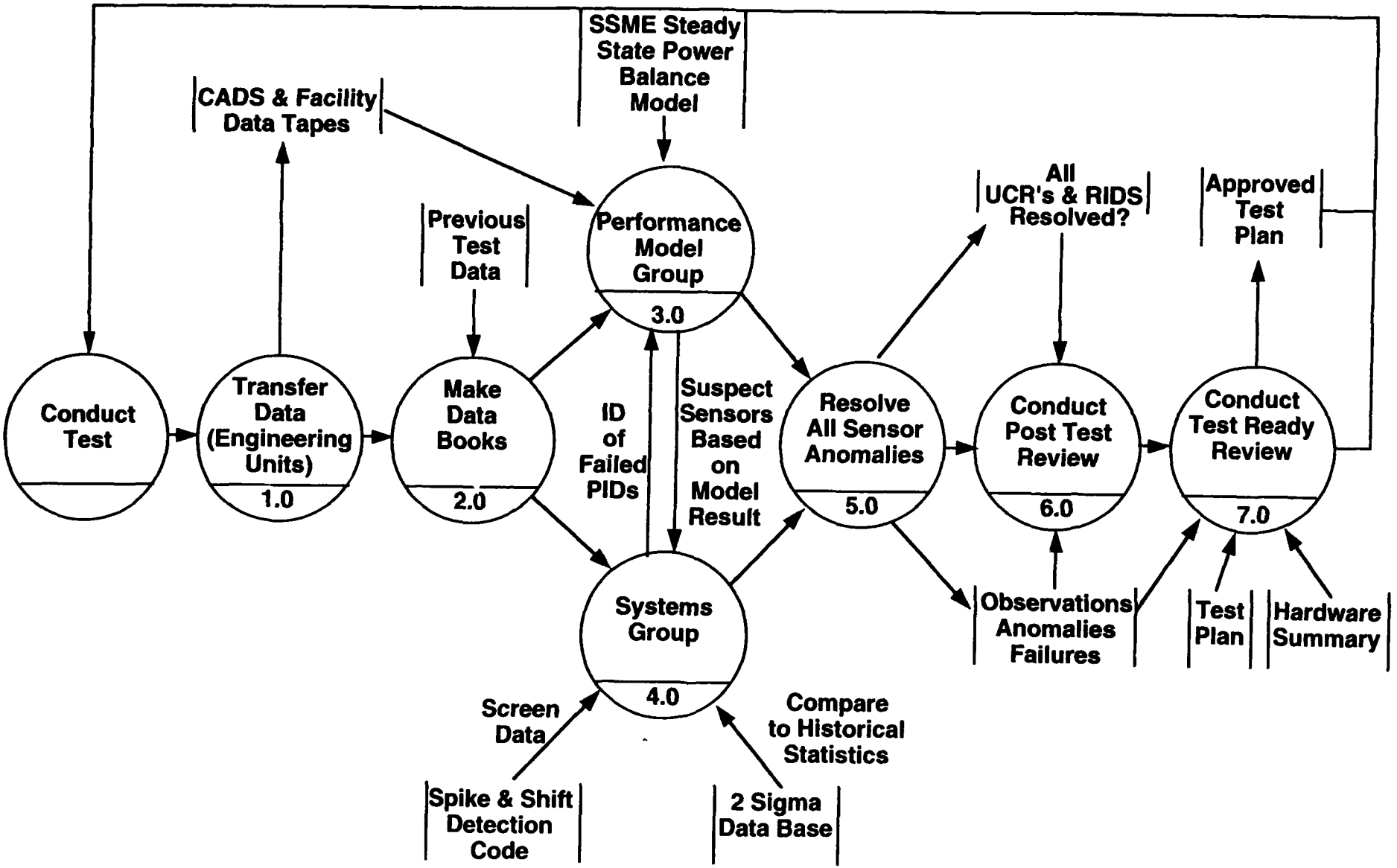

Figure 3. Current NASA MSFC Data Review Process

3.0 The test data packages and data files are simultaneously reviewed by two groups. The first group is the performance analysis group which uses the test data as input to the SSME steady state power balance model.

4.0 Concurrent with the power balance analysis the Systems Analysis Group (typically one lead analyst and one support analyst) performs a manual review of the data and use existing data validation codes to screen the data. The group currently uses two FORTRAN computer codes to screen data to detect faulty data.

- Two Sigma Comparison Code:
- Spike Detection and Shift Code:

5.0 Comparison of results are made between the two groups to identify potential faulty data. By the conclusion of process 5.0 (typically an eight hour shift), all anomalies detected in the data are attributed to engine behavior or transducer malfunction.

6.0/7.0 The results of the test data analysis process (3.0 , 4.0, and 5.0) are presented in the post test review. Instrumentation action items are flagged for the next pretest review.

Sensor data validation occurs in steps 3.0 and 4.0. As indicated on the process flow diagram results from the power balance calculation and the manual data review are shared. It is not uncommon for the initial run of the power balance model to produce anomalous results (typically a noticeable change in calculated specific impulse). After detailed inspection of the input PIDS and intermediate calculations of the model, failed sensors are identified and excluded from the input deck of the model. Soft failures present a particular problem to the power balance model because their magnitude is often not large enough to violate currently employed limit checking procedures, but can significantly impact calculation of key performance parameters.

When a sensor is suspected of a failure, a "confirmation" procedure is used to confirm failure. The experienced data analyst will look at the following evidence to determine a sensors validity.

1. Pre and post test values indicate if the transducer was scaled, calibrated, or installed improperly. Additionaly, if a sensor does assume a normal steady post test value, then transient effects such as thermal drifts may have caused the failure.

2. Related sensors (such as upstream and downstream pressures and temperatures) are inspected to see if they agree with the failed sensor.

3. The signal is compared to previous measurements made with the same engine components.

Several aspects of the current NASA MSFC data validation procedure have been adopted in the Sensor Data Validation and Signal Reconstruction System described in section 4.0. These key features are:

1. integration of many sources of information for determining sensor validity (see Section 3.3);
2. use of calculated engine system parameters to indicate an inconsistent sensor reading (see Section 3.2 on characteristic equations);
3. comparison of data patterns to known "nominal" patterns.

3.1.3 SSME Sensor Failure Modes

A wide range of sensor failure modes exist for the SSME digital data sets as summarized in Table 1. The general requirements of the senser data validation and reconstruction system to detect these diffent types of failure modes is described in the Systems Users Requirements Summary Report in Appendix A. During the task, data from 20 recent SSME test firing was reviewed to identify common failure modes Table 4 lists 22 sensors which were documented as failed in the 20 tests reviewed. Of the 22 sensors, 13 failed only once in the 20 tests examined and a few sensors such as the Fuel Preburner Chamber Pressure, PID 158, which has history of thermal drift, failed on 85% of the tests. Extension of the sensor failure frequency data to a larger number of tests will allow a more comprehensive database of sensor reliability to be constructed. The use of such data can be incorporated into the SDV&SR data system as described in Section 3.3.

Figure 4 illustrates four common failure signatures of the SSME pressure and flow transducers. Thermal drift of the FPB Pc and the OPB Pc are common failure modes due to their installation on the SSME. The characteristic behavior is for the signal to appear normal during startup, but during mainstage to begin to decay due to icing. Intermittent or "hashy" signals are typically due to poor electrical connections as noted in Table 1. These signals generally appear normal except for large spikes off scale either over or under the scaled range. Fuel turbine flow meters and pump speed transducers can exhibit signal aliasing such that false signal fluctuations appear in the data. During power level transitions many pressure and temperature transducers experience over and under shoot causing their data to be invalid during a brief period of time while recovery occurs. This type of behavior is considered a sensor failure because the data is not valid, even though there is not a problem with the transducer. Figure 5 shows some of the documented SSME sensor failures.

Table 4 Documented Sensor Failures Indicate Reliability

PID		Test Number																				
		A1-618	A1-619	A1-620	A1-622	A2-493	A2-495	A2-496	A2-497	B1-055	B1-064	B1-065	B1-066	B1-067	B1-069	B1-070	B1-071	B1-072	B1-073	B1-074	B1-075	Total
LPOP SPD B	30		•	•																		2
HPFD DS PR A	152				•																	1
FPB CHMBR PR A	158				•	•	•	•	•	•	•	•	•	•	•	•	•	•	•	•	•	17
LBOP DS PR B	210															•						1
HPOP DS PR	334									•												1
PBP DS PR	341												•					•	•		•	4
MCC HG INJ PR	371	•																				1
M INJ LOX PR	395																			•	•	2
FPB CHMBR PR	410		•	•		•	•	•	•	•	•	•	•	•	•	•	•	•	•	•	•	18
LPFT IN PR	436				•																	1
HPFTP DS PR	459			•																		1
OPB PC	480				•		•		•													3
HPFP CLNT L TEMP	650											•										1
HPFP DR PR	657				•																	1
HPFP DS TEMP	659	•	•																			2
LPFP SPD	754	•																•				2
FAC LH2 OUT T	1017																		•			1
ENG FL IN T	1021					•																1
FUEL PRESS INT T	1035																	•				1
FAC OX FLOW 2	1213																				•	1
AMB PH E TEMP	1489																	•				1
MCCLINER CAV PR	1951										•			•	•	•						4
	Total	3	3	3	5	3	3	2	3	3	3	3	3	3	3	4	2	6	4	3	5	

Source: SSME Test Review Summaries

M16/D31/SVC-2

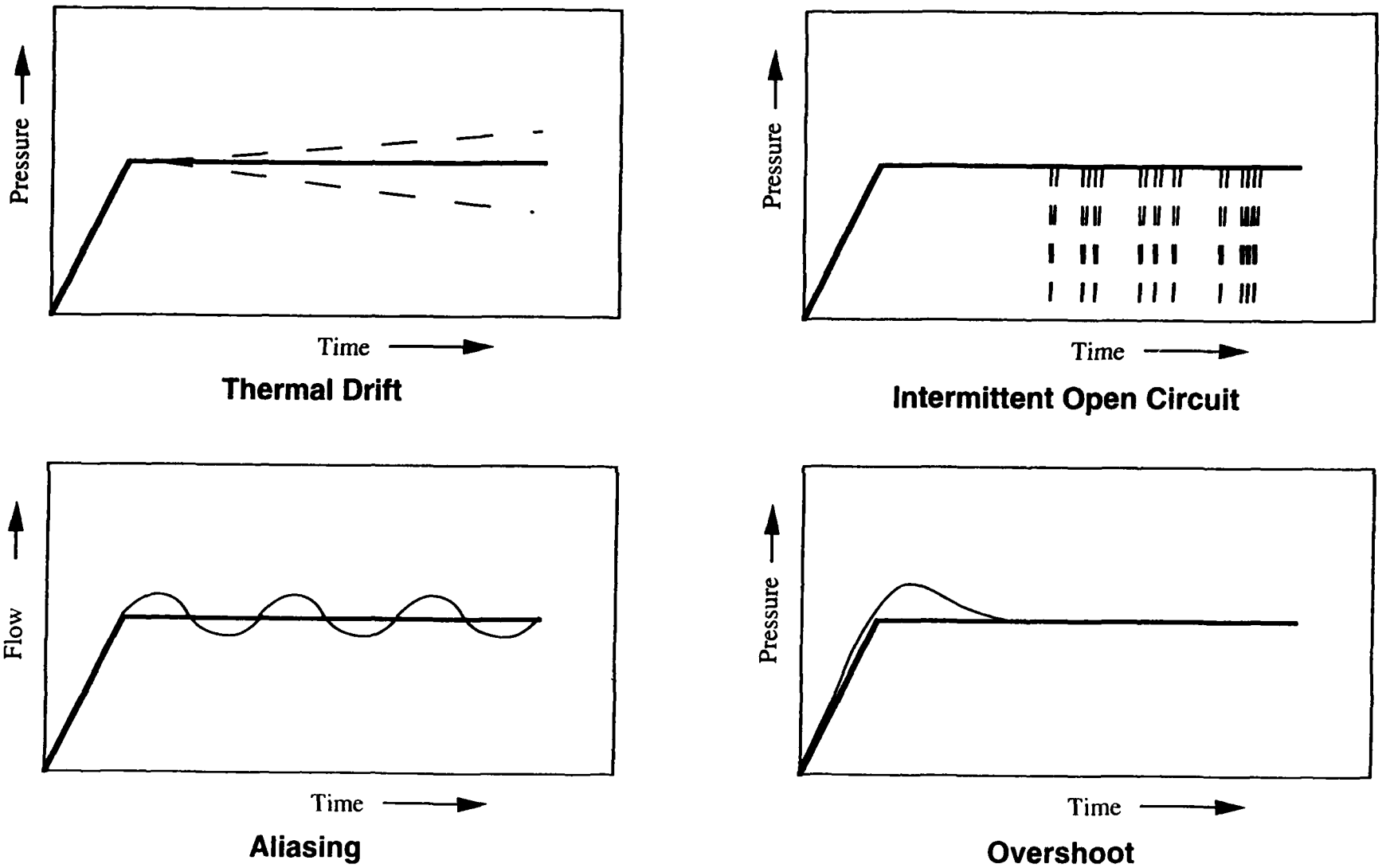

Figure 4. Typical SSME Sensor Failure Modes

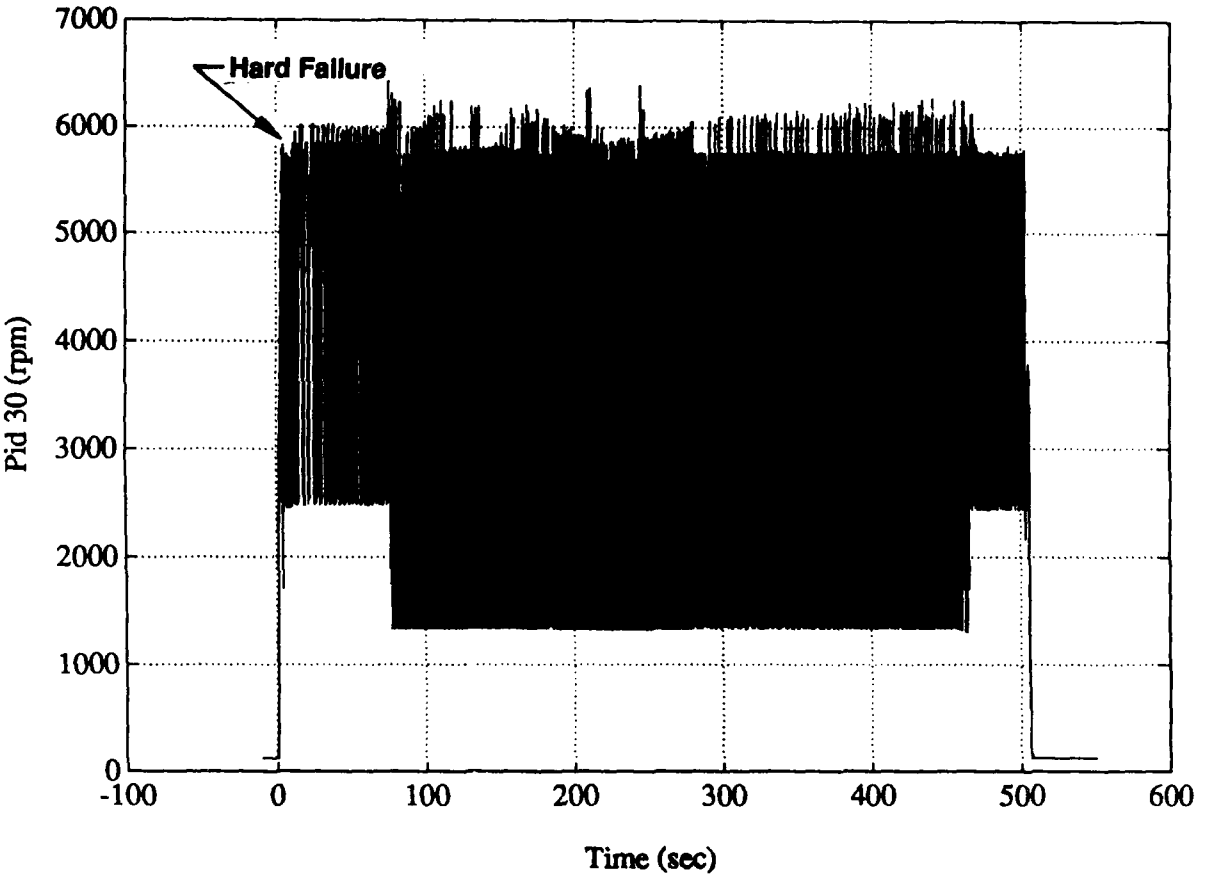

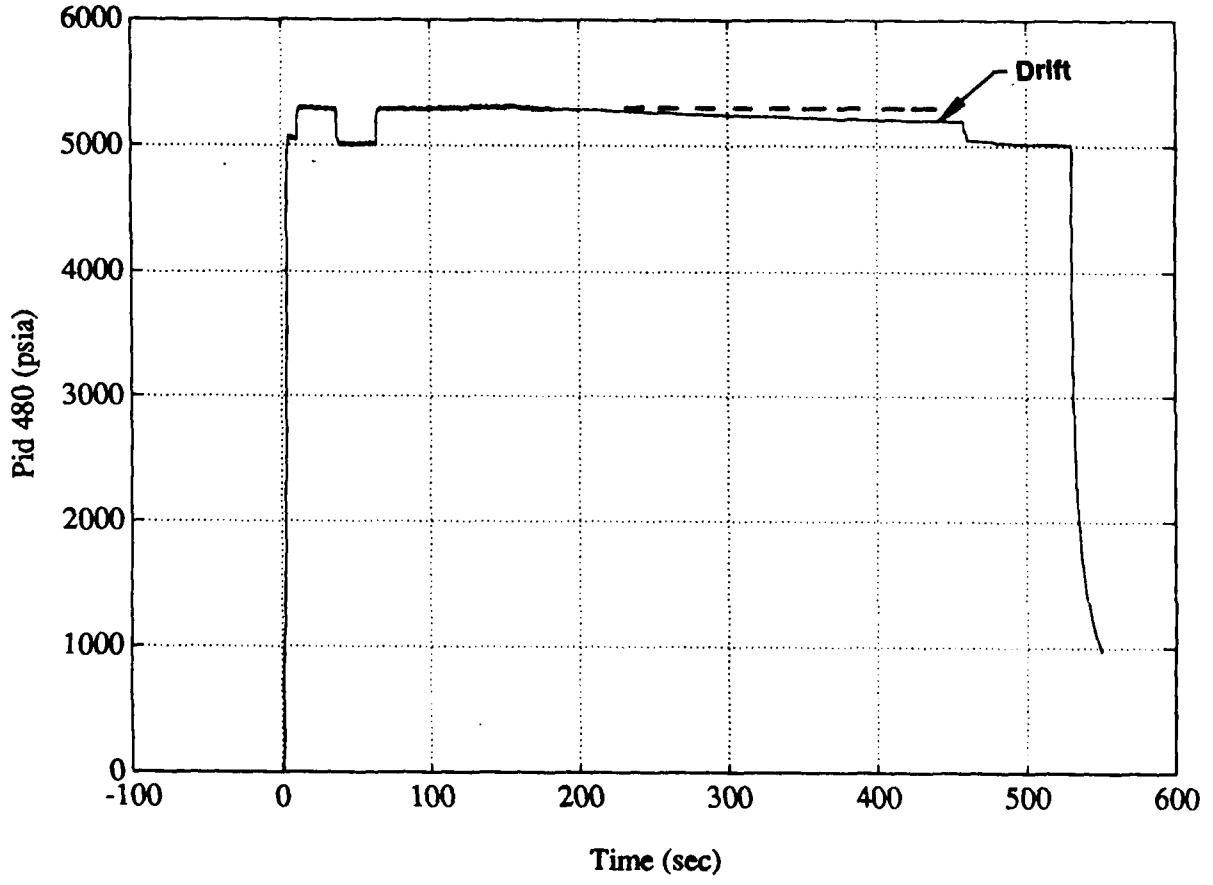

Figure 5. Examples of Failed SSME Sensor Signals

3.2 Evaluation of Fault Detection and Signal Reconstruction Techniques

Table 2 summarizes the various fault detection and isolation techniques which were reviewed during the task. As noted in the table, applicable literature for the various techniques has been reviewed and in some cases demonstrated with available SSME test data at Aerojet. A description of the applicability and limitations of each of these techniques as applied to SSME data is given below.

3.2.1 Statistical Comparison Techniques

Statistical comparison techniques cover the class of techniques where the signal value or statistics of the transducer signal are compared to known "acceptable" values. Three of these techniques which are suitable for SSME data validation are described below. The first technique is limit checking tests which serves as a basic indicator if a transducer signal is within the expected envelope of "nominal" operation. The second technique discussed is an extreme value exceedance test which can differentiate true signal behavior from spurious spikes in the data. The third statistical comparison test is a moving average test which indicates if a significant trend exists in the data.

Limit Checking

Comparison of a signal to predefined limits constitutes the simplest form of sensor data validation [3,4]. If the signal exceeds the limit it is considered "out of family" and indicates either an instrumentation error or an engine component failure. Common limits used in data validation schemes are:

1. High and low data ranges of the transducer
2. Two or three standard deviation variation from the mean
3. Comparison of signal statistical values to "family" averaged values.

Limit checking is for sensor failure detection is limited to severe hard failures. In order to detect soft failures such as drifts, simple limits must be set so tight that an unacceptably high number of false detections occur. Currently the SSME test data is compared to the "Two Sigma" database as part of the data analysis. Figure 6 shows some typical data plot with the two sigma limits indicated.

A table of the "Two Sigma" database is given in Appendix C. In order to rationally compare different tests, the average values of parameters are taken at (1) the maximum fuel turbine temperature, (2) the maximum oxidizer turbine temperature, and (3) at the

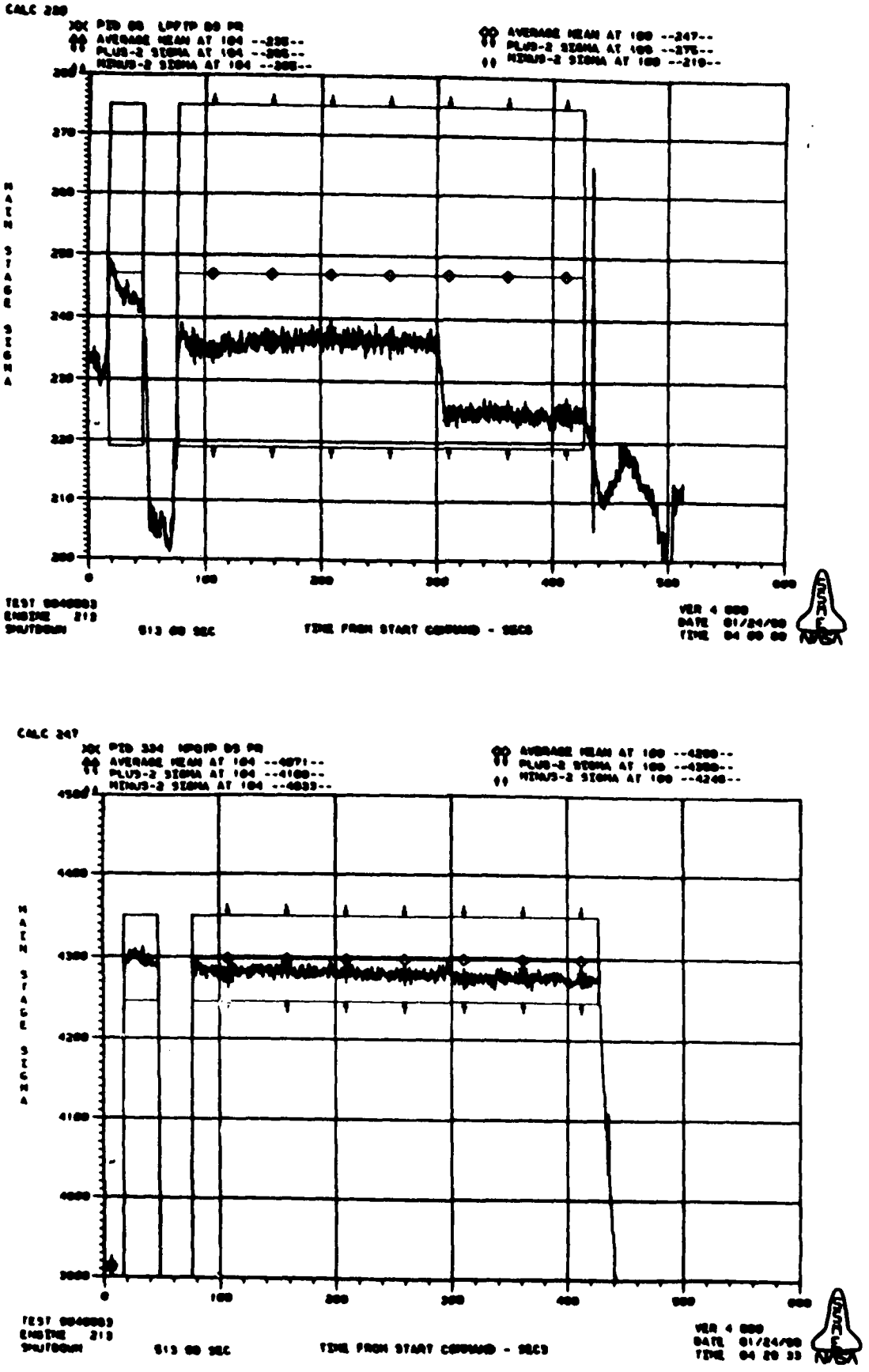

Figure 6. Typical Data Package Plots With Family-Averaged Two Sigma Limits

nominal 104% LOX vent. Figure 7 shows a typical thrust profile and the locations of each of the conditions listed above.

The "sigma" bands reflect a wide variation in "nominal" operating conditions for some parameters. This variability is due to the averaging effect obtained by using data from various engines and test stands when populating a statistical database. While these statistically based techniques are relatively effective in detecting signals that have a large drift or a low signal to noise ratio, it is possible that a noisy signal can lie within the "sigma" band and go undetected. This is shown graphically in Figure 3.

Data Spikes Detection

Data spikes are sharp and significant changes in data, not attributable to measurable physical phenomena, but due to a instrumentation anomaly, such as a malfunctioning A/D converter. Removal of spurious spikes from measured data is necessary to improve quality of the data and therefore any conclusions drawn from the data.

One approach to identifying such spurious signals is with extreme value probability theory [5]. Extreme value theory is concerned with the probability distribution of the extreme value of a sample of n independent observations of a random variable. Given this extreme value probability distribution, a detection limit can be established with an arbitrarily low probability of exceedance for the largest value of n independent observations.

The theoretically exact distribution of the extreme largest value (Y) from n independent observations of a random variable (X) is defined in terms of cumulative distribution functions:

$$F_y(y) = [F_x(y)]^n$$

The particular value of Y=y corresponding to a cumulative probability p can then be determined from the distribution of X as follows:

$$[F_x(y)]^n = p$$
$$F_x(y) = p^{1/n}$$
$$y = F_x^{-1}(p^{1/n})$$

Thus y is determined directly from the inverse cumulative distribution function of X.

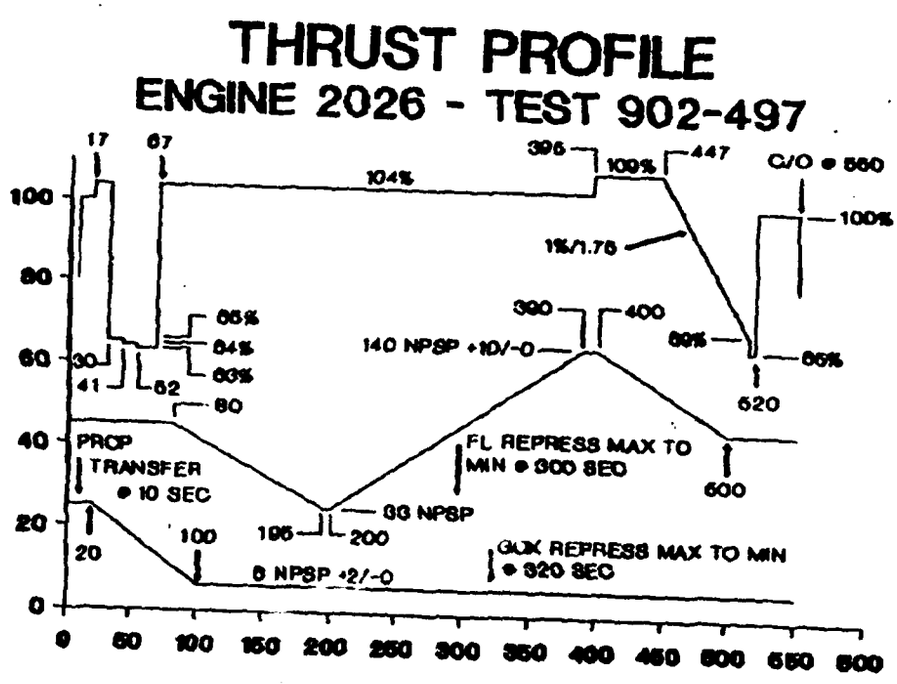

Figure 7. Typical SSME Thrust Profile

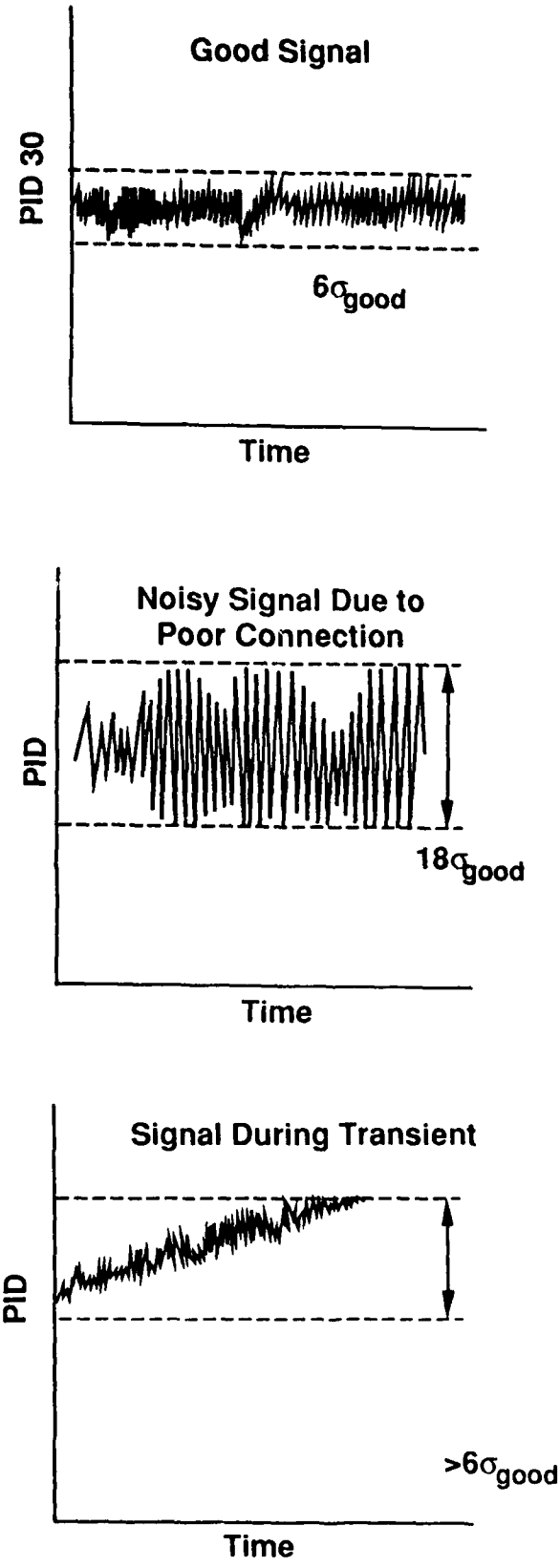

Figure 8. **Illustration Of The Use of Standard Deviation Test For Sensor Validation**

For example, let n = 10,000 be independent observations of a normal variate X and let p = 0.99 define the arbitrarily established detection limit. Then this detection limit (y) is calculated as follows in terms of standard deviations from the mean.

$$y = F_X^{-1}(p^{1/n}) = F_X^{-1}(0.999999) = 4.76$$

The inverse of the normal cumulative distribution function is conveniently tabulated.

Therefore if the detection limit is set at 4.76 standard deviations above the mean of a normal distribution and if 10,000 independent observations are made of this normal random variate, then the single largest of these observations will be expected to exceed this detection limit, on the average, one percent of the time. More realistically, many sensors which are prone to spiked data will usually have an exceedance probability much greater than one percent. This higher probability can be determined by examination of previously obtained data, and reflected by lowering P to a more realistic value. Such application of extreme value theory can be used to define a detection limit, the exceedance of which may reasonably be assumed to constitute a spurious data spike.

Moving Averages

As discussed in Section 3.1.3, soft failures usually manifest themselves as slowly changing drifts typical of thermally sensitive failure modes. As seen in Figure 6, varying amounts of dynamic fluctuations of the signals about their mean values occur during steady power level operation of the SSME. The sources of these fluctuations are (1) quantitization error during A/D conversion, (2) electrical noise induced by mechanical vibration of engine, and (3) dynamic excursions of the engine resulting from the closed loop control logic of the engine. In order to extract the true trend data signal a simple moving average of the data can be calculated [6,7]. Some SSME failure detection algorithms such as the System For Anomaly and Failure Detection (SAFD) [8] algorithms are based on monitoring the moving average of many parameters. Figure 9 illustrates the smoothing effect of a noisy signal by applying a moving average calculation. The simplest moving average can be defined as:

$$Y_i = \Sigma\, Y_i/N$$

where: N = a fixed number of previous points (25 for a 1 second average of CADS data)
Y_i = sensor reading at a given time slice

The moving average smooths the signal and reveals the true trend of the data. While the overall trend is apparent to a trained expert, evaluation of the time derivative from the raw signal at a given time slice can yield a meaningless result (e.g. a positive value when the true trend has a negative slope).

The moving average computation provides a good means of extracting trend data from signals. For sensor fault detection the signal trend is insufficient to identify a bad signal. The trends (transients) in sensor values of the SSME can be caused by factors other than power level change, such as (1) engine component anomalies, (2) propellant transfer which causes changes in propellant inlet temperatures, and (3) propellant tank venting and repressurization, which causes pump inlet pressure changes.

3.2.2 Analytical Redundancy Techniques

Analytical redundancy for sensor data validation consists of three parts, (1) parameter estimation, (2) parameter fault detection, and (3) fault isolation [10, 11, 12]. The principle advantage of analytical redundancy techniques over the statistical comparison techniques discussed above is that the parameter estimation model provides a means of signal reconstruction which is a key element of the SDV&SR system.

The major uncertainties regarding the development of an analytical redundancy capability for the SSME sensors have been addressed. These issues are the following:

1. How many of the Sensor PIDs of interest can be can be modeled as linear or nonlinear combinations of other parameters?
2. Is the accuracy of these models sufficient to enable reasonable fault detection?
3. Can a robust fault isolation methodology be developed for the resulting models?

Issues (1) and (2) above involve a basic tradeoff model complexity (i.e. number of terms in equations and form of model) and the accuracy of the estimate, as illustrated in

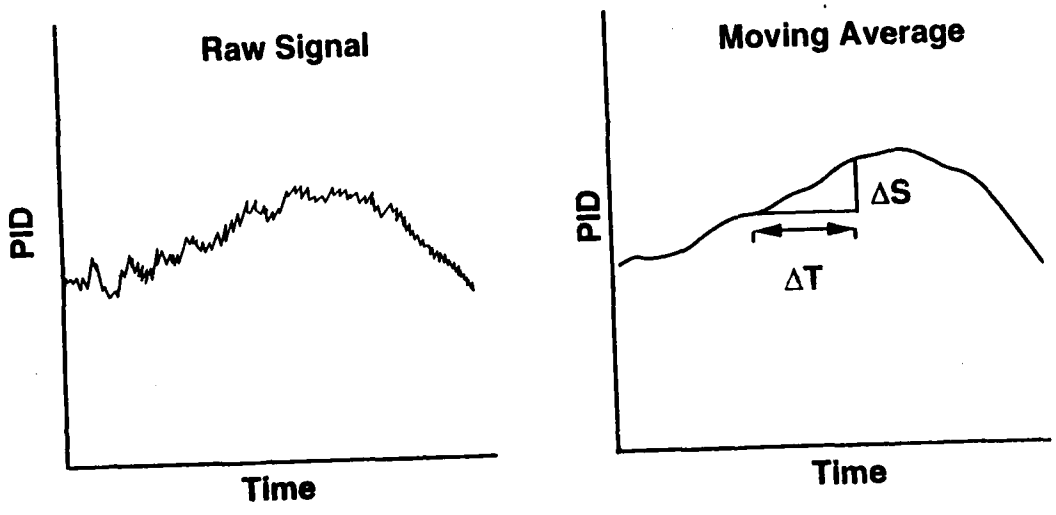

Figure 9. **Moving Average Calculations Provide Data Smoothing For Determining True Signal Trend**

Figure 10. Two schemes which represent the limits of this tradeoff are (1) the "dedicated observer scheme" (DOS) [13] and (2) the "generalized observer scheme" (GOS) [14] shown Figure 11. The DOS technique performs sensor fault detection by assigning a dedicated estimator to each of the sensors. Each estimator (e.g. a least squares fit of another sensor output to previous test data or an ARMA model [15]) is driven by only a single sensor output The output of the estimator, Y', is then compared to the sensor measurement, Y, to produce a residual r. The residual is then compared to a threshold limit, ϕ, to determine if a fault has occurred.

The "generalized observer scheme" is similar to DOS except that it is constructed such that the estimator is driven by all the output sensors except that of the respective sensor. In theory, the "generalized observer scheme" provides the most accurate estimate (for a given class of estimators, such as linear regression models) of sensor output and therefore the best fault detection because it makes use of all available information in the system. The obvious draw back of the GOS approach is that fault isolation becomes difficult since a single point failure may cause failure of many estimators. On the other hand, the "dedicated observer scheme" can easily accommodate single point and most multi-point failure instances provided the large number of different PIDs used as the independent variables is approximately the same as the number of equations.

Parameter Estimation

Two approaches were investigated to generate estimator models for each of the SSME CADS and facility parameters specified for validation and reconstruction. The first approach was the use of engine characteristic equations which physically relate parameters. The second approach was to generate empirical regression equations based on existing SSME test data. Each of these techniques is discussed below.

Engine Characteristics

Engine characteristics are parameters which describe the performance of a particular engine and its components (Table 5 shows some examples of engine characteristics). The set of characteristics for an engine form a "fingerprint" which describes the engine's idiosyncrasies relative to all other engines in the same family tested thus far.

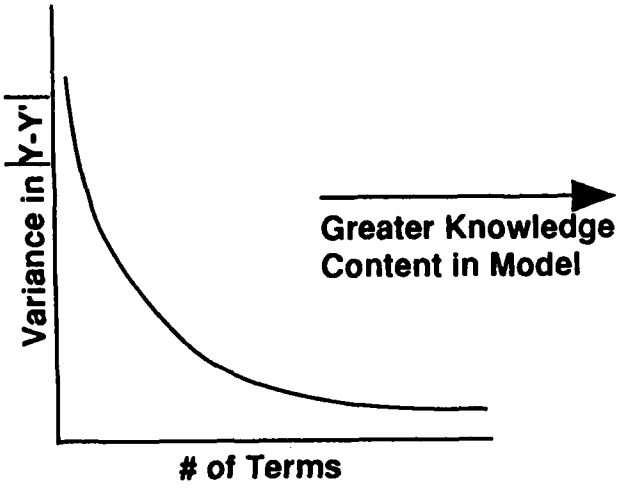

Figure 10. Increasing The Complexity Of Estimator Models Improves Model Accuracy

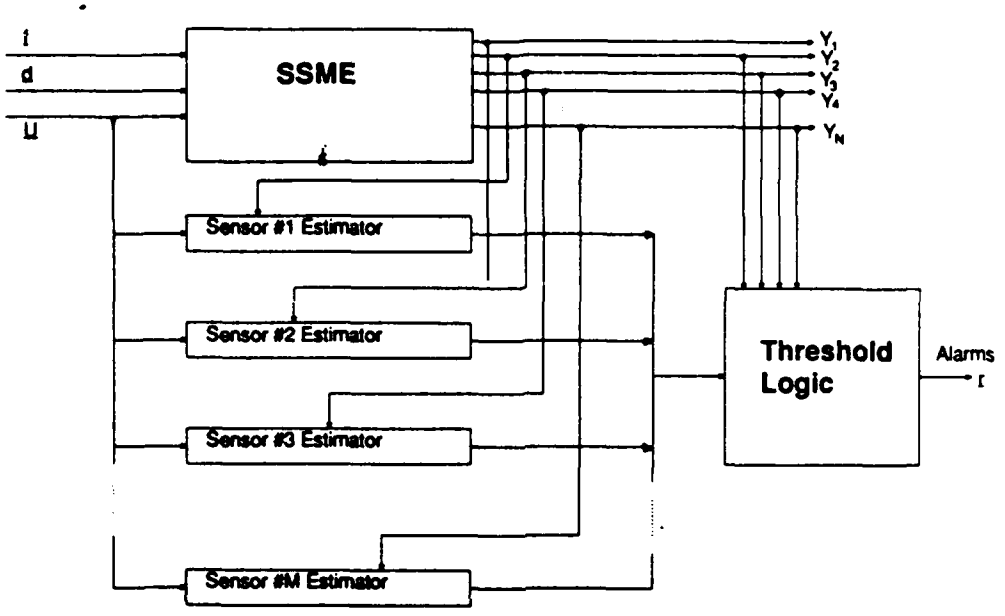

Dedicated Observer Scheme (DOS)

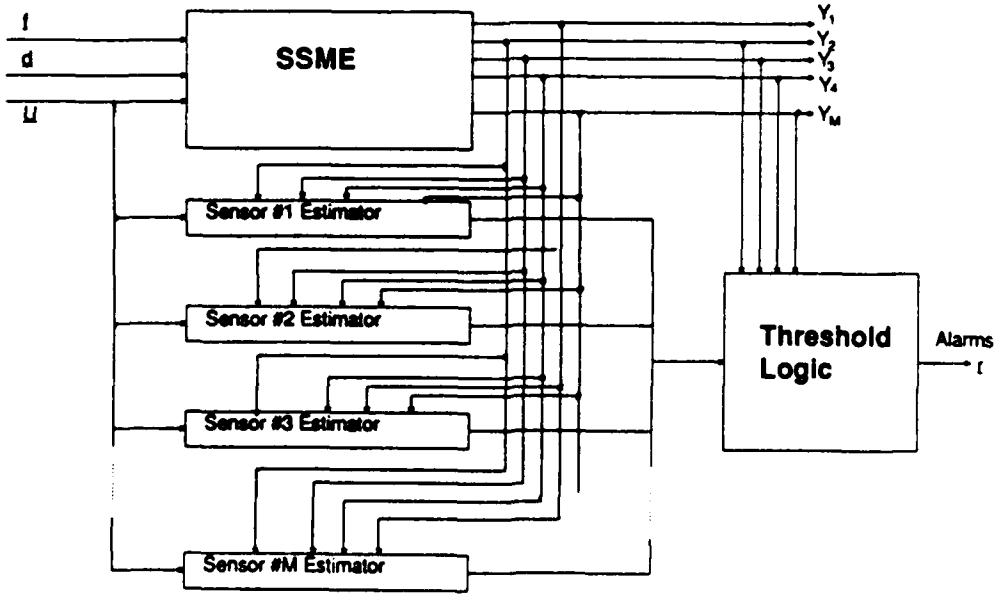

Generalized Observer Scheme (GOS)

Figure 11. Schemes For Generating Estimates of Sensors Based on Input From Other Sensors

Table 5. Typical Liquid Rocket Engine Characteristics

Line Resistance	$\Delta P/(\text{Density Flow}^2)$
Pump Affinity	Flow/Speed
Pump Affinity	Head/Speed^2
C^*	PC A $_t$/Flow

Characteristics can be computed for every engine and then entered into a database for comparison with the characteristics from all engines in the family. Any characteristic which is "out of family" (the largest or smallest value seen, or close to it) warrants investigation. Armed with the equations for computing characteristics, and the assumption that only one sensor or component can fail at a given time, analysts can quickly narrow in on the sources of anomalies. In the example shown in Figure 12, three line resistances are calculated given readings from three pressure sensors, a temperature sensor (for computing specific gravity), and a flow sensor. In this example the two partial resistances R1-2 and R2-3 are out-of-family, while the overall resistance R1-3 is normal. The only explanation for this, assuming a single-point failure, is that pressure sensor P2 has failed (i.e., biased high). Had all three resistances been out-of-family in the same direction (i.e., high or low) then either the temperature or flow sensors would be suspect.

Engine characteristics provide relatively invariant relationships among small sets of sensors, thus they are good predictors for use in sensor validation. One approach to using characteristics for sensor validation is the following:

1. Sample a small segment of data for the engine under test and compute all characteristics.
2. If any characteristic is out-of-family, then suspect all sensors involved in its calculation (i.e., there was a possible sensor failure in the initial sample data).
3. The engine's characteristics are computed for each time slice and compared to the sampled characteristics. If the residual between any sampled and computed characteristic is larger than a threshold (say 2 sigma), then the sensors involved in the calculation are suspect.

(See Section 3.3 for a discussion of how these "suspicions" can be integrated into a final decision regarding sensor failure.)

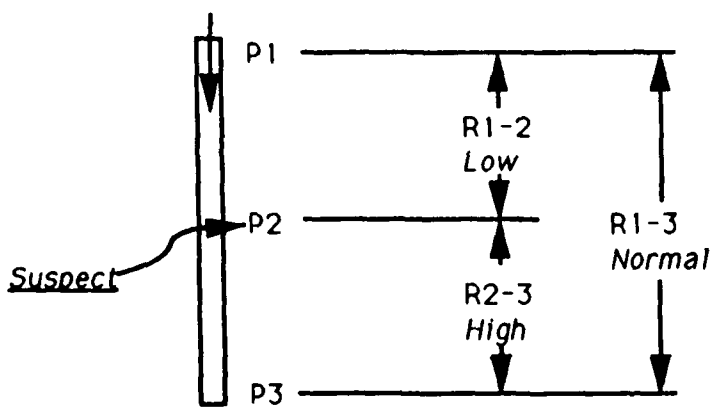

$$R = \frac{\Delta P}{Q^2 \bullet S.G.}$$

Figure 12. Example Characteristic-Based Diagnostics

To evaluate the approach outlined above for use on the SSME data, 15 characteristics relating 19 non-redundant PIDs were derived and tested to see how well they would perform as predictors.

To derive the characteristics, SSME flow diagrams were annotated with available PIDs, and the characteristic relations were then encoded through analysis of these diagrams. Figure 13 and 16 show examples of annotated flow diagrams along with its derived characteristics, and Table 6 shows the complete list of characteristics evaluated.

To evaluate whether family-averaged characteristics could be used as predictors, characteristics were computed for three test data sets at 109% steady-state power levels (A2492, A2493, and A2495). Characteristics were averaged over these three runs and then used as predictors for a fourth test data set (A2497) at its 109% steady-state power level. The results of this experiment are shown in columns 3 and 4 of Table 7.

As discussed above, an alternative approach to family-averaged characteristics is to take a small sample of data from the test set, compute engine-specific characteristics from this sample, and then use these characteristics as predictors. A second experiment was performed to evaluate this approach. A sample of the 109% steady-state data was taken (10 seconds of test A2497) and then used to predict PID values for the remainder of the 109% steady-state data. The results of this experiment are shown in columns 5 and 6 of Table 7.

In almost every PID prediction in the two experiments the sampled characteristic performed significantly better as a predictor than the family-averaged one (i.e., the residuals-the difference between the sensed value and the predicted value-were larger for averaged characteristics than for sampled ones). This can also be seen graphically from plots of sensed vs. predicted PID values. Figure 15 shows a prediction and residual for PID 1205 using a family-averaged characteristic (LPFP Q/N). Figure 16 shows the same prediction using a sampled, engine-specific characteristic.

A final test was conducted to determine how well characteristic-based predictions would perform on transient test data. The characteristics sampled at the 109% power level in the previous experiment (for test A2497) were used to predict PID values during the first 30 seconds of the same test. Unfortunately, only 5 of the 42 predictions performed well enough to be usable during transient conditions. Figure 17 shows a typical prediction whose residual is too large during the transient conditions to make it usable for sensor validation.

The characteristic model development work is contained in Appendix B.

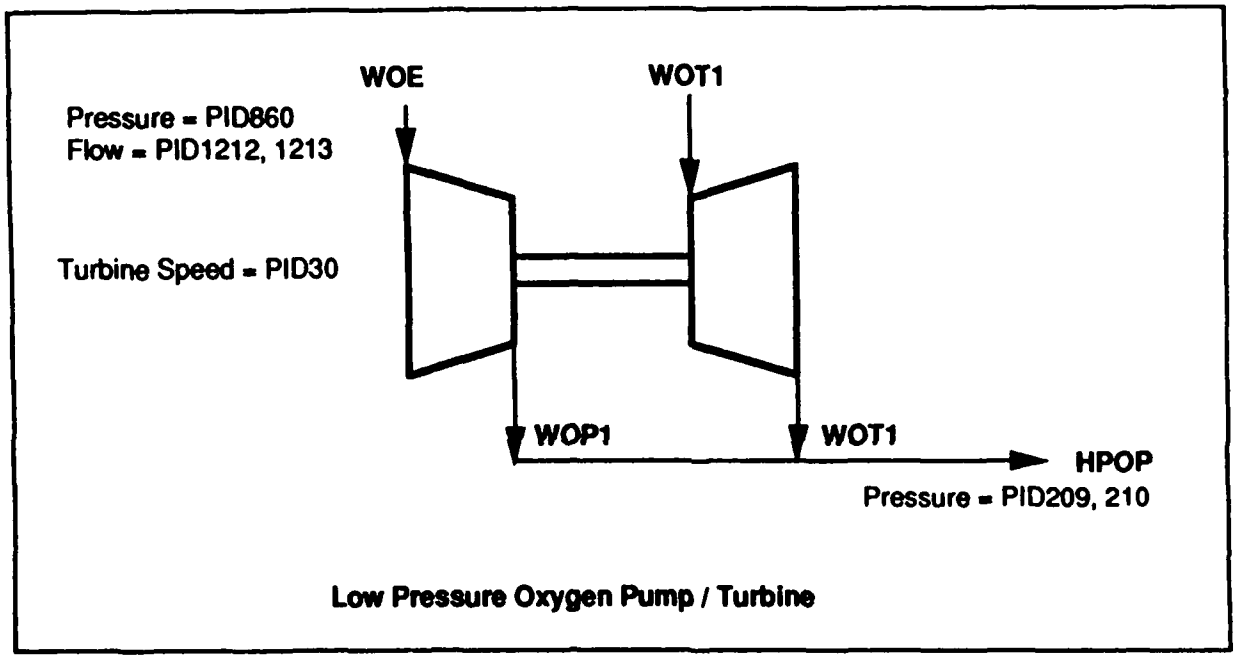

Characteristic	Equation	PID Relation
Pump Flow/Speed	Q/N = Constant	P1212/P30 = Constant
Pump ΔHead/Speed^2	ΔP/N^2 = Constant	(P209-P860)/P30^2 = Constant

Figure 13. Example of Flow Diagram and Derived Characteristics for Low Pressure Oxygen Pump/Turbine

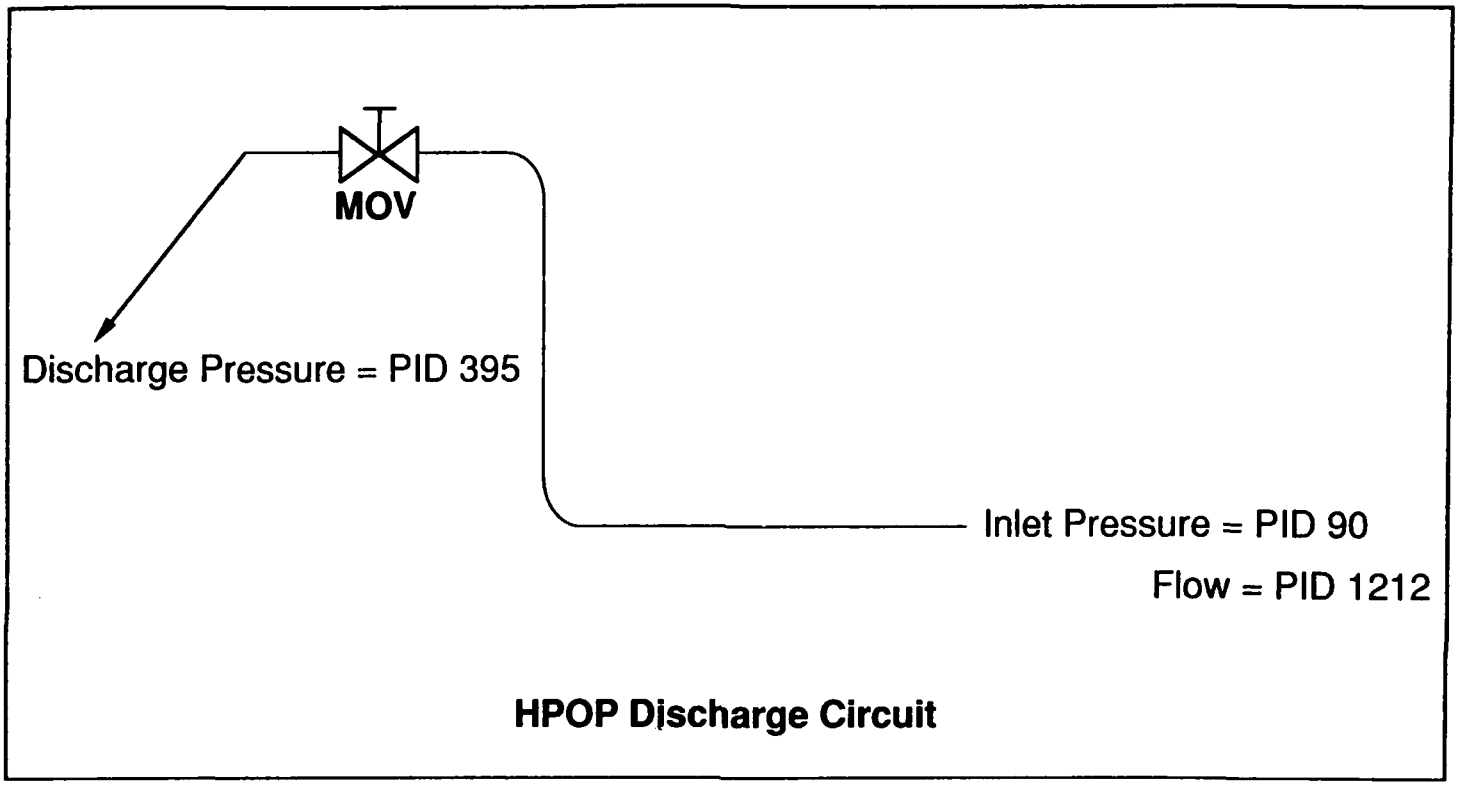

Characteristic	Equation	PID Relation
Line Resistance	$\Delta P/Q^2 \approx$ Constant	$(P90-P395)/P1212^2 \approx$ Constant

15-16-46

Figure 14. Example of Flow Diagram and Derived Characteristics For HPOP Discharge Circuit

Table 6 Characteristic PID Relations Evaluated

Characteristic	Equation	PID Relation	Label
Pump Flow/Speed	Q/N ~ Constant	P1212/P30 ~ Constant P1205/P32 ~ Constant P133/P260 ~ Constant	LPOP Q/N LPFP Q/N HPFP Q/N
Pump ΔHead/Speed^2	ΔP/N^2 ~ Constant	(P209-P860)/P30^2 ~ Constant (P203-P819)/P32^2 ~ Constant (P52-P133)/P260^2 ~ Constant	LPOP H/N2 LPFP H/N2 HPFP H/N2
Line Resistance	ΔP/Q^2 ~ Constant	(P90-P395)/P1212^2 ~ Constant (P52-P129)/P133^2 ~ Constant (P52-P17)/P133^2 ~ Constant (P17-P436)/P133^2 ~ Constant (P52-P436)/P133^2 ~ Constant (P59-P58)/P1212^2 ~ Constant (PP59-P480)/P1212^2 ~ Constant (P209-P90)/P1212^2 ~ Constant (P209-P395)/P1212^2 ~ Constant	HPOP R1 MC R1 MC R2 MC 43 MC R4 PRE R1 PRE R2 HPOP R2 HPOP R3

Table 7 Results of Steady-State Characteristic Experiments

Predicted PID	Characteristic Used	Averaged Characteristics		Sampled Characteristics		PID Rating (3S)
		Observed Residual Avg	Observed Residual 3S	Observed Residual Avg	Observed Residual 3S	
P1212	LPOPQ/N	4.26E+1	8.32E+1	-1.36E+1	7.98E+1	8.50E+1
P30		-3.67E+1	7.16E+1	1.16E+1	6.81E+1	5.89E+1
P209	LPOPH/N2	3.00E+0	6.94E+0	6.33E-1	6.94E+0	1.20E+1
P860		-3.00E+0	6.94E+0	-6.33E-1	6.94E+0	5.00E+0
P30		-2.95E+1	6.83E+1	-6.19E+0	6.78E+1	5.89E+1
P90	HPOPR1	5.45E+0	3.14E+1	1.27E+0	3.16E+1	1.40E+2
P395		-5.45E+0	3.14E+1	-1.27E+0	3.16E+1	2.50E+1
P1212		-4.78E+1	2.79E+2	-1.05E+1	2.78E+2	8.50E+1
P1205	LPFPQ/N	-6.51E+2	1.25E+2	-4.42E+0	1.21E+2	2.20E+2
P32		6.33E+2	1.21E+2	4.47E+0	1.22E+2	1.98E+2
P203	LPFPH/N2	8.57E+0	4.76E+0	3.70E-3	4.88E+0	6.00E+0
P819		-8.57E+0	4.76E+0	-3.70E-3	4.88E+0	2.00E+0
P32		-2.92E+2	1.62E+2	-9.70E-2	1.62E+2	1.98E+2
P133	HPFPQ/N	-6.18E+0	8.41E+2	-5.18E+1	8.46E+2	1.69E+2
P260		1.33E+1	1.81E+3	1.11E+2	1.82E+3	3.15E+1
P52	HPFPH/N2	-1.48E+1	1.02E+3	6.93E+1	1.04E+3	1.90E+2
P133		1.48E+1	1.02E+3	-6.93E+1	1.04E+3	1.69E+2
P260		-3.10E+1	1.81E+3	1.17E+2	1.82E+3	3.15E+1
P52	MC R1	-4.29E+1	6.71E+1	-1.99E+0	6.62E+1	1.90E+2
P129		4.29E+1	6.71E+1	1.99E+0	6.62E+1	7.00E+1
P133		1.08E+2	1.69E+2	5.03E+0	1.69E+2	1.69E+2
P52	MC R2	-1.98E+2	4.58E+1	-1.20E+0	4.33E+1	1.90E+2
P17		1.98E+2	4.58E+1	1.20E+0	4.33E+1	1.40E+2
P133		9.09E+2	2.10E+2	5.98E+0	2.16E+2	1.69E+2
P17	MC R3	-7.26E+0	2.43E+1	-4.94E-1	2.47E+1	1.40E+2
P436		7.26E+0	2.43E+1	4.94E-1	2.47E+1	5.00E+1
P133		7.91E+2	2.63E+3	8.15E+1	2.79E+3	1.69E+2
P52	MC R4	-2.05E+2	4.73E+1	-1.68E+0	4.45E+1	1.90E+2
P436		2.05E+2	4.73E+1	1.68E+0	4.45E+1	5.00E+1
P133		9.03E+2	2.08E+2	8.03E+0	2.13E+2	1.69E+2
P59	PRE R1	1.40E+2	6.24E+1	1.68E+1	6.04E+1	1.90E+2
P58		-1.40E+2	6.24E+1	-1.68E+1	6.04E+1	1.40E+2
P1212		-1.96E+2	8.71E+1	-2.27E+1	8.13E+1	8.50E+1
P59	PRE R2	7.02E+1	5.77E+1	1.22E+1	5.63E+1	1.90E+2
P480		-7.02E+1	5.77E+1	-1.22E+1	5.63E+1	2.00E+2
P1212		-1.03E+2	8.41E+1	-1.75E+1	8.05E+1	8.50E+1
P209	HPOP R2	2.33E+1	6.83E+1	-1.10E+1	6.48E+1	1.20E+1
P90		-2.33E+1	6.83E+1	1.10E+1	6.48E+1	1.40E+2
P1212		1.84E+1	5.39E+1	-8.75E+0	5.15E+1	8.50E+1
P209	HPOP R3	2.90E+1	5.61E+1	-9.59E+0	5.33E+1	1.20E+1
P395		-2.90E+1	5.61E+1	9.59E+0	5.33E+1	2.50E+1
P1212		2.51E+1	4.86E+1	-8.40E+0	4.66E+1	8.50E+1

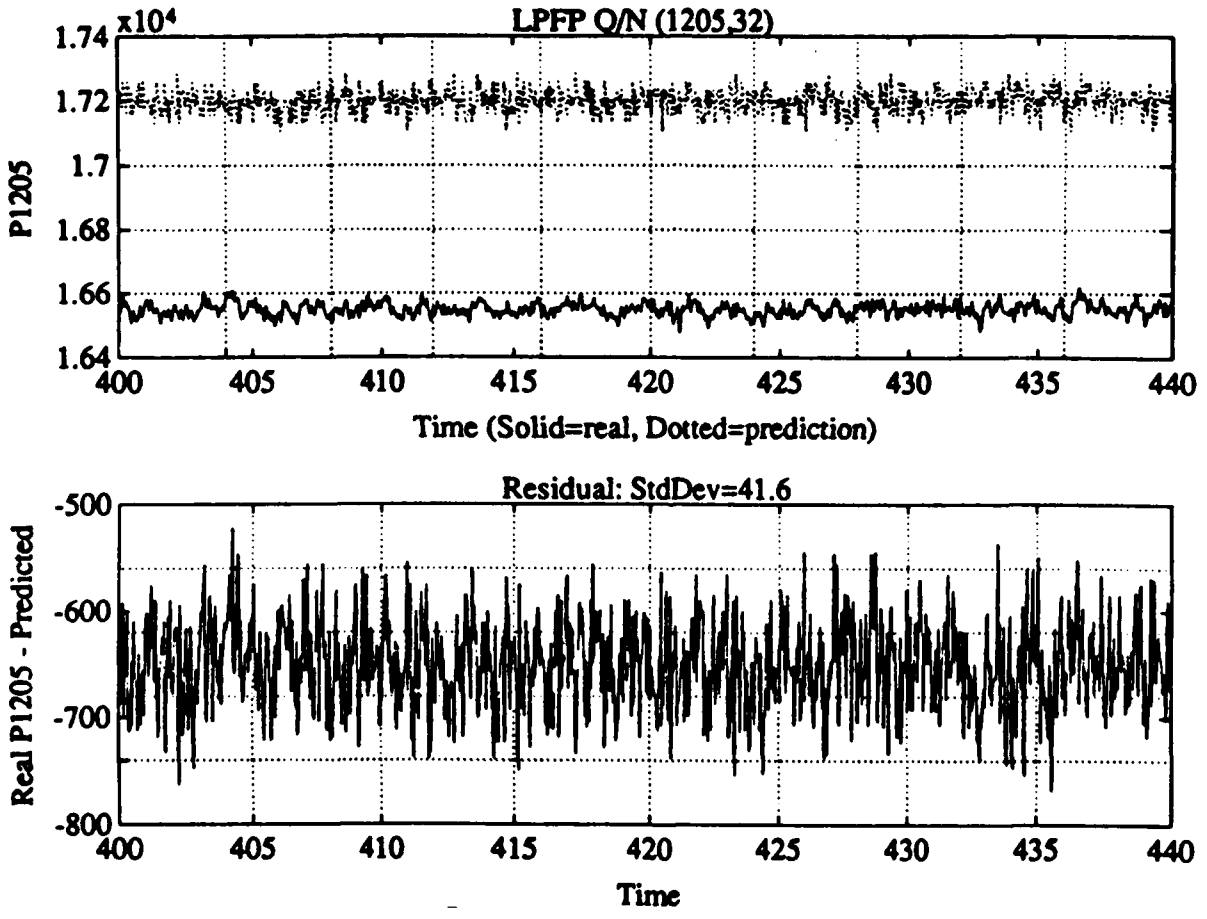

Figure 15. Familiy-Averaged Characteristic-Based Prediction

Empirical Regression Equations

The principle advantages of linear models are that they can usually be solved by a single matrix inversion and are relatively straightforward to derive. Linear regression models have been successfully employed on the Advanced Propulsion Monitoring System Program [3] to detect sensor failures in jet engines. Linear models of dynamic systems can display poor accuracy when applied over a wide range of dynamic response, however during steady state operation of the SSME, linear models appear to work well in tracking the relatively small amplitude of dynamic perturbations of the engine. A typical SSME thrust profile is comprised of over 90% commanded steady state operation.

The procedure being followed for developing the regression equations is shown in Figure 18. "Nominal" test data sets were partitioned into startup, shutdown, 65%, 100%,104% and 109% power levels. The SSME test summaries for the data sets on hand at Aerojet were reviewed for known sensor failures (summarized in Table 4) and excluded from the partitioned sets. The steady state data has been further screened to isolate the data sets during LOX venting, repressurization, and propellant transfer operations.

Using the partitioned data sets, the one to one correlations between all the sensors in the CADS data set have been determined using the Matlab software on the GFE Sun workstation [16]. As expected excellent correlation (correlation coefficient greater than 0.95) was found between redundant sensor channels and some reasonable correlation (correlation coefficient greater than 0.5) was found between over half of the sensors. The sole fact of a high correlation coefficient is not sufficient to guarantee that a true and significant physical correlation exists between signals. These sensors have been down selected based on physical reasonableness determined by subjective reasoning regarding physical interactions of the SSME. A summary of the correlation coefficients is included in Appendix C.

From analysis of the correlation coefficients, 42 potential linear regression relationships were identified and evaluated versus SSME data. Test were conducted similar to those described above for the characteristic equations. First, the coefficients of the regression models were developed using "family" data derived from four different tests at the same power level. Second, the coefficients were evaluated using a small sampling of data from the beginning of the specific test. The results of these experiments are summarized below. Typical test results are included in Appendix B.

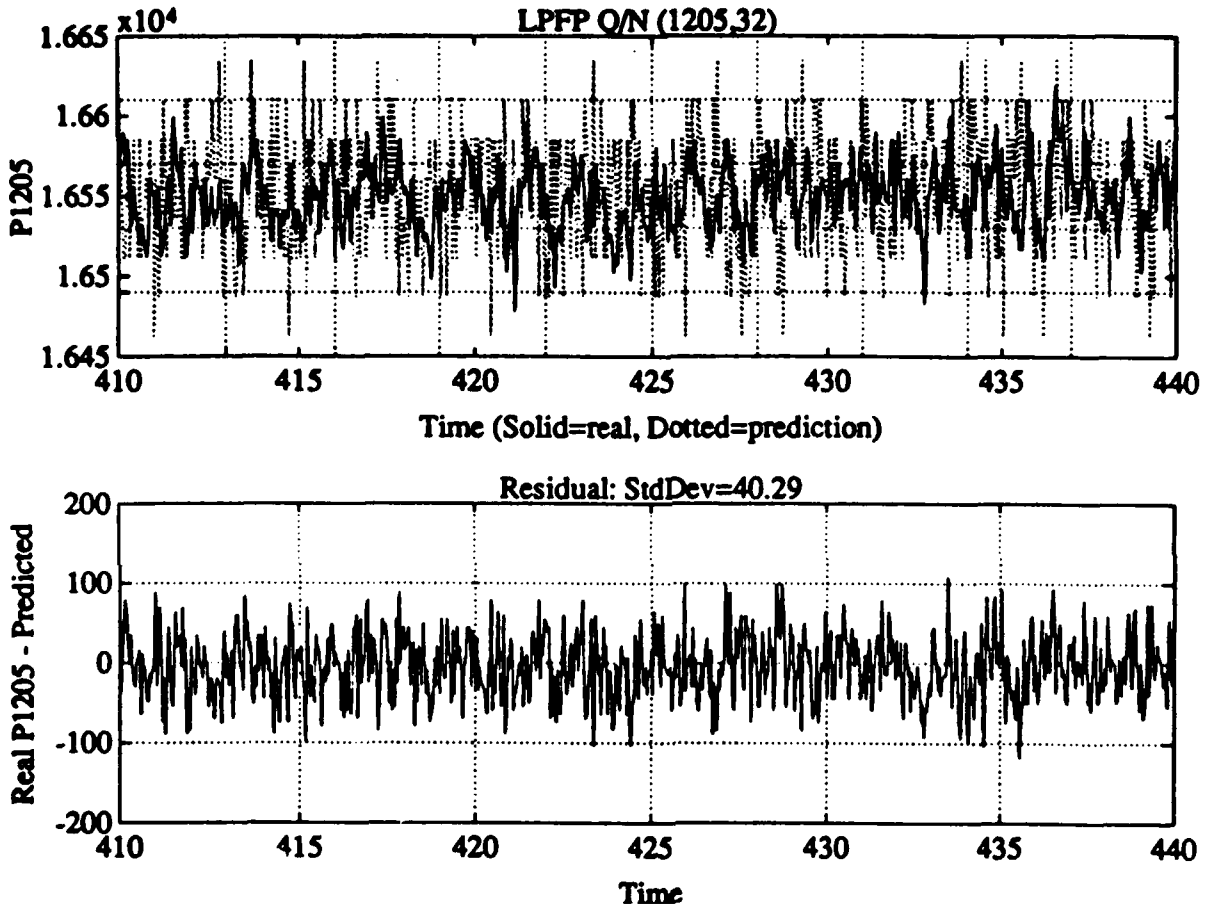

Figure 16. Sampled Characteristic-Based Prediction

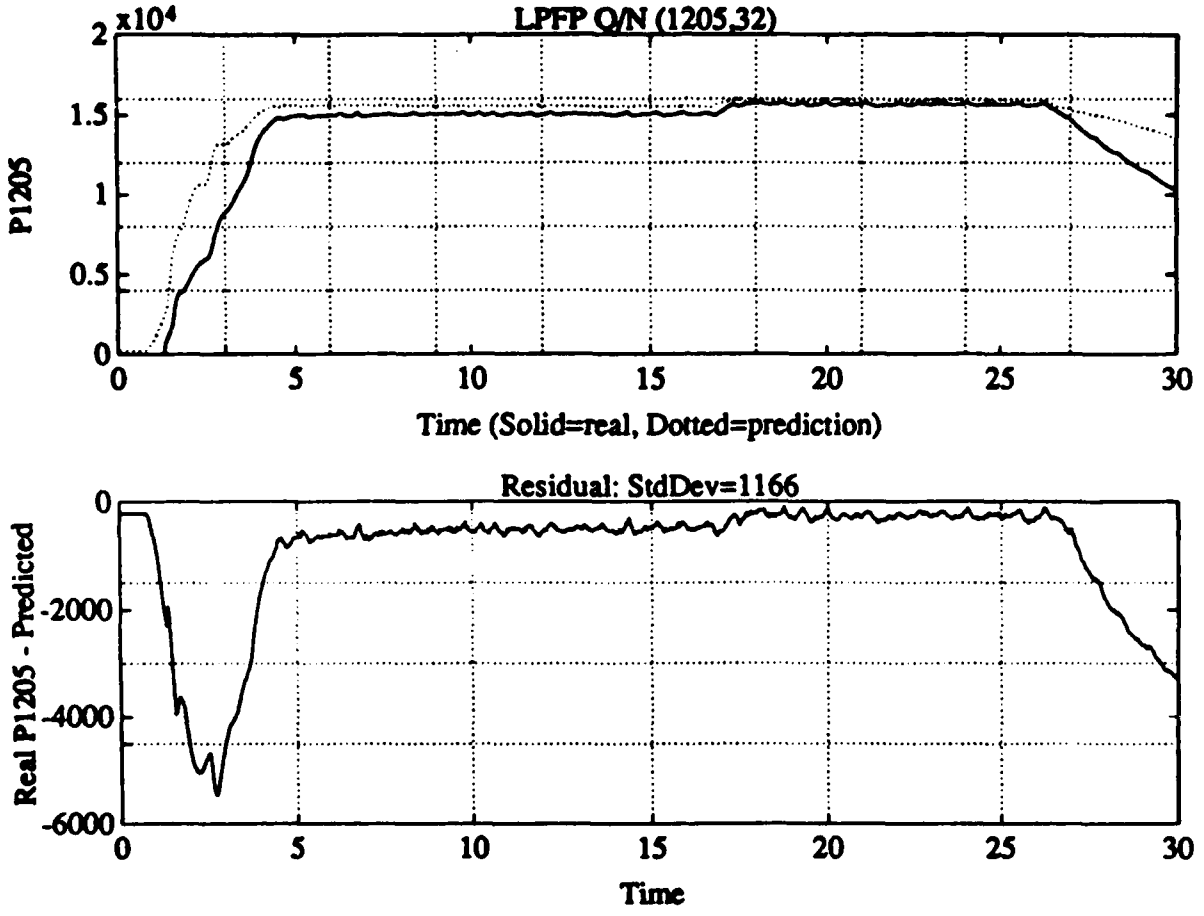

Figure 17. Example Transient Prediction

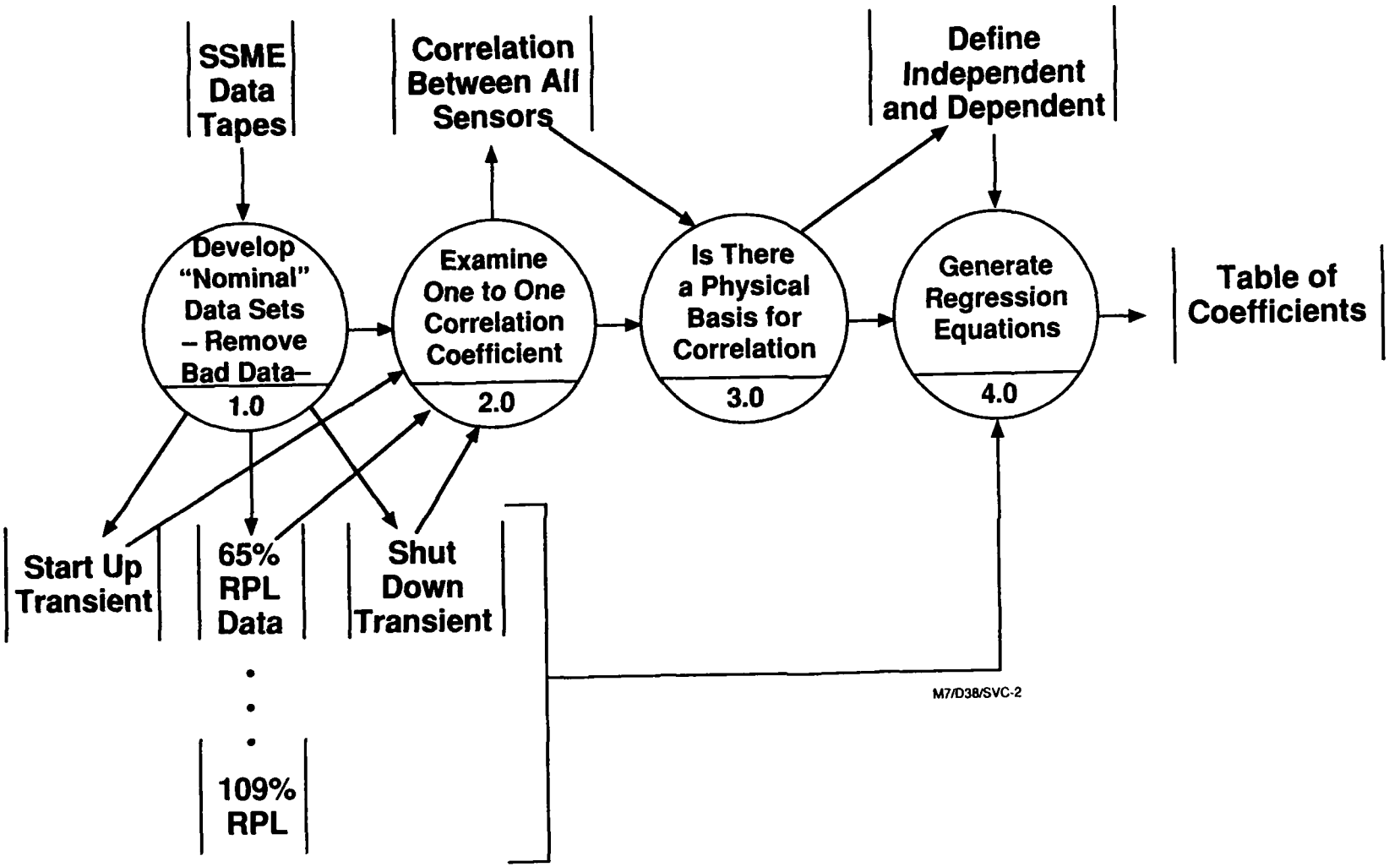

Figure 18. Procedure For Generating Regression Equations

Two typical residuals (true signal minus the predicted) generated using "family" data are shown in Figure 19. In the first example the Heat Exchanger Exit Pressure (PID 34) is calculated as a function of the POGO Precharge Pressure, HPOPT Intermediate Purge Pressure, and the HPOPT Secondary Seal Cavity Pressure. The equation was derived from 109% power level data from test A1-619 and tested on 109% power level data from test A1-620. The residual shows a slight offset from zero which is a common feature of many of the equations tested. This offset is approximately 10% of the documented SSME sigma for the parameter. The second example is for the POGO Precharge Pressure (PID 221) as a function of how many other parameters which includes its redundant channel. As might be expected, the inclusion of a redundant channel produces very good correlations with little shift from zero. Equations such as that in first example appear promising for providing sensor predictions considering no redundant parameters were included. Equations which include redundant channels such as the second example are heavily weighted by the redundant channel and will work for data validation and reconstruction only when the sensor failure mode is such that the loss of one sensor channel does not influence the other sensor channel (e.g. poor cable connection). These results often show a fixed offset of the signal representative of the variance of the particular engine to the family. This offset can not be predicted a priori and may trigger false alarms in a simple fault tree logic isolation scheme.

The use of engine specific data to generate the regression equations yielded more accurate models. The regression coefficients were derived using a 2 second (50 data points) time slice at the beginning of a given steady state portion of the test. Using sampled data from the beginning of the steady state time slice virtually eliminates the offset because the coefficients of the equations are calibrated for the particular engine. Of the empirical equations evaluated, 28 equations yielded a standard deviation less than that of each of the variables and significantly less than the family two sigma database. Figure 20 shows two typical examples of the linear regression equations derived by sampling the power level.

Conclusions Of Parameter Estimation

Engine characteristic and empirical equations provide a good source of analytical redundancy. Although only a small set of all potential relations have been evaluated, a larger set covering most of the PIDs on the SSME should be derivable. Table 8

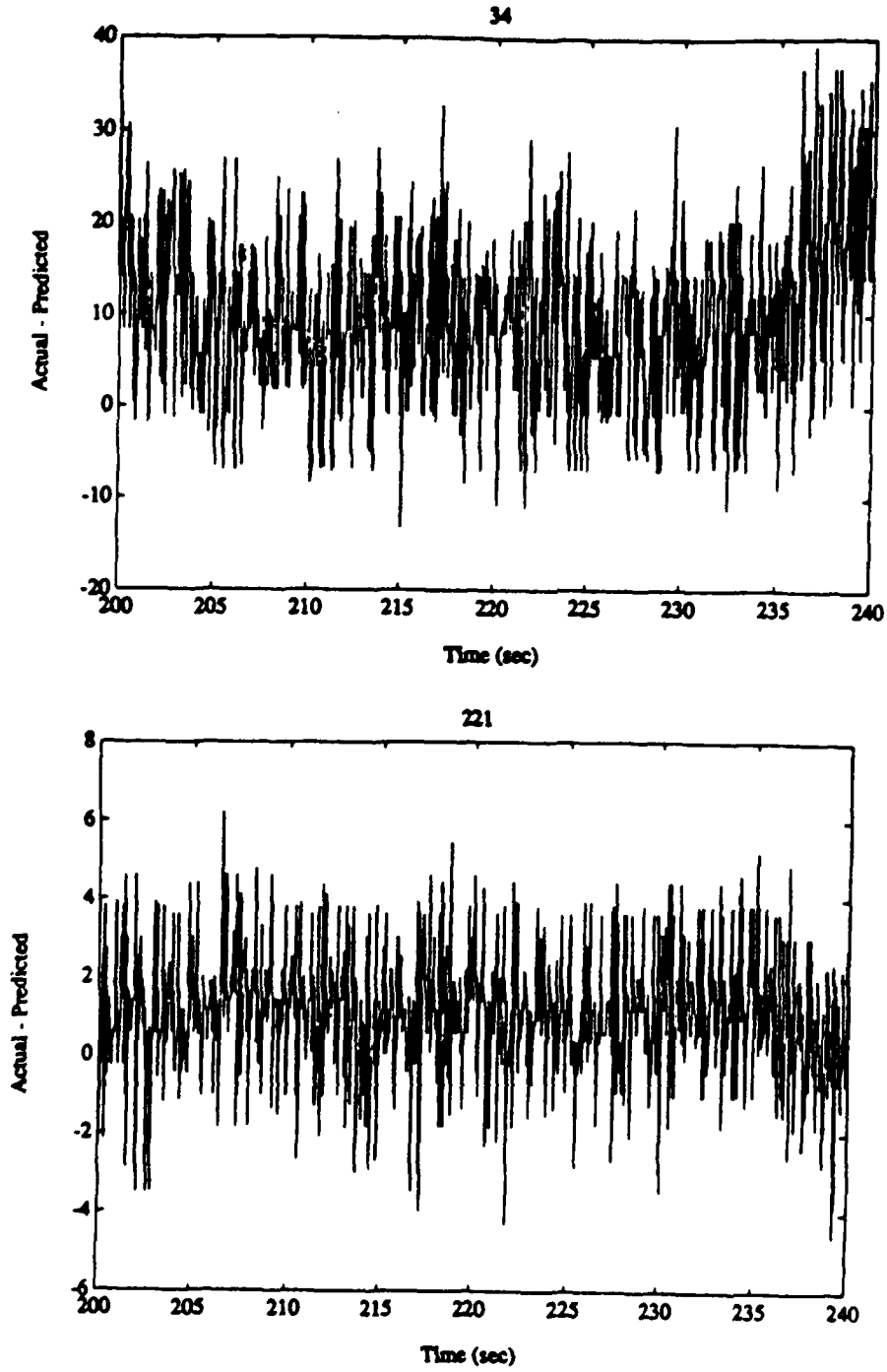

Figure 19. Example of Familiy-Averaged Regression Results With a) Nonredundant and b) Redundant Parameters Included

summarizes the CADS PIDs (based on the sensor set selected for validation) for which characteristic and empirical equations have been developed. In addition, PIDs for which hardware redundant channels are available are also indicated. In summary:

Characteristics and empirical equations computed from samples of data from the engine being evaluated work better than family-averaged ones.
Sampled equations can be checked for reasonableness by comparison to a database of family characteristics.
The characteristic and empirical equations work better during steady state operation than during engine transients.

Fault Detection

Once a set of equations (empirical or characteristic) have been developed for the sensors, fault detection is accomplished by comparing the true signal to the prediction. If the resulting difference (the residual) exceeds a predefined threshold value then a failure of the equation is declared. The cause of the equation failure may be a failure of any of the sensors in the equation. Figure 21 illustrates how a residual could violate predefined thresholds, each of which represents a different confidence level as to the existence of a failure. If the three threshold levels are taken to be the standard deviation of the residual computed from nominal data, then the probability of failure could be assigned by assuming Gaussian statistics. Spikes in the data which tend to cross the threshold level for only a single cycle can be filtered from true violations of the threshold limits by applying statistical tests.

Statistical hypothesis tests can be used to define detection limits for sensors measuring well-behaved random data. The most common hypothesis tests are concerned with the mean and standard deviation of a normal distribution. If the data of interest is approximately normally distributed or if the data can be transformed into approximately normal random variables, such hypothesis tests could be applied directly. Detection limits could be established either to one side or to both sides, using standard methodology, and the probability of false alarm and the probability of detection could be rigorously determined. The one-sided binomial confidence limit can be used with sequences of observed exceedances of the detection limits to interpret the significance of the exceedances. If the exceedances are interpreted as not being false alarms, the sensor can be confidently classified as failed.

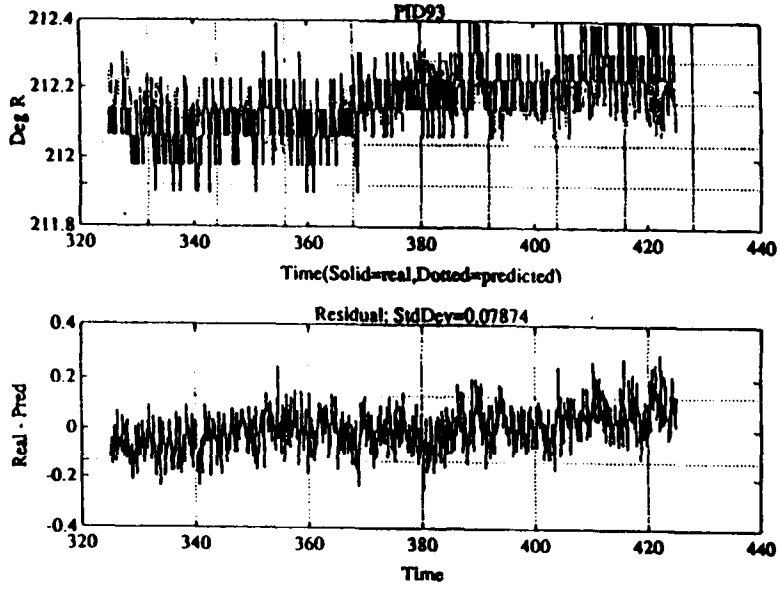

PID 93=fnc(40,42,59,210)

Data Calibrated With 320-322 second Time Slice

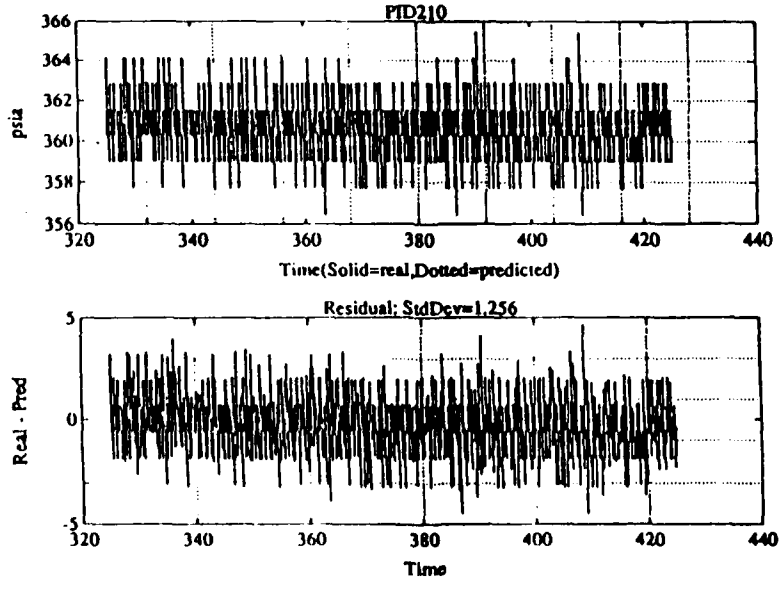

PID 210=fnc(34,90)

Data Calibrated With 320-322 second Time Slice

Figure 20. Example Sampled Regression Results of SSME Data

Table 8 Applicable Techinques For ~~CADS~~ Selected PIDs

MEASUREMENT	MEAS SET	PID	UNITS	DATA LOW	DATA HIGH	DISCRIPTION	LIMIT CHECK & SIGNAL ANALYSIS	REDUNDANT CHANNEL AVAILABLE	EMPIRICAL EQUATION IDENTIFIED	CHARACTERISTIC EQUATION IDENTIFIED
MCC COOLANT DISCH PRESS CH A1	C	17	PSIA	0	7000	Pressure	YES			YES
MCC COOLANT DISCH TEMP CH B	C	18	DEG R	360	760	Temperature	YES			
MCC OXID INJ TEMP	C	21	DEG R	110	610	Temperature	YES			
MCC HOT GAS INJ PRESS CH A	C	24	PSIA	0	7000	Pressure	YES			
LPOP SPD CH B	C	30	RPM	180	6000	Rate	YES			YES
LPFP SPD CH A	C	32	RPM	600	20000	Rate	YES			YES
HEX DS PR (A49P9655H)	C	34	PSIA	0	7000	Pressure	YES		YES	
HPFP COOLANT PRESS CH A	C	53	PSIA	0	4500	Pressure	YES			
HPFP COOLANT PRESS CH B	C	54	PSIA	0	4500	Pressure	YES			
HPOTP SEC SEAL CAV PRESS CH A	C	91	PSIA	0	300	Pressure	YES	YES		
HPOTP SEC SEAL CAV PRESS CH B	C	92	PSIA	0	300	Pressure	YES	YES		
PBP DISCH TEMP CH A	C	93	DEG R	160	210	Temperature	YES	YES	YES	
PBP DISCH TEMP CH B	C	94	DEG R	160	210	Temperature	YES	YES	YES	
MCC PRESSURE CH A2	C	129	PSIA	0	3500	Pressure	YES	YES		YES
MCC PRESSURE CH A1	C	130	PSIA	0	3500	Pressure	YES	YES		YES
FUEL FLOWRATE CH A1	C	133	GPM	1080	18000	Rate	YES	YES		YES
MFV ACTUATOR POSITION CH A	C	136	PCT	-5	105	Position/Disp.	YES	YES		
MFV ACTUATOR POSITION CH B	C	137	PCT	-5	105	Position/Disp.	YES	YES		
MOV ACTUATOR POSITION CH A	C	138	PCT	-5	105	Position/Disp.	YES	YES		
MOV ACTUATOR POSITION CH B	C	139	PCT	-5	105	Position/Disp.	YES	YES		
OPOV ACTUATOR POSITION CH A	C	140	PCT	-5	105	Position/Disp.	YES	YES	YES	
OPOV ACTUATOR POSITION CH B	C	141	PCT	-5	105	Position/Disp.	YES	YES	YES	
FPOV ACTUATOR POSITION CH A	C	142	PCT	-5	105	Position/Disp.	YES	YES		
FPOV ACTUATOR POSITION CH B	C	143	PCT	-5	105	Position/Disp.	YES	YES	YES	
CCV ACTUATOR POSITION CH A	C	145	PCT	-5	105	Position/Disp.	YES	YES		
CCV ACTUATOR POSITION CH B	C	146	PCT	-5	105	Position/Disp.	YES	YES		
HYDRAULIC SYS PRESSURE A	C	147	PSIA	0	4000	Pressure	YES			
FUEL PREBURN PGE PRESS CH A	C	148	PSIA	0	1500	Pressure	YES			
OXID PREBNR PGE PRESS B	C	149	PSIA	0	1500	Pressure	YES			
HPFP DISCH PRESS CH A	C	152	PSIA	0	9500	Pressure	YES			YES
FPB CHMBR PR A	C	158	PSIA	0	7000	Pressure	YES		YES	YES
PBP DISCH PRESS CH B	C	159	PSIA	0	9500	Pressure	YES		YES	YES
MCC PRESSURE B2	C	161	PSIA	0	3500	Pressure	YES	YES		
MCC PRESSURE B1	C	162	PSIA	0	3500	Pressure	YES	YES		
HPOP DISCH PRESS CH A	C	190	PSIA	0	7000	Pressure	YES			YES
LPFP DISCH PRESS CH A	C	203	PSIA	0	300	Pressure	YES	YES	YES	YES
LPFP DISCH PRESS CH B	C	204	PSIA	0	300	Pressure	YES	YES	YES	YES
LPOP DISCH PRESS CH A	C	209	PSIA	0	600	Pressure	YES	YES	YES	YES
LPOP DISCH PRESS CH B	C	210	PSIA	0	600	Pressure	YES	YES	YES	YES
HPOTP I-SEAL PGE PRESS CH A	C	211	PSIA	0	600	Pressure	YES	YES	YES	
HPOTP I-SEAL PGE PRESS CH B	C	212	PSIA	0	600	Pressure	YES	YES	YES	
HYDRAULIC SYS PRESSURE CH B	C	214	PSIA	0	4000	Pressure	YES	YES		
FUEL SYS PGE PRESS CH A	C	219	PSIA	0	600	Pressure	YES	YES		
FUEL SYS PGE PRESS CH B	C	220	PSIA	0	600	Pressure	YES	YES		
POGO PRECHG PRESS CH A	C	221	PSIA	0	1500	Pressure	YES	YES	YES	
POGO PRECHG PRESS CH B	C	222	PSIA	0	1500	Pressure	YES	YES	YES	
EMERG SHT DN PRESS CH A	C	223	PSIA	0	1500	Pressure	YES	YES		
EMERG SHT DN PRESS CH B	C	224	PSIA	0	1500	Pressure	YES	YES		
LPFP DISCH TEMP CH A	C	225	DEG R	30	55	Temperature	YES	YES		

MEASUREMENT	MEAS SET	PID	UNITS	DATA LOW	DATA HIGH	DISCRIPTION	LIMIT CHECK & SIGNAL ANALYSIS	REDUNDANT CHANNEL AVAILABLE	EMPIRICAL EQUATION IDENTIFIED	CHARACTERISTIC EQUATION IDENTIFIED
LPFP DISCH TEMP CH B	C	226	DEG R	30	55	Temperature	YES	YES		
HPFT DISCH TEMP CH A	C	231	DEG R	460	2760	Temperature	YES	YES		
HPFT DISCH TEMP CH B	C	232	DEG R	460	2760	Temperature	YES	YES		
HPOT DISCH TEMP CH A	C	233	DEG R	460	2760	Temperature	YES	YES		
HPOT DISCH TEMP CH B	C	234	DEG R	460	2760	Temperature	YES	YES		
MFV HYD TEMP CH A	C	237	DEG R	360	760	Temperature	YES	YES		
MFV HYD TEMP CH B	C	238	DEG R	360	760	Temperature	YES	YES		
MOV HYD TEMP CH A	C	239	DEG R	360	760	Temperature	YES	YES		
MOV HYD TEMP CH B	C	240	DEG R	360	760	Temperature	YES	YES		
FUEL FLOWRATE CH A2	C	251	GPM	1080	18000	Rate	YES	YES		
FUEL FLOWRATE CH B2	C	253	GPM	1080	18000	Rate	YES	YES		
FUEL FLOWRATE CH A1	C	258	GPM	1080	18000	Rate	YES	YES		
HPFP SPD A	C	260	RPM	1350	45000	Rate	YES	YES		YES
HPFP SPD B	C	261	RPM	1350	45000	Rate	YES	YES		YES
ANTI-FLOOD VLV POS CH A	C	268	PCT	-5	105	Position/Disp.	YES	YES	YES	
ANTI-FLOOD VLV POS CH B	C	269	PCT	-5	105	Position/Disp.	YES	YES	YES	
FUEL FLOWRATE CH B1	C	301	GPM	1080	18000	Rate	YES	YES		
LVL S BARO PR	F	316				Pressure	YES			
HPOP DS PR NFD	F	334	PSIA	0	7000	Pressure	YES	YES		
PBP DS PR NFD	F	341	PSIG	0	9500	Pressure	YES	YES		
MAIN INJECTOR LOX INJECTION PR N	F	395	PSIG	0	5000	Pressure	YES			YES
LPFT IN PR	F	436	PSIG	0	10000	Pressure	YES	YES		
HPFTP DISCH PR NFD	F	459	PSIA	0	9500	Pressure	YES	YES		
OPB PC	F	480	PSIS	0	10000	Pressure	YES	YES		YES
MFV DIS SKIN T1	F	553	DEG R	35	560	Temperature	YES	YES		
MFV DIS SKIN T2	F	554	DEG R	35	560	Temperature	YES	YES		
MCC LOX DOME T NO 3 (NOT APPROV	F	595	DEG R	110	610	Temperature	YES			
HPFP CLNT LINER TEMP	F	650	DEG R	0	560	Temperature	YES			
HPFP DS TEMP	F	659	DEG R	30	1200	Temperature	YES			
ENGINE FUEL FLOW NFD (A49R8038A)	F	722	GPM	0	29000	Rate	YES	YES		
LPOP SPD NFD (A49R8651A)	F	734	RPM	0	6400	Rate	YES	YES		
LPFP SPD NFD (A49R8001A)	F	754	RPM	0	24000	Rate	YES	YES		
HPFP SPD NFD (A49R8101A)	F	764	RPM	0	48000	Rate	YES	YES	YES	
ENG FL IN PR 2	F	819	PSIS	0	100	Rate	YES	YES		YES
ENG FL IN PR 1	F	821	PSIS	0	100	Pressure	YES	YES		YES
ENG FL IN PR 3	F	827	PSIS	0	100	Pressure	YES	YES		YES
ENG OX IN PR 1	F	858	PSIS	0	250	Pressure	YES	YES		YES
ENG OX IN PR 2	F	859	PSIS	0	250	Pressure	YES	YES		YES
ENG OX IN PR 3	F	860	PSIS	0	250	Pressure	YES	YES		YES
HEAT EXCHANGER INTERFACE PRESS	F	878	PSIS	0	5000	Pressure	YES			
HEAT EXCHANGER INTERFACE TEMP	F	879	DEG F	160	1900	Temperature	YES			
HPOP PR SL DR PR 1	F	951	PSIG	0	100	Pressure	YES	YES	YES	
HPOP PR SL DR P2	F	952	PSI	0	100	Pressure	YES	YES	YES	
HPOP PR SL DR P3	F	953	PSI	0	100	Pressure	YES	YES	YES	
ENGINE GN2 PURGE INTRF PRESS	F	957	PSIS	0	1000	Pressure	YES			
HPOT PR SL DR PR	F	990	PSIG	0	100	Pressure	YES		YES	
FAC LH2 FLOWMETER OUTLET TEMP	F	1017	DEG R	-430	-380	Temperature	YES	YES		
LPTOP INLET TEMP	F	1058	DEG R	160	180	Temperature	YES			
FAC FUEL FLOW 1	F	1205	GPM	0	22000	Rate	YES	YES		YES

MEASUREMENT	MEAS SET	PID	UNITS	DATA LOW	DATA HIGH	DISCRIPTION	LIMIT CHECK & SIGNAL ANALYSIS	REDUNDANT CHANNEL AVAILABLE	EMPIRICAL EQUATION IDENTIFIED	CHARACTERISTIC EQUATION IDENTIFIED
FAC FUEL FLOW 2	F	1206	GPM	0	22000	Rate	YES	YES		YES
FAC OX FLOW 1	F	1212	GPM	0	8500	Rate	YES	YES		YES
FAC OX FLOW 2	F	1213	GPM	0	8500	Rate	YES	YES		YES
HORZ F1A	F	1345	KLB	0	100	Force	YES	YES		
HORZ F2A	F	1350	KLB	0	100	Force	YES	YES		
VERT F1A	F	1360	KLB	0	225	Force	YES	YES		
VERT F1B	F	1361	KLB	0	225	Force	YES	YES		
VERT F2A	F	1365	KLB	0	225	Force	YES	YES		
VERT F3A	F	1370	KLB	0	225	Force	YES	YES		
VERT F3B	F	1371	KLB	0	225	Force	YES	YES		
AFV DIS SKIN TEMP NO 1	F	1420	DEG R	160	560	Temperature	YES	YES		
AFV DIS SKIN TEMP NO 2	F	1421	DEG R	160	560	Temperature	YES	YES		
GIM BR LNG 1 (A49D8607A)	F	1543	GRMS	0	30	Vibration	YES	YES	YES	
GIM BR LNG 2 (A49D8608A)	F	1544	GRMS	0	30	Vibration	YES	YES	YES	
GIM BR LNG 3 (A49D8609A)	F	1547	GRMS	0	30	Vibration	YES	YES	YES	
MCC LINER CAV P2	F	1956	PSI	0	200	Pressure	YES	YES	YES	
MCC LINER CAV P3	F	1957	PSI	0	200	Pressure	YES	YES	YES	

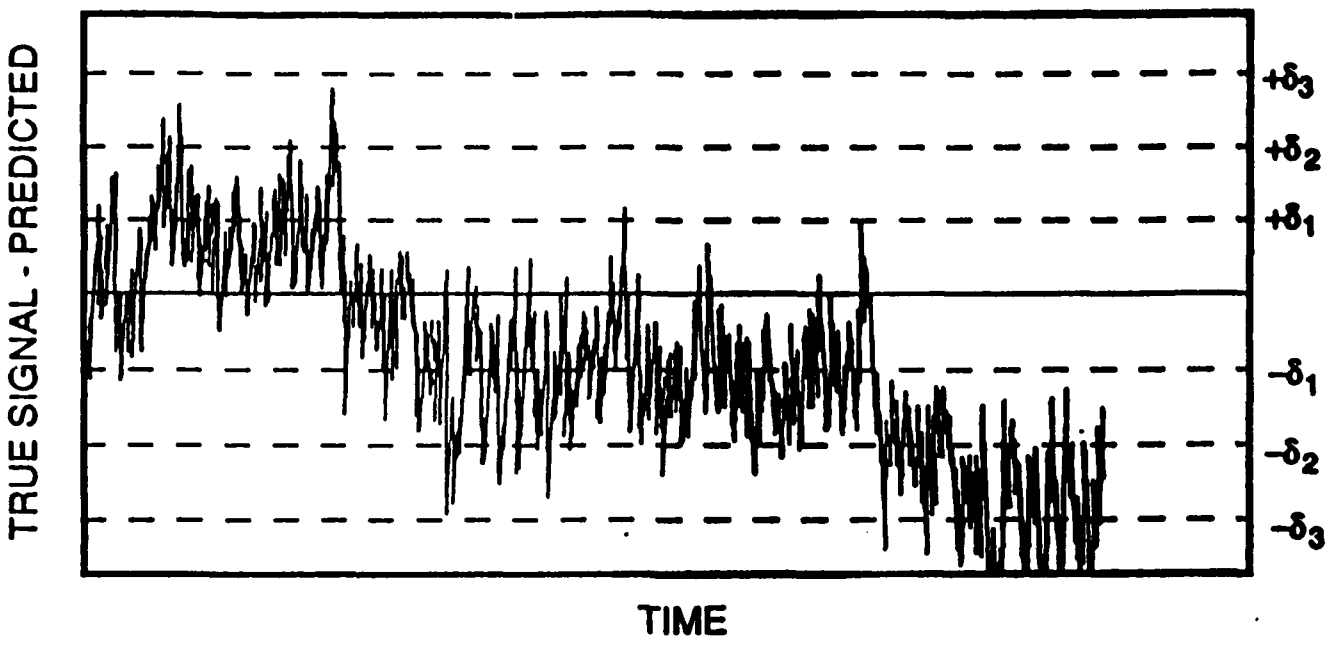

- **Confidence Levels (i.e. Probabilities) Can Be Assigned To Different Level**

Example

Assuming Gaussian Statistics

δ_1 = 1 sigma = 68 % confidence of failure if thresold is violated

δ_2 = 2 sigma = 95 % confidence of failure if thresold is violated

δ_3 = 3 sigma = 99 % confidence of failure if thresold is violated

(sigma based on analysis of model residual against "nominal engine data")

Figure 21. The Probability of Sensor Failure Based On Model Results Is Related To Statistics Of Residual Vector

In any hypothesis test, two types of errors are possible. The Type I error is rejecting the hypothesis when it is true. The Type II error is accepting the hypothesis when it is false. If the null hypothesis is defined as the condition that the sensor and the relevant component are functioning properly, then the probability of the Type I error is the probability of false alarm. This probability may be determined whether there is one detection limit (one-sided test) or two detection limits (two-sided test). In most cases of sensor failure detection, the two-sided limit test would be the correct one to use. Similarly, the probability of the Type II error is the complement of the detection probability.

For a particular application, as the probability of false alarm is decreased, the probability of detection is also decreased. The detection limits must therefore be set with appropriately balanced values of these two probabilities. If the probability of false alarm cannot be made negligible, additional logic may be used to interpret the observed exceedances relative to the theoretical probability of false alarm. Appropriate methodology for the interpretation of the observed exceedances is the one-sided binomial confidence limit.

Fault Isolation

Following the occurrence of a detected parameter fault (i.e. a failed equation), the failed PID(s) must be isolated. An approach suitable for the SDV&SR system is based on fault tree logic [3]. In this scheme, a system of equations for the SSME sensor is specified such as that shown in Figure 22. An incidence matrix which codes the occurrence of independent and dependent parameters in the model is then constructed. Rows of the incidence matrix correspond to the equations and each column of the matrix represents a PID. The matrix is built by entering a one if a PID is present as an independent variable in an equation or a zero if it is not as shown in Figure 22. Each column of the incidence matrix represents a fault detection vector for its specific PID as shown in Figure 22. If the threshold limits are set such that a failed PID causes a failure of all equations in which it appears with equal probability, then single point failure detection can be isolated by comparing the vector of failed equations to the each of the fault detection vectors for a match. The ability to isolate multi-point failures is dependent on the specific structure of the incidence matrix (i.e. the system of equations).

Step 1. Define Model: Example 8 equations (2 based on hardware redundancy) 12 Parameters

Model #		
1	HEX DS PR	PID 34 = fnc(40,59,210,221,234)
2	OPOV ACT POS CH A	PID 40 = fnc(59,94,210)
3	FPOV ACT POS CH A	PID 42 = fnc(40,59,94)
4	PBP DIS PR CH A	PID 59 = fnc(58,94,210)
5	PBP DIS TEMP CH B	PID 94 = fnc(40,42,59,210,234)
6	LPOP DIS PR CH B	PID 210 = fnc(34,90)
7	LPOP DIS PR CH A	PID 209 = fnc(210)
8	PBP DIS TEMP CH A	PID 93 = fnc(94)

Figure 22. Fault Tree Logic for Isolating Sensor Failures

Step 2. Form an Incidence Matrix With 1's and 0's Indicating Appearance of PID in Model

	PID Number											
Model No.	34	40	42	58	59	90	93	94	209	210	221	234
1	0	1	0	0	1	0	0	0	0	1	1	1
2	0	0	0	0	1	0	0	1	0	1	0	0
3	0	1	0	0	1	0	0	1	0	0	0	0
4	0	0	0	1	0	0	0	1	0	1	0	0
5	0	1	1	0	1	0	0	0	0	1	0	1
6	1	0	0	0	0	1	0	0	0	0	0	0
7	0	0	0	0	0	0	0	0	0	1	0	0
8	0	0	0	0	0	0	0	1	0	0	0	0

Step 3. – If Failed PID Fails All Equations Then Comparison of Fault Detection Vectors to Failed Models Enables Isolation

– Multiparameter Isolation Depends on Structure of Incidence Matrix

PID #	34	40	• • •	234
	1	1		1
	0	0		0
	0	0		0
	0	0		0
	0	1		1
	1	0		0
	0	0		0
	0	0		0

Figure 22 cont.

2.2.4 Pattern Matching Techniques

Those sensors whose status cannot be effectively determined using linear or non-linear regression techniques, or engine characteristic equations, can be analyzed using pattern matching tools. Areas of potential application include start, shutdown, and power level transients, as well as thermal drifts and other highly non-linear phenomena. Pattern clustering appears to be a good candidate for the reconstruction of data which cannot be accurately reconstructed by using regression or engine characteristic modeling. Pattern matching techniques fall into two basic categories: pattern matching algorithms and artificial neural networks. Even though the mechanics of the two methods are different, the resultant output is similar for both. Neural networks are useful for both sensor validation and data reconstruction purposes and have been demonstrated with SSME data [17].

The two primary types of pattern matching algorithms are categorized as decision-theoretic and semantic. For this study, only the decision-theoretic algorithms were investigated. This family of algorithms operates roughly as follows: An exemplar pattern of interest is input to the algorithm, along with a sample test pattern. The algorithm reduces the two patterns into their respective vector components and computes the matching score between the two. The matching score is a statistical measure of the relative likeness between the vectors. This technique can be used to validate sensors in the following manner: patterns of data, such as the startup transient of the MCC pressure, which are known to be good, can be input into the algorithm as sample exemplar patterns. As more samples are used to train the algorithm, the algorithm is increased. Once the algorithm has "learned" the pattern, suspect data (data where no validity determination has been made), can be input into the algorithm. The matching score is then computed, and if it falls below a predetermined threshold, the sensor (in this case PID 130) is classified as failed. The most well known of the decision-theoretic algorithms is the K-nearest neighbor classifier [18, 19, 20]. This algorithm works on the principal that the probability of any particular point being part of the pattern of interest is directly proportional to a specified number of points nearby (K), and inversely proportional to the sample space volume containing k number of points.

Artificial neural networks appear to be good candidates for both sensor validation and data reconstruction. Neural networks are a highly parallel computational architecture which is roughly modeled on the physical structure of the brain. The basic

building blocks of all artificial neural nets are layers of nodes (neurons) which have weighted connections to other nodes. A number of specialized architectures, in which the number and configuration of inputs, nodes, layers, connections, and outputs are varied, have been developed for a variety of specialized purposes [21, 22, 23]. Connection weights can either be variable or fixed, depending on which particular architecture is selected. Nodes in a particular layer can be connected to specific nodes in the adjacent layers, or they can be connected to all of the nodes in adjacent layers (fully connected). The first layer of nodes in any net is called the input layer, the last layer is called the output layer, and all intermediate layers are called hidden layers. In the case of a two layer network, one input is presented to each of the nodes in the first layer. Each of the inputs is then output to a node in the following layer as the product of the original input value and the appropriate connection weight. These products are then combined algorithmically by the second node (known as a processing unit) and that output is compared to a target value. The difference of the two is the residual error. As in algorithmic pattern matching, if the residual error is within the required threshold, the computation is complete and the final output, in this case a sensor signal, is considered good. If not the connection weights are modified algorithmically, and the neural net process is repeated, and continues until an acceptable residual error level has been reached.

For the purposes of pattern recognition and data reconstruction, the best neural net architecture appears to be the multi-layer perceptron [22]. This architecture is better known as the back-error propagation or simply the back propagation network. This name refers to the algorithm which is used to reset the connection weights after each complete pass through the network. Figure 23 shows a flowchart representation of this architecture. The perceptron has variable connection weights, is fully connected throughout, and uses supervised learning. For the complex pattern matching and data reconstruction tasks on this program, at least four layers of nodes (two hidden layers) are desirable. The number of nodes in the hidden layers should be three times the number of input nodes, so that sufficient pattern definition is achieved [22]. This approach is identical to that taken by Guo and Nurre, who were successfully able to diagnose a simulated SSME sensor failure and reconstruct the lost data [17].

Another architecture which appears to have promise for pattern classification is known as competitive learning [21]. This architecture is very similar to the multi-layer perceptron, except that the former uses unsupervised learning, and only the weight of

the highest valued or "winning" output node is modified during the recursive phase of the process. This process continues until the value of the "winning" node no longer changes.

Due to the complexity of both the neural network and pattern matching/pattern clustering approaches to sensor validation and reconstruction, designing and implementing either system from scratch is relatively resource intensive. There are several commercial software products, representing both pattern matching paradigms, which are currently available and listed in Appendix D. These packages contain networks or algorithms which can perform pattern classification tasks.

3.3 Knowledge Fusion Approaches

As shown in the previous section, there are several possible sources of information about a PID's failure (Table 9 summarizes the sources of information that have been investigated so far). Given all of these pieces of information about a sensor, which may be conflicting and have varying degrees of uncertainty associated with them, the sensor validation system must be able to make (and justify) a decision about the status of each sensor. This is the problem addressed by a sub-discipline of Artificial Intelligence referred to as *information fusion* (also known as *evidential reasoning* or *reasoning with uncertainty*).

Information fusion involves the combination of evidence from several sources into a single, consistent model. Uncertainties in the sources of evidence (i.e., inaccuracies in the sensors or uncertainties in the fault detection algorithms themselves) are explicitly modeled and accounted for. There is a spectrum of information fusion techniques available, ranging from computationally efficient but unsound approaches, to those guaranteeing semantically correct results but having a high computational overhead and implementation complexity associated with them. In addition, for any given technique chosen there are typically many algorithms available for implementation. The following section will describe and evaluate the four most popular techniques currently used for information fusion, and evaluate which is the most appropriate for use in the sensor validation system.

Survey of Techniques

Four approaches to information fusion were evaluated for the sensor validation system. These approaches were selected based on their frequency of use in fielded systems and their mention in the literature. These measures of popularity indicate the

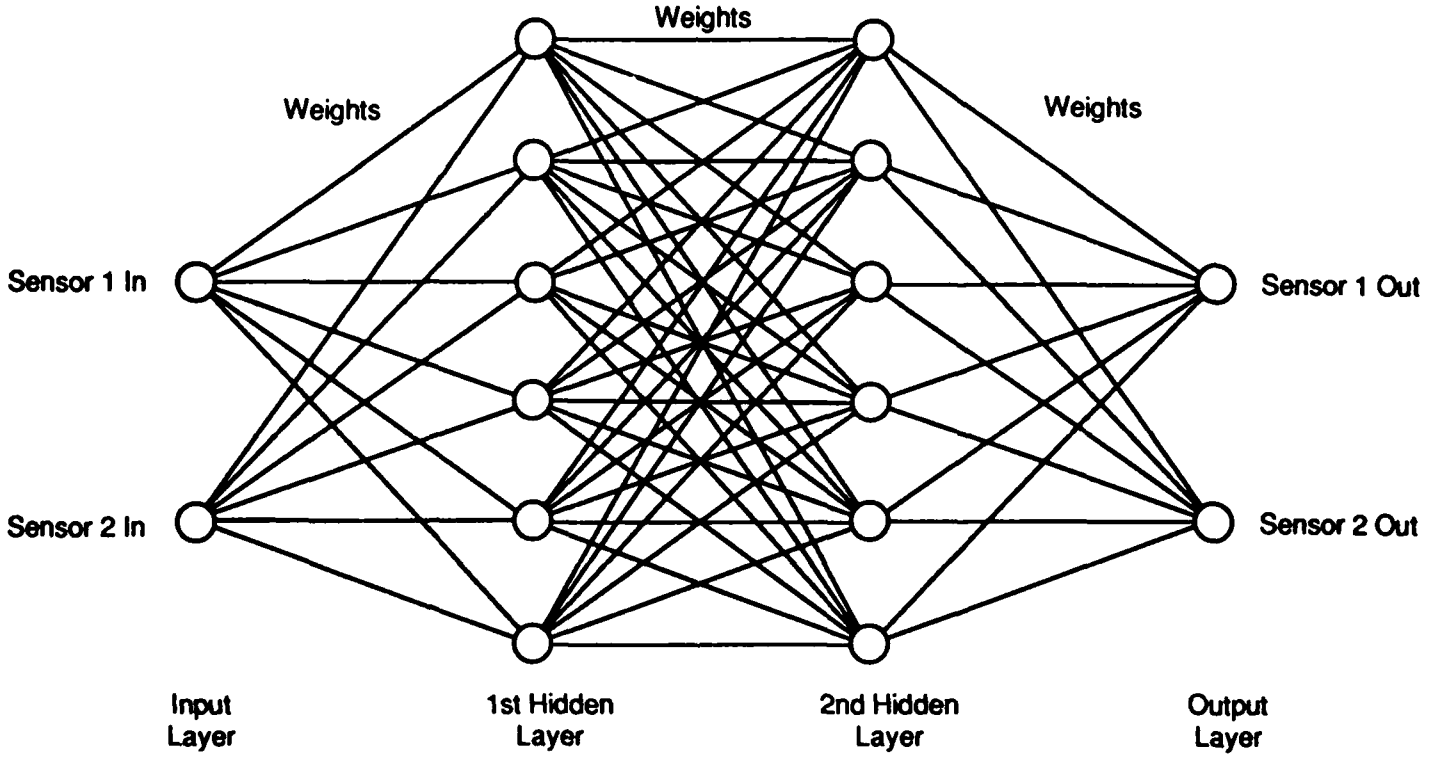

13.11.8

Figure 23. Multi-layer Perceptron Circuit Showing Two Sensor Imputs and Outputs

degree of confidence held in the techniques by the Artificial Intelligence community. These techniques have also been in use long enough to ensure their maturity: The MYCIN approach was developed in the 1970's; Dempster-Shafer theory was developed in the 1970's and has seen wide use and mention in the literature in the 1980's; and the Bayesian Belief Network approach was developed in the 1980's, although its foundation can be traced to the roots of probably theory (1500's).

Binary Logic

Binary Logic represents the most common approach to information fusion, and involves decision-making based on hard-coded rules, such as those in NEXPERT. Examples of such rules are:

Voting redundant sensors.

- Redlining (thresholding).

Fixed prioritization of sources of evidence. For example: "If two physically redundant sensors differ by more than a threshold amount, then suspect the one with lower variance."

Fault tree isolation logic.

Binary logic does not address uncertainties in the sensors or the sources of evidence. More importantly, it is highly susceptible to making wrong decisions (false alarms or undetected failures) since exhaustive enumeration of all possible exceptions to rules is extremely difficult, if not impossible[1]. The major advantages to binary logic are its computational efficiency and ease of implementation (once the rules have been defined).

MYCIN Certainty Factors

Several attempts have been made to add the capability to reason with uncertainty to rule-based systems. One example of such an approach is MYCIN certainty factors[2] MYCIN is a rule-based medical diagnostic system. In order to address uncertainties both in the observation of symptoms and in the diagnostic rules themselves, the developers of MYCIN devised an ad-hoc technique for representing and reasoning with uncertainty which could be layered onto their rule-based approach. This approach can be summarized as follows:

Table 9. Sources of Information about Sensor Failures

A-Priori Knowledge about Likelihood of Failures Reliability of Sensor Class Sensor Failure History Sensor Time in Service Pre- and Post- Test Calibration	**Physical Redundancy** Alternate Sensors
Reasonableness Checks Red, Yellow, and "Reasonable" Lines Rate of Change Standard Deviation	**Known Failure Mode Analysis** "Universal" Failure Modes Hard Open Circuit Intermittent Open Circuit Short Circuit / Shutdown Spikes Speed and Flow Sensors Aliasing
Signal Analysis Moving Average Time Series	 Pressure Sensors Thermal Drift Overshoot Loss of Reference Vacuum
Analytical Redundancy Empirical Correlation Models Engine Characteristic Models	 Temperature Sensors Thermal Expansion

Each proposition (fact) in the knowledge base has a certainty factor associated with it, which is a real number between -1 (indicating that the fact is definitely false) to +1 (indicating that the fact is definitely true).

Each rule has an *attenuation* , a real number between 0 and 1, indicating the uncertainty in the rule (a value of 1 indicates that if the rule's antecedents are known with absolute certainty, then the rule's consequents can be concluded with absolute certainty).

Given antecedents *a1, a2, , an* , and a consequent *c* for a rule:

$$Certainty[c] = Minimum(Certainty[a_1], Certainty[a_2],...Certainty[a_n]) \; Attenuation$$

If two rules assert certainty factors for the same proposition, the resulting certainty factor is found by:

$$\begin{cases} x + y - xy & \text{if } x,y > 0 \\ (x + y)/(1 - Minimum(x,y)) & \text{if } x,y \text{ different sign} \\ x + y + xy & \text{if } x,y < 0 \end{cases}$$

Where *x* and *y* are the certainty factors assigned by the two rules.

This approach is better than binary logic in that it attempts to deal with uncertainty in an explicit way, and provides a means for combining multiple sources of evidence. As with binary logic, this approach is also computationally efficient and straightforward to implement (it can easily be added onto a NEXPERT rule base). However, since the approach is based on ad-hoc formulas there are cases in which it will produce non-intuitive results.

One case in which it will give incorrect results is when the sources of evidence contributing to a proposition are correlated. An example of this from the Chernobyl disaster is shown in Figure 24 (the example is due to Henrion[3]). Pearl says about this example, "Multiple, independent sources of evidence would normally increase the credibility of the hypothesis (*Thousands dead*), but the discovery that these sources have a common origin should reduce the credibility. Extensional systems are too local to recognize the common origin of the information, and they would update the credibility of the hypothesis as if it were supported by three independent sources."[4]

Dempster-Shafer Theory

The Dempster-Shafer theory of evidential reasoning[5] has experienced a wide

popularity in the Artificial Intelligence community in the last 10 years. In contrast with approaches such as MYCIN certainty factors, it is a mathematically sound approach.

The Dempster-Shafer formalism maintains a body of evidence about a set of mutually exclusive hypotheses (in sensor validation, the hypotheses would be of the form *PIDi_Failed*). In this theory, a source of information can assign probabilities to disjuncts of hypotheses. For example, if evaluation of the engine characteristic

LPOPH/N2 = (P209-P860)/P30^2

at a particular time point indicates that the characteristic is anomalous (e.g., the residual is greater than 3 sigma), the following probability assignment could be made:

Confirm({p209,p860,p30}, 0.9)

This assignment indicates that either P209 or P860 or P30 has failed with a 0.9 probability. A formal method, *Dempster's Rule of Combination*, exists to combine two *statistically independent* bodies of evidence formed by statements of the form shown above. Once all sources of evidence have been combined, the *Belief* and *Plausibility* of any disjunction of hypotheses can be found.

Belief in a hypothesis is the probability that a logical proof for the hypothesis exists (i.e. if evidence assignments are interpreted as constraints, this is the probability that the constraints allow the hypothesis to be deduced). This can also be interpreted as the degree to which the evidence supports the proposition.

Plausibility of a hypothesis is the probability that it is compatible with the evidence (i.e. the probability that it cannot be disproved and is therefore possible). Thus, this is the degree to which the evidence fails to refute the proposition.

Plausibility(H) = 1 - Belief(H)

Thus, once all sources of information about a sensor have been combined, the Belief in each sensor's failure hypothesis could be examined and acted upon if over some threshold.

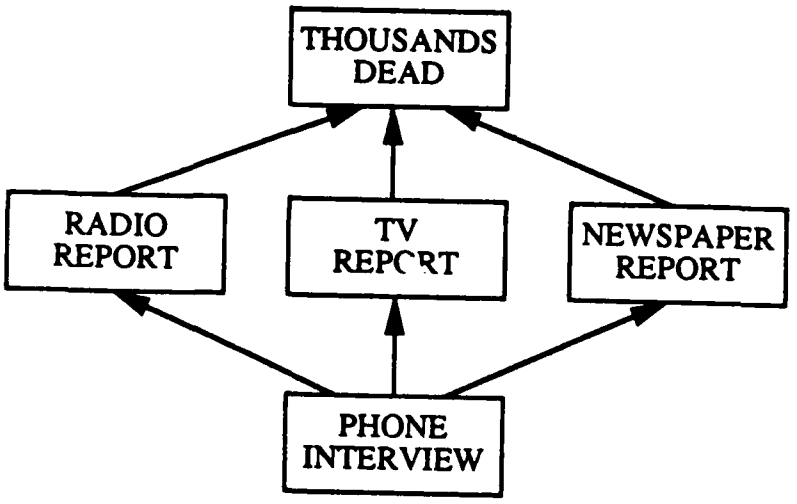

Figure 24. Chernobyl Disaster Example Shows Why Rules Cannot Combine Locally

Dempster-Shafer Theory has several disadvantages when applied to the sensor validation information fusion problem:

The theory assumes that all sources of evidence are statistically independent (this is not true if any PIDs are used in more than one test).

The theory assumes that exactly one of its hypotheses is true; thus, it will not detect multiple-point failures. (However, if the method is used for every time slice of data this should not be a problem, since the probability of having more than one failure at a given instance is extremely small.)

Each application of Dempster's rule can be computationally very expensive. Direct implementation is exponential in the number of hypotheses, although approximate solutions have been developed.

Finally, Dempster-Shafer theory is good for reasoning about problems in which constraints are stated explicitly, such as in design or planning, since the objects that are reasoned over are constraints among its hypotheses.

Bayesian Belief Networks

Bayesian probability theory, like the Dempster-Shafer theory described above, is mathematically sound. However, prior to the development of graphical representations and efficient network solution algorithms, its application to non-trivial problems (with more than a few dozen random variables) was extremely awkward if not intractable. Graphical representations of joint probability distributions provide a very intuitive knowledge representation format, and the Bayesian network formalism allows the requisite probabilities to be specified in a very concise and painless manner.

A Bayesian network consists of nodes which represent discrete-valued random variables. Examples of such nodes in the sensor validation system are shown in Figure 25. The node/random variable-P209-represents the current state of PID 209, and can be in one of five mutually exclusive states: OK, Hard_Open, Intermittent_Open, Drift, or Bias. Associated with this node is a probability distribution which describes the probability of the node being in each of its possible states given all available information. The LPOPH/N2 node represents the outcome of the engine characteristic test:

LPOPH/N2 = (P209-P860)/P30^2

This is computed from a time slice of data and compared to a sampled baseline characteristic. The states for this node represent the residual from comparison, and thus the outcome of the test.

Directed arcs lines between nodes in a Bayesian Belief Network represent *influences*. In particular, an arc from node A to node B indicates that knowledge of node A's state can change the probability distribution for node B. Figure 26 shows the three arcs influencing node LPOPH/N2, namely those coming from the three PIDs involved in the test (a change in the status of any of the PIDs involved can change the outcome of the test). The nodes and arcs in a Belief Network must form a Directed Acyclic Graph (DAG), that is, the nodes can be connected in any manner as long as you cannot start at a node and get back to the same node by following directed arcs through the network.

Once the topology of a network has been defined, two types of probabilities must be specified to complete the network. First, all nodes which do not have any influencing arcs (i.e., no arcs coming into them) must have default probability distributions for their states defined (P209 in Figure 27 shows an example of this). In the Belief Networks used for sensor validation, these nodes typically represent random variables specifying the status of each PID. The default probability distributions would be obtained from historical reliability data for each sensor (e.g., PID xyz has exhibited a 0.99 reliability over the last 30 tests with a 0.005 probability of failing hard open circuit and a 0.005 probability of failing by drift), coupled with time in service, and pre- and post-test calibration.

Second, every node which has influencing arcs must have probability distributions conditioned on the states of their influencing nodes specified (see LPOPH/N2 in Figure 27). In the Belief Networks used for sensor validation, these nodes typically represent random variables specifying the outcomes of diagnostic test. The probabilities distributions can be obtained analytically by analysis of each test used.

A fully specified Belief Network can be used to answer queries in the following manner:

1. "Observables" are instantiated (in the example above, this consists setting the state of the LPOPH/N2 node to reflect the test outcome).
2. A network update algorithm is run.[6,7,8]
3. The probability distributions of nodes of interest are examined (in the example

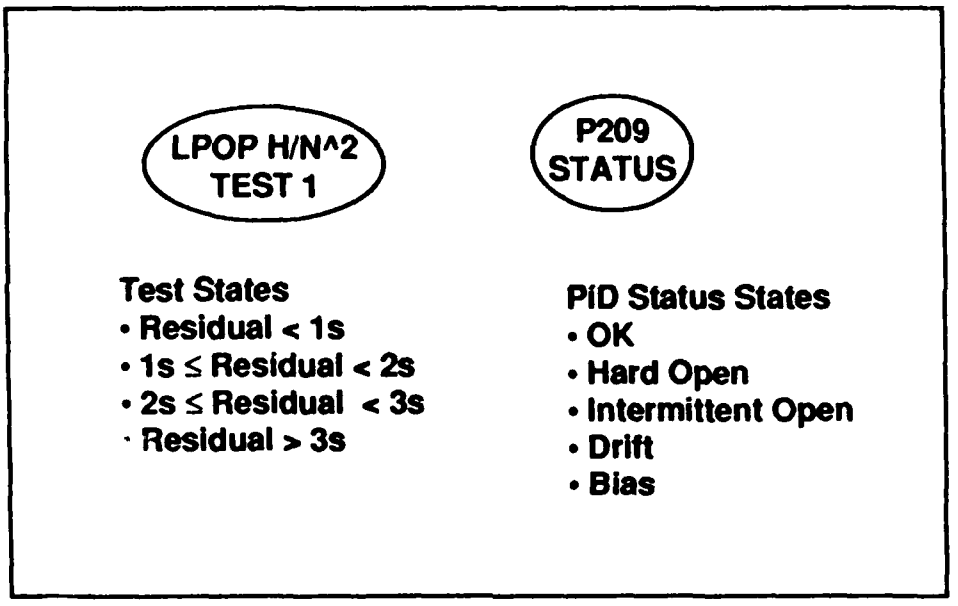

Figure 25. Example Bayesian Belief Network Nodes

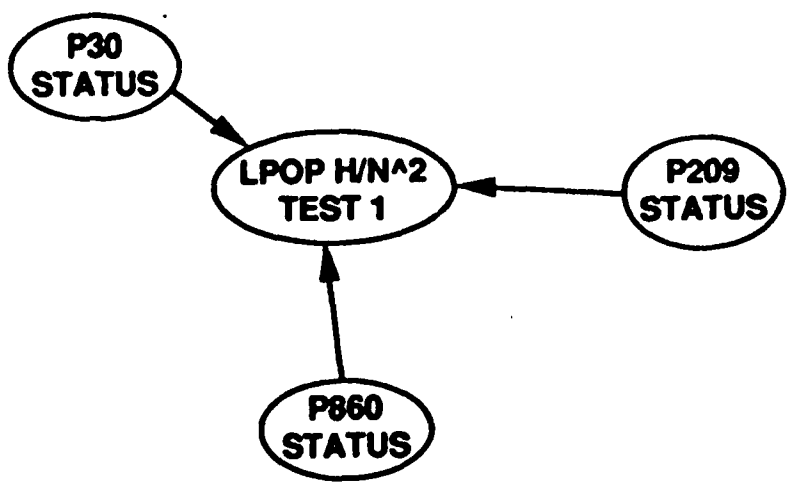

Figure 26. Example Belief Network Influences

above, this consists of examining the distributions for P209, P860, and P30 to see if the probability of any fault state exceeds a threshold).

The major advantage of Bayesian Belief Networks is that they are the most semantically correct way to perform information fusion. For analysis problems such as diagnosis, Bayesian probability theory is better suited than the Dempster-Shafer approach, since the objects that it reasons over are probabilistic models (there are no explicit constraints known a-priori).[9] However, the Belief Network solution algorithms can be complex to implement and computationally expensive.

Evaluation of Techniques

Table 10 shows the results of a trade study on the four techniques discussed above for use in sensor validation information fusion. In the trade, the "soundness" criterion was given the highest weighting because the whole purpose of information fusion is to give the best possible evaluation of all sources of information. The "Ease of Implementation" criterion includes not only implementation of the fusion algorithm, but the encoding of all requisite knowledge to perform the sensor validation information fusion task (i.e., specification of probabilities, certainty factors, logic rules, etc.). Based on this trade, Bayesian Belief Networks are the recommended approach to information fusion for sensor validation.

Application to Sensor Data Validation

Figure 28. shows how all of the information available about the state of P209 (LPOP discharge pressure) might be integrated using Belief Networks. Given the research performed in Phase I, it is known that P209 can be evaluated by two characteristic tests (LPOPH/N2, HPOPR2), by an empirical test (relating P209 to P211 and P91), by range tests (e.g., 2sigma bands), by pattern-matching techniques which look for specific failure modes such as spikes and drifts, and by comparison to P210 (channel B). In addition, information about P209's failure history, time in service, pre- and post-test calibration, and the reliability of the transducers used to measure LPOP discharge pressure can be combined into an initial probability distribution for P209 and combined with the evidence gathered for each time slice of the test data analyzed.

The specification of the Belief Networks needed should be very straightforward. A preliminary analysis of the networks required indicates that most of the probabilities, and

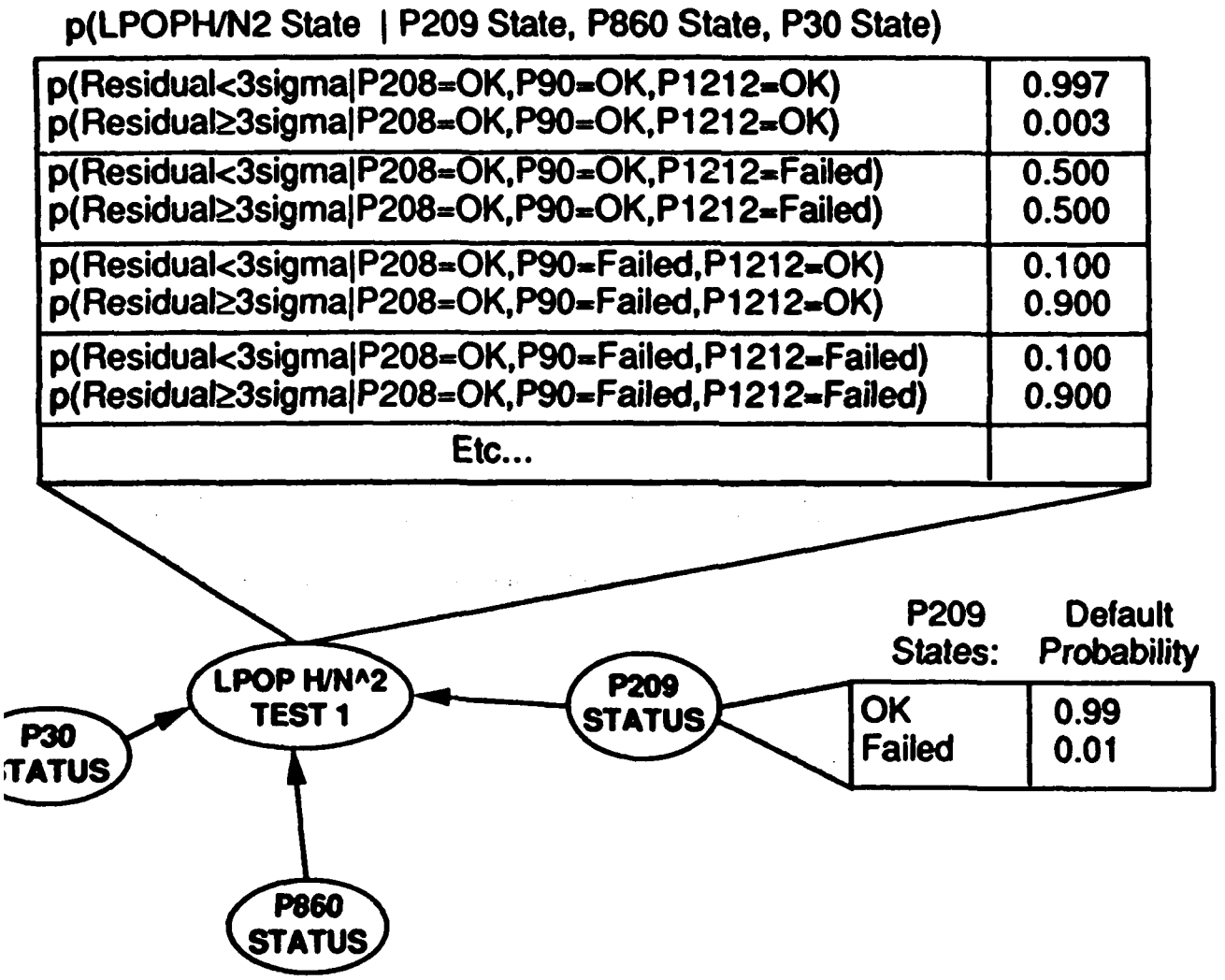

Figure 27. Example Belief Network Probability Specification

	Ease of Implementation $ (0 = Most Expensive)	Computational Efficiency	Soundness	Handles Simultaneous Multiple-Point Failures	Development Risk (0 = High)	Totals
Weight	5	5	10	3	7	
Boolean Logic	4	10	1	2	9	5.0
MYCIN	8	8	3	6	9	6.4
Dempster-Shafer	7	4	7	0	7	5.8
Belief Networks	3	5	10	10	6	7.1

Figure 28. Information Fusion Techniques Trade Offs

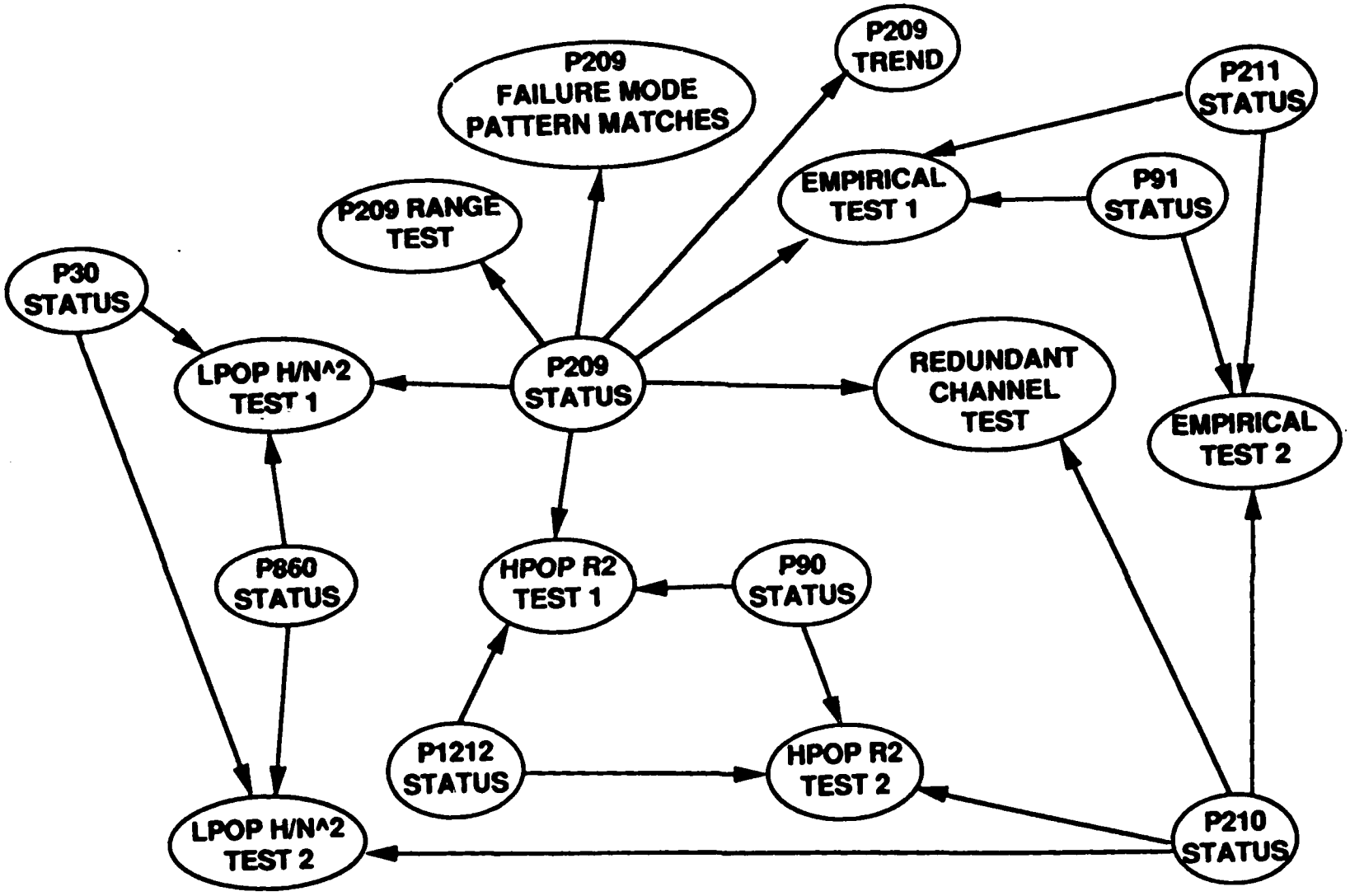

Figure 29. Example Belief Network Segment Around P209

possibly the network topology itself, can be automatically compiled from descriptions of the various sources of information (e.g., engine characteristic and empirical PID relations).

4.0 System Software Specification

4.1 Scope

4.1.1 System Objective

The major objective of the Sensor Validation system is to automatically detect sensor malfunctions in the SSME test data, and to reconstruct the data for any malfunctioned sensors using alternate sources of information. The system will run in two major stages; an initial batch processing mode, followed by an interactive post-processing mode (see Figure 30). In the batch mode, the sensor data from the SSME test (in engineering units) is thoroughly analyzed by the sensor validation system, with PID failures flagged and PID value reconstructions automatically run. The purpose of the interactive mode is to allow analysts to quickly understand the results of the batch mode processing, and either confirm or override the failure and reconstruction decisions made by the sensor validation system.

Batch Processing Mode

In the batch processing mode the SSME data is analyzed and acted on according to three user-specified thresholds:

Report threshold - the system will write a report whenever the estimated probability of any sensor failing crosses this threshold (in either direction). The report will be produced in two parts: a brief summary stating which PID(s) changed state and when, and a detailed report describing how the system arrived at the estimated probability.

Reconstruction threshold - the system will reconstruct the value for a sensor using alternate sources of information whenever its probability of failure exceeds this threshold. If several viable methods for reconstruction exist, the system will pick the method with the highest probability of being correct (based on the failure probabilities of any other sensors involved in the reconstruction and the accuracy of the method).

Failure threshold-when a sensor's probability of failure exceeds this threshold, the system will assume that its value cannot be used to cross-check other sensors or in reconstruction of other sensor values.

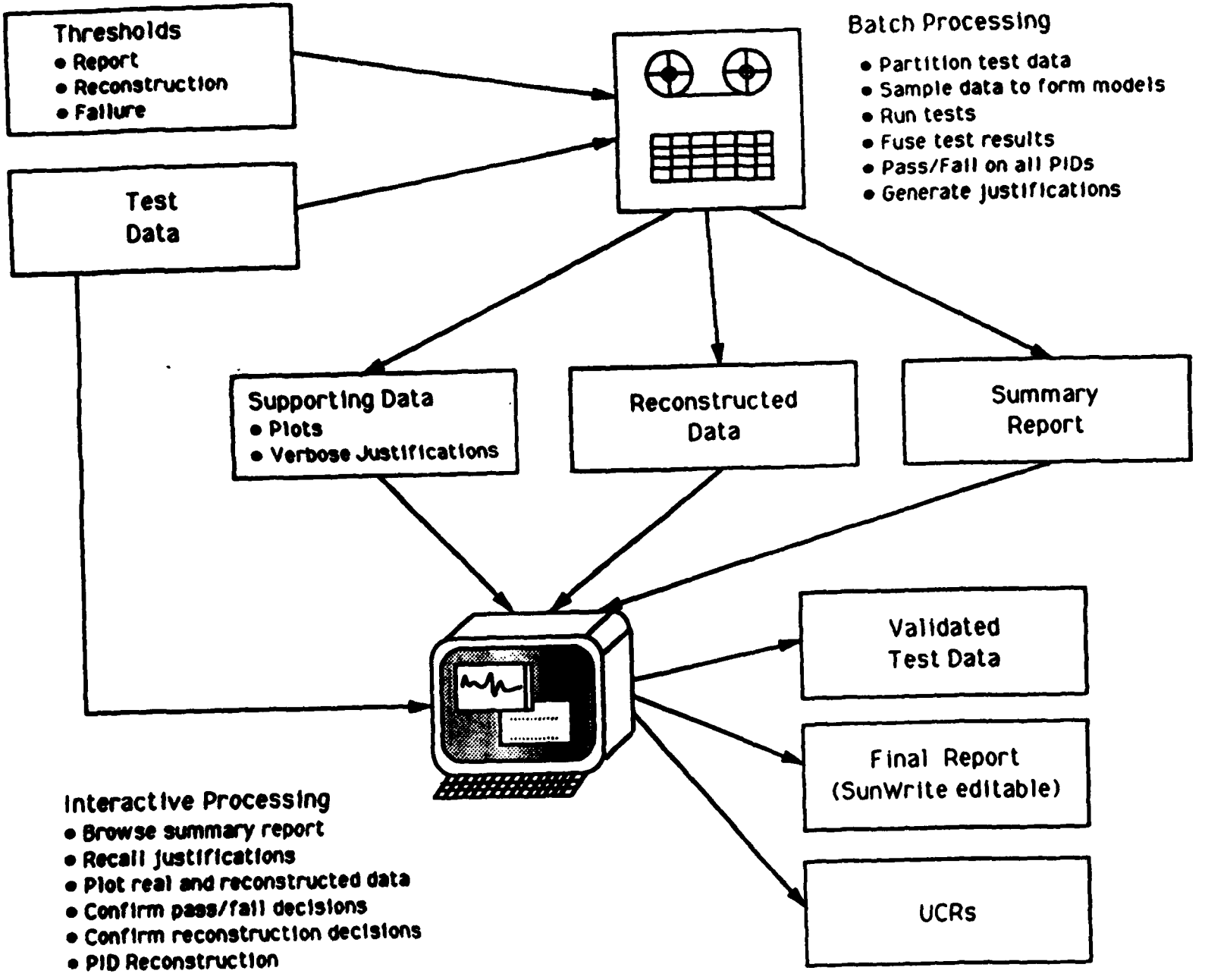

Figure 30. Data Flow Diagram

Although users are free to set the thresholds at any values, it is expected that typically the following relative settings will be used:

$$\text{Report} \leq \text{Reconstruction} \leq \text{Failure}$$

Using these settings, the system would typically generate reports whenever a sensor exhibits any questionable behavior. Additionally, reconstructed values will be produced in cases when the system does not conclude that the sensor has failed, but simply derives an unusually high probability of failure. Thus, the user still has pre-computed reconstructed values to use in case he or she overrides the system's judgement about the failure status of a sensor.

Batch mode processing is expected to take place immediately following an SSME test, with results available within an hour for use by the rest of the Life Prediction System and for use in Interactive mode analysis. Thus, this processing will not exceed one hour in duration on a Sun SPARCStation.

In batch mode, all sources of available information will be analyzed and fused to reach the best possible decision about the status of a sensor. The tests incorporated into the initial version of the sensor validation system will include:

Empirical models
Characteristic models
Red-line test
Sensor class reliability
Sensor failure history
Some form of pattern-matching
Comparison with redundant channels

The system will be constructed in such a way so that tests can be added or modified with minimum effort. Bayesian Belief Networks will be used as the approach to information fusion. An approach to specifying the networks will be developed which minimizes the effort required to define the network(s) required and the associated probabilities.

In addition to flagging sensor failures and performing reconstructions, the batch mode software will determine the best source of information to use for each physical

measurement (e.g., channel A, channel B, reconstruction method 1, reconstruction method 2, family-averaged historical value, etc.). This designation can then be used by other modules in the SSME Life Prediction system (e.g., expert diagnostic modules) so that they only need to look at a single source of data for each measurement and not concern themselves with evaluating the different possible sources of information. Thus, this provides a form of data reduction for the entire Life Prediction system.

Interactive Post-Processing Mode

The Interactive post-processing mode is intended to provide an analyst with an environment in which he or she can quickly understand the conclusions reached by the system during its batch processing, and either confirm or override the decisions made by the system. The analyst will also be able to display arbitrary PID value vs. time plots, and run any available reconstruction algorithm. The interactive software will make maximum use of a mouse-driven, color, graphical user interface to convey the sensor validation system's results as efficiently as possible, and to minimize the analysts' learning time.

The post-processing software will have three main displays (in addition to a "main menu" for specifying test numbers, top-level operations, etc.). The first display will show a color plant diagram of the SSME with icons representing all CADS PIDs (see Figure 30). Sensors which had been flagged as failed during batch processing (according to the failure threshold) will be highlighted on the display. This display gives the analyst a quick, global view of problems detected by the sensor validation system. In addition, the highlighting can reflect a single instant in time during the test, and the analyst will be able to move a scrollbar along the bottom of the display to advance forward or backward in time to get a quick feel for the chronology of events during the test. If a PID icon is clicked on with the mouse, a pop-up window will appear showing a brief summary of the PID's status. Further, if this window is clicked on a justification display will appear to give a complete description of the sensor validation system's evaluation of that PID at the indicated time.

The justification display is the second main display in the interactive system (see Figure 31). When requested by the analyst, a display will appear showing a verbal description of the evaluation of a PID at a specific time, and any supporting graphics (e.g., plots) will also be displayed.

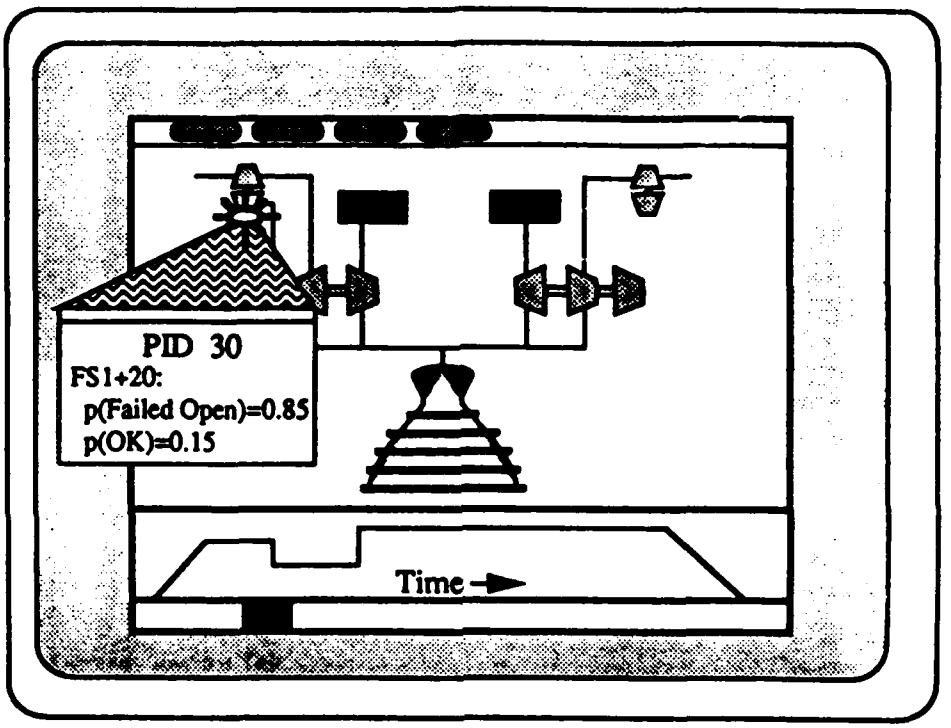

Figure 31. Interactive Plant Display

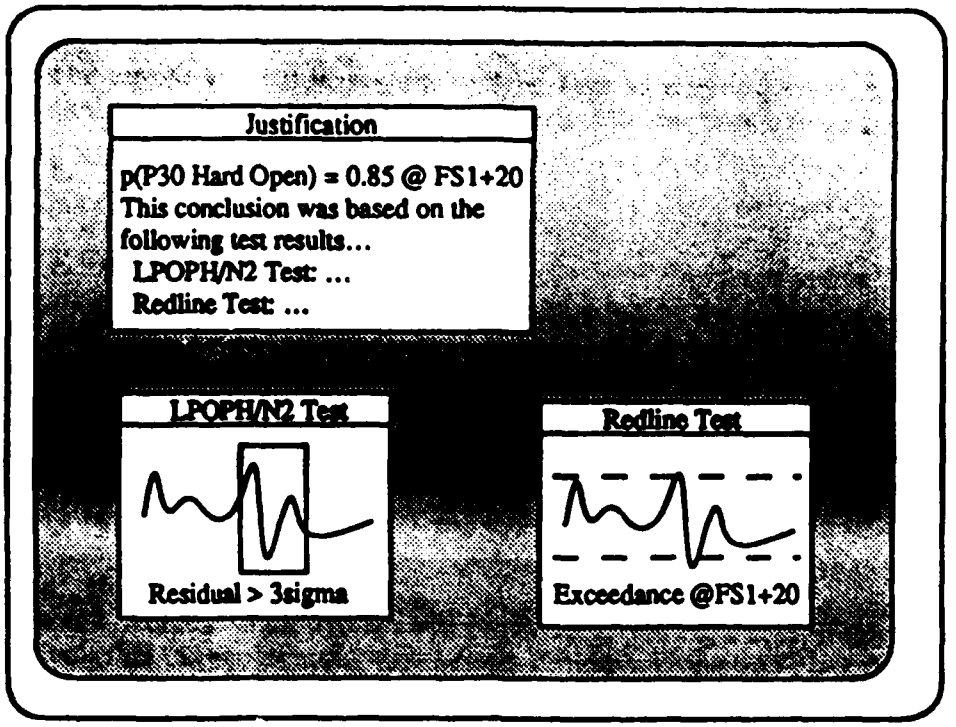

Figure 32. Interactive Justification Display

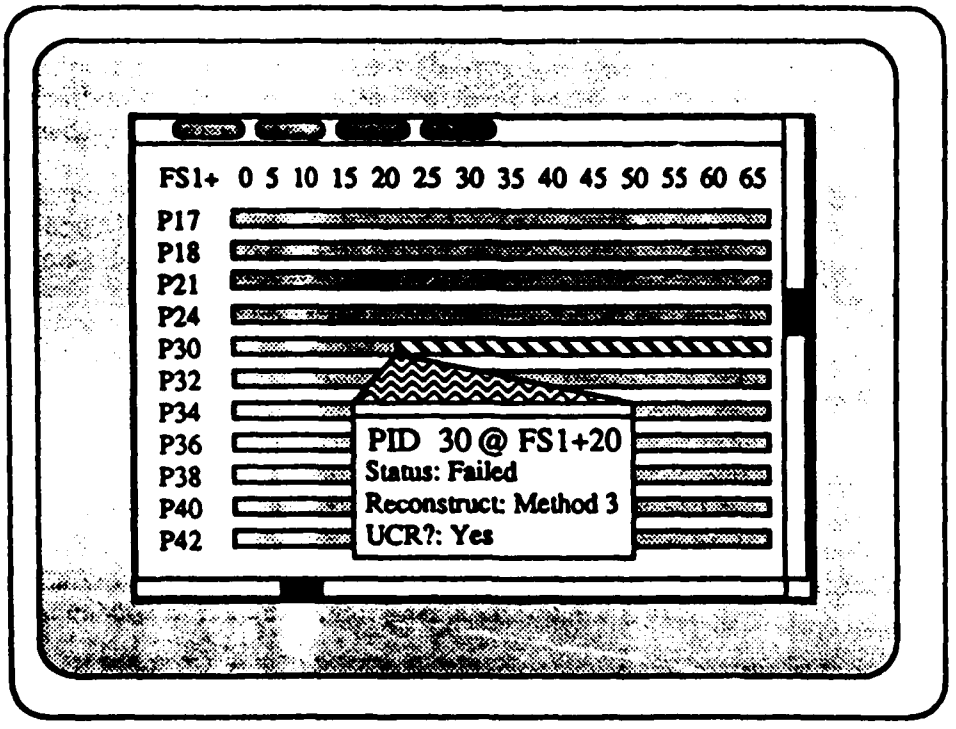

Figure 33. Interactive PID Matrix Display

The third main display in the interactive system is the "PID Matrix" (see Figure 32). This display shows a concise summary of the system's conclusions and recommendations, and allows the analyst to override any of the entries. Each PID is displayed on a timeline, with the color of the display indicating the status of the PID (e.g., green for OK, red for failed). Although the initial display represents the validation system's batch mode conclusions, the user can click the mouse on any segment of the display and modify the status of the sensor. Additionally, if the sensor is declared failed, the user can specify the reconstruction method used and whether a UCR should be generated or not.

Once the analyst OKs the PID Matrix, the sensor validation system automatically assembles a test data file with all selected reconstructions, generates all requested UCRs, and generates a final report. The report includes the justifications for all failed sensors (including text and graphics), and is editable by the analyst using SunWrite.

Global Objectives

In addition to the objectives mentioned above, the following objectives apply:

Although the Sensor Validation system will eventually have to interact with the Session Manager to obtain its data and to interface with the user, it will initially be designed as a stand-alone system since it is the first module in the SSME Life Prediction system planned to be completed. However, a clear migration path from standalone to embedded processing will be maintained.

The sensor validation system will be designed so as to minimize the effort required to modify engine data (e.g., PID lists, sensor specifications, sampling rates, etc.).

The sensor validation system will be kept as engine-generic as possible so as to minimize effort in porting the system to a different engine (e.g., the SBE).

4.1.2 Hardware

The sensor validation system will be implemented on a Sun SPARCStation.

4.1.3 Software

The sensor validation system will be implemented using the following software languages, tools, and environment:

Operating System: Unix

Procedural Language: C
Expert System Shell: NEXPERT Object
Windowing/Graphics System: Motif or Dataviews
CAE Package: PV-WAVE

4.1.4. Human Interface

The human interface to the system will provide a graphical, mixed-initiative interface to the set of tools that the sensor validation system provides. Point-and-click functionality will be used throughout (including the use of pop-up menus) to initiate all functions so that the analyst does not need to remember commands and their parameters. Different activities (e.g., plant display, justification, default modification, etc.) will take place in separate windows so that the user can visually cross-reference information when desired. A mixed-initiative interface will be used so that at any time either the system can lead the user (e.g., with a suggested action or a query) or the user can direct the system (e.g., with a new command or volunteered information).

The display format of data (e.g., test data plots) will adhere as closely as possible to the formats used in current hardcopies to minimize the users' effort in orienting to the system.

The user will be able to index PIDs either by PID number, by Rocketdyne number, by label (e.g., "MCC COOLANT DISCH PRESS CH A1"), or by clicking on the appropriate plant display icon.

Stylistically, the system will adhere to the OPEN LOOK Graphical User Interface specification through the use of Sun's OpenWindows window system.

4.1.5. Major Software Functions

Batch Mode

Import and partition Engine Test Data. The system will import test data from an Ingres data base and partition it into steady-state and transient intervals.

Import PID Reliability and Failure History. The system will import the failure history for all PIDs and the reliability figures for all PIDs from an Ingres database, and integrate this information into its decision about the status of PIDs.

Import Family-Averaged Models. The system will import all summarized characteristic and empirical (regression equation) information about previous tests from an Ingres database, and integrate this information into its decision about the status of PIDs. This information includes:

- True Engine Characteristics.
- Empirical model constants.
- PID value means and standard deviations as a function of power level (for computing yellow and red-lines, and as a "last resort" method for reconstruction).

Assess sensor status. The system will determine the probability of each PID's likelihood of failure at each time point in the test data.

Report sensor failures. Whenever a sensor's probability of failure exceeds a user-specified Report Threshold, a brief statement will be output to a Batch Report file, and a detailed justification of the probability assessment will be output to a Justification Data file. The Justification Data file can not only contain textual descriptions, but specifications for generating supporting plots as well.

Reconstruct sensor values. Whenever a sensor's probability of failure exceeds a user-specified Reconstruction Threshold, the system will reconstruct the sensor's value from that time point until the end of the test using alternate sources of information. There are different thresholds for reconstruction and failure to support efficient interactive processing, so that an analyst can use reconstructed data for a "borderline" sensor, even though the system did not declare it as failed. If several viable reconstruction methods exist, the system will pick the one with the highest probability of being correct (based on the failure probabilities of any other sensors involved in the reconstruction and the accuracy of the method). Once reconstruction has started, the method used may be changed dynamically as the probability of other sensors (i.e., those used in the reconstruction method) change. All reconstructed data will be output to an Ingres database.

Conclude sensor failure. Whenever a sensor's probability of failure exceeds a user-specified Failure Threshold, the system will not use the sensor's value in any

further reconstructions or cross-checks for other sensors. In addition, a brief statement describing the failure will be output to the Batch Report for use in the Interactive Mode.

Generate Engine-Specific Models. Characteristics (as described in the Import Family Characteristics function above), empirical model constants, and mean and 2-sigma values, computed and averaged per power level for the engine under test will be written to an Engine Characteristics Ingres database.

Select best source of information. For each physical measurement (e.g., PC, LPFP DISCH PRESS, etc.), the system will determine the best source of information at every time point based on its sensor analyses. The sources may include not only redundant channels, but any available reconstruction methods. This information will be output to the Batch Report file.

Generate validated data set. When this option is selected at the start of the batch mode processing, the system will assemble a final validated data set, integrating real and reconstructed values according to the user-specified Failure threshold (i.e., whenever the probability of a sensor's failure exceeds this threshold it is replaced with the best reconstruction method available).

Interactive Mode

Display PID Matrix. The system will display a graphical matrix indicating the assessed status of each PID at each time point in the test (e.g., a green bar will indicate that the PID is functioning normally, while a red bar will indicate a failure). When an entry is clicked on with the mouse, a popup window will appear showing a brief summary of the PIDs status and, if a failure is indicated, the reconstruction method used and whether a UCR will be issued or not (see Figure 32). The matrix will be initialized from data in the Batch Report, but the user can modify any of the entries via the popup window. If the user changes a PID's status, all ramifications of this must be determined by the system (in particular, if the user declares a PID as failed, then any reconstructions based on that PID must be invalidated). In addition, the popup window will have a "Justify" button which will

cause a justification for the system's assessment to be displayed if it is clicked on (see Display Justification below).

Display plant summary. The system will display a picture of the SSME plant diagram with all PIDs depicted by icons which indicate assessed status (e.g., a red icon will indicate a sensor failure, while green will indicate that the sensor is OK). The plant display will have two modes: summary and chronological. In summary mode the maximum failure probabilities over the duration of the test will be used for the icon display (i.e., the display indicates the worst-case status of all PIDs over the duration of the test). In chronological mode, the user will be able to step forward or backward through the test time by moving a scrollbar along the bottom of the plant display (see Figure 31) with the icons updated so as to display their status at that point in the test. If an icon is clicked on, a summary of its status over the duration of the test will appear in a pop-up window. If one the entries in this summary is clicked on, a justification for the system's assessment is displayed (see Display Justification below). The plant summary is generated from information in the PID Matrix.

Display Justification. The system will display the justification data for a given PID assessment when requested by the user. The justification information will be imported from the Justification Data file generated during batch mode. Text and supporting graphics (i.e., plots) will be displayed in separate windows.

Plot Generation. The system will plot any PID value, reconstructed PID value, or any combination of these over any requested time interval. If a reconstruction is requested which was not run during batch mode, the reconstruction is run immediately using information from the engine test data, and the family and engine characteristics databases.

Authorization. Once the user is satisfied that the PID Matrix is correct, he or she can authorize the system to complete its processing. This includes the following functions:

- The system generates all UCRs specified in the PID Matrix.

- The system updates the Failure History database according to the sensor failures indicated in the PID Matrix.
- The system updates the Family Characteristics database using the information in the Engine Characteristics database output in batch mode, and using information in the PID Matrix to determine what should *not* be updated (due to sensor failures).
- A final report will be generated. This includes a brief textual summary describing all PID failures, followed by all justification information for each PID failure. The report will be output in SunWrite format so that it can be edited by the user.

4.2. Reference Documents

IR&D Proposal AMP 91-03: Integrated Controls & Health Monitoring, Aerojet
NEXPERT Object User's Manuals (vol I and II). Neuron Data, Inc.
OpenWindows 1.0 User's Guide, Sun Microsystems
XView 1.0 Reference Manual: Summary of the XView API, Sun Microsystems
SunWrite 1.1 User's Guide, Sun Microsystems
SunOS Reference Manual (vol I, II, and III), Sun Microsystems
PV-WAVE User's Manual

Programming Language C, X3.159-1989, ANSI

4.3. Preliminary Design Description

4.3.1. Batch Mode

Data Flow

Figure 33 shows the top-level, formal data flow diagram for the batch mode processing modules in the sensor validation system. Figure 34 shows the next level data flow diagram for the Sensor Failure Detection module. The software modules in these diagrams are described next.

Software Modules

Steady-State/Transient Partitioning. The test data will be partitioned into steady-state and transient intervals.

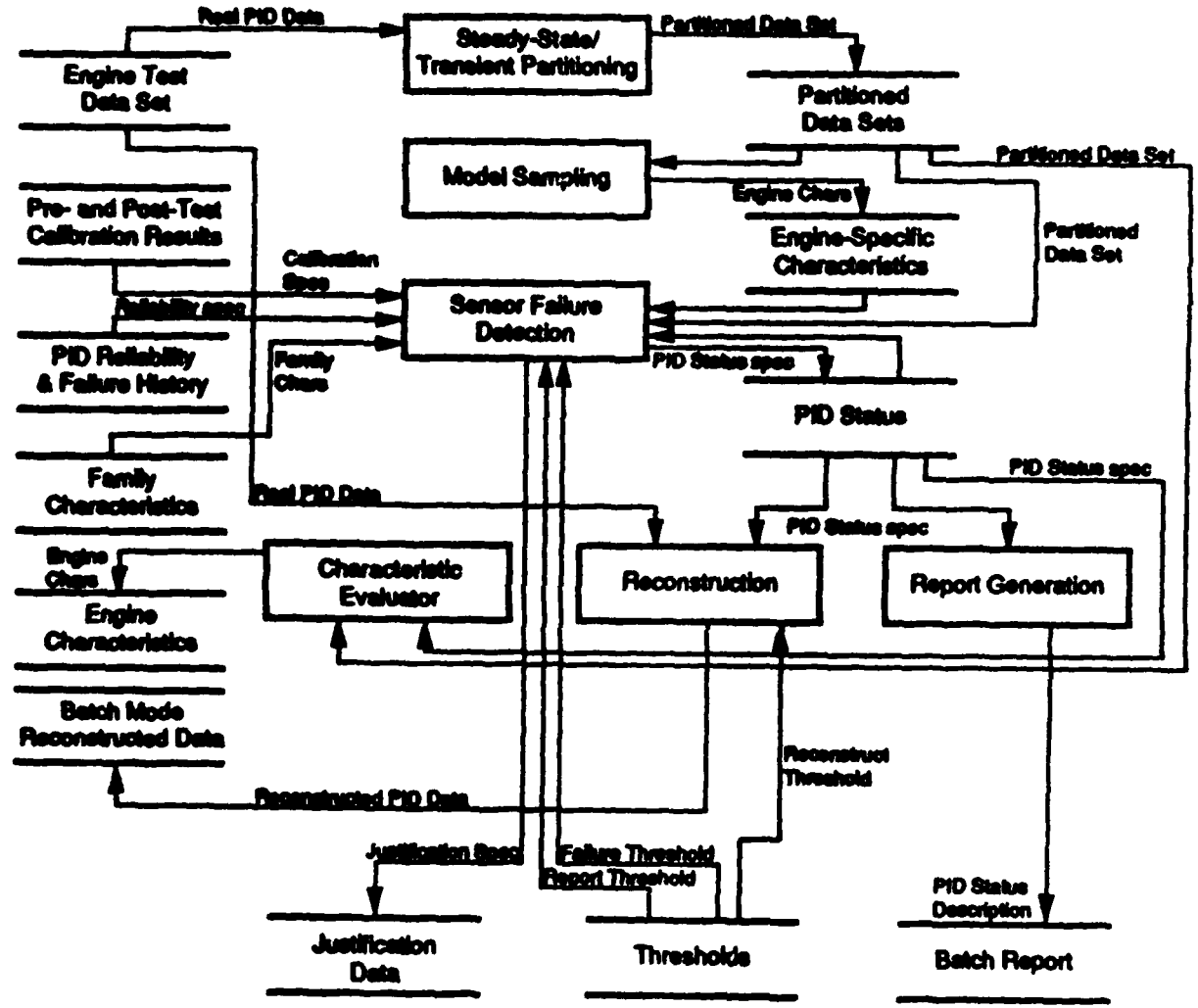

Figure 34. Top Level Batch Mode Data Flow Diagram

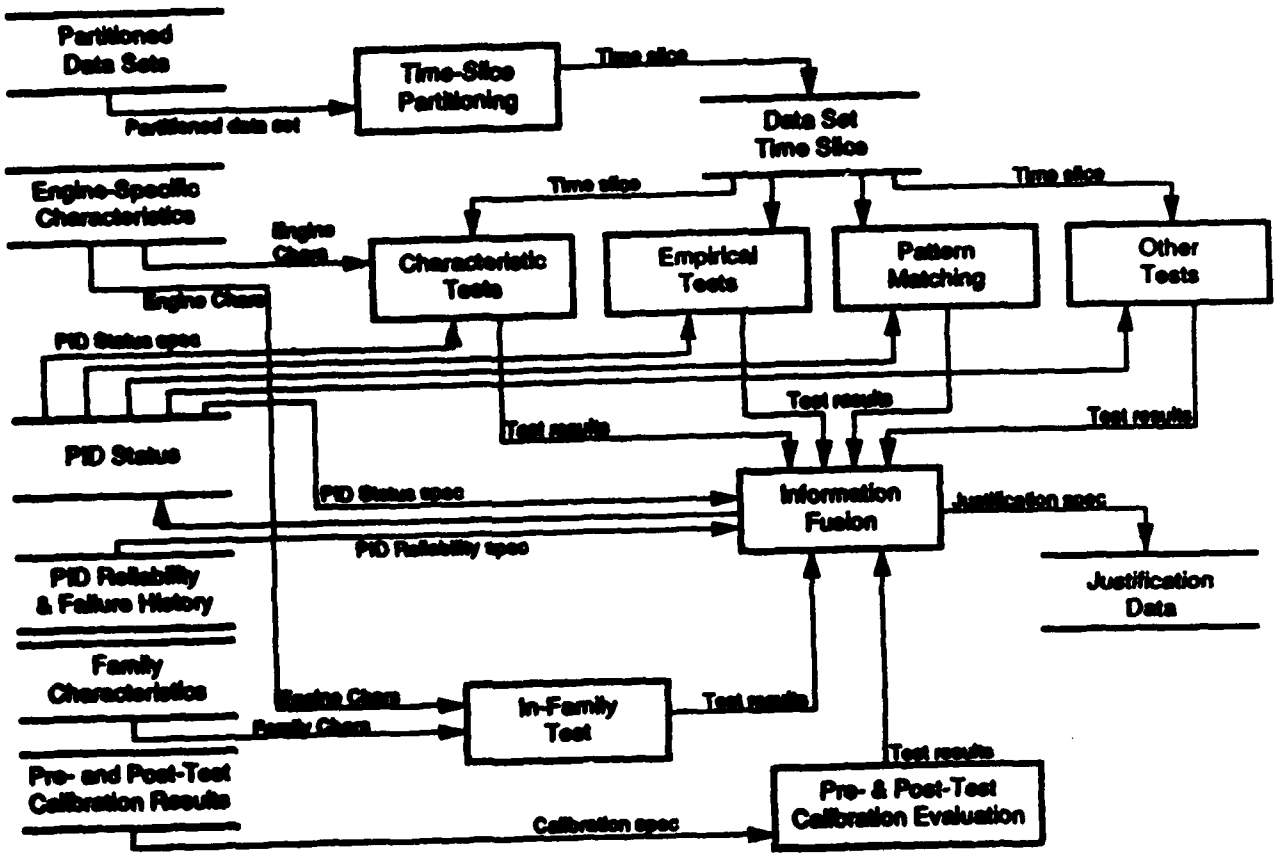

Figure 35. Sensor Failure Detection Module Data Flow Diagram

Model Sampling. Data samples required by the characteristic and empirical models (and any other models requiring engine-specific tuning for other tests) will be taken from each data set partition.

Sensor Failure Detection. The probability of failure for each PID at each time point will be assessed based on the fusion of all available information and tests and output to the PID Status table. For each crossing of the Report Threshold, a justification will also be output to the Justification Data file.

Characteristic Evaluator. The characteristics for the engine under test (including true engine characteristics, and PID means and standard deviations) are computed and output to the Engine Characteristics database.

Reconstruction. For each crossing of the Reconstruction Threshold, a reconstructed sensor value will be generated and output to the Batch Mode Reconstructed Data database.

Report Generation. The contents of the PID Status table will be output to the Batch Report file.

In-Family Test. Each engine-specific characteristic sampled by the Model Sampling module will be compared with family values in the Family Characteristics database. If the engine-specific characteristic is "out-of-family" then that characteristic will not be used for further sensor assessment, and information about the out-of-family condition will be passed to the Information Fusion module.

Time-Slice Partitioning. All PID values for a given test sampling time will be extracted for use by the various assessment tests.

Characteristic Tests, Empirical Tests. All viable characteristics and empirical models will be evaluated and compared to their corresponding sampled baseline values. Information about the degree of disagreement (i.e., the size of the

residual) will be passed to the Information Fusion module. Whenever the probability of a sensor's failure exceeds the Failure Threshold (based on the PID status table), tests involving that sensor's values will no longer be used.

Pattern Matching. Any pattern-matching techniques will be run, with the results passed to the Information Fusion module.

Information Fusion. All sources of information about the status of each PID at each time point in the test will be fused together using the technique of Bayesian Belief Networks. The resulting probability of failure for each PID will be compared to the Reporting Threshold and, if exceeded, justification data based on the tests involved in the assessment and the Bayesian analysis will be written to the Justification Data file. The best source of information to use for each physical measurement, and the best reconstruction method to use for each PID are also determined.

4.3.2. Interactive Mode

Data Flow

Figure 35 shows the formal data flow diagram for the interactive mode processing modules in the sensor validation system. The software modules in this diagram are described next.

Software Modules

Plant Browser. Performs the "Display Plant Summary" function described in section III.1.e.

Justification Browser. Performs the "Display Justification" function described in section III.1.e.

PID Matrix Authorizer. Performs the "Display PID Matrix" function described in section 1.e.

Plot Generator. Performs the "Plot Generation" function described in section 1.e.

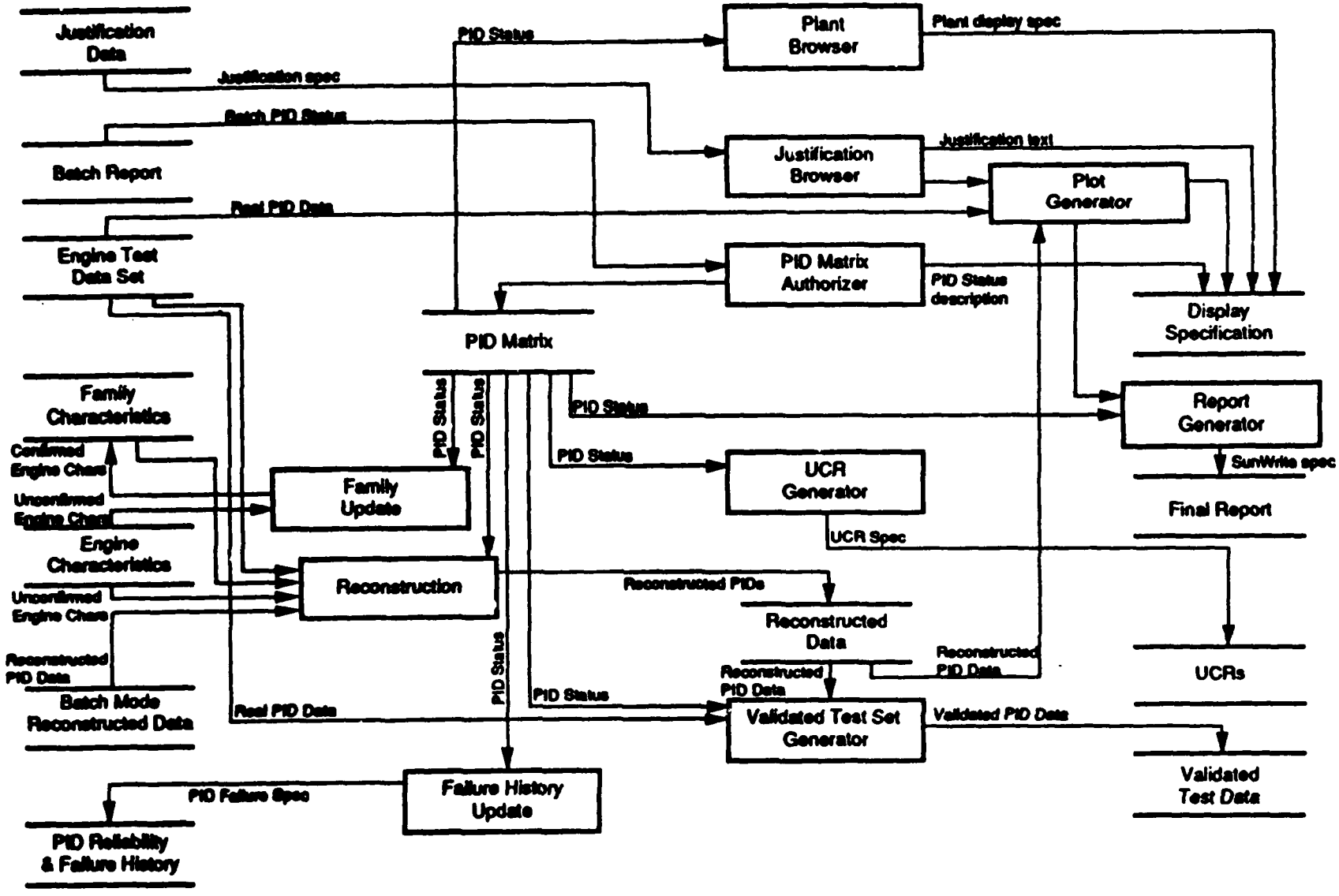

Figure 36. Interactive Mode Data Flow Diagram

Family Update. Some or all of the characteristics for the engine under test will be added to the Family Characteristics database, once the PID Matrix has been authorized.

Reconstruction. PID values not reconstructed during batch mode may be generated in real time if requested by the user.

Failure History Update. The PID Reliability & Failure History database will be updated with the failed PIDs in the PID Matrix, once it has been authorized.

UCR Generator. UCRs will be generated as specified in the PID Matrix, once it has been authorized.

Validated Test Set Generator. A final engine test data set will be assembled from real and reconstructed PID values according to the PID Matrix, once it has been authorized.

Report Generator. A final report will be generated, consisting of a brief summary of all failed PIDs, followed by a justification for each failure assessment. The report is based on the PID Matrix and the Justification Data file, and is generated once the PID Matrix has been authorized.

4.3.3 External File Structure

Engine Test Data Set - Ingres database containing the raw data from the test under analysis, with all values converted into engineering units.

PID Reliability & Failure History - Ingres database containing the reliability (manufacturer's statement) of each sensor, in addition to the failure history for each particular PID.

Family-Averaged Models - Ingres database containing the characteristics, summarized at each power level, for all engines.

Engine Models - Ingres database containing the characteristics, summarized at each power level, for the engine under test.

Batch Mode Reconstructed Data - Ingres database containing all reconstructed PID values (same as Engine Test Data Set, except that the start and stop times and reconstruction method used are also recorded).

Justification Data - An ASCII file containing text and plot generation information for each PID whose probability of failure exceeded the Report Threshold.

Batch Report - ASCII text file, formatted for ease of reading into the interactive mode system, but also sufficiently annotated to make it usable as a hardcopy report.

Validated Test Data - Ingres database; same format as Engine Test Data Set.

. Thresholds - Text file containing the report, reconstruction, and failure threshold values.

4.4 Test Provisions

The sensor assessment capabilities of the system will be evaluated by the following methods:

Review of heuristics and strategies with experts.

Running several test cases through the system, using real or simulated failures as necessary to obtain broad test coverage.

Running two new test cases provided by NASA LeRC through the system.

in the system will be evaluated during

In addition, the overall capabilities of the system, including the interactive mode user interface, will be evaluated during demonstrations (as scheduled in section IV) to members of NASA LeRC.

5.0 SYSTEM DEVELOPMENT PLAN

The Phase II development plan for the Sensor Validation system is shown in Figure 36. The development spans two and one-half years, at the end of which a fully functional software module, integrated with the Session Manager of the SSME Life Prediction system, will be delivered. The Sensor Validation system architecture, as described above, allows for incremental addition of validation tests, thus validation techniques can be developed and implemented by several groups (e.g., neural network and time series approaches by NASA Lewis) and integrated into the system before delivery.

5.1. 1991 Development Tasks

Batch System Design, NASA Review

The architecture of the Batch Processing system will be designed. The result of this task will be a detailed design document, specifying data structures, software modules and their interfaces. This design document will be reviewed and approved by NASA before implementation proceeds.

Information Fusion Implementation

The Information Fusion module will be implemented, using the Bayesian Belief Network approach. This module will consist of procedure calls to define the network, to run the update/solution algorithm, and to extract results (probability distribution for any node in the network).

Redline and Redundant Channel Test Implementation

The Redline and Redundant Channel Test modules will be the first validation techniques implemented, since they are the most straightforward to implement and their results are easily verifiable. In addition to the test modules themselves, the Steady-State/Transient Partitioning, Time-Slice Partitioning, and Batch Report Generation modules will be implemented and integrated with the Information Fusion module so that the test modules can be fully tested. The Redline and Redundant channel tests will be fully functional for all 114 critical PIDs described in Section 3.1.1.

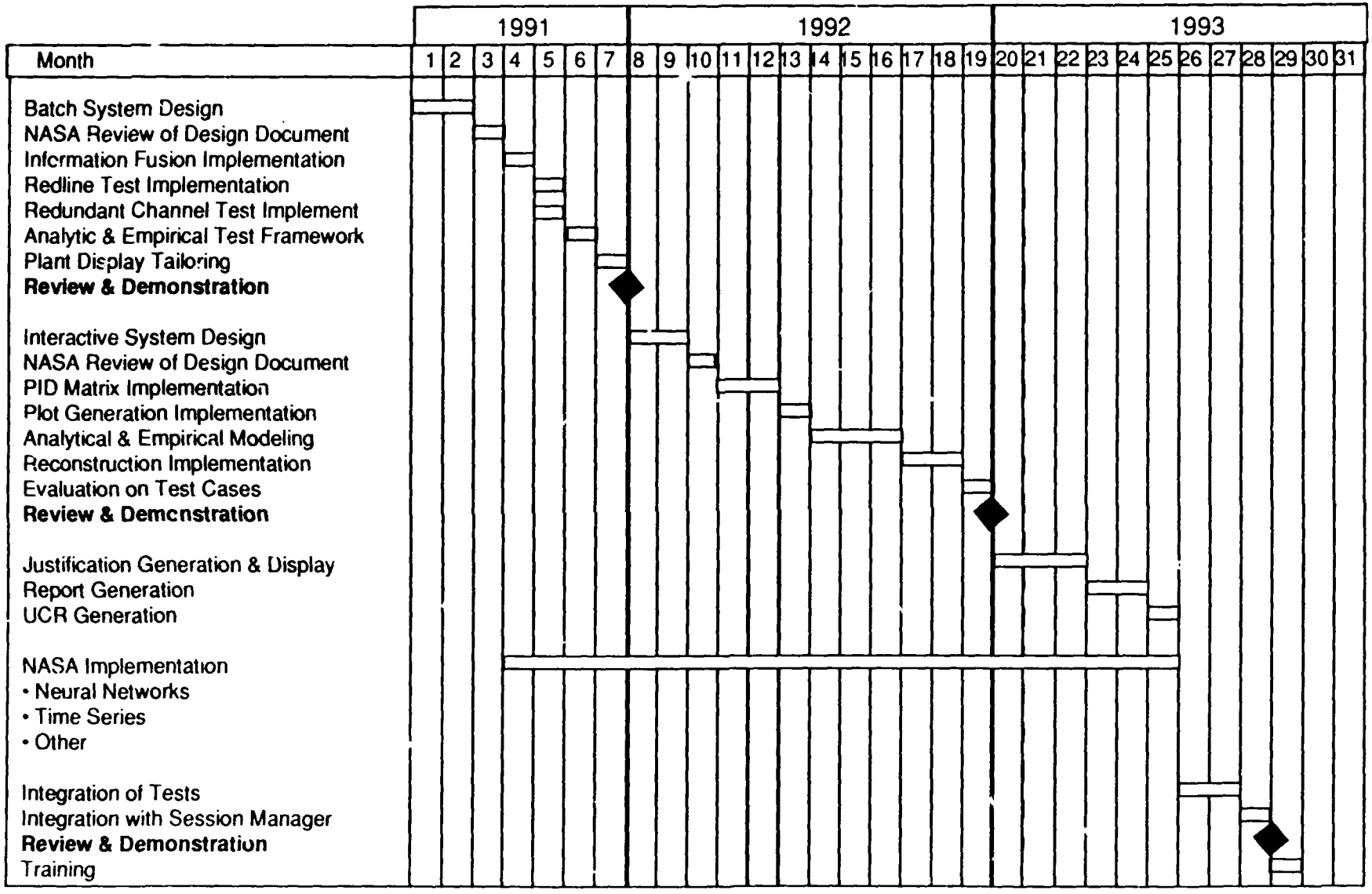

Figure 37. Software Implementation Schedule

Analytic & Empirical Test Framework Implementation

The Analytic and Empirical Test modules will be implemented. This initial implementation will utilize family-averaged characteristic values (the Model Sampling module will not be implemented), and the tests will only be used on steady-state test data segments. In addition, only those models developed in Phase I will be implemented (covering approximately 50 PIDs). The Model Sampling module, characteristic database, and remaining models will be developed in 1992.

Plant Display Tailoring

An existing prototype of the Interactive Mode Plant Browser will be modified to display the results of the Batch Processing system for all 131 PIDs.

Review and Demonstration

A final review will be conducted at Aerojet Propulsion Division in Sacramento, California. The review will include a demonstration of the Sensor Validation system on the test data sets currently in Aerojet's possession. A report of the 1991 activities will be delivered to NASA TBD days following the final review.

Summary

In 1991 a minimally-functional Batch Processing system will be developed, which will perform validation on all 131 critical PIDs. A very simple graphical user interface (consisting of the Plant Browser module of the Interactive System) will be developed for displaying the results of the Batch processing. This development is expected to take approximately 5-1/2 person-months of effort.

5.2 1992 Development Tasks

Interactive System Design, NASA Review of Design Document

The architecture of the Interactive Processing system will be designed. The result of this task will be a detailed design document, specifying data structures, software modules and their interfaces. This design document will be reviewed and approved by NASA before implementation proceeds.

PID Matrix Implementation

The PID Matrix Authorizer module will be implemented, allowing the analyst to browse and modify the results of the Batch Mode processing.

Plot Generation Implementation

The Plot Generation module will be implemented for plotting PID values (as requested by the analyst) and for displaying graphical elements of Batch Mode justifications.

Analytical & Empirical Modeling

The Model Sampling module in the Batch Processing system and the Family Update module in the Interactive Processing system will be implemented, in addition to the Family and Engine characteristic databases. A complete set of analytical and empirical models, covering all 114 critical PIDs, will be developed and implemented.

Reconstruction Implementation

The Reconstruction module (used in both the Batch and Interactive systems) and the Validated Test Set Generator modules will be implemented.

Evaluation on Test Cases

The Sensor Validation system (the Batch Mode module of which will be essentially complete) will be evaluated on test cases provided by NASA Lewis.

Review and Demonstration

A final review will be conducted at NASA Lewis Research Center in Cleveland, Ohio. The review will include a demonstration of the Sensor Validation system on the test cases provided by NASA. A report of the 1992 activities will be delivered to NASA TBD days following the final review.

Summary

In 1992 the Sensor Validation system will be complete, except for the ability to justify conclusions, and without the integration of validation techniques developed by other groups. At this point, the system can be fielded at MSFC for initial evaluation.

5.3. 1993 Development Tasks

Justification Generation and Display

The ability for the Batch Mode system to generate justifications, and for the Interactive Mode system to display them will be implemented.

Report Generation

The Report Generation module in the Interactive Mode system will be implemented to produce SunWrite-editable reports describing and justifying the conclusions reached by the Sensor Validation system.

UCR Generation

The UCR Generation module in the Interactive Mode system will be implemented to produce UCRs as requested by the analyst.

Integration of Tests

Sensor validation techniques developed by other groups will be integrated into the final sensor validation system. This includes extending the Information Fusion module to incorporate the results from these tests.

Integration with Session Manager

Both the Batch and Interactive mode systems will be integrated with the Session Manager, so that the Sensor Validation system can be run from the unified Life Prediction system interface.

Review and Demonstration

A final review will be conducted at NASA Lewis Research Center in Cleveland, Ohio. The review will include a demonstration of the Sensor Validation system on additional test cases provided by NASA. A report of the 1993 activities will be delivered to NASA TBD days following the final review.

Training

One-week of on-site training will be provided to analysts wishing to use the Sensor Validation system. The training will not only cover how to run both modes of the system, but will cover how to modify the system's parameters (i.e., Batch thresholds, Test parameters, and Belief Network probabilities).

References

1. Gage, M., and De Hoff, R., Diagnostic System Architecture Study: Final Report, NAS 3-25883, August 1990.

2. SSME Failure Modes and Effects Analysis, SSME FMEA-RSS-8553-11, July 1988.

3. Smith, C., Broadie, M., and DeHoff, R., Turbine Engine Fault Detection and Isolation Program:Final Report, Systems Control Technology, AFWAL-TR-82-2058, August 1982.

4. Basseville, M., "Detecting Changes in Signals and Systems- A Survey", Automatica, Volume 24, 1988

5. Gumbel, E. J., Statistics of Extremes. Columbia University Press: New York, 1958

6. Freund, J. E., Statistics, A First Course. Prentice-Hall: Englewood Cliffs, New Jersey, 1970

7. Lipson and Sheth, Statistical Design and Analysis of Engineering Experiments. McGraw-Hill: New York 1973

8. Speigel, M. R., Probability and Statistics. Schaum's, McGraw-Hill:1975

9. Taniguchi, M. H., Failure Control Techniques for the SSME Phase II: Final Report, NASA CR-179231, 1987.

10. Frank, P. N., "Fault Diagnosis in Dynamic Systems Using Analytical and Knowledge-based Redundancy- A Survey and Some New Results", Automatica, Volume 25, 1989

11. Merill, W. C., DeLaat J. C., and Bruton, W. M., "Advanced Detection, Isolation, and Accommodation of Sensor Failures- Real-Time Evaluation", NASA Technical Paper 2740, 1987

12. Isermann, R. "Process Fault Detection Based on Modeling and Estimation Methods- A Survey", Automatica, Volume 20, Number 4, 1984

13. Clark, R. N., "Instrument fault detection", *IEEE Trans. Aerospace Electron Syst.*, 14, 456-465, 1978.

14. Frank, P. M., "Advanced fault detection and isolation schemes using nonlinear and robust observers," Presented at *10th IFAC World Congress*, Munich, July 1987.

15. Meyer, C. M. and Zakrajsek, J. F., "Rocket Engine Failure Detection Using System Identification Techniques", 26th Joint Propulsion Conference: Orlando, Florida 1990

16. Pro-Matlab User's Guide. The Math Works Inc.: Massachusetts 1990

17. Guo, T H. and Nurre, J., "Sensor Failure Detection and Recovery By Neural Networks", NASA Lewis Research Center, January 1991

18. Cover, T. M. and Hart, P. E., "Nearest Neighbor Pattern Classification", IEEE Tran. Information Theory, January 1967

19. James, M., Classification Algorithms. John Wiley & Sons: London, 1985

20. Fu, K. S. and Rosenfeld, A., "Pattern Recognition and Computer Vision", IEEE Computer Magazine, October 1984

21. Dayhoff, J., Neural Network Architectures. Van Nostrand Reinhold: New York, 1990

22. Lippmann, R. P.,"An Introduction to Computing With Neural Nets", IEEE ASSP Magazine, April 1987

23. Wasserman, P. D., Neural Computing. Van Nostrand Reinhold: New York, 1990

24. Pearl, J., Probabilistic Reasoning in Intelligent Systems: Networks of Plausible Inference. Morgan Kaufmann: San Mateo, California 1988

25. Shortliffe, E., Computer-Based Medical Consultations: MYCIN. Elsvier, New York, 1976

26. Henrion, M., "Should We Use Probability In Uncertain Inference Systems?", Proceedings, Cognitive Science Society Meeting, Amherst, MA, August 1986

27. Shafer, G., A Mathematical Theory of Evidence. Princeton Press, Princeton, New Jersey 1976

28. Morawski, P., "Understanding Bayesian Belief Networks", AI Expert Magazine, Volume 4, Issue 5, May 1989

29. D'Ambrosio, B., Symbolic Probabilistic Inference in Belief Nets. Department of Computer Science, Oregon State University, 1989

30. Lauritzen, S. and Spiegelhalter, D., "Local Computations With Probabilities On Graphical Structures and their Application to Expert Systems", Journal of Royal Statistical Society B, 1988

31. Pearl, J., "Fusion, Propagation and Structuring in Belief Networks", Artificial Intelligence, 1986

32. Arthur, L. J., UNIX Shell Programming. John Wiley & Sons: New York,1990

33. Groff, J. R. and Weinberg, P. N., Understanding UNIX, A Conceptual Guide. Que Corporation: Indianapolis, 1983

34. Kernighan, B. W. and Ritchie, D. M., The C Programming Language. Prentice-Hall, Englewood Cliffs, New Jersey 1978

35. Leithauser, D., Artificial Intelligence Programming Techniques In Basic. Wordware Publishing, Inc.: Dallas, 1987

30. Reitman, E., Exploring the Geometry of Nature. Windcrest Books, 1989

31. Scarl, E. A., Jamieson, J. R., Delaune, C. I., "Diagnosis and Sensor Validation through Knowledge of Structure and Function", IEEE Tran. Systems, Man, and Cybernetics, Vol. SMC-17, No. 3, May/June 1987

34. Specht, D., "Probabilistic Neural Networks for Classification, Mapping, or Associative Memory", Proceedings IEEE International Conference on Neural Networks, San Diego, California, July 1988

37. Widrow, B. and Winter, R., "Neural Nets for Adaptive Filtering and Adaptive Pattern Recognition", IEEE Computer Magazine, March 1988

Appendix A: INTERVIEWS WITH DATA VALIDATION EXPERTS

A trip was taken to NASA MSFC on 4-7 June to meet with SSME data analysts and engine experts. The interviews were conducted with both Martin Marietta and NASA personnel. In addition two post test data review were attended. The results of these interviews have been used to prepare the Users Requirements Document (URD.) In addition, interviews have been conducted with Aerojet personnel knowledgable with sensor data validation.

A brief summary of key interviews and comments from the trip to NASA MSFC are given below. The following questions were asked of the NASA MSFC personnel during the interviews.

(1) What is the current data validation procedure?
(2) How is previous test data used in the validation procedure?
(3) How are test stand, engine, and component variations accounted for?
(4) What types of computer interfaces are used or would be most useful (i.e. hardcopy plots, databases, on-line plots and zooms)?
(5) Which sensors historically are prone to failure?
(6) What records of failed PID's are maintained?
(7) What I/O format is required to handle data at MSFC?
(8) What analytical models of the SSME might be available?
(9) Who at MSFC would be principle users of this system?
(10) Who at MSFC would be interested in receiving status updates on the progress of the system?
(11) Who at MSFC could ask questions regarding specific PID's on recent tests?

General Comments

All the NASA MSFC and Martin Marietta personnel interviewed were extremely helpful, interested, and generous with their time during the trip to Huntsville. Two types of meeting were conducted. First, general overview meetings were held with Darby Makel and Mark Gage of Aerojet, and Ron De Hoff of SCT, along with a given MSFC interviewee. In these meetings the program objectives and the relationships between Task 3 and Task 4 were explained. These meetings were then followed up

with one on one meetings between Darby Makel and the various SSME data analysts.

Interview with David Vaughn:

David Vaughn is the manager of the Martin Marietta Data Analysis Group. He was very supportive of the program objectives and stated that there is a "real need" for the sensor data validation code as soon as possible. He said he would be the contact person for providing information and data regarding the historical behavior of particular PID's and test firings. David described their current sensor data validation procedure as a "confirmation procedure," where the data analysts have sufficient experience and intuition that they can inspect other transducer readings to confirm a failrd sensor reading. While this procedure is qualitative it appears to be a gooo starting place for a rule based approach. While David did not provide specifics regarding system requirements, he emphasized the need to link the Sun into their overall data flow.

Interview with David Foust:

David Foust is the lead engineer in the Data Analysis Group, he reports to David Vaughn. David's group has the primary responsibility for detecting sensor failures as part of their overall responsibility to review engine operation from test to test. The data analysis group examines a standard set of data plots for each test. If anomalies are detected other plots are requested after the initial review or previous test records are examined. Sensor failure detection depends on the analysts' manual review of the plots. In addition, not all of the CADS and Facility PIDs are plotted. Failed PIDs not plotted may never be detected (however, these PIDs are not very important for assessing engine operation). Once a failed PID is detected, a confirmation procedure is used to determine if the signal is the result of a sensor problem or an engine problem. If the anomalous signal occurs during main stage, the sensor reading during pretest and post test is examined to see if erratic behavior or scaling problems exist. In addition, other sensors which should be similarly affected by off nominal engine behavior are examined. A typical confirmation is to examine pressures and temperatures upstream and downstream of an anomalous sensor. The sensor reading will also be compared to previous test data. The previous test data must always be from the same test stand and preferably with the same engine

and the same turbopumps. If data with the same engine is not available, then data from an engine with as many of the same pumps as possible is used. The degree of variation in a sensor reading is judged based on a two sigma data base maintained by David Foust's group. A different 2 sigma data base exists for each of the three NASA SSC test stands. As a general rule an "typical" transducer will fail once in every 10 tests and small number of "problem" transducers fail on more than 50% of tests. David Foust viewed an automated sensor data validation procedure as a significant improvement to the efficiency of the current data review process.

Interview with Brian Pierkarski:

Brian Pierkarski is the lead engineer in the Model Analysis Group, he reports to David Vaughn. The Model Analysis group is responsible for calculating the performance for each test. This group uses the test data as an input to the steady state performance model. Brain's group is very sensitive to the issue of sensor failures and are very supportive of the data validation and signal reconstruction code. The calculation of specific impulse is very sensitive to slight errors in the model input PID's. Slight sensor drifts which are within the 2 sigma band, and may not appear significant to the data analysts assess engine operation, can cause appreciable errors in the performance calculation. Signal reconstruction is of particular interest to the model group. Currently, if a PID needed for the steady state model is missing due to a sensor failure, an approximate average value is input by the operator.

Interview with Marc Neely:

Marc Neely is a NASA MSFC engineer and works in the Liquid Propulsion Branch. Marc was very interested in the sensor data validation program and offered to provide help as the program evolved. He reiterated much the same technical information as discussed above. In addition, he feels that an expert system approach is the most suitable based the current state of knowledge of the SSME and the lack of a good model which can yield data that accurately predicts sensor readings. He expressed the opinion that the it would be necessary to bring a beta-test version of the code to MSFC, with on-site support from Aerojet. This task would be needed to test out its operation and build confidence among the analysts and NASA management in the codes operation and reliability.

Interview with Bill Baker (Aerojet)

- Bill Baker is in Data Services. Bill performs data analysis for about 15 programs (including Titan) in the test area.

- The primary function of Data Services is to provide 'Qualified Data' to Engineering. Thus, the detection and resolution of sensor anomalies is their responsibility (although, they frequently work together with Engineering in resolving problems which turn out to be sensor malfunctions).

- Procedure:

  -Sensors are calibrated in the lab to specifications.

  -Sensors are installed on the stand and hooked up to electrical and recording equipment.

  -A pre-test electrical calibration is run. Each sensor is stepped through four voltage levels (25, 50, 75, and 100% of maximum nominal value) to simulate its output. The sensor's response to these excitations are recorded and the absolute value, linearity, and return to zero are computed for each test.

  -Immediately following a test a post-test electrical calibration is run.

  -Approximately one hour after the test (when the engine has completely de-pressurized) another post-test electrical calibration is run.

  (All of the above data is available for diagnostic purposes.)

- For each sensed parameter the following values are computed for each steady-state summarized time slice for post-test analysis:

  -Standard deviation for each sensor.

  -Variance of each sensor from a family nominal value.

  -For duplex sensors: Difference and percent difference from each other (compared to historical difference).

- No hard "redlines" are used to automatically discredit sensors (although Bill mentioned that a 3-sigma variance warranted investigation).

- If two duplex sensors differ by too much and one is especially noisy, then you tend to discredit the noisy one.

- There are two kinds of noise:
  -Random (positive and negative variance).
  -Spike (positive OR negative variance at periodic intervals); indicative of an electrical problem.

- If you suspect a sensor problem, check the values upstream and downstream from it.

- Bill always looks at computed performance data first. If there is a problem, then he starts looking at suspect sensors on an as-needed basis.

- If there is a serious sensor problem, will often re-calibrate the sensor in the metrology lab and apply a correction factor (derived from the re-calibration procedure) to the sensor data.

- Unless a problem is detected, Bill typical does not look at:
  -Facility sensors.
  -Post-test calibration data.
  -Transient data plots.

- Try to look at invariant relationships among sensors to diagnose problems (e.g., ΔP or computed resistance). Example:

Interview with Joe Berroteran (Aerojet)

- Joe is head of Aerojet's Instrumentation group in Design Engineering. He used to work for Rocketdyne and performed failure analysis on the SSME instrumentation.

- Current SSME controller sensor validation procedure:

  -Each sensor has yellow lines, red lines, and reasonableness lines (piecewise models for all steady-state and transient conditions, see below), expressing upper and lower bounds for the sensor's values. A yellow line represents the normal operating range. Red lines demarcate abnormal (often unsafe) operating ranges. Reasonableness lines demarcate regions which are physically impossible for the sensor's value to fall within.

  -Duplex sensors (including most SSME sensors): If either sensor is above the red line but below the reasonableness line for two consecutive samples, then the engine is shut down (for certain critical sensors). Otherwise, if either sensor is over the reasonable line for two consecutive counts then that sensor is assumed to have failed and is ignored.

- SSME test procedures do include a pre- and post- test calibration.

- There are five major classes of sensors on the SSME: temperature, pressure, flow, speed, and acceleration.

- Open circuits (both hard and intermittent, caused by a broken wire, e.g.) are probably the most common sensor failure. Typically an open circuit will cause a sensor's value to go to zero (or some very small constant "offset" value). Intermittent open circuits show up as instantaneous variations from normal to zero (or offset).

- Short circuits (e.g., due to contamination) are very rare (Joe has only seen one or two in over 10 years). Instrument circuitry is typically designed to shut down the sensor if a short occurs.

- "Spikes" - sensor readings which change faster than their measured parameters could physically change - are indicative of sensor failures.

- Speed and flow sensors are subject to "aliasing" in which the sensor reading has a low frequency sine wave superimposed onto it. This is fundamentally due to a timing problem, but can be caused by mis-alignments of the sensors (e.g., Joe had an example of a flow meter which suffered from aliasing due to its four impellor blades not being at perfect right angles to each other). This is a very rare problem.

- Pressure sensors are subject to drift due to thermal effects. Drift typically shows up as a constantly increasing or decreasing bias.

- Pressure sensors are also subject to "overshoot" of about 3-5psi. It can take around 15 seconds for them to settle to their correct value.

- Temperature sensors can go out of calibration due to thermal expansion. This results in a constant bias (1% FS) in the open circuit direction.

- Pressure sensors have a "reference vacuum" on the inner side of their diaphragm. These sensors can lose this vacuum, resulting in a constant bias (this should show up as a difference between pre- and post- test calibrations).

- Sensor accuracy specs for SSME:

  -All sensor <u>systems</u> must be accurate to within 2% FS (including transmission, A/D conversion, etc.).

  -Pressure and temperatures transducers must be accurate to within 1/4% FS.

  -Flow and speed transducers must be accurate to within 1/2% FS (?).

<u>Interview with Bill Ferrell (Aerojet)</u>

- Bill Ferrell has 31 years' experience at Aerojet (including 5 years in the test area), mostly on the Titan program. He currently analyzes data from Titan flights and acceptance tests, particularly when an anomaly is discovered.

- Bill confirmed that the primary way sensor malfunctions are currently detected and diagnosed on Titan is through analysis of the engine characteristics (resistances, performance biases, etc.). These characteristics should be relatively constant across the range of engine performance, and should have a predictable variance from engine to engine, both making anomaly detection easier.

- Bill showed me plots of three related characteristics from the most recent Titan acceptance test which clearly demonstrate the usefulness of using characteristics for anomaly detection and diagnosis (see the two pages attached to this report). These three parameters are:

  ROT - Total resistance from turbopump discharge to chamber.

  ROL - Resistance from turbopump discharge to injector.

  ROJ - Resistance across injector (also called ROTCA for "Chamber Assembly").

  Resistance = (Pressure drop across line)*(Specific Gravity) / $(\text{Flow})^2$

  In the most recent test, the values for ROL, ROJ, and ROT were as shown on the first graph. ROT stayed constant, but ROJ and ROJ varied. However, their variance was equal in magnitude and opposite in direction, indicating a problem with the POJ sensor. Note that if *all* resistances are high or low, then the sensors used for computing Specific Gravity or Flow should be suspect.

- Bill mentioned that accuracy of computed characteristics depends on the accuracy of the sensors involved and the formulas used in their derivation. For example, if the pressure drop between two pressure sensors is very small (e.g., across a pipe) then the computed resistance will have a high variance because a small change in either pressure will have a large effect on computed resistance.

- A second method for detecting sensor failures used by Ferrell is to look at the transient curves of characteristics (even though they don't change much, they still experience small transients on engine startup and shutdown). The second chart

attached shows ROJ for the last five Titan turbopump tests over time. The most recent test clearly shows a deviation from family norms.

- Another diagnostic method that Ferrell suggested (given that an engine has already been tested once to derive an initial set of characteristics) involves taking a few critical sensor values (at steady-state) and deriving what all other sensor values should be using the engine's characteristics as true. Deviations of sensors from these "reconstructed" values are then used for anomaly detection.

- Bill also mentioned that the pre-test and post-test calibrations for sensors should be compared (see the 1/17/91 interview notes for Bill Baker); any mismatches are indicative of malfunction.

- Two other heuristics that Bill mentioned were:

  -If a sensed value has an unusually high variance it typically indicates a sensor problem (Bill visually inspects transient plots and knows what normal variances "look" like, see the third chart attached to this write-up).

  -If a sensed value has an unusually high frequency it typically indicates a sensor problem, especially if the signal is changing faster than the process could physically change.

Appendix B: CHARACTERISTIC AND REGRESSION MODELS

Results of characteristic equations based on family average characteristics

Test A2497

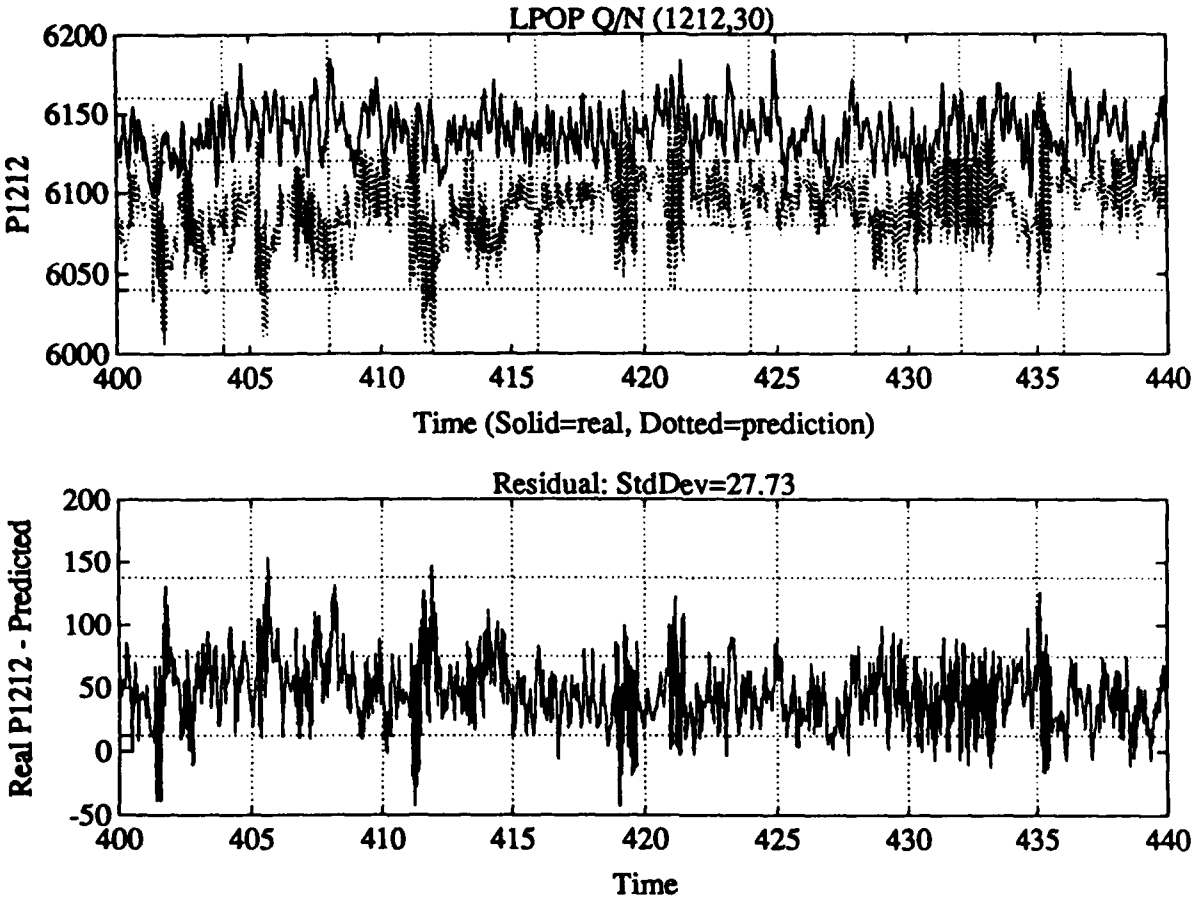

Test AJ497

Based on Family Avg. characteristic

Steady-State

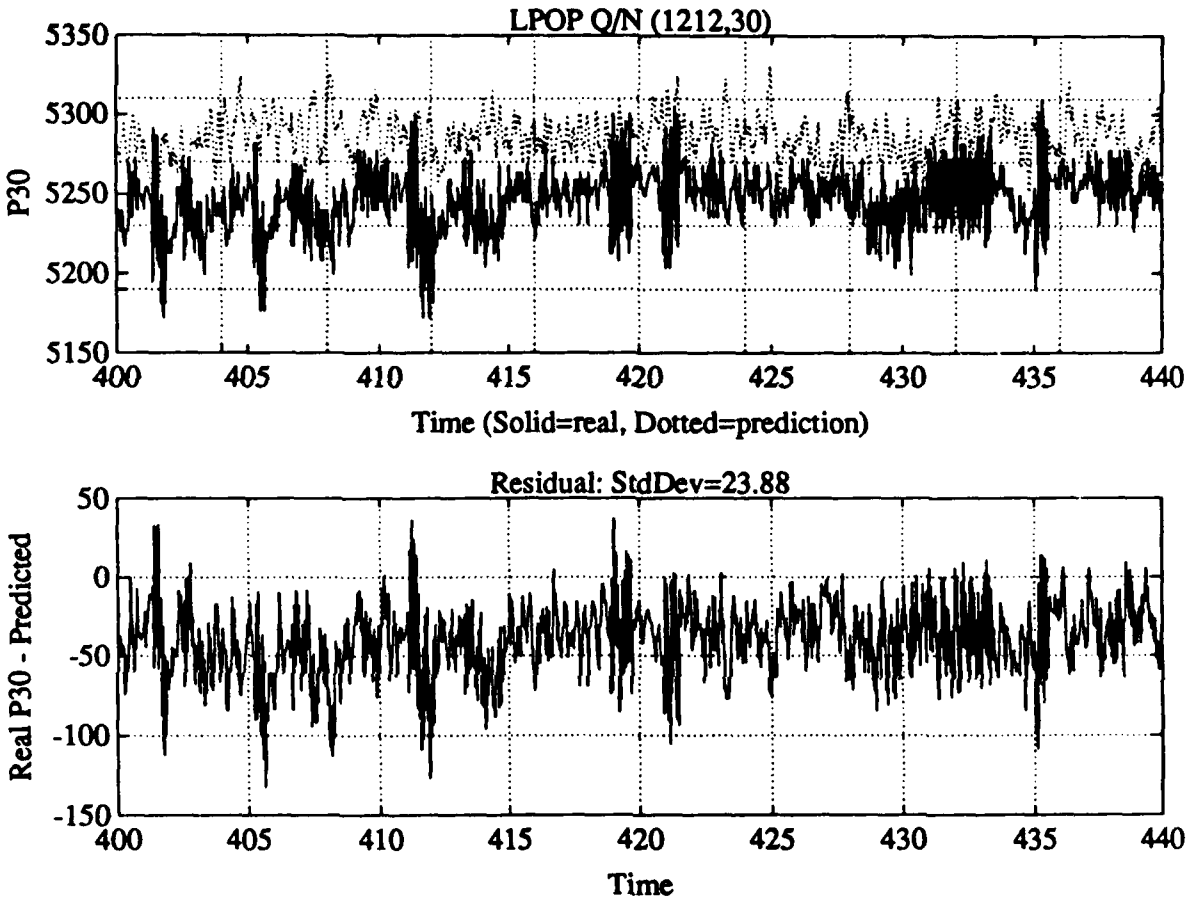

Family / Steady-state

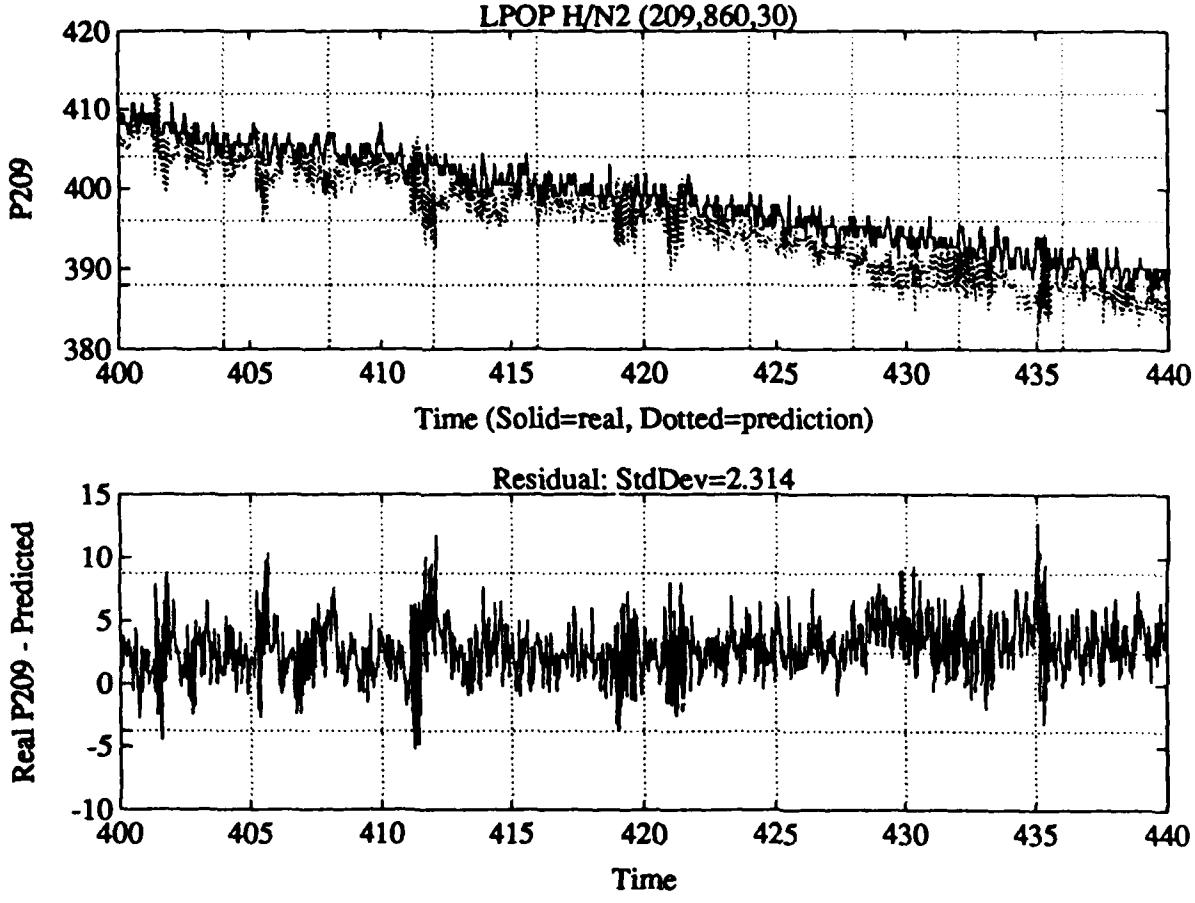

Family / Steady - State

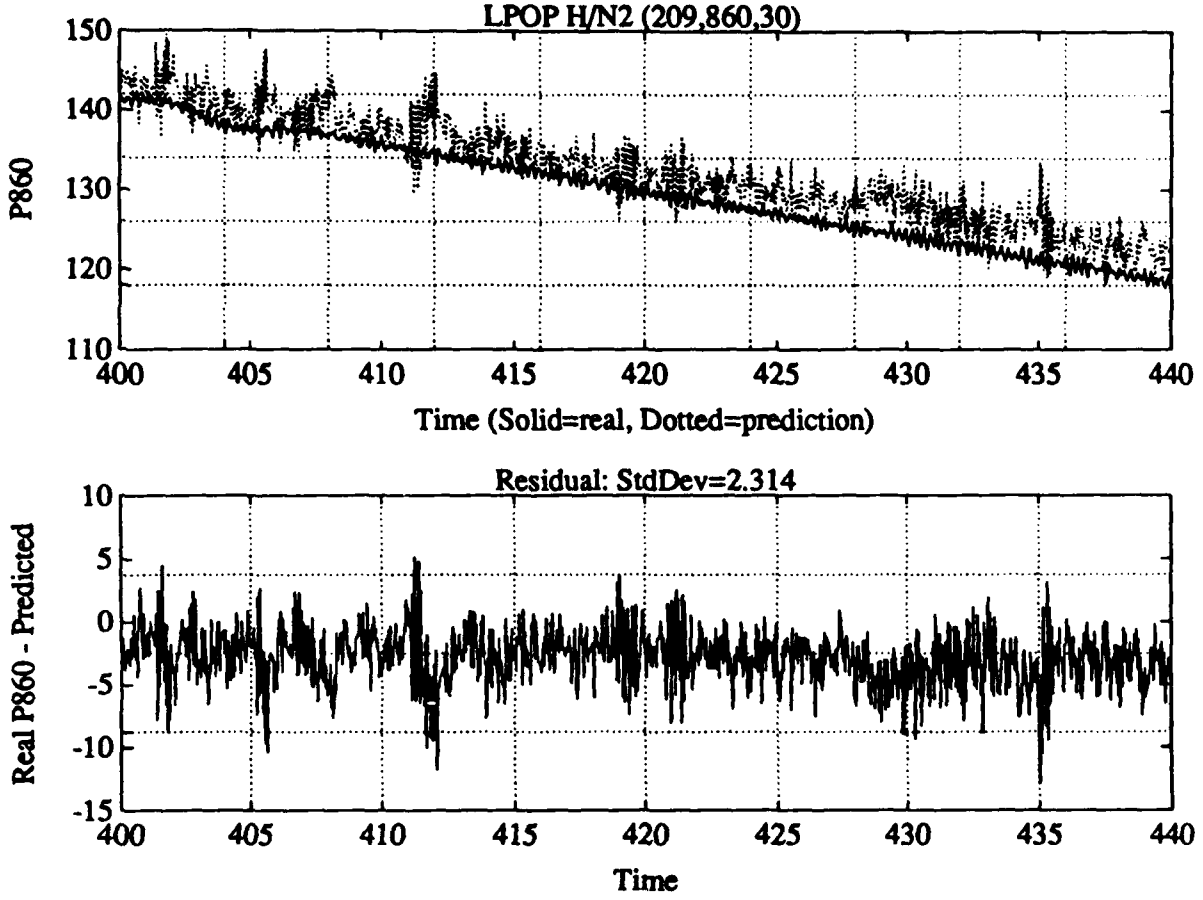

Family / Steady State

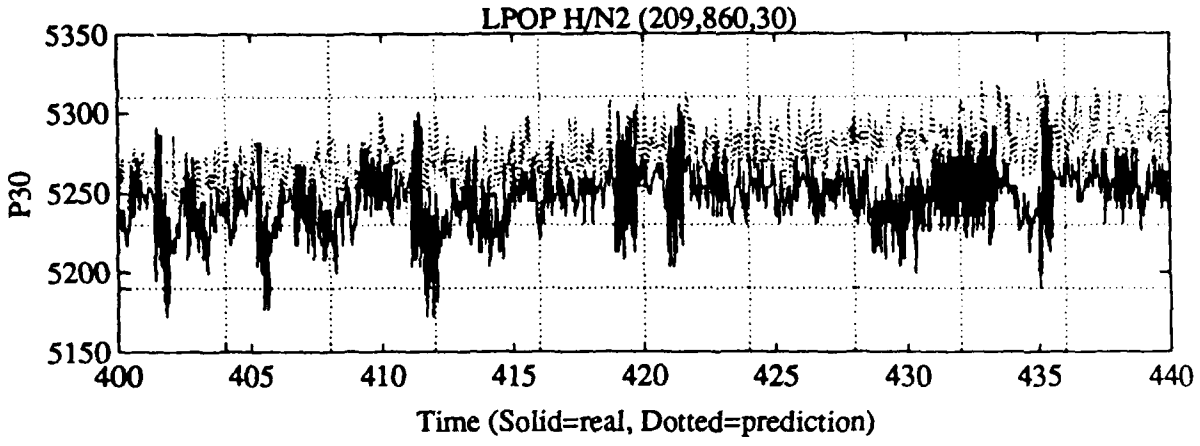
LPOP H/N2 (209,860,30)
P30
5350
5300
5250
5200
5150
400
405
410
415
420
425
430
435
440
Time (Solid=real, Dotted=prediction)

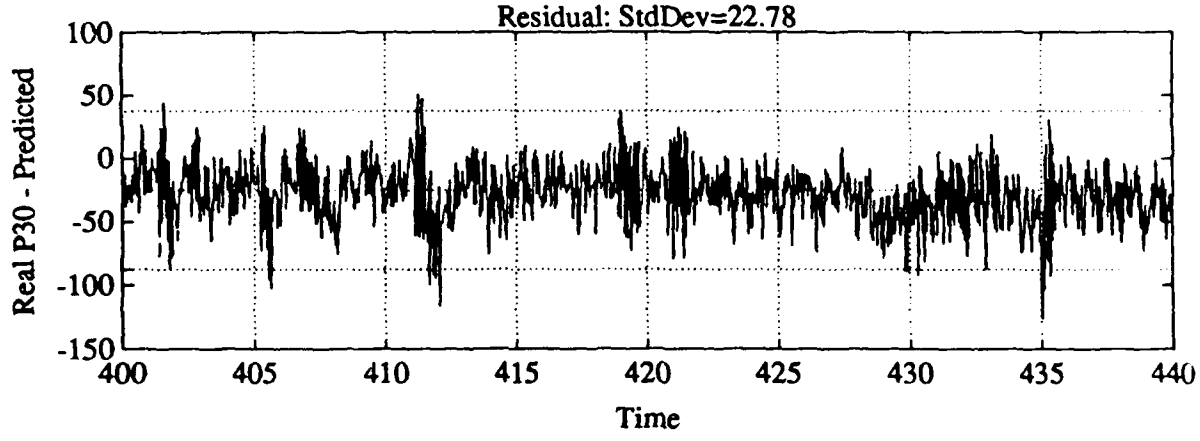
Residual: StdDev=22.78
Real P30 - Predicted
100
50
0
-50
-100
-150
400
405
410
415
420
425
430
435
440
Time

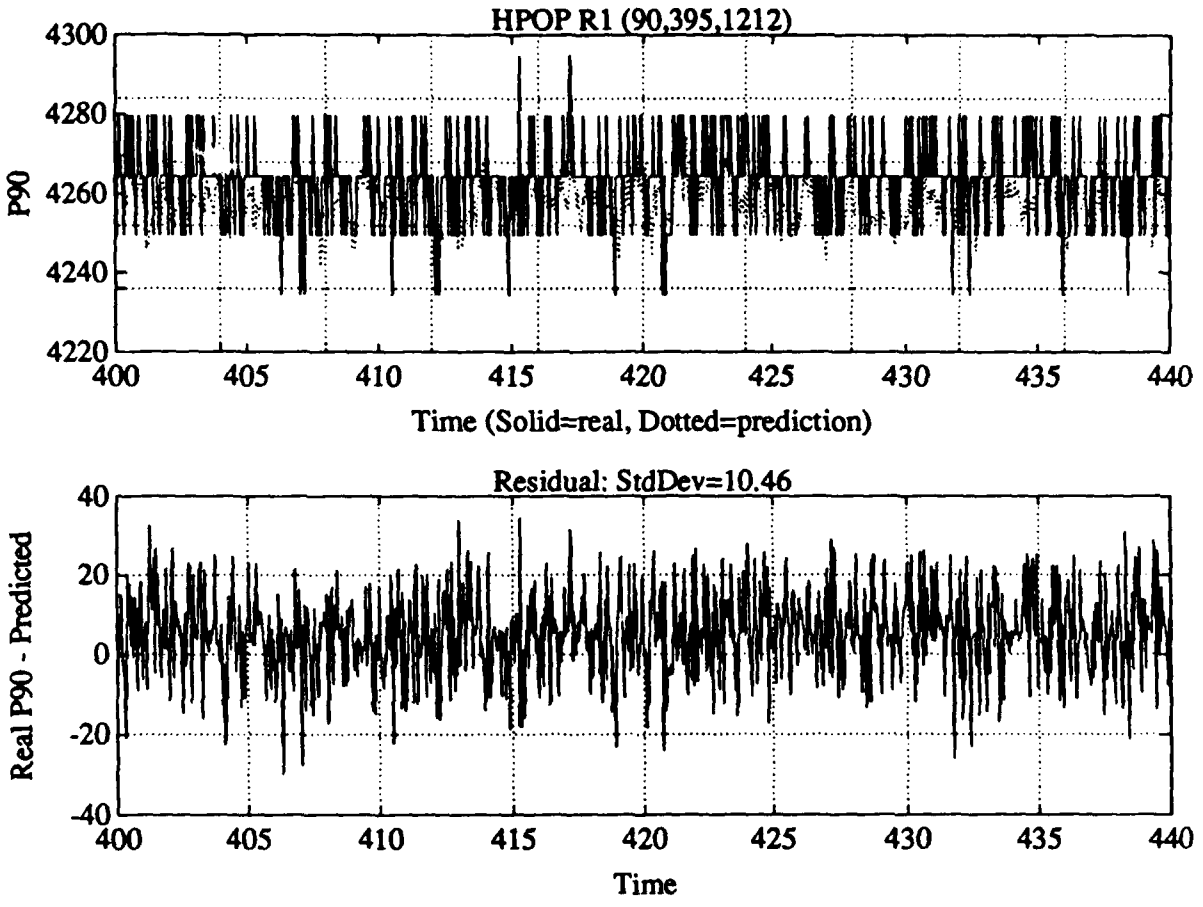

Family / Steady State

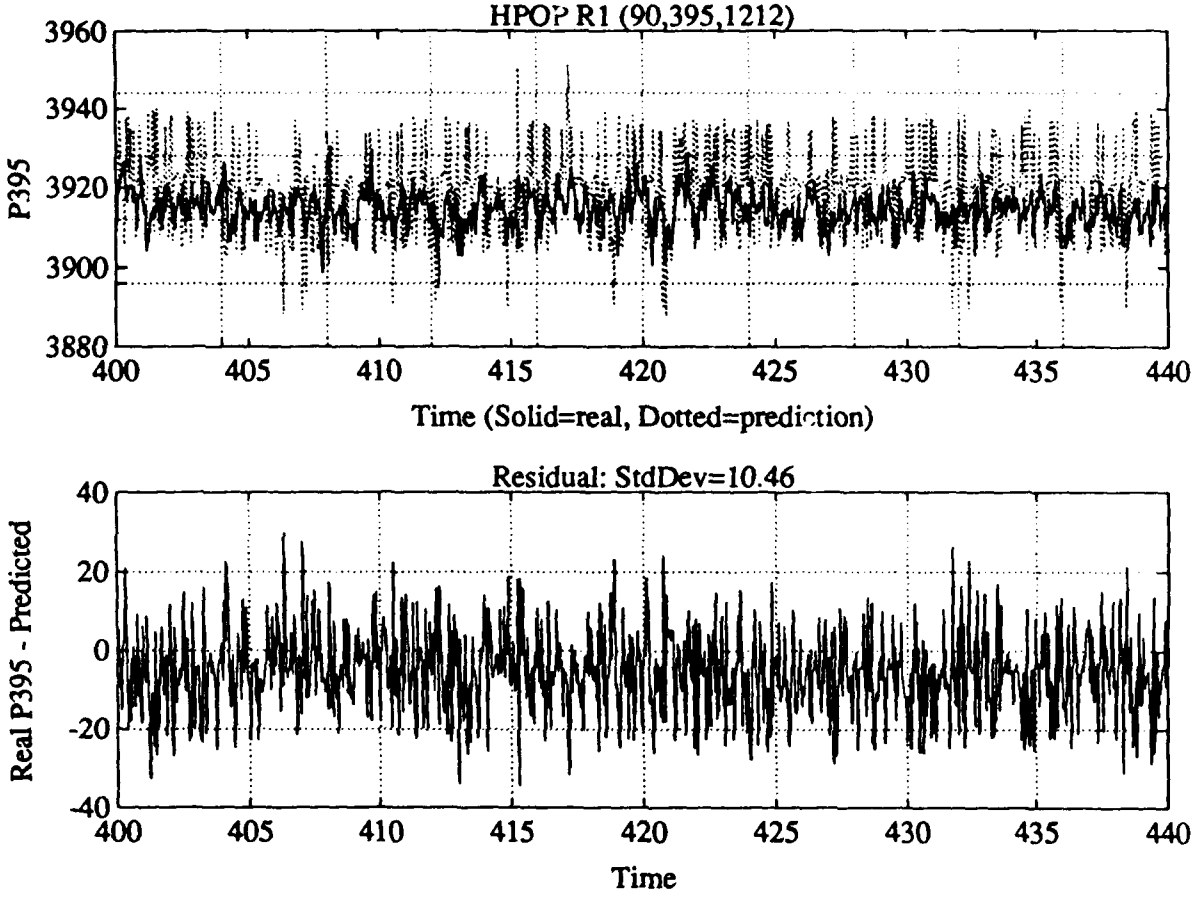

Family / Steady-State

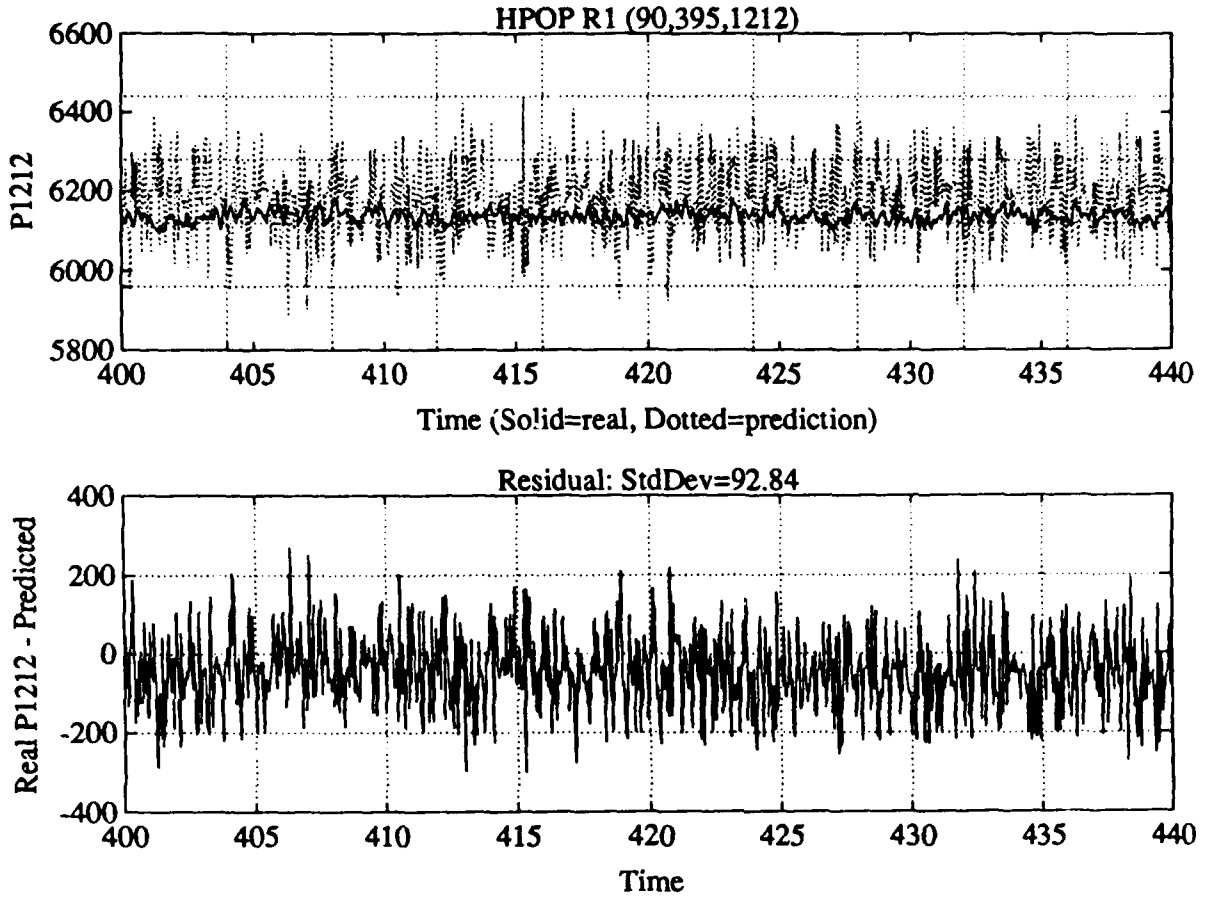
HPOP R1 (90,395,1212)
P1212
6600
6400
6200
6000
5800
400
405
410
415
420
425
430
435
440
Time (Solid=real, Dotted=prediction)
Residual: StdDev=92.84
Real P1212 - Predicted
400
200
0
-200
-400
Time

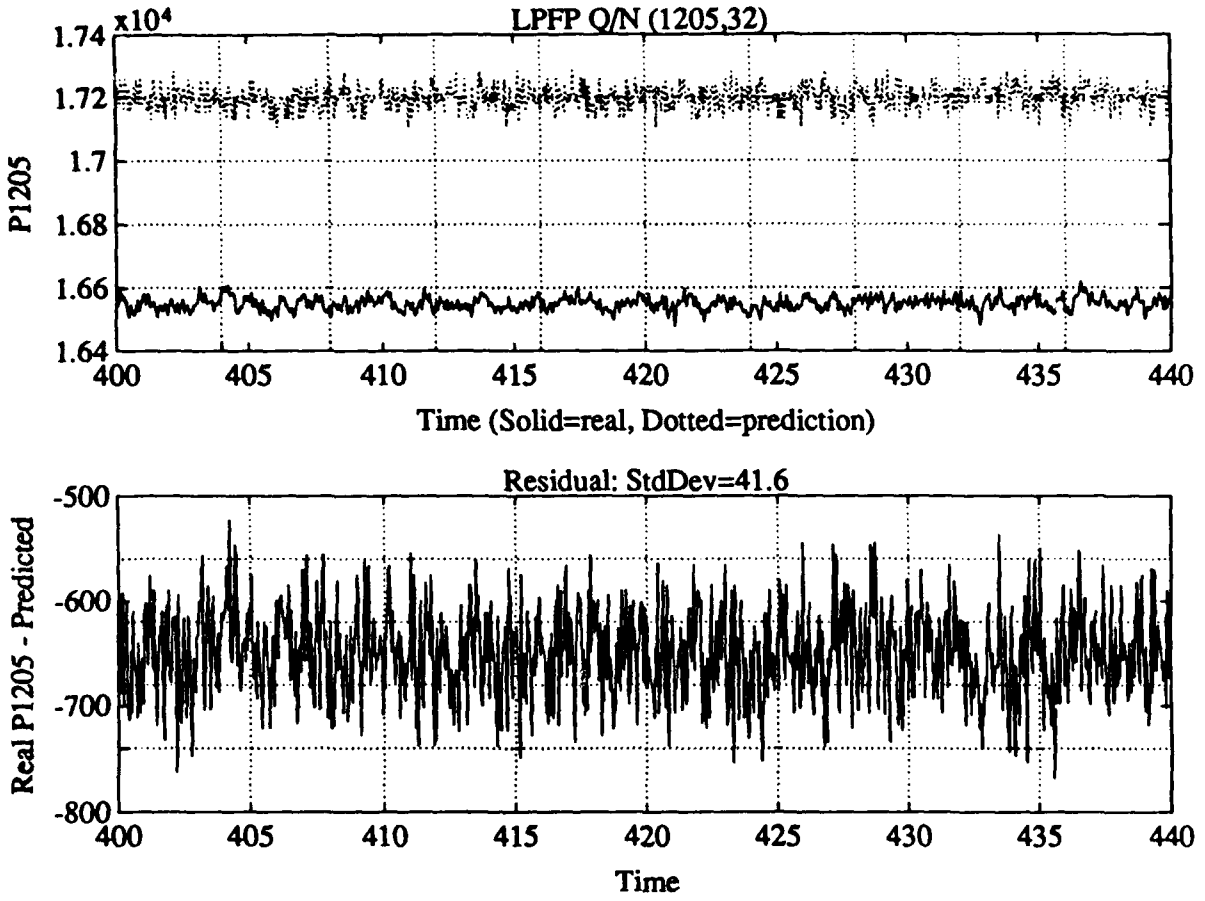

Fig 3

Family / Steady-state

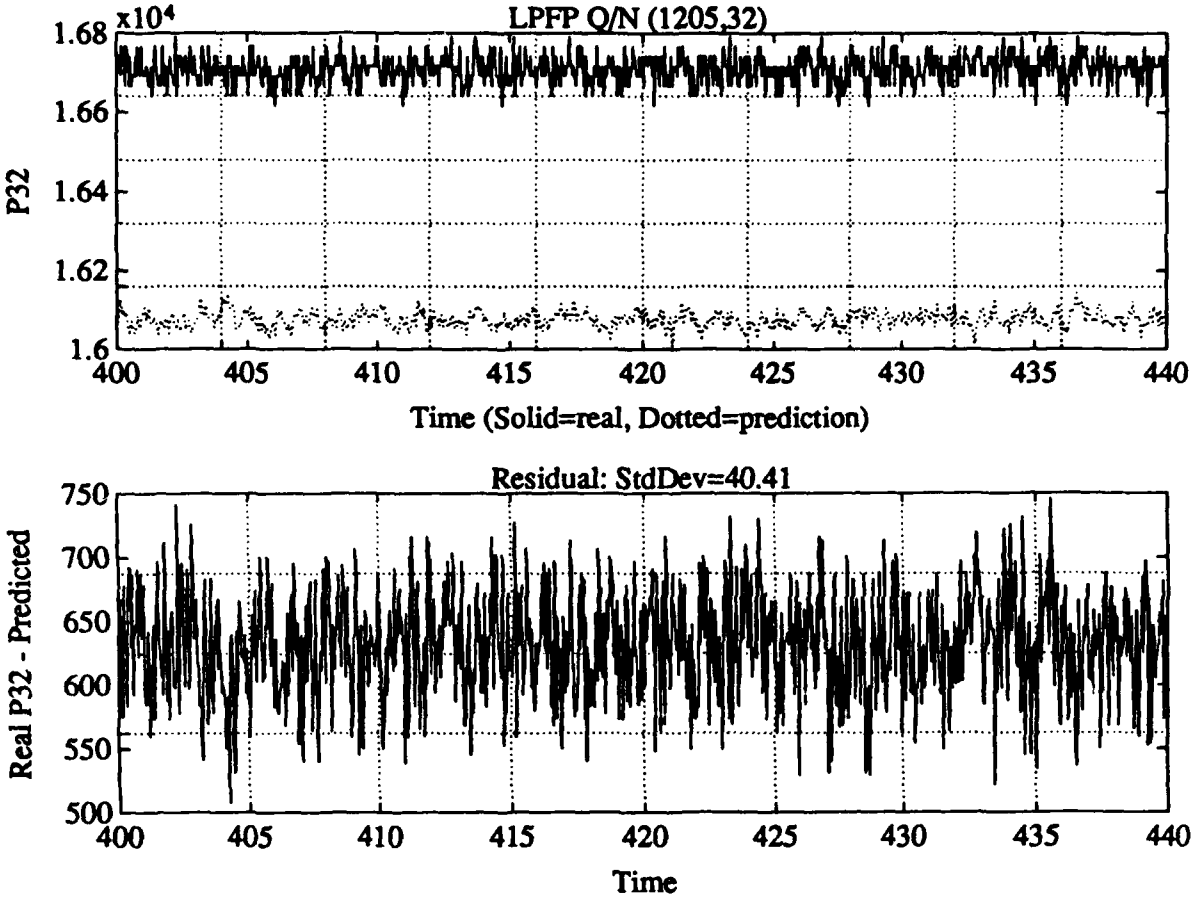

Fourier / Steady-State

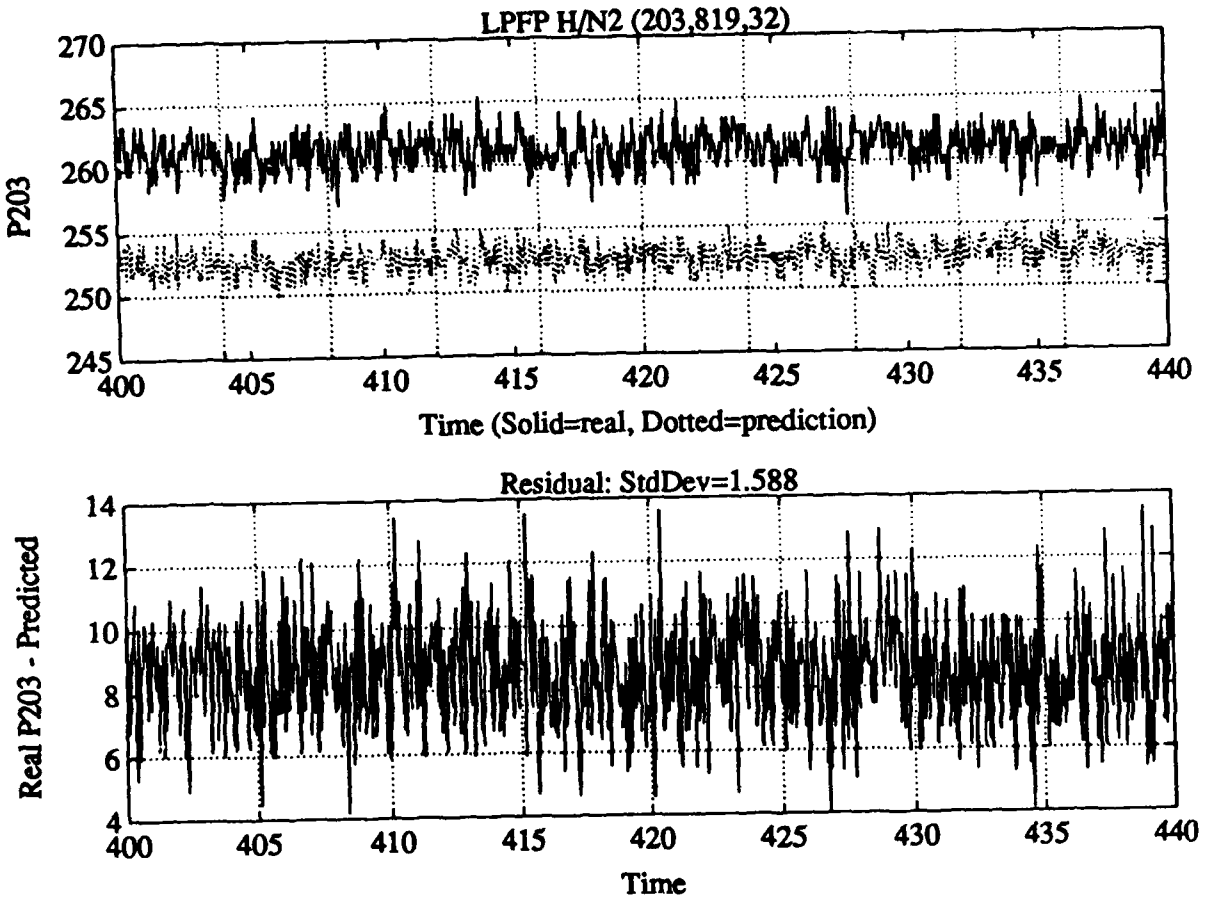

Family / Steady-state

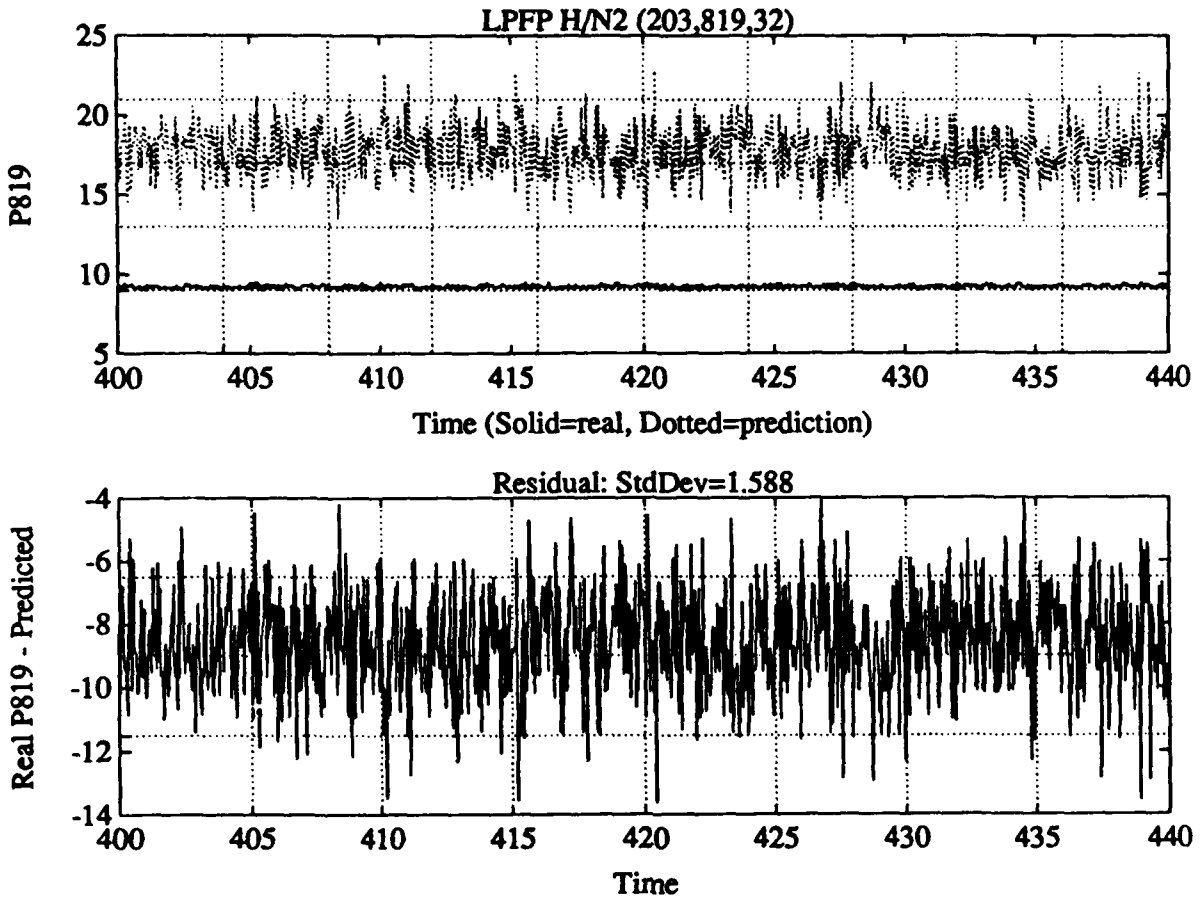

Family / Steady-state

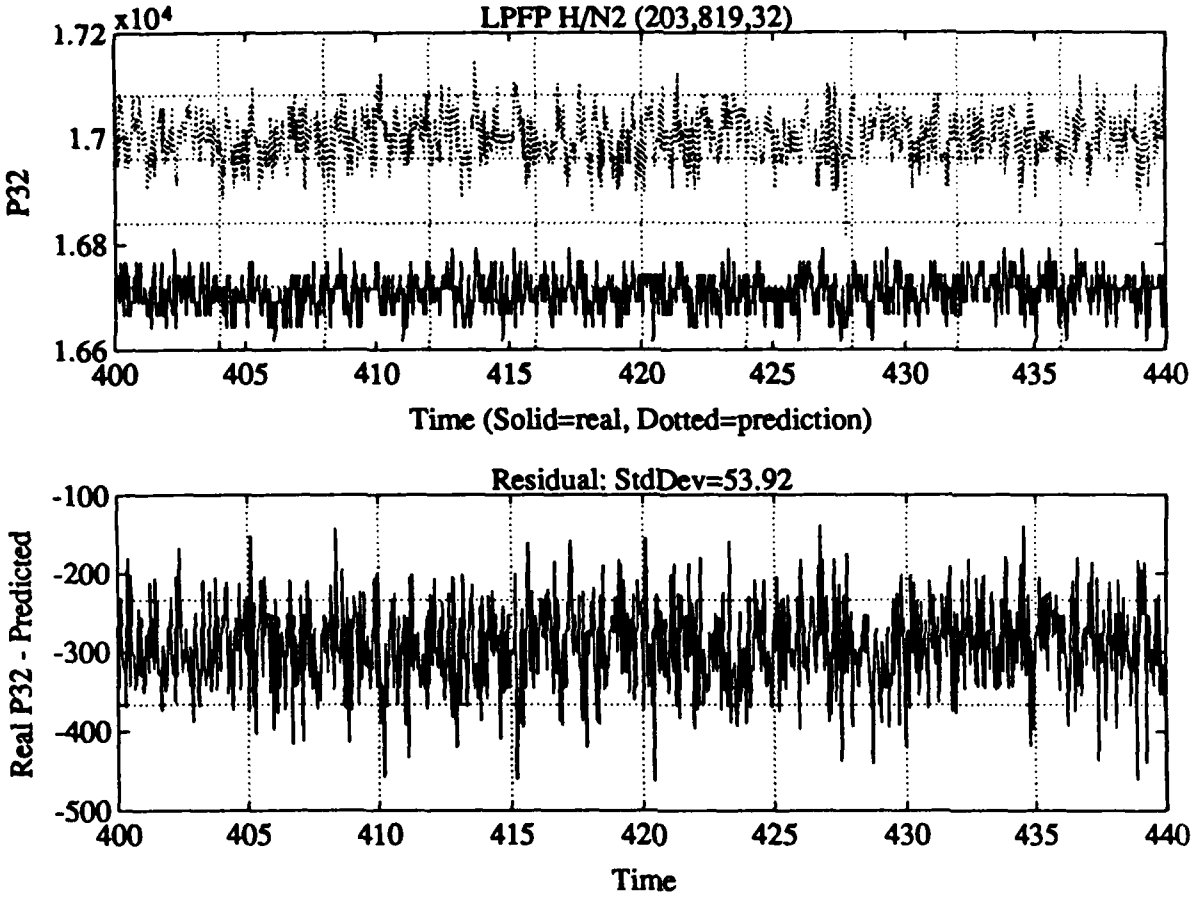
LPFP H/N2 (203,819,32)
x10^4
1.72
1.7
1.68
1.66
P32
400
405
410
415
420
425
430
435
440
Time (Solid=real, Dotted=prediction)
Residual: StdDev=53.92
-100
-200
-300
-400
-500
Real P32 - Predicted
400
405
410
415
420
425
430
435
440
Time

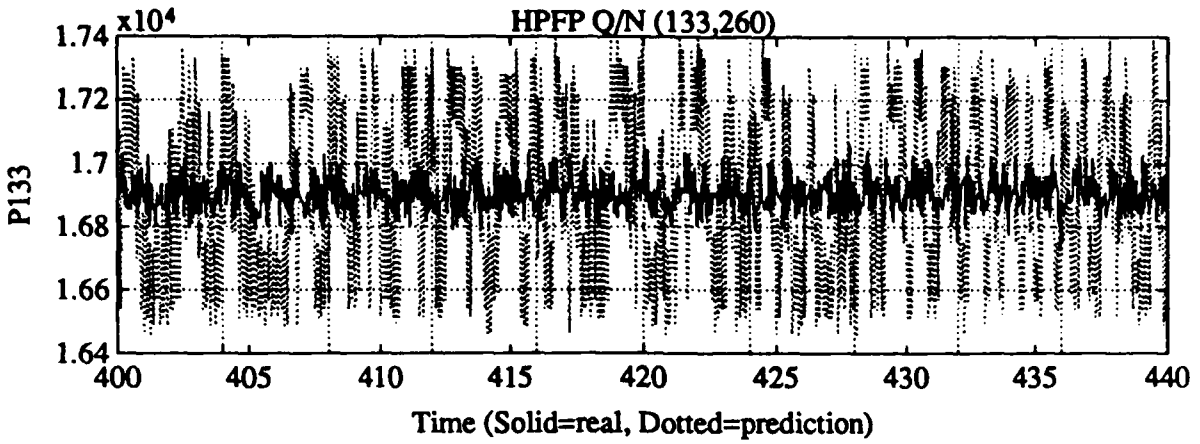

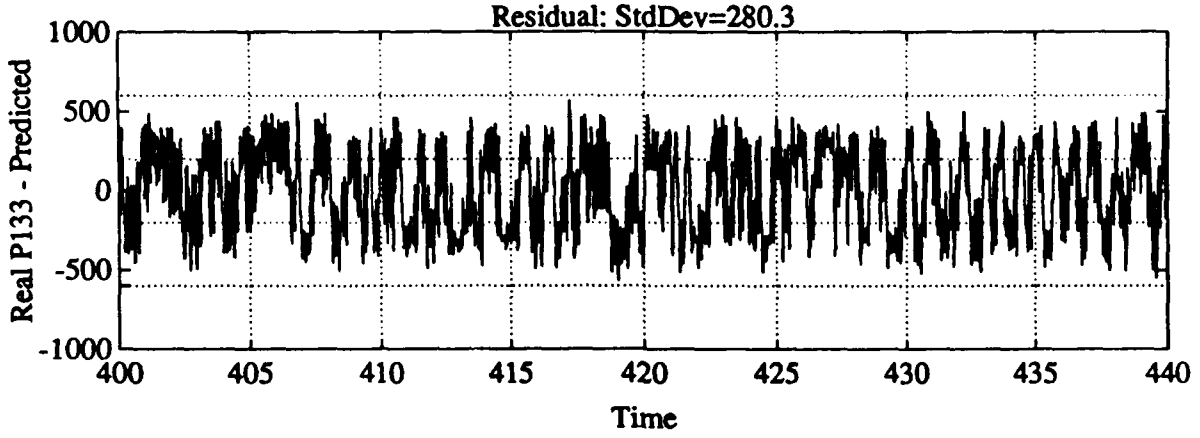

Family / Steady-State

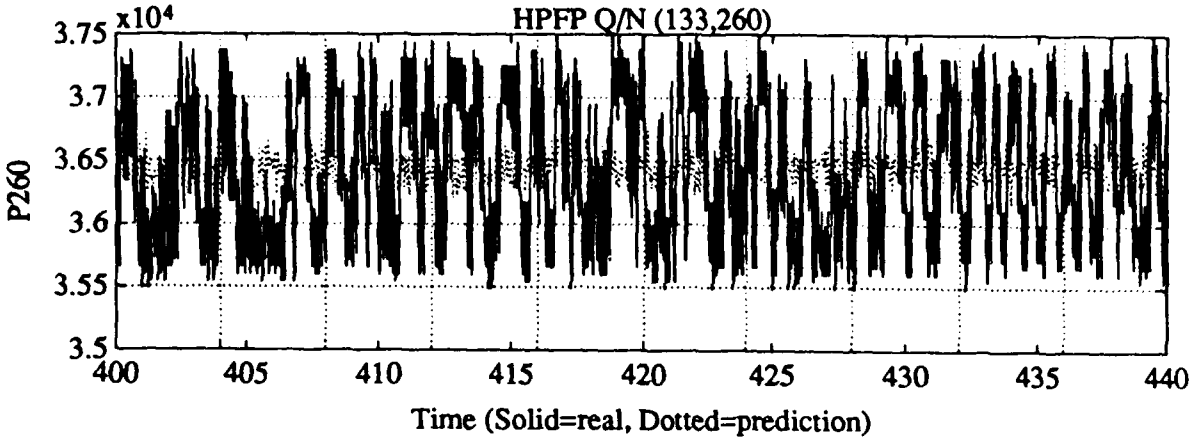

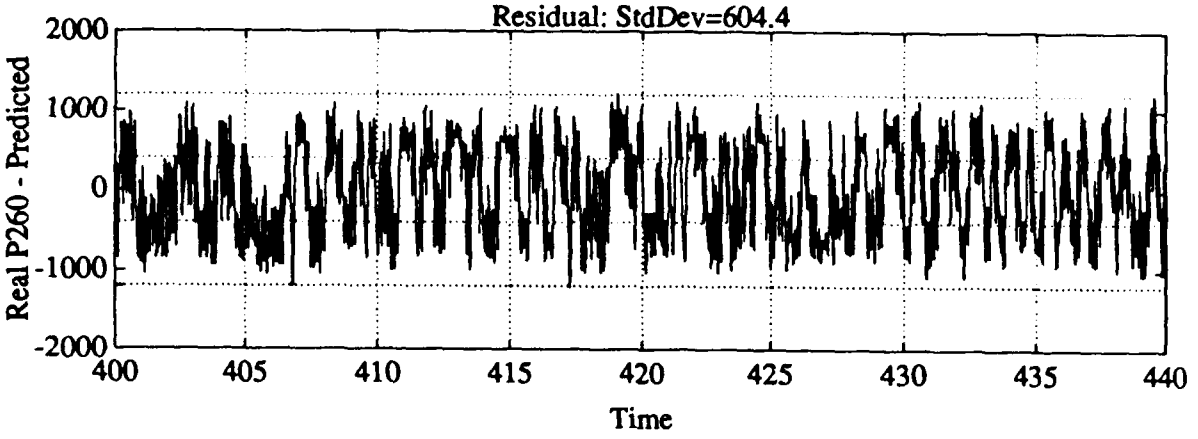

Family / Steady-State

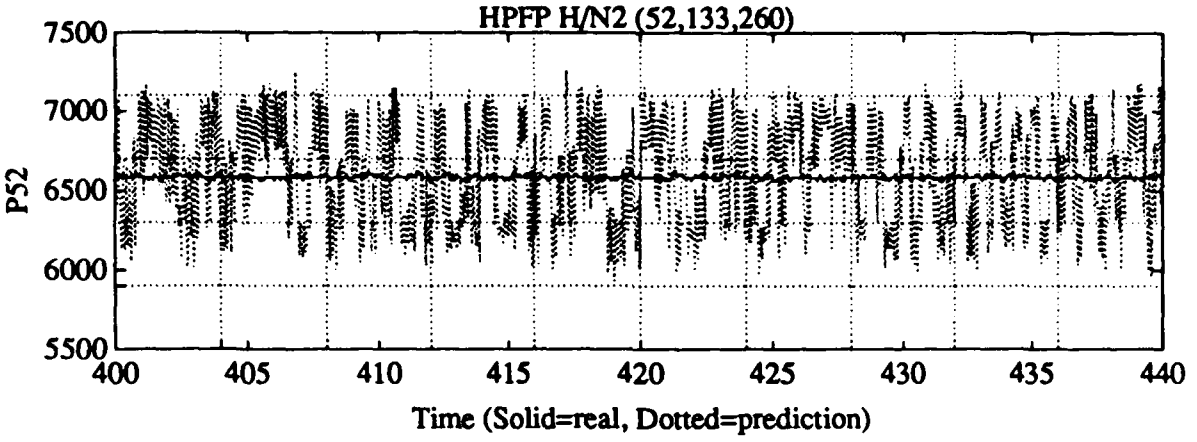

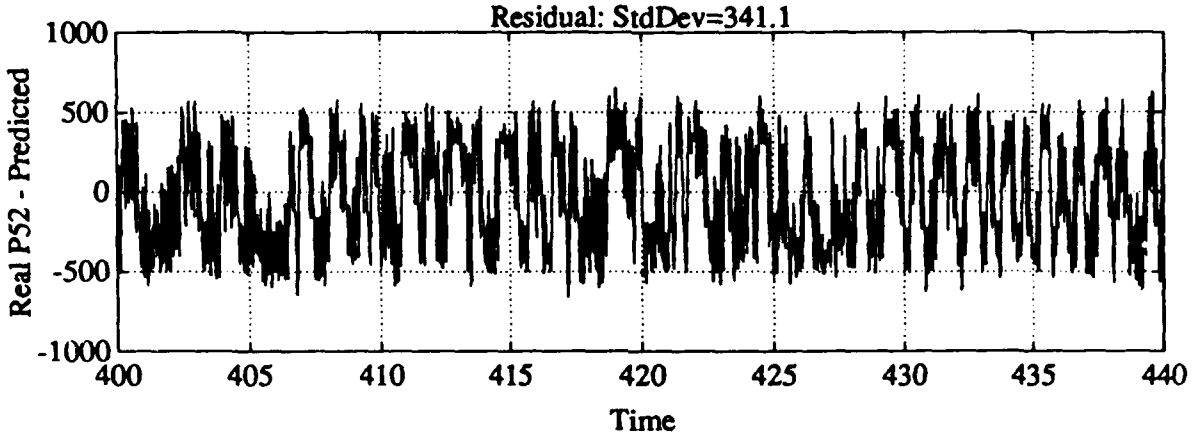

Family / Steady-State

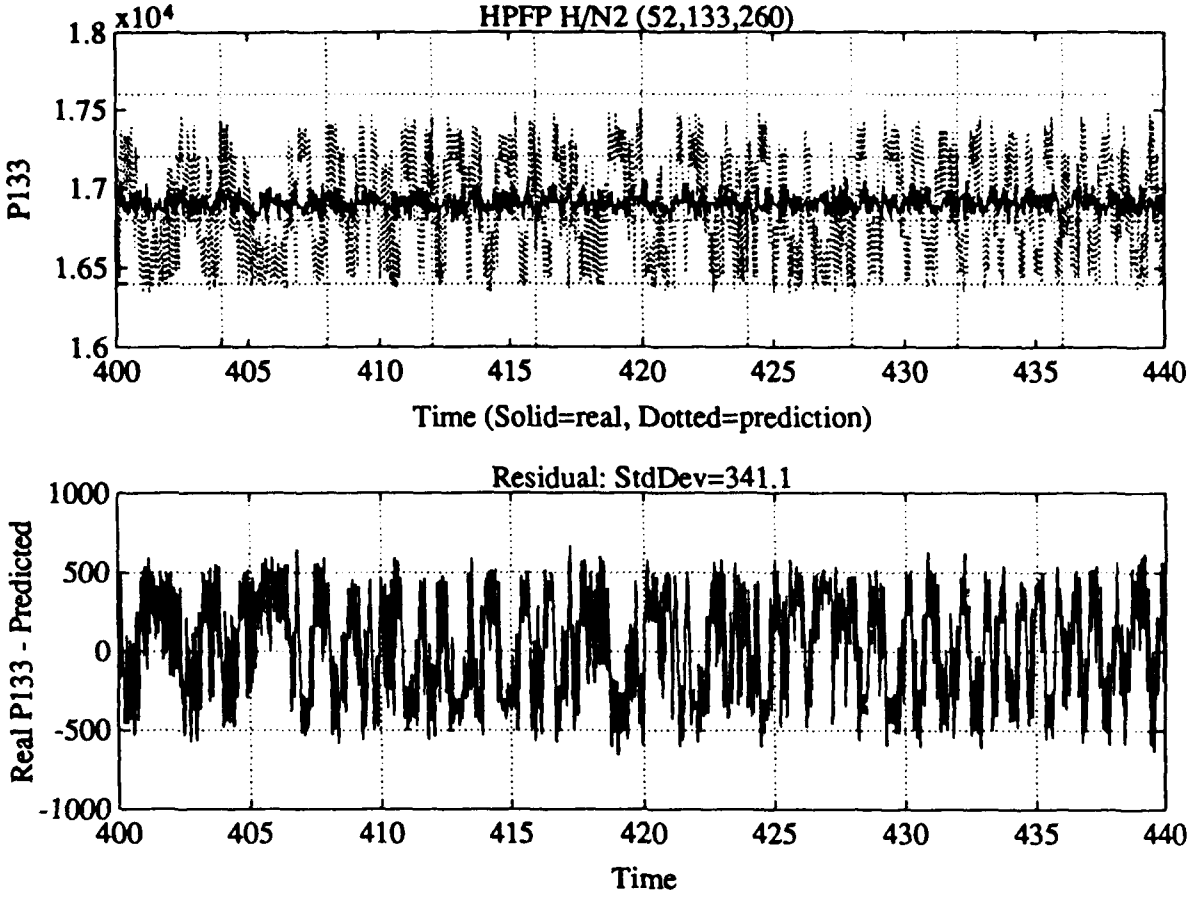

Faulty/ Steady-State

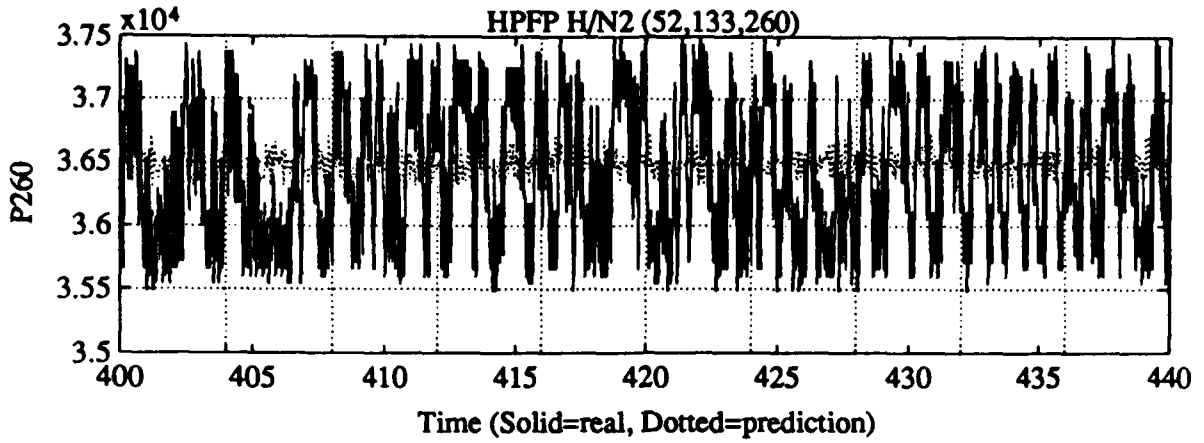
HPFP H/N2 (52,133,260)
x10^4
3.75
3.7
3.65
3.6
3.55
3.5
P260
400
405
410
415
420
425
430
435
440
Time (Solid=real, Dotted=prediction)

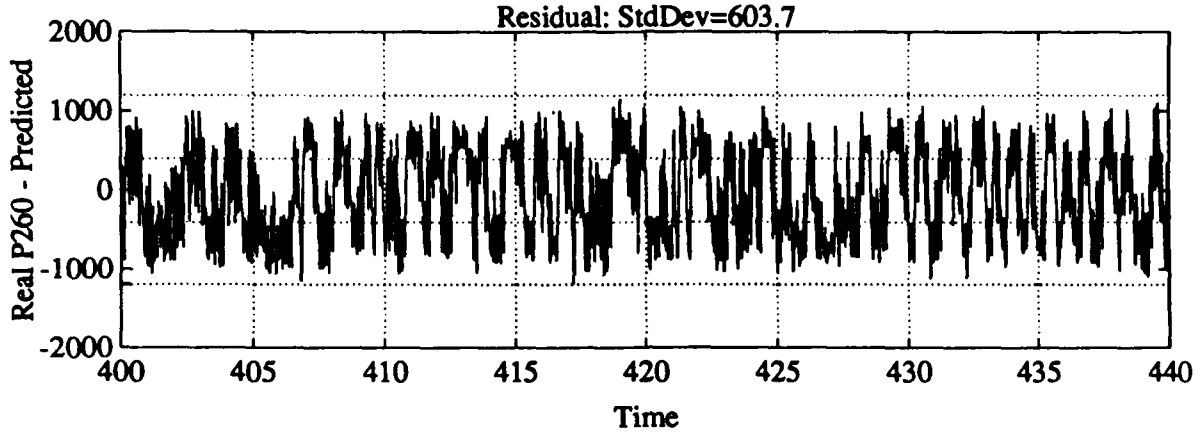
Residual: StdDev=603.7
2000
1000
0
-1000
-2000
Real P260 - Predicted
400
405
410
415
420
425
430
435
440
Time

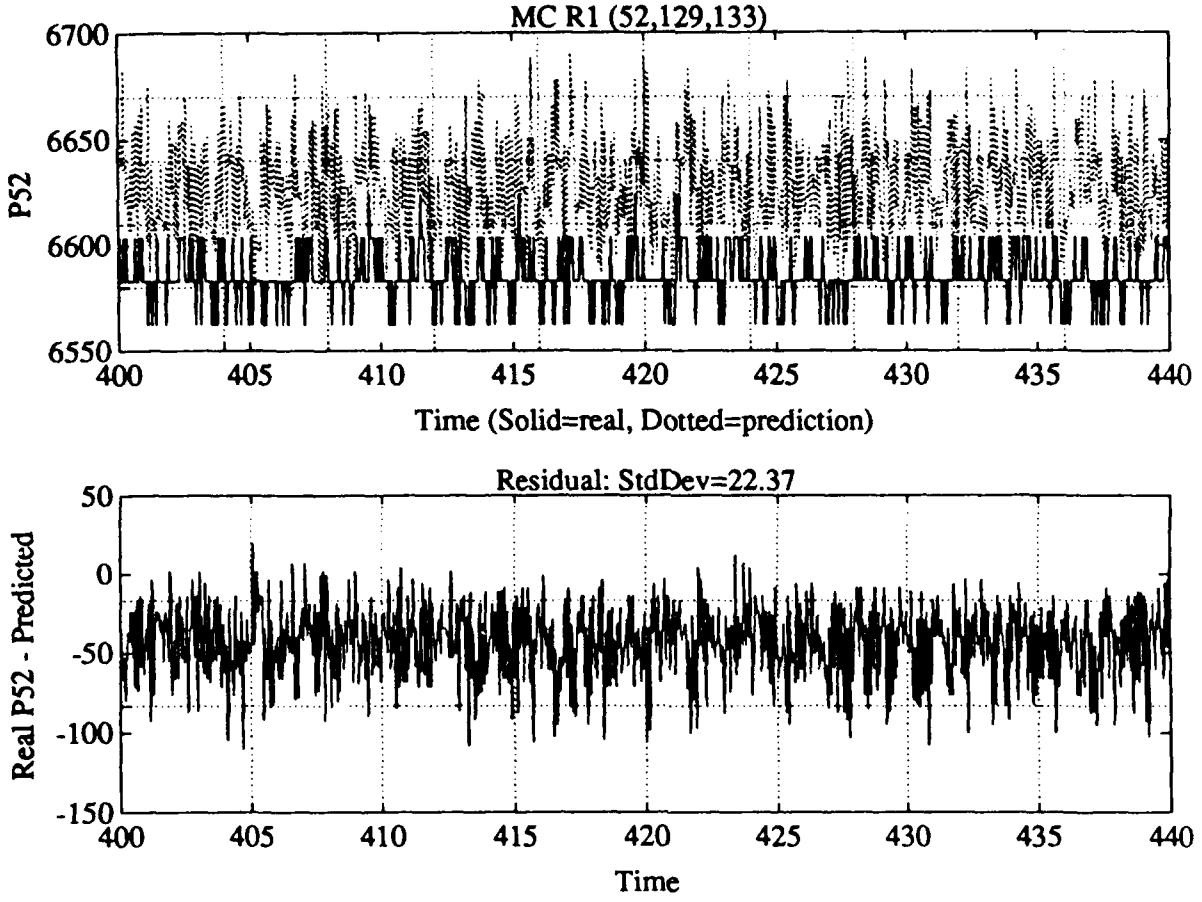

Family / Steady-state

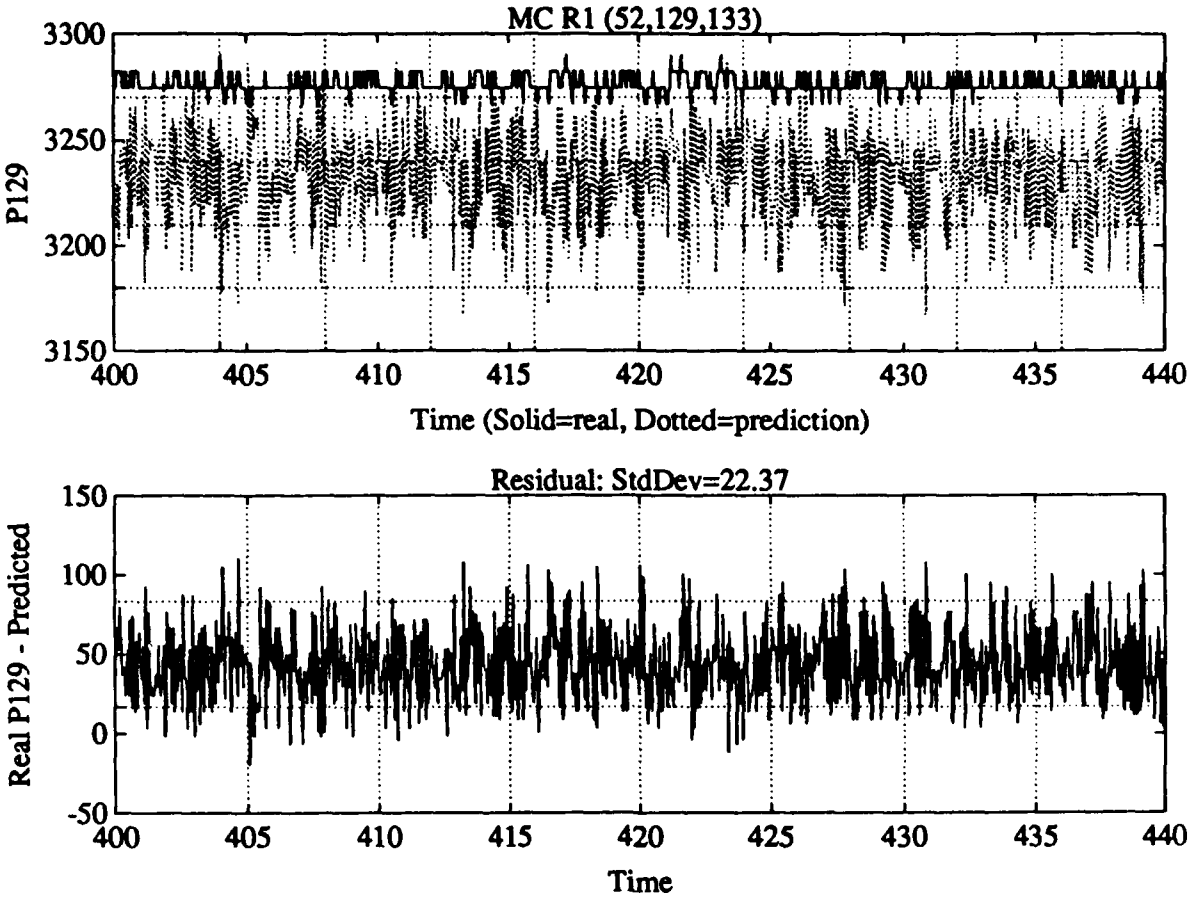

Family / Steady-State

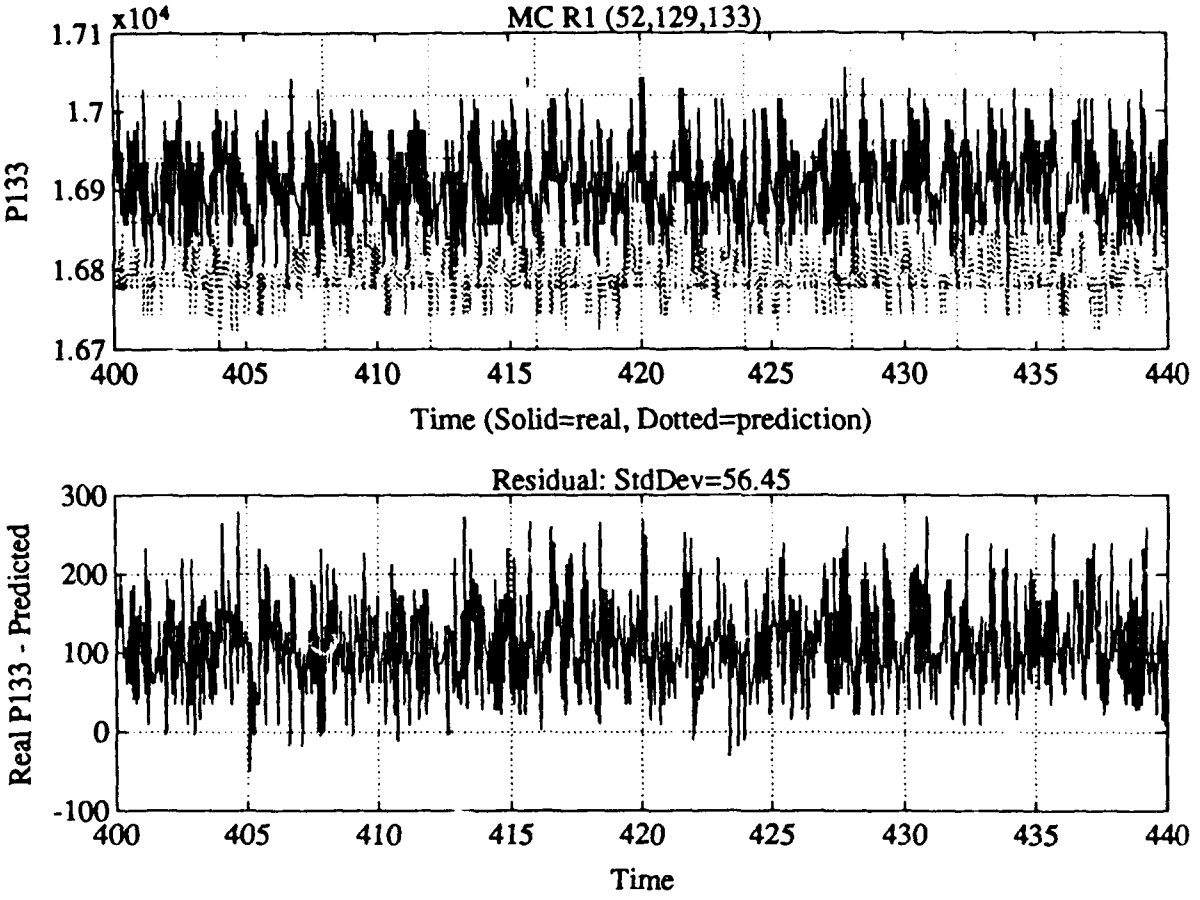
MC R1 (52,129,133)
x10^4
1.71
1.7
1.69
1.68
1.67
P133
400
405
410
415
420
425
430
435
440
Time (Solid=real, Dotted=prediction)
Residual: StdDev=56.45
300
200
100
0
-100
Real P133 - Predicted
400
405
410
415
420
425
430
435
440
Time

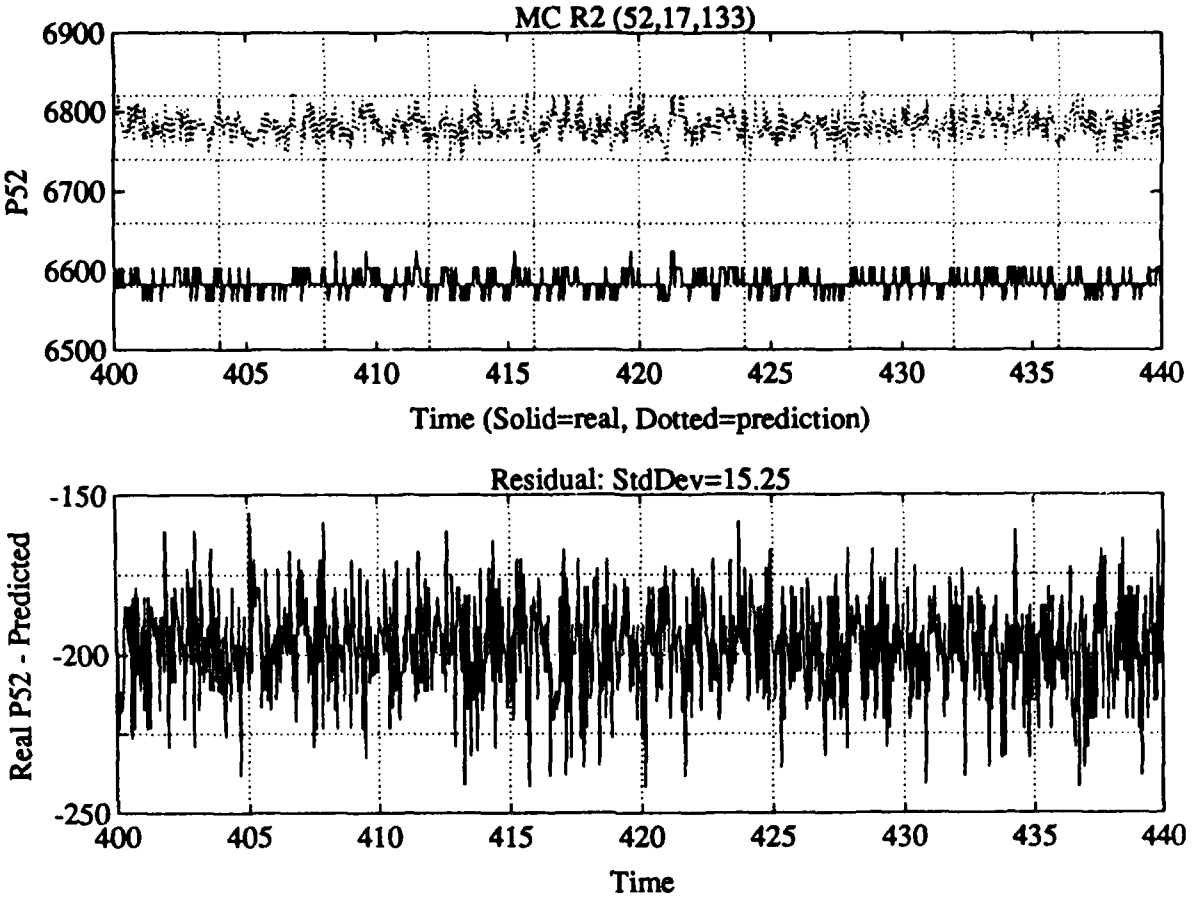

Family / Steady-State

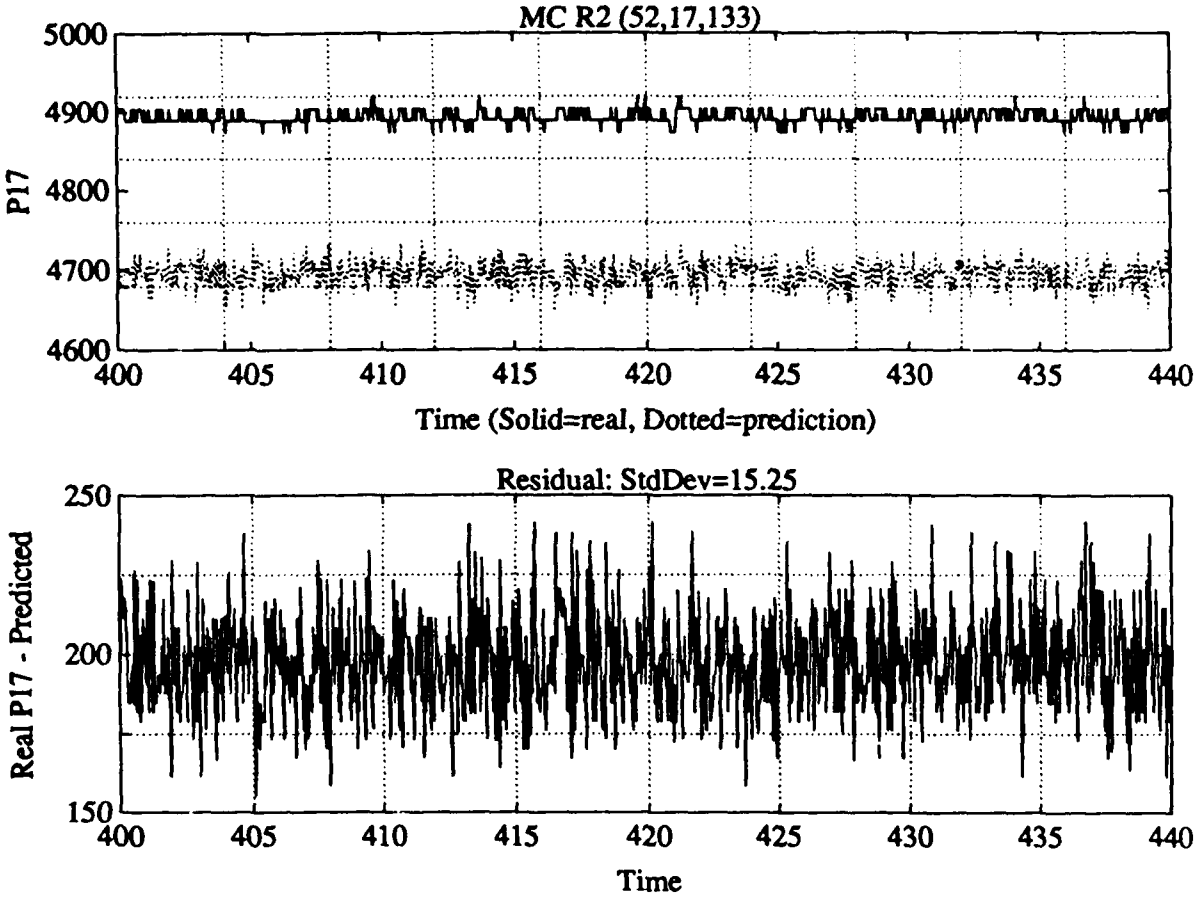

Family / steady-state

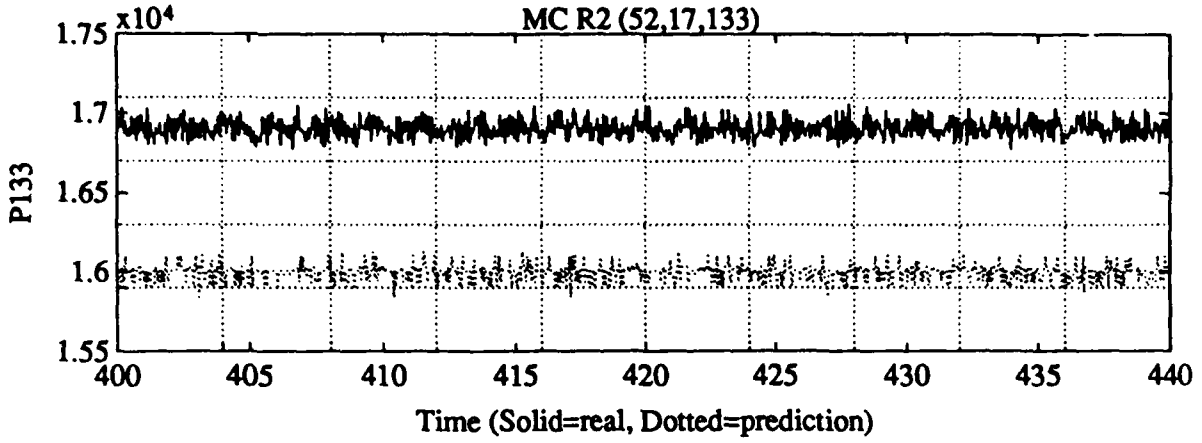
MC R2 (52,17,133)
x10^4
1.75
1.7
1.65
1.6
1.55
P133
400
405
410
415
420
425
430
435
440
Time (Solid=real, Dotted=prediction)

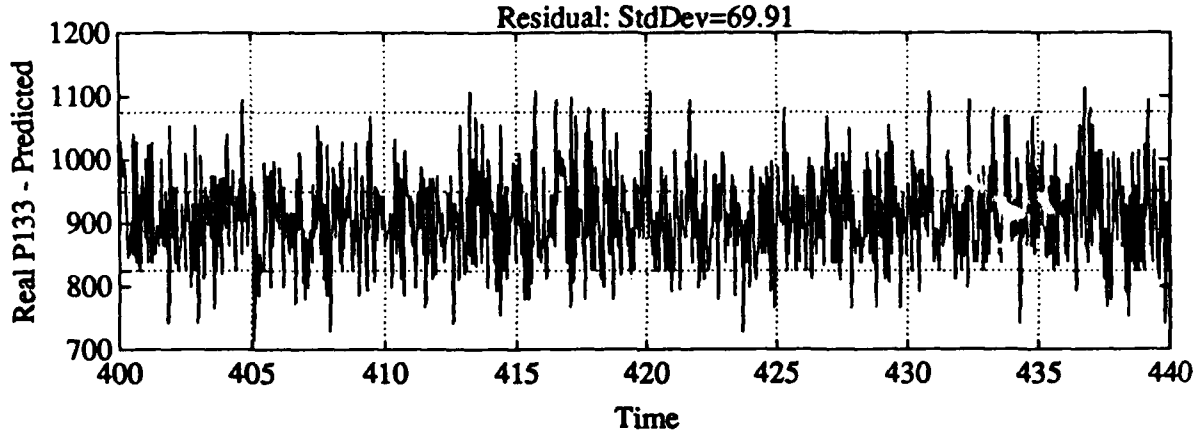
Residual: StdDev=69.91
1200
1100
1000
900
800
700
Real P133 - Predicted
400
405
410
415
420
425
430
435
440
Time

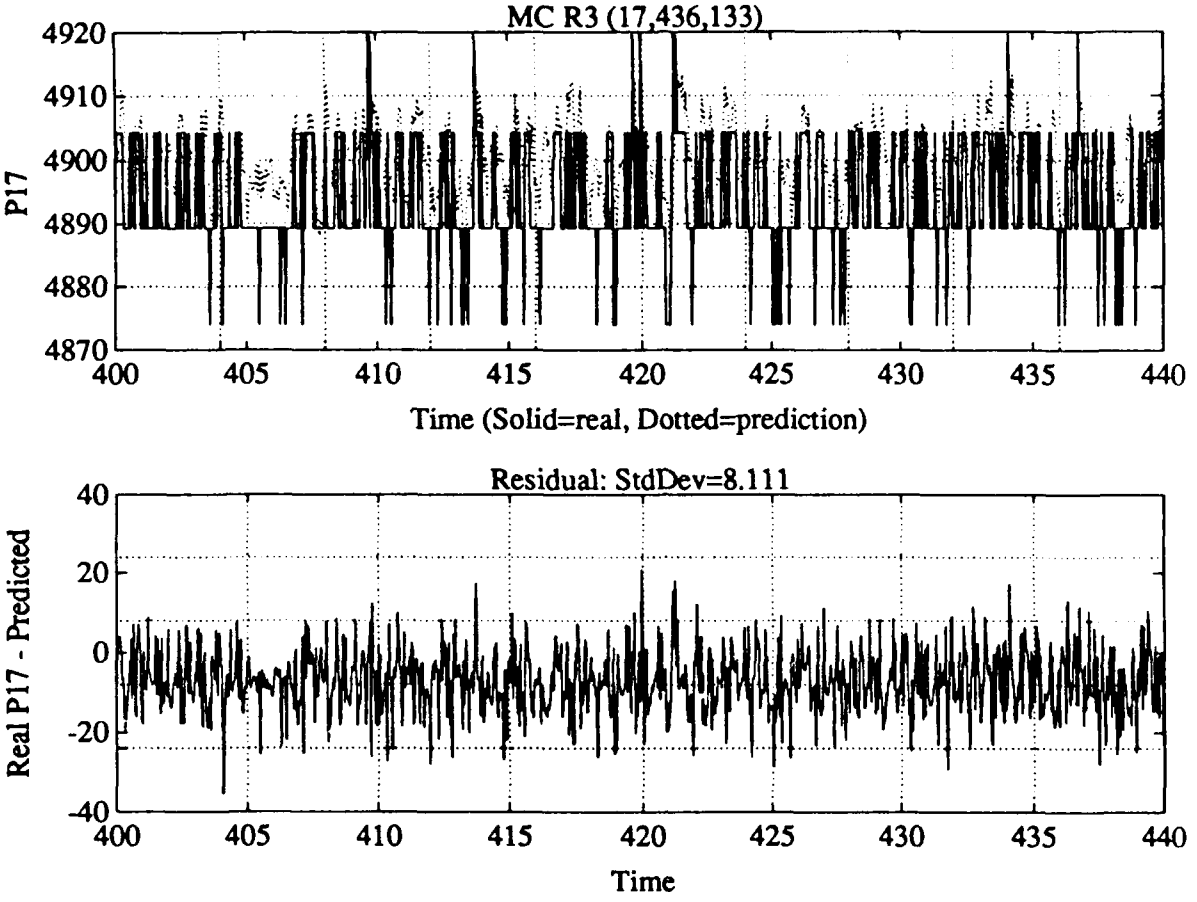

Family/Steady State

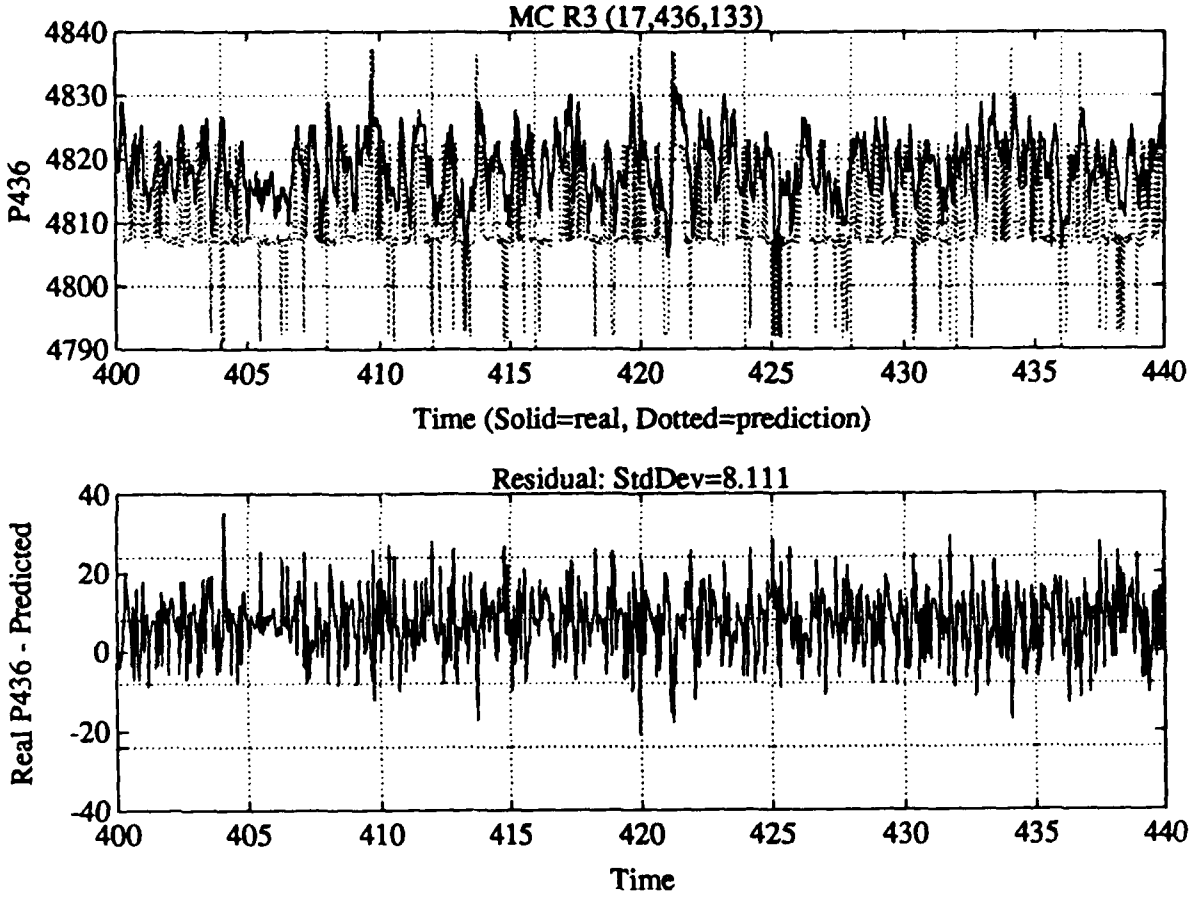

Family / Steady-State

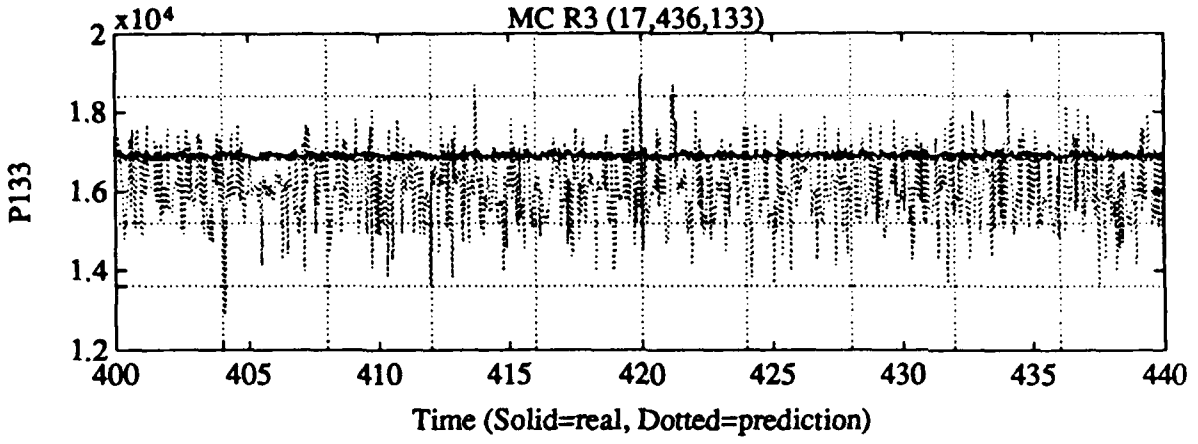
MC R3 (17,436,133)
x10^4
2
1.8
1.6
1.4
1.2
P133
400
405
410
415
420
425
430
435
440
Time (Solid=real, Dotted=prediction)

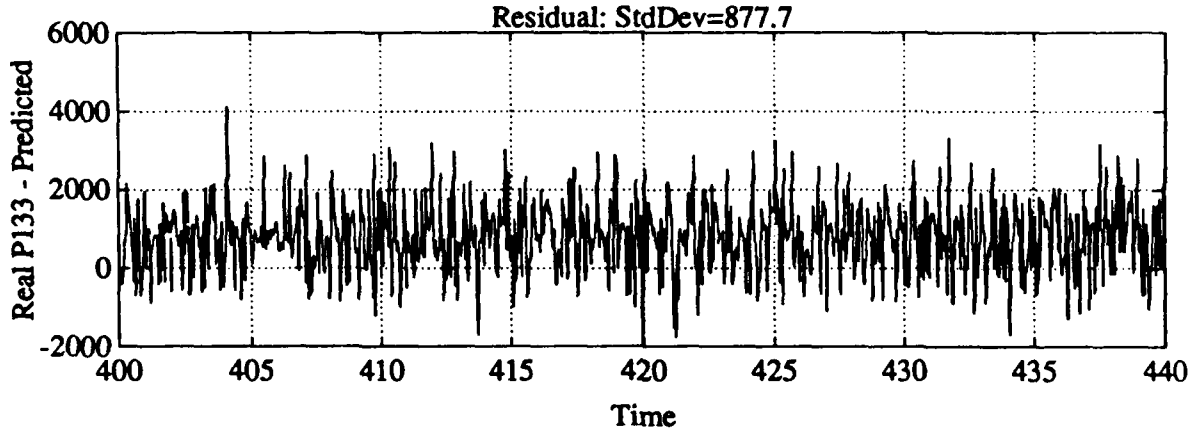
Residual: StdDev=877.7
6000
4000
2000
0
-2000
Real P133 - Predicted
400
405
410
415
420
425
430
435
440
Time

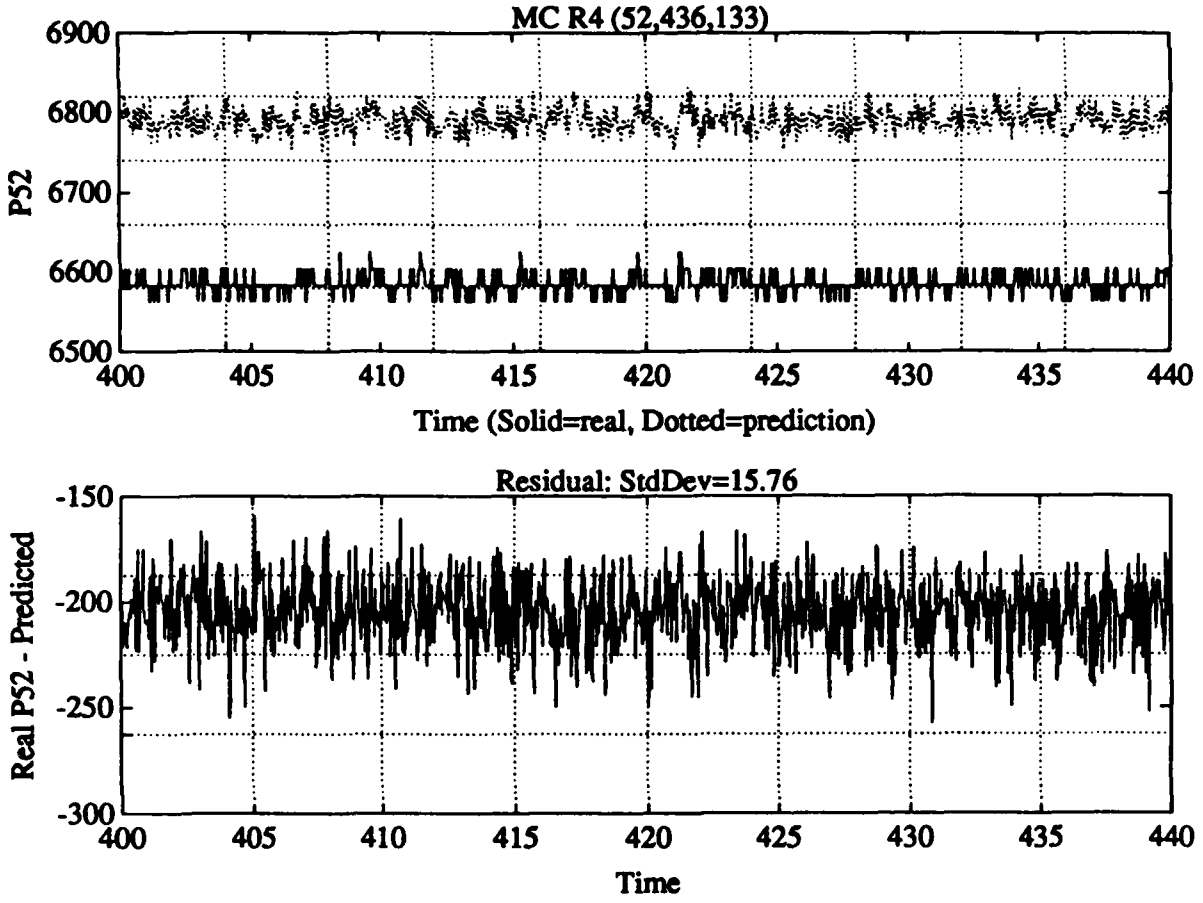
MC R4 (52,436,133)
P52
6900
6800
6700
6600
6500
400
405
410
415
420
425
430
435
440
Time (Solid=real, Dotted=prediction)
Residual: StdDev=15.76
Real P52 - Predicted
-150
-200
-250
-300
Time

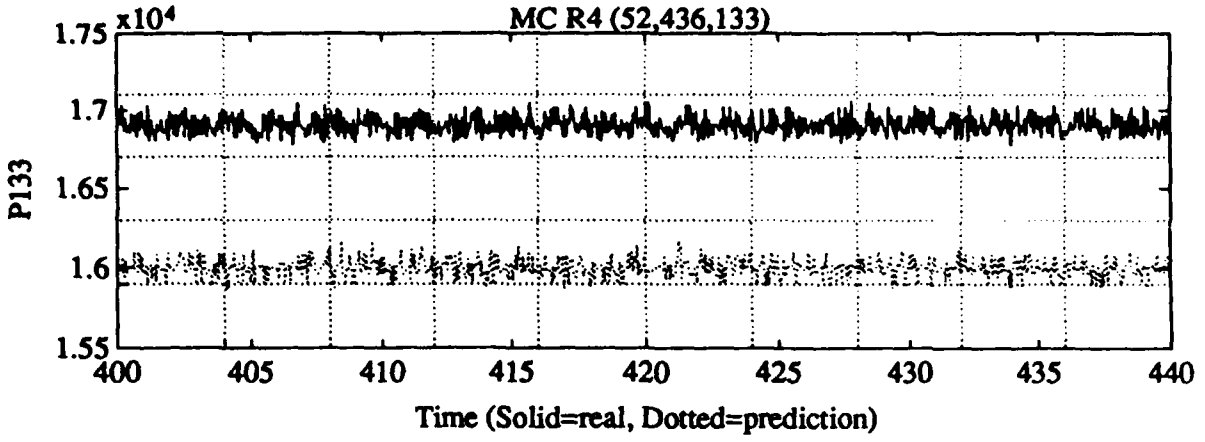
MC R4 (52,436,133)
x10^4
1.75
1.7
1.65
1.6
1.55
P133
400
405
410
415
420
425
430
435
440
Time (Solid=real, Dotted=prediction)

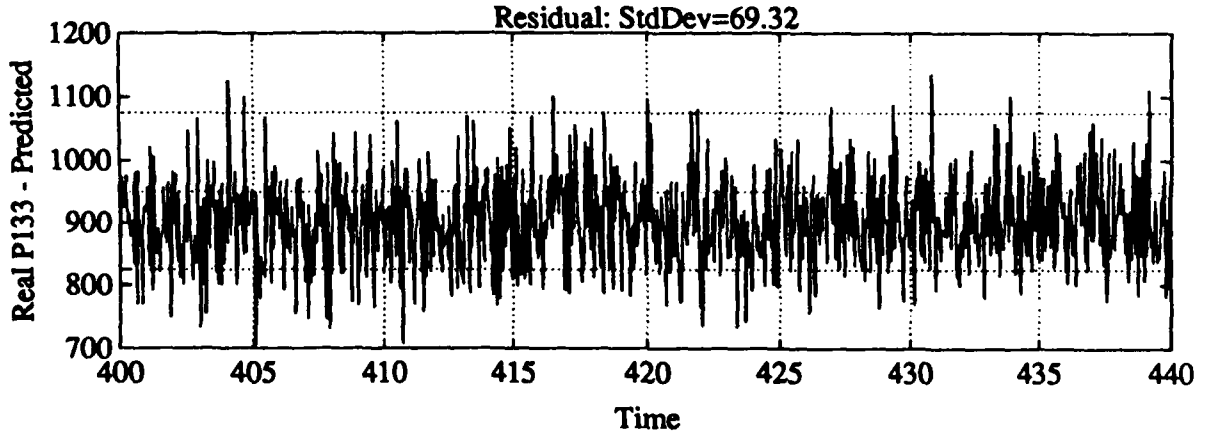
Residual: StdDev=69.32
1200
1100
1000
900
800
700
Real P133 - Predicted
400
405
410
415
420
425
430
435
440
Time

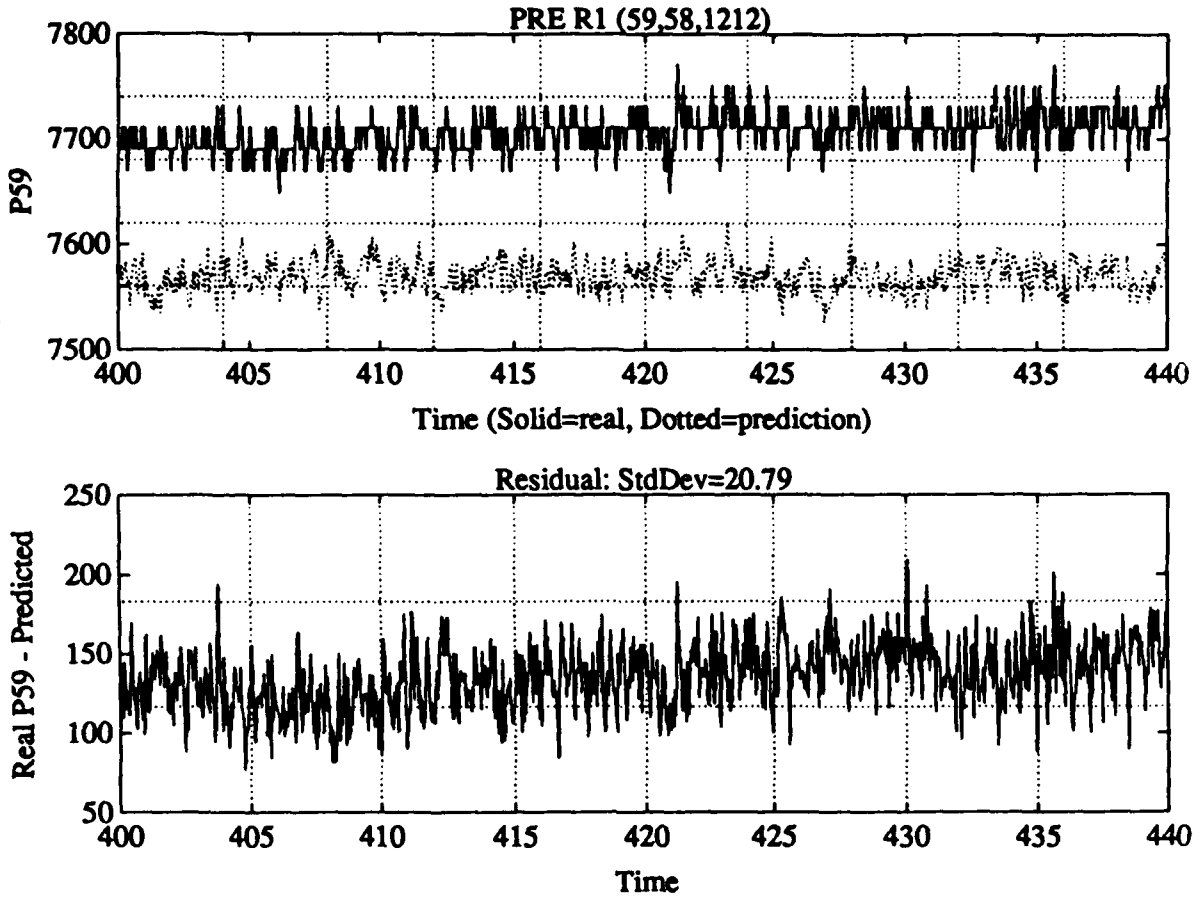
PRE R1 (59,58,1212)
7800
7700
7600
7500
P59
400
405
410
415
420
425
430
435
440
Time (Solid=real, Dotted=prediction)
Residual: StdDev=20.79
250
200
150
100
50
Real P59 - Predicted
400
405
410
415
420
425
430
435
440
Time

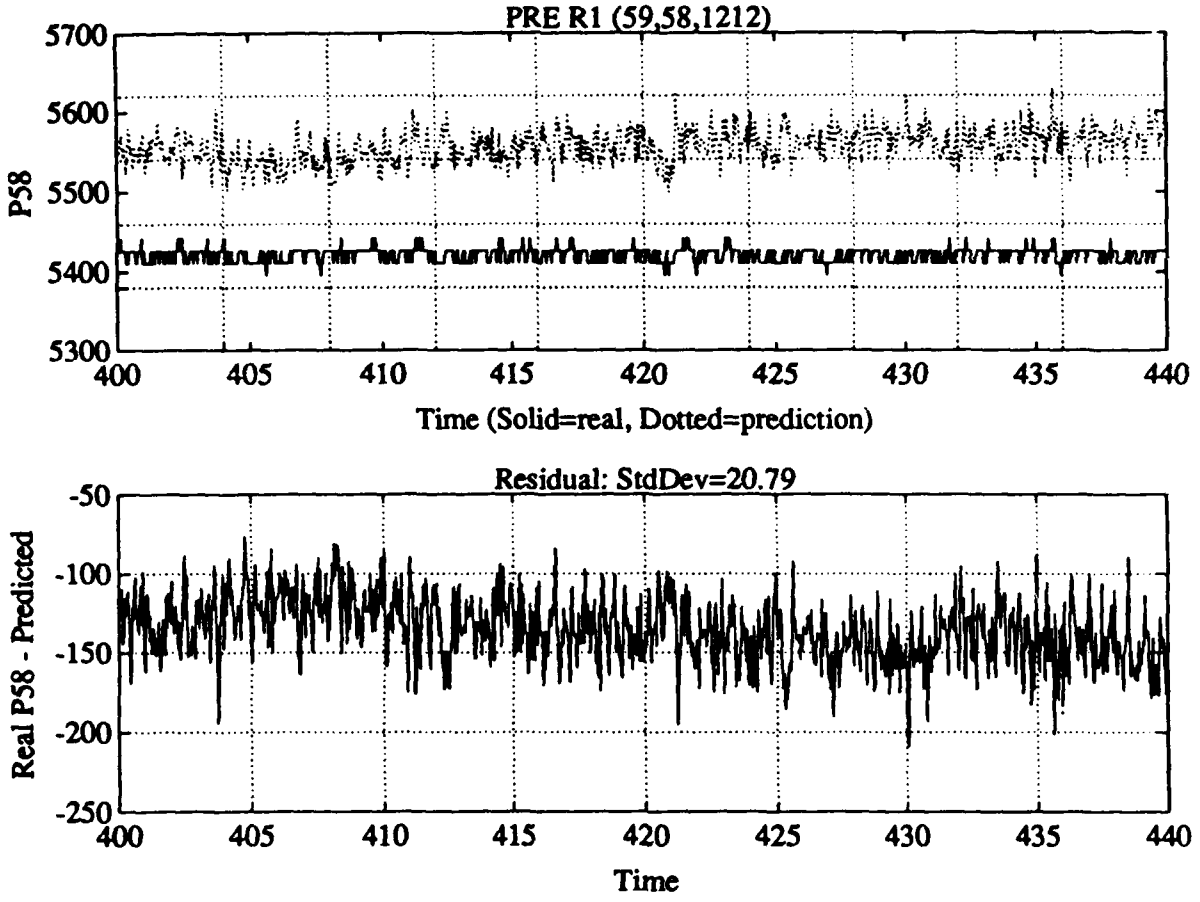
PRE R1 (59,58,1212)
P58
5700
5600
5500
5400
5300
400
405
410
415
420
425
430
435
440
Time (Solid=real, Dotted=prediction)
Residual: StdDev=20.79
Real P58 - Predicted
-50
-100
-150
-200
-250
400
405
410
415
420
425
430
435
440
Time

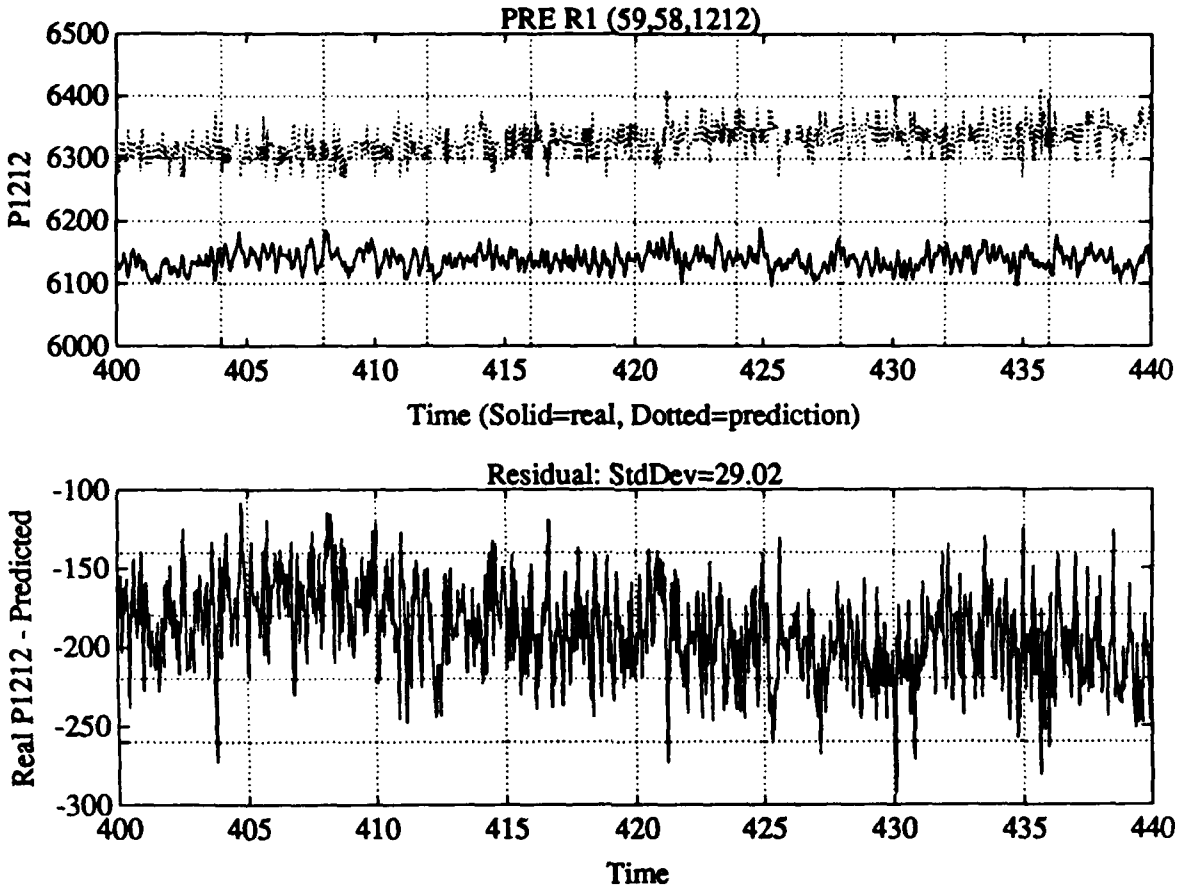
PRE R1 (59,58,1212)
P1212
6500
6400
6300
6200
6100
6000
400
405
410
415
420
425
430
435
440
Time (Solid=real, Dotted=prediction)

Residual: StdDev=29.02
Real P1212 - Predicted
-100
-150
-200
-250
-300
400
405
410
415
420
425
430
435
440
Time

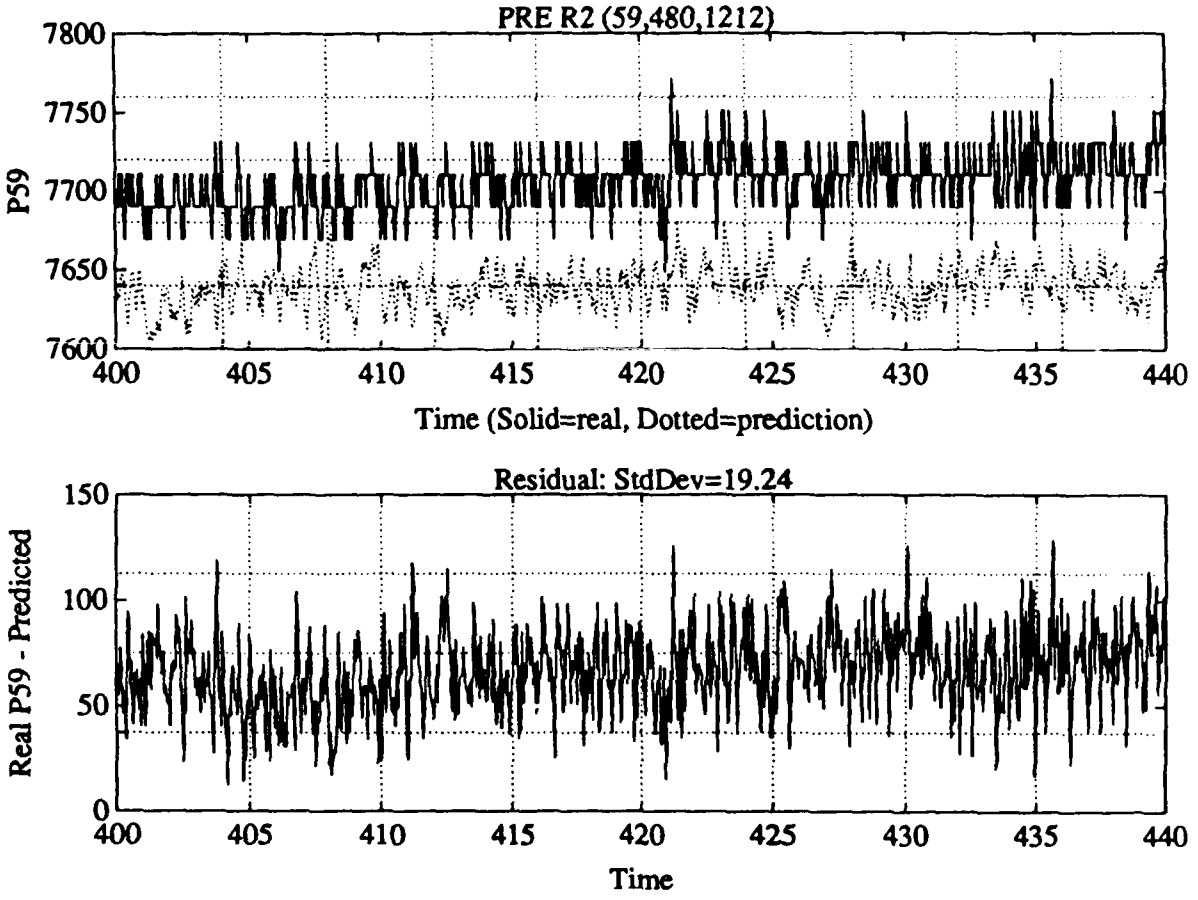
PRE R2 (59,480,1212)
P59
7800
7750
7700
7650
7600
400
405
410
415
420
425
430
435
440
Time (Solid=real, Dotted=prediction)
Residual: StdDev=19.24
Real P59 - Predicted
150
100
50
0
400
405
410
415
420
425
430
435
440
Time

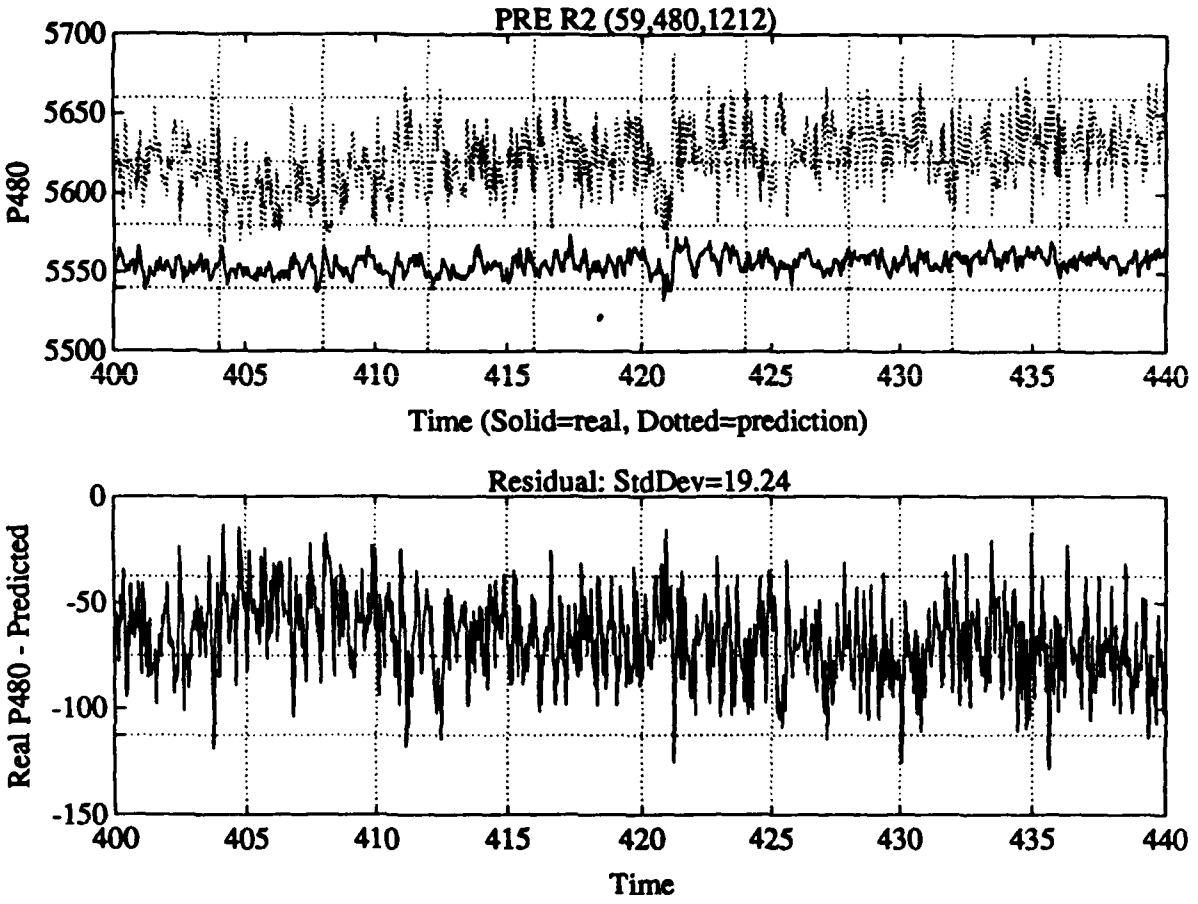
PRE R2 (59,480,1212)
P480
5700
5650
5600
5550
5500
400
405
410
415
420
425
430
435
440
Time (Solid=real, Dotted=prediction)
Residual: StdDev=19.24
Real P480 - Predicted
0
-50
-100
-150
Time

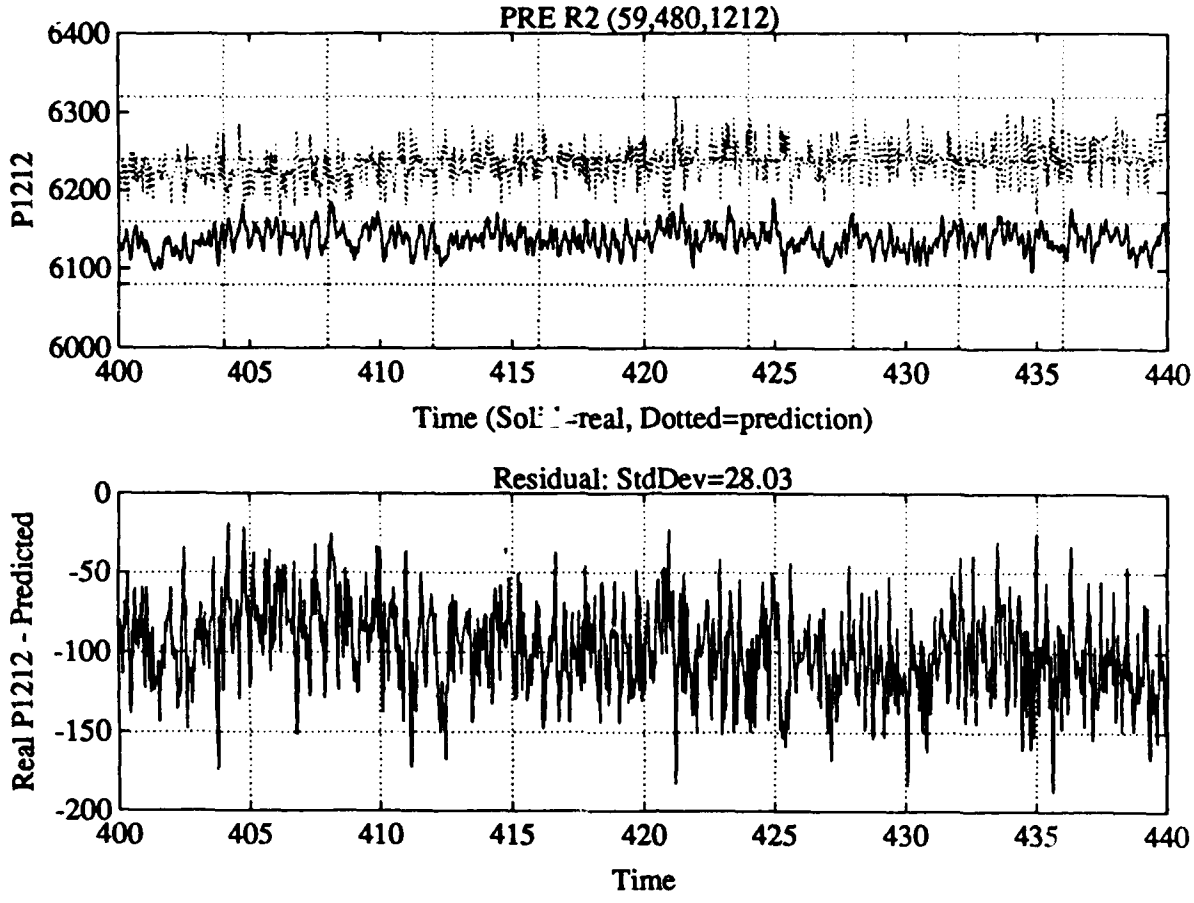
PRE R2 (59,480,1212)
P1212
6400
6300
6200
6100
6000
400
405
410
415
420
425
430
435
440
Time (Sol: -real, Dotted=prediction)
Residual: StdDev=28.03
Real P1212 - Predicted
0
-50
-100
-150
-200
Time

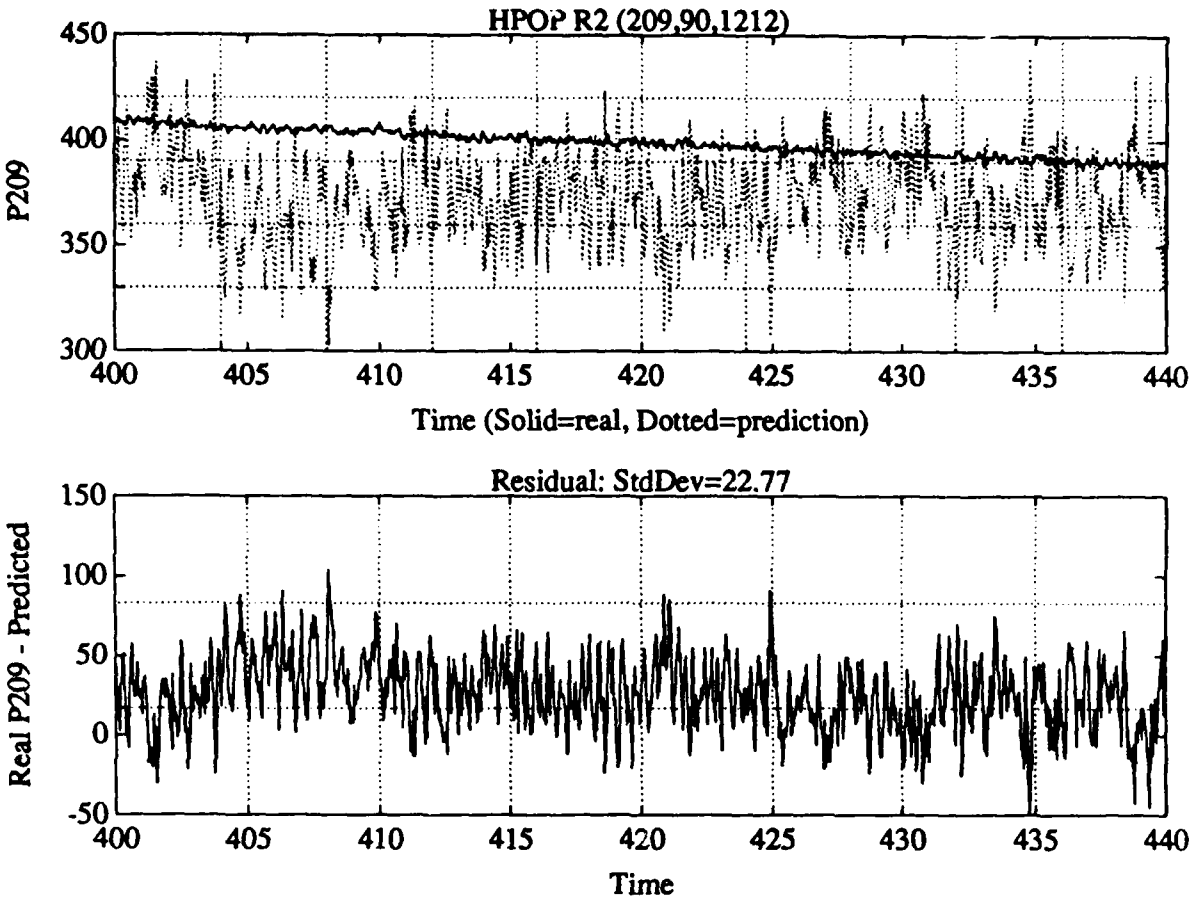
HPOP R2 (209,90,1212)
P209
450
400
350
300
400
405
410
415
420
425
430
435
440
Time (Solid=real, Dotted=prediction)
Residual: StdDev=22.77
Real P209 - Predicted
150
100
50
0
-50
400
405
410
415
420
425
430
435
440
Time

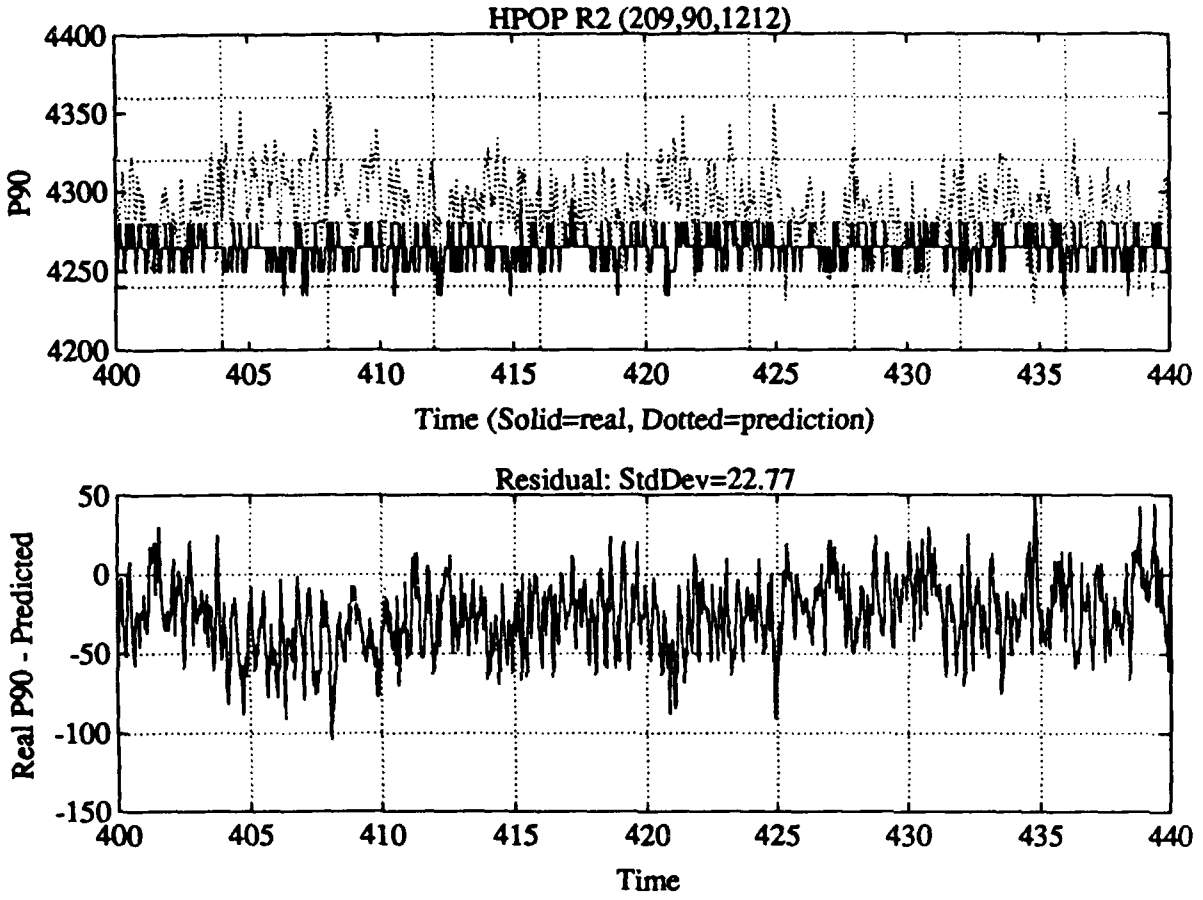
HPOP R2 (209,90,1212)
P90
4400
4350
4300
4250
4200
400
405
410
415
420
425
430
435
440
Time (Solid=real, Dotted=prediction)
Residual: StdDev=22.77
Real P90 - Predicted
50
0
-50
-100
-150
400
405
410
415
420
425
430
435
440
Time

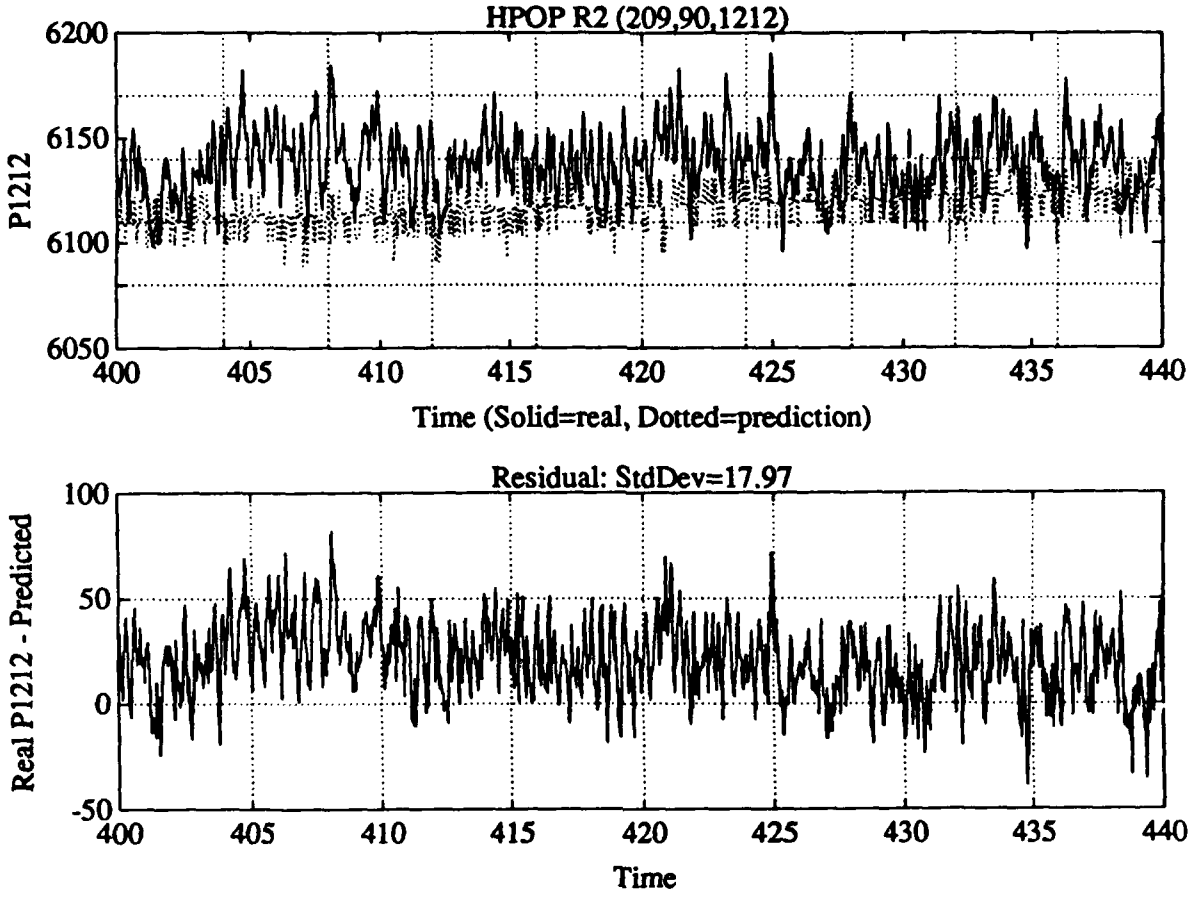
HPOP R2 (209,90,1212)
P1212
6200
6150
6100
6050
400
405
410
415
420
425
430
435
440
Time (Solid=real, Dotted=prediction)
Residual: StdDev=17.97
Real P1212 - Predicted
100
50
0
-50
400
405
410
415
420
425
430
435
440
Time

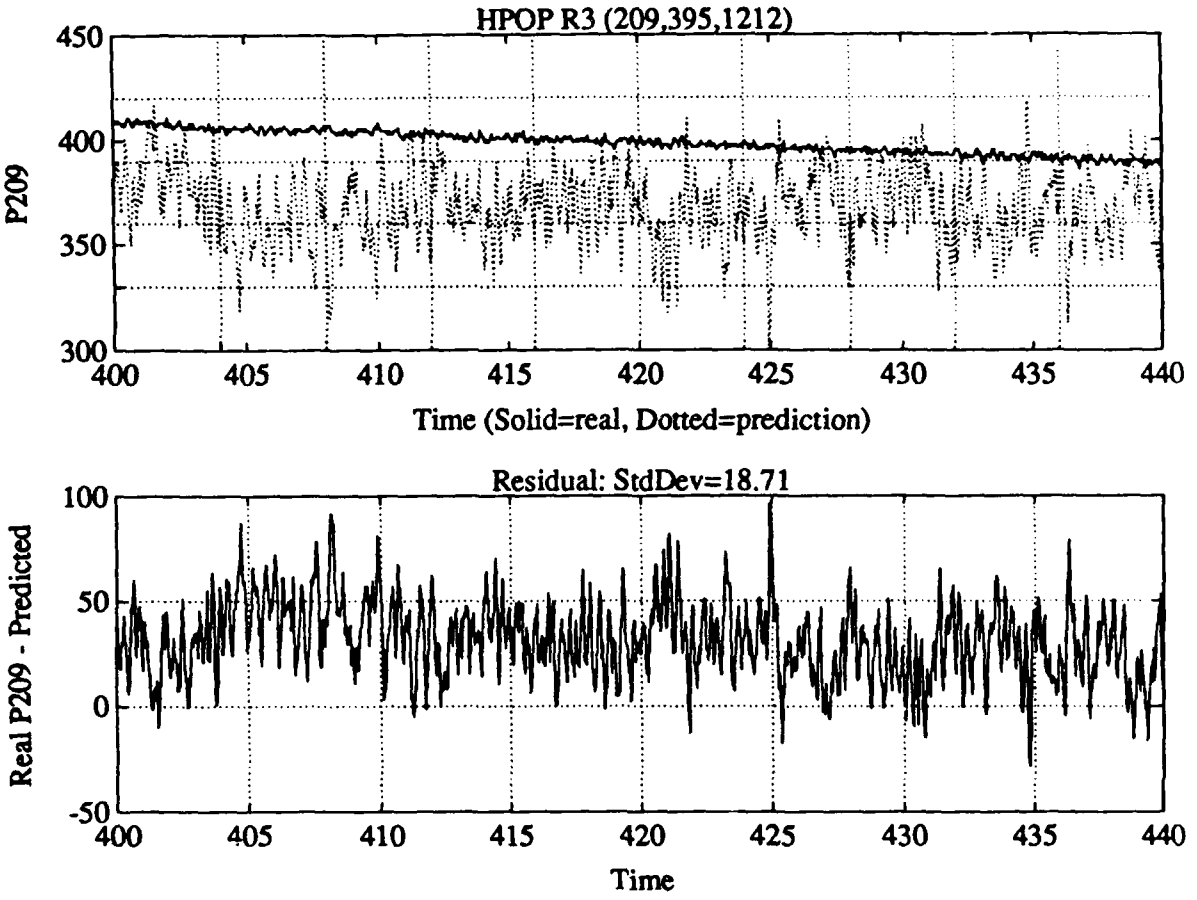
HPOP R3 (209,395,1212)
P209
450
400
350
300
400
405
410
415
420
425
430
435
440
Time (Solid=real, Dotted=prediction)
Residual: StdDev=18.71
Real P209 - Predicted
100
50
0
-50
400
405
410
415
420
425
430
435
440
Time

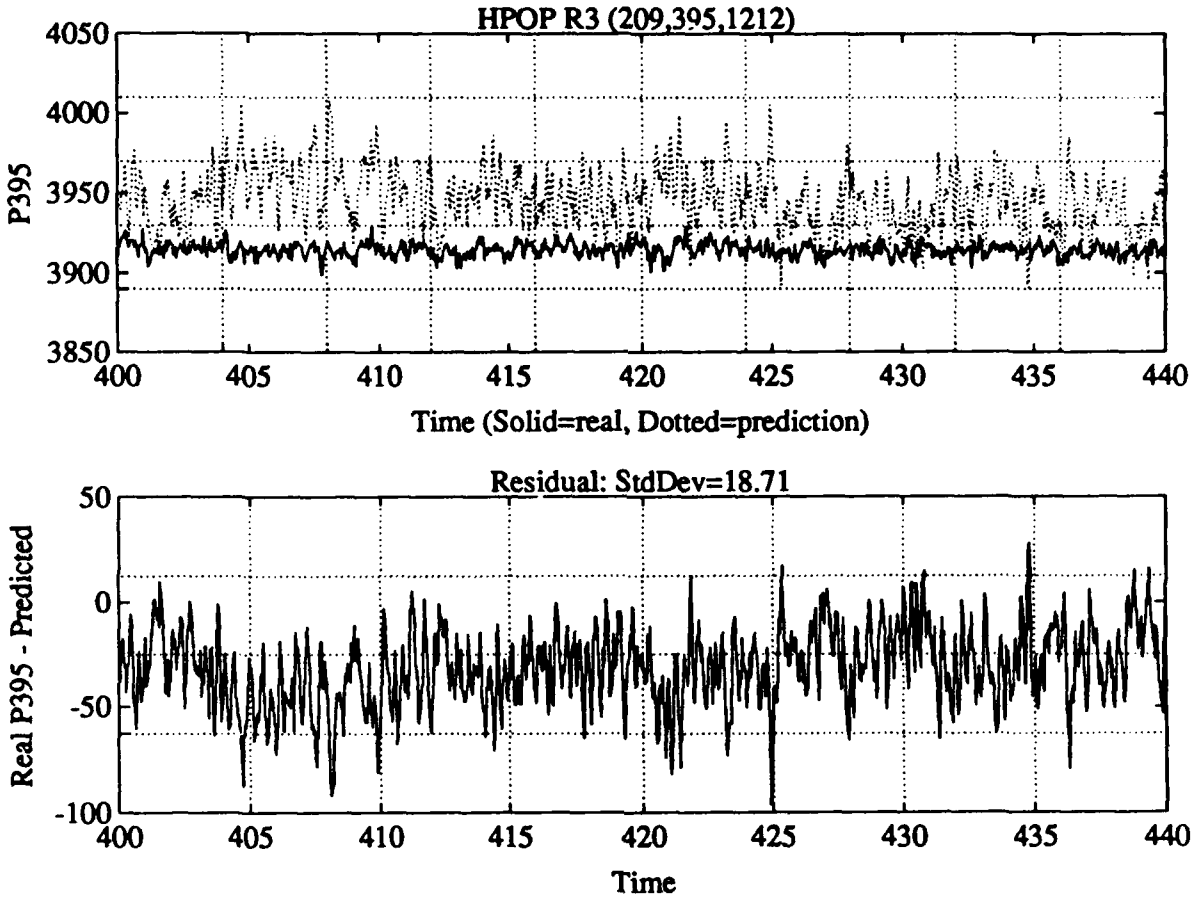
HPOP R3 (209,395,1212)
P395
4050
4000
3950
3900
3850
400
405
410
415
420
425
430
435
440
Time (Solid=real, Dotted=prediction)
Residual: StdDev=18.71
Real P395 - Predicted
50
0
-50
-100
Time

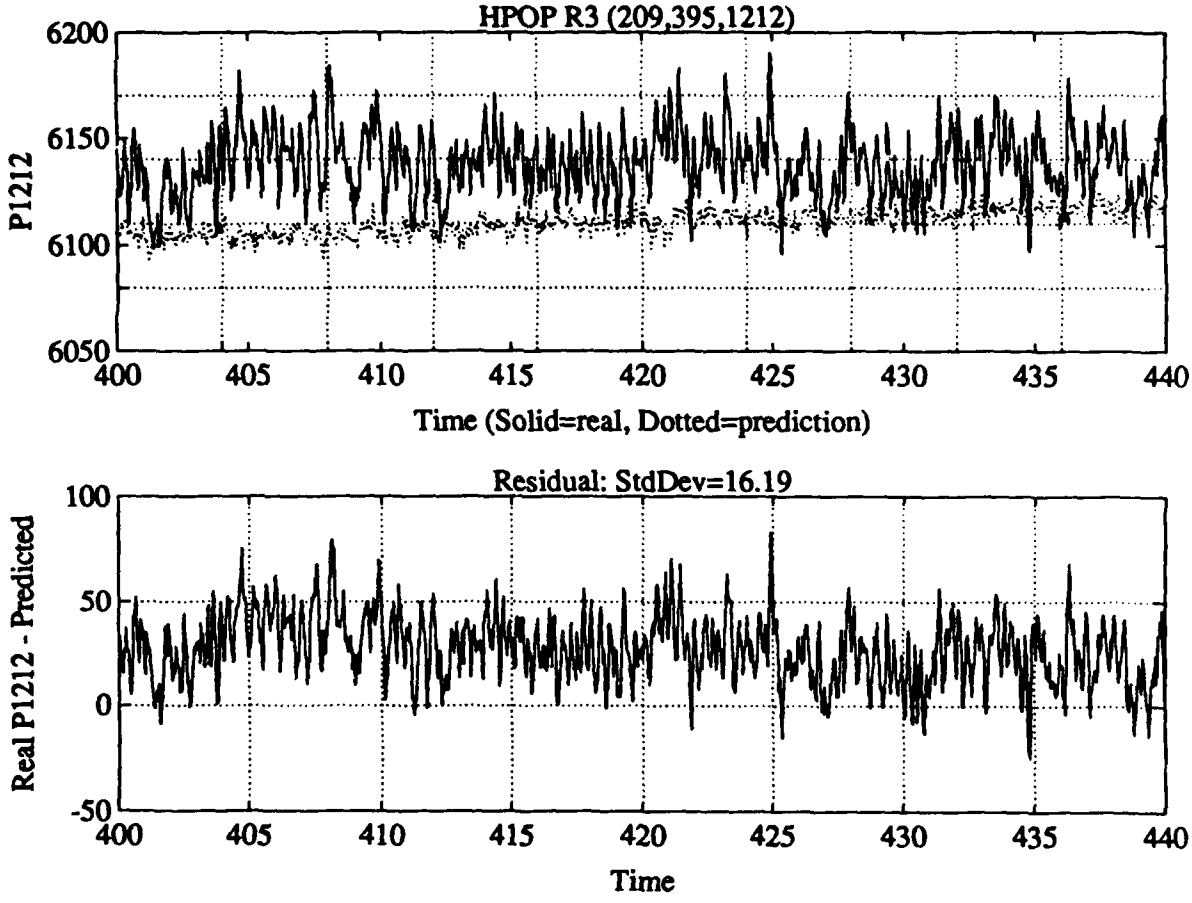
HPOP R3 (209,395,1212)
P1212
6200
6150
6100
6050
400
405
410
415
420
425
430
435
440
Time (Solid=real, Dotted=prediction)
Residual: StdDev=16.19
Real P1212 - Predicted
100
50
0
-50
400
405
410
415
420
425
430
435
440
Time

Results of characteristic equations using engine specific data

Test A2497

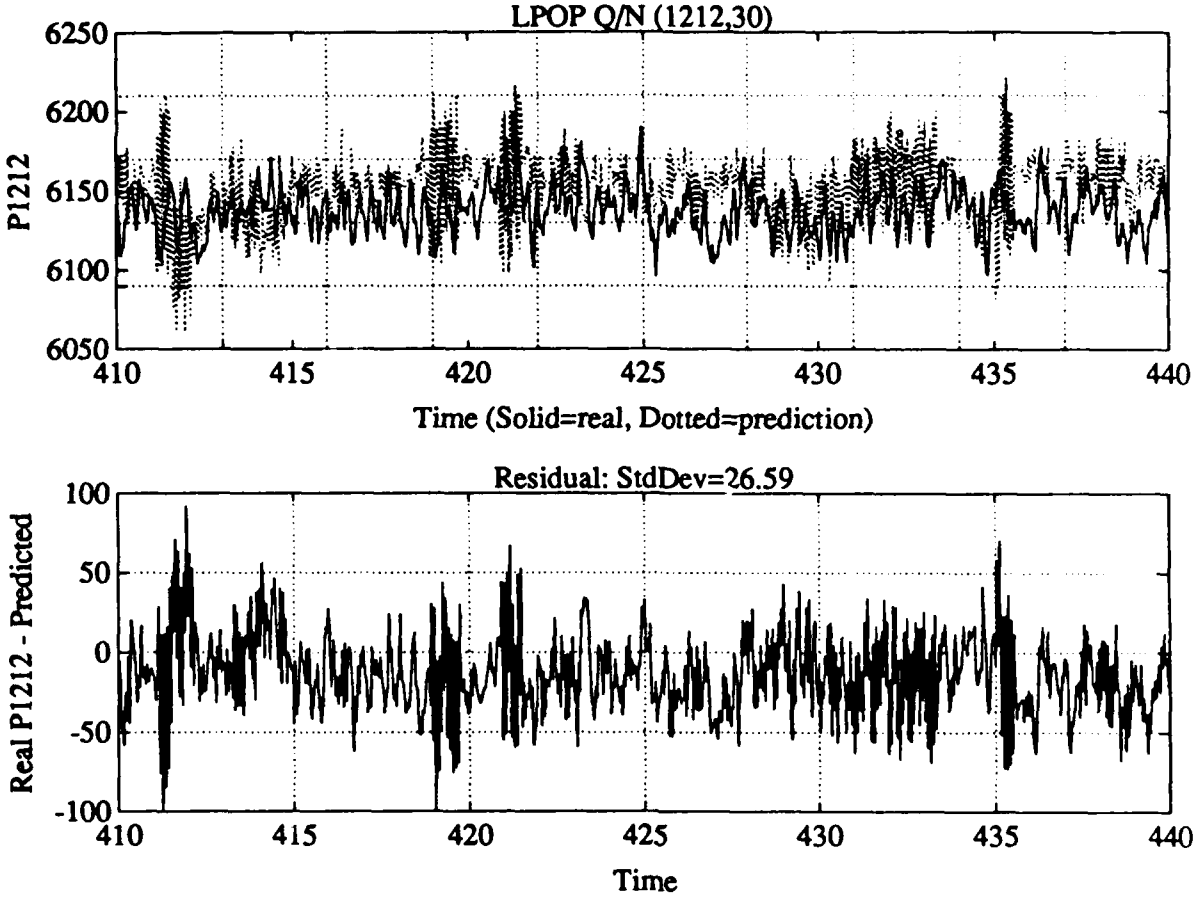

P1212 +/- 85

Prediction +/- 80

Best Possible +/- 68

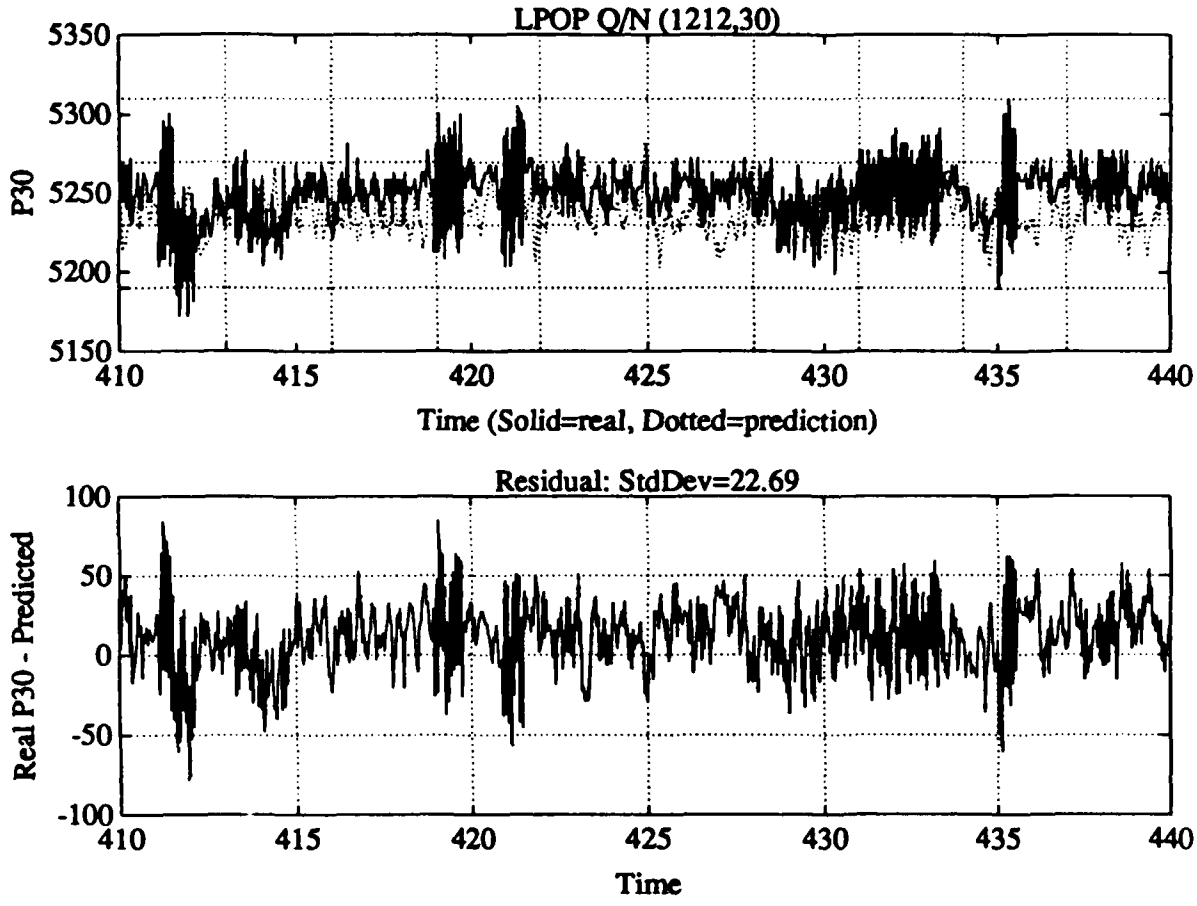

· P30 +/- 58.92

Prediction +/- 68.07

Best Possible +/- 50.4

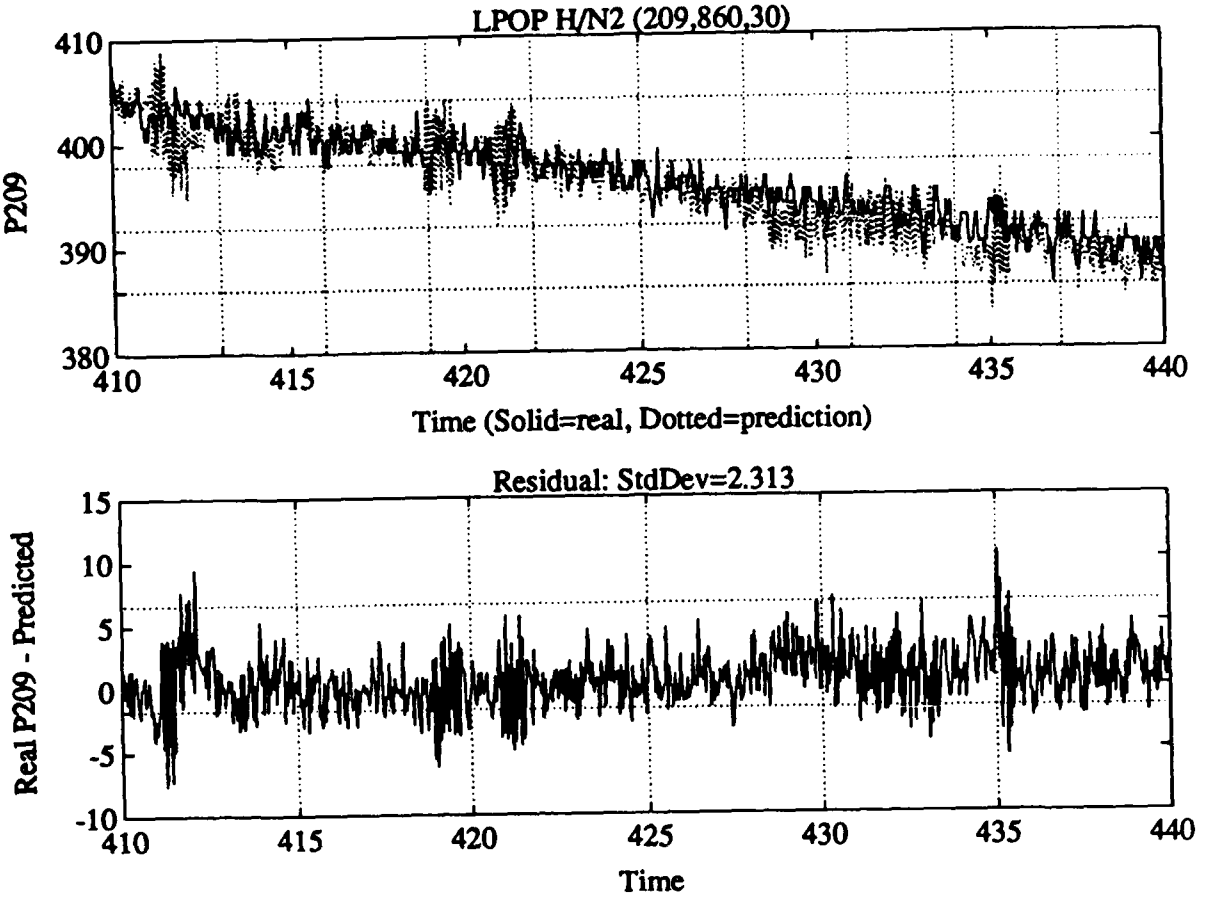

P209 +/- 12
Prediction +/- 6.9.

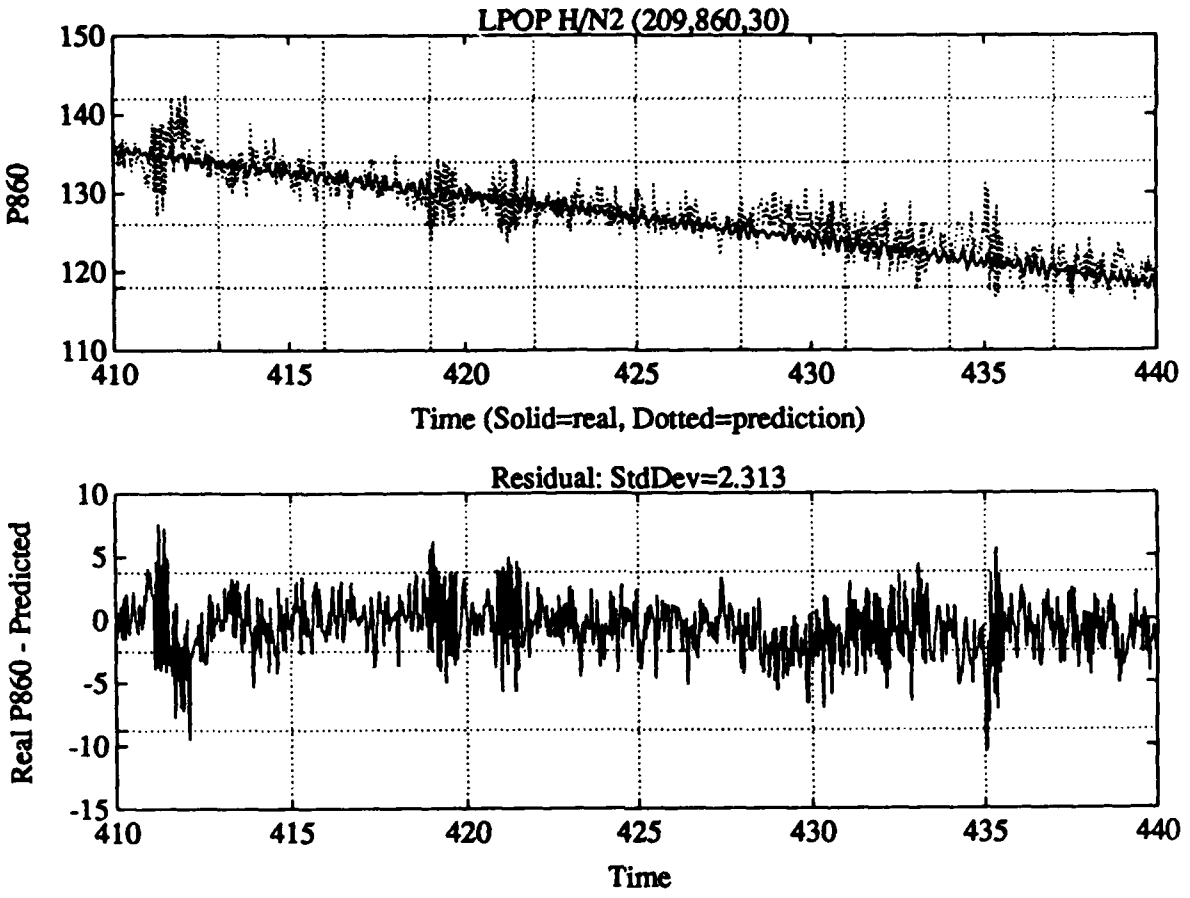

P860 +/- 5

Predictor +/- 6.9

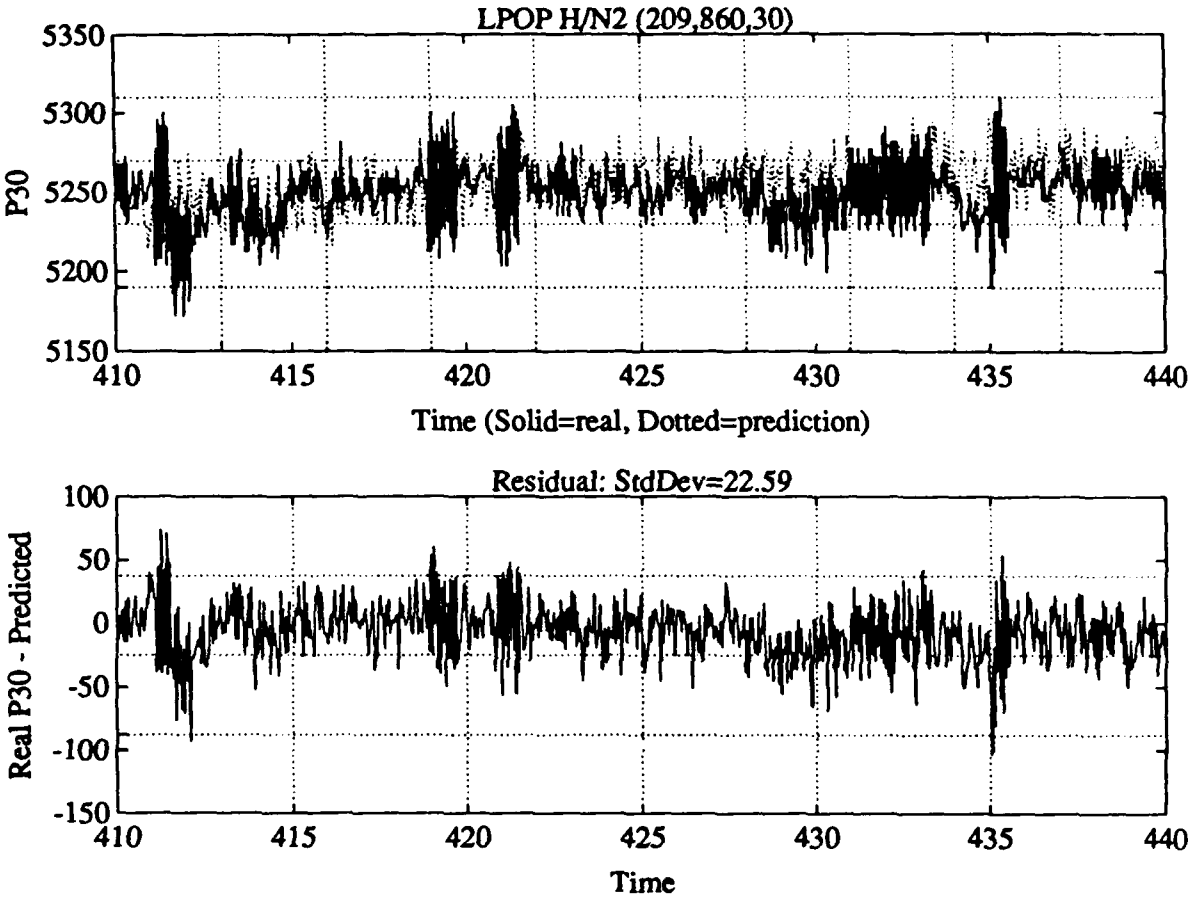

P30 +/- 58.92
Prediction +/- 67

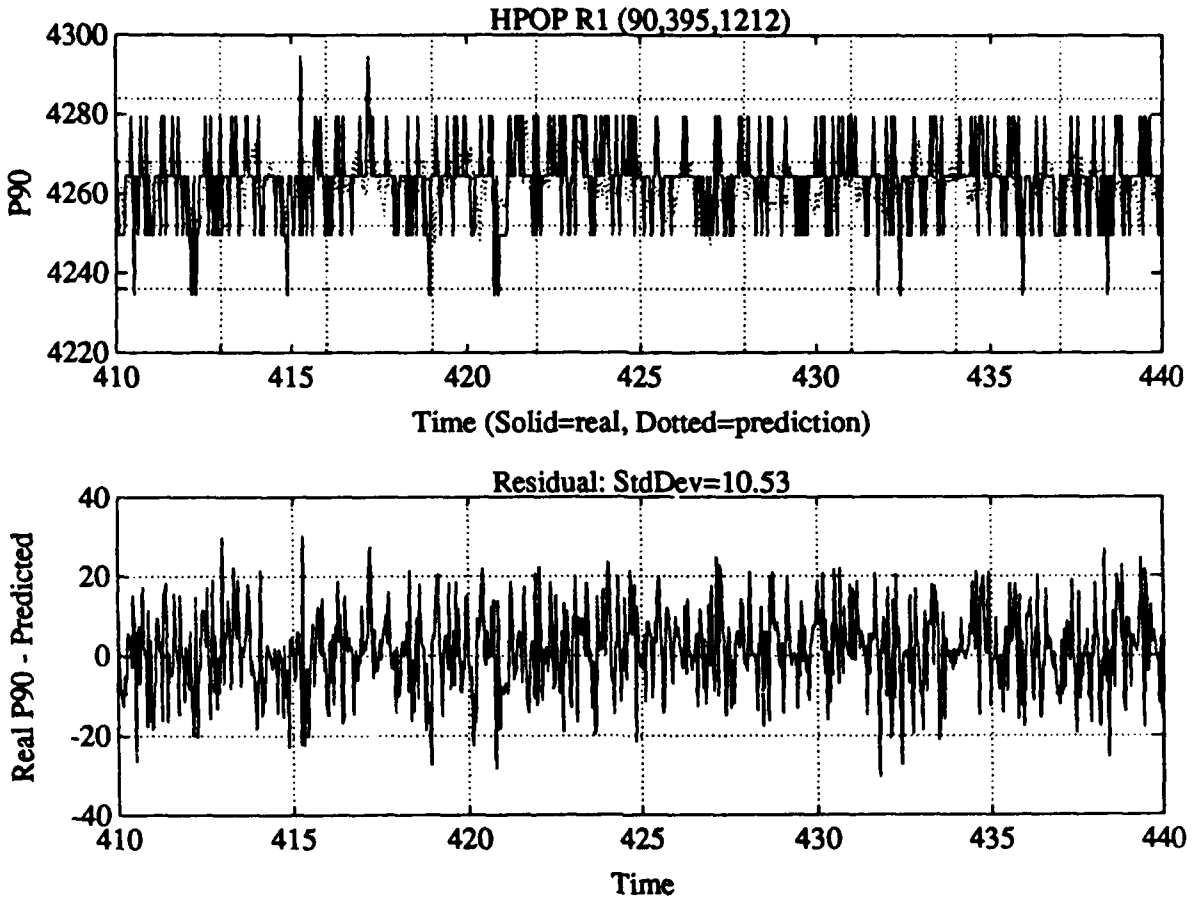

P90 +/- 140

Prediction +/- 31

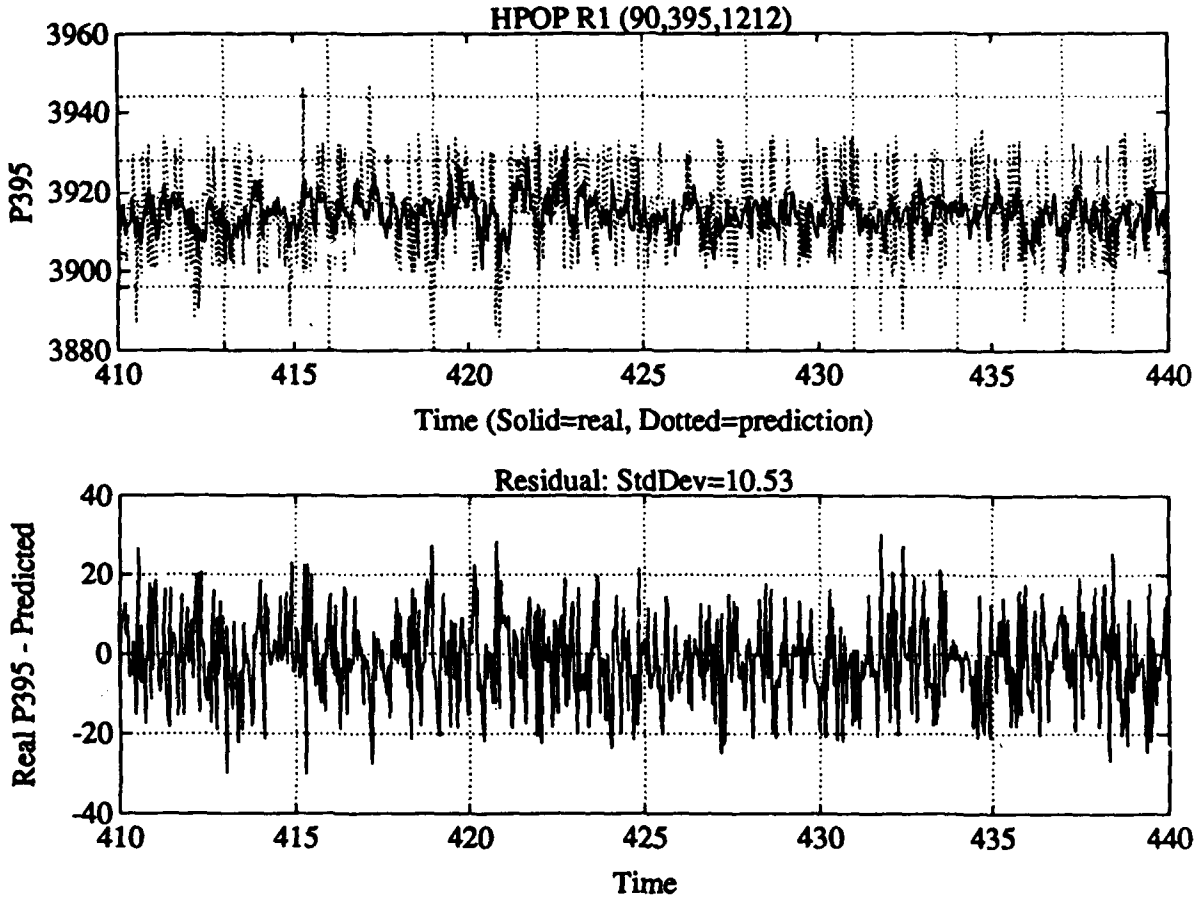

P395 +/- 25
Prediction +/- 31

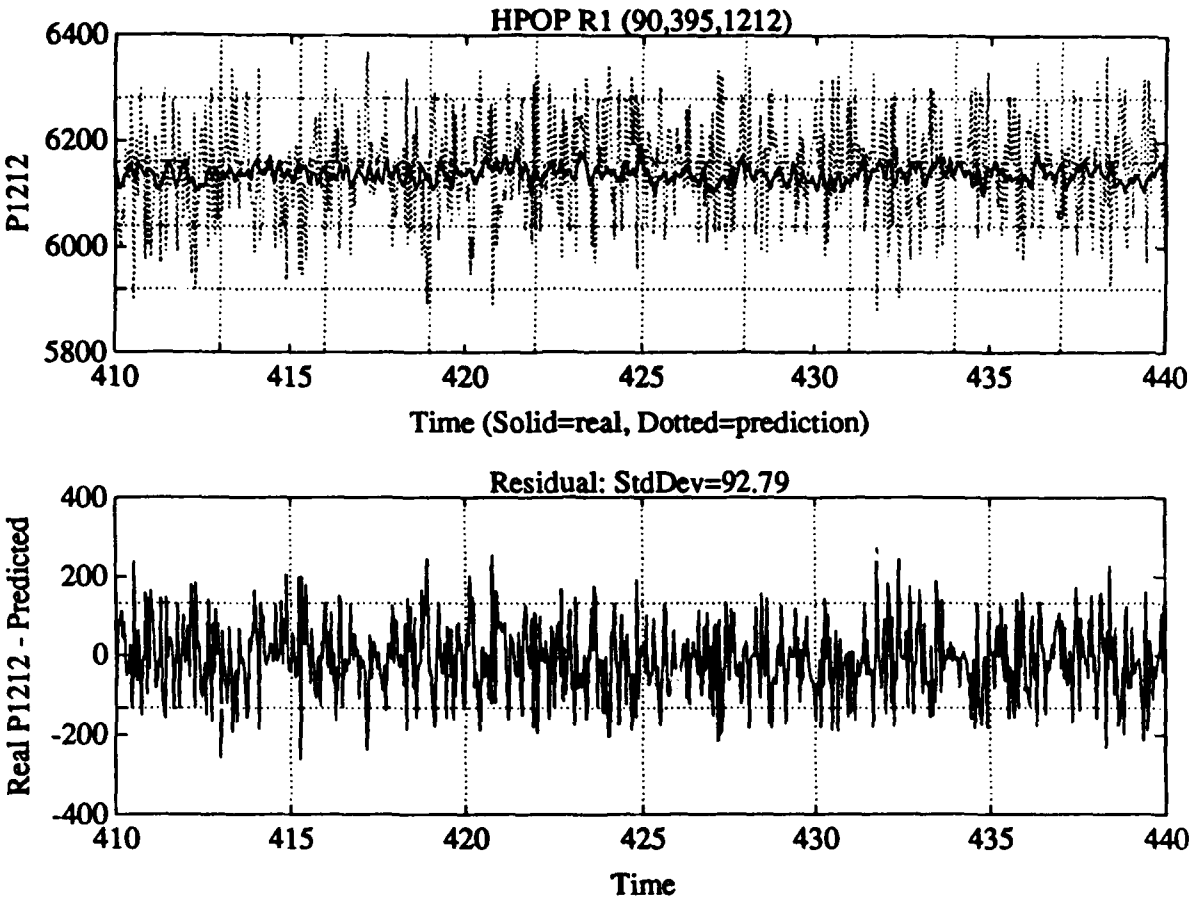

P1212 +/- 85
Prediction +/- 278

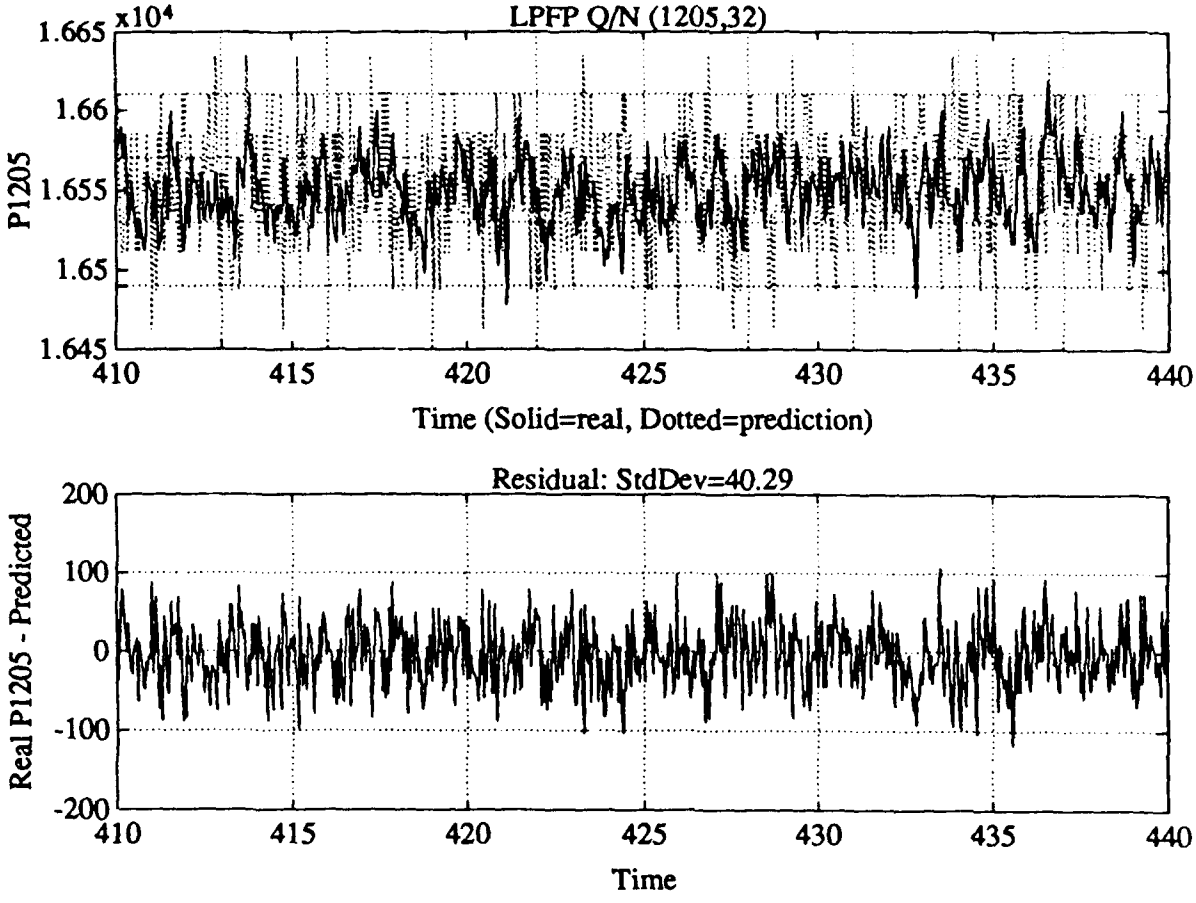

Fig 4.

P1205 +/- 220
Prediction +/- 120

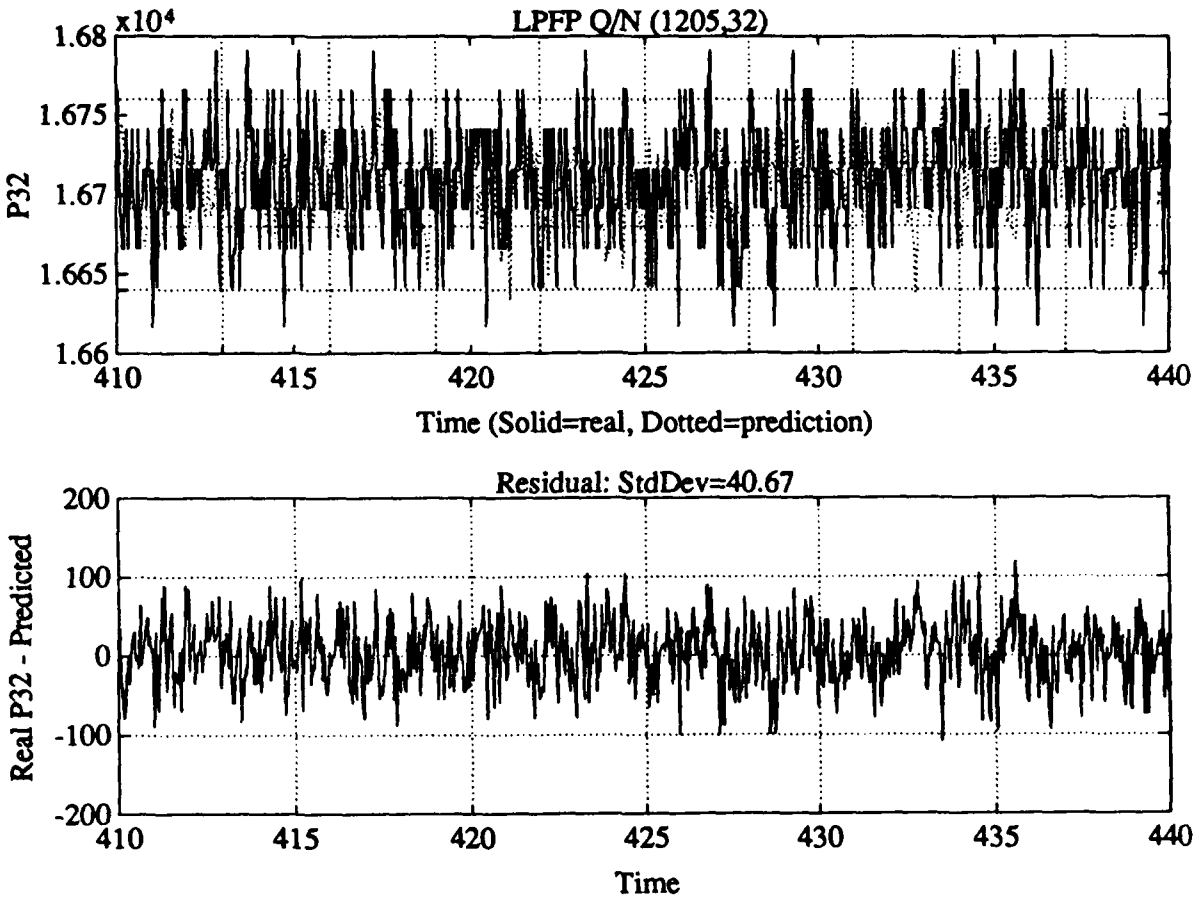

P32 +/- 198
Prediction +/- 121

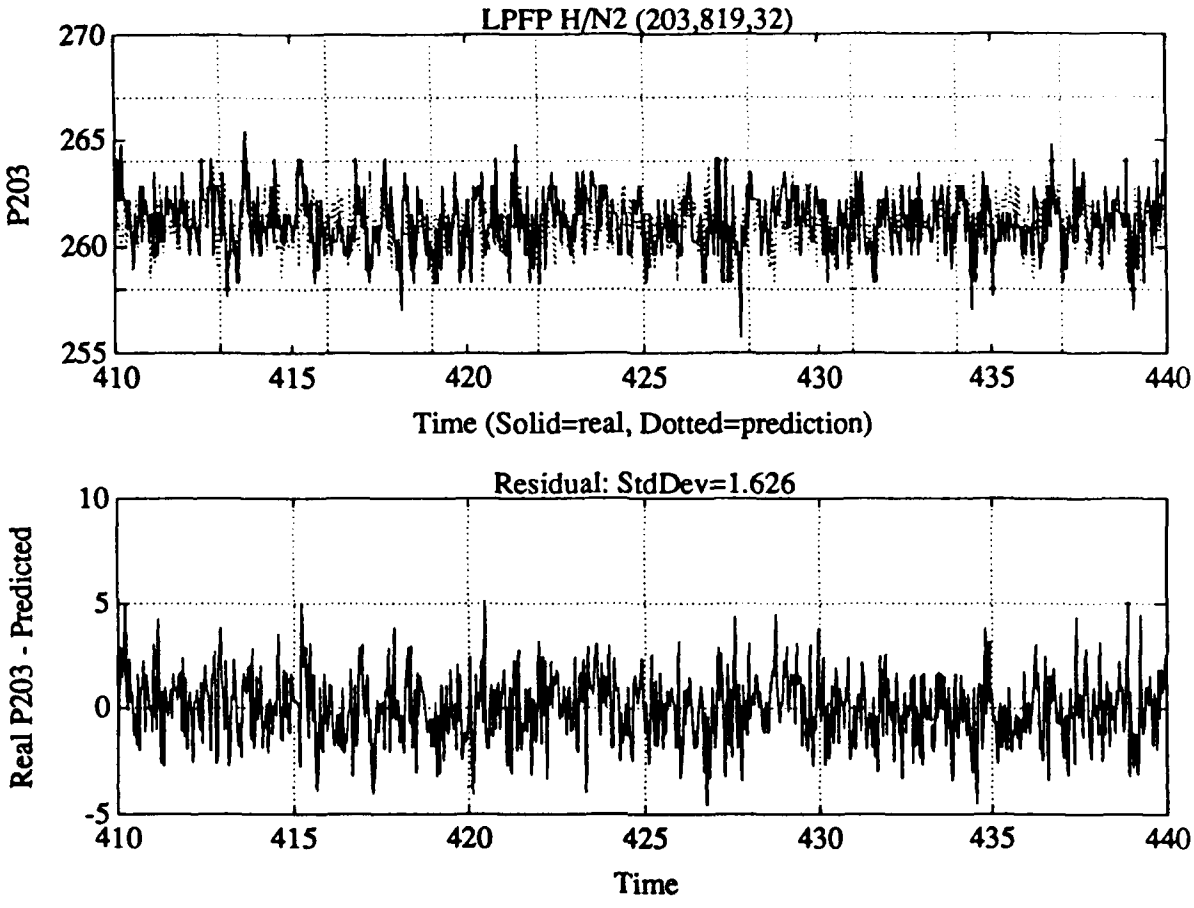

P203 +/- 6

Prediction +/- 4.8

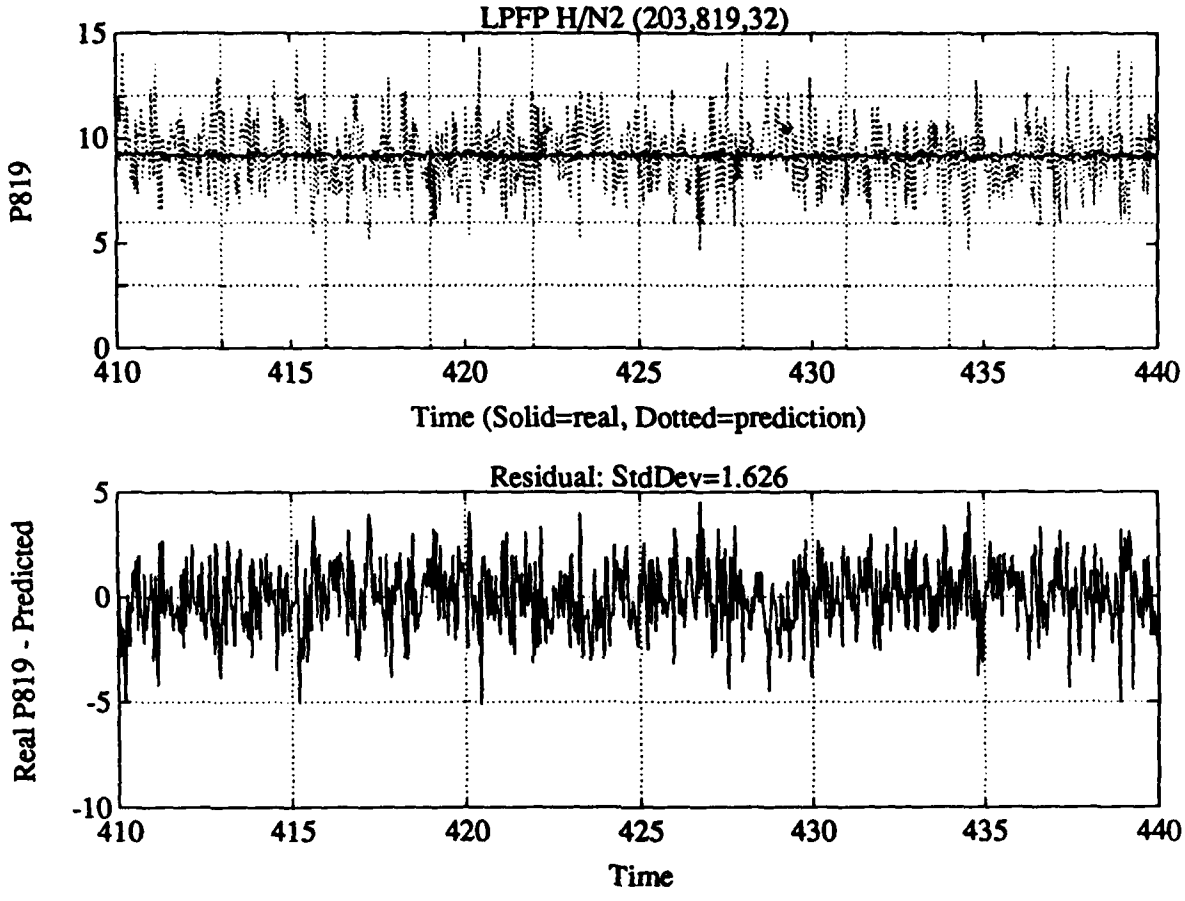

P819 +/- 2
Prediction +/- 4.8

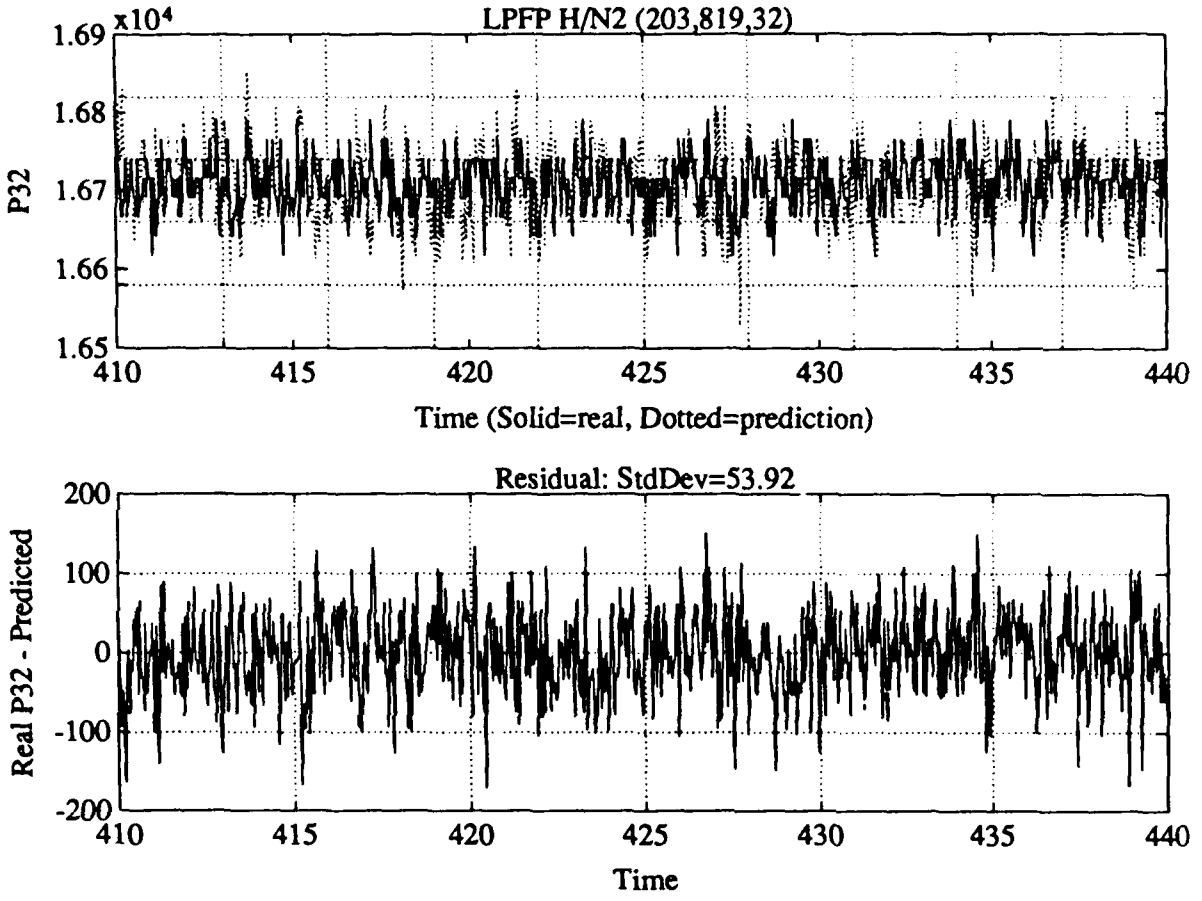

P32 +/- 198
Prediction +/- 162

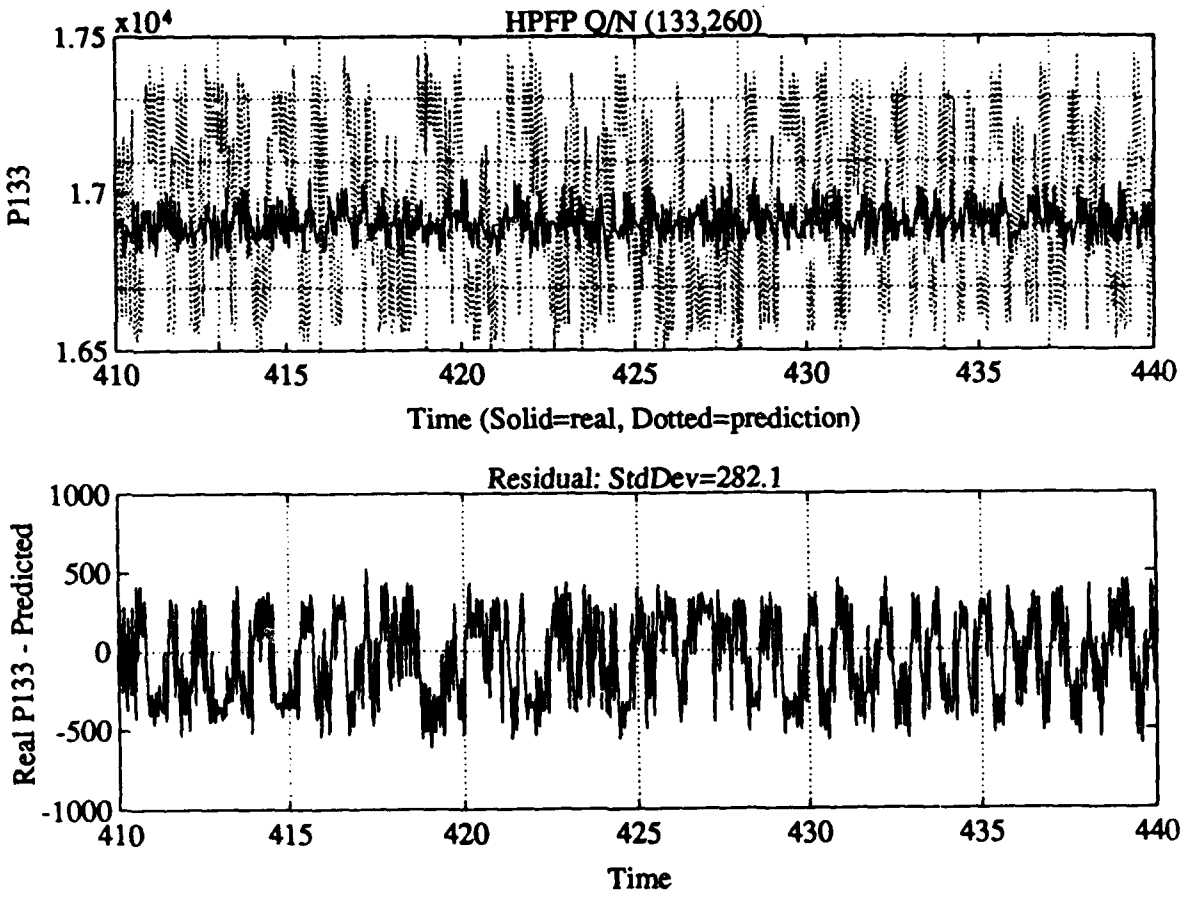

P133 +/- 169
Prediction +/- 846

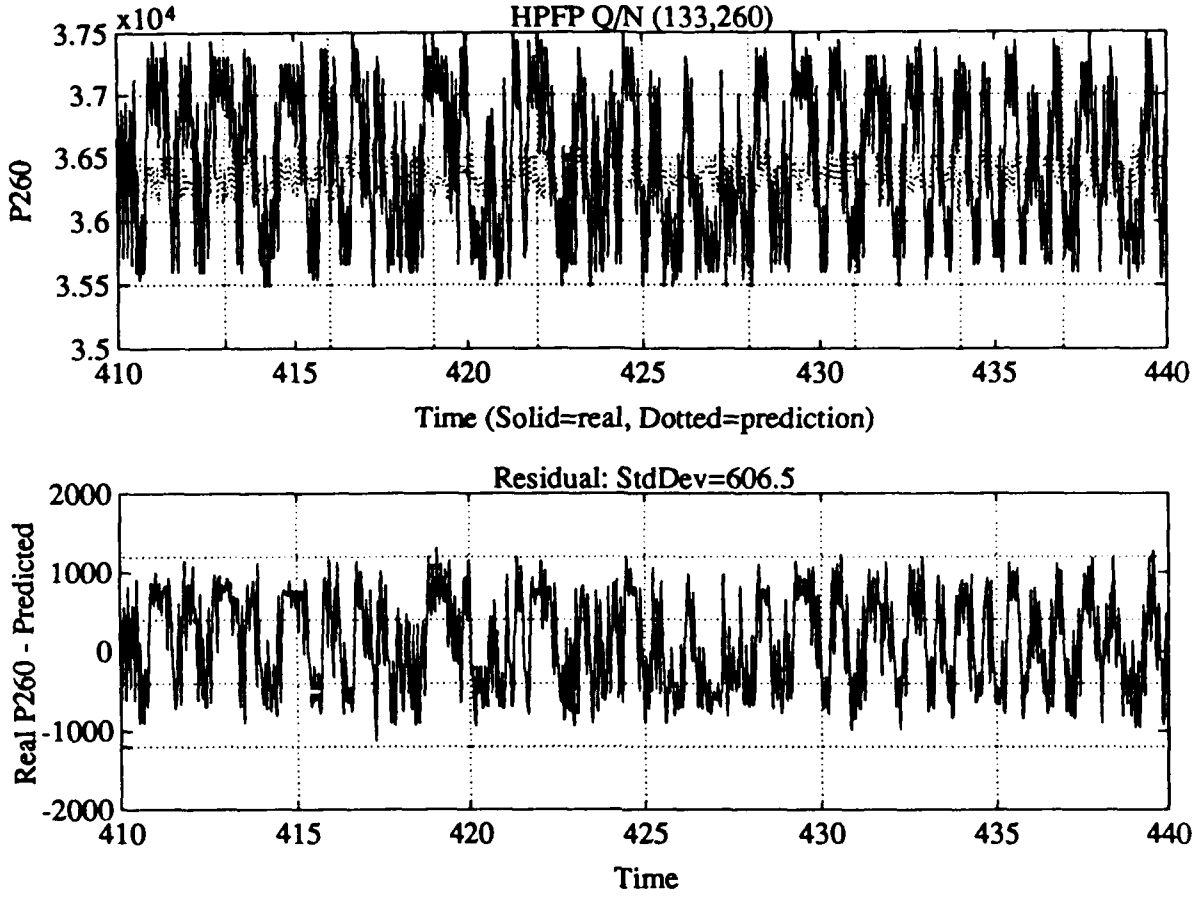

P260 +/- 31.5

~~P60~~

Prediction +/- 1819

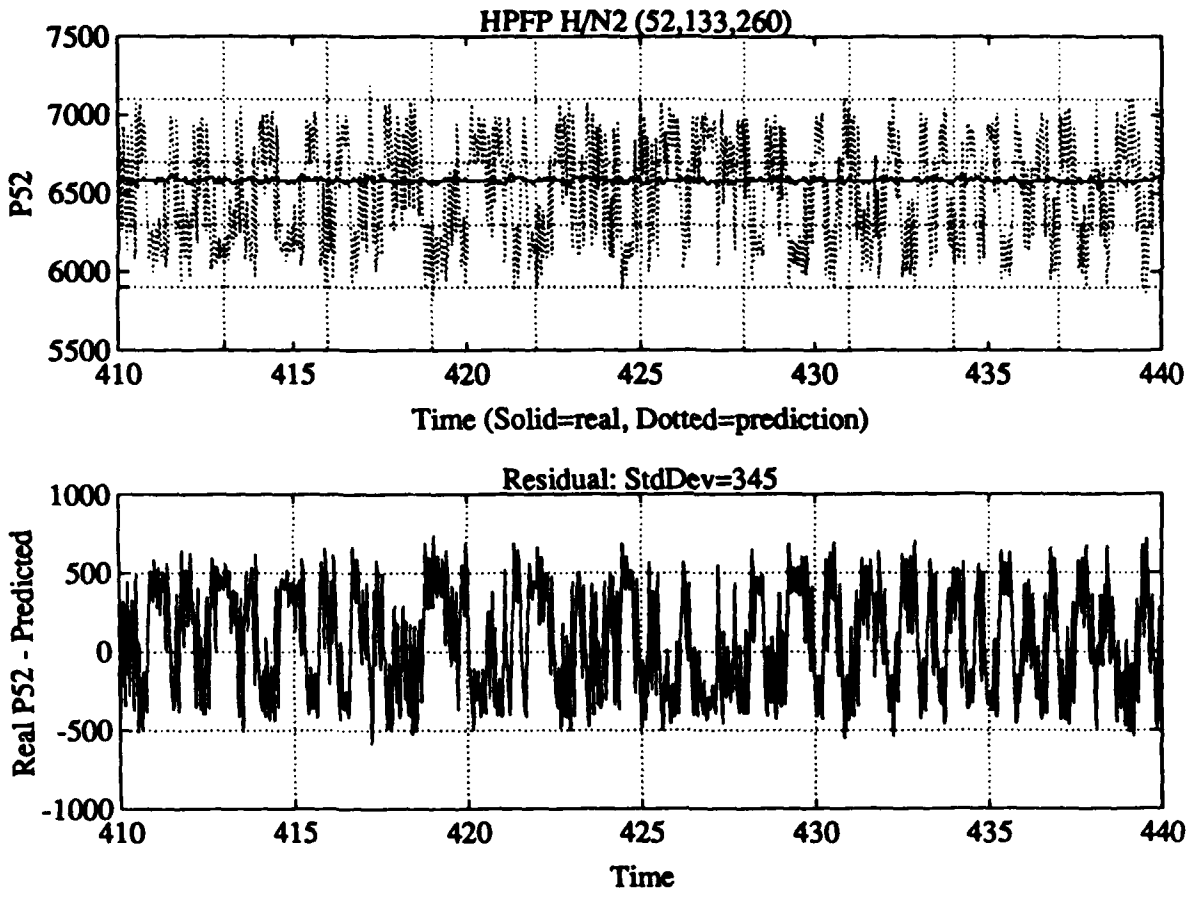

P52 +/- 190
Prediction +/- 1035

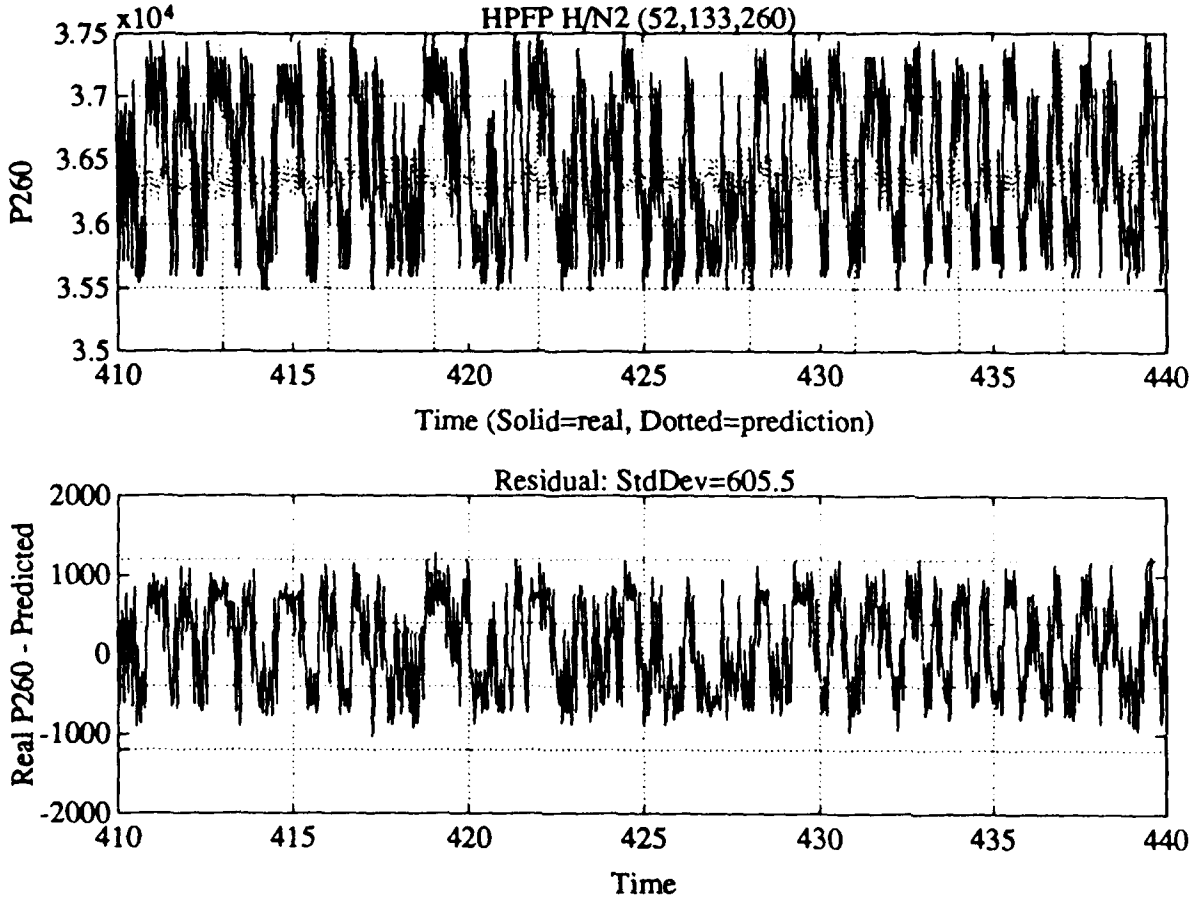

P260 +/- 31.5

Prediction +/- 1816

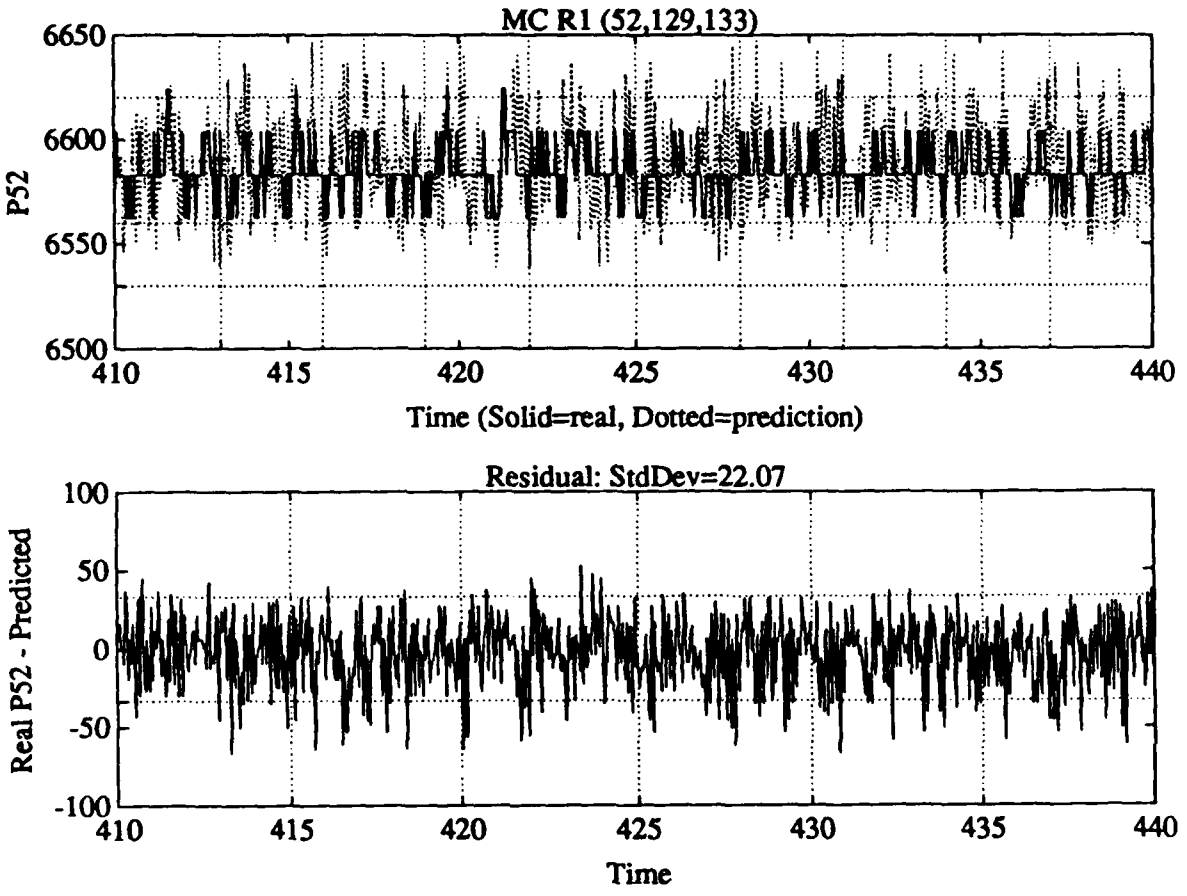

P52 +/- 190

Prediction +/- 66

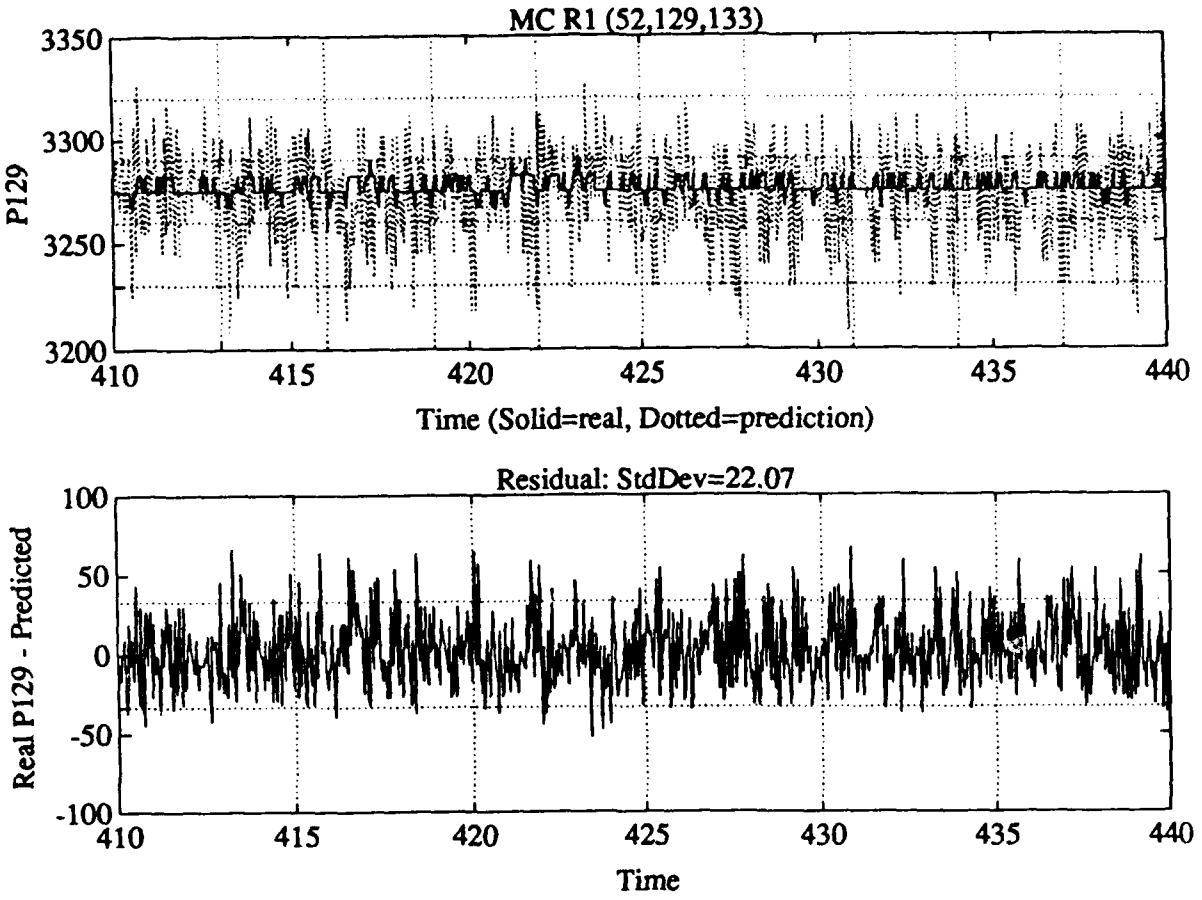

P129 +/- 70

Prediction +/-66

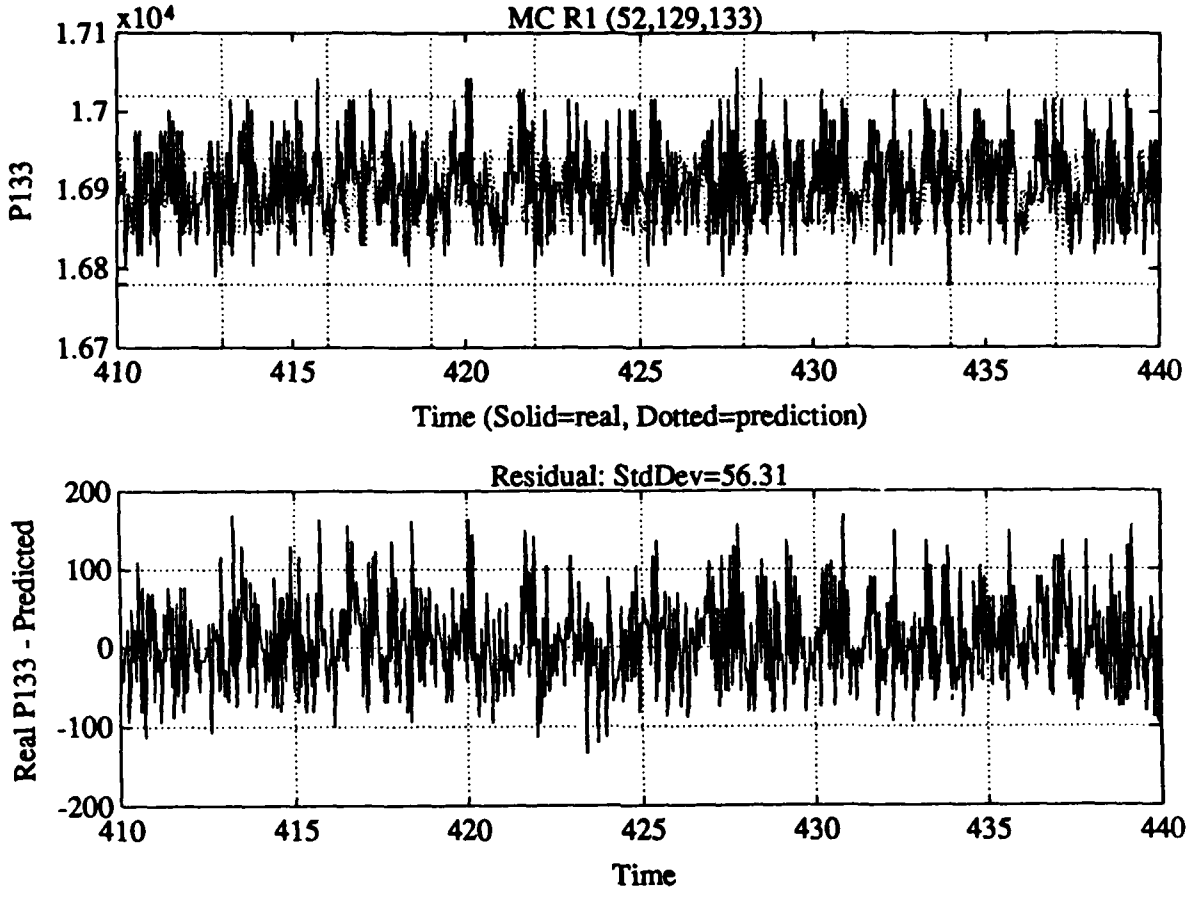

P133 +/- 169

Prediction +/- 168

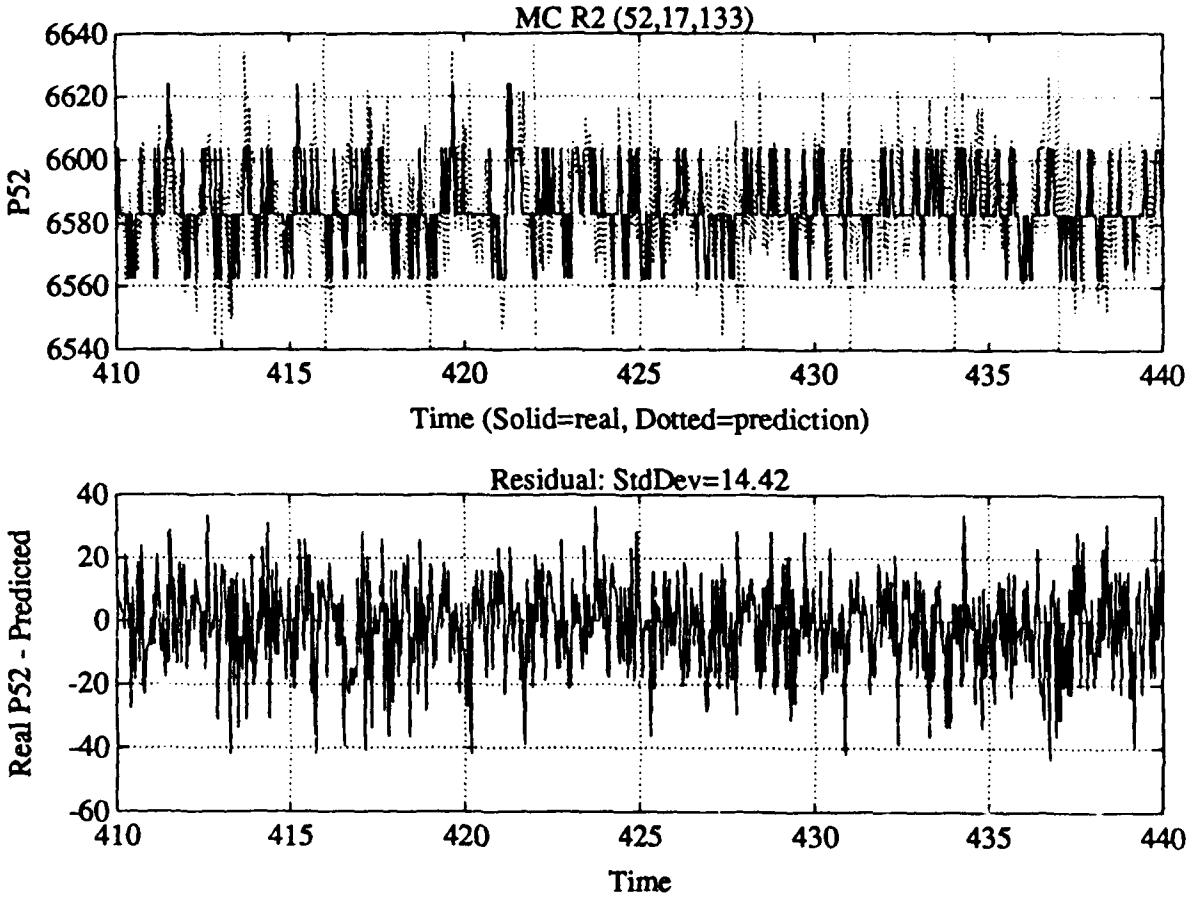

P52 +/- 190

Prediction +/- 43

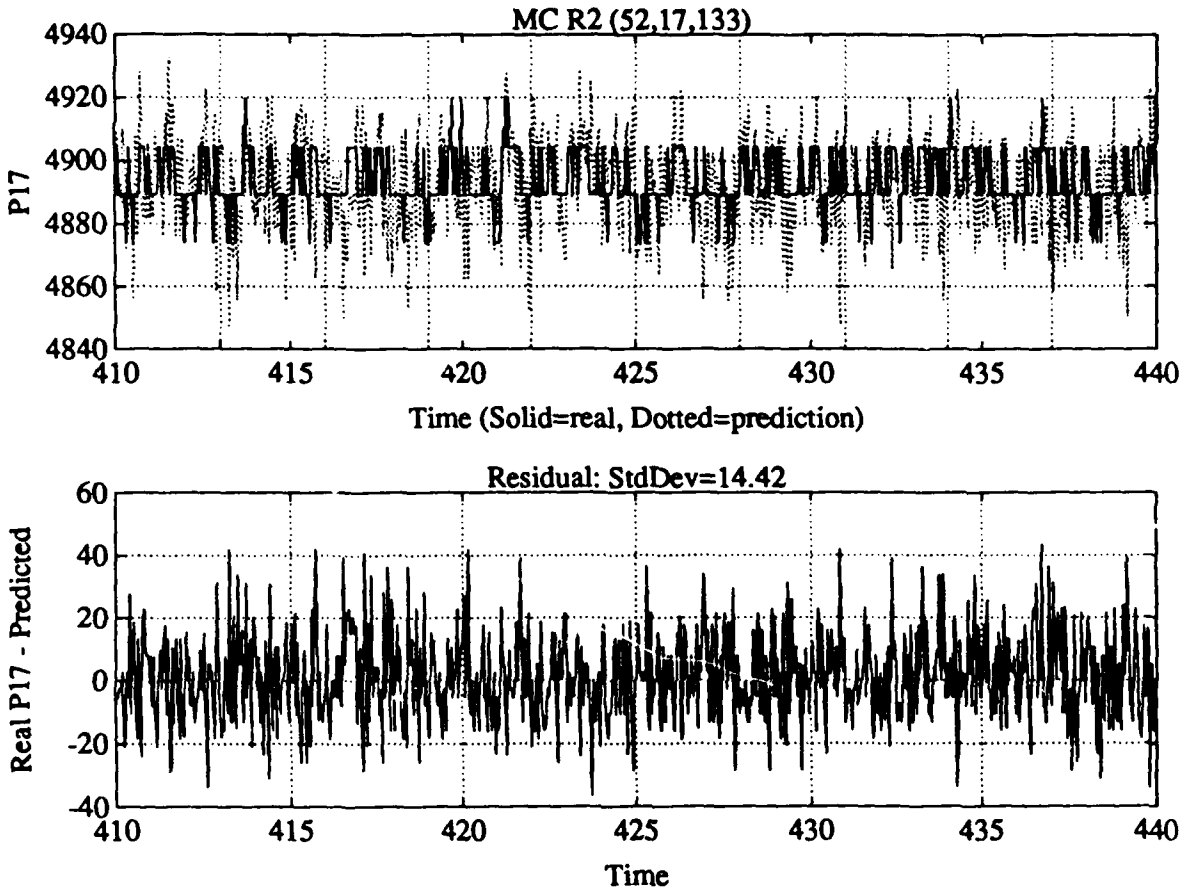

P17 +/- 140

Prediction +/- 43

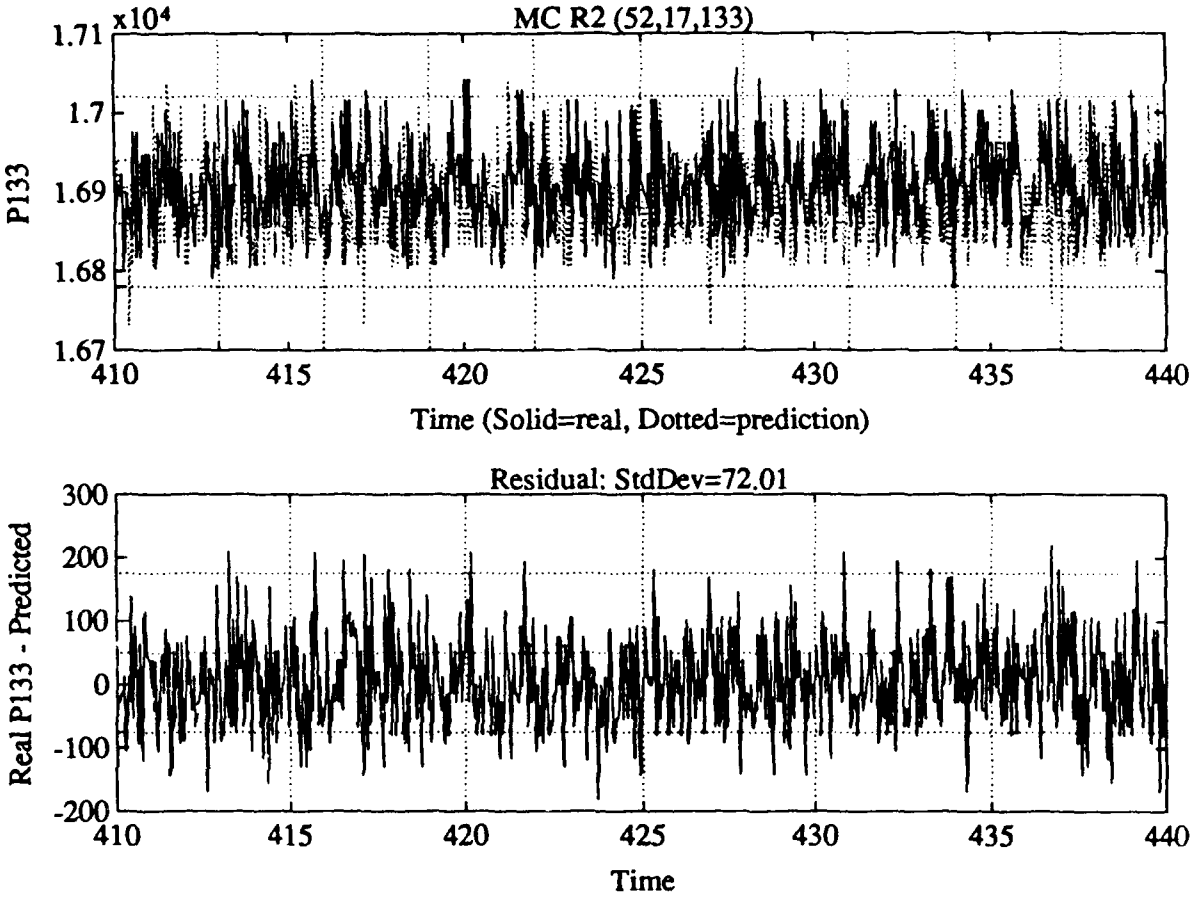

P133 +/- 169

Prediction +/- 216

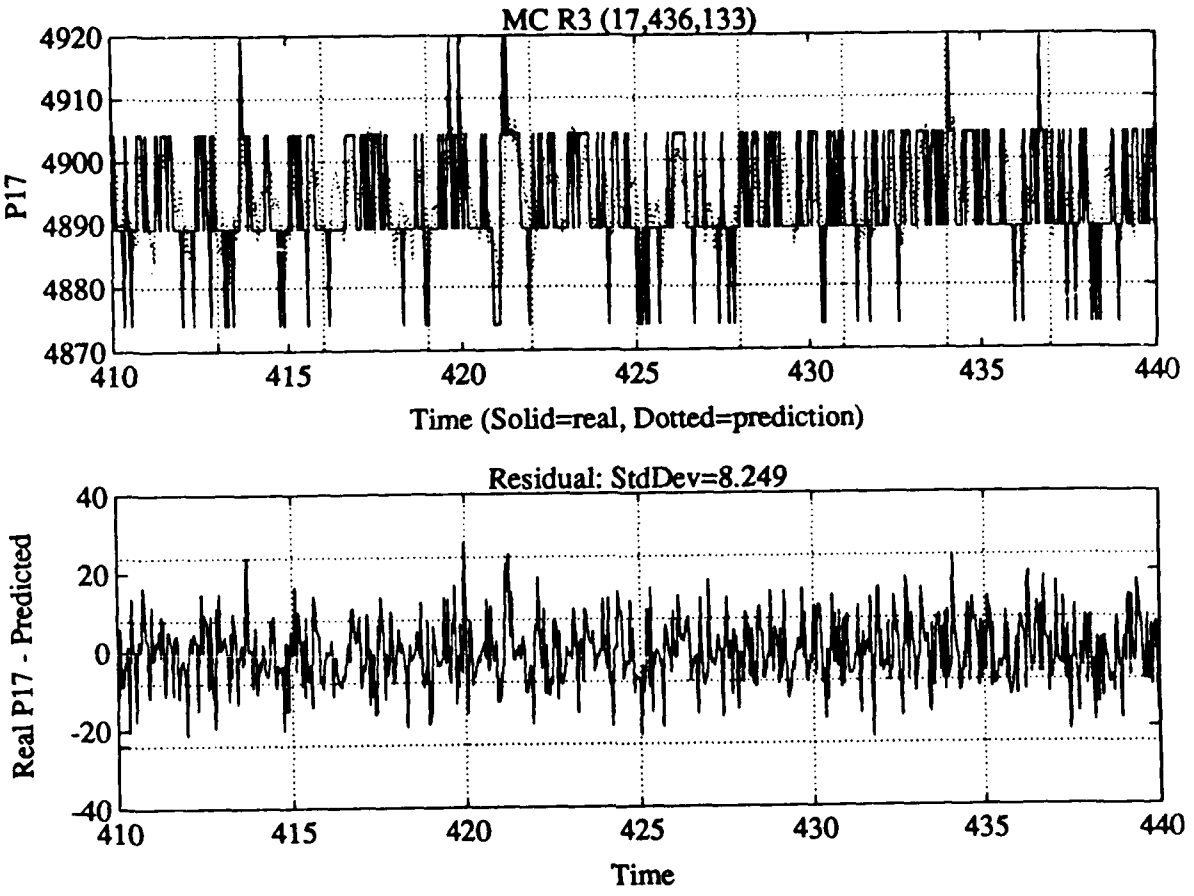

P17 +/- 140
Prediction +/- 25

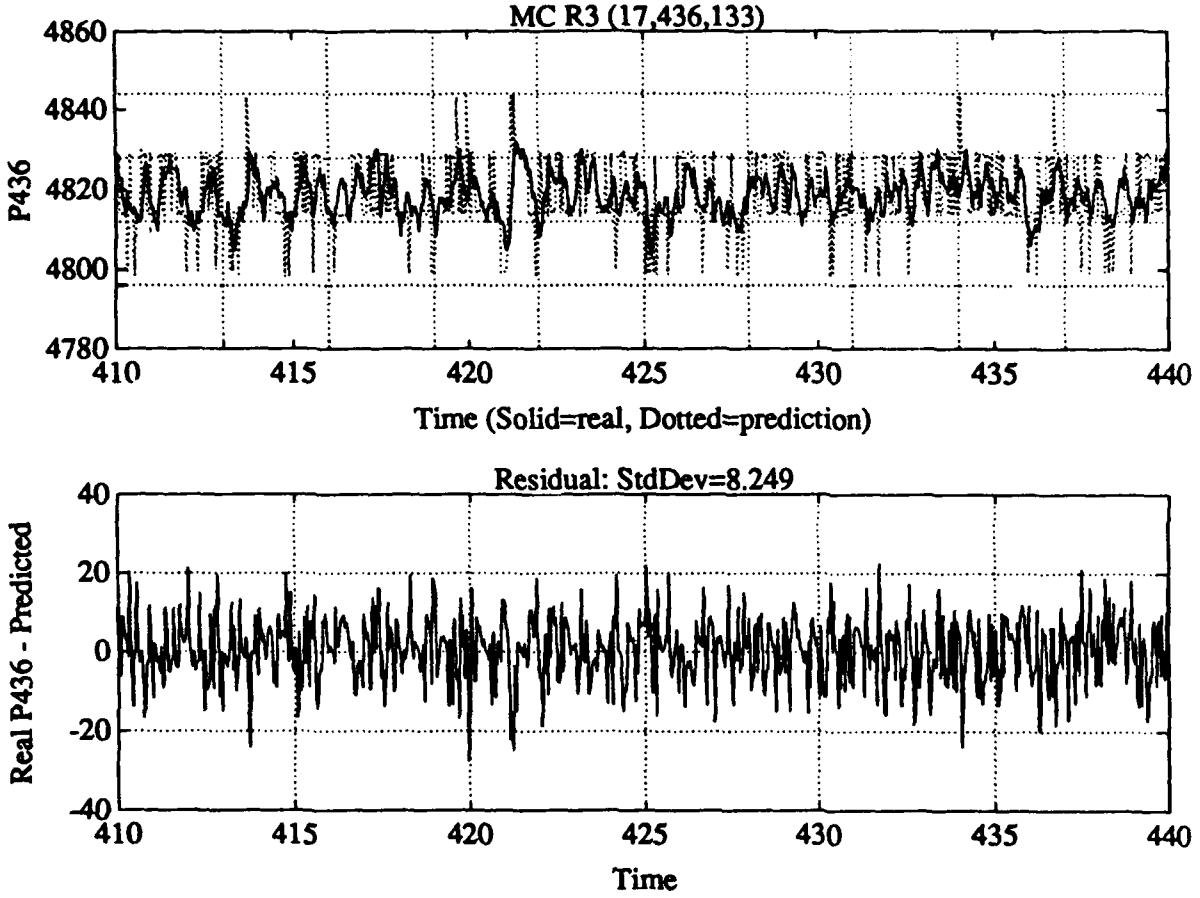

P436 +/- 50

Prediction +/- 25

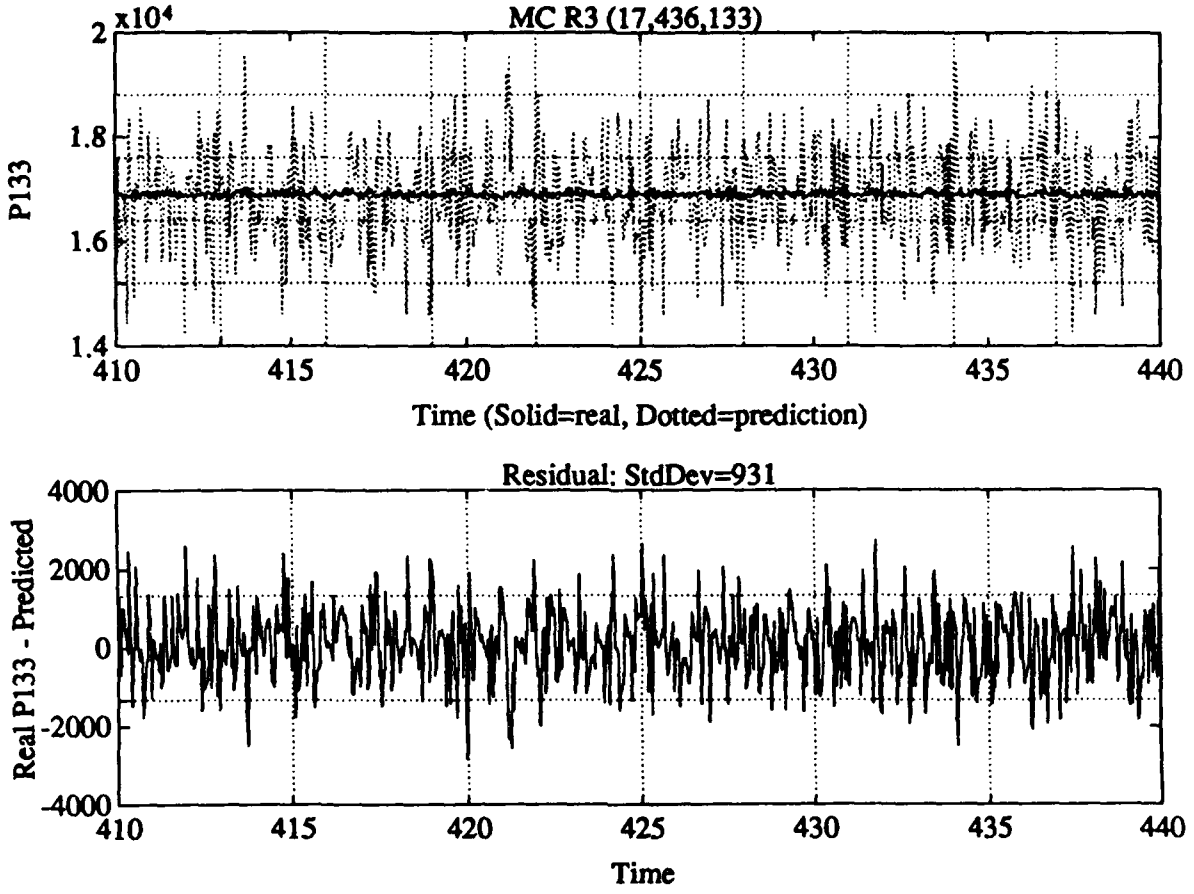

P133 +/- 169
Prediction +/- 2793

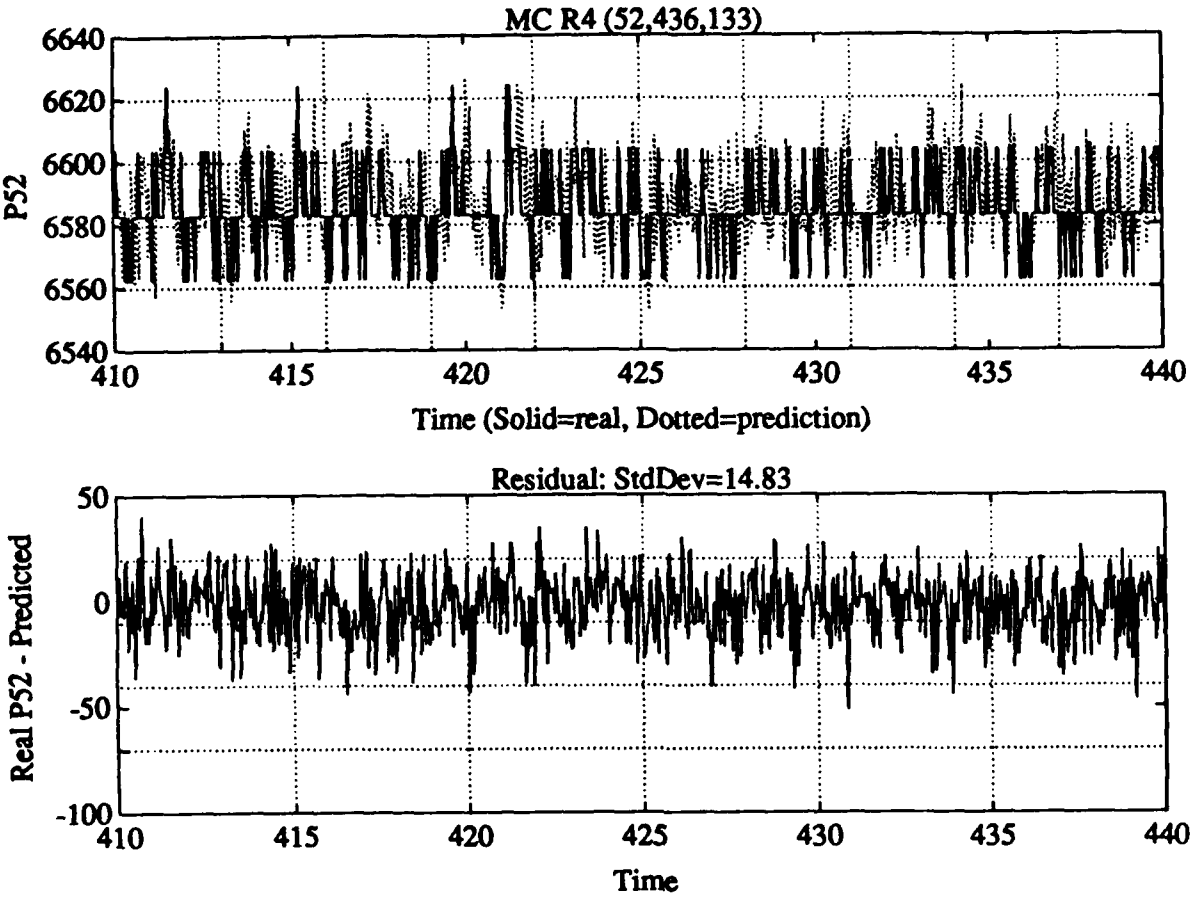

P52 +/- 190
Prediction +/- 44

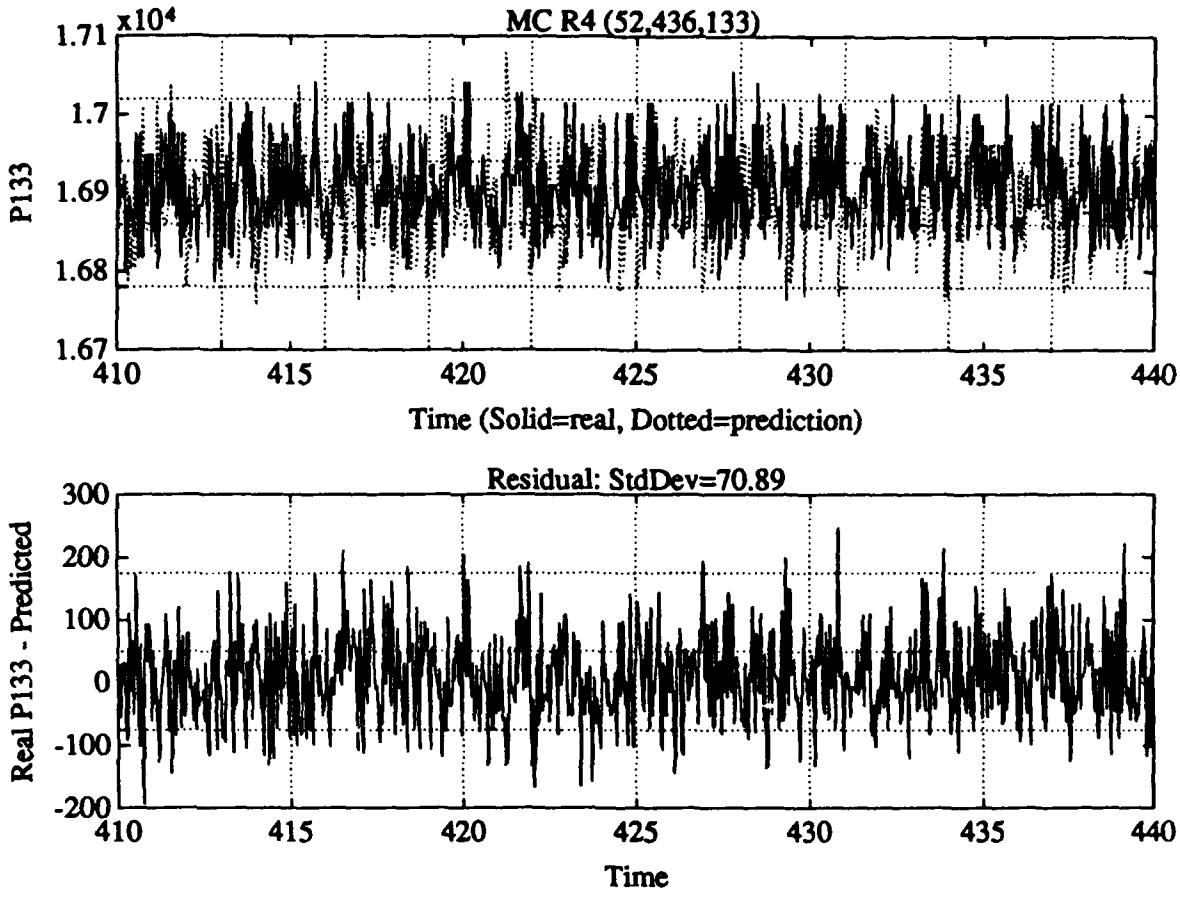

P133 +/- 169

Prediction +/- 213

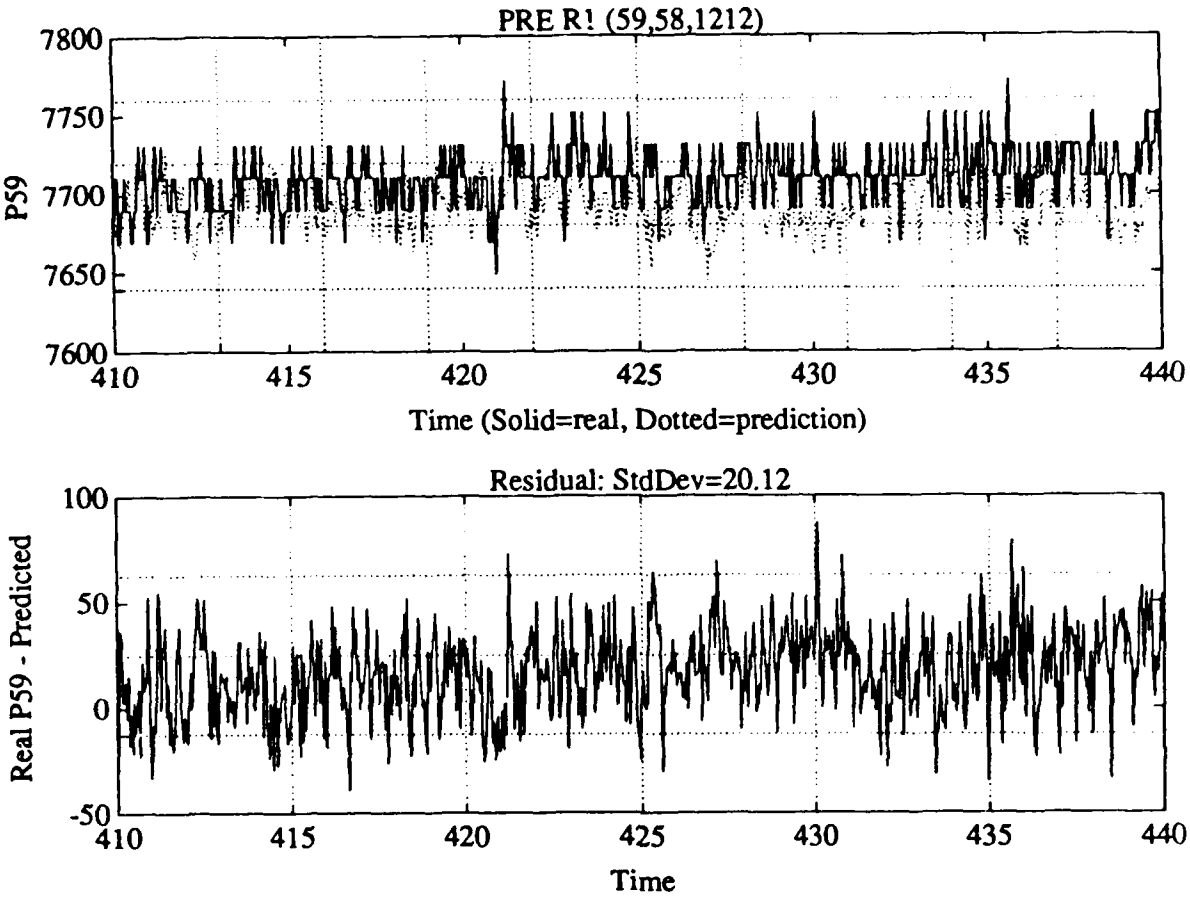

P59 +/- 190

Prediction +/- 60

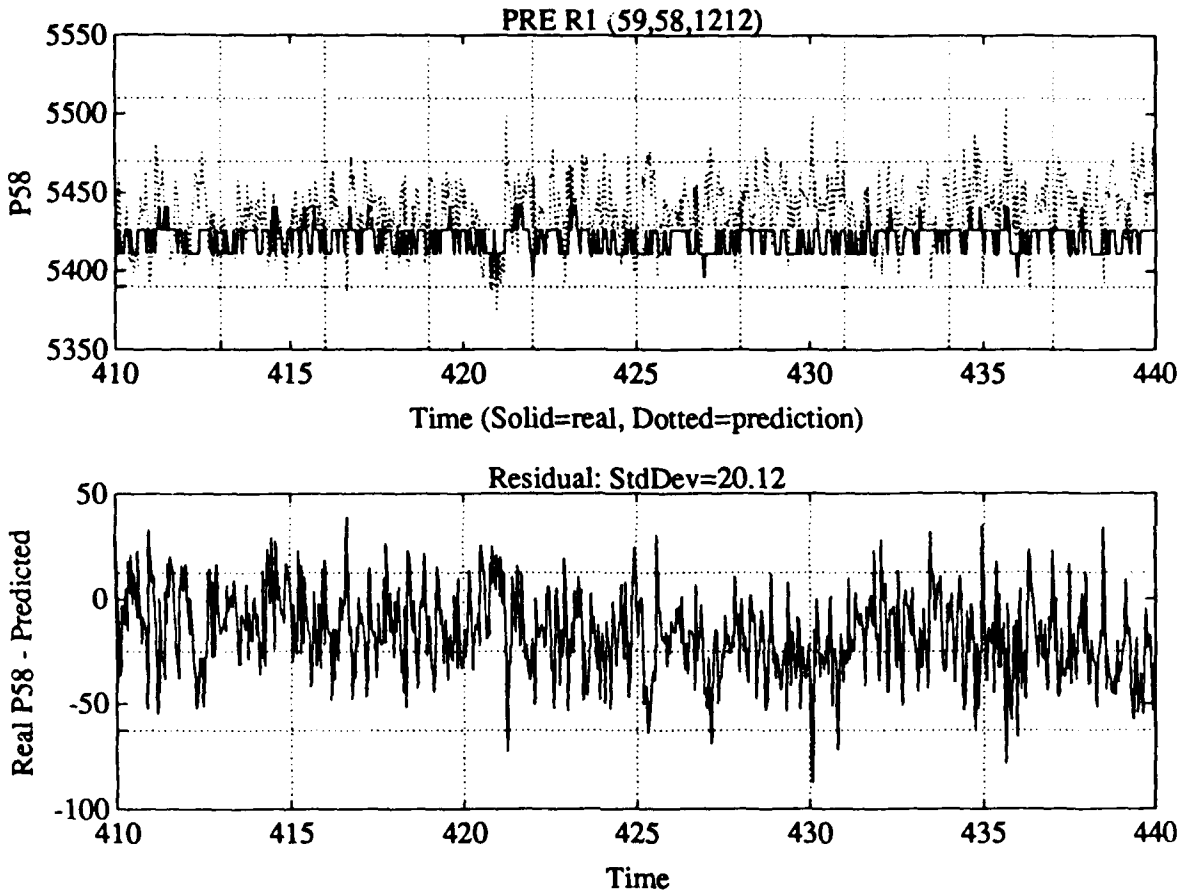

P58 +/- 140
Prediction +/- 60

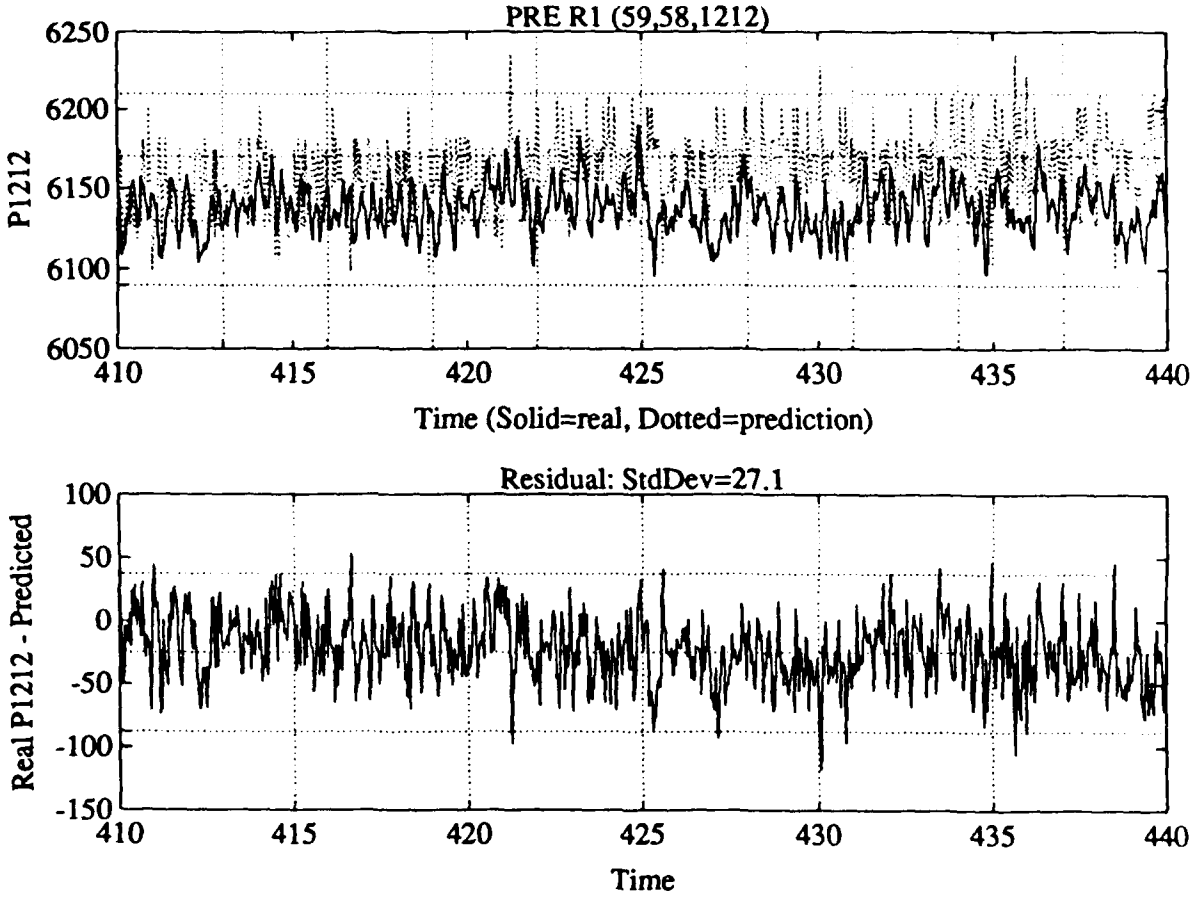

P1212 +/- 85

Prediction +/- 81

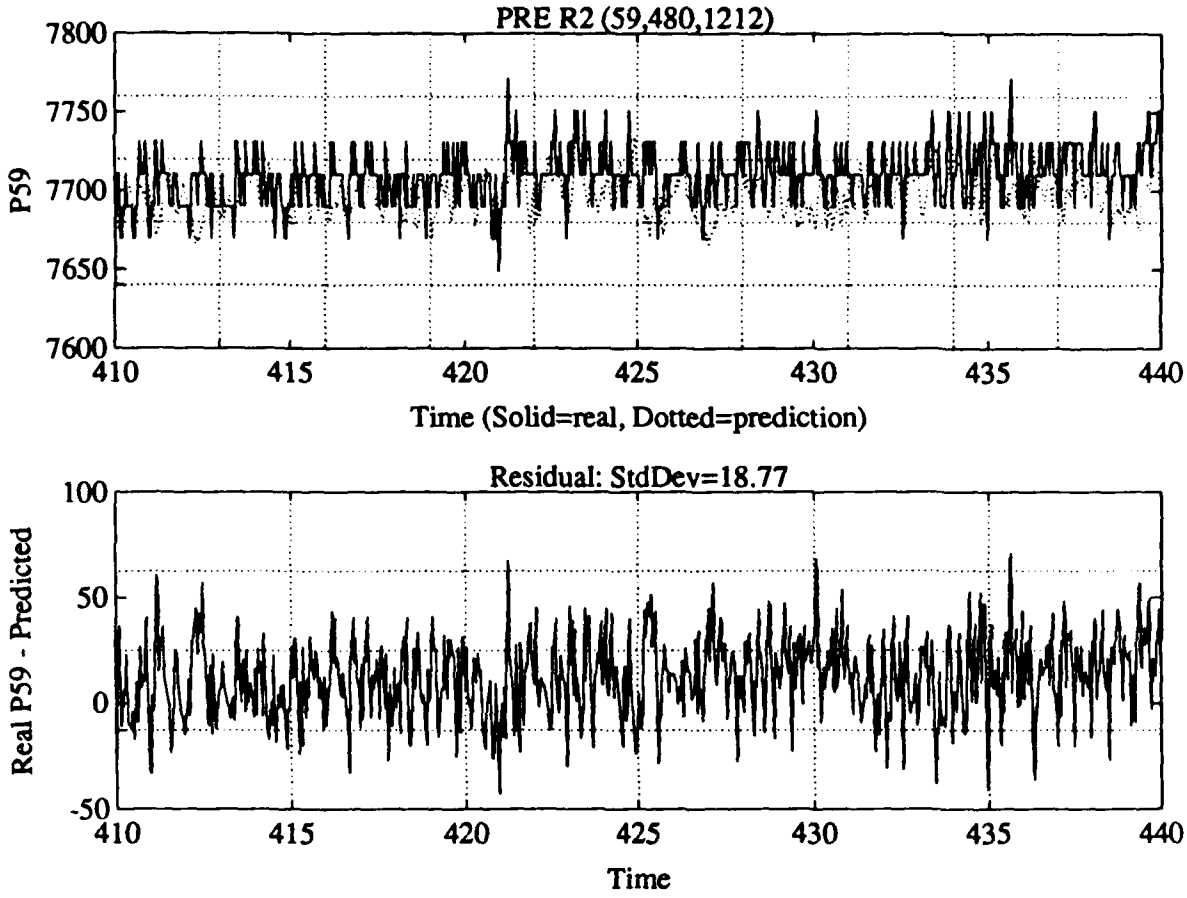

P59 +/- 190

Prediction +/- 56.4

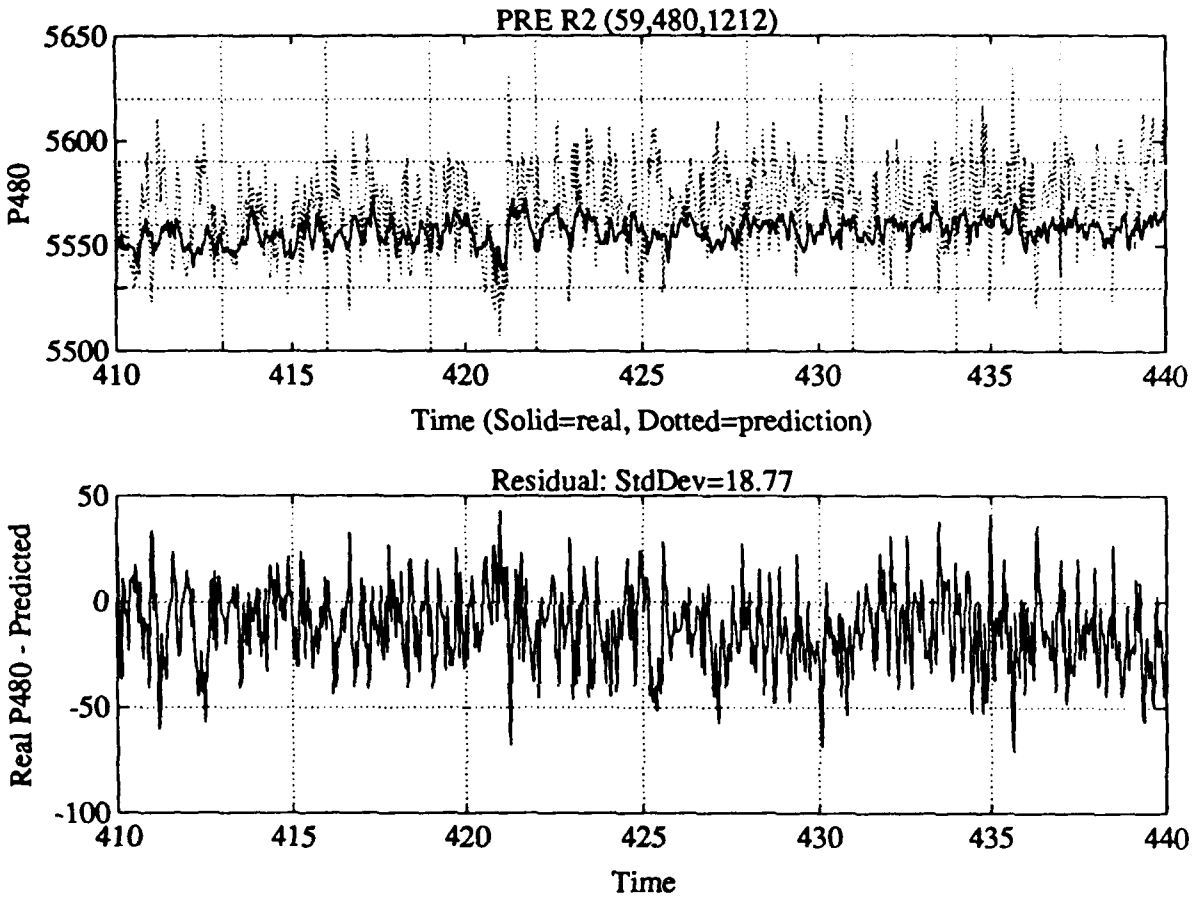

P480 +/- 200

Prediction +/- 56.4

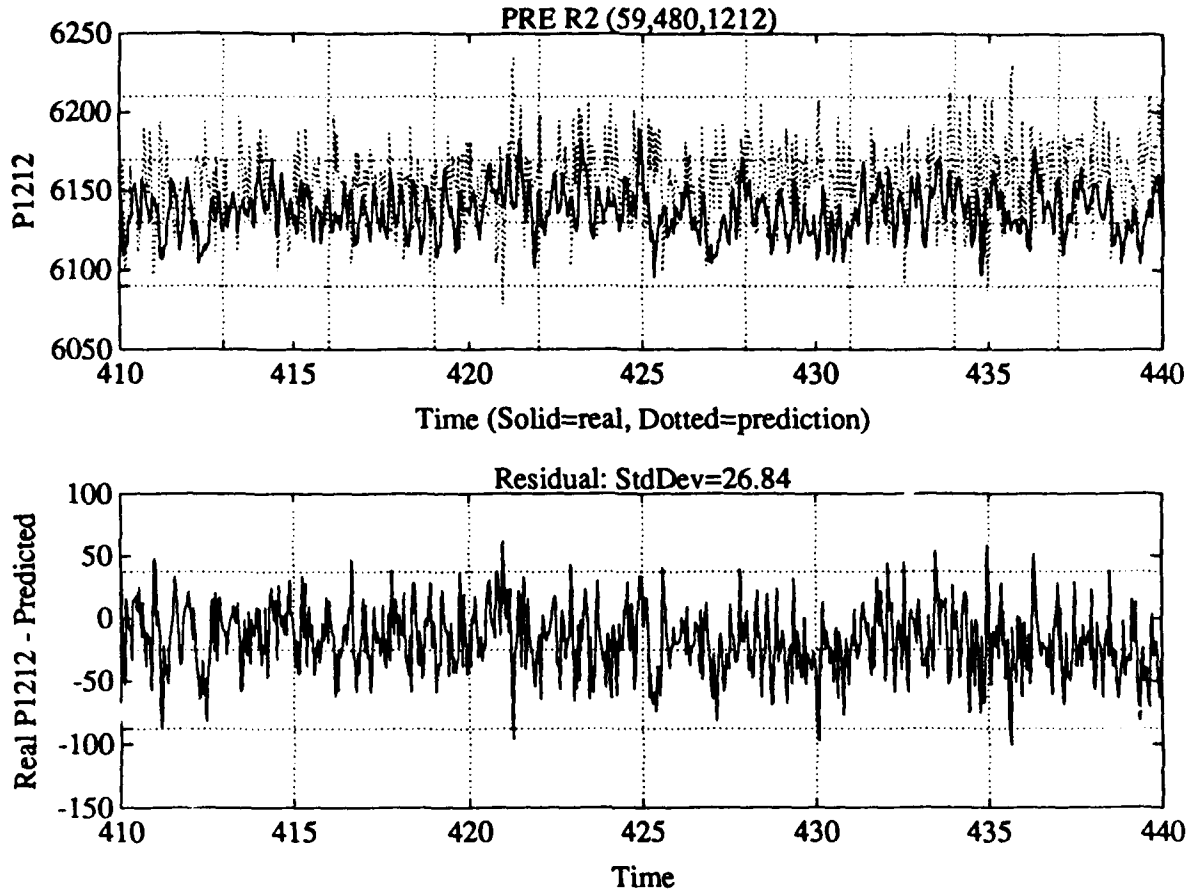

P1212 +/- 85

Prediction +/- 80

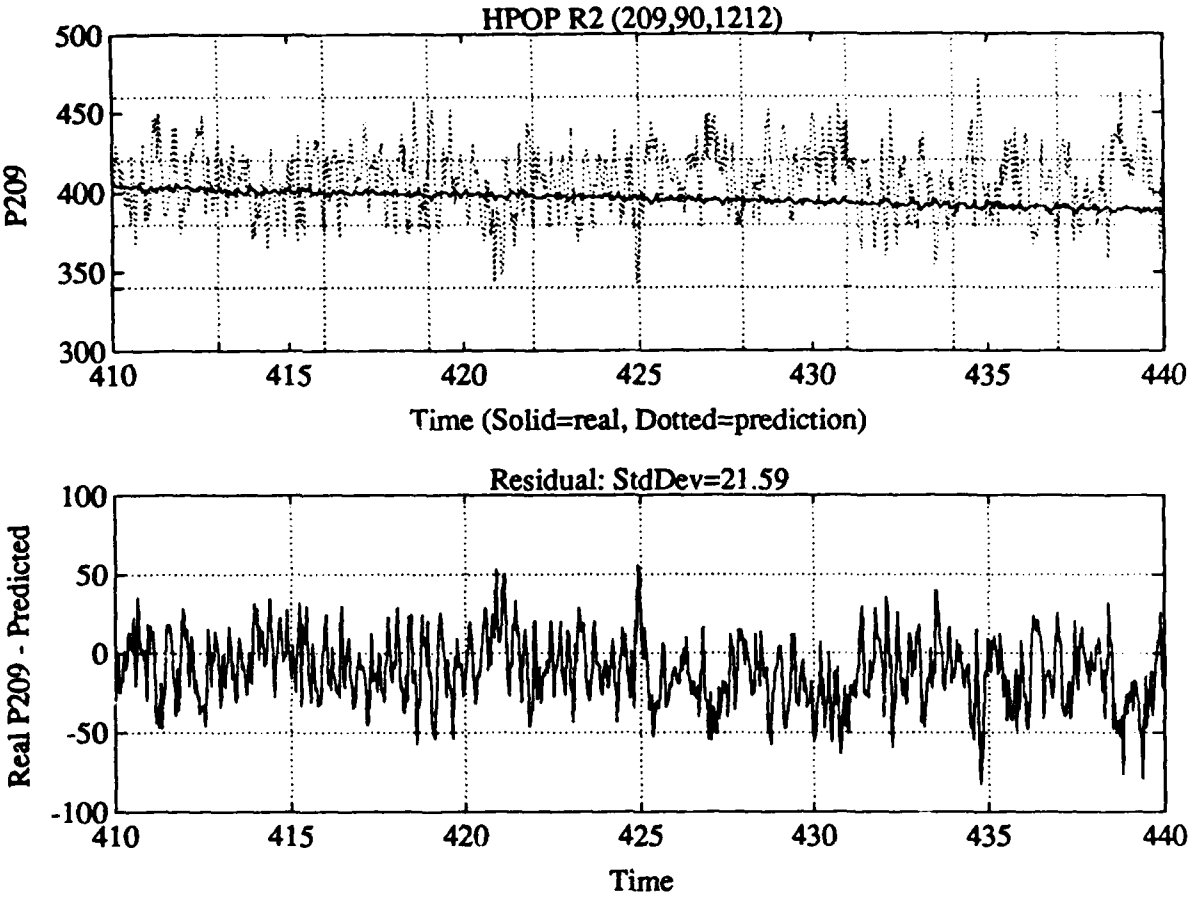

P209 +/- 15
Prediction +/- 65

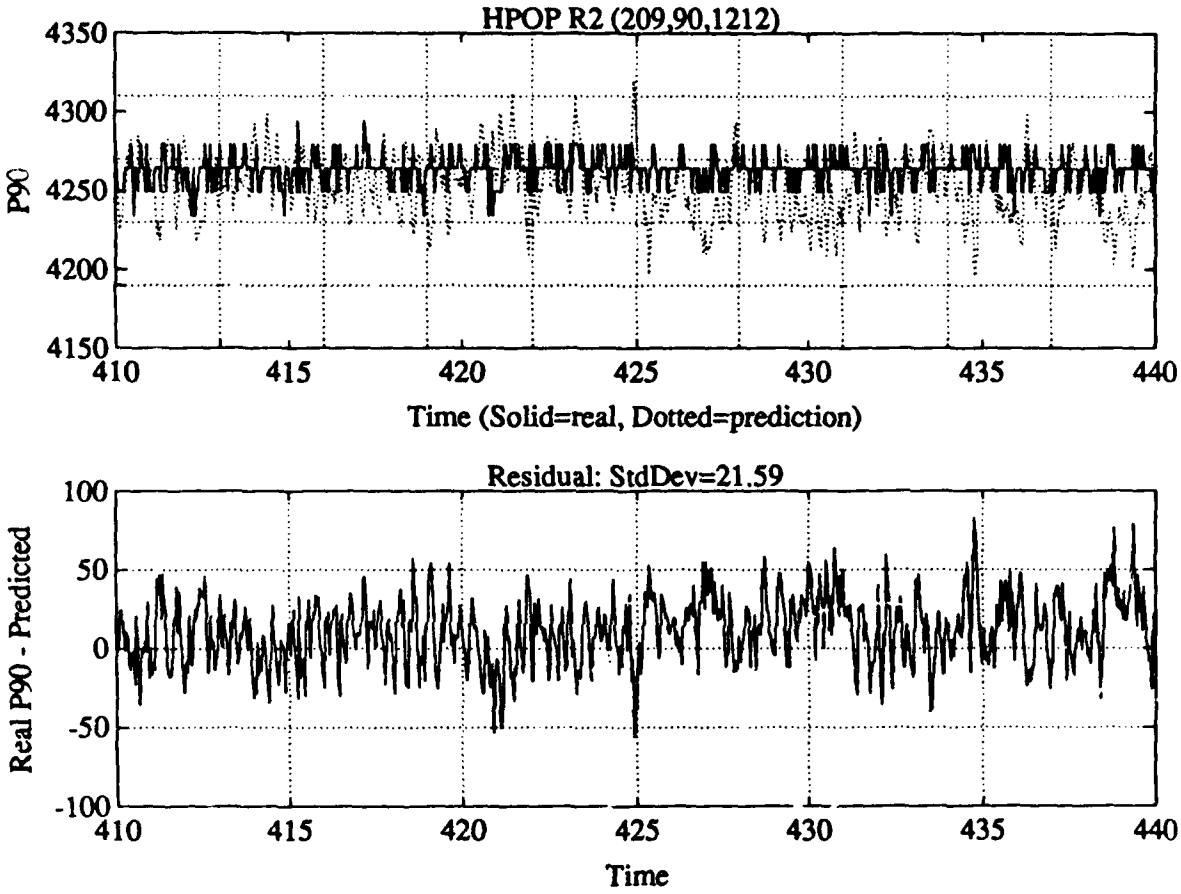

P90 +/- 140
Prediction +/- 65

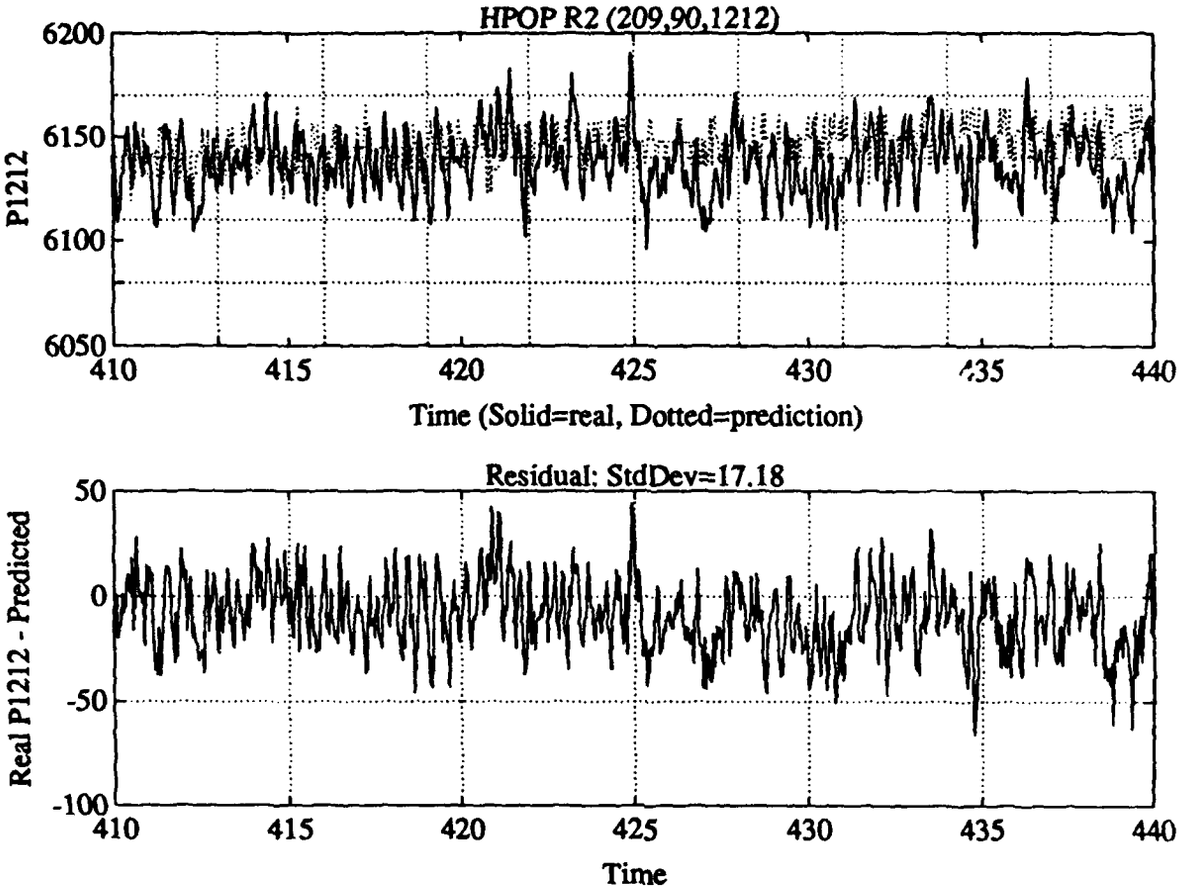

P1212 +/- 85
Prediction +/- 51

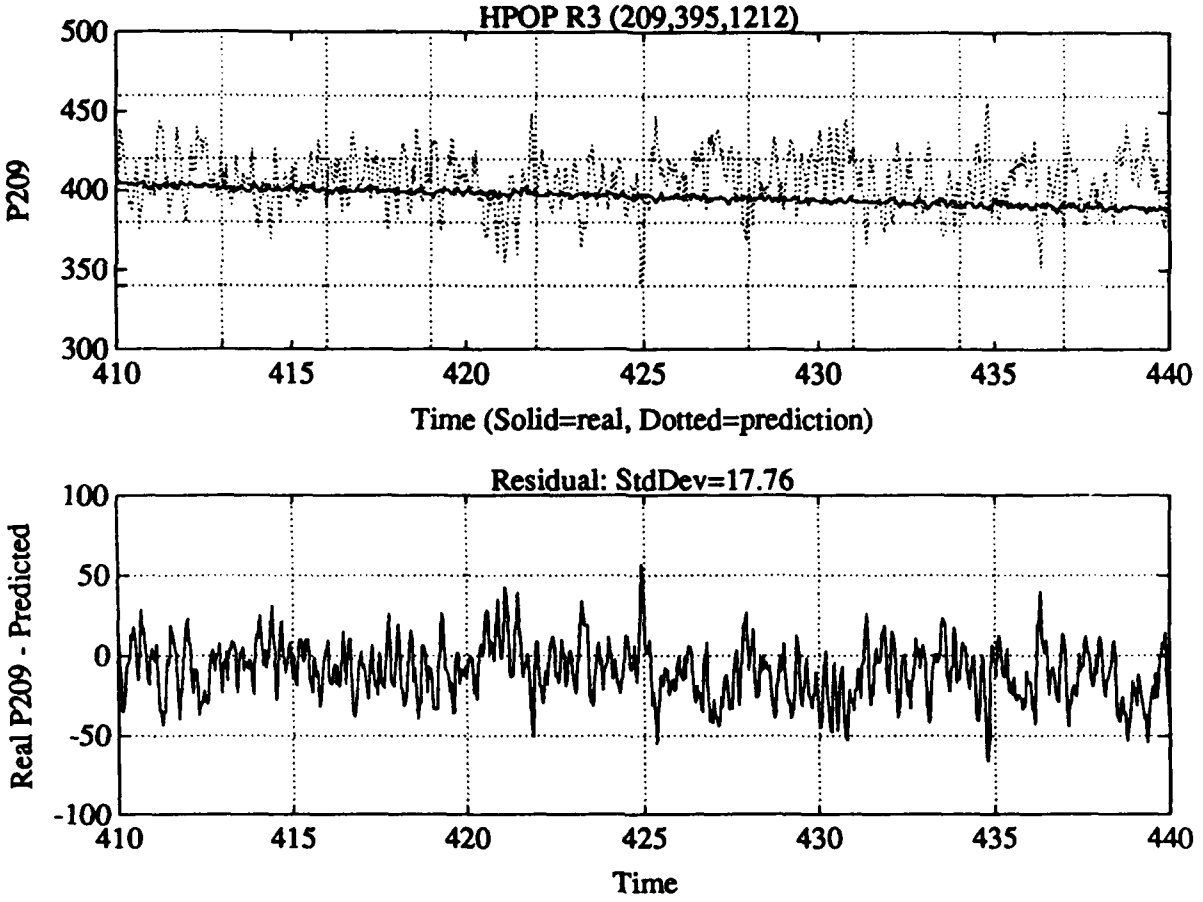

P209 +/- 2-
Prediction +/- 53

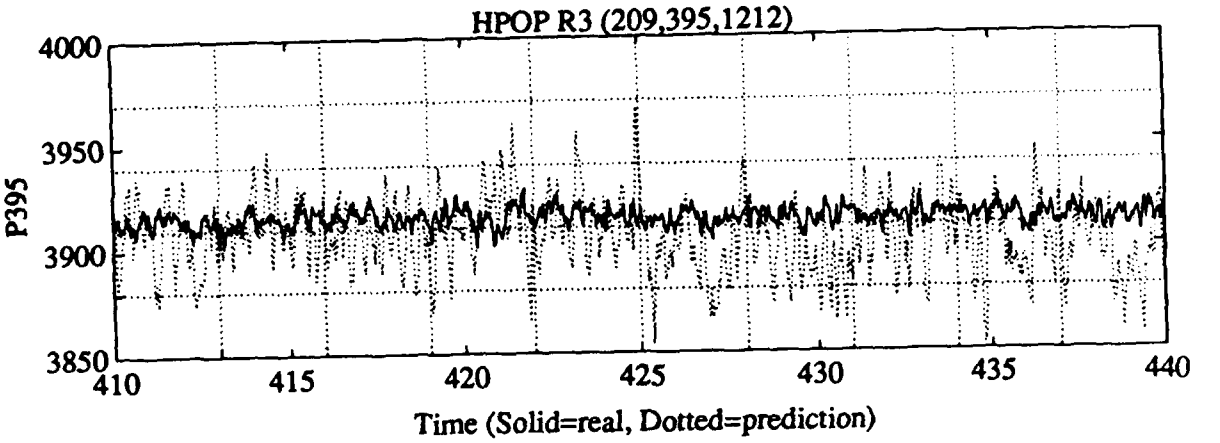

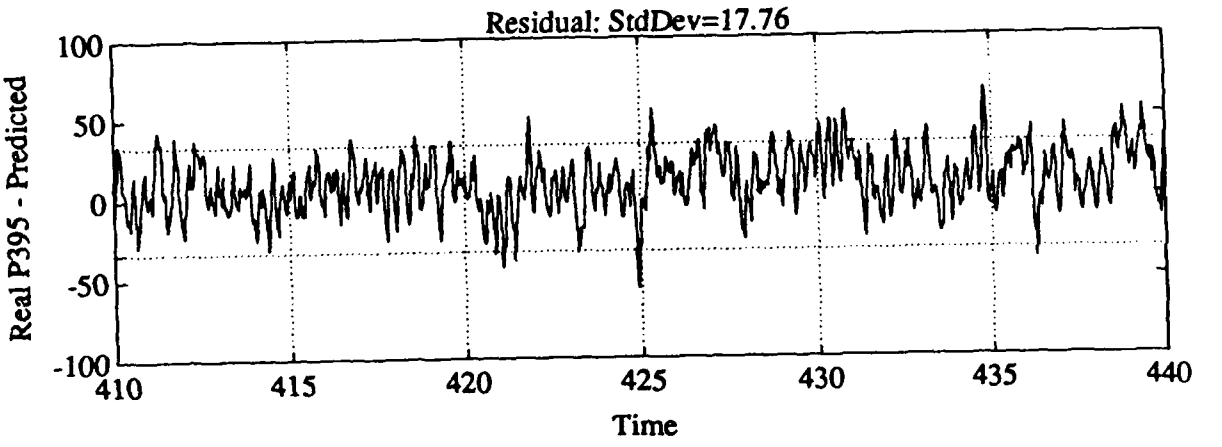

P395 +/- 25

Prediction +/- 53

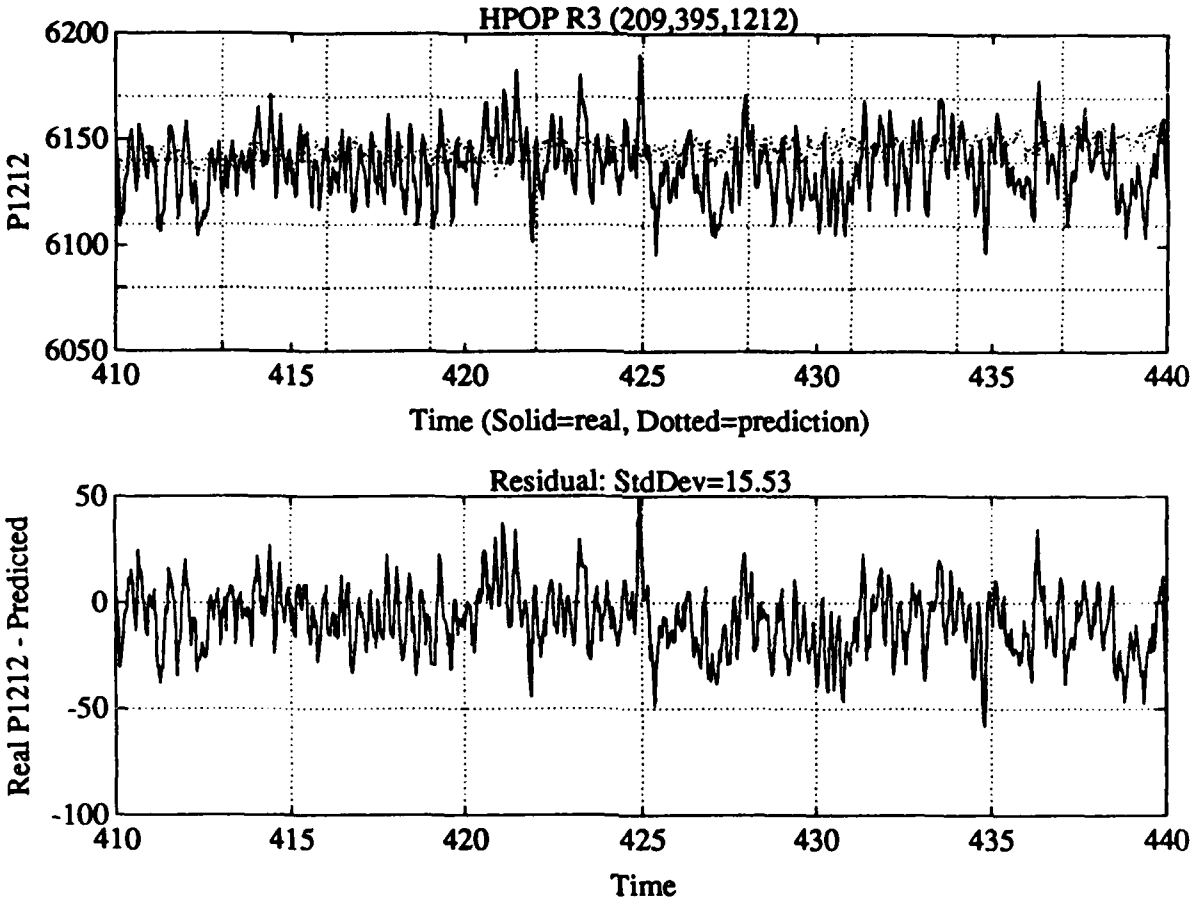

P1212 +/- 85

Prediction +/- 47

Results of characteristic equations applied to engine start transient using engine specific characteristics derived from steady state

Test A2497

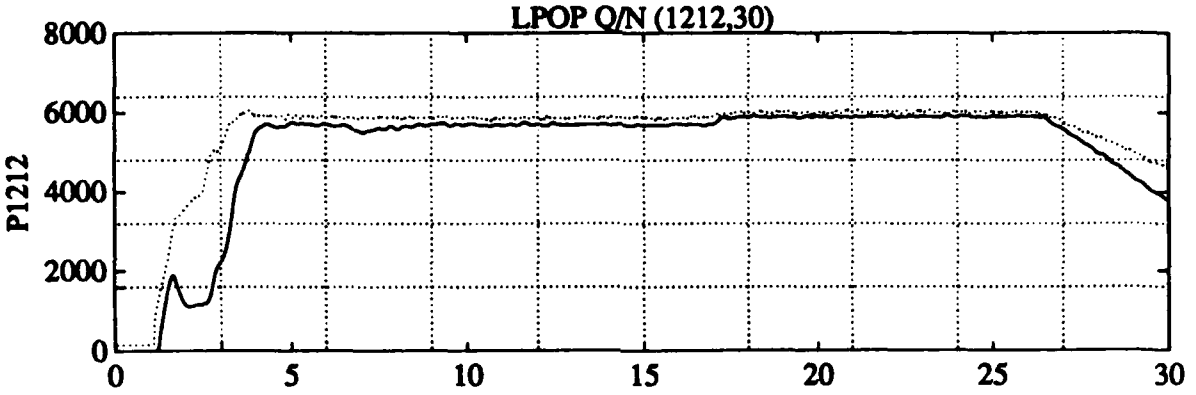

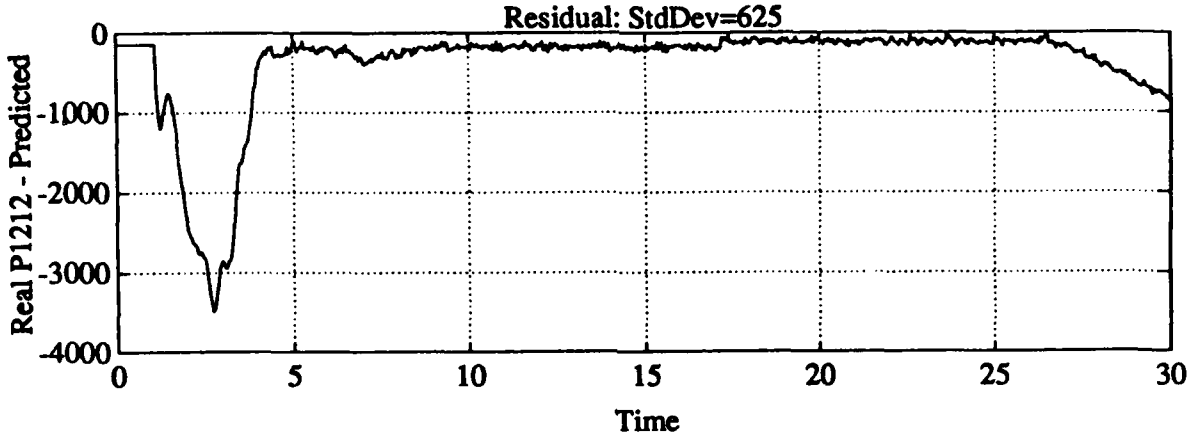

A2497 0-30
(Start Transient)

Using Engine-Specific characteristics
Sampled at 400-410

P4-85

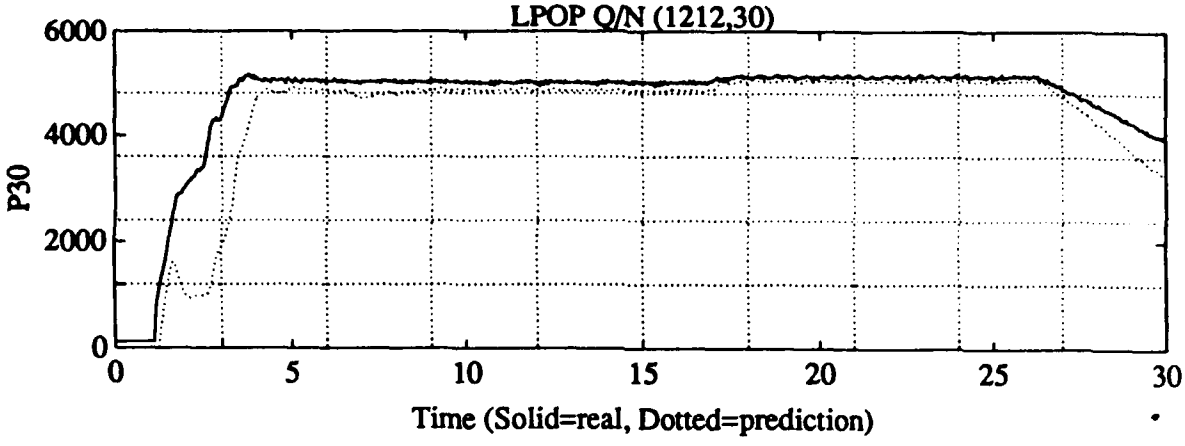
LPOP Q/N (1212,30)
P30
6000
4000
2000
0
0
5
10
15
20
25
30
Time (Solid=real, Dotted=prediction)

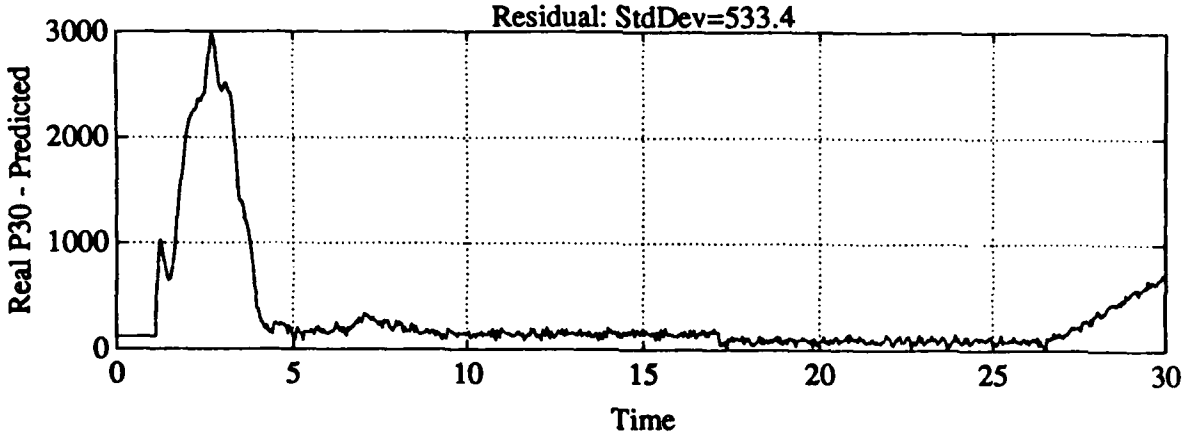
Residual: StdDev=533.4
Real P30 - Predicted
3000
2000
1000
0
0
5
10
15
20
25
30
Time

PTL 59

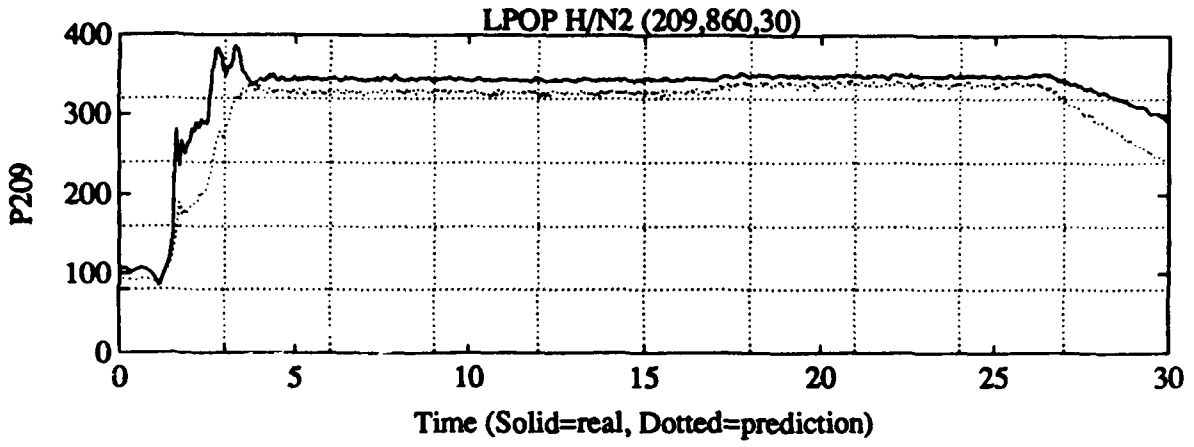
LPOP H/N2 (209,860,30)
P209
400
300
200
100
0
0
5
10
15
20
25
30
Time (Solid=real, Dotted=prediction)

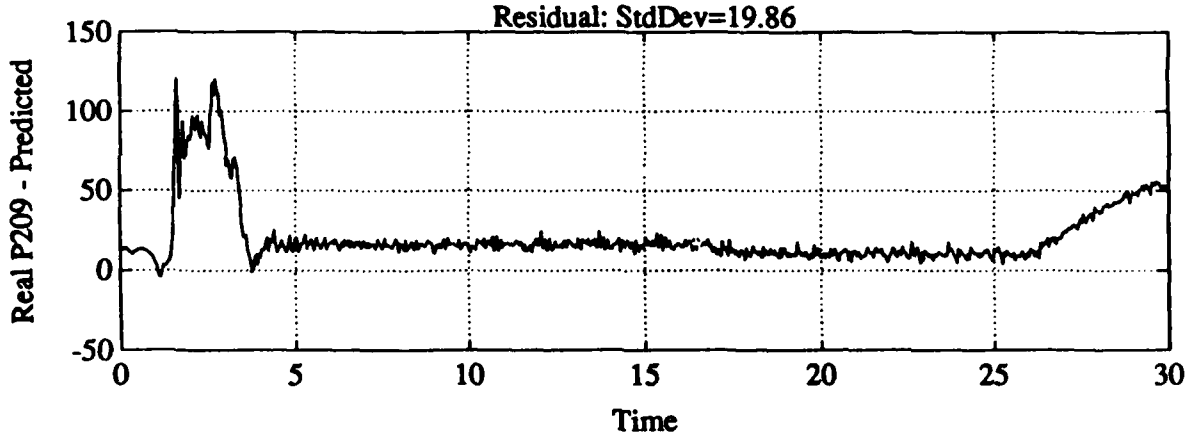
Residual: StdDev=19.86
Real P209 - Predicted
150
100
50
0
-50
0
5
10
15
20
25
30
Time

P7/-12

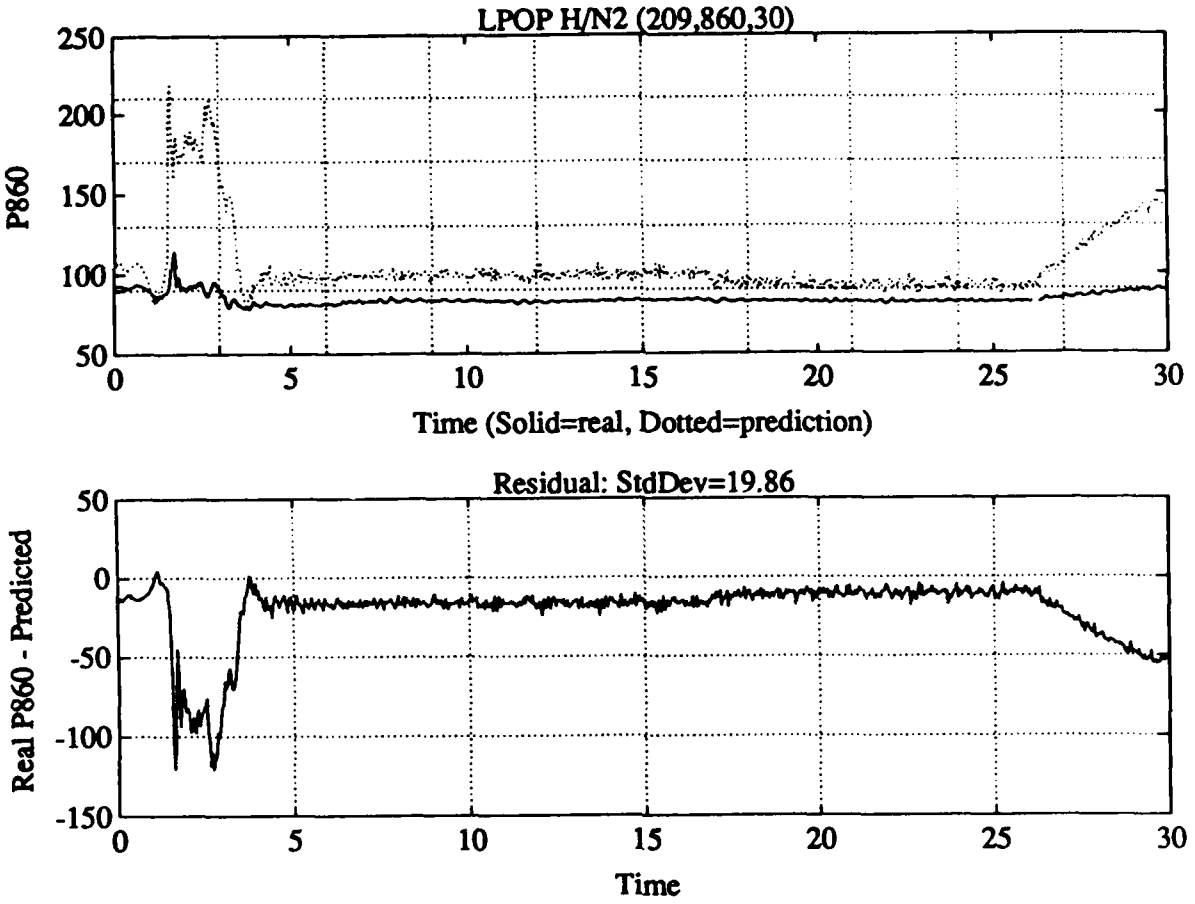
LPOP H/N2 (209,860,30)
P860
250
200
150
100
50
0
5
10
15
20
25
30
Time (Solid=real, Dotted=prediction)
Residual: StdDev=19.86
Real P860 - Predicted
50
0
-50
-100
-150
0
5
10
15
20
25
30
Time

P+L-5

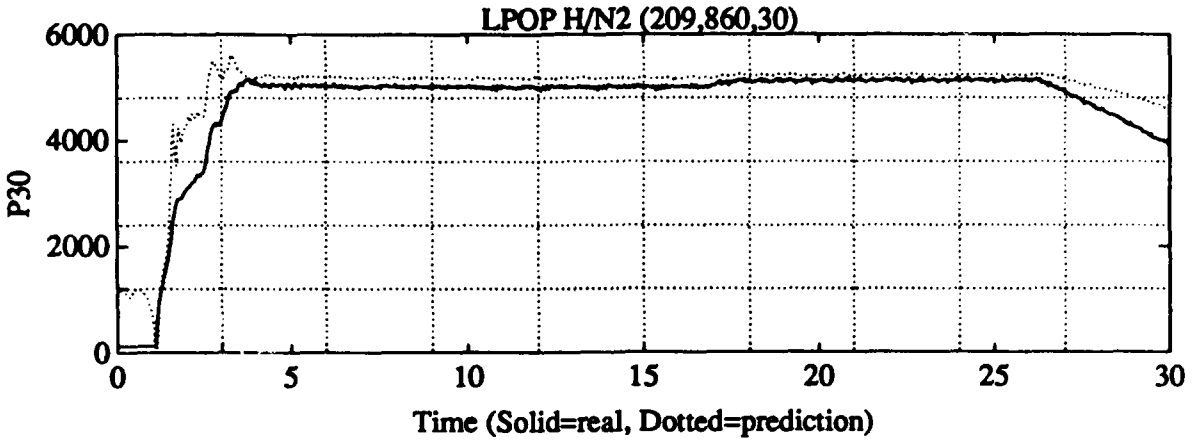
LPOP H/N2 (209,860,30)
P30
6000
4000
2000
0
0
5
10
15
20
25
30
Time (Solid=real, Dotted=prediction)

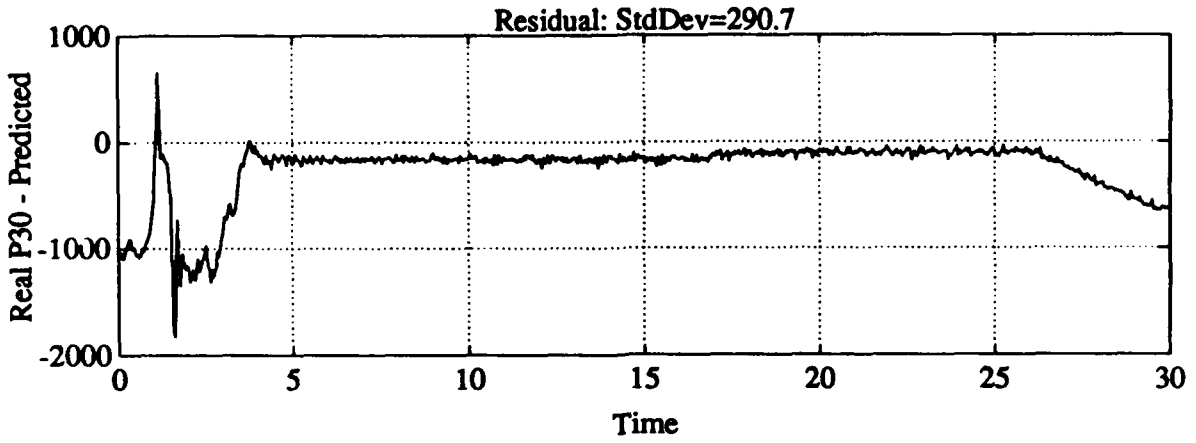
Residual: StdDev=290.7
Real P30 - Predicted
1000
0
-1000
-2000
0
5
10
15
20
25
30
Time

PTL59

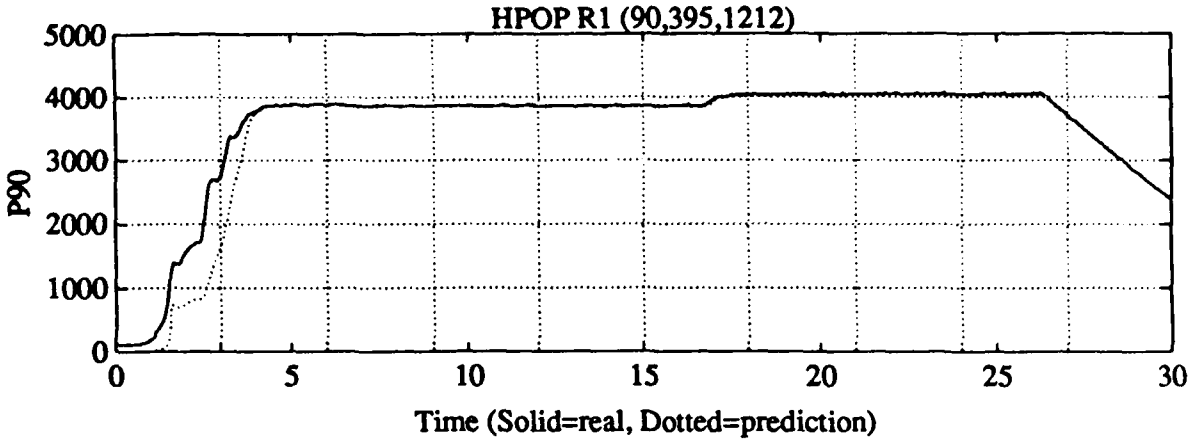
HPOP R1 (90,395,1212)
P90
5000
4000
3000
2000
1000
0
0
5
10
15
20
25
30
Time (Solid=real, Dotted=prediction)

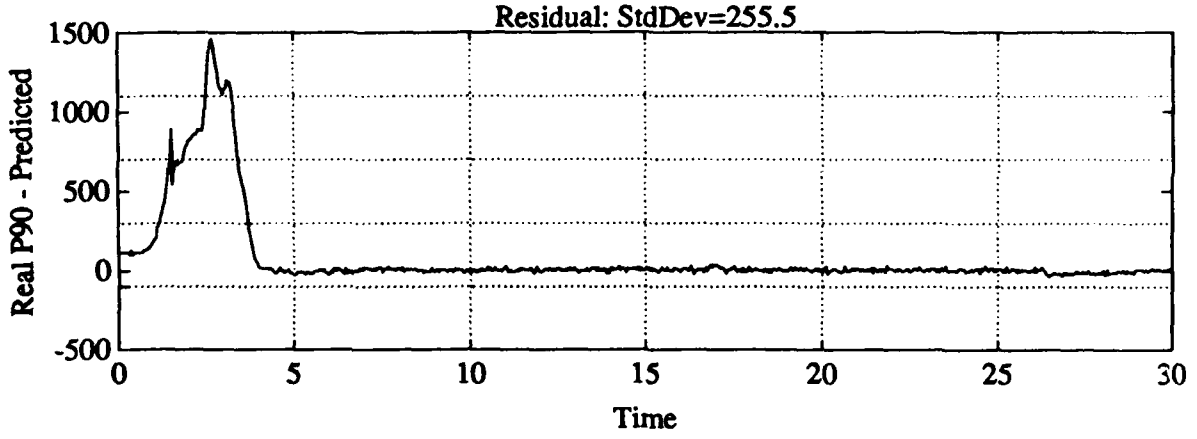
Residual: StdDev=255.5
Real P90 - Predicted
1500
1000
500
0
-500
0
5
10
15
20
25
30
Time

P+/-140

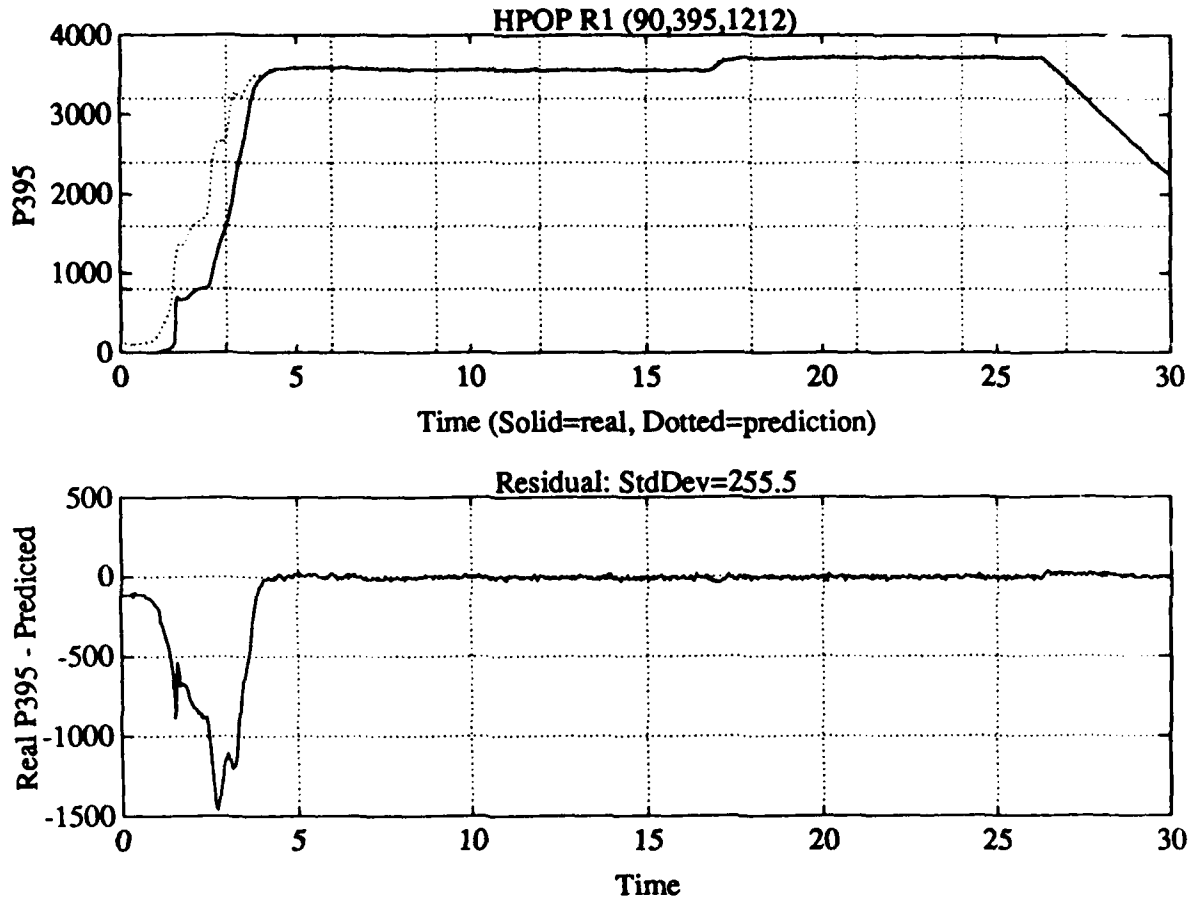
HPOP R1 (90,395,1212)
P395
4000
3000
2000
1000
0
0
5
10
15
20
25
30
Time (Solid=real, Dotted=prediction)
Residual: StdDev=255.5
Real P395 - Predicted
500
0
-500
-1000
-1500
0
5
10
15
20
25
30
Time

P+/-25

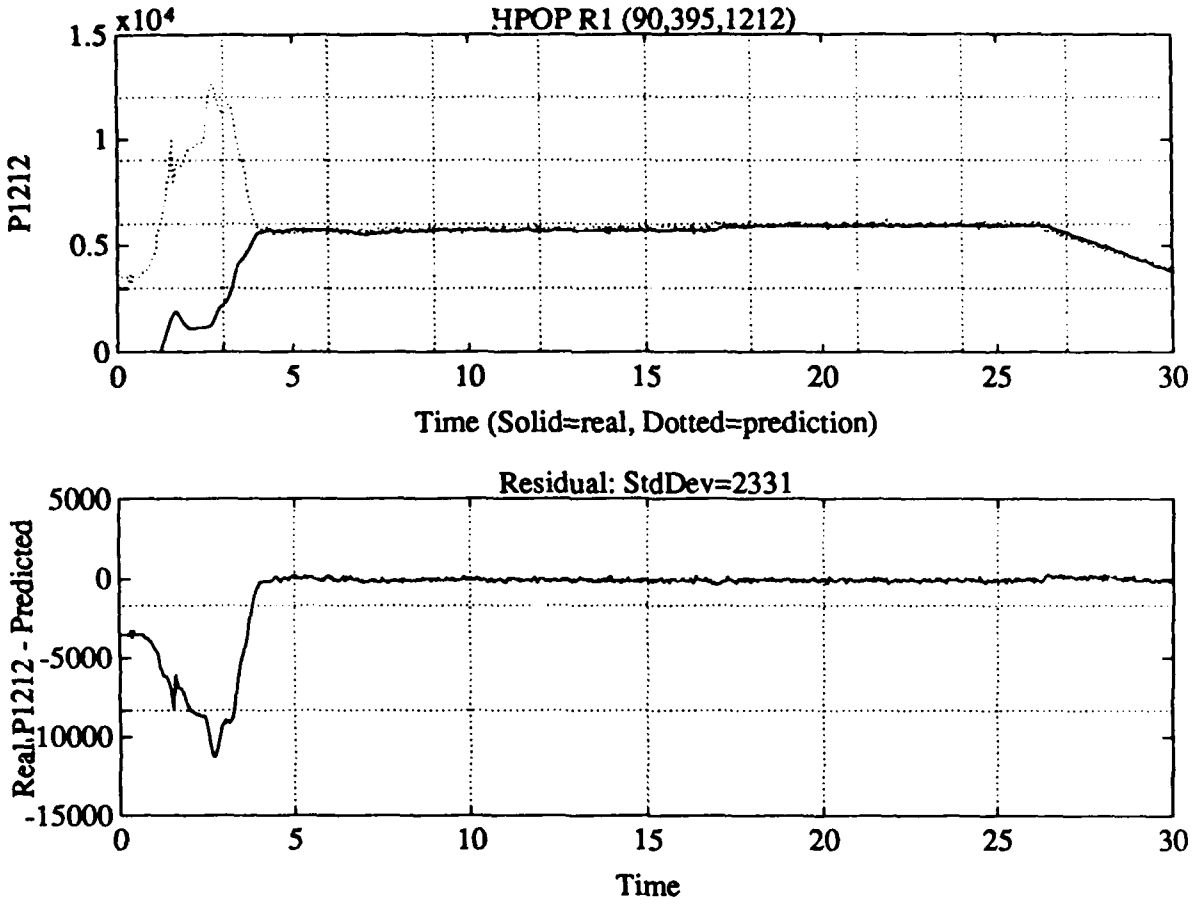
HPOP R1 (90,395,1212)
x10^4
1.5
1
0.5
0
P1212
0
5
10
15
20
25
30
Time (Solid=real, Dotted=prediction)
Residual: StdDev=2331
5000
0
-5000
-10000
-15000
Real P1212 - Predicted
0
5
10
15
20
25
30
Time

PM-85

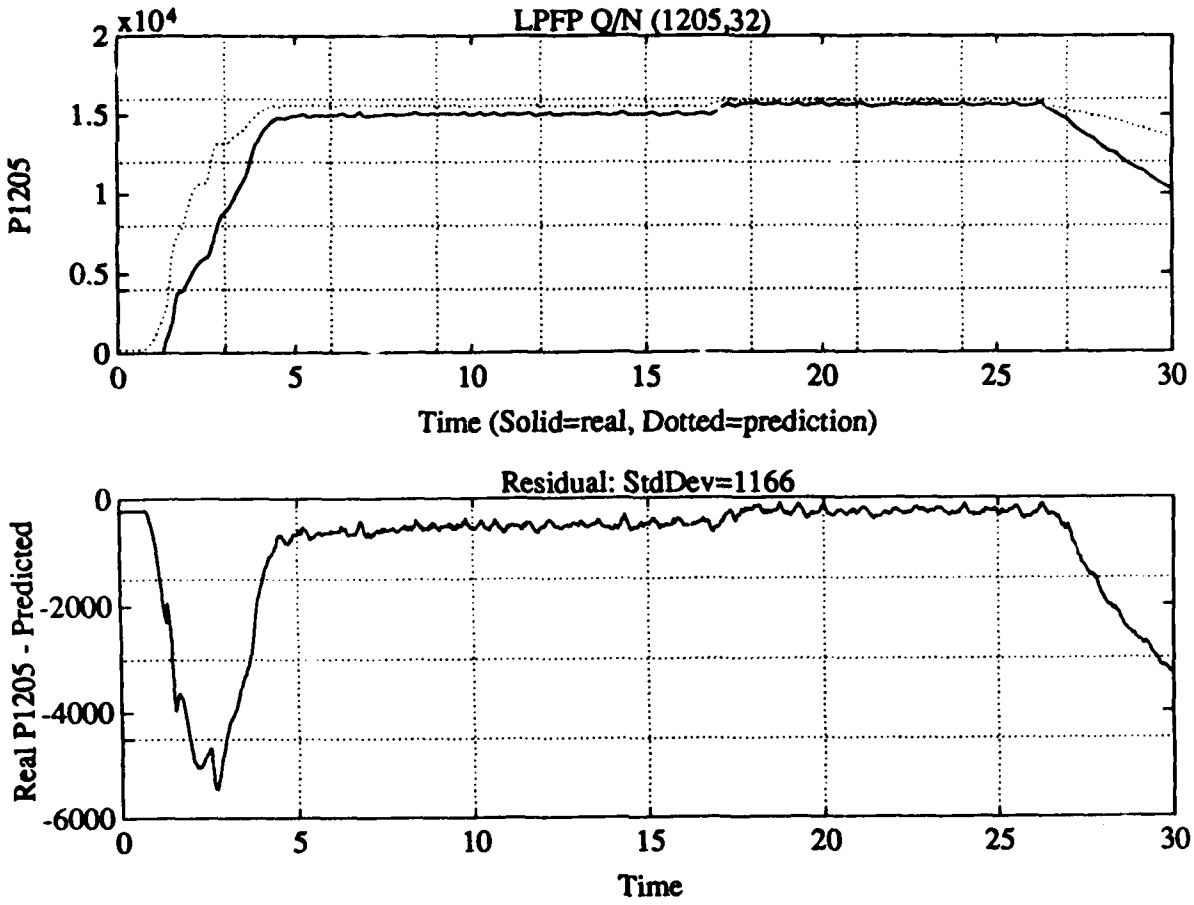
LPFP Q/N (1205,32)
x10^4
P1205
Time (Solid=real, Dotted=prediction)
Residual: StdDev=1166
Real P1205 - Predicted
Time

Fig 5

P +/- 200

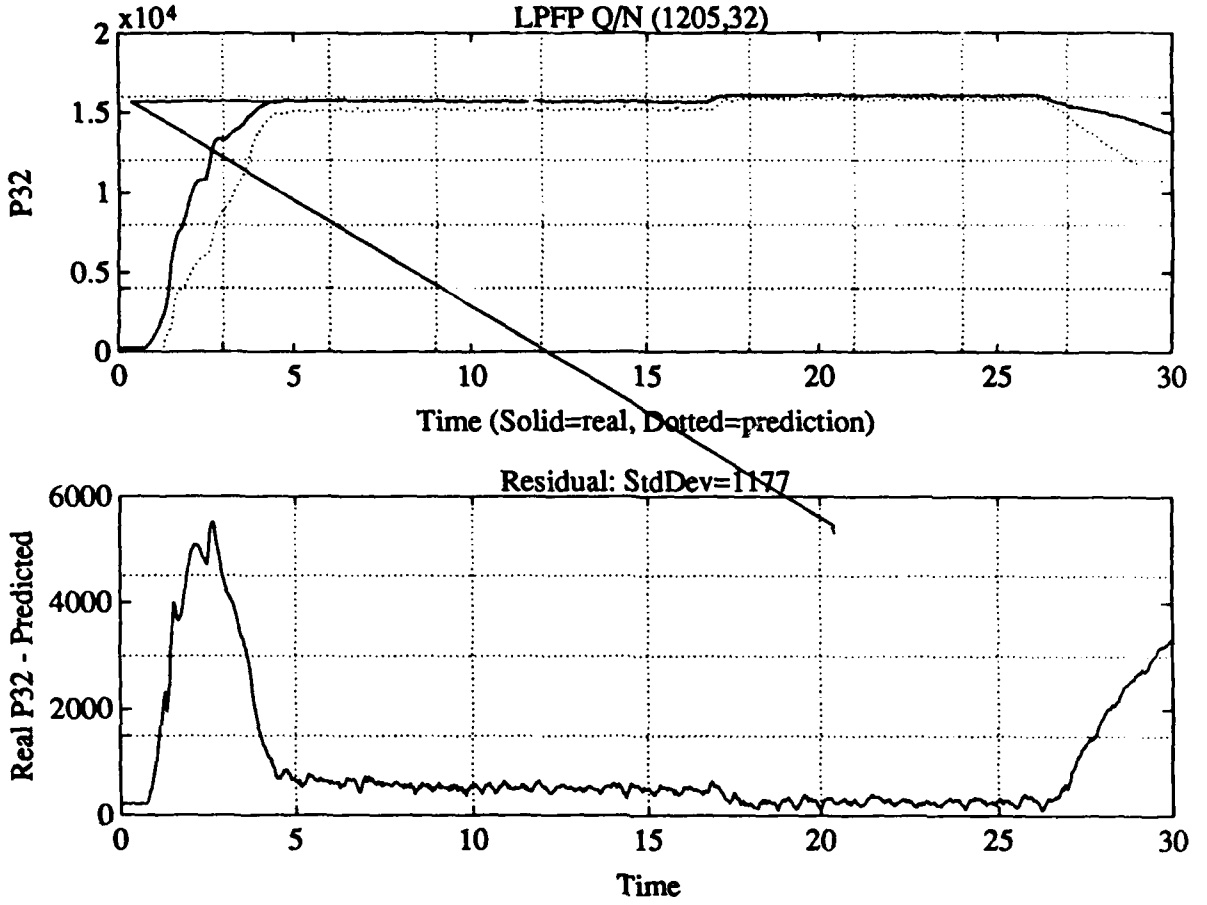
LPFP Q/N (1205,32)
x10^4
P32
Time (Solid=real, Dotted=prediction)
Residual: StdDev=1177
Real P32 - Predicted
Time

P +/- 198

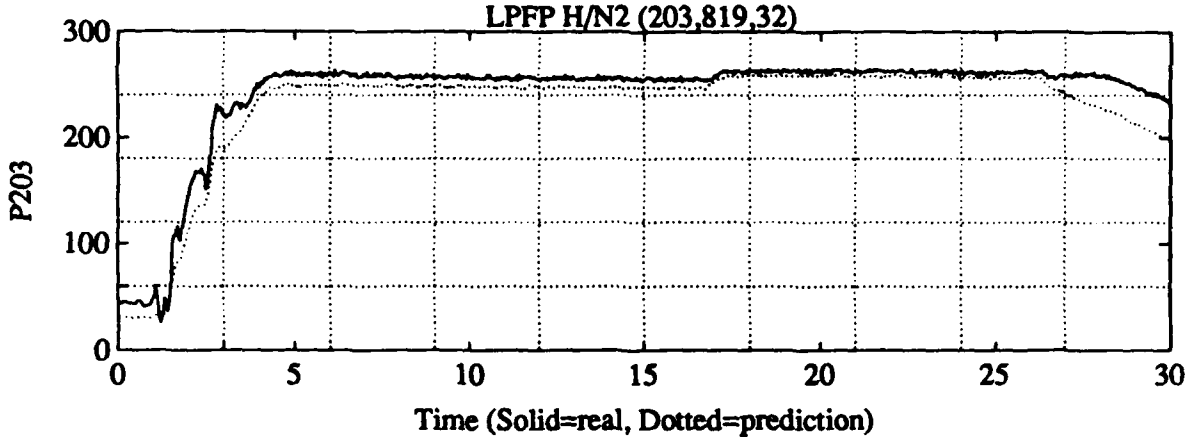
LPFP H/N2 (203,819,32)
P203
300
200
100
0
0
5
10
15
20
25
30
Time (Solid=real, Dotted=prediction)

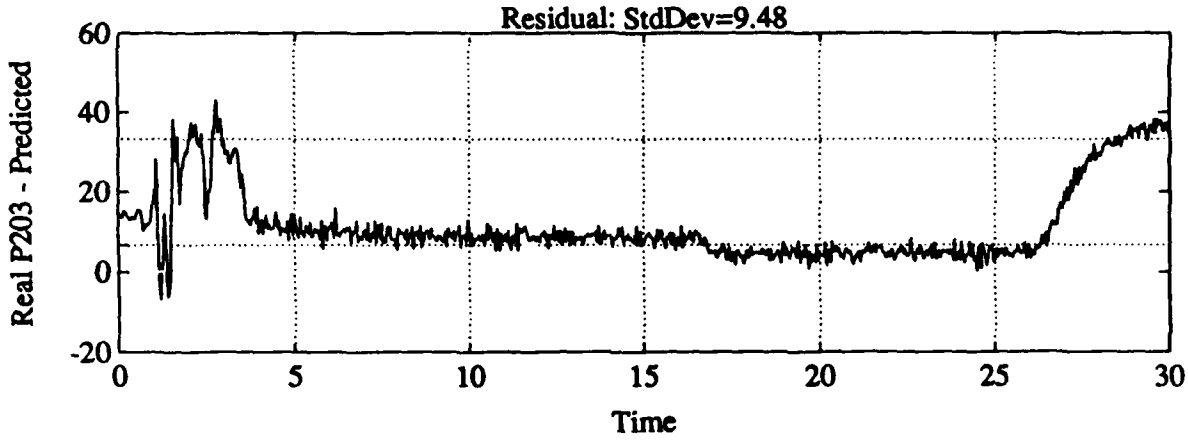
Residual: StdDev=9.48
Real P203 - Predicted
60
40
20
0
-20
0
5
10
15
20
25
30
Time

PT-6

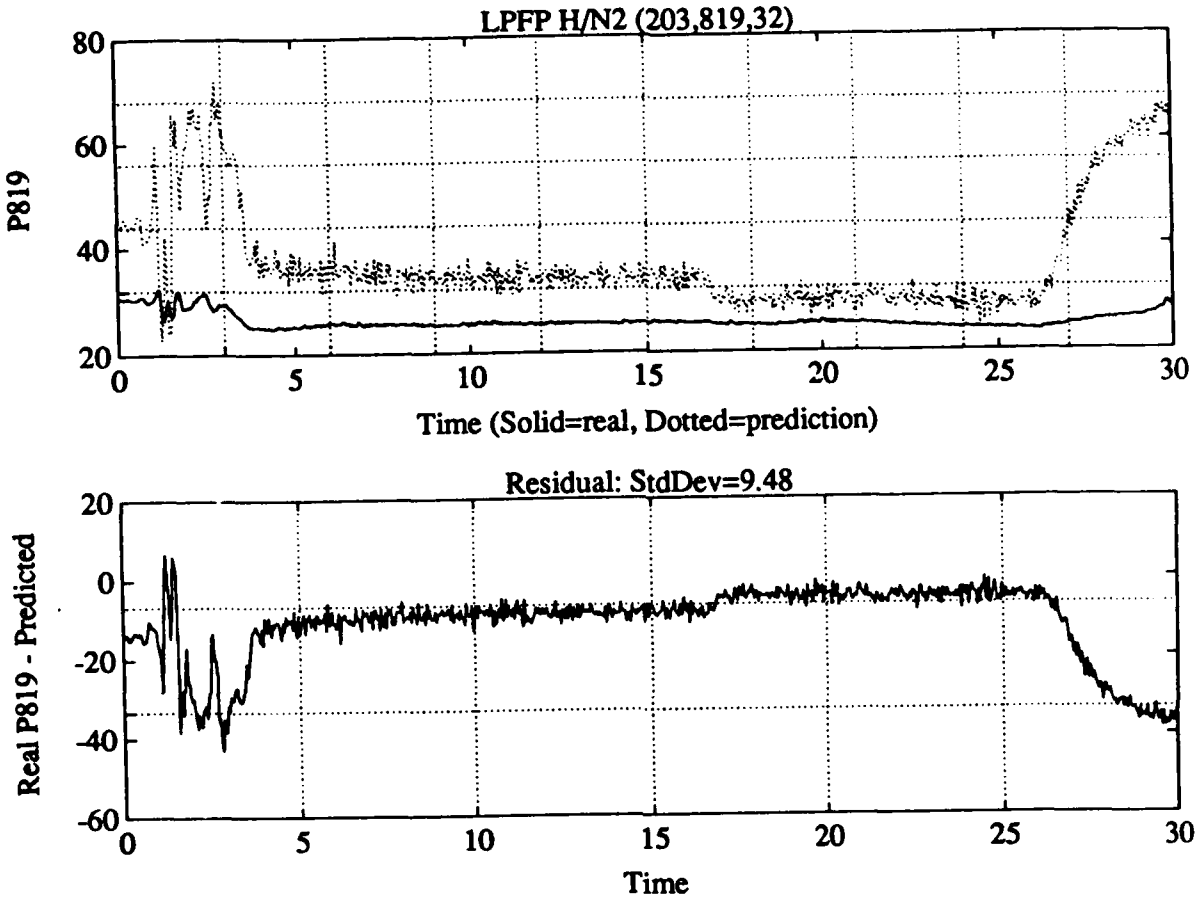
LPFP H/N2 (203,819,32)
P819
80
60
40
20
0
5
10
15
20
25
30
Time (Solid=real, Dotted=prediction)
Residual: StdDev=9.48
Real P819 - Predicted
20
0
-20
-40
-60
0
5
10
15
20
25
30
Time

P7/-2

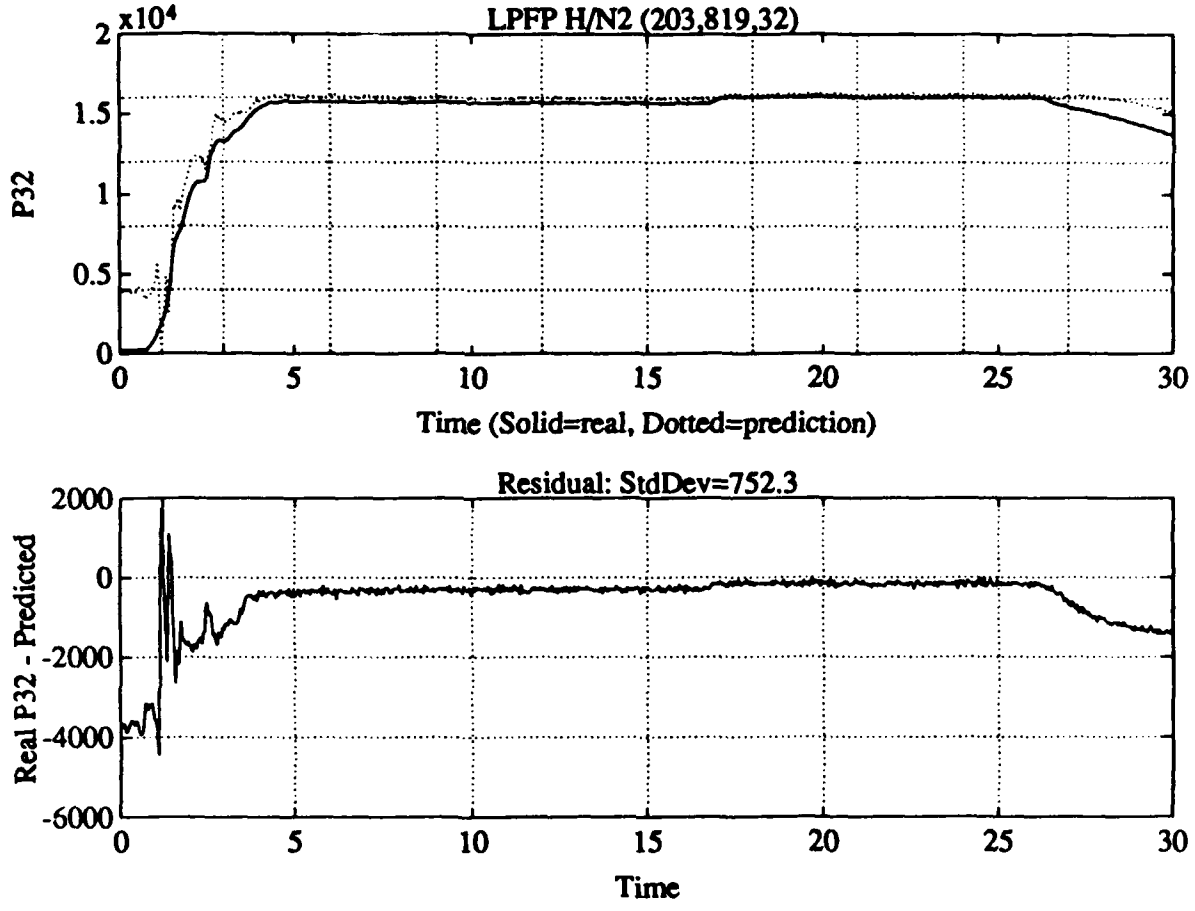
LPFP H/N2 (203,819,32)
x10^4
P32
Time (Solid=real, Dotted=prediction)
Residual: StdDev=752.3
Real P32 - Predicted
Time

P+/- 198

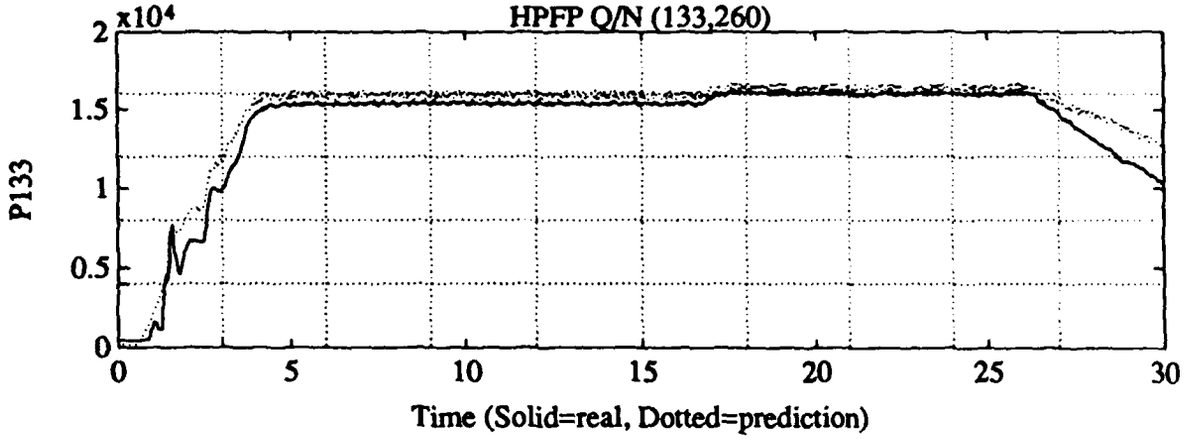
HPFP Q/N (133,260)
x10^4
P133
Time (Solid=real, Dotted=prediction)

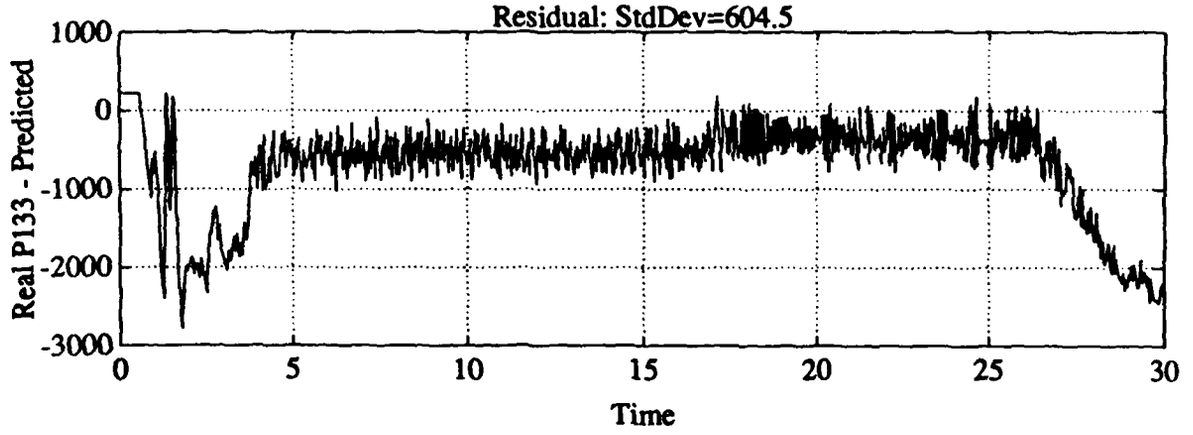
Residual: StdDev=604.5
Real P133 - Predicted
Time

PT-169

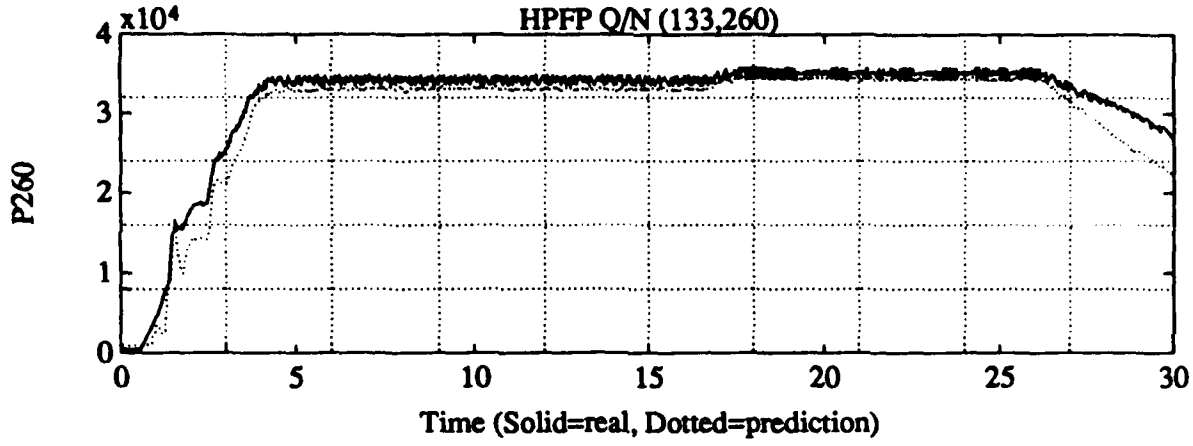
HPFP Q/N (133,260)
x10^4
P260
Time (Solid=real, Dotted=prediction)

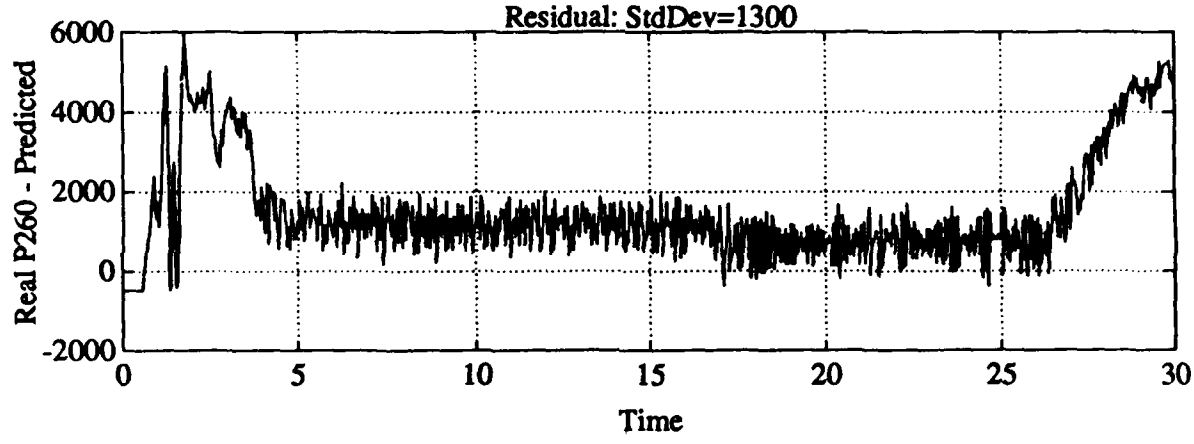
Residual: StdDev=1300
Real P260 - Predicted
Time

PT1-32

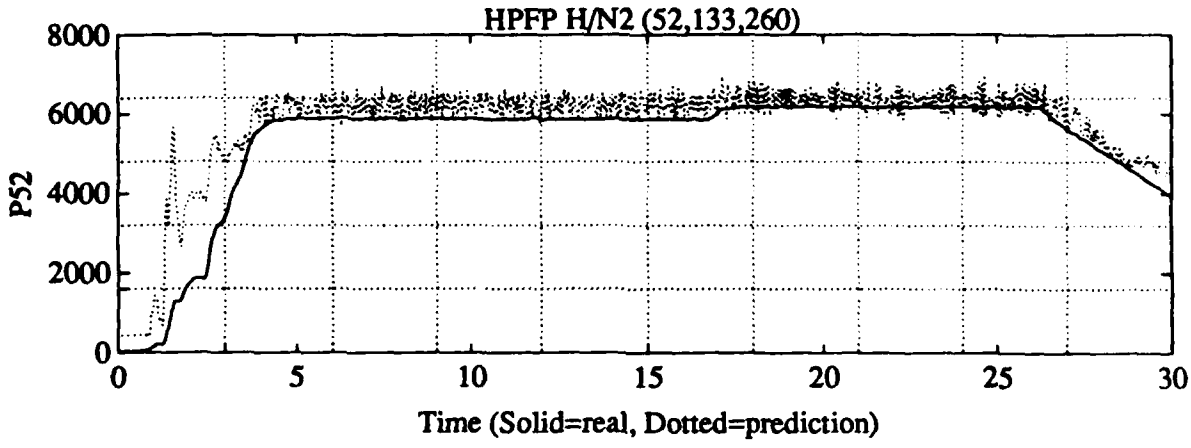
HPFP H/N2 (52,133,260)
P52
8000
6000
4000
2000
0
0
5
10
15
20
25
30
Time (Solid=real, Dotted=prediction)

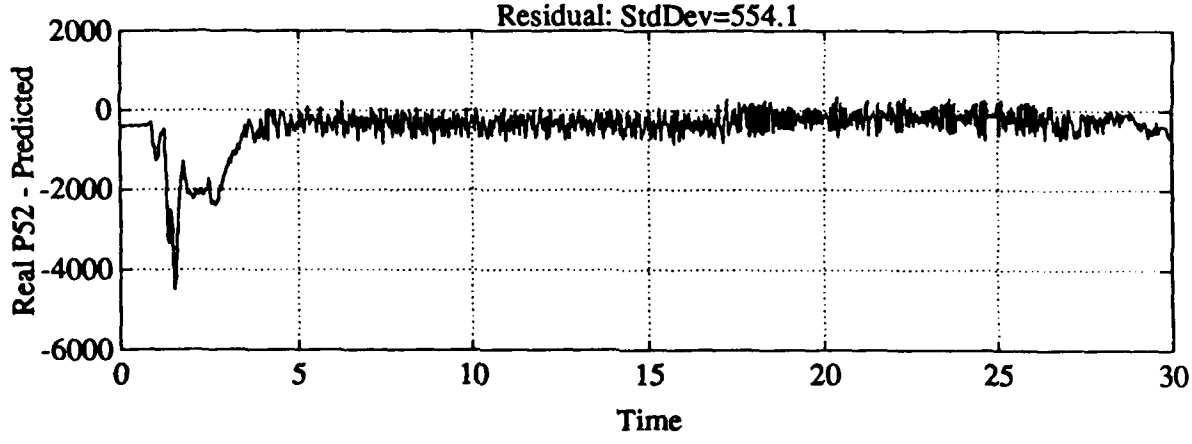
Residual: StdDev=554.1
Real P52 - Predicted
2000
0
-2000
-4000
-6000
0
5
10
15
20
25
30
Time

P+/- 190

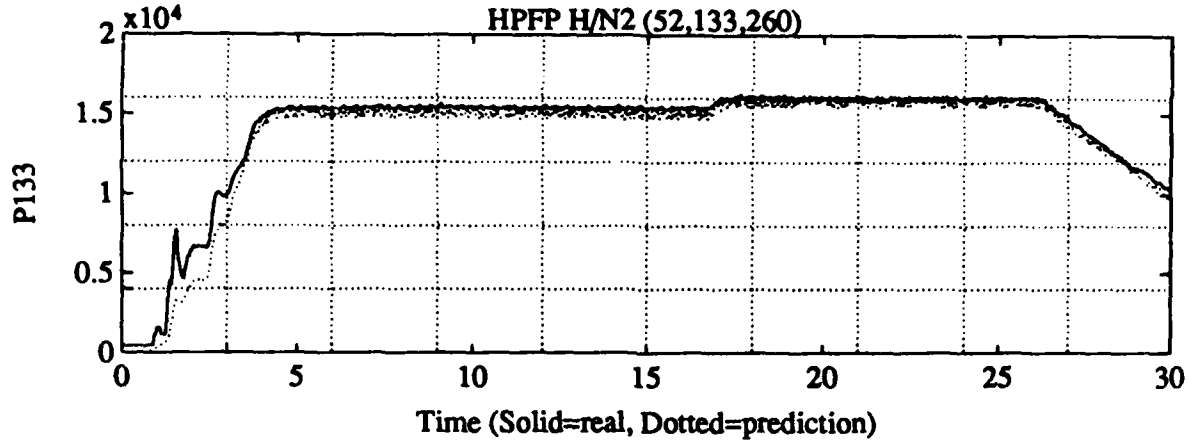
HPFP H/N2 (52,133,260)
x10^4
P133
Time (Solid=real, Dotted=prediction)

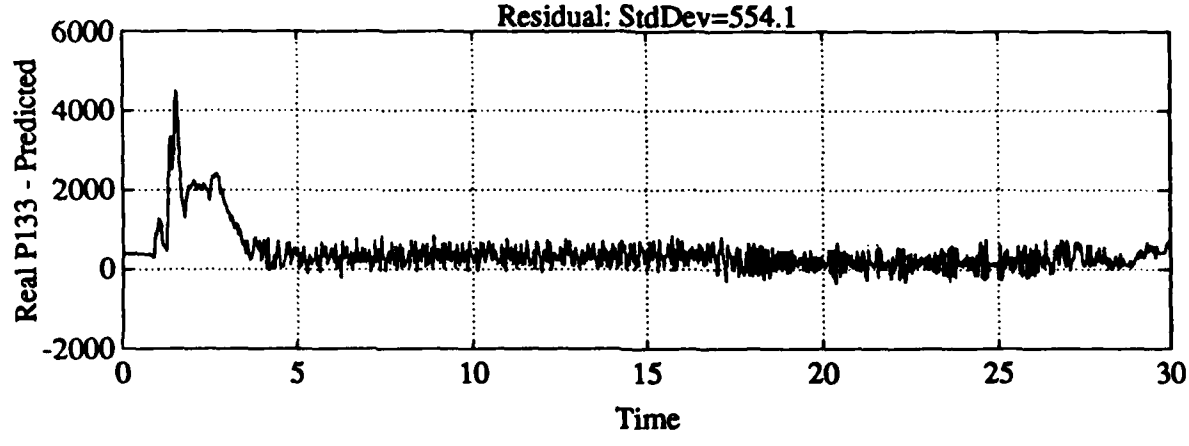
Residual: StdDev=554.1
Real P133 - Predicted
Time

P+/- 169

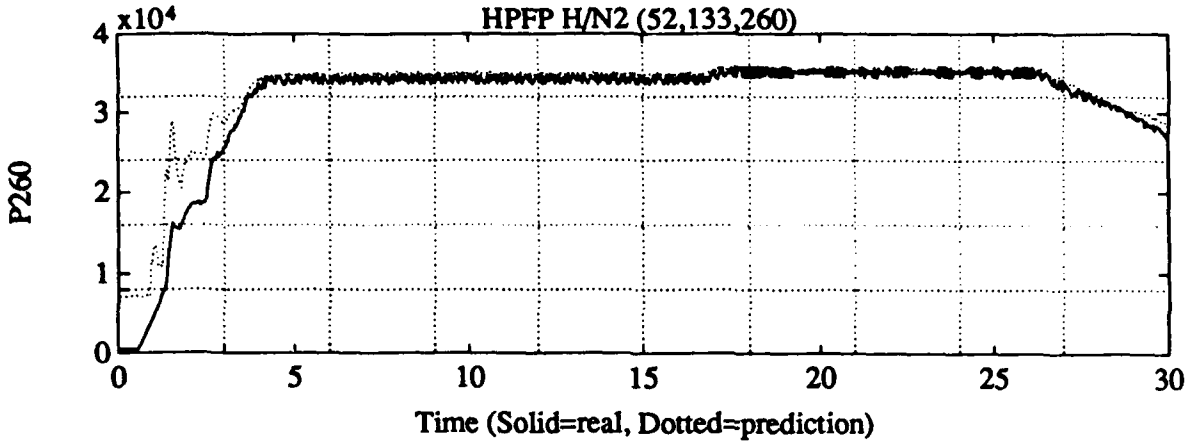
x10^4
HPFP H/N2 (52,133,260)
P260
4
3
2
1
0
0
5
10
15
20
25
30
Time (Solid=real, Dotted=prediction)

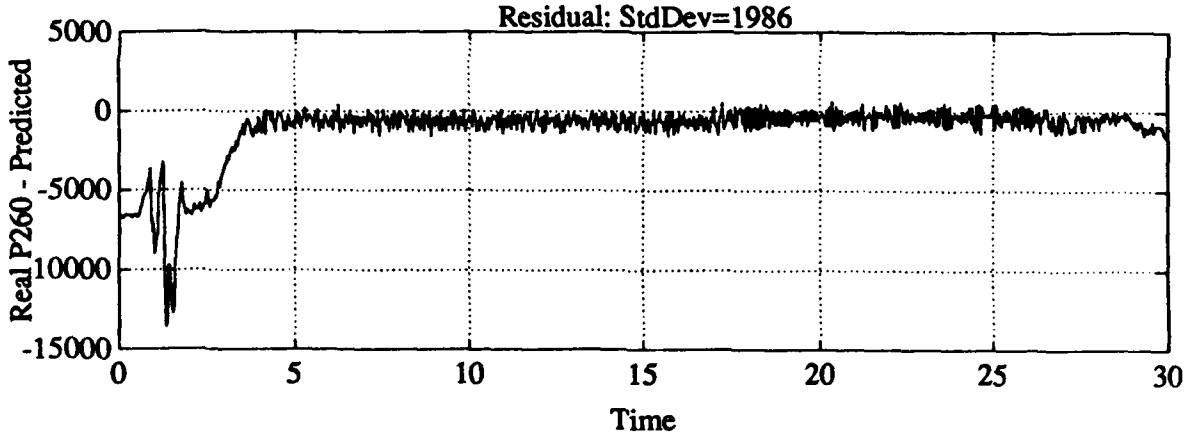
Residual: StdDev=1986
Real P260 - Predicted
5000
0
-5000
-10000
-15000
0
5
10
15
20
25
30
Time

P+/- 31.5

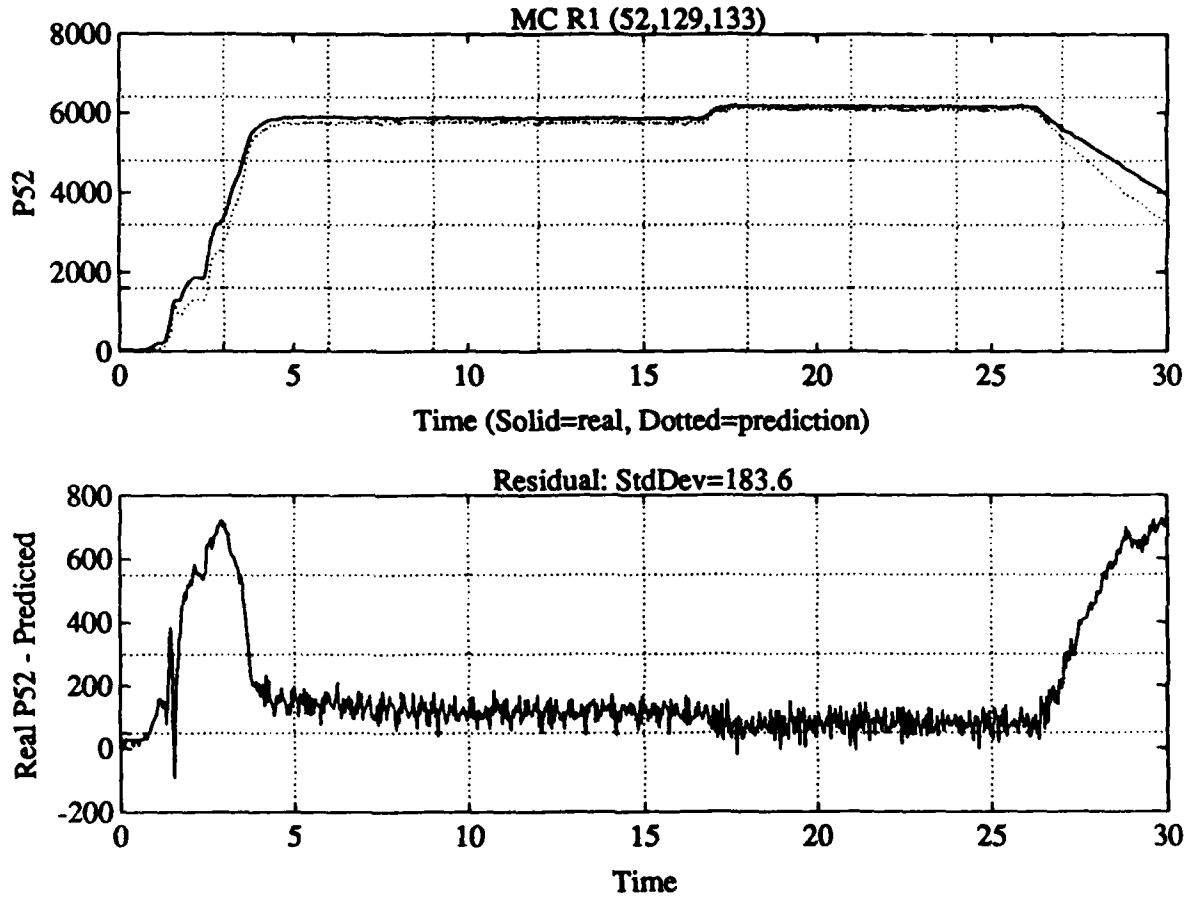
MC R1 (52,129,133)
P52
8000
6000
4000
2000
0
0
5
10
15
20
25
30
Time (Solid=real, Dotted=prediction)
Residual: StdDev=183.6
Real P52 - Predicted
800
600
400
200
0
-200
0
5
10
15
20
25
30
Time

P +/- 190

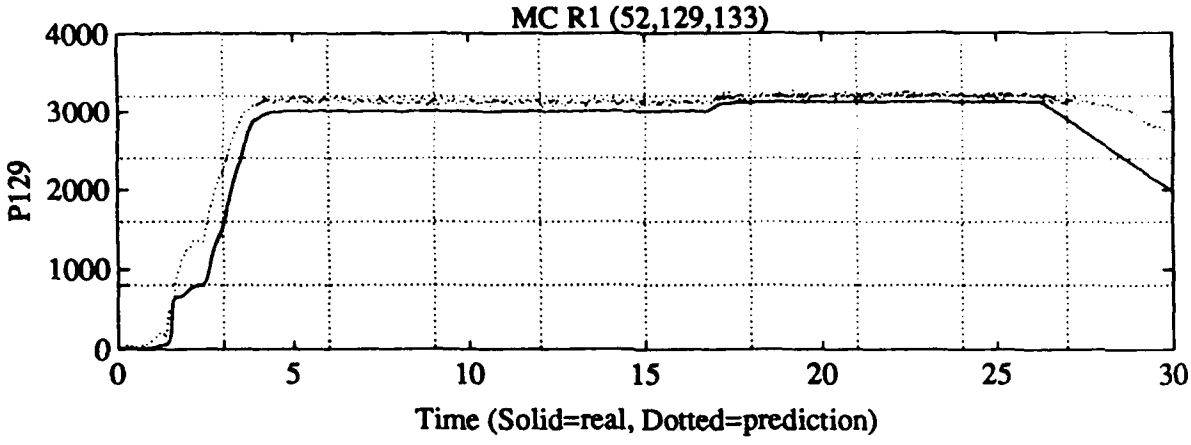
MC R1 (52,129,133)
P129
4000
3000
2000
1000
0
0
5
10
15
20
25
30
Time (Solid=real, Dotted=prediction)

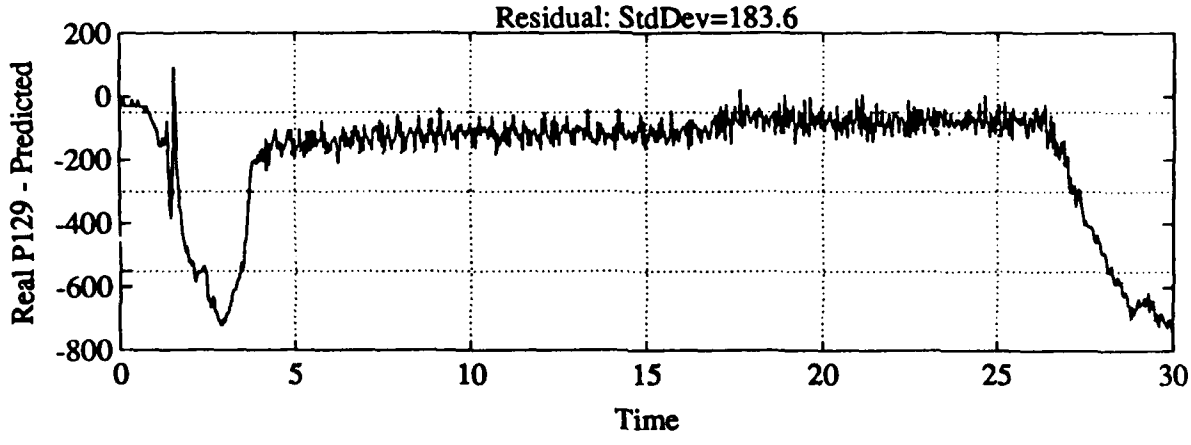
Residual: StdDev=183.6
Real P129 - Predicted
200
0
-200
-400
-600
-800
0
5
10
15
20
25
30
Time

P+/-70

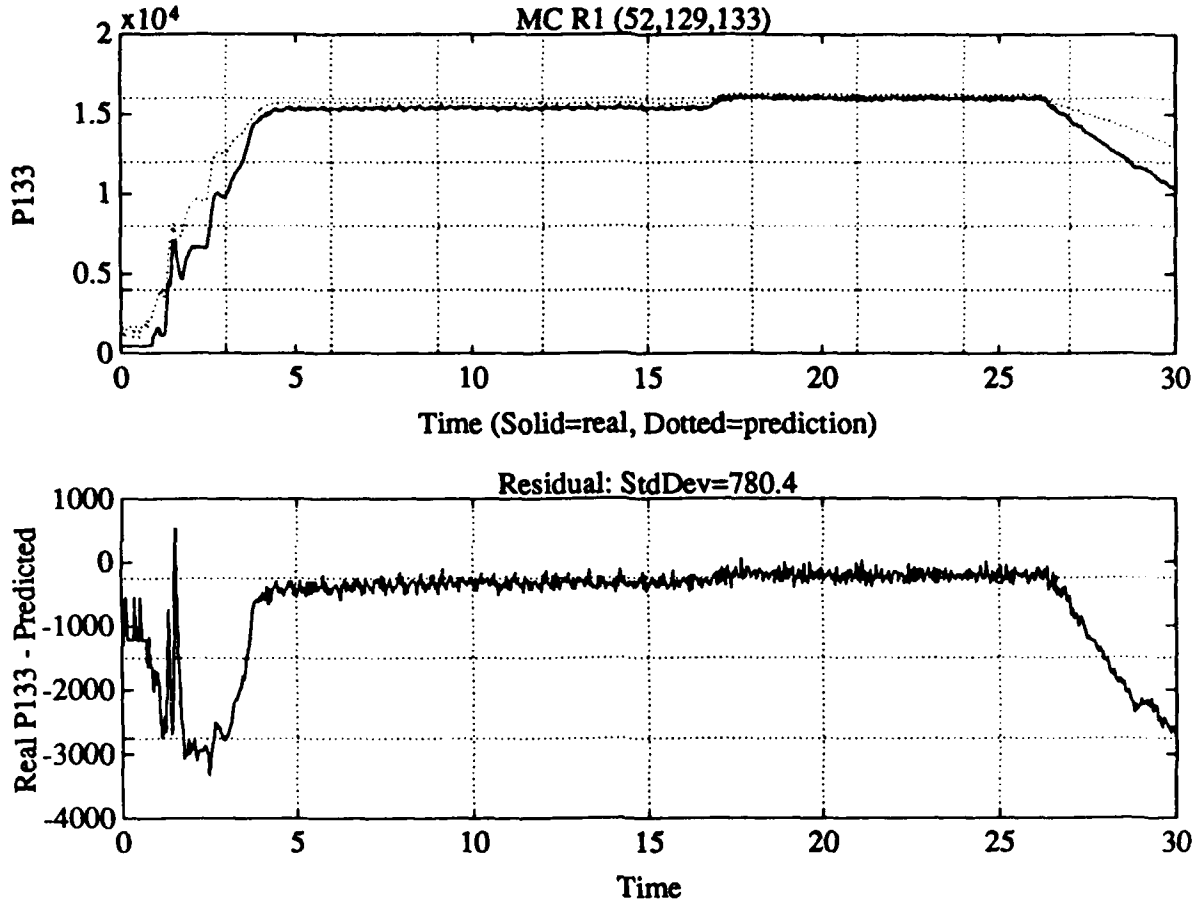
MC R1 (52,129,133)
x10^4
P133
Time (Solid=real, Dotted=prediction)
Residual: StdDev=780.4
Real P133 - Predicted
Time

p+/- 169

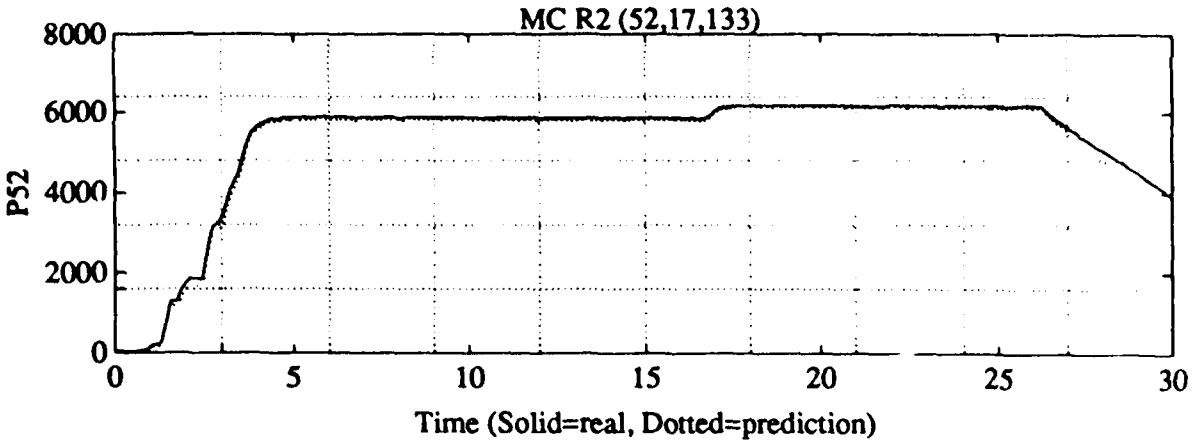
MC R2 (52,17,133)
P52
8000
6000
4000
2000
0
0
5
10
15
20
25
30
Time (Solid=real, Dotted=prediction)

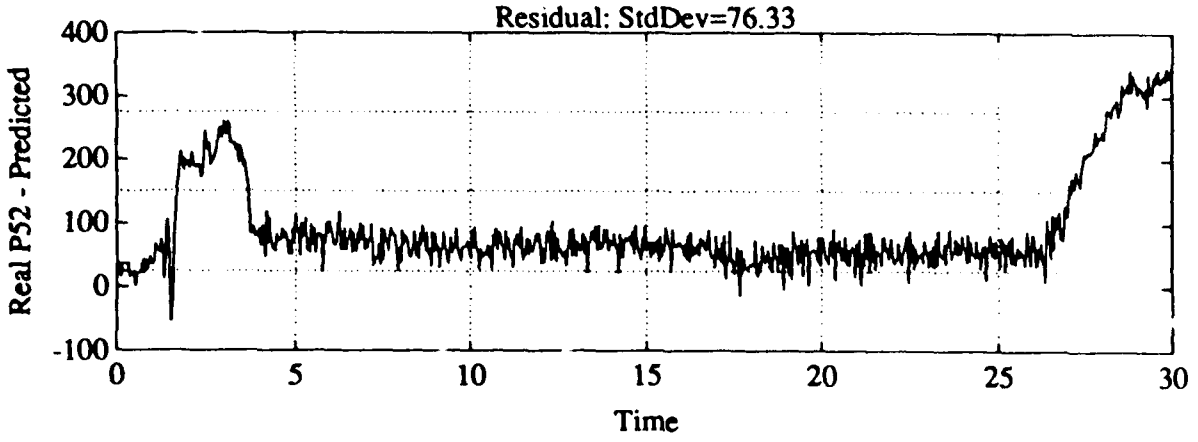
Residual: StdDev=76.33
Real P52 - Predicted
400
300
200
100
0
-100
0
5
10
15
20
25
30
Time

P+/-190

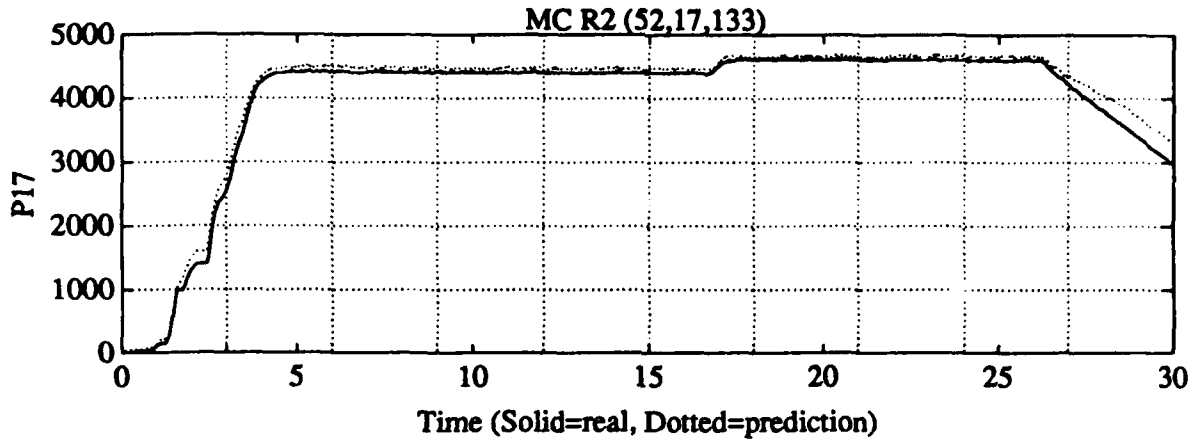
MC R2 (52,17,133)
P17
5000
4000
3000
2000
1000
0
0
5
10
15
20
25
30
Time (Solid=real, Dotted=prediction)

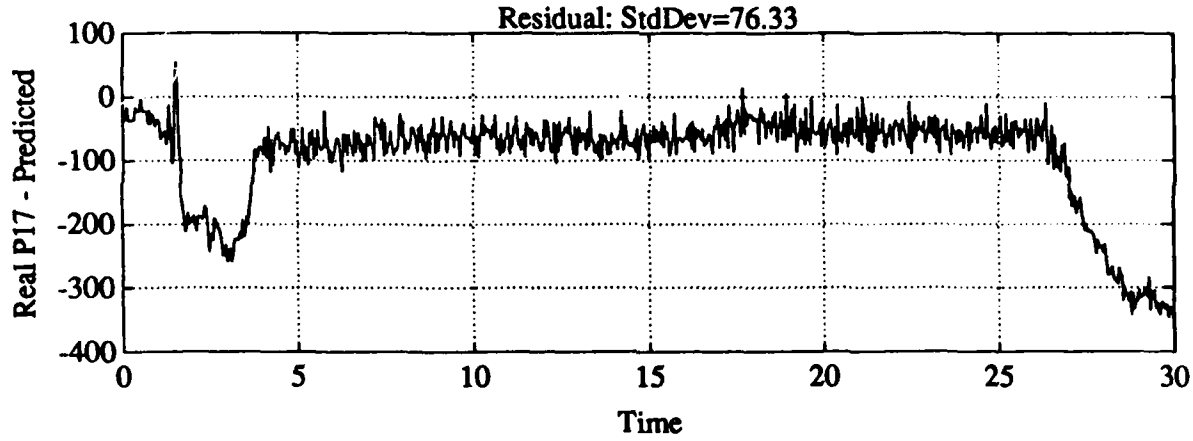
Residual: StdDev=76.33
Real P17 - Predicted
100
0
-100
-200
-300
-400
0
5
10
15
20
25
30
Time

PT/-140

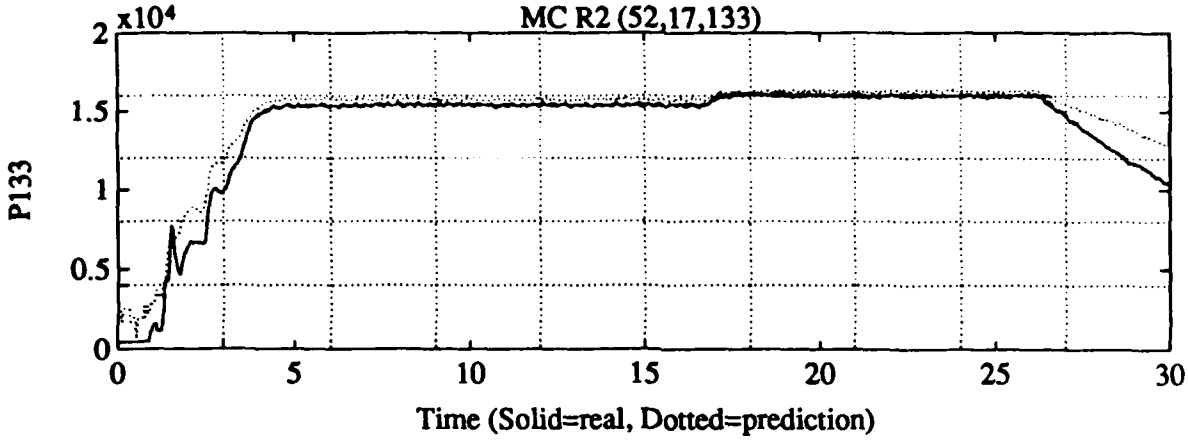
MC R2 (52,17,133)
x10^4
P133
Time (Solid=real, Dotted=prediction)

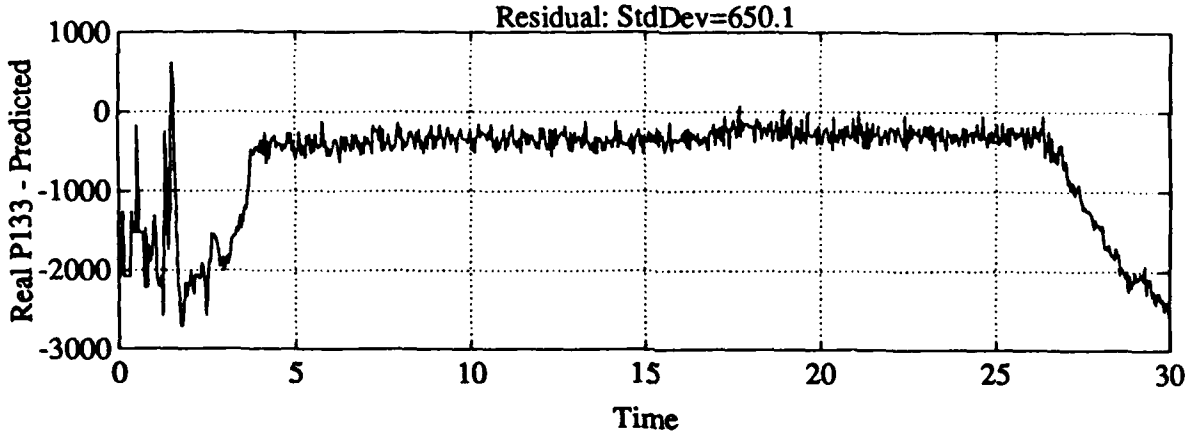
Residual: StdDev=650.1
Real P133 - Predicted
Time

P+/-169

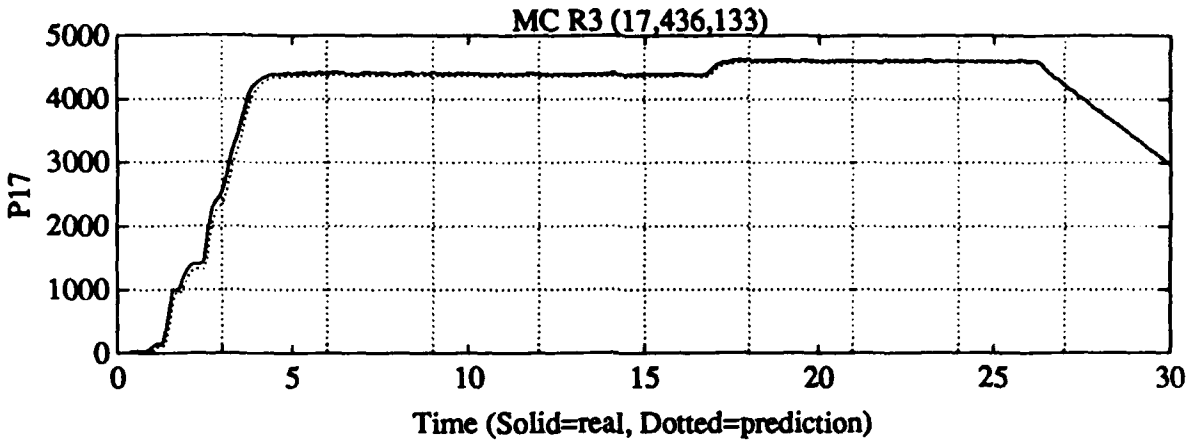
MC R3 (17,436,133)
P17
5000
4000
3000
2000
1000
0
0
5
10
15
20
25
30
Time (Solid=real, Dotted=prediction)

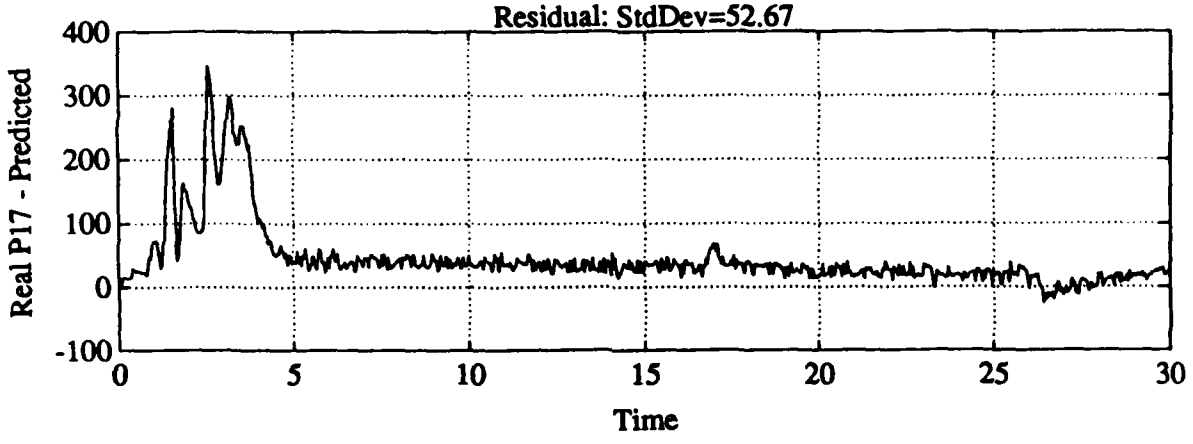
Residual: StdDev=52.67
Real P17 - Predicted
400
300
200
100
0
-100
0
5
10
15
20
25
30
Time

P +/- 140

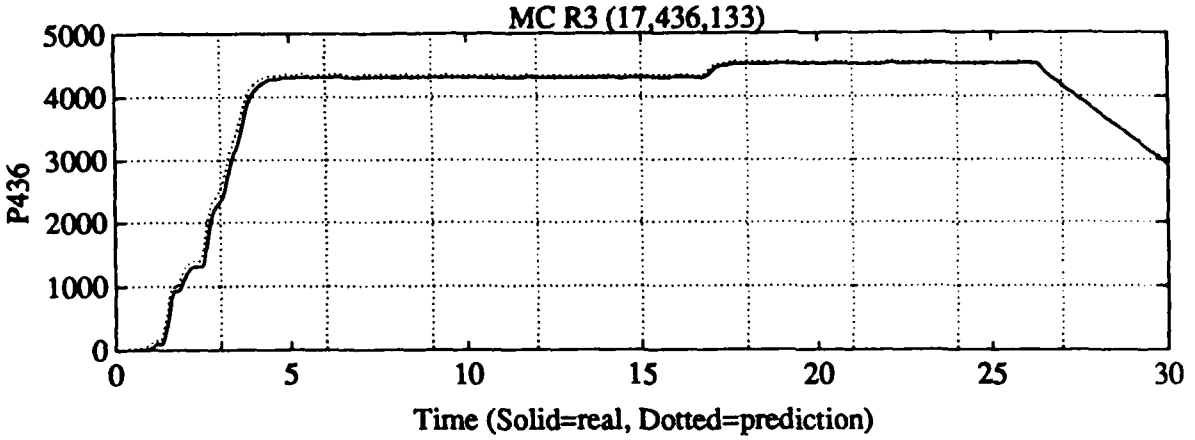
MC R3 (17,436,133)
P436
5000
4000
3000
2000
1000
0
0
5
10
15
20
25
30
Time (Solid=real, Dotted=prediction)

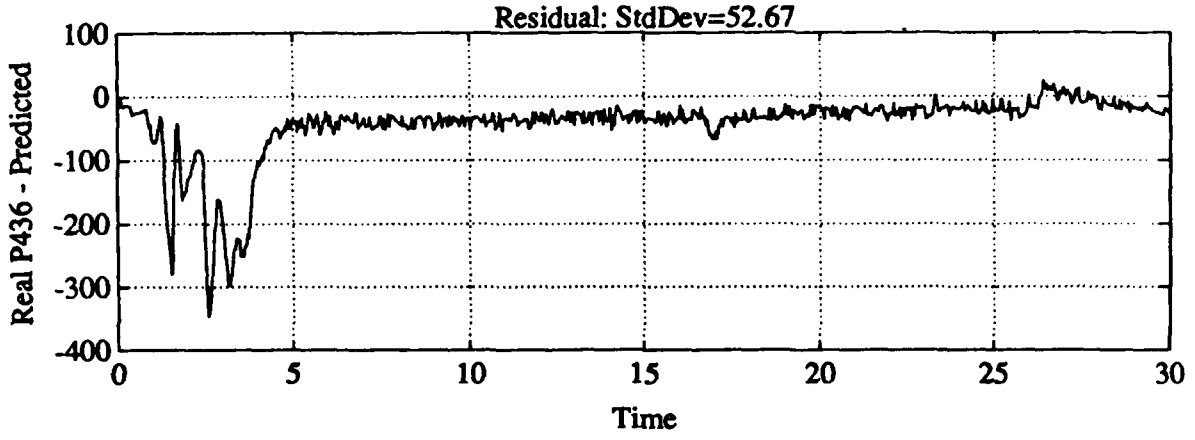
Residual: StdDev=52.67
Real P436 - Predicted
100
0
-100
-200
-300
-400
0
5
10
15
20
25
30
Time

P+/- 50

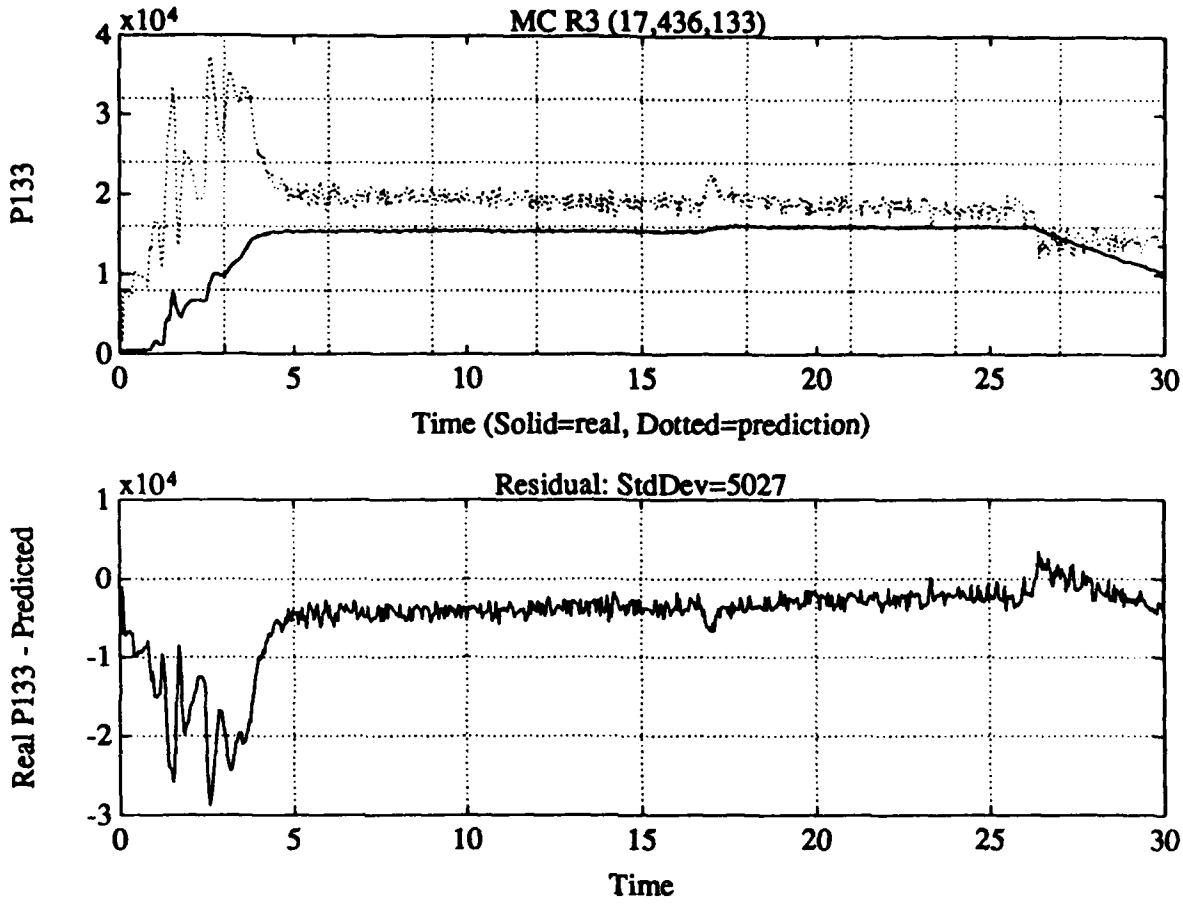
MC R3 (17,436,133)
x10^4
P133
Time (Solid=real, Dotted=prediction)
Residual: StdDev=5027
x10^4
Real P133 - Predicted
Time

8+1-169

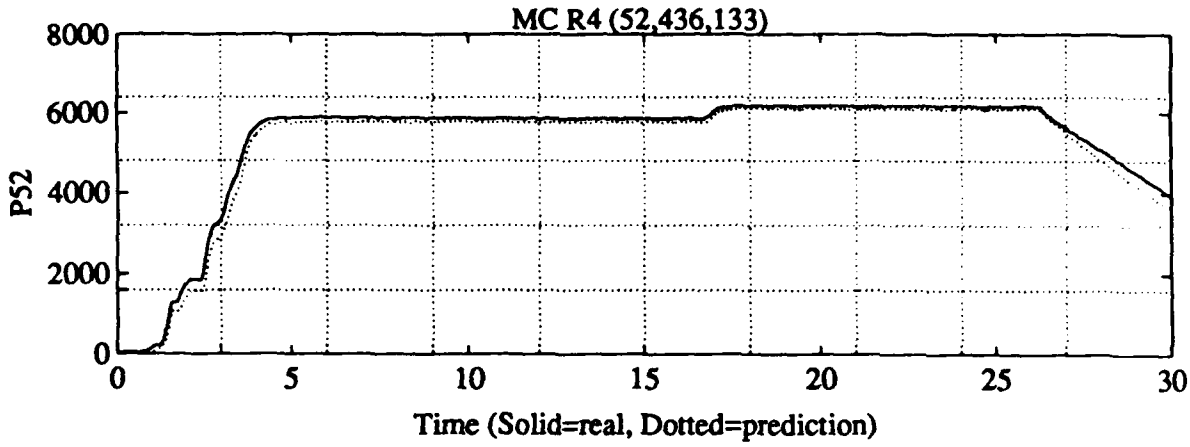
MC R4 (52,436,133)
P52
8000
6000
4000
2000
0
0
5
10
15
20
25
30
Time (Solid=real, Dotted=prediction)

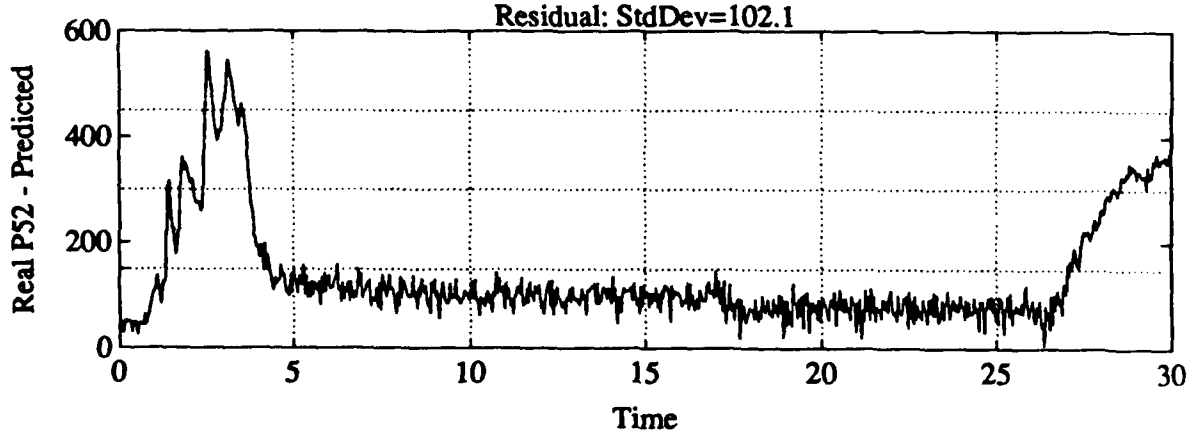
Residual: StdDev=102.1
Real P52 - Predicted
600
400
200
0
0
5
10
15
20
25
30
Time

P+/-190

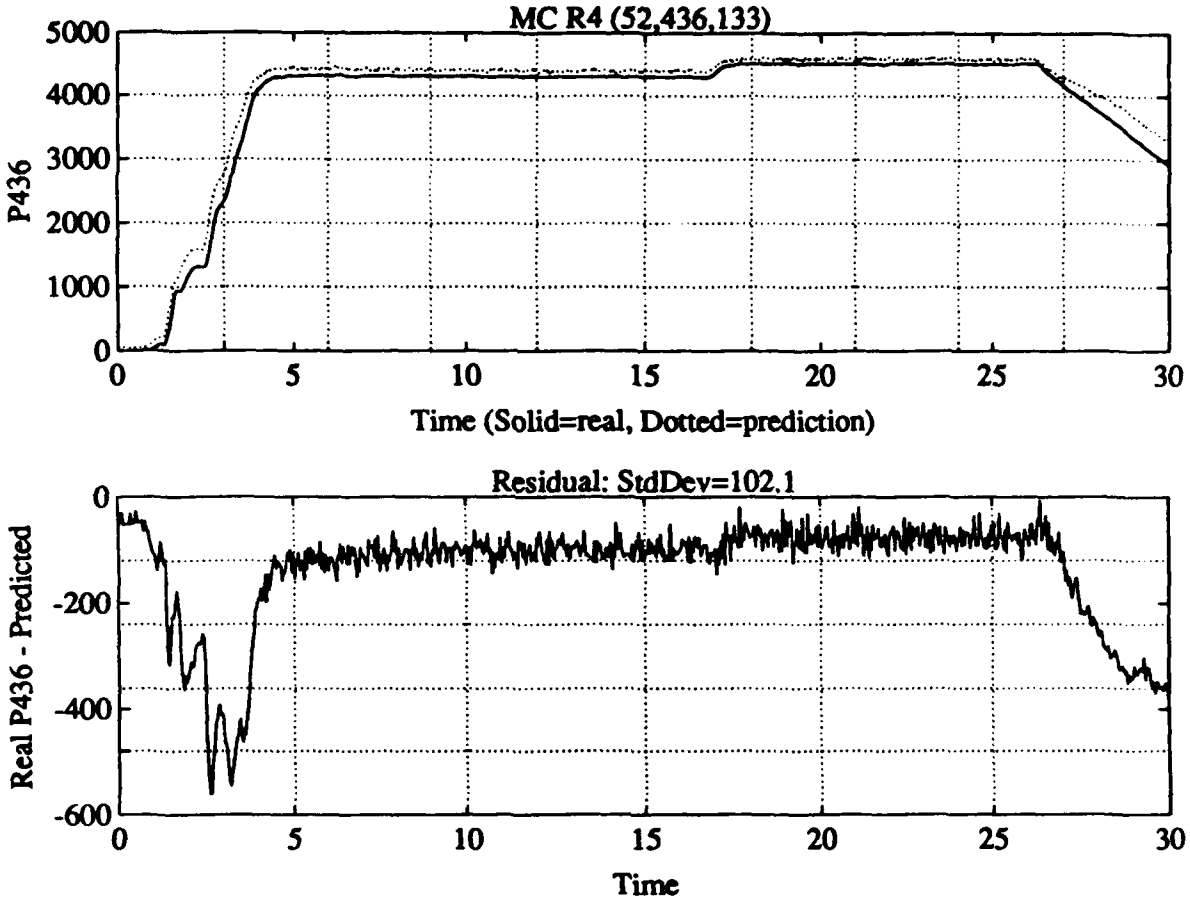
MC R4 (52,436,133)
P436
5000
4000
3000
2000
1000
0
0
5
10
15
20
25
30
Time (Solid=real, Dotted=prediction)
Residual: StdDev=102.1
Real P436 - Predicted
0
-200
-400
-600
0
5
10
15
20
25
30
Time

P+/- 50

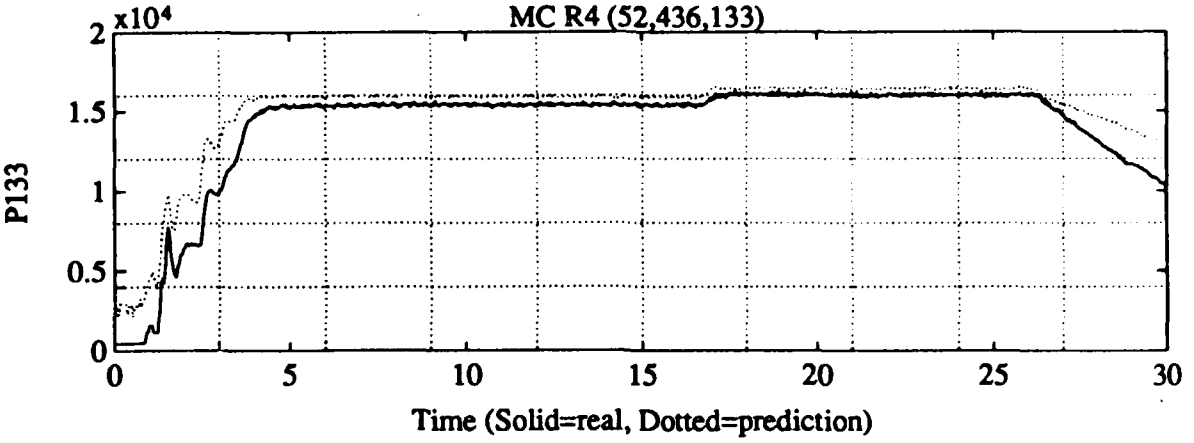
MC R4 (52,436,133)
x10^4
P133
Time (Solid=real, Dotted=prediction)

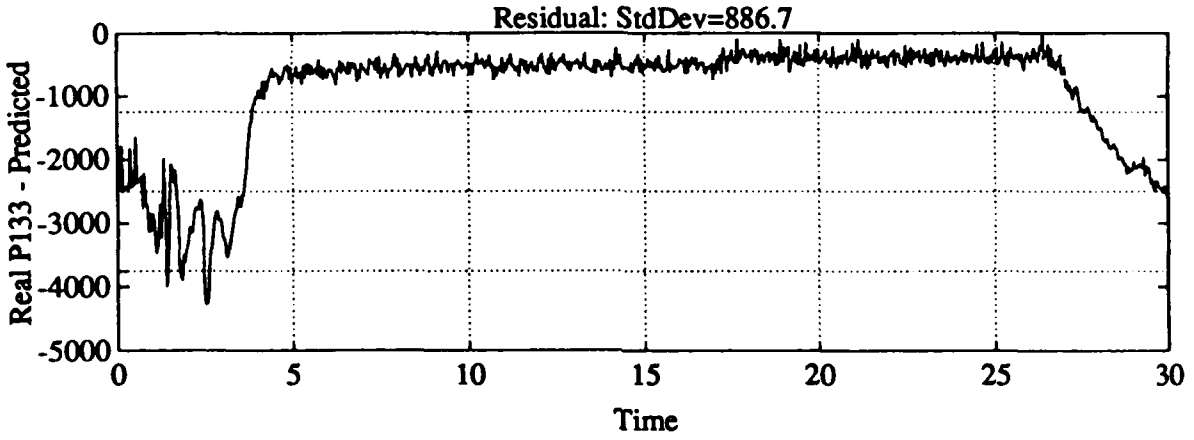
Residual: StdDev=886.7
Real P133 - Predicted
Time

87/-169

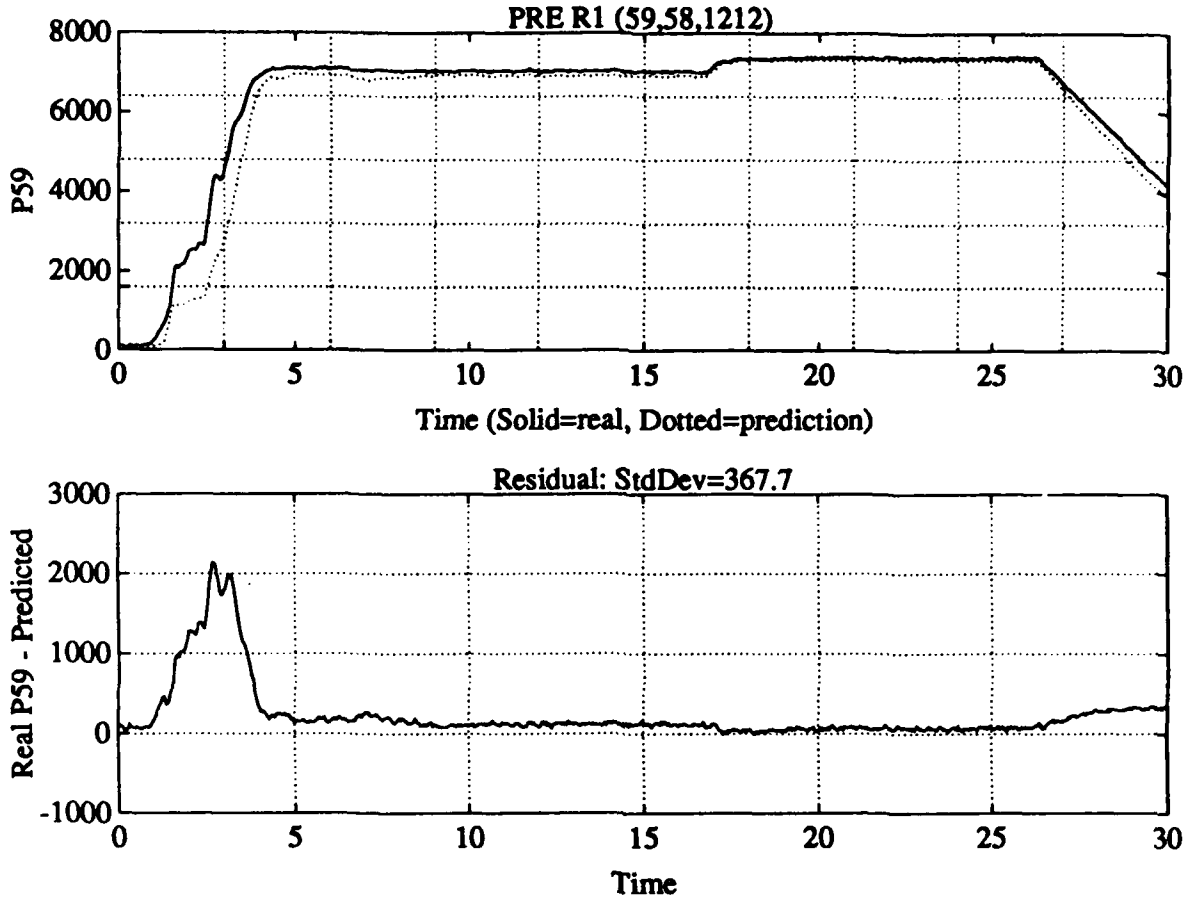
PRE R1 (59,58,1212)
P59
Time (Solid=real, Dotted=prediction)
Residual: StdDev=367.7
Real P59 - Predicted
Time

P +/- 100

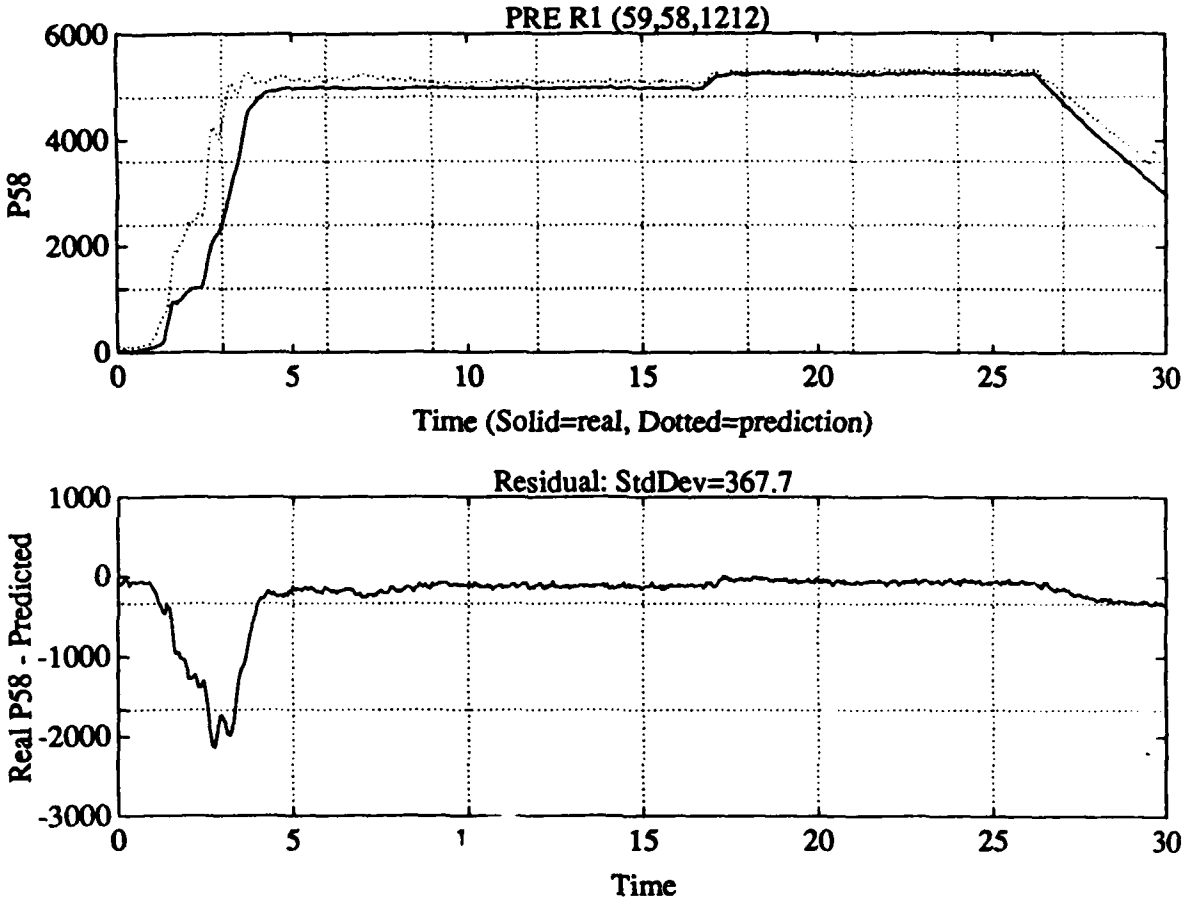
PRE R1 (59,58,1212)
P58
Time (Solid=real, Dotted=prediction)
Residual: StdDev=367.7
Real P58 - Predicted
Time

P+/- 140

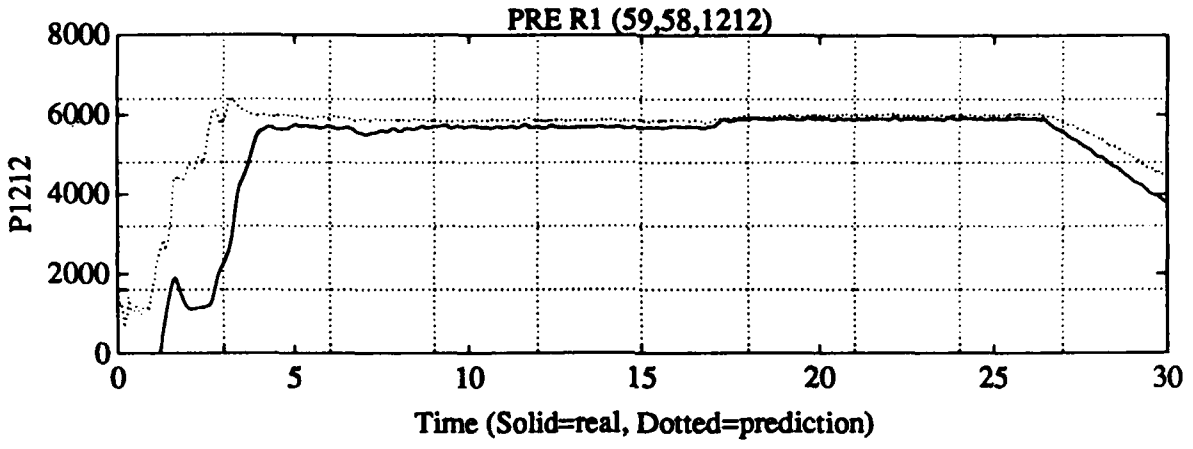
PRE R1 (59,58,1212)
P1212
8000
6000
4000
2000
0
0
5
10
15
20
25
30
Time (Solid=real, Dotted=prediction)

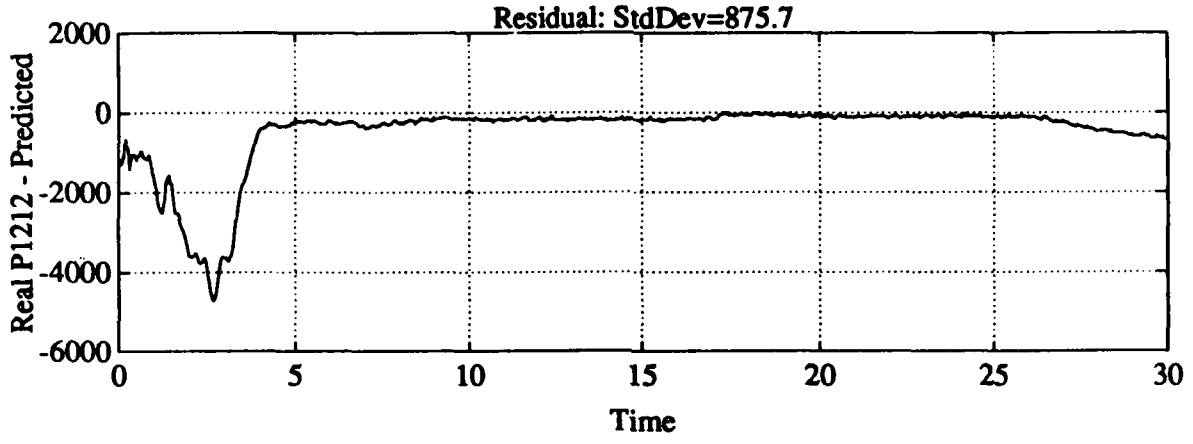
Residual: StdDev=875.7
Real P1212 - Predicted
2000
0
-2000
-4000
-6000
0
5
10
15
20
25
30
Time

P+/- 85

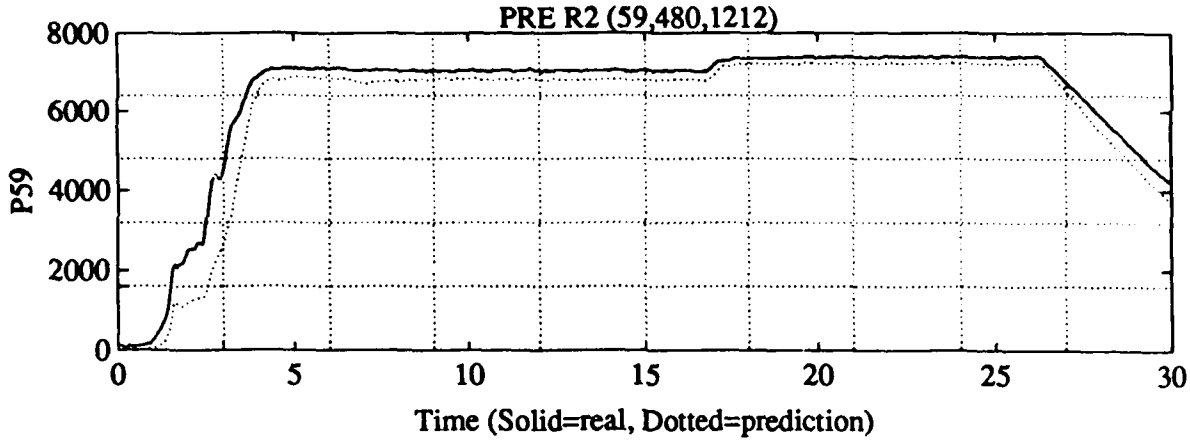
PRE R2 (59,480,1212)
P59
8000
6000
4000
2000
0
0
5
10
15
20
25
30
Time (Solid=real, Dotted=prediction)

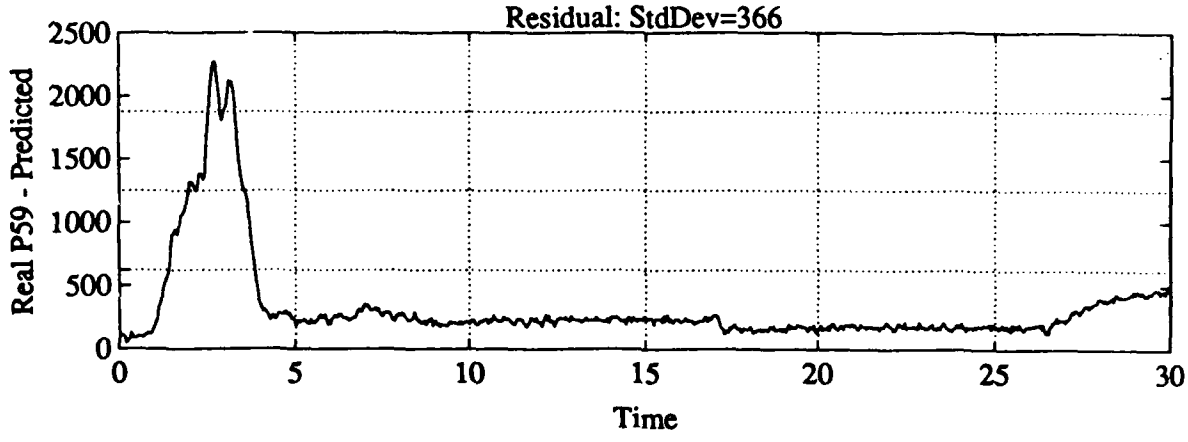
Residual: StdDev=366
Real P59 - Predicted
2500
2000
1500
1000
500
0
0
5
10
15
20
25
30
Time

PT/-190

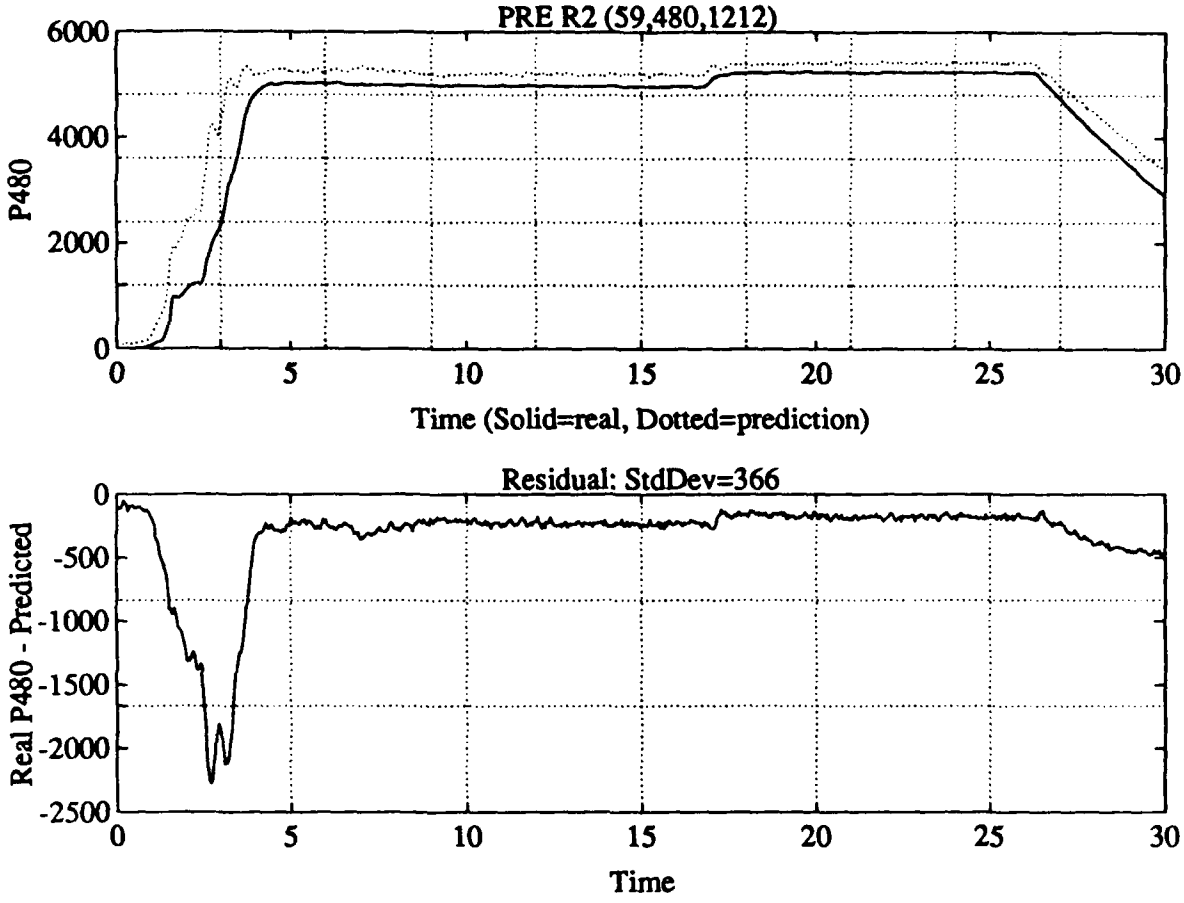
PRE R2 (59,480,1212)
6000
4000
2000
0
P480
0
5
10
15
20
25
30
Time (Solid=real, Dotted=prediction)
Residual: StdDev=366
0
-500
-1000
-1500
-2000
-2500
Real P480 - Predicted
0
5
10
15
20
25
30
Time

P+/-200

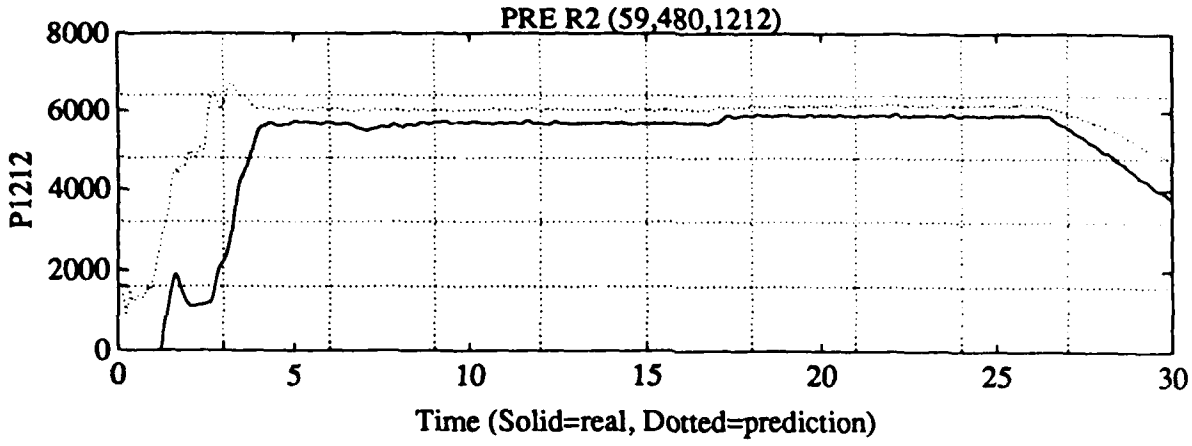
PRE R2 (59,480,1212)
P1212
8000
6000
4000
2000
0
0
5
10
15
20
25
30
Time (Solid=real, Dotted=prediction)

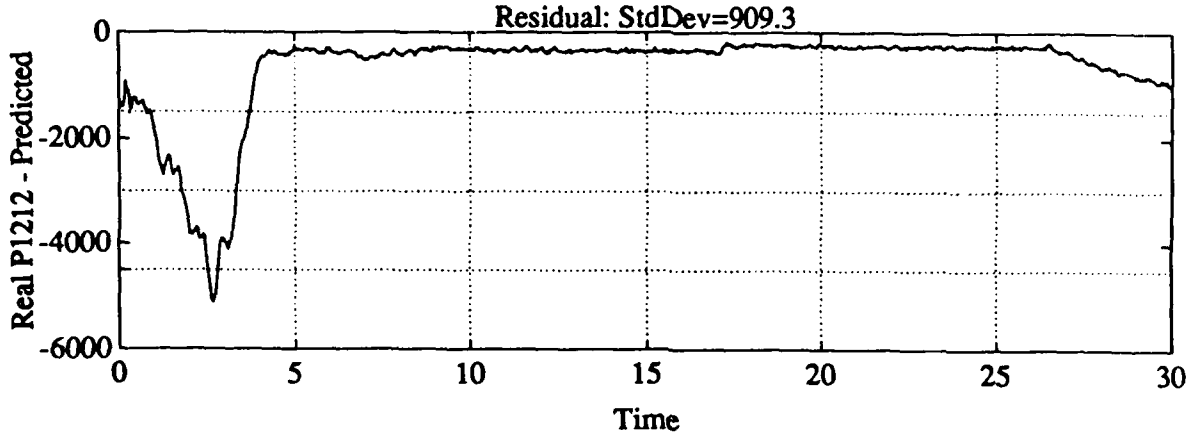
Residual: StdDev=909.3
Real P1212 - Predicted
0
-2000
-4000
-6000
0
5
10
15
20
25
30
Time

P4-85

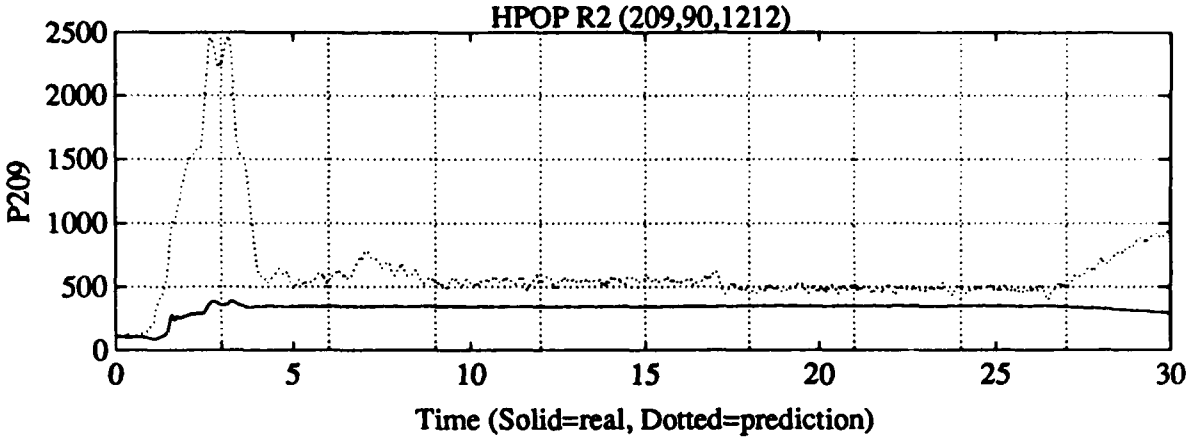
HPOP R2 (209,90,1212)
P209
2500
2000
1500
1000
500
0
0
5
10
15
20
25
30
Time (Solid=real, Dotted=prediction)

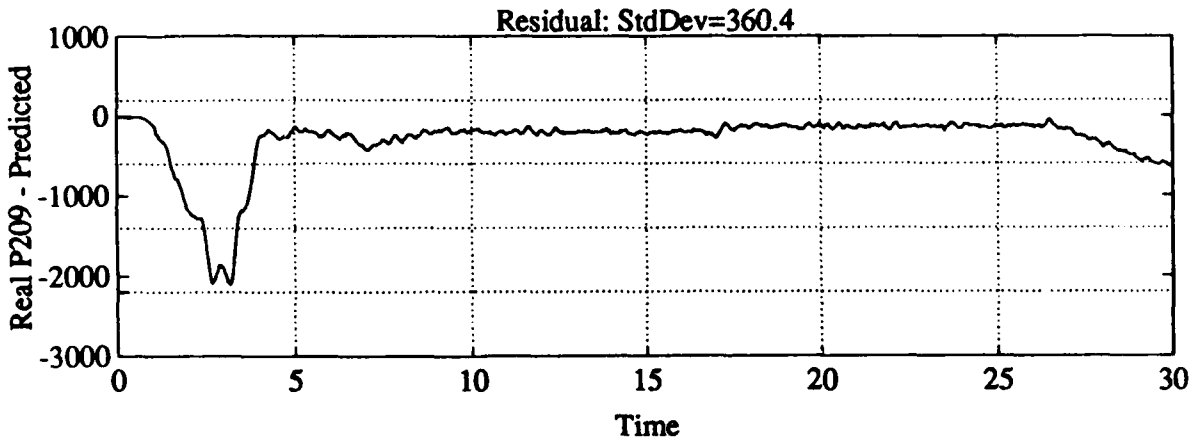
Residual: StdDev=360.4
Real P209 - Predicted
1000
0
-1000
-2000
-3000
0
5
10
15
20
25
30
Time

PH-18

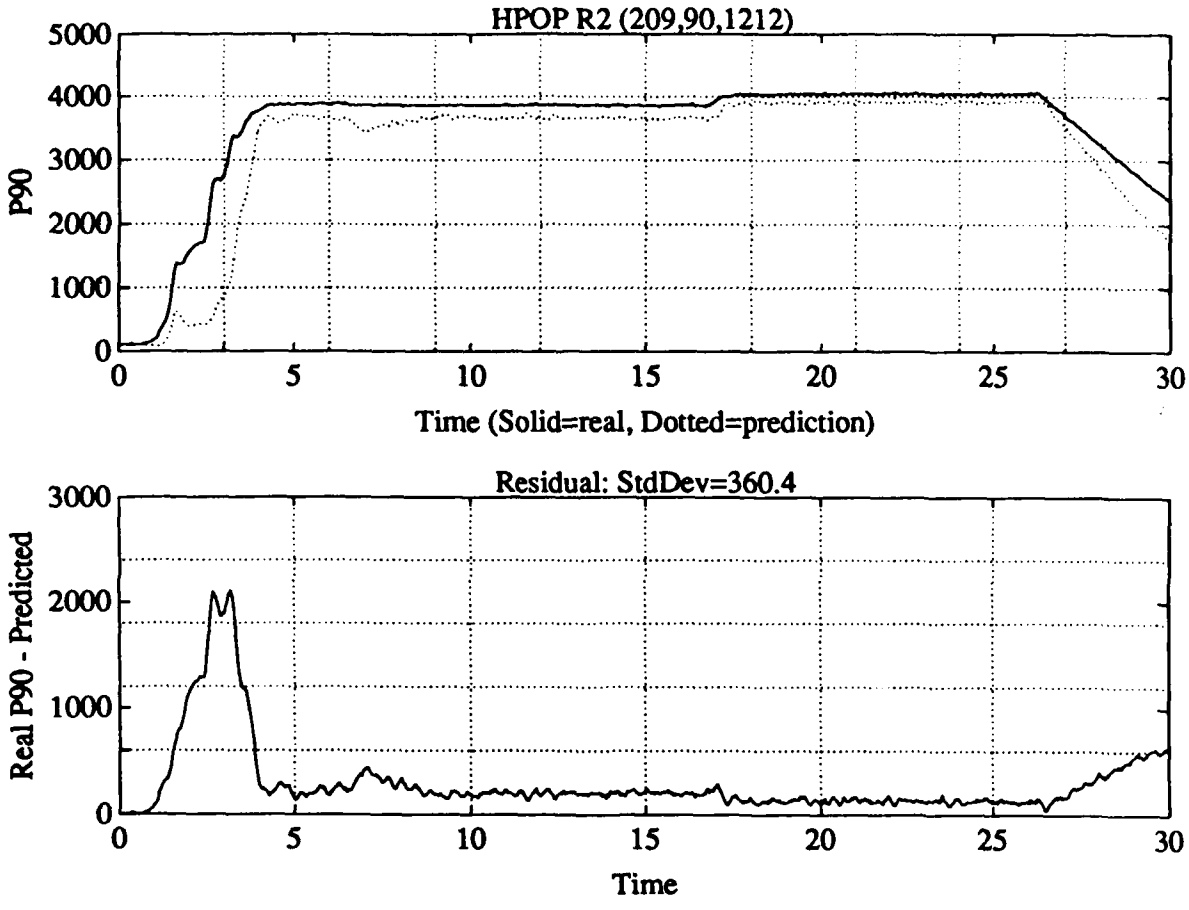
HPOP R2 (209,90,1212)
P90
5000
4000
3000
2000
1000
0
0
5
10
15
20
25
30
Time (Solid=real, Dotted=prediction)
Residual: StdDev=360.4
Real P90 - Predicted
3000
2000
1000
0
0
5
10
15
20
25
30
Time

8 +/- 140

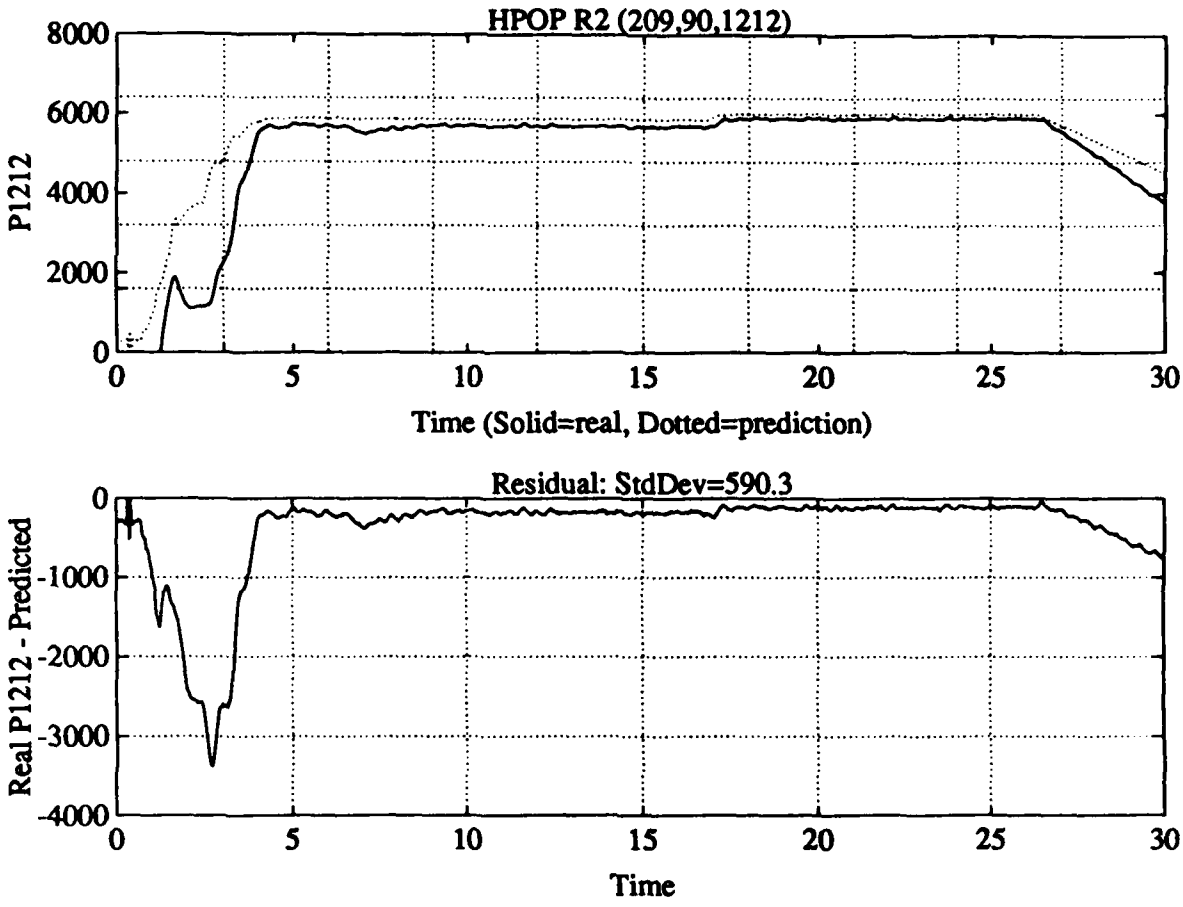
HPOP R2 (209,90,1212)
P1212
8000
6000
4000
2000
0
0
5
10
15
20
25
30
Time (Solid=real, Dotted=prediction)
Residual: StdDev=590.3
Real P1212 - Predicted
0
-1000
-2000
-3000
-4000
0
5
10
15
20
25
30
Time

P+/- 6T

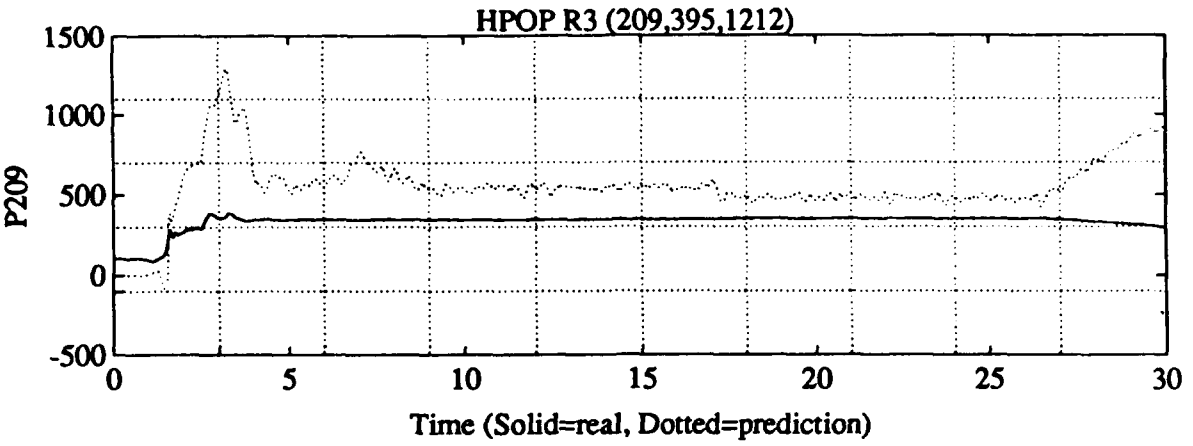
HPOP R3 (209,395,1212)
P209
1500
1000
500
0
-500
0
5
10
15
20
25
30
Time (Solid=real, Dotted=prediction)

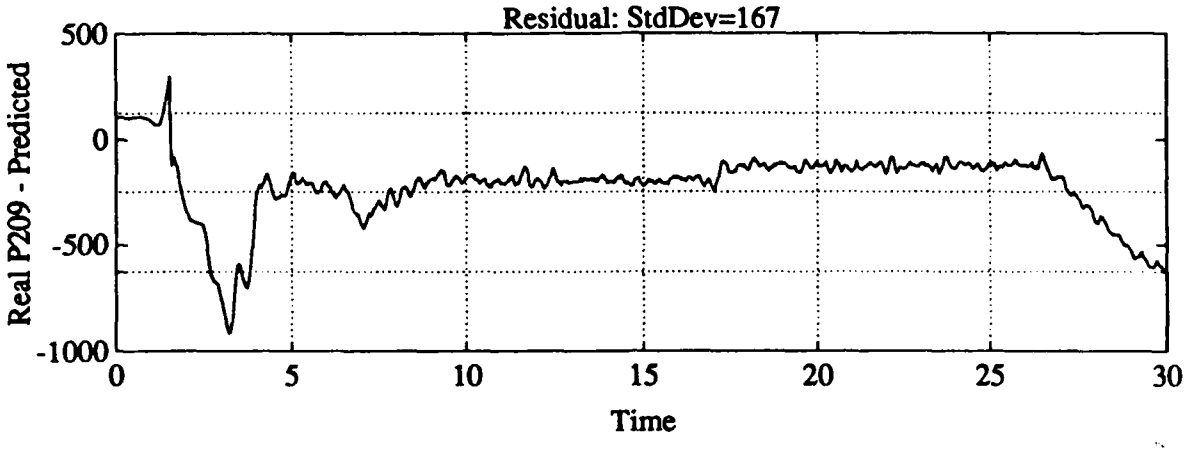
Residual: StdDev=167
Real P209 - Predicted
500
0
-500
-1000
0
5
10
15
20
25
30
Time

97-10

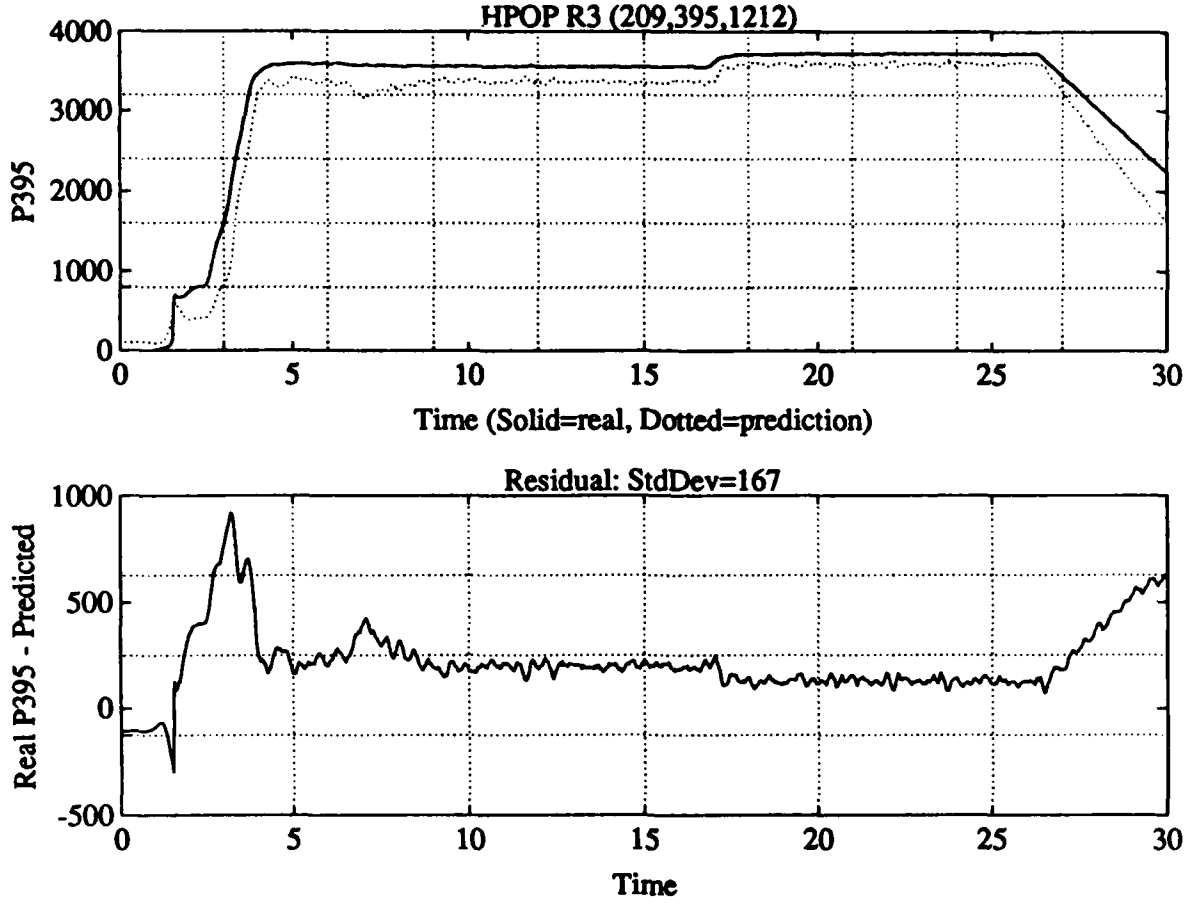
HPOP R3 (209,395,1212)
P395
4000
3000
2000
1000
0
0
5
10
15
20
25
30
Time (Solid=real, Dotted=prediction)
Residual: StdDev=167
Real P395 - Predicted
1000
500
0
-500
0
5
10
15
20
25
30
Time

P+/- 25

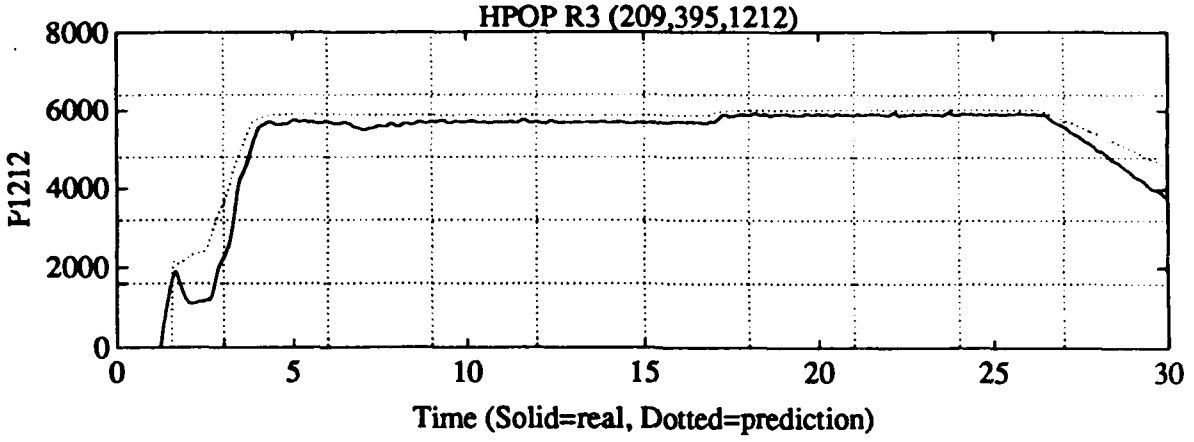
HPOP R3 (209,395,1212)
P1212
8000
6000
4000
2000
0
0
5
10
15
20
25
30
Time (Solid=real, Dotted=prediction)

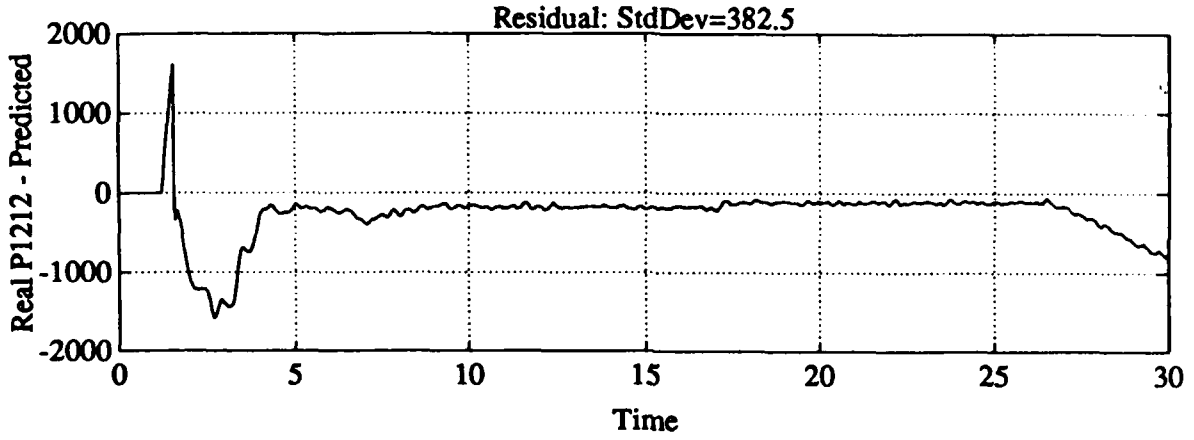
Residual: StdDev=382.5
Real P1212 - Predicted
2000
1000
0
-1000
-2000
0
5
10
15
20
25
30
Time

P+/-85

Regression equation results using best correlating parameters including redundants.
Correlation coefficients based on "*family average*" *derived coefficients.*

Test A2497 @109% RPL

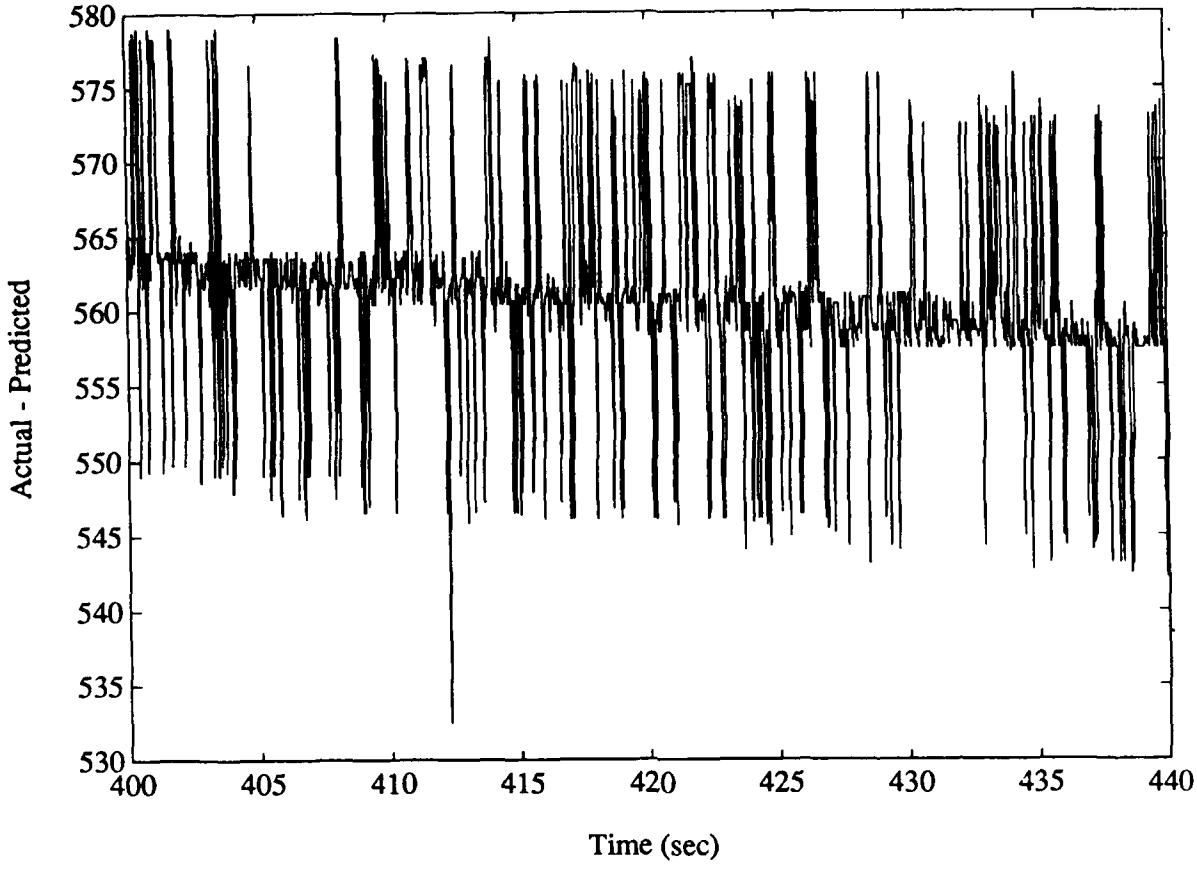
580
575
570
565
560
555
550
545
540
535
530
400
405
410
415
420
425
430
435
440
Actual - Predicted
Time (sec)

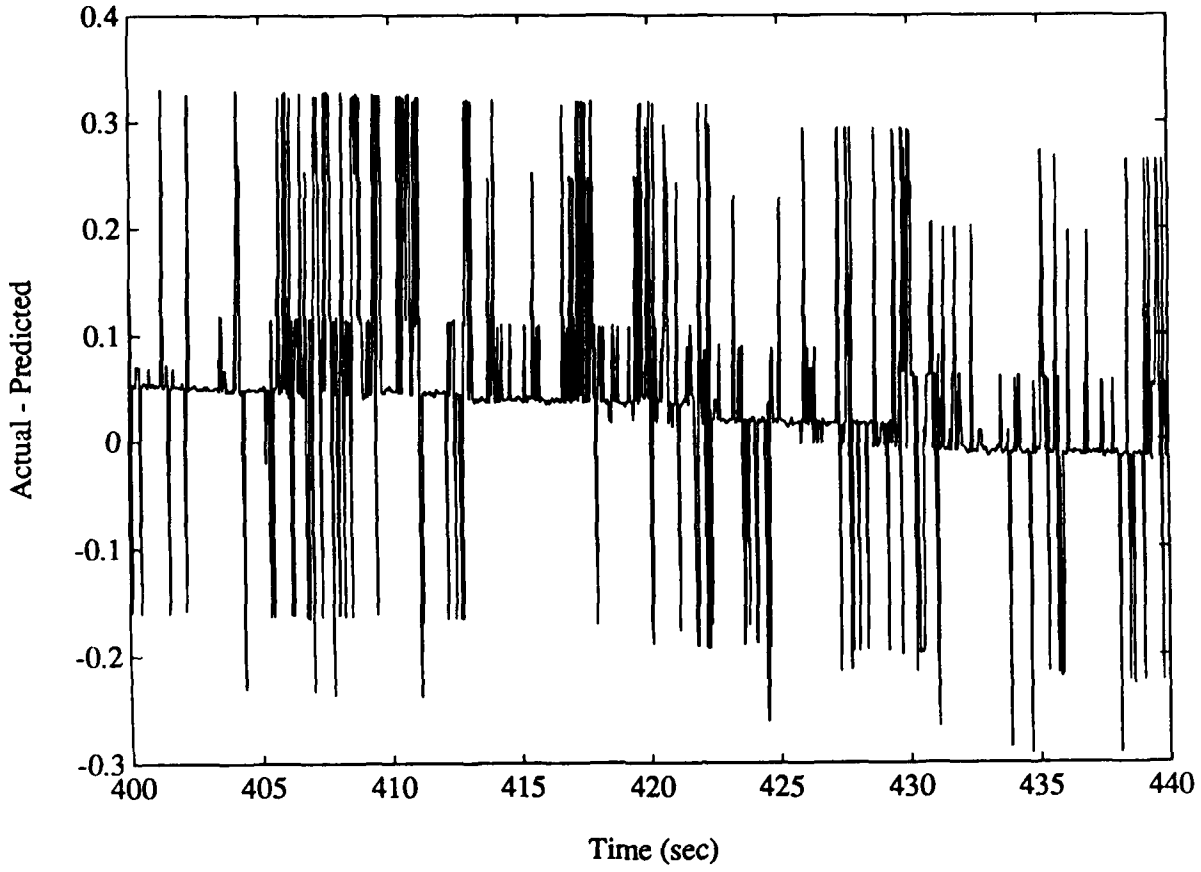
0.4
0.3
0.2
0.1
0
-0.1
-0.2
-0.3
Actual - Predicted
400
405
410
415
420
425
430
435
440
Time (sec)

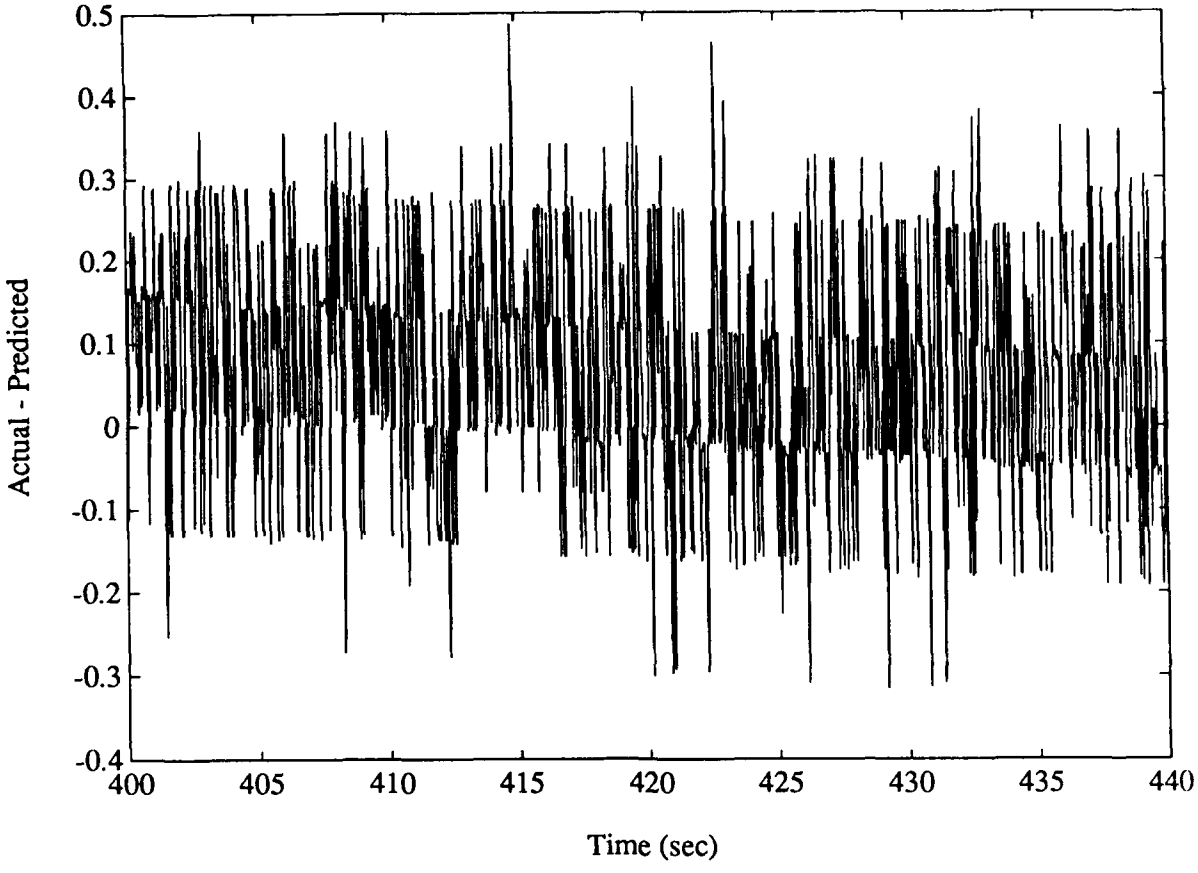
0.5
0.4
0.3
0.2
0.1
0
-0.1
-0.2
-0.3
-0.4
Actual - Predicted
400
405
410
415
420
425
430
435
440
Time (sec)

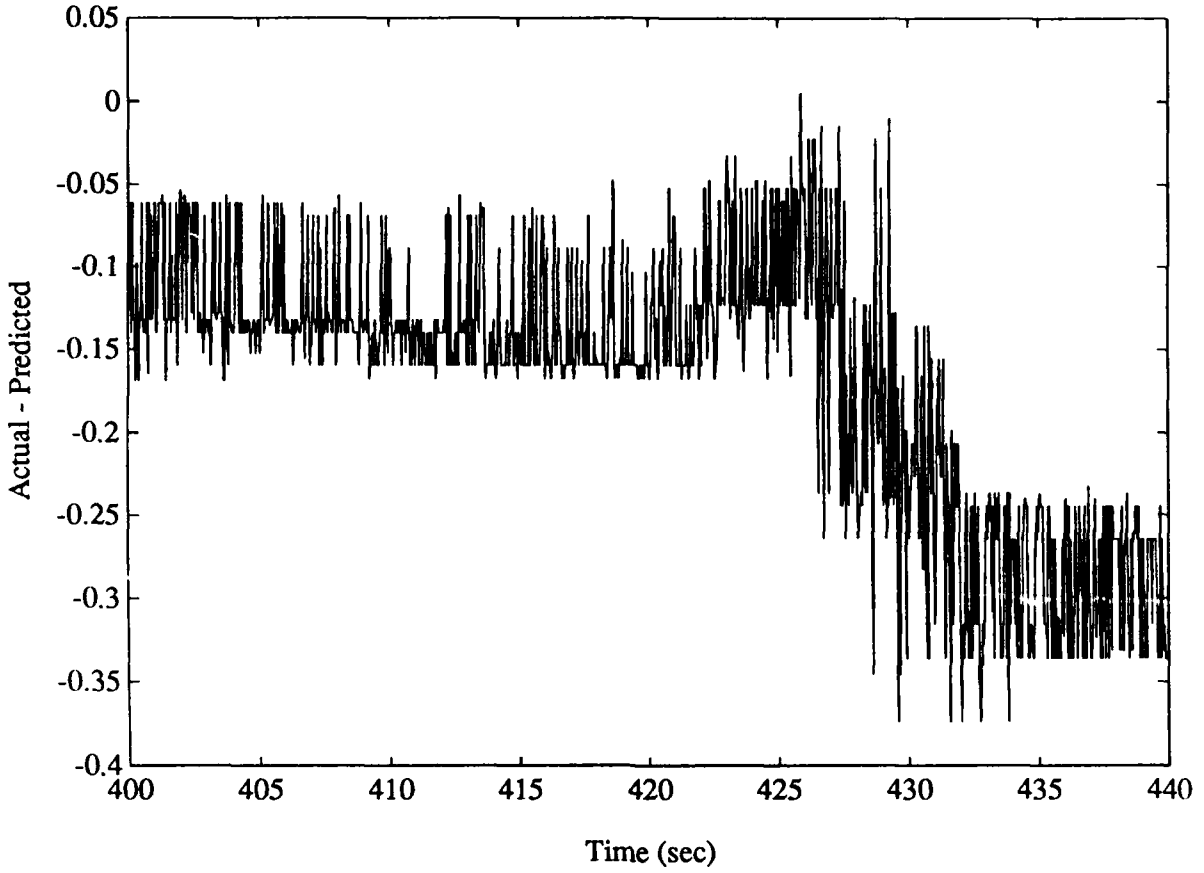
0.05
0
-0.05
-0.1
-0.15
-0.2
-0.25
-0.3
-0.35
-0.4
Actual - Predicted
400
405
410
415
420
425
430
435
440
Time (sec)

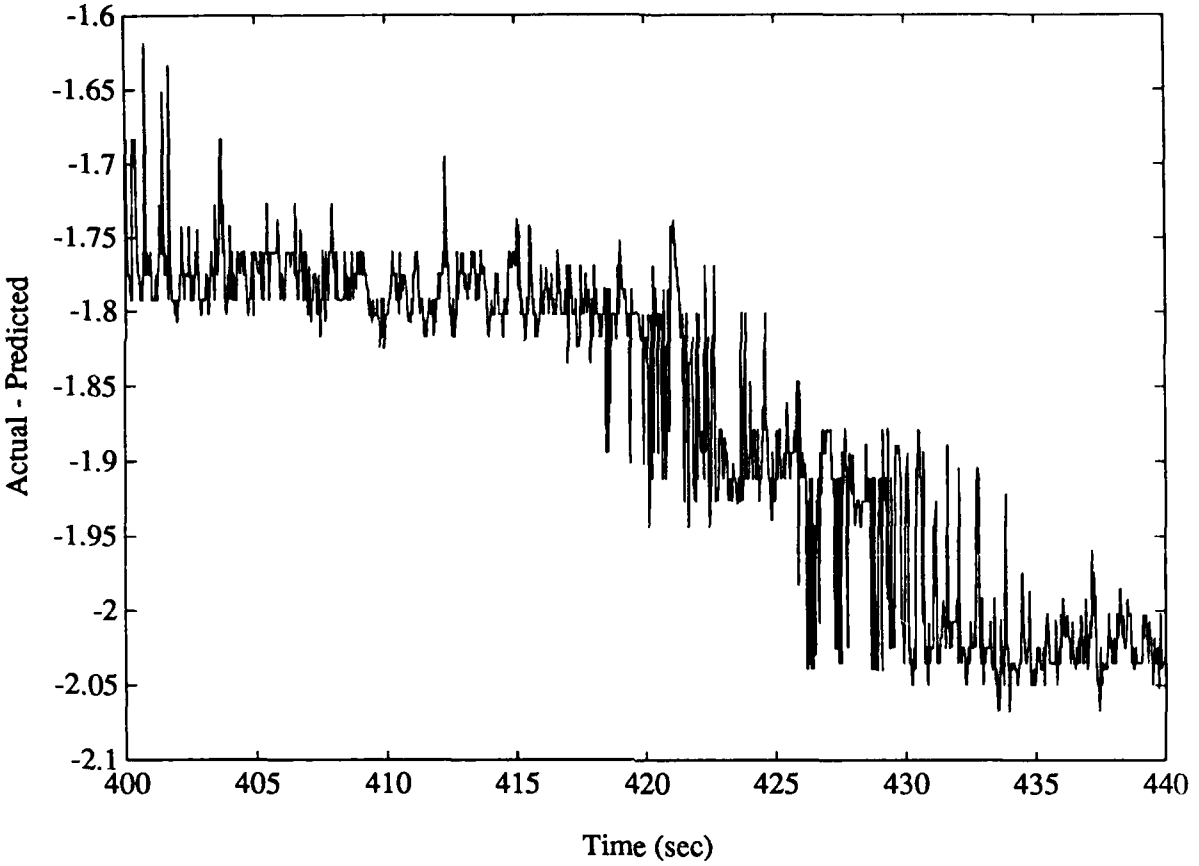
-1.6
-1.65
-1.7
-1.75
-1.8
-1.85
-1.9
-1.95
-2
-2.05
-2.1
Actual - Predicted
400
405
410
415
420
425
430
435
440
Time (sec)

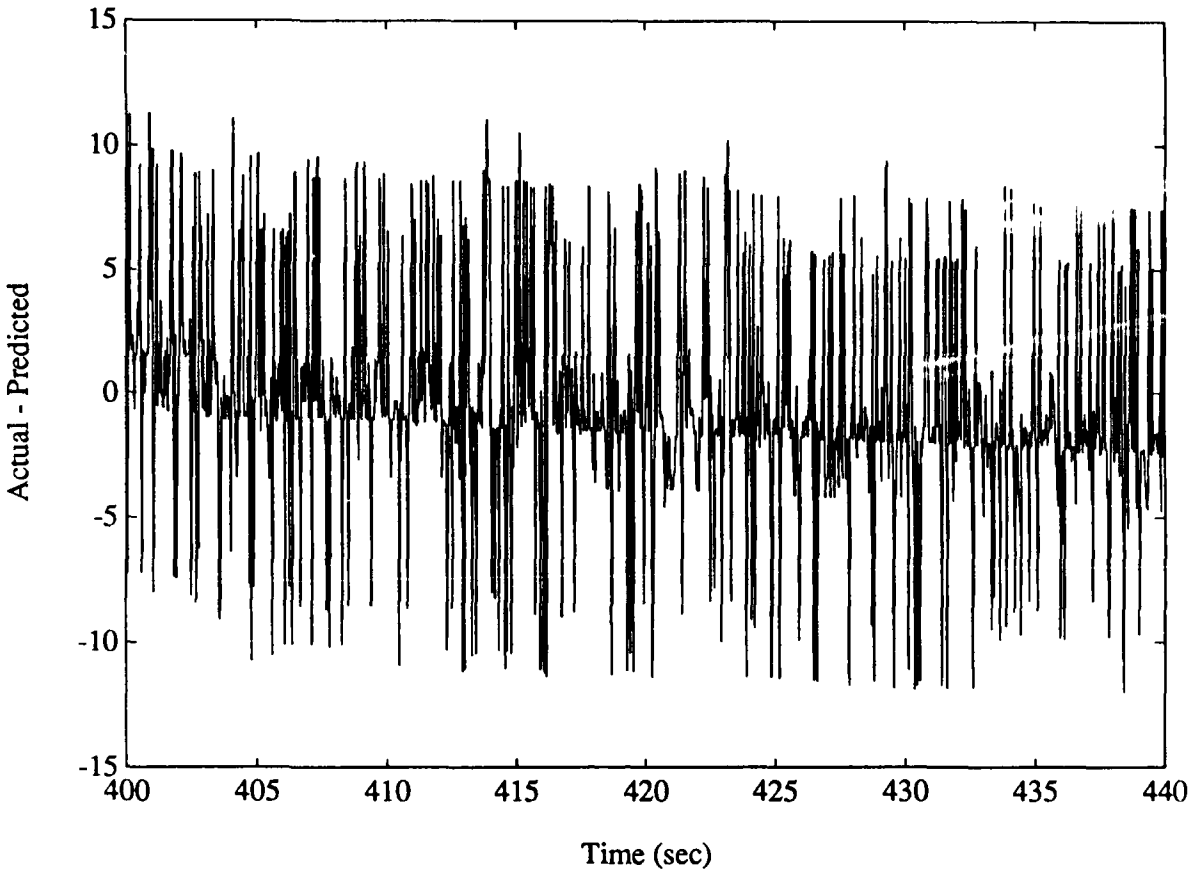
15
10
5
0
-5
-10
-15
400
405
410
415
420
425
430
435
440
Actual - Predicted
Time (sec)

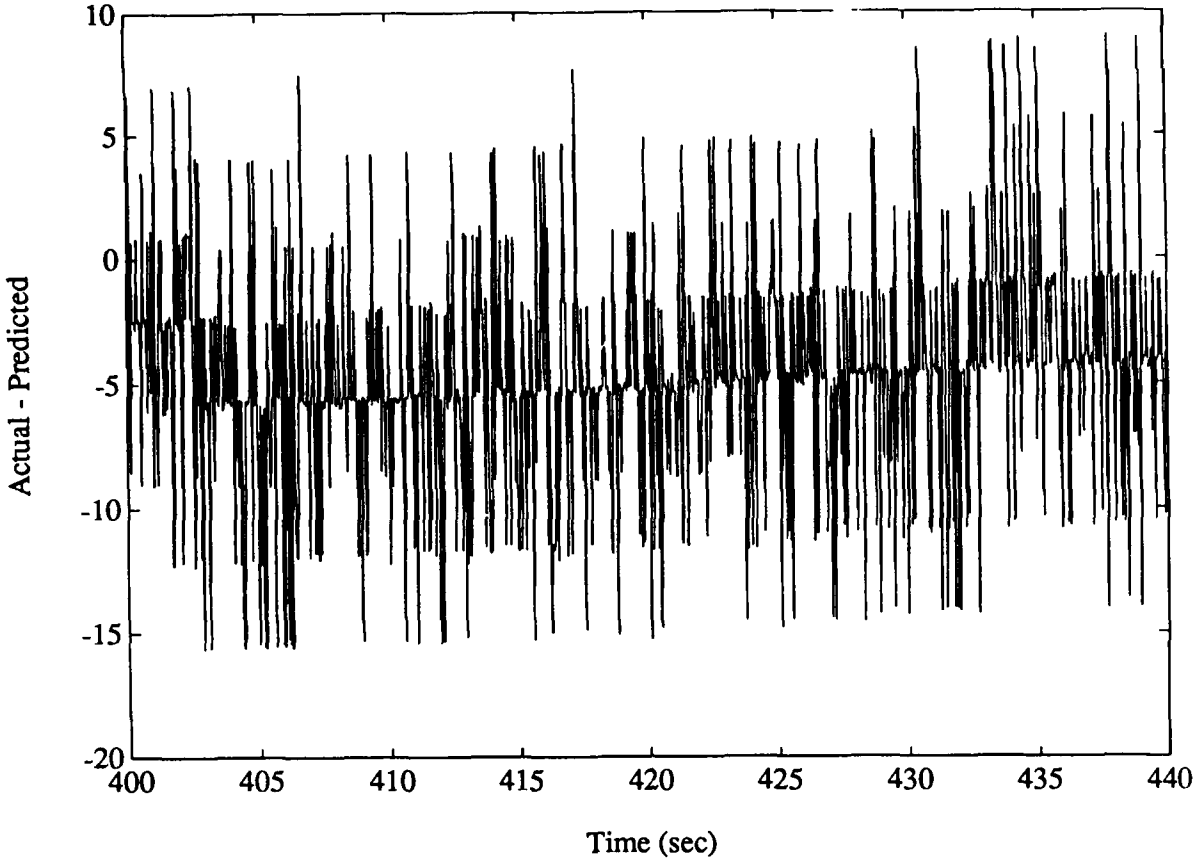
10
5
0
-5
-10
-15
-20
400
405
410
415
420
425
430
435
440
Actual - Predicted
Time (sec)

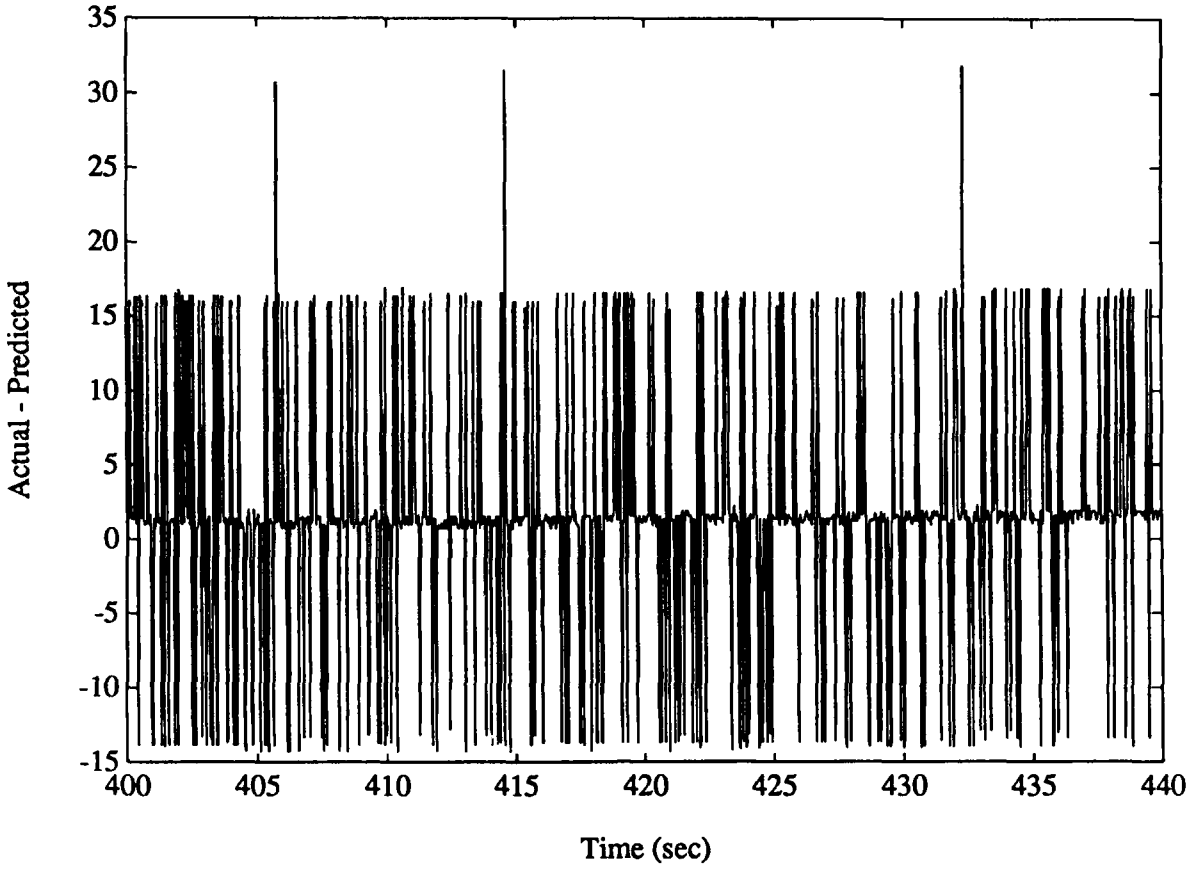
35
30
25
20
15
10
5
0
-5
-10
-15
400
405
410
415
420
425
430
435
440
Actual - Predicted
Time (sec)

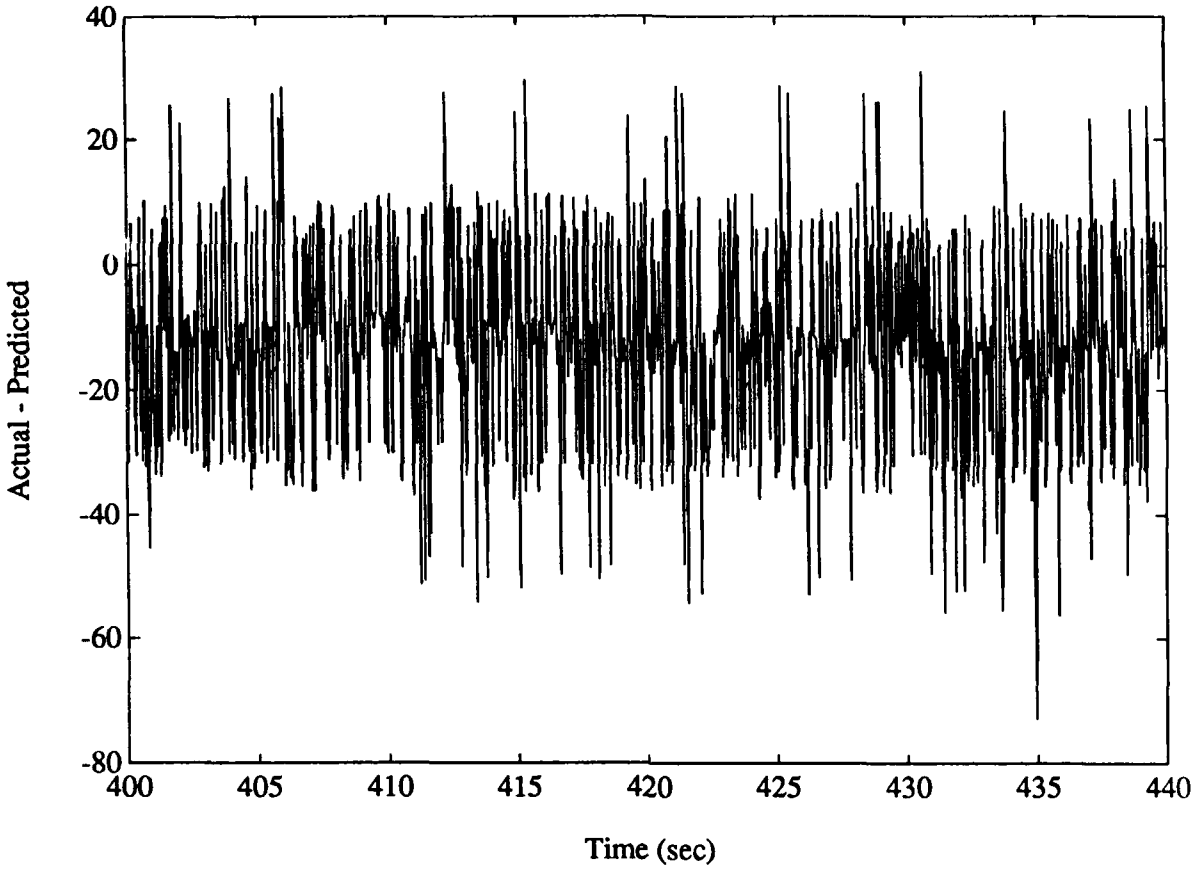
40
20
0
-20
-40
-60
-80
400
405
410
415
420
425
430
435
440
Actual - Predicted
Time (sec)

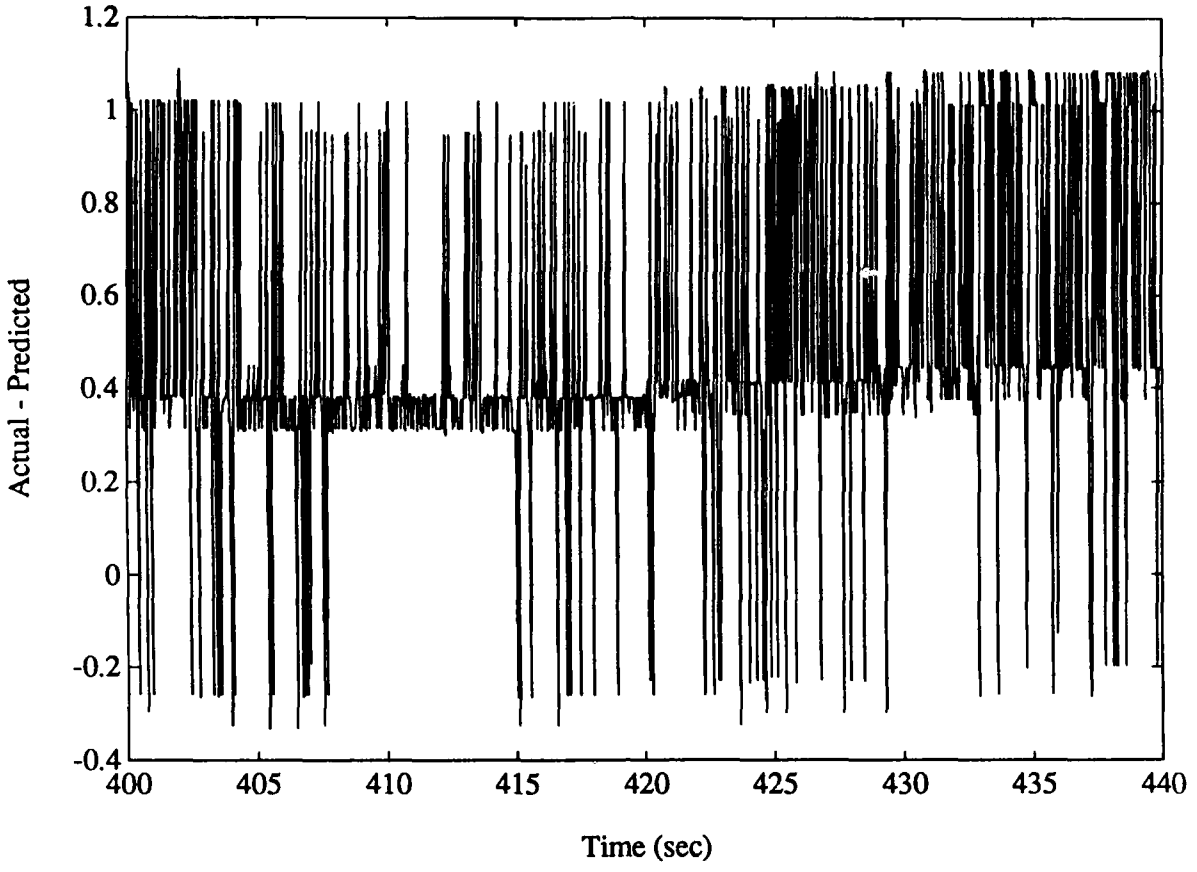
1.2
1
0.8
0.6
0.4
0.2
0
-0.2
-0.4
Actual - Predicted
400
405
410
415
420
425
430
435
440
Time (sec)

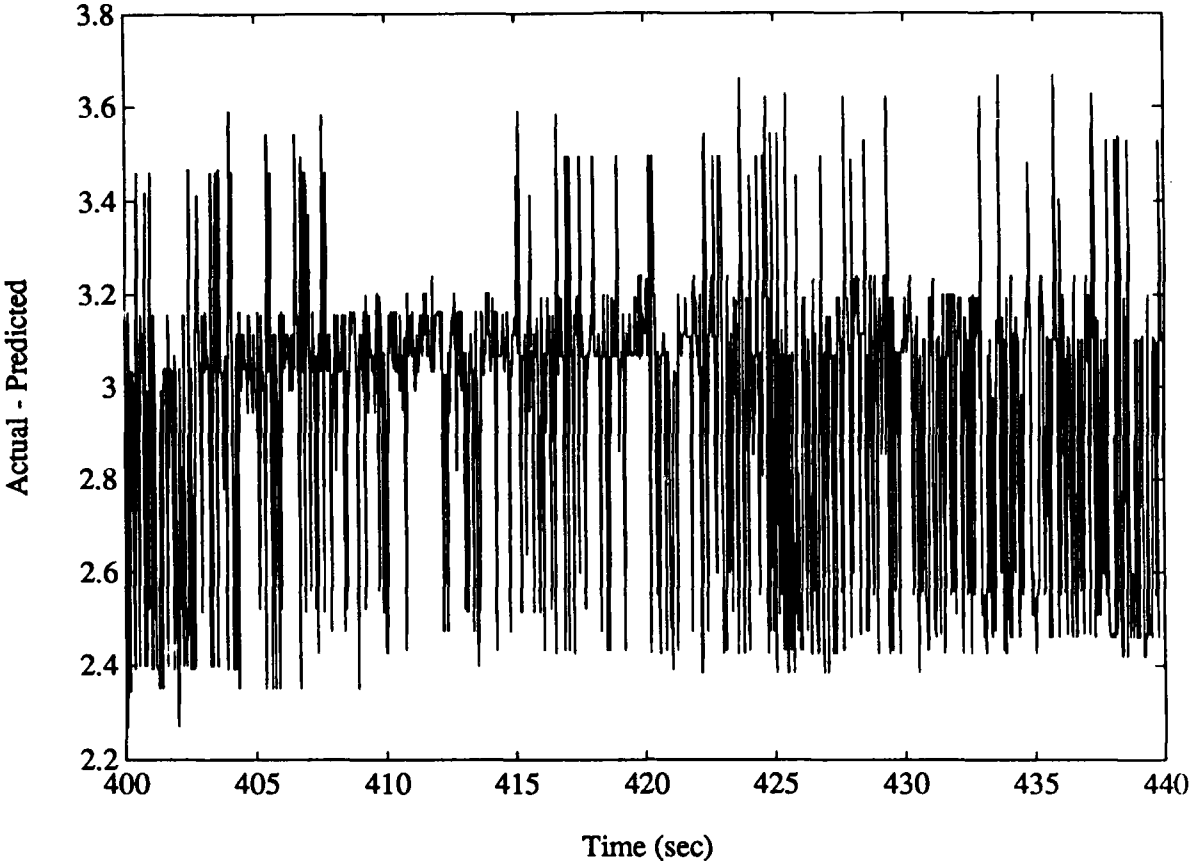
3.8
3.6
3.4
3.2
3
2.8
2.6
2.4
2.2
Actual - Predicted
400
405
410
415
420
425
430
435
440
Time (sec)

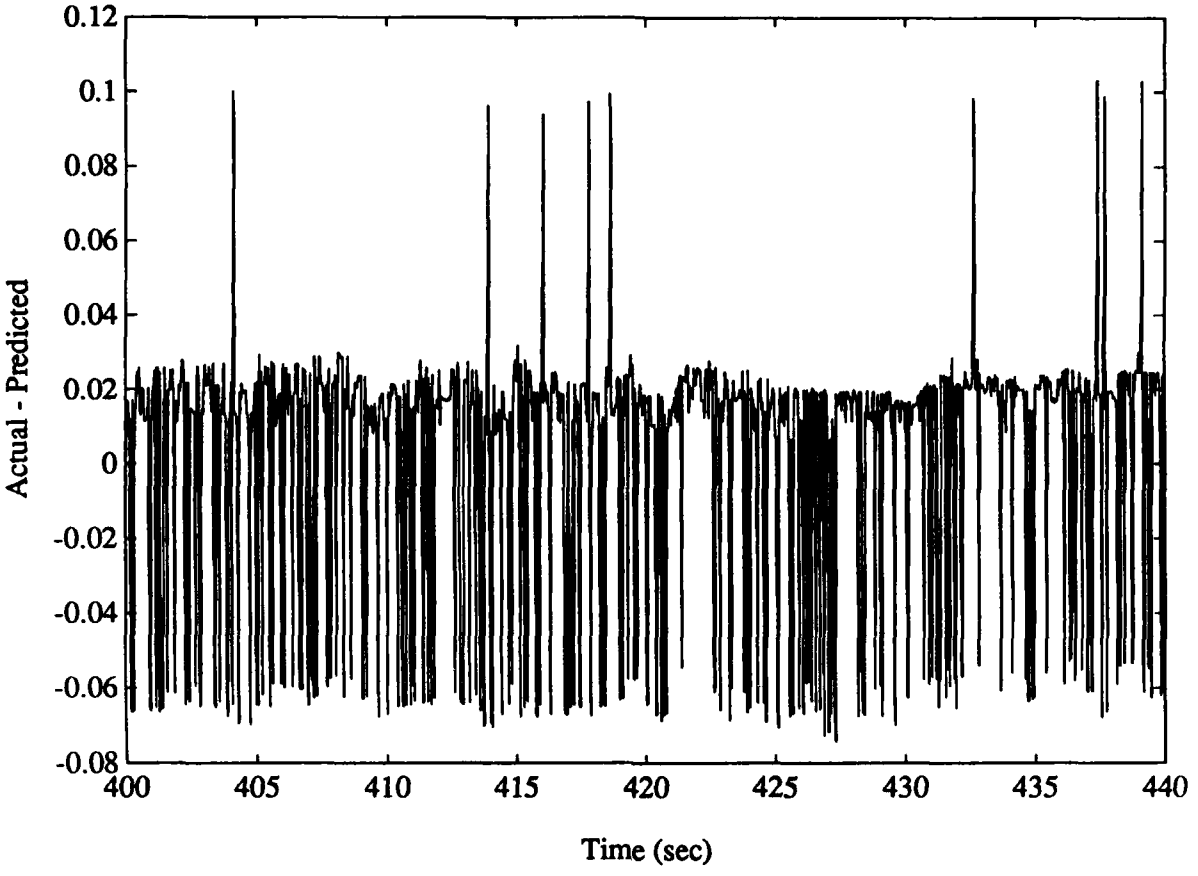
0.12
0.1
0.08
0.06
0.04
0.02
0
-0.02
-0.04
-0.06
-0.08
Actual - Predicted
400
405
410
415
420
425
430
435
440
Time (sec)

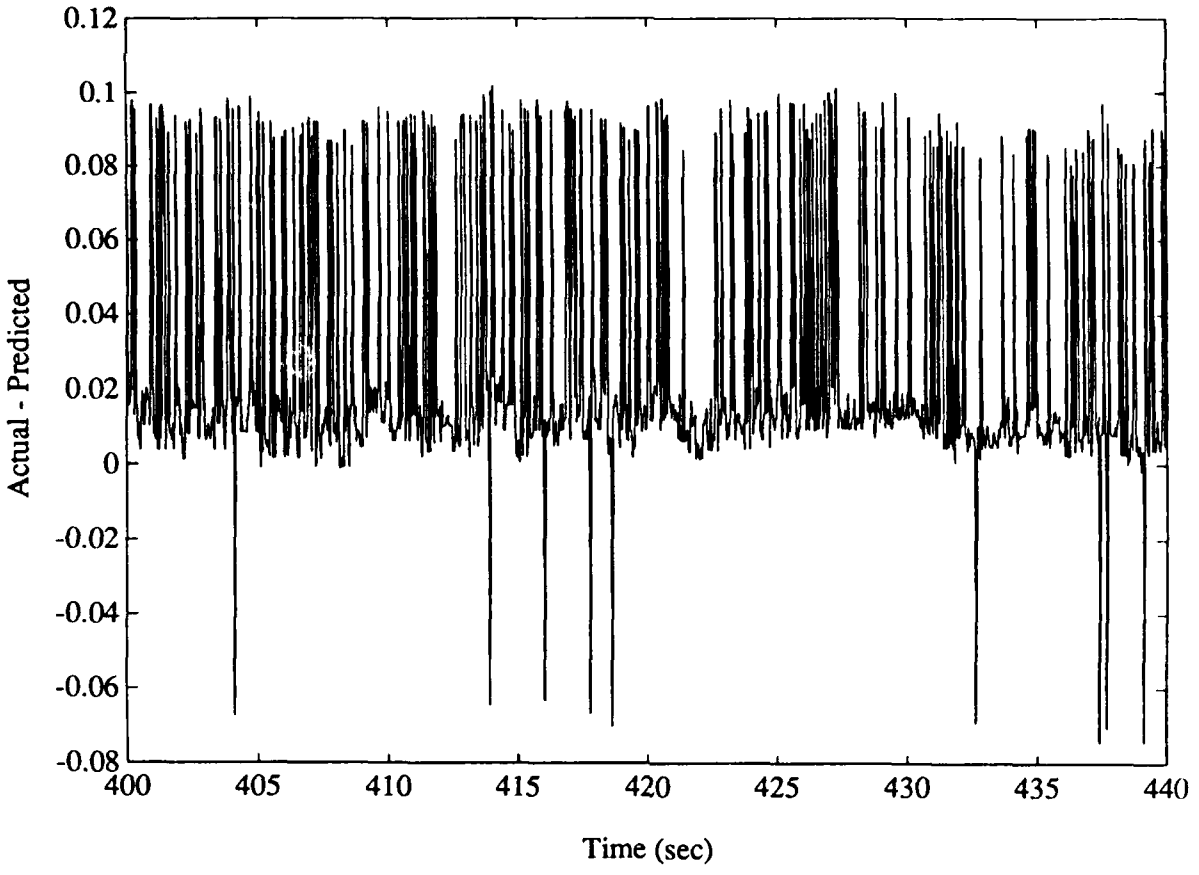
0.12
0.1
0.08
0.06
0.04
0.02
0
-0.02
-0.04
-0.06
-0.08
Actual - Predicted
400
405
410
415
420
425
430
435
440
Time (sec)

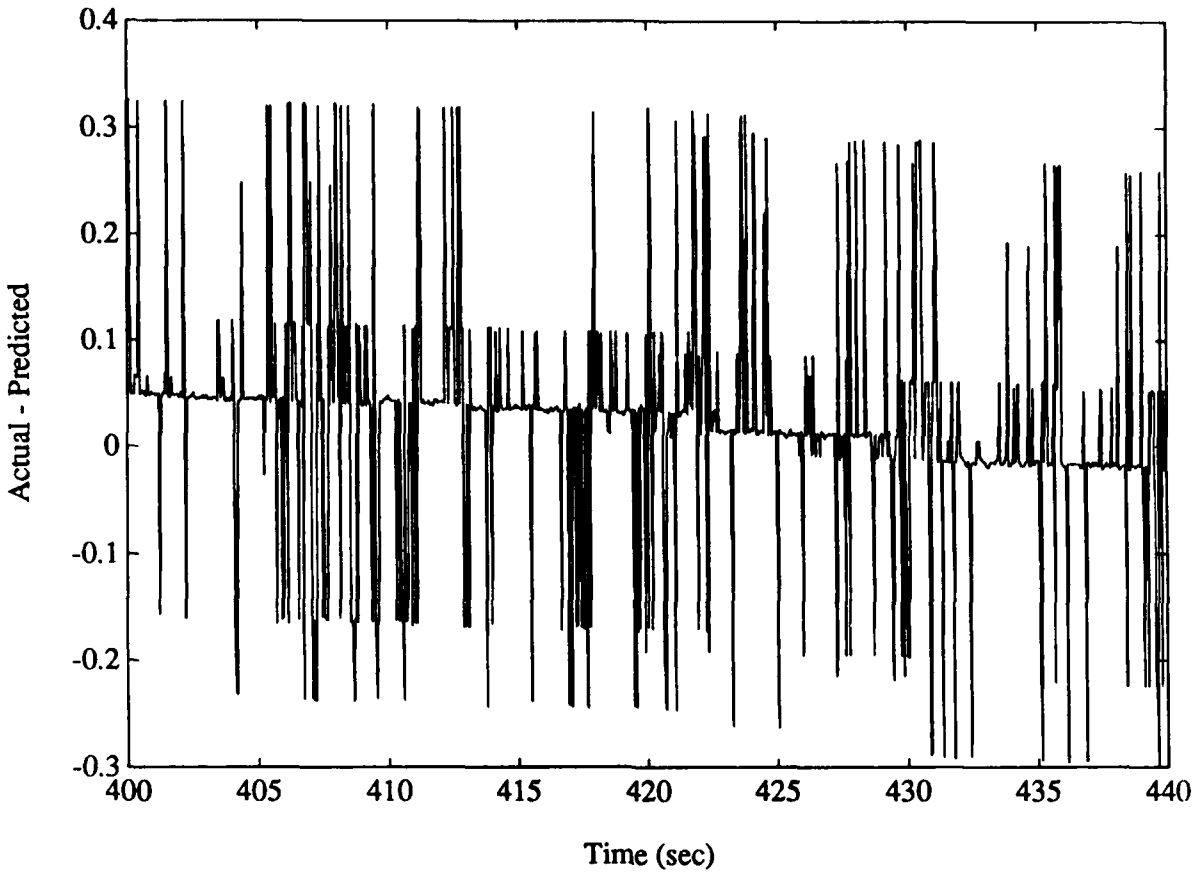
0.4
0.3
0.2
0.1
0
-0.1
-0.2
-0.3
Actual - Predicted
400
405
410
415
420
425
430
435
440
Time (sec)

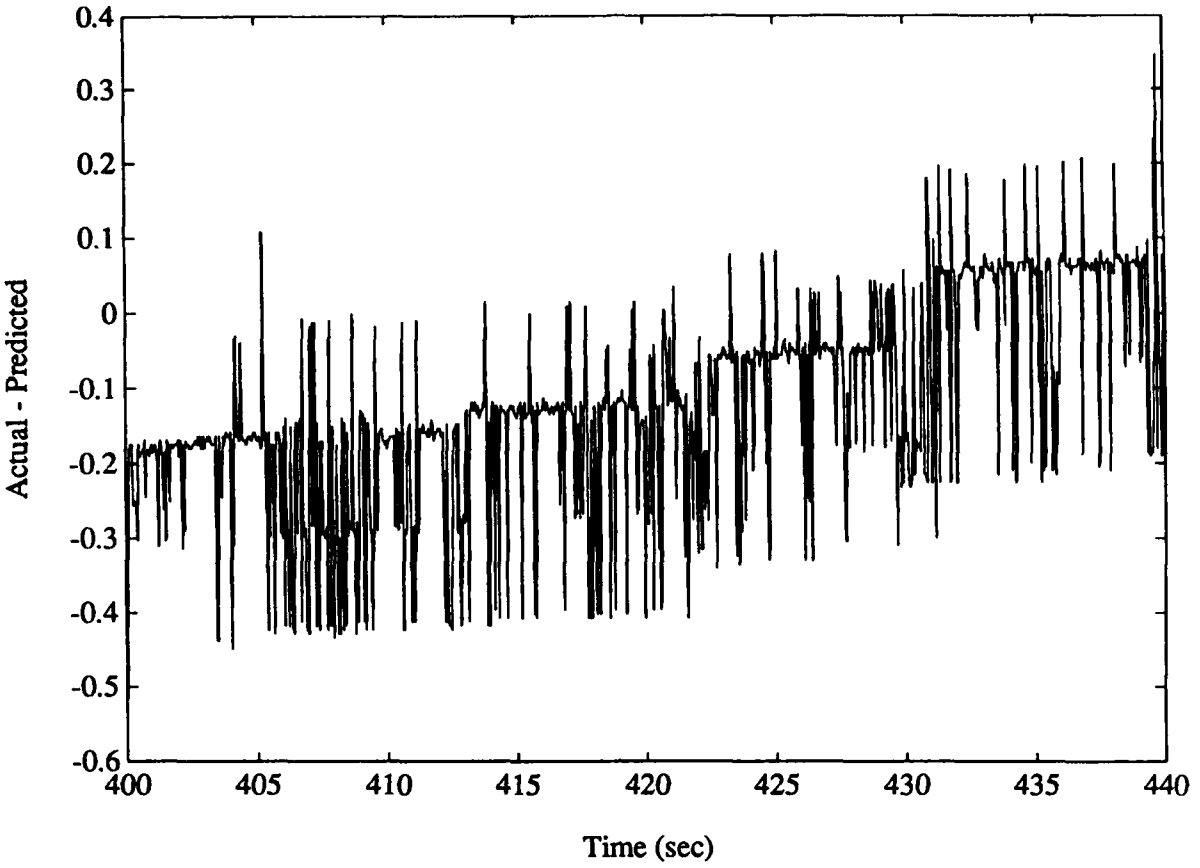
0.4
0.3
0.2
0.1
0
-0.1
-0.2
-0.3
-0.4
-0.5
-0.6
Actual - Predicted
400
405
410
415
420
425
430
435
440
Time (sec)

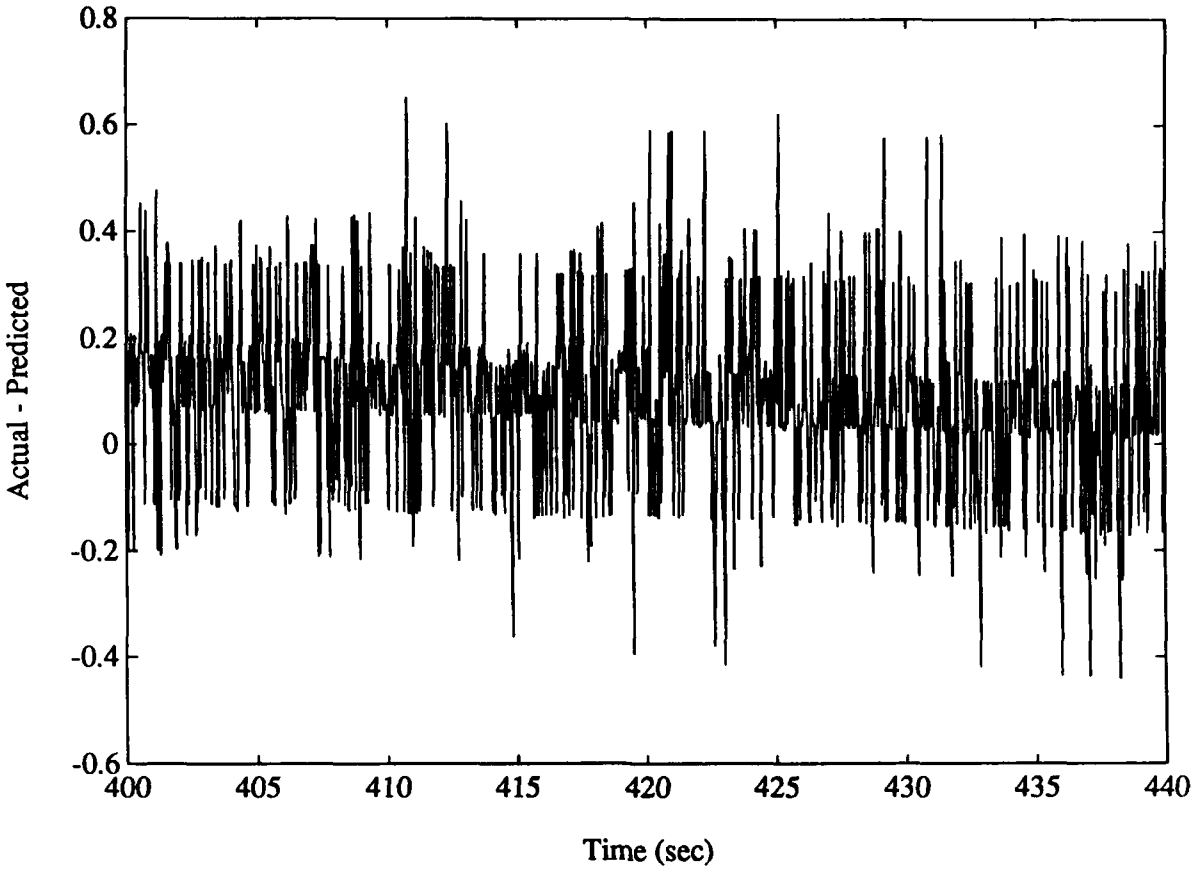
0.8
0.6
0.4
0.2
0
-0.2
-0.4
-0.6
Actual - Predicted
400
405
410
415
420
425
430
435
440
Time (sec)

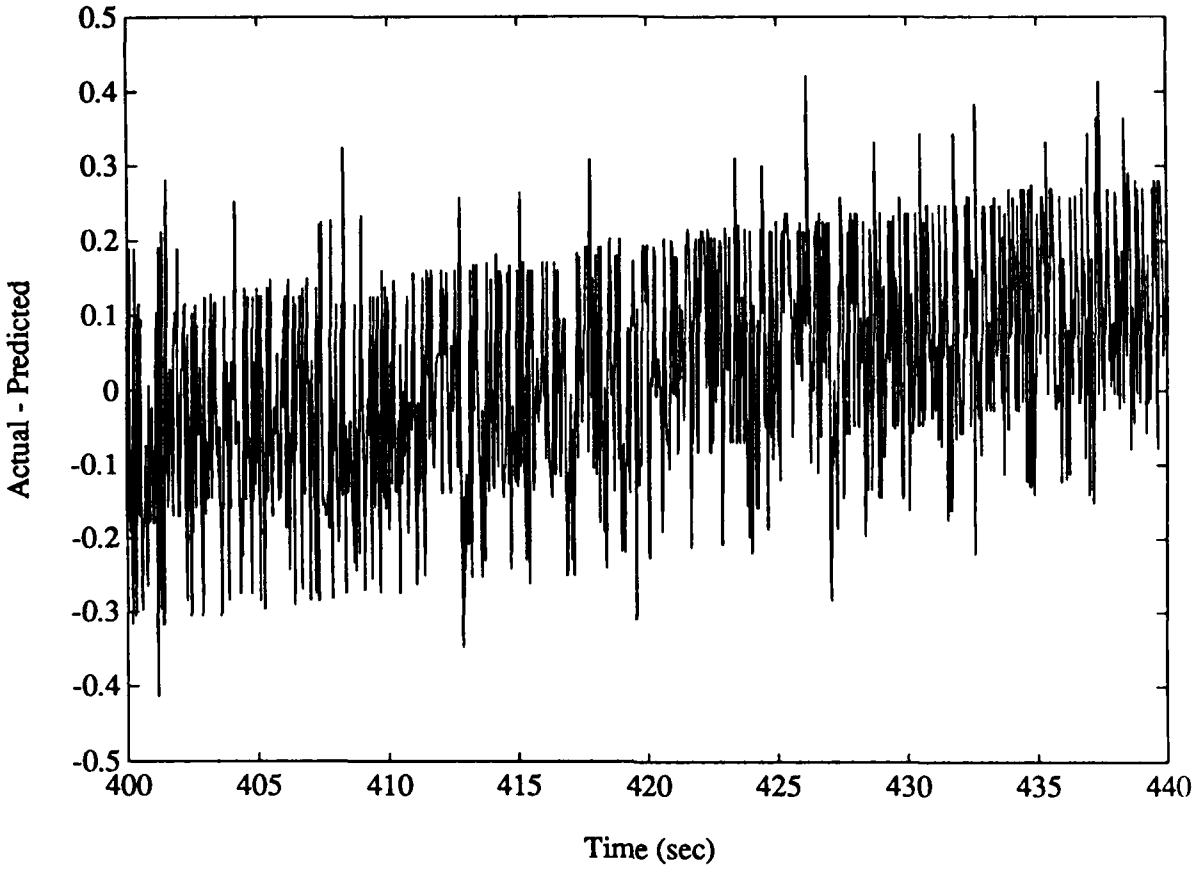
0.5
0.4
0.3
0.2
0.1
0
-0.1
-0.2
-0.3
-0.4
-0.5
Actual - Predicted
400
405
410
415
420
425
430
435
440
Time (sec)

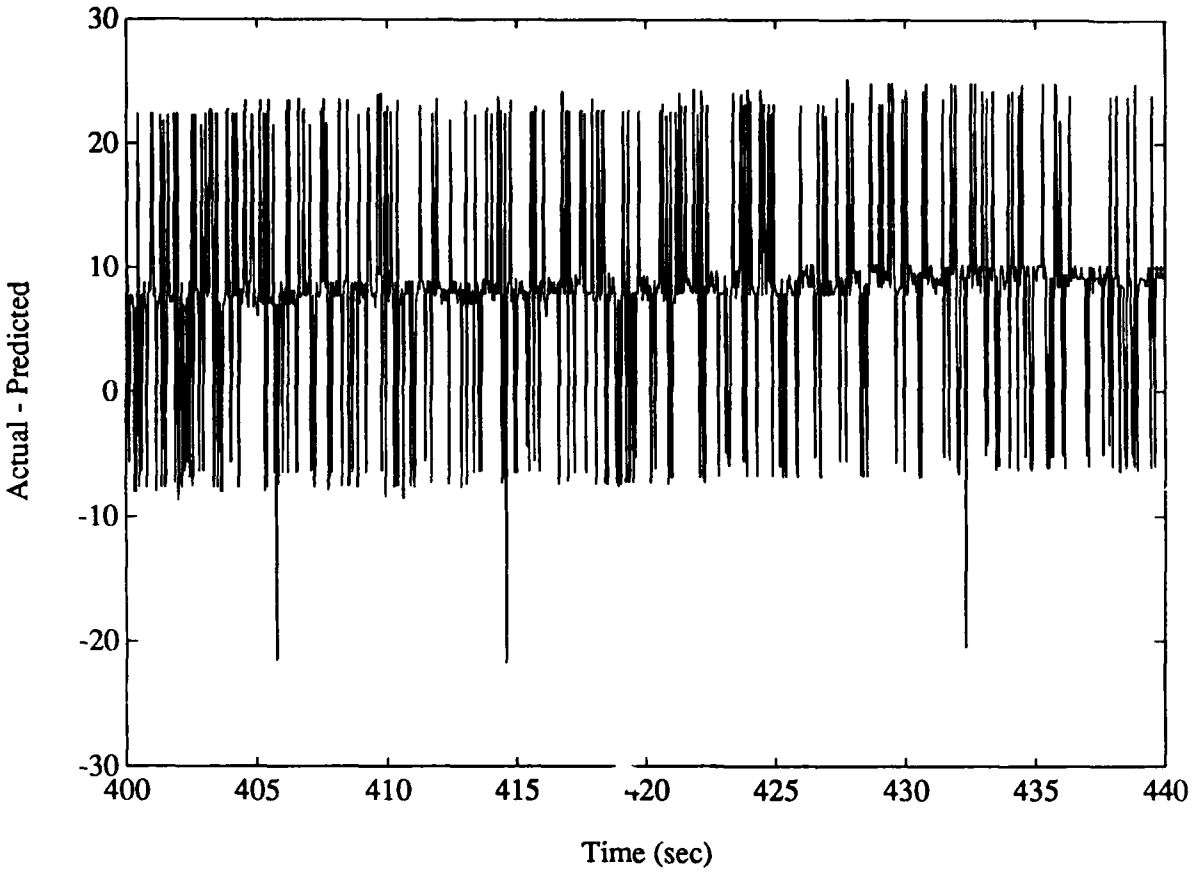
30
20
10
0
-10
-20
-30
400
405
410
415
420
425
430
435
440
Actual - Predicted
Time (sec)

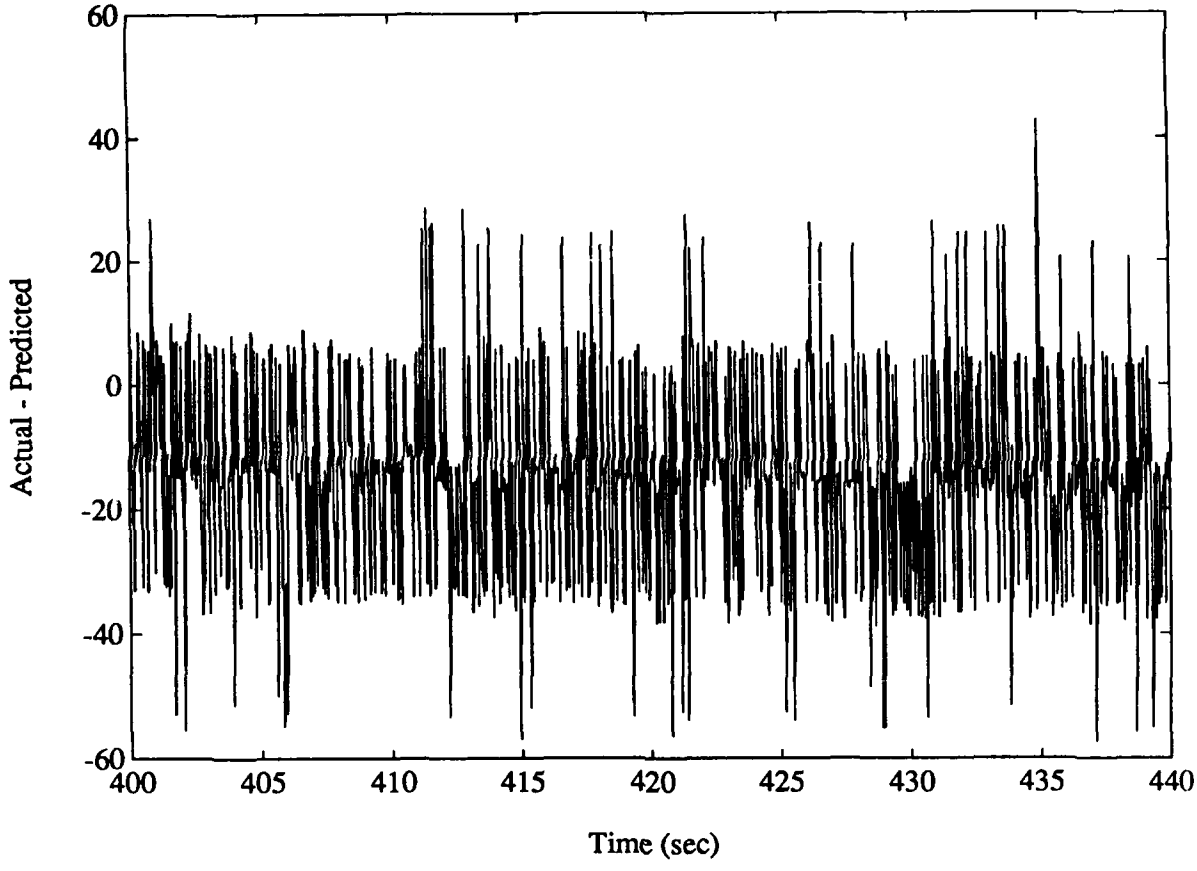
60
40
20
0
-20
-40
-60
400
405
410
415
420
425
430
435
440
Actual - Predicted
Time (sec)

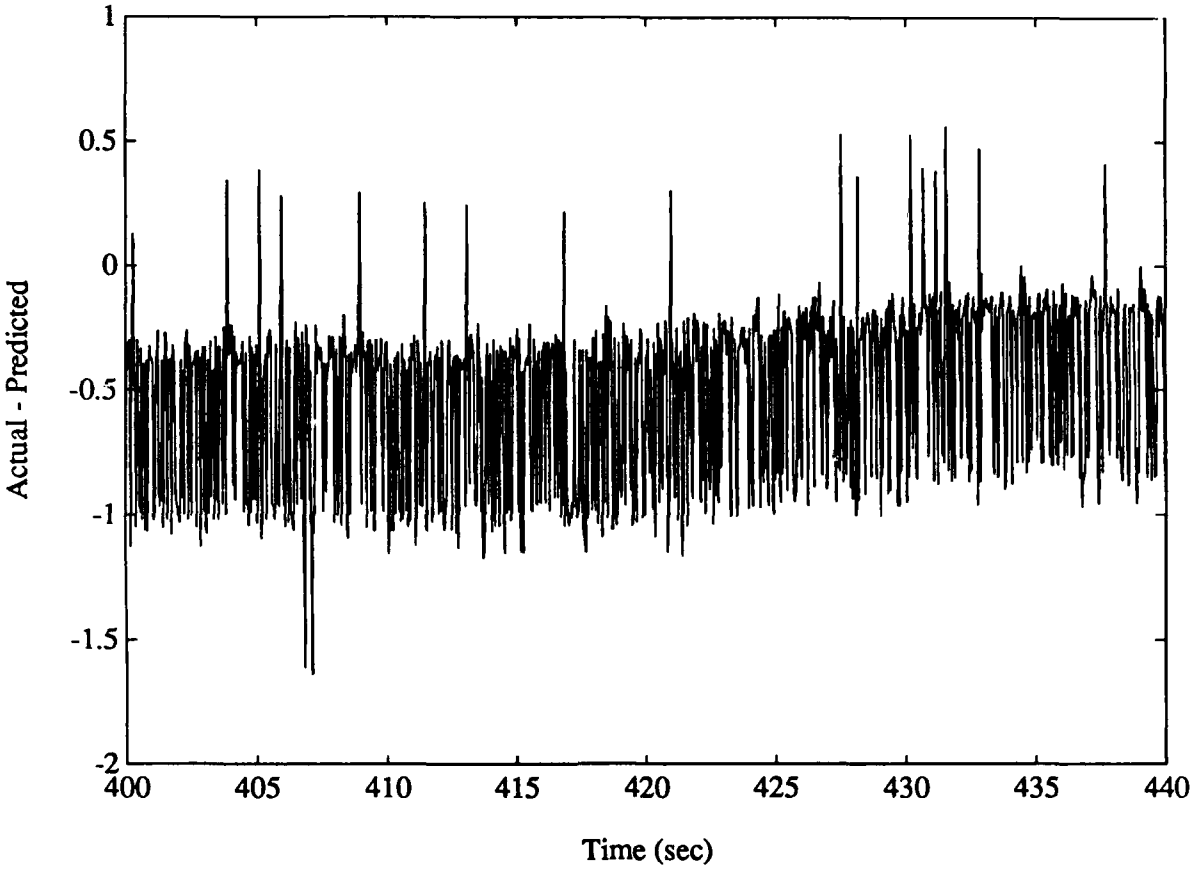
Actual - Predicted
1
0.5
0
-0.5
-1
-1.5
-2
400
405
410
415
420
425
430
435
440
Time (sec)

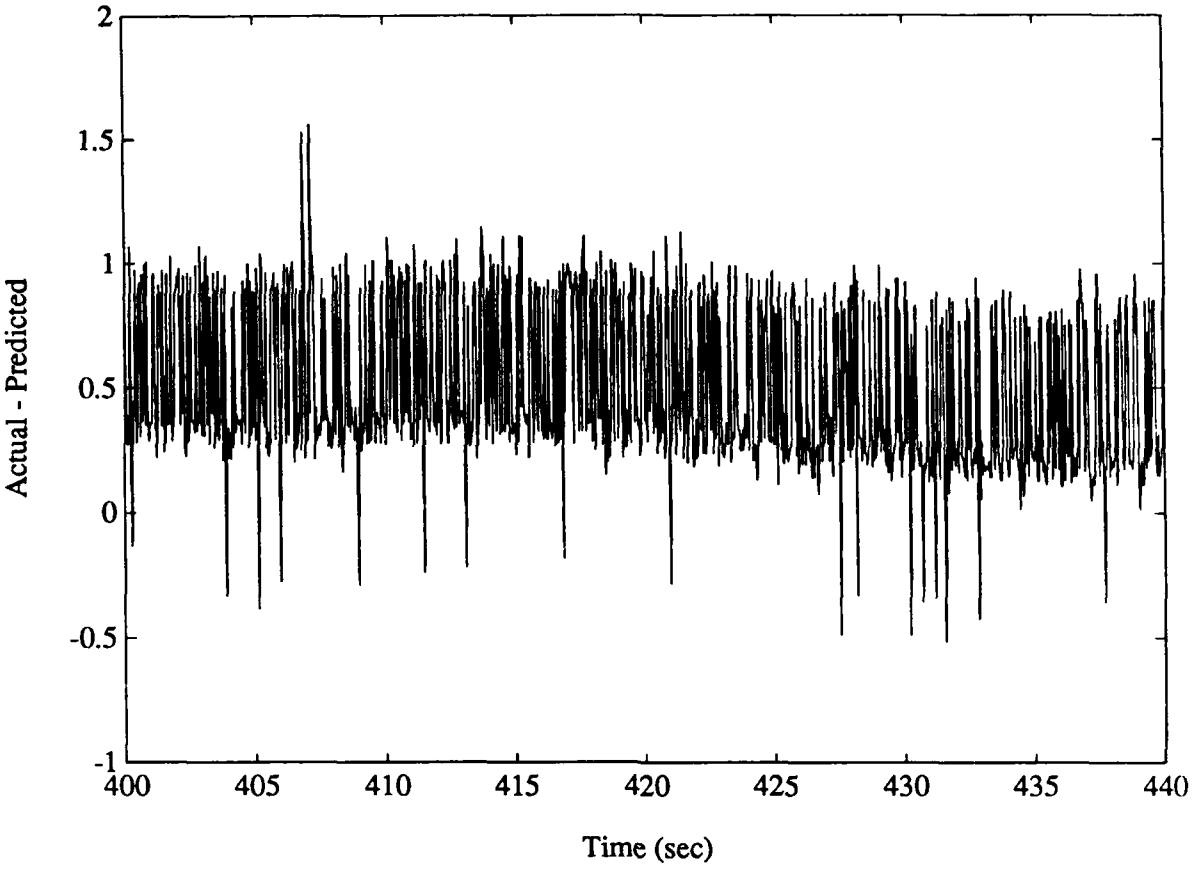
2
1.5
1
0.5
0
-0.5
-1
Actual - Predicted
400
405
410
415
420
425
430
435
440
Time (sec)

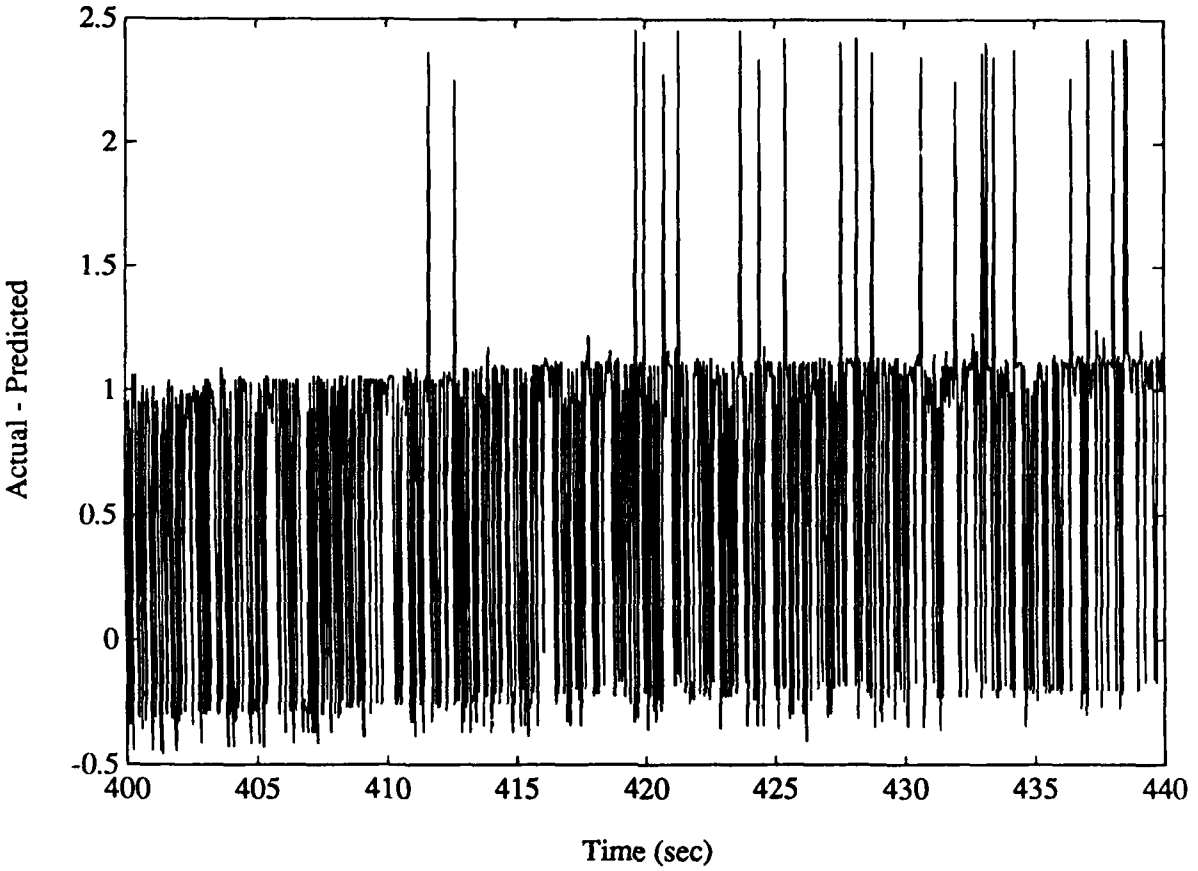
2.5
2
1.5
1
0.5
0
-0.5
400
405
410
415
420
425
430
435
440
Actual - Predicted
Time (sec)

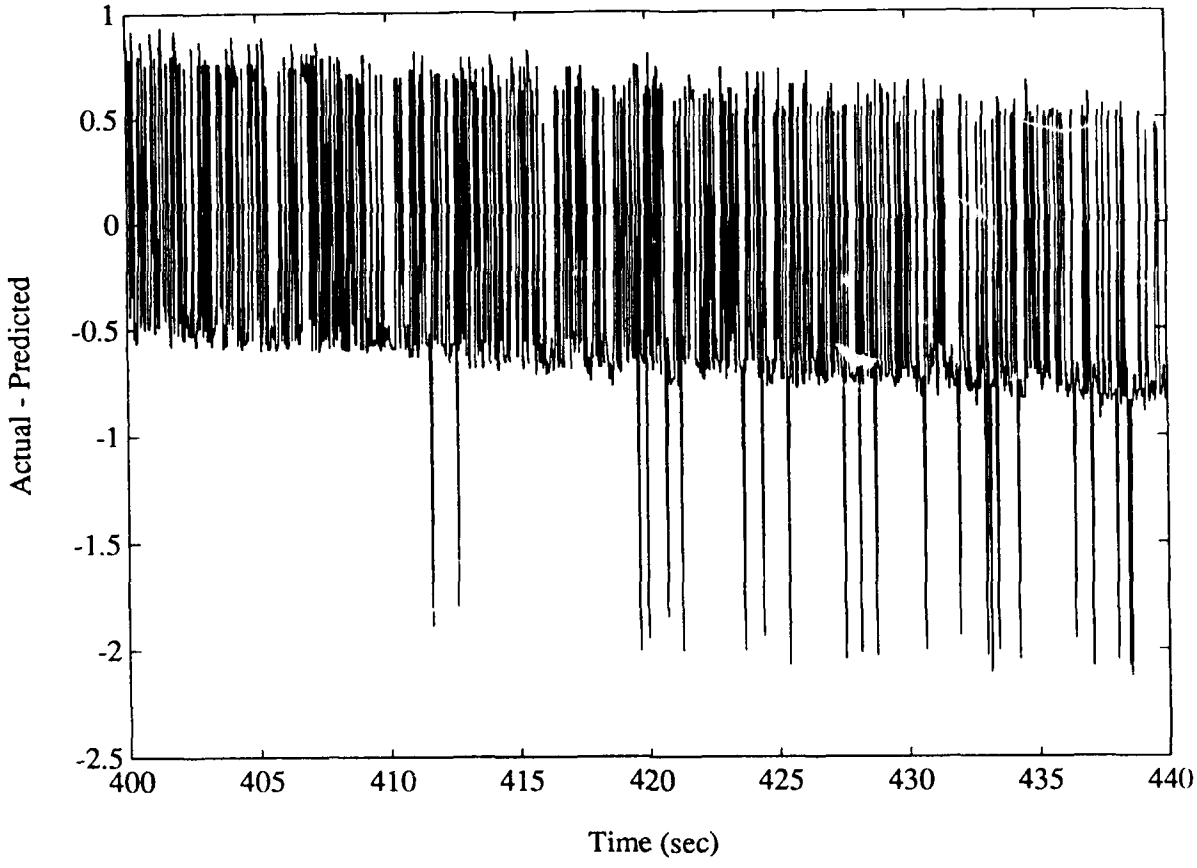
Actual - Predicted
1
0.5
0
-0.5
-1
-1.5
-2
-2.5
400
405
410
415
420
425
430
435
440
Time (sec)

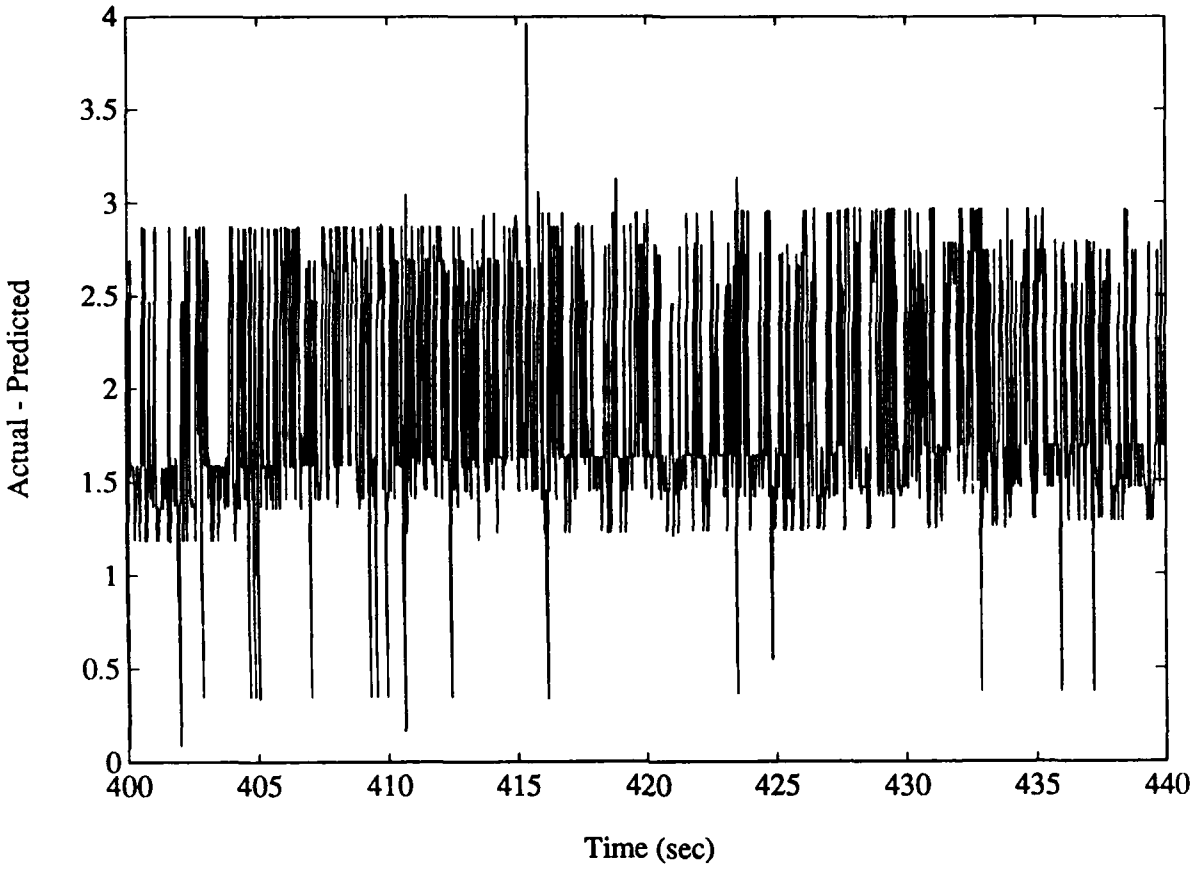
Actual - Predicted
Time (sec)
4
3.5
3
2.5
2
1.5
1
0.5
0
400
405
410
415
420
425
430
435
440

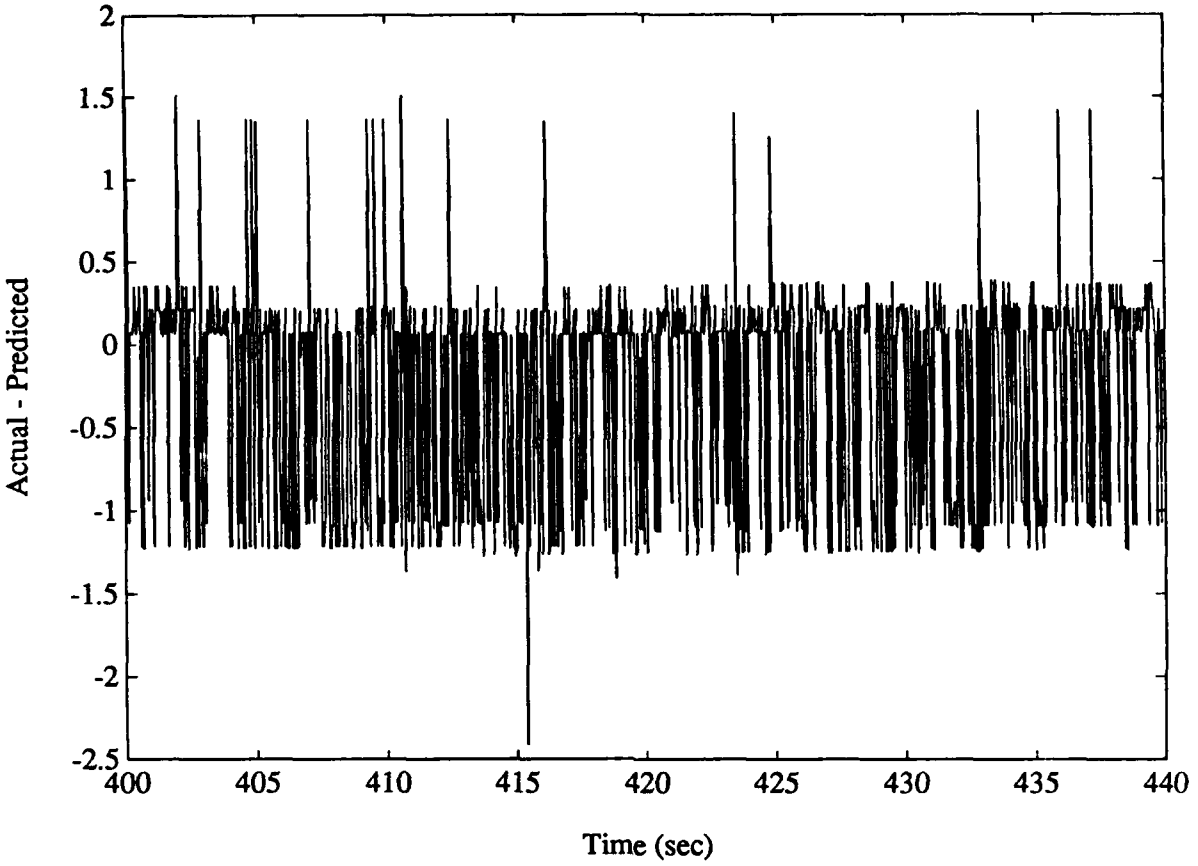
Actual - Predicted
Time (sec)
2
1.5
1
0.5
0
-0.5
-1
-1.5
-2
-2.5
400
405
410
415
420
425
430
435
440

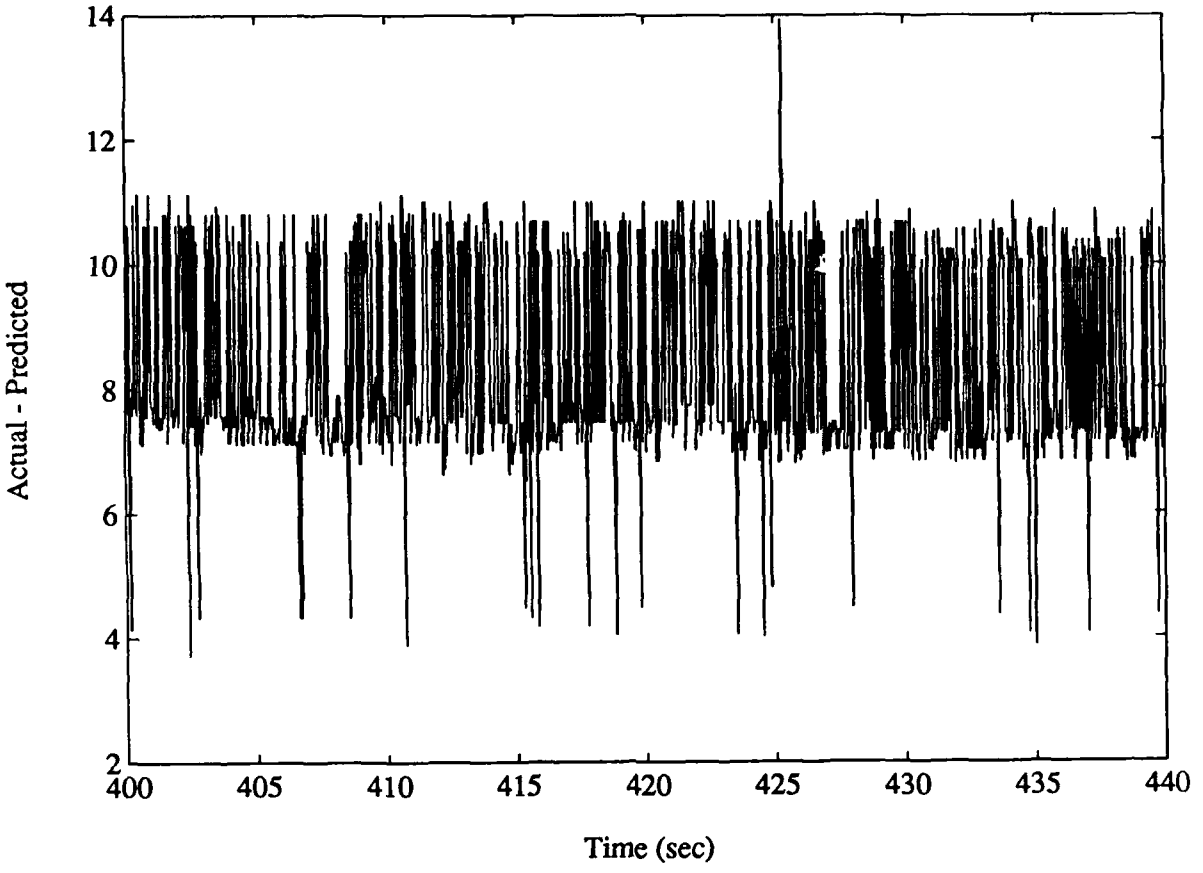
14
12
10
8
6
4
2
Actual - Predicted
400
405
410
415
420
425
430
435
440
Time (sec)

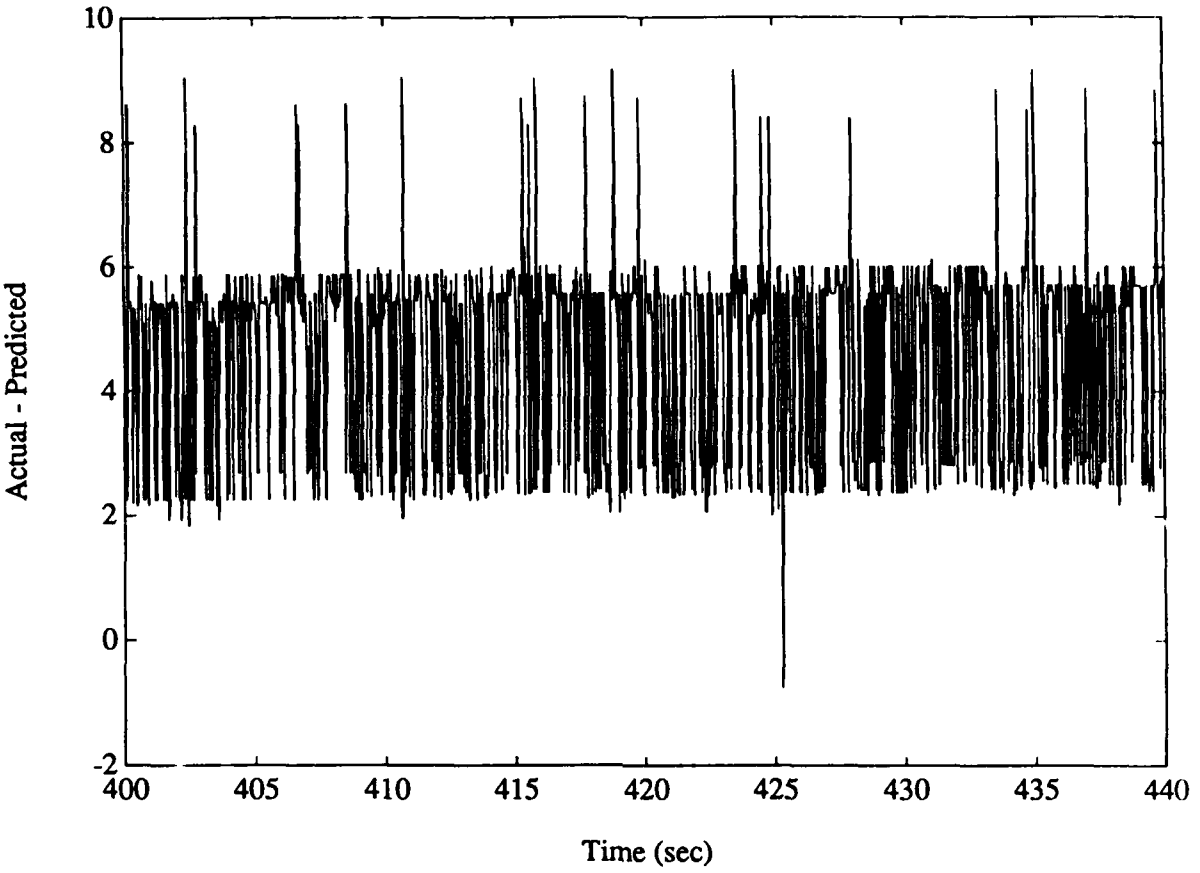
10
8
6
4
2
0
-2
Actual - Predicted
400
405
410
415
420
425
430
435
440
Time (sec)

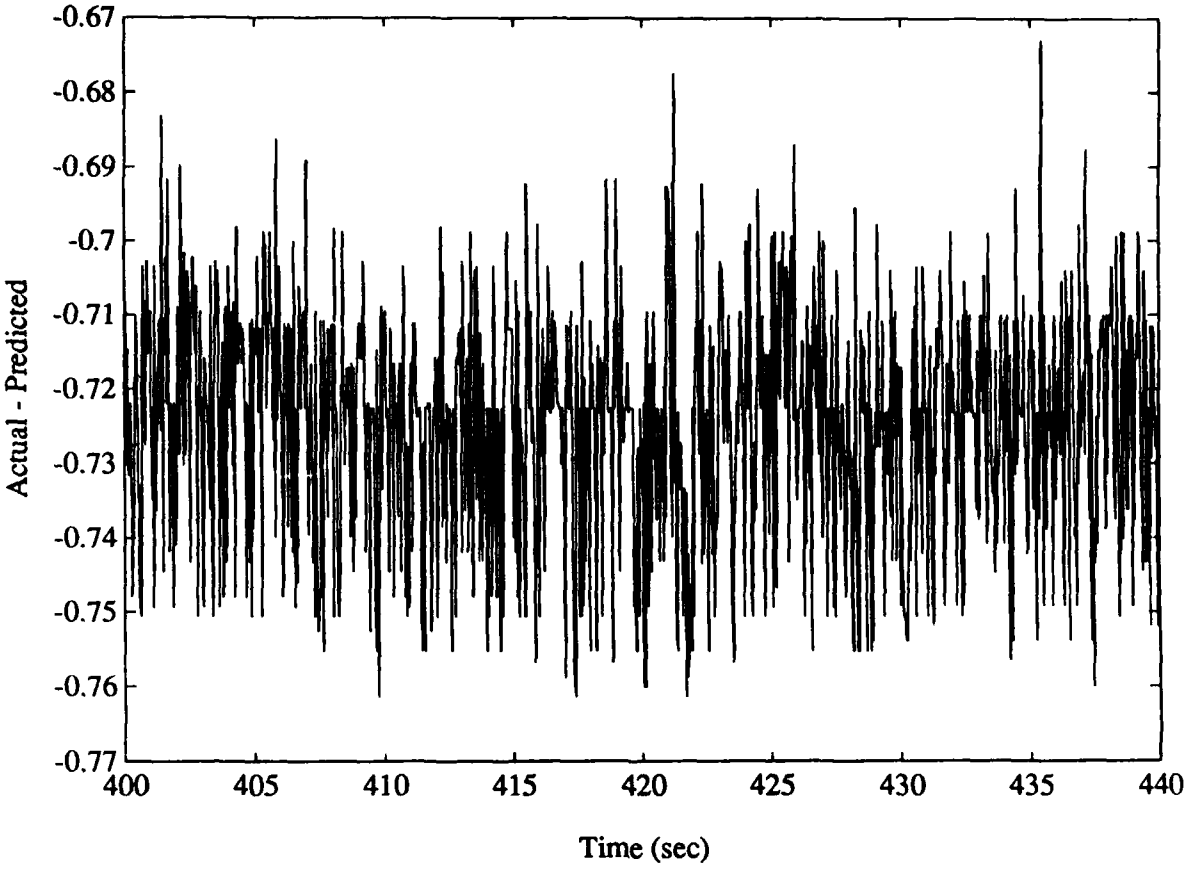
-0.67
-0.68
-0.69
-0.7
-0.71
-0.72
-0.73
-0.74
-0.75
-0.76
-0.77
Actual - Predicted
400
405
410
415
420
425
430
435
440
Time (sec)

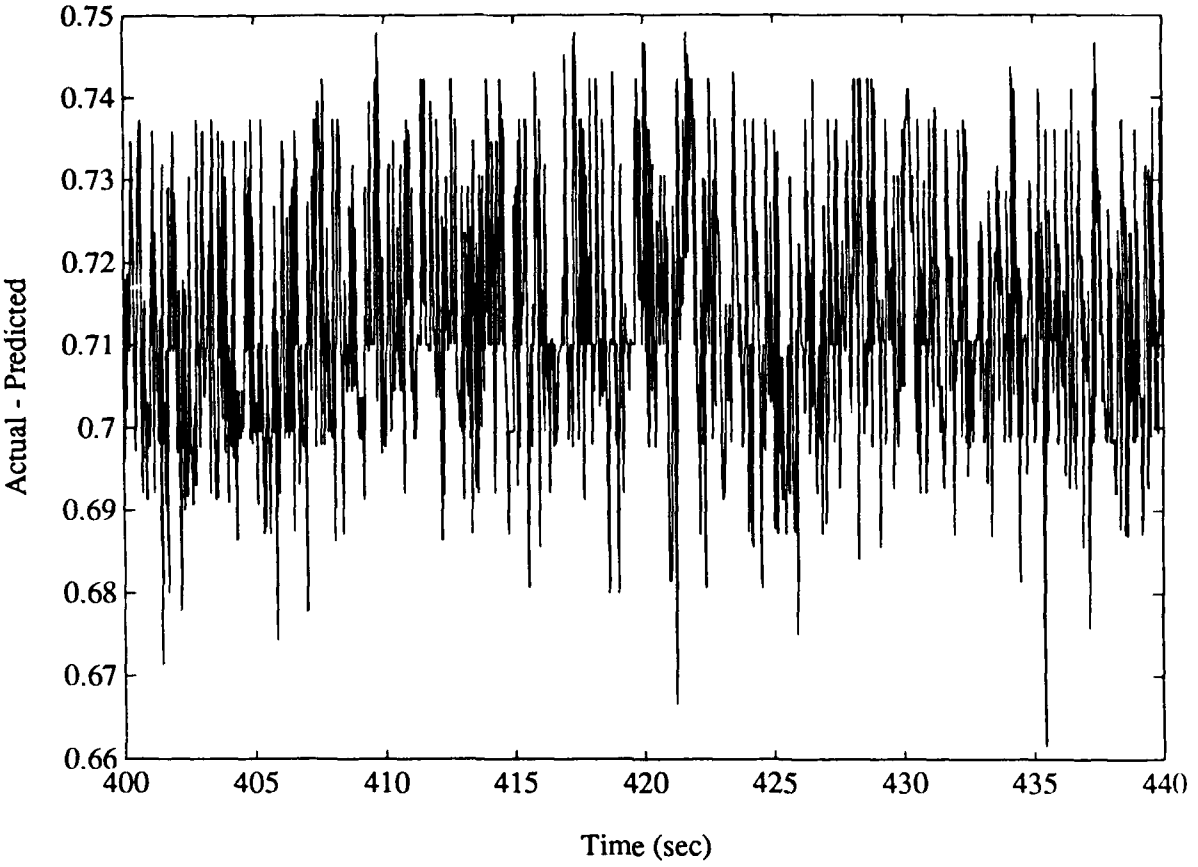
0.75
0.74
0.73
0.72
0.71
0.7
0.69
0.68
0.67
0.66
Actual - Predicted
400
405
410
415
420
425
430
435
440
Time (sec)

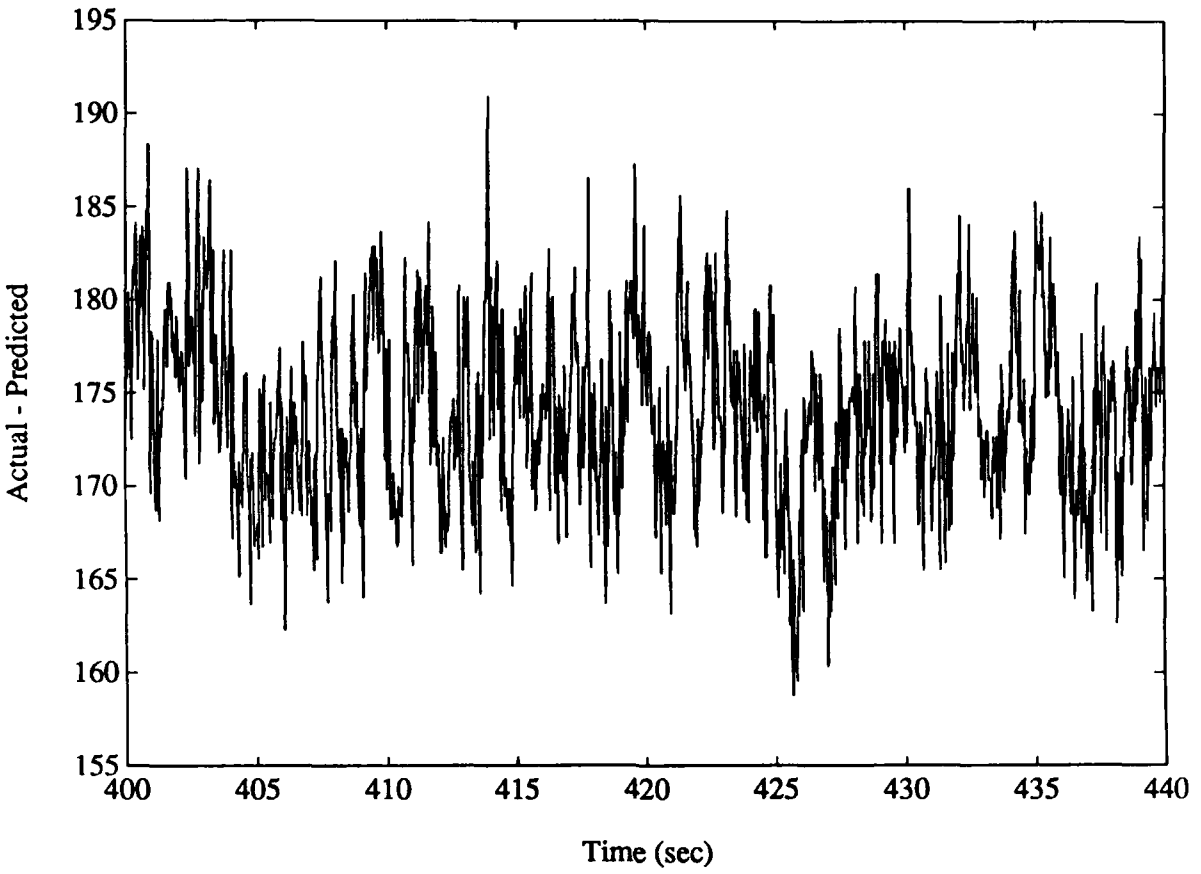
195
190
185
180
175
170
165
160
155
400
405
410
415
420
425
430
435
440
Actual - Predicted
Time (sec)

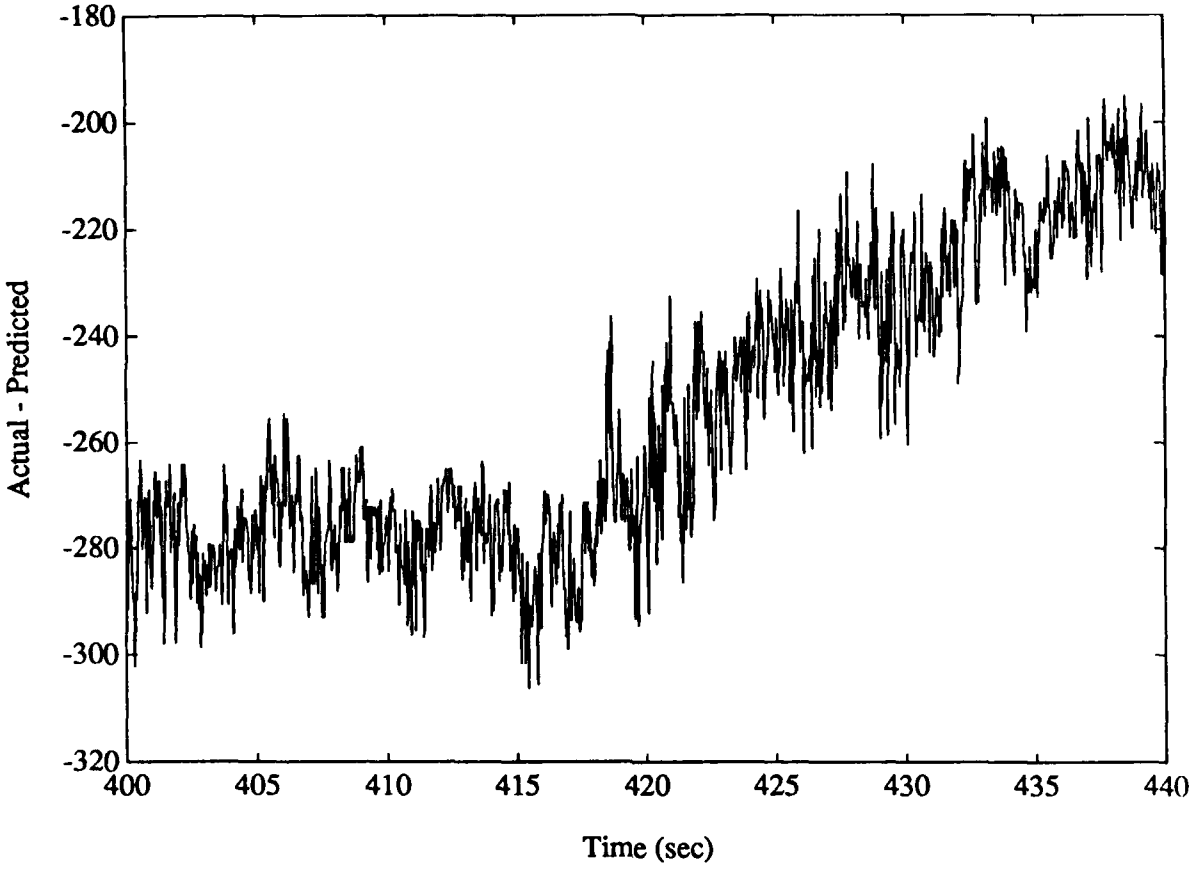
-180
-200
-220
-240
-260
-280
-300
-320
Actual - Predicted
400
405
410
415
420
425
430
435
440
Time (sec)

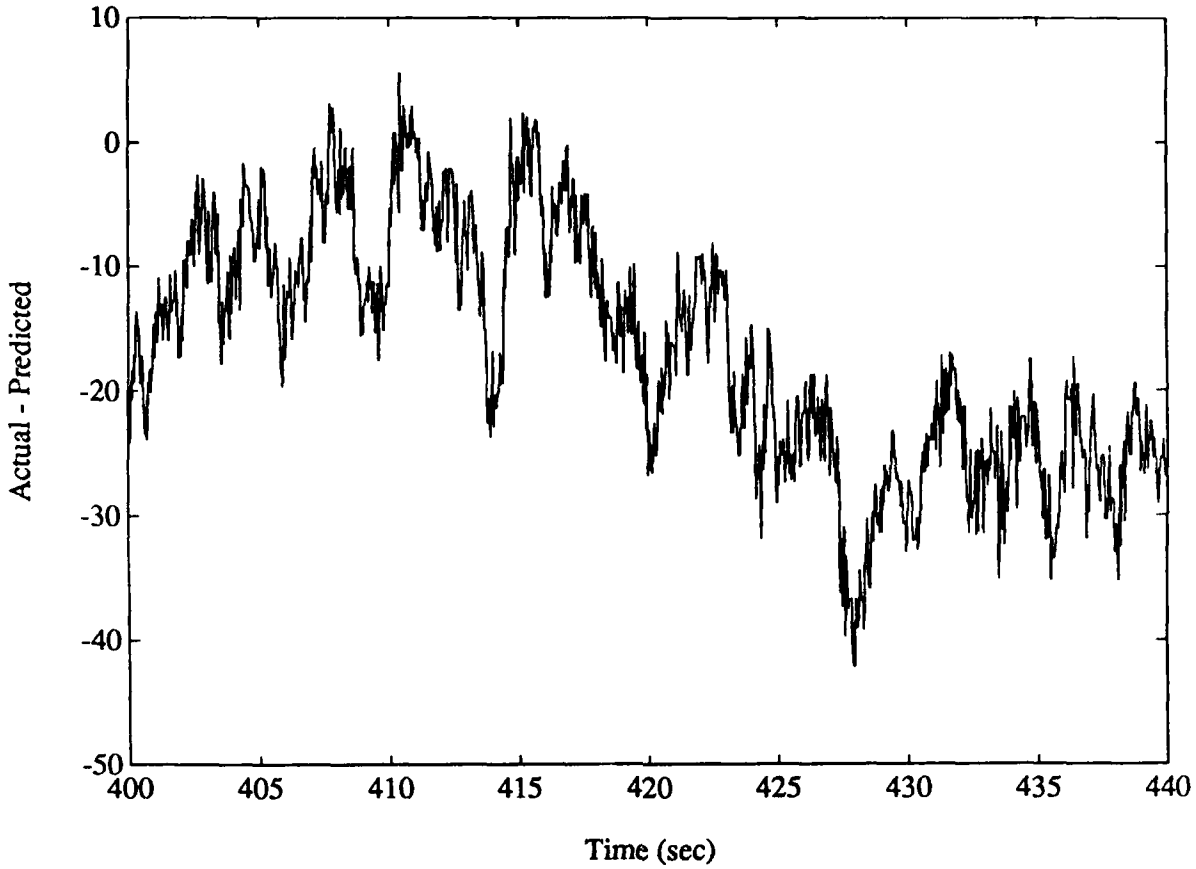
10
0
-10
-20
-30
-40
-50
400
405
410
415
420
425
430
435
440
Actual - Predicted
Time (sec)

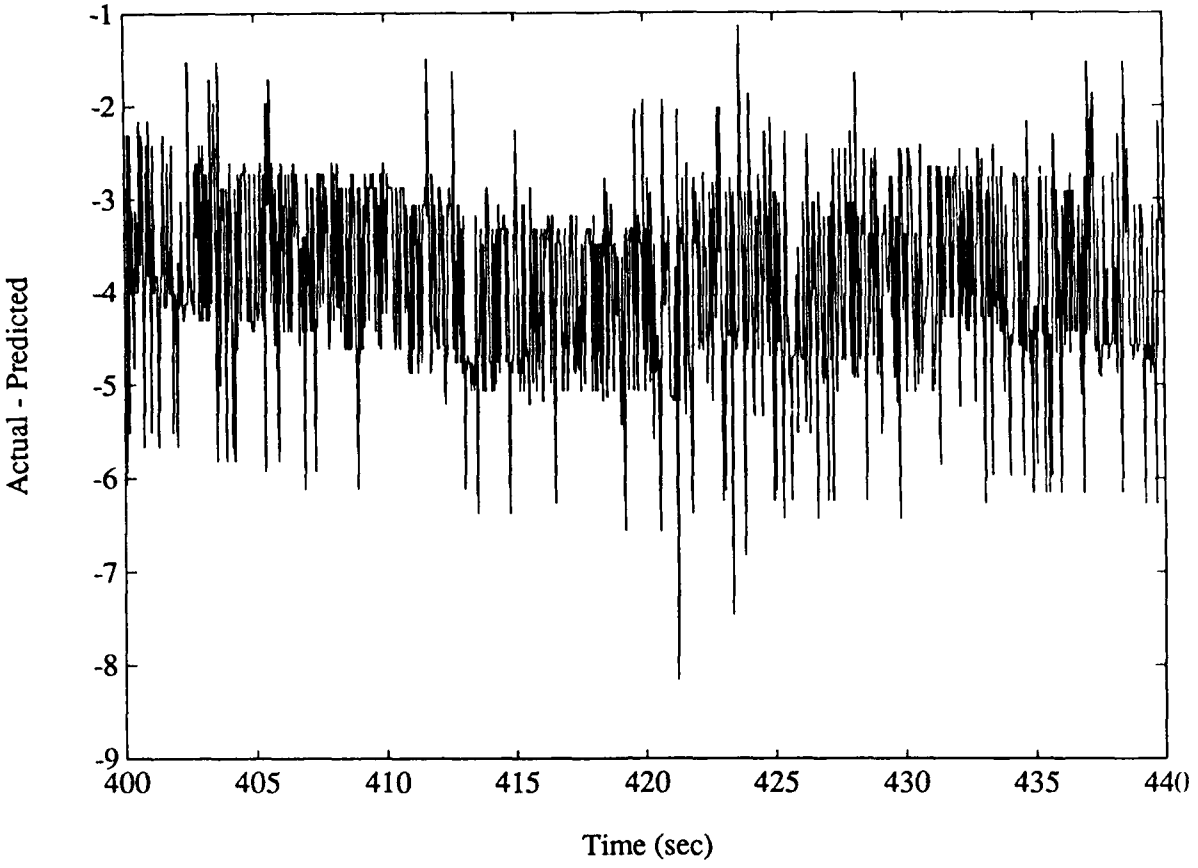
Actual - Predicted
-1
-2
-3
-4
-5
-6
-7
-8
-9
400
405
410
415
420
425
430
435
440
Time (sec)

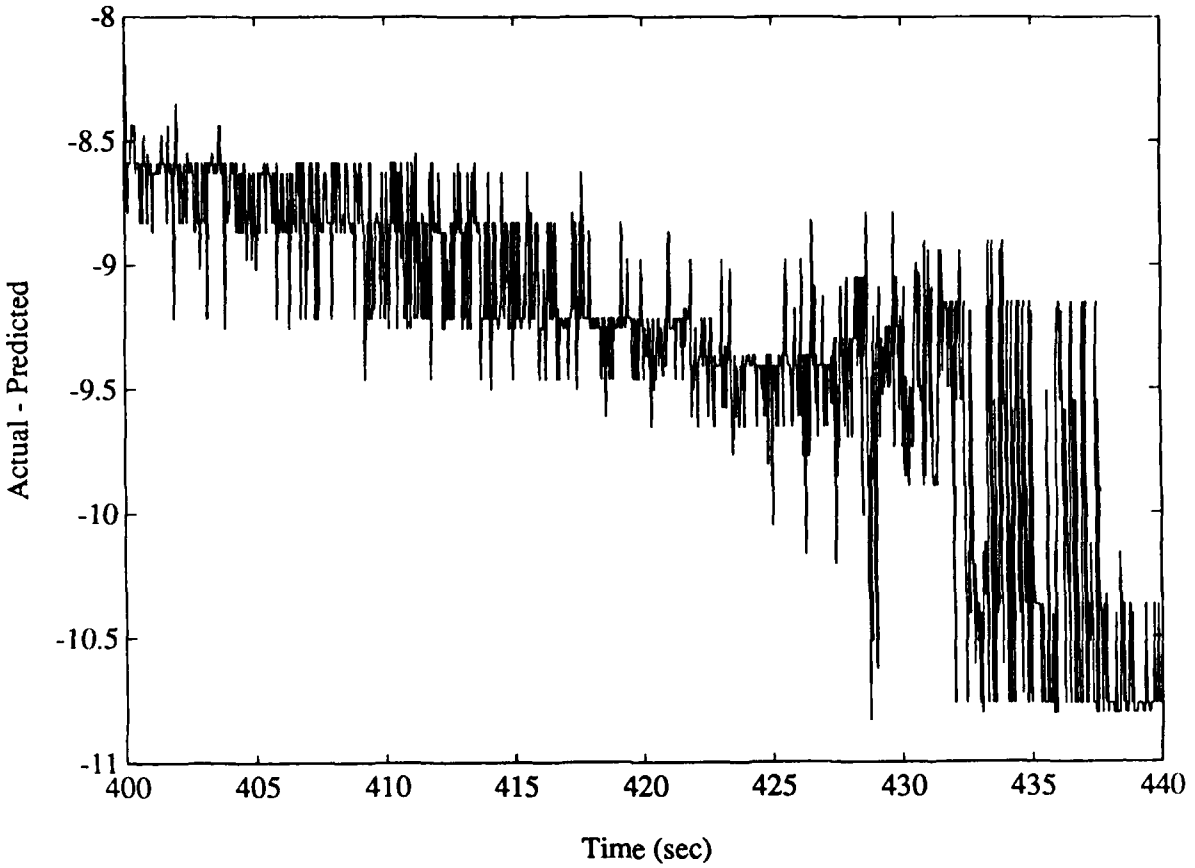
-8
-8.5
-9
-9.5
-10
-10.5
-11
Actual - Predicted
400
405
410
415
420
425
430
435
440
Time (sec)

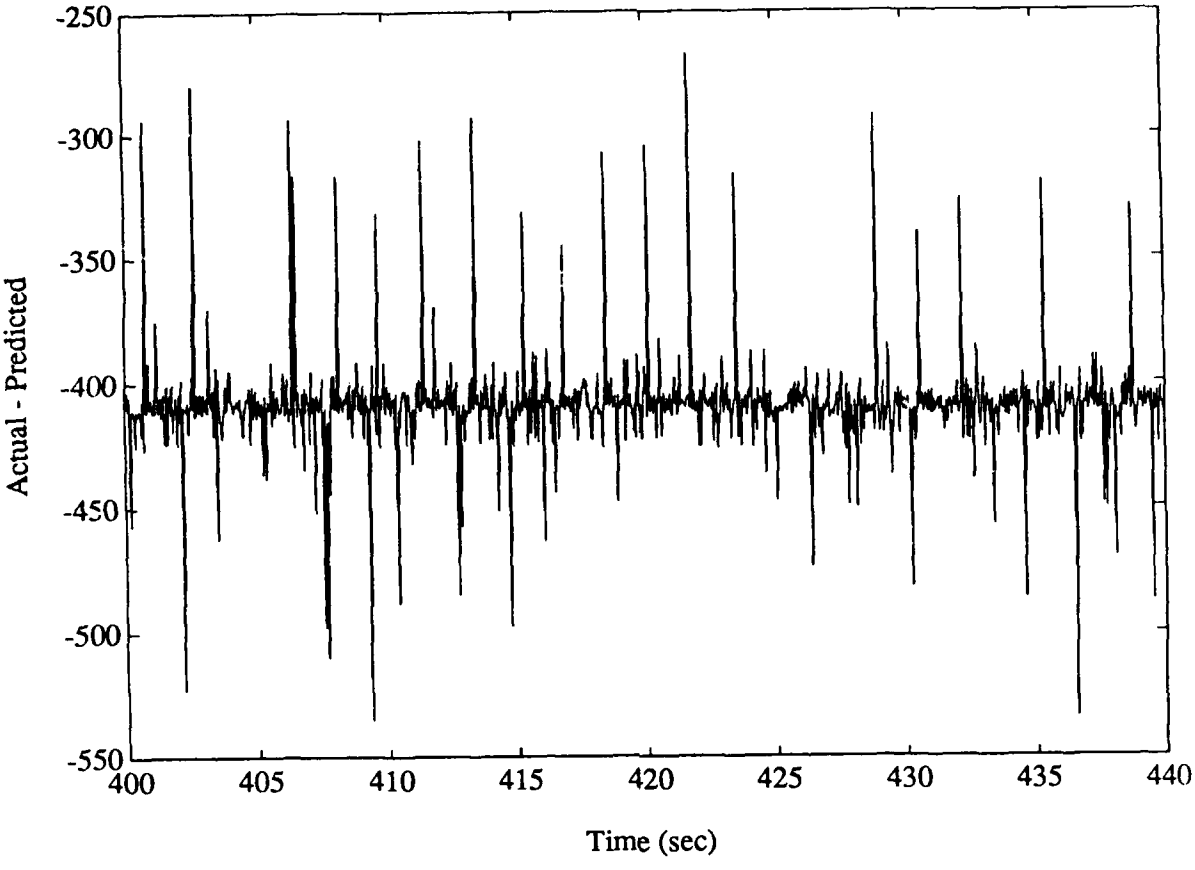
-250
-300
-350
-400
-450
-500
-550
Actual - Predicted
400
405
410
415
420
425
430
435
440
Time (sec)

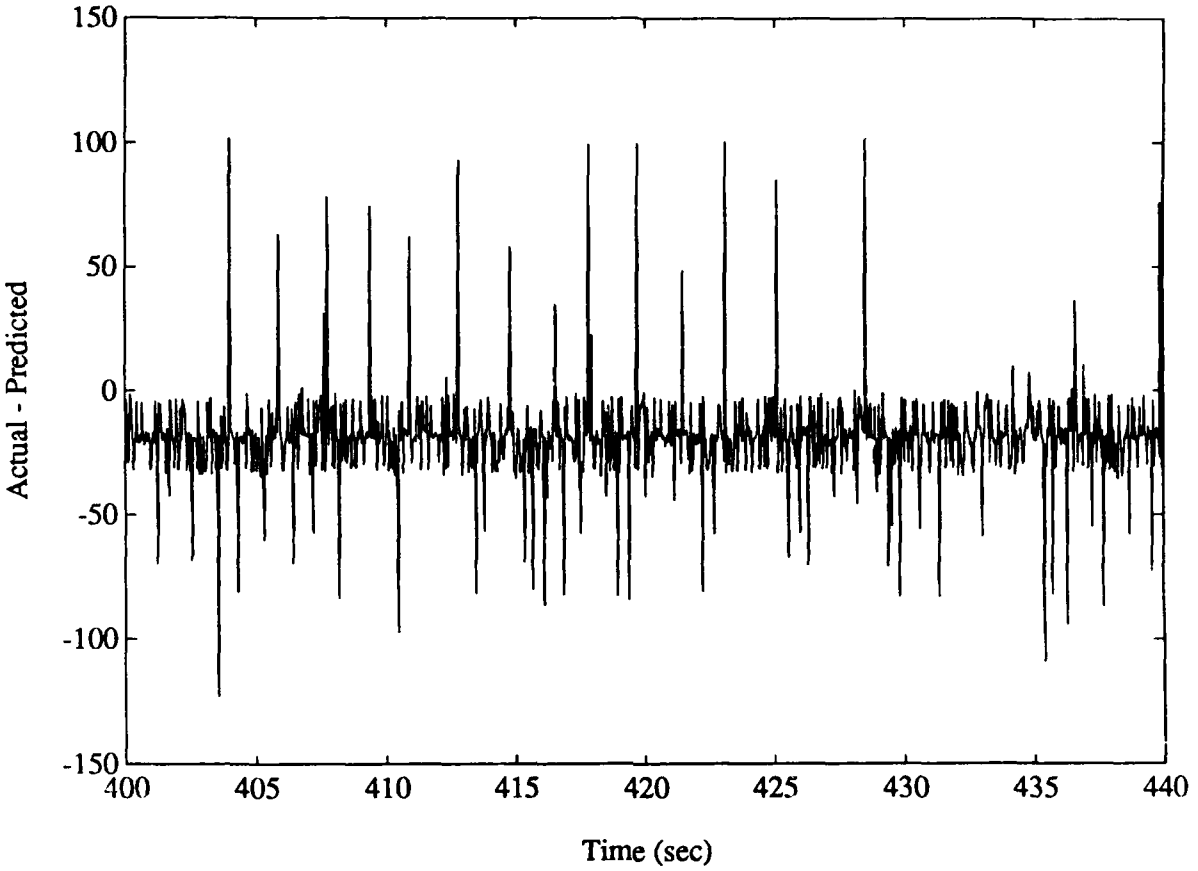
150
100
50
0
-50
-100
-150
400
405
410
415
420
425
430
435
440
Actual - Predicted
Time (sec)

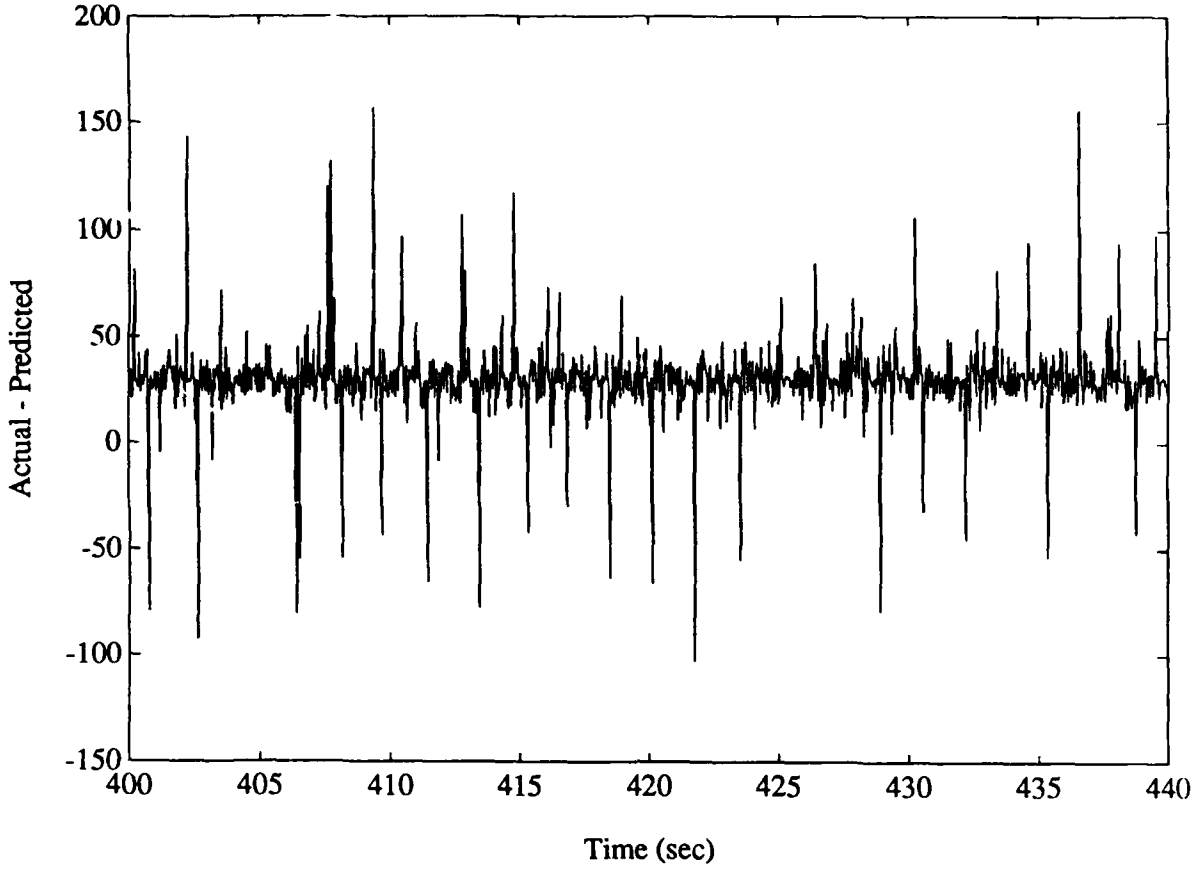
200
150
100
50
0
-50
-100
-150
Actual - Predicted
400
405
410
415
420
425
430
435
440
Time (sec)

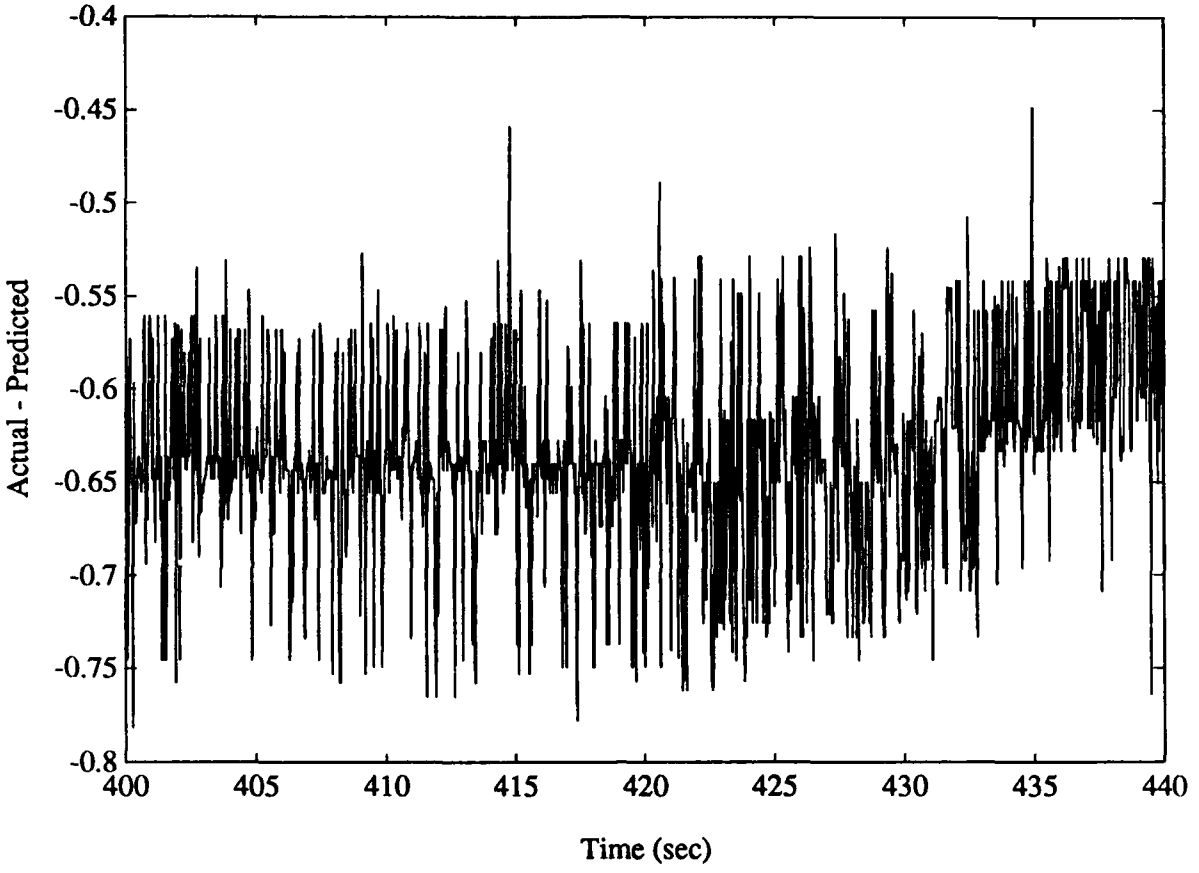
-0.4
-0.45
-0.5
-0.55
-0.6
-0.65
-0.7
-0.75
-0.8
Actual - Predicted
400
405
410
415
420
425
430
435
440
Time (sec)

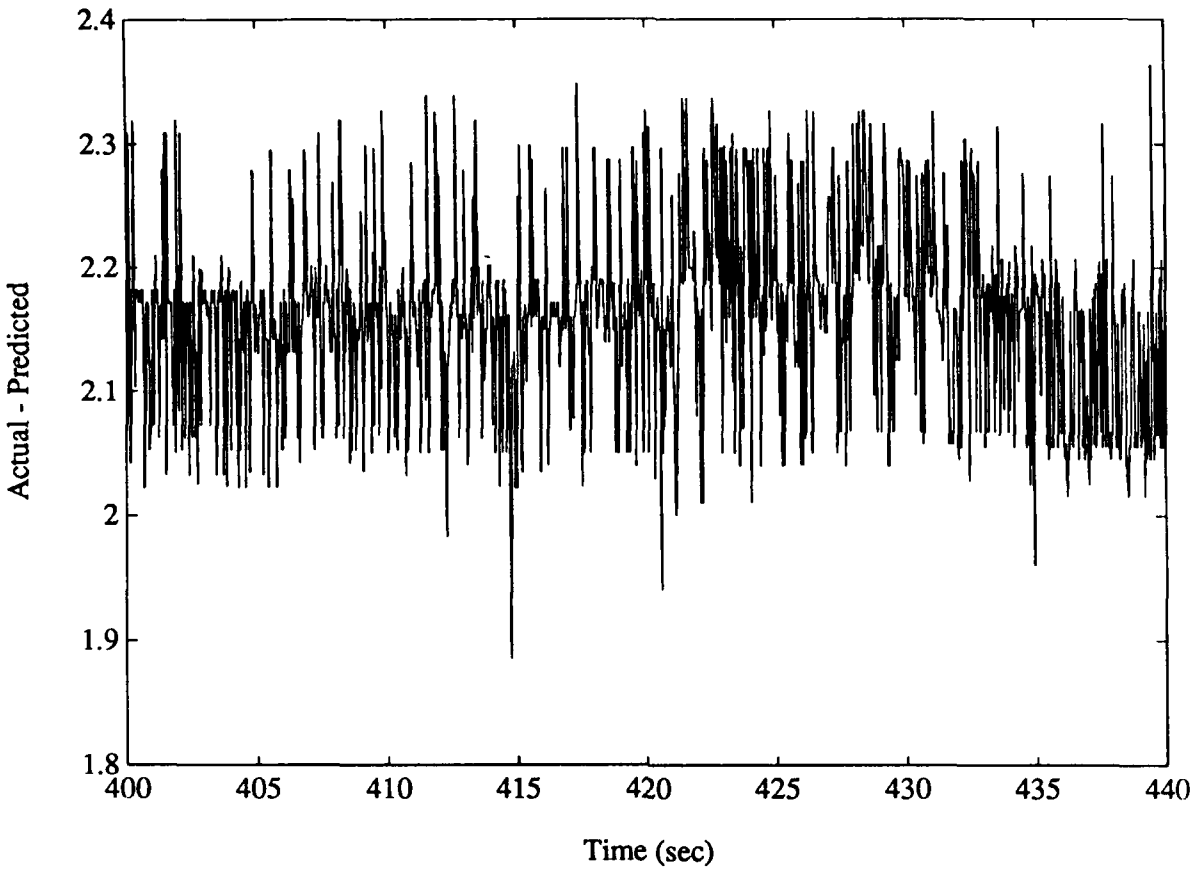
2.4
2.3
2.2
2.1
2
1.9
1.8
Actual - Predicted
400
405
410
415
420
425
430
435
440
Time (sec)

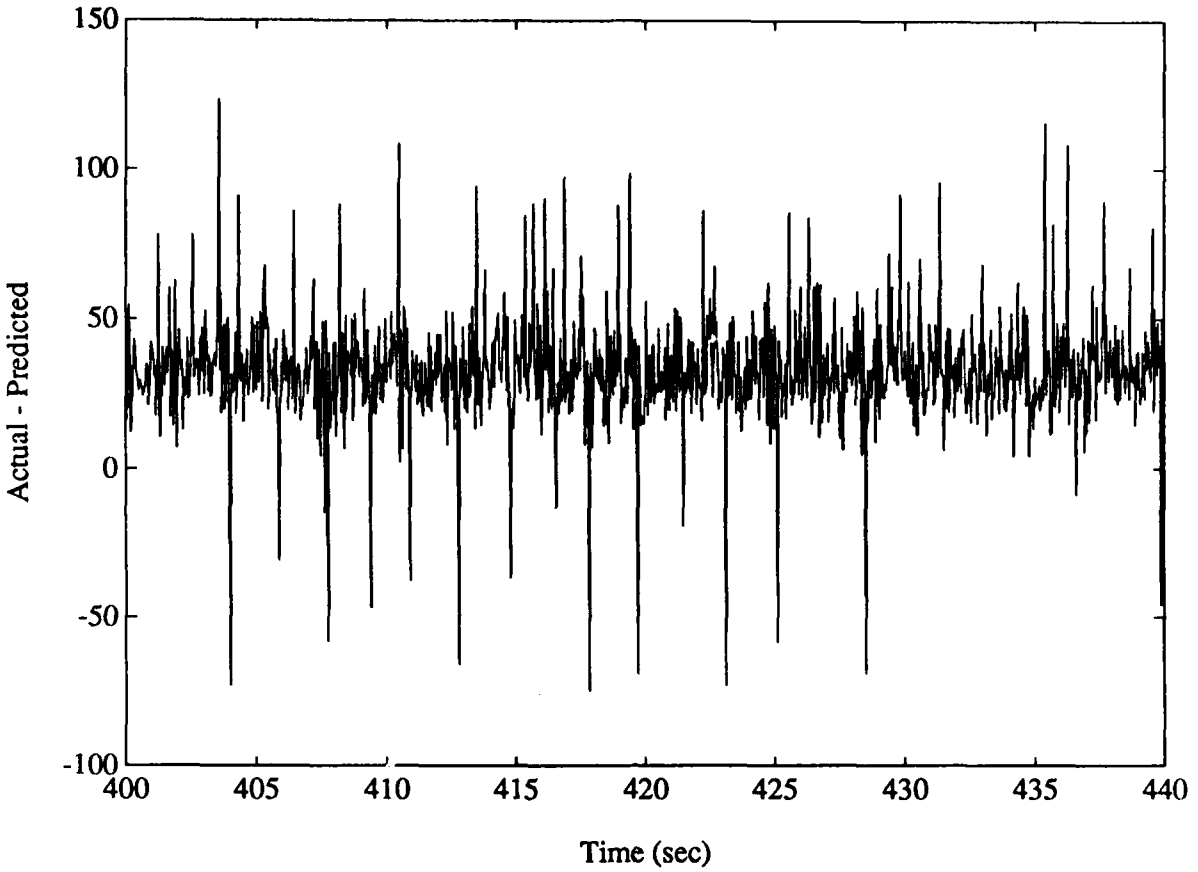
150
100
50
0
-50
-100
400
405
410
415
420
425
430
435
440
Actual - Predicted
Time (sec)

Regression equation results using best non-redundant parameters and "family average" coefficients.

Test A1619 @104% RPL

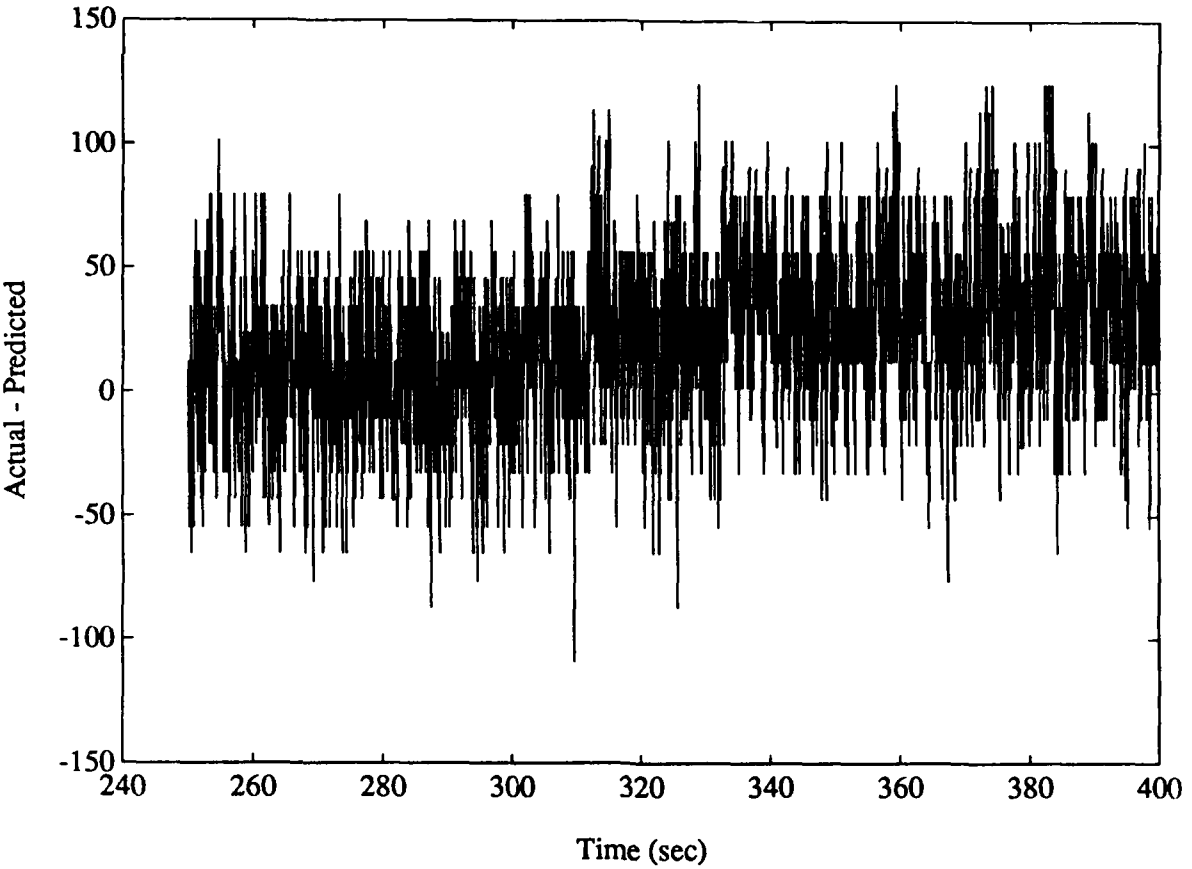
150
100
50
0
-50
-100
-150
240
260
280
300
320
340
360
380
400
Actual - Predicted
Time (sec)

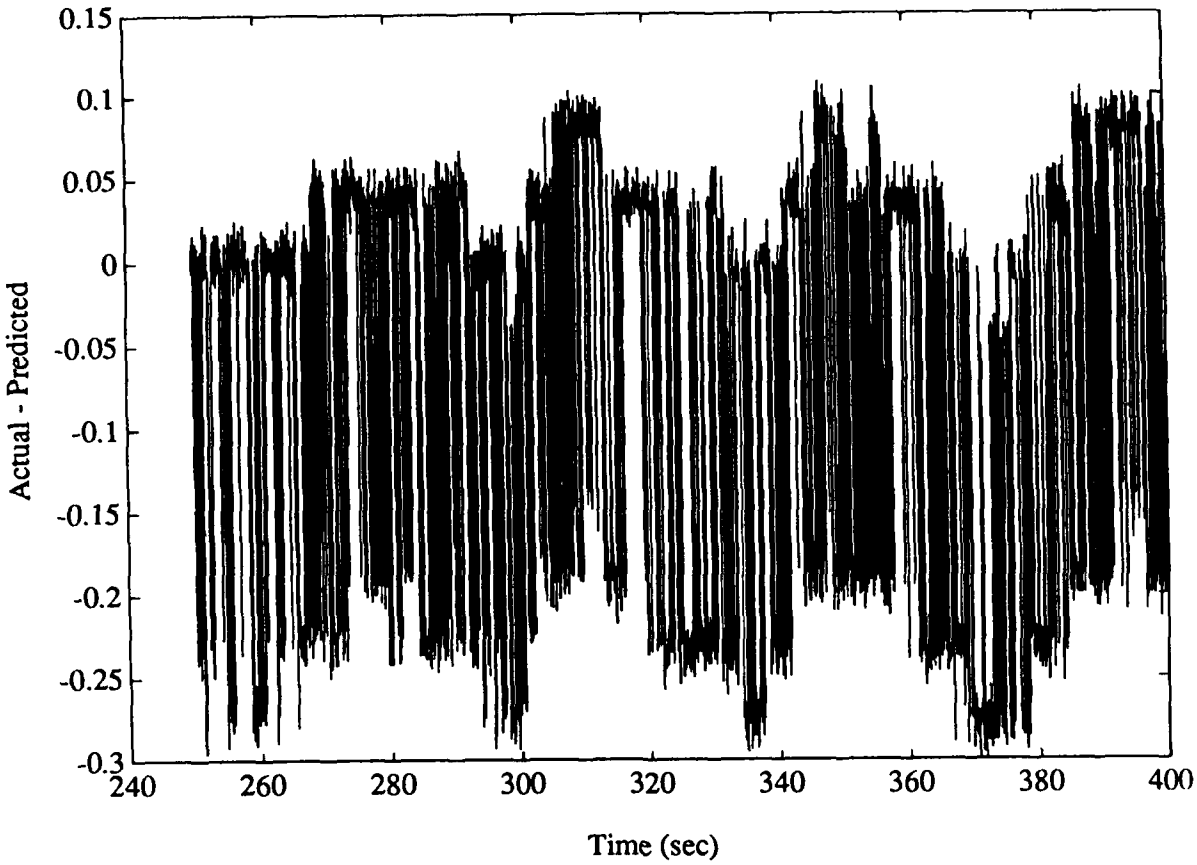
0.15
0.1
0.05
0
-0.05
-0.1
-0.15
-0.2
-0.25
-0.3
Actual - Predicted
240
260
280
300
320
340
360
380
400
Time (sec)

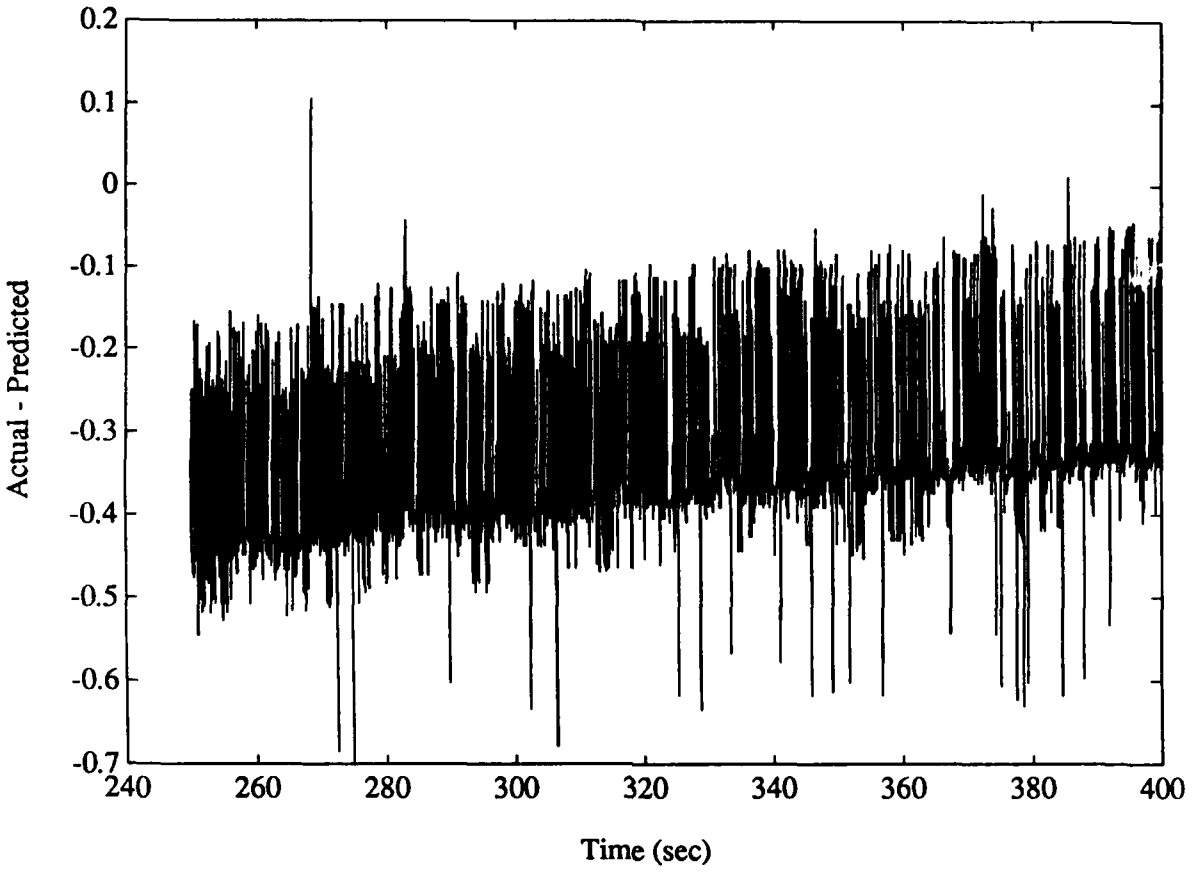
0.2
0.1
0
-0.1
-0.2
-0.3
-0.4
-0.5
-0.6
-0.7
Actual - Predicted
240
260
280
300
320
340
360
380
400
Time (sec)

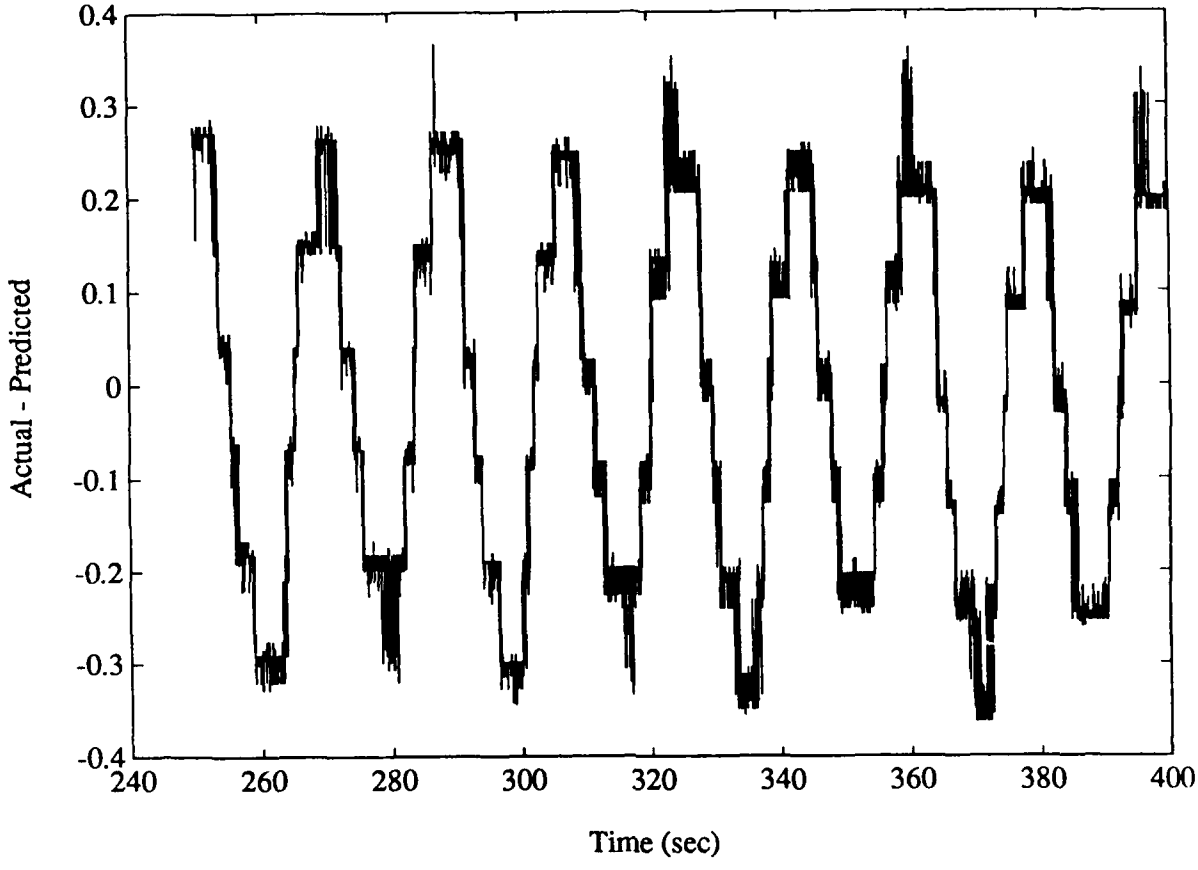
0.4
0.3
0.2
0.1
0
-0.1
-0.2
-0.3
-0.4
Actual - Predicted
240
260
280
300
320
340
360
380
400
Time (sec)

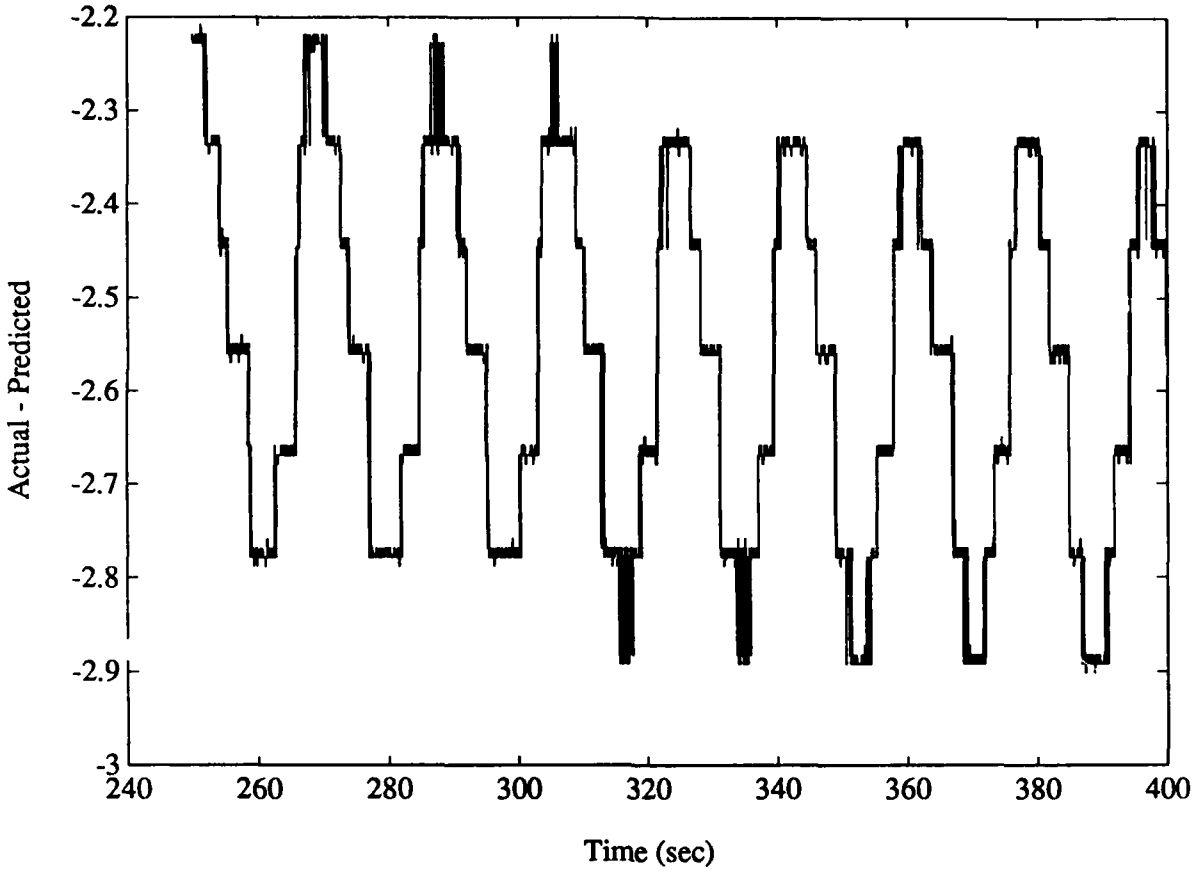
-2.2
-2.3
-2.4
-2.5
-2.6
-2.7
-2.8
-2.9
-3
Actual - Predicted
240
260
280
300
320
340
360
380
400
Time (sec)

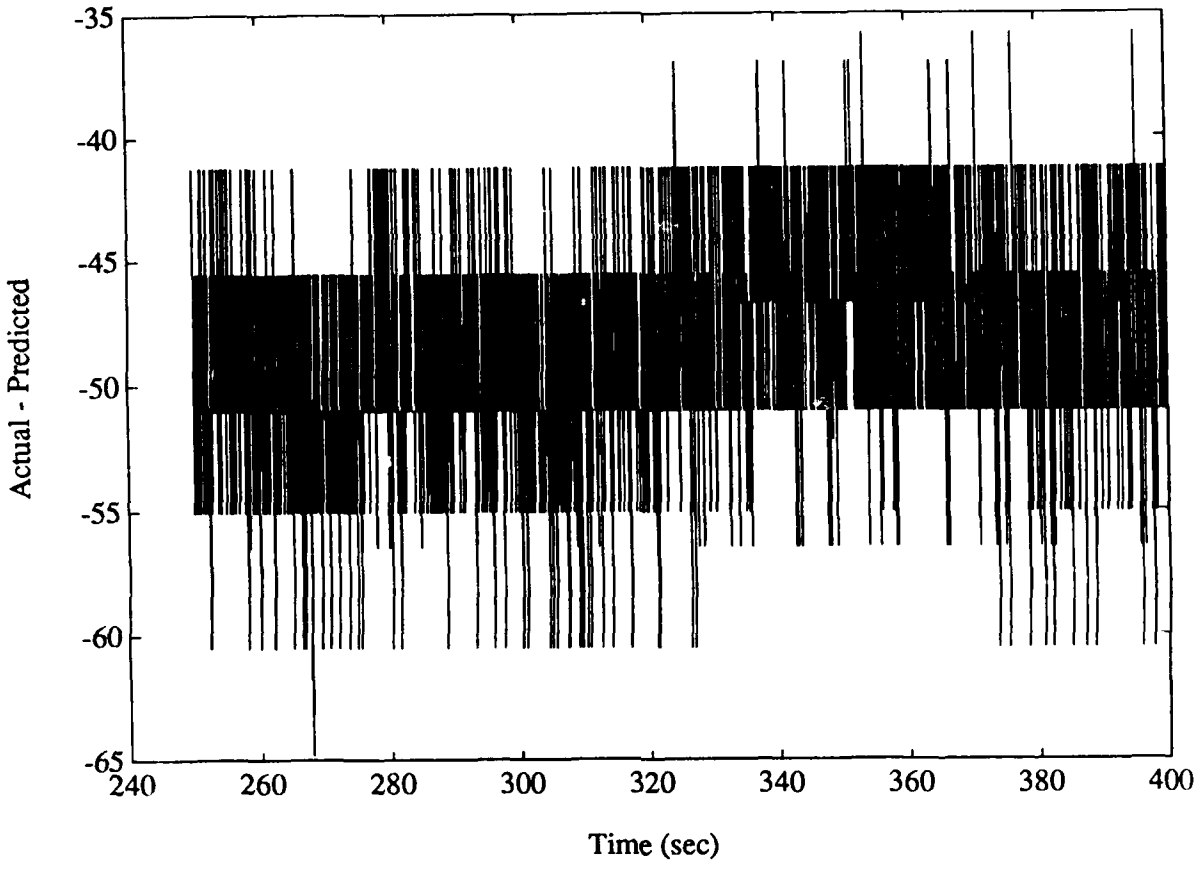
-35
-40
-45
-50
-55
-60
-65
240
260
280
300
320
340
360
380
400
Actual - Predicted
Time (sec)

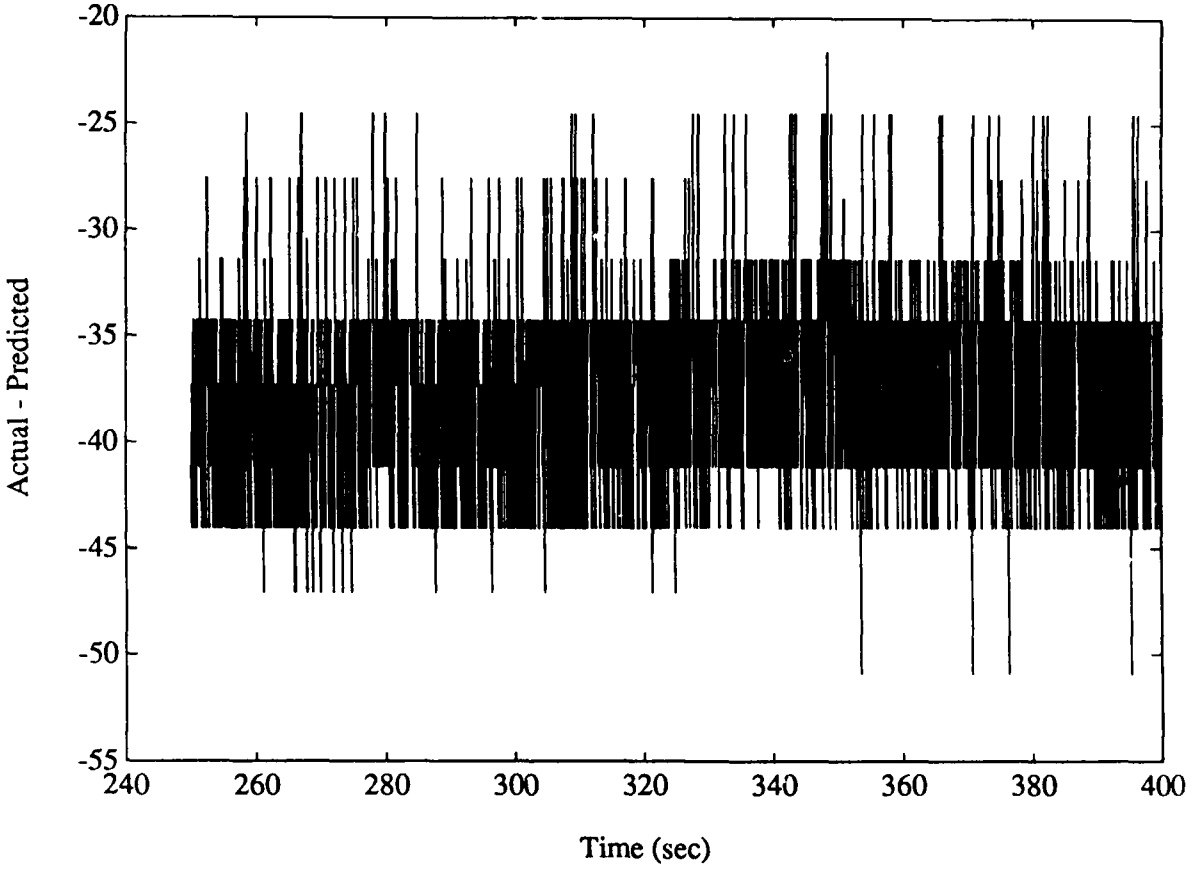
-20
-25
-30
-35
-40
-45
-50
-55
240
260
280
300
320
340
360
380
400
Actual - Predicted
Time (sec)

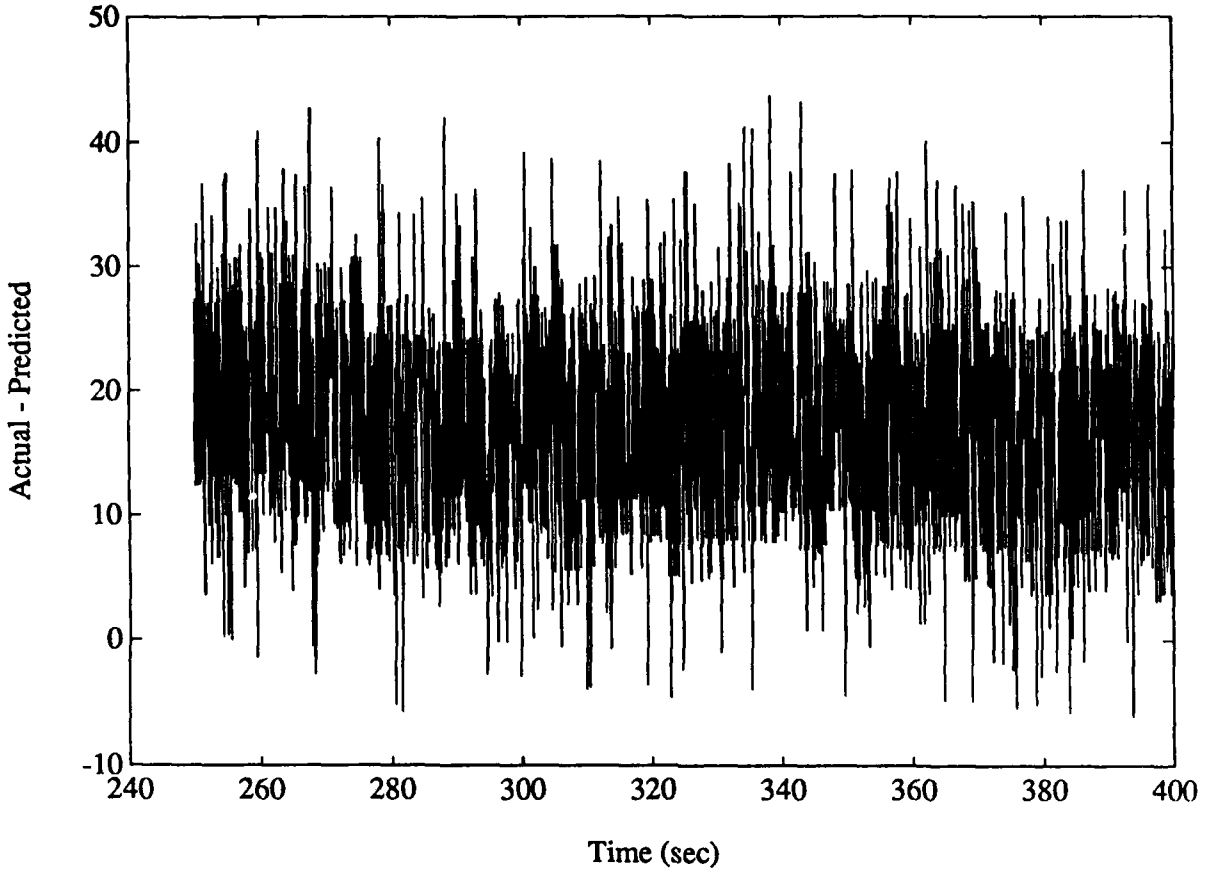
50
40
30
20
10
0
-10
240
260
280
300
320
340
360
380
400
Actual - Predicted
Time (sec)

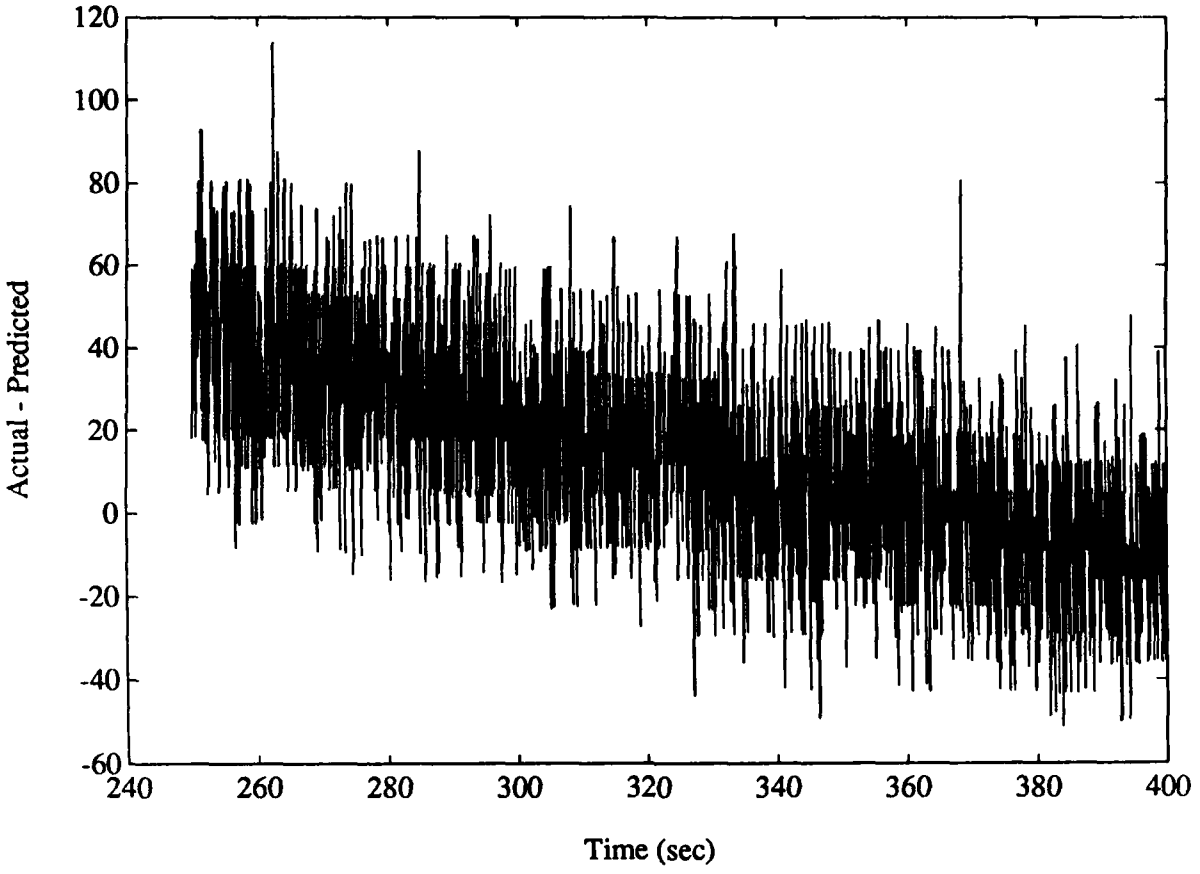
120
100
80
60
40
20
0
-20
-40
-60
240
260
280
300
320
340
360
380
400
Actual - Predicted
Time (sec)

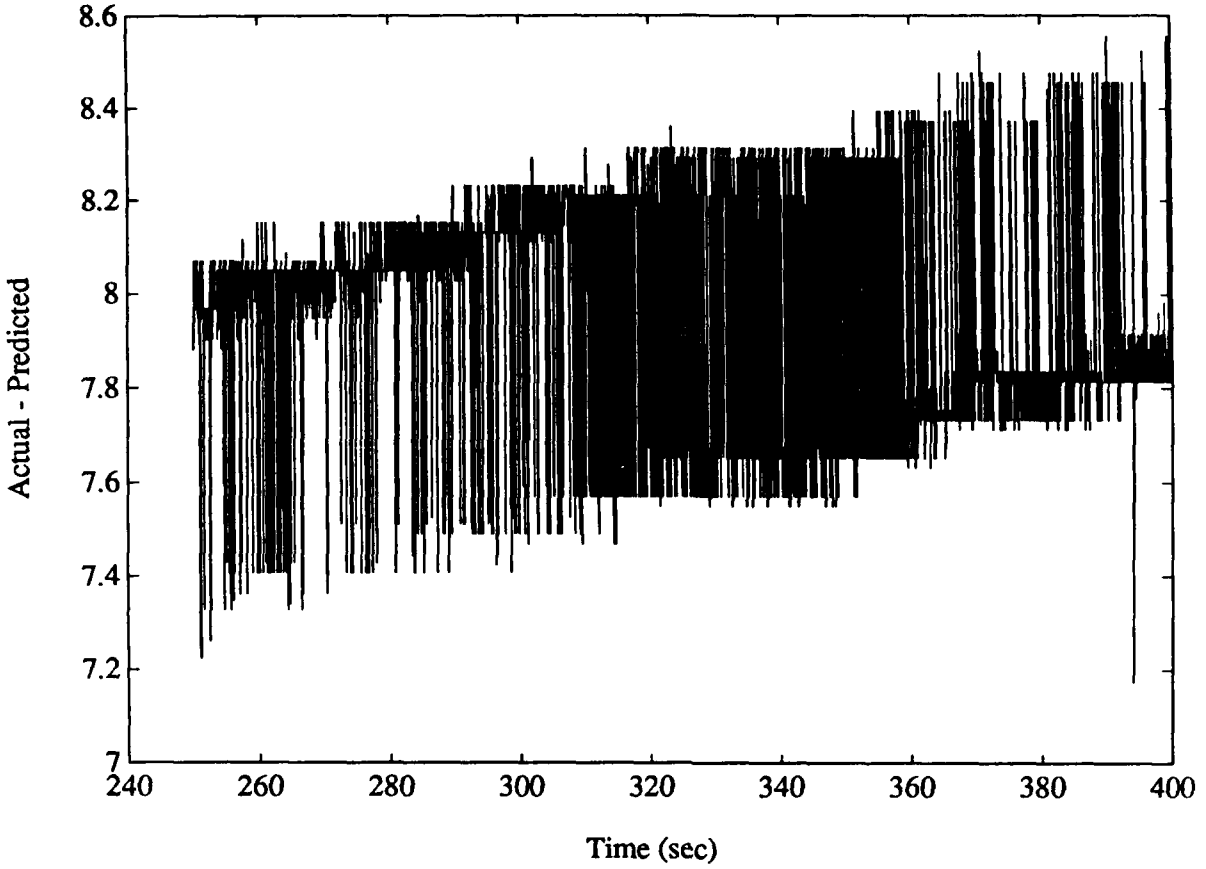
8.6
8.4
8.2
8
7.8
7.6
7.4
7.2
7
240
260
280
300
320
340
360
380
400
Actual - Predicted
Time (sec)

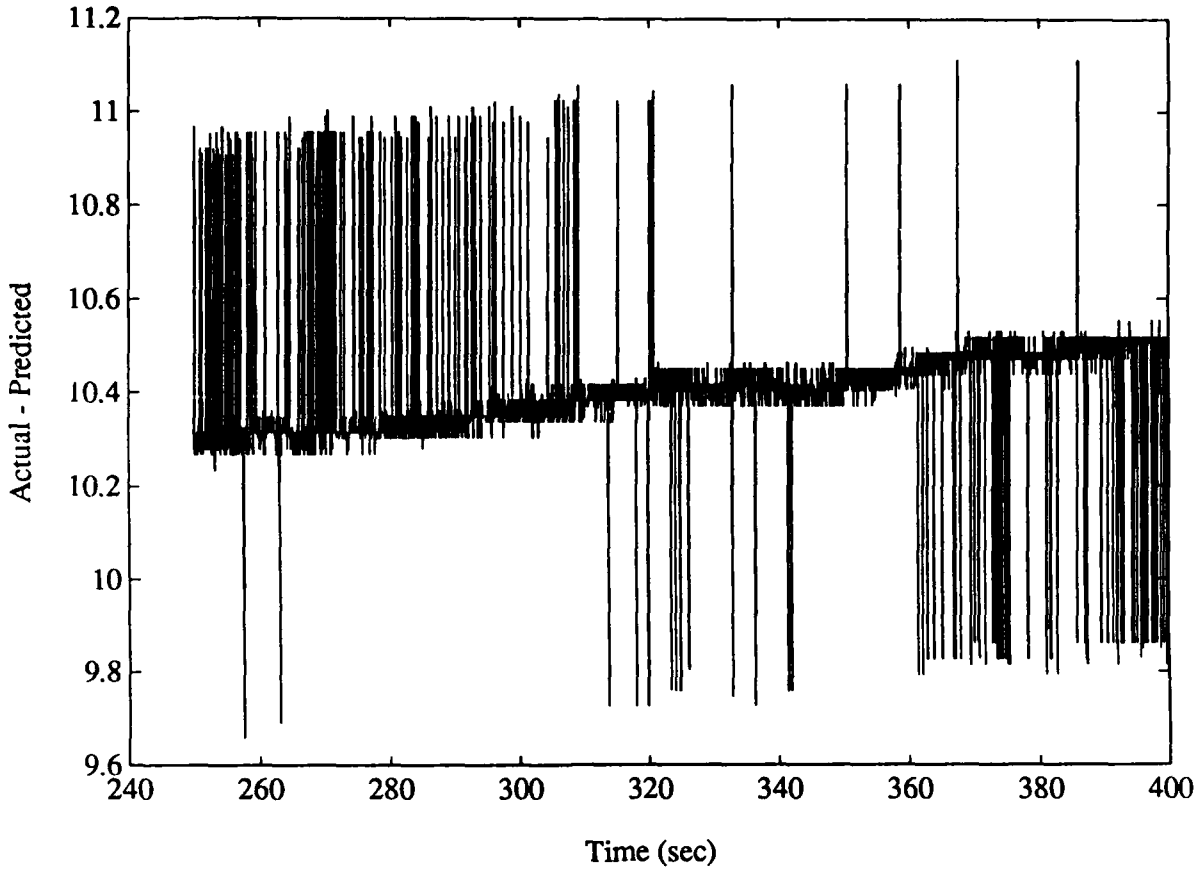
11.2
11
10.8
10.6
10.4
10.2
10
9.8
9.6
Actual - Predicted
240
260
280
300
320
340
360
380
400
Time (sec)

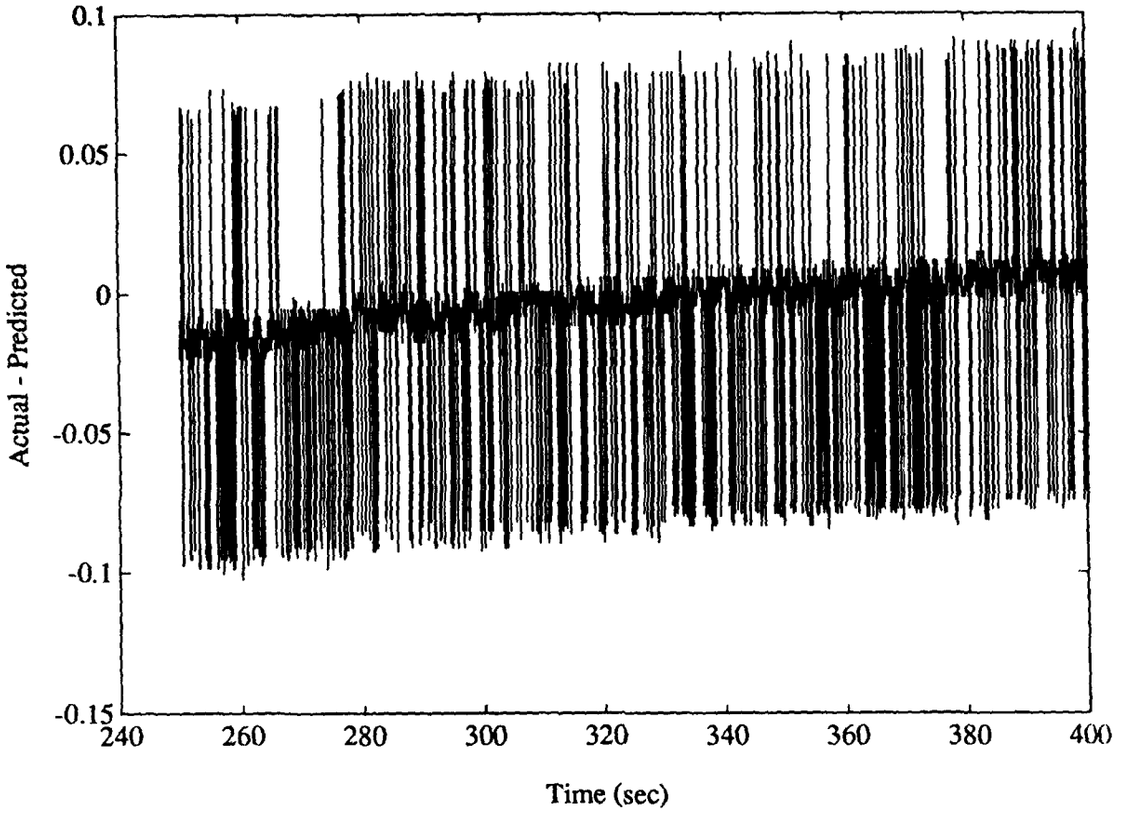
0.1
0.05
0
-0.05
-0.1
-0.15
Actual - Predicted
240
260
280
300
320
340
360
380
400
Time (sec)

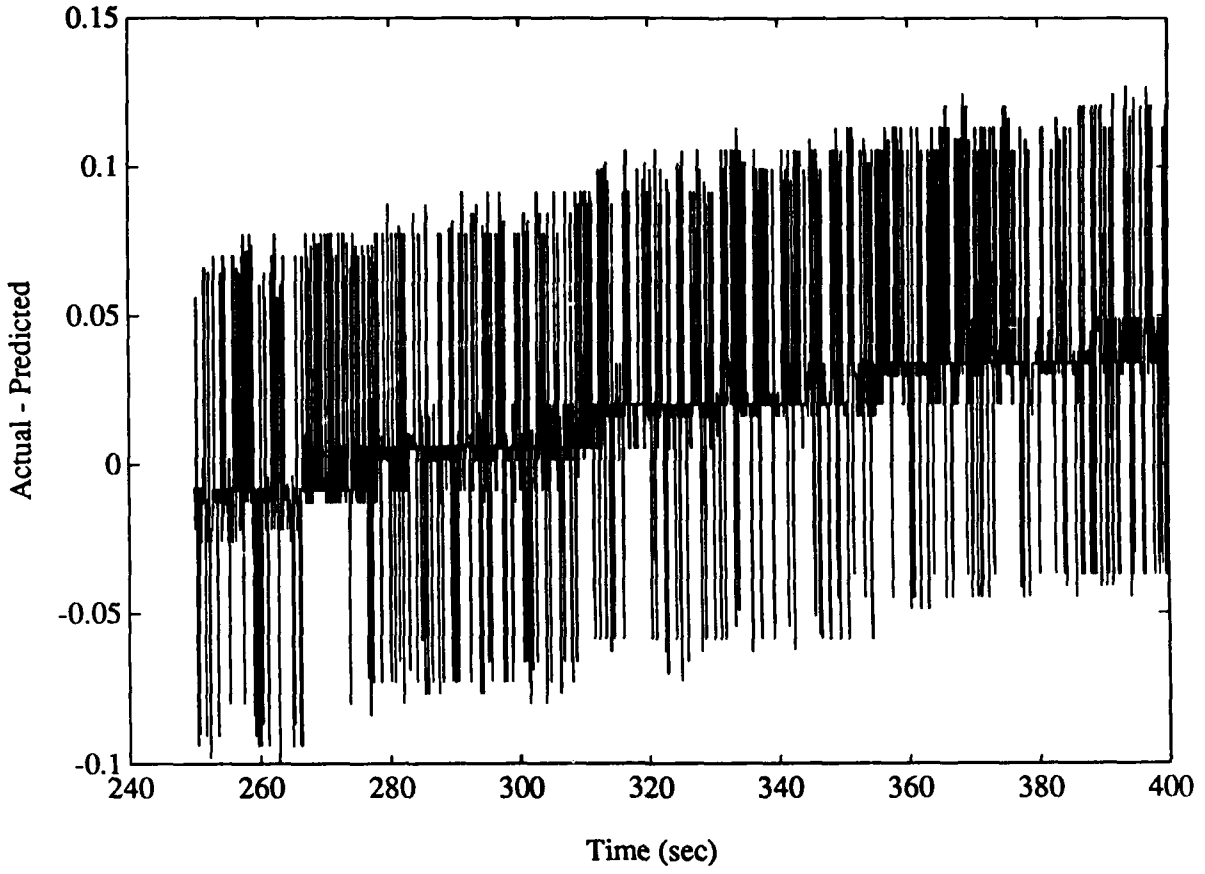
0.15
0.1
0.05
0
-0.05
-0.1
Actual - Predicted
240
260
280
300
320
340
360
380
400
Time (sec)

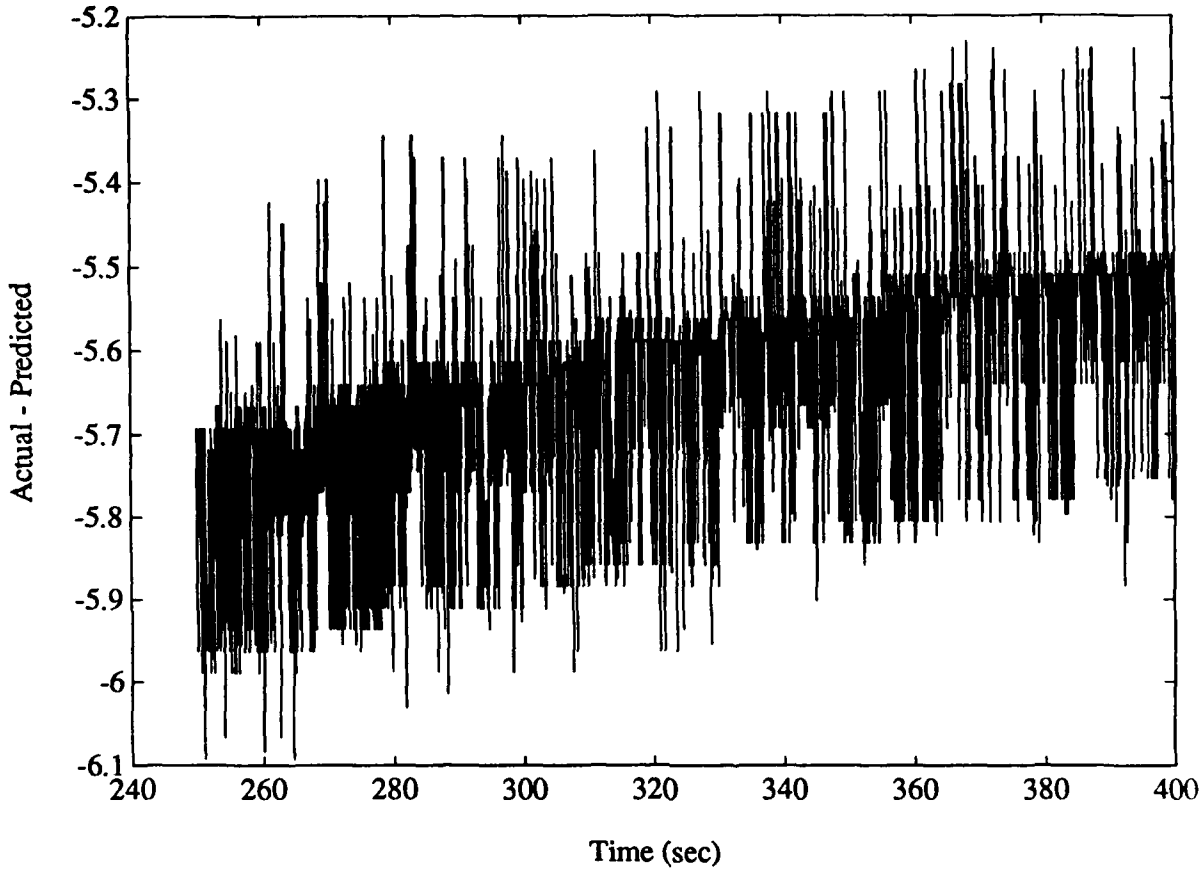
-5.2
-5.3
-5.4
-5.5
-5.6
-5.7
-5.8
-5.9
-6
-6.1
Actual - Predicted
240
260
280
300
320
340
360
380
400
Time (sec)

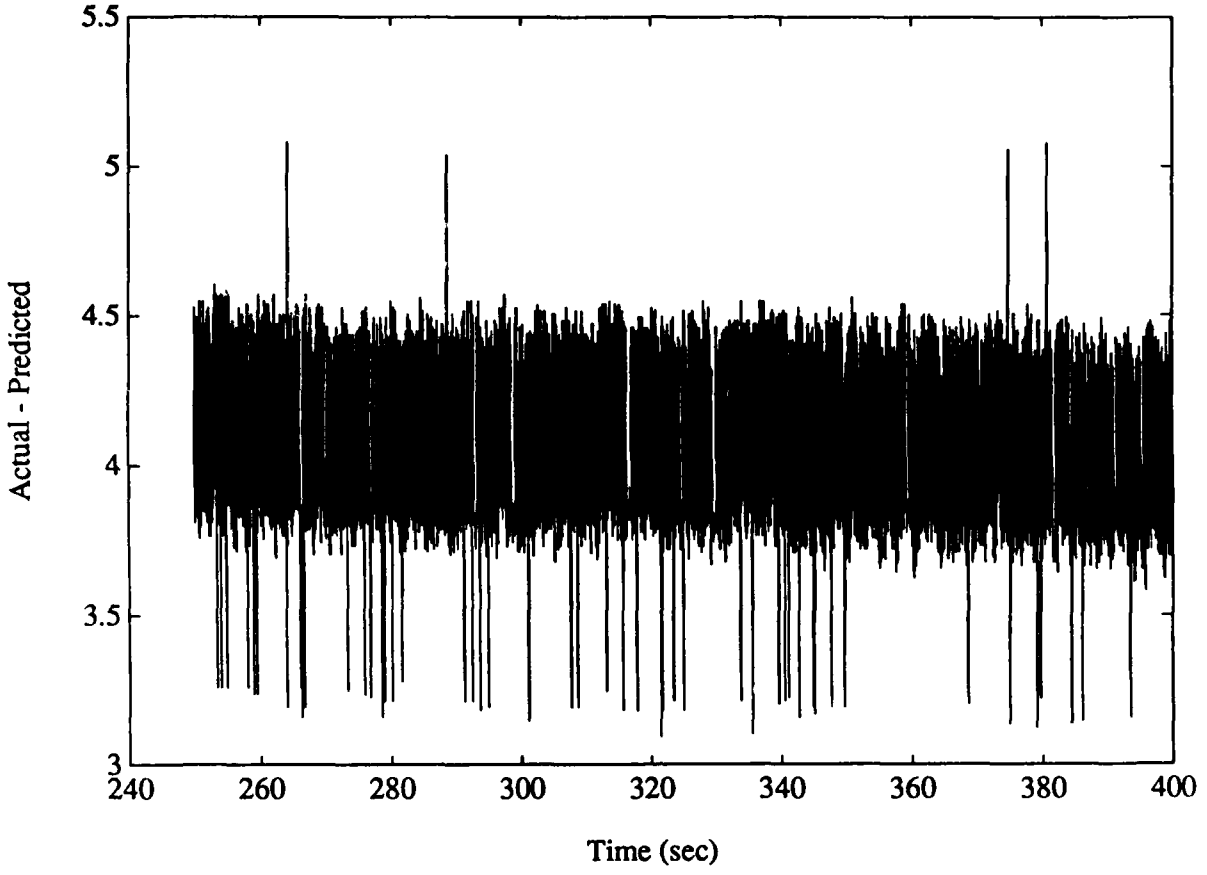
5.5
5
4.5
4
3.5
3
240
260
280
300
320
340
360
380
400
Actual - Predicted
Time (sec)

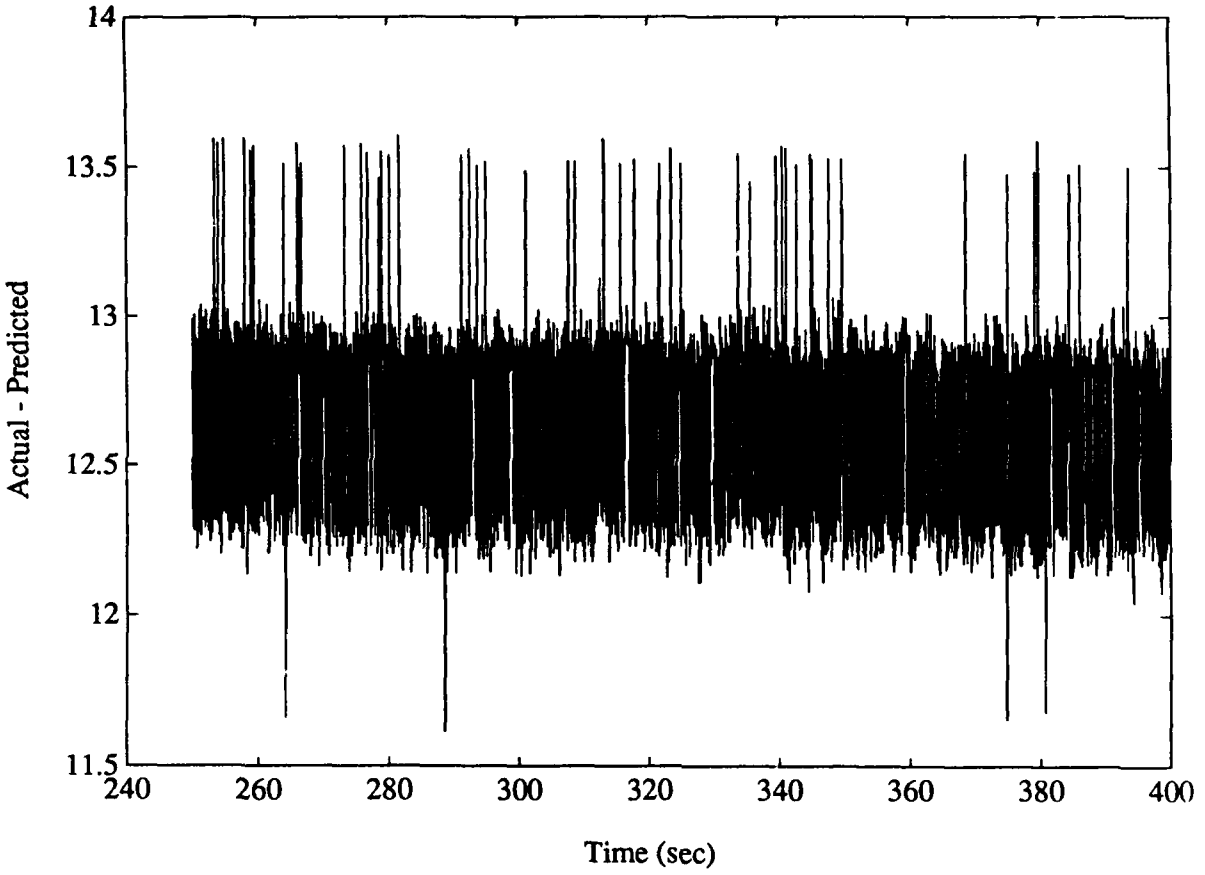
14
13.5
13
12.5
12
11.5
Actual - Predicted
240
260
280
300
320
340
360
380
400
Time (sec)

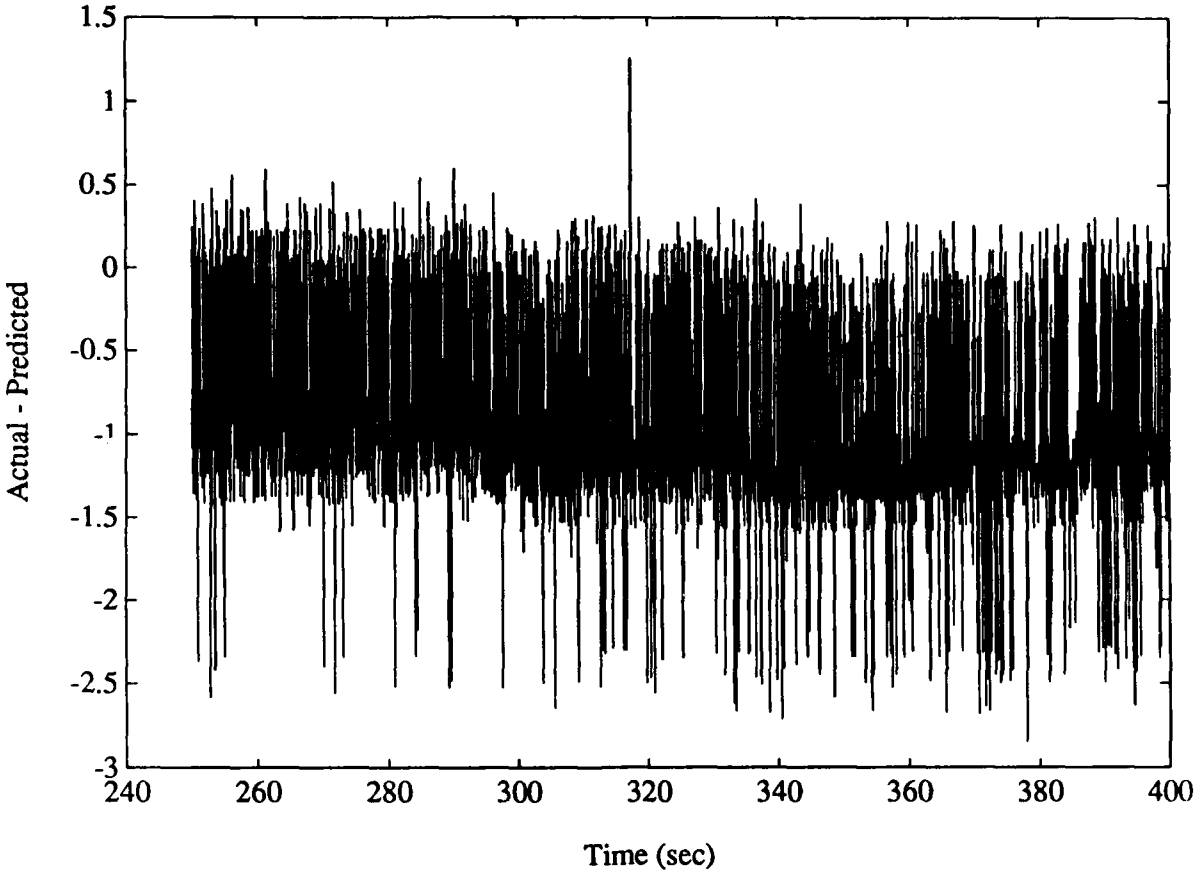
1.5
1
0.5
0
-0.5
-1
-1.5
-2
-2.5
-3
240
260
280
300
320
340
360
380
400
Actual - Predicted
Time (sec)

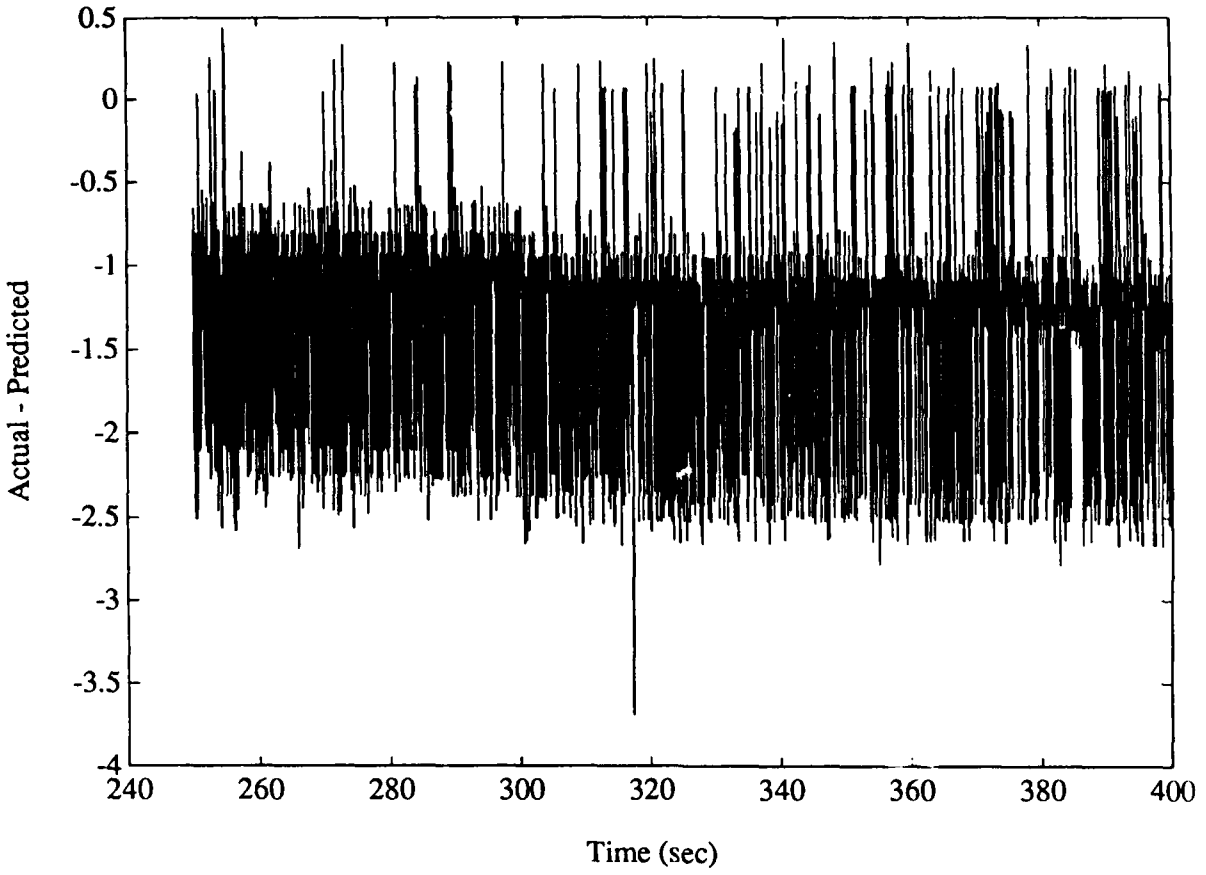
0.5
0
-0.5
-1
-1.5
-2
-2.5
-3
-3.5
-4
240
260
280
300
320
340
360
380
400
Actual - Predicted
Time (sec)

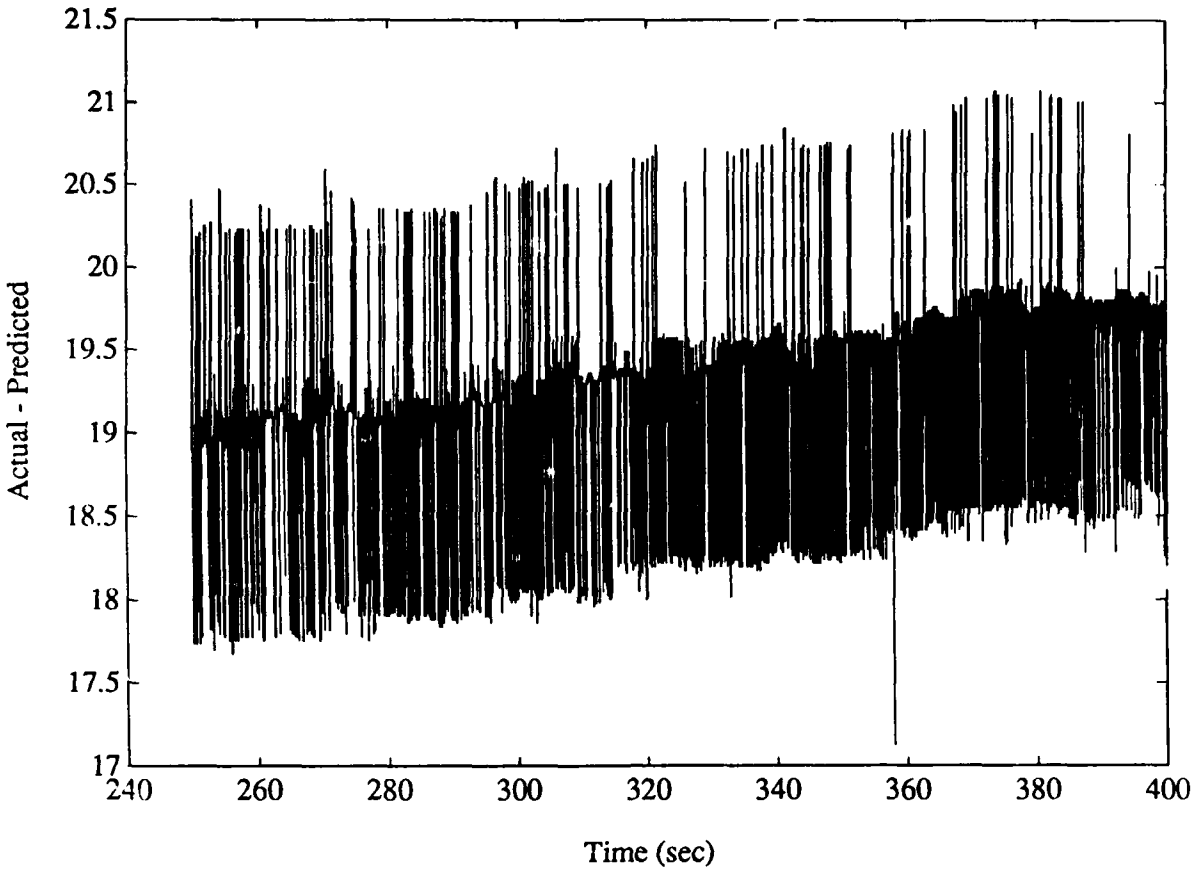
21.5
21
20.5
20
19.5
19
18.5
18
17.5
17
240
260
280
300
320
340
360
380
400
Actual - Predicted
Time (sec)

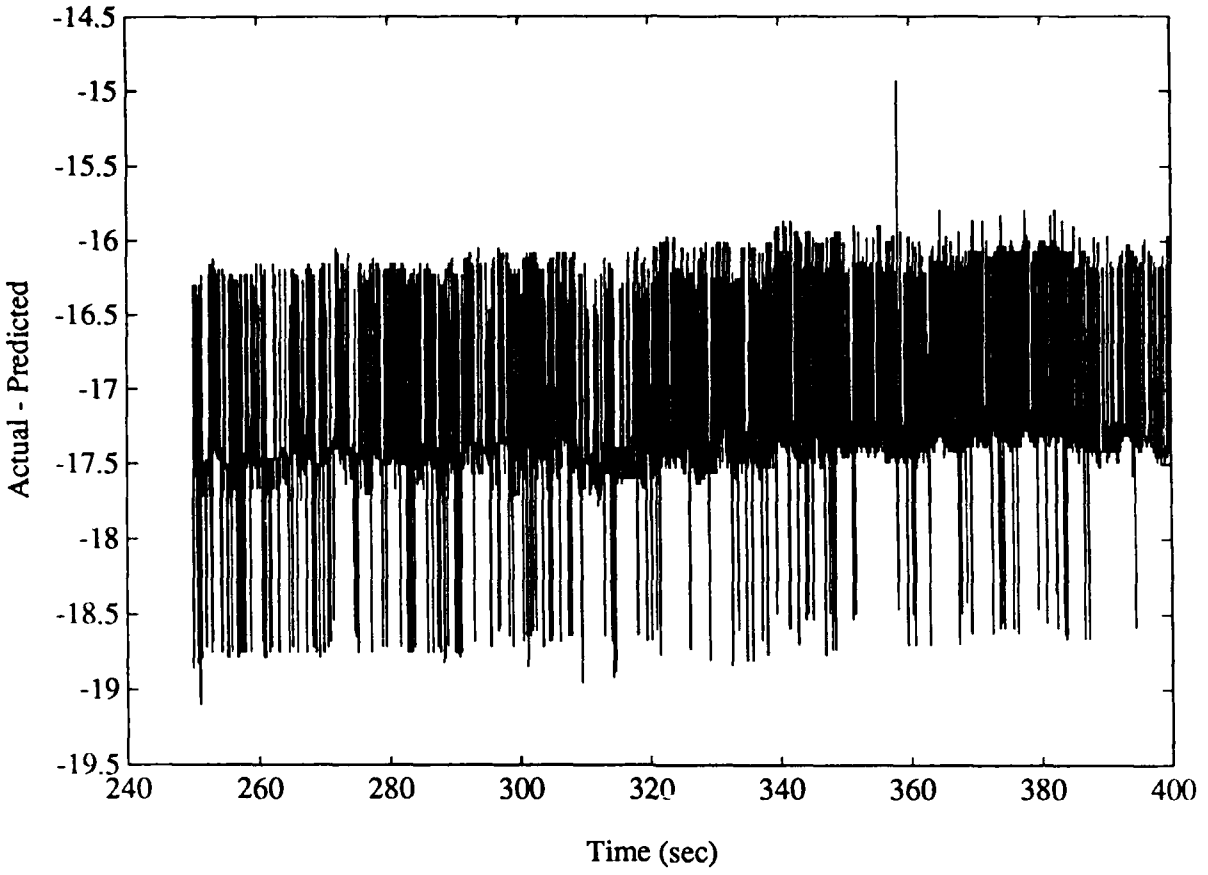
-14.5
-15
-15.5
-16
-16.5
-17
-17.5
-18
-18.5
-19
-19.5
Actual - Predicted
240
260
280
300
320
340
360
380
400
Time (sec)

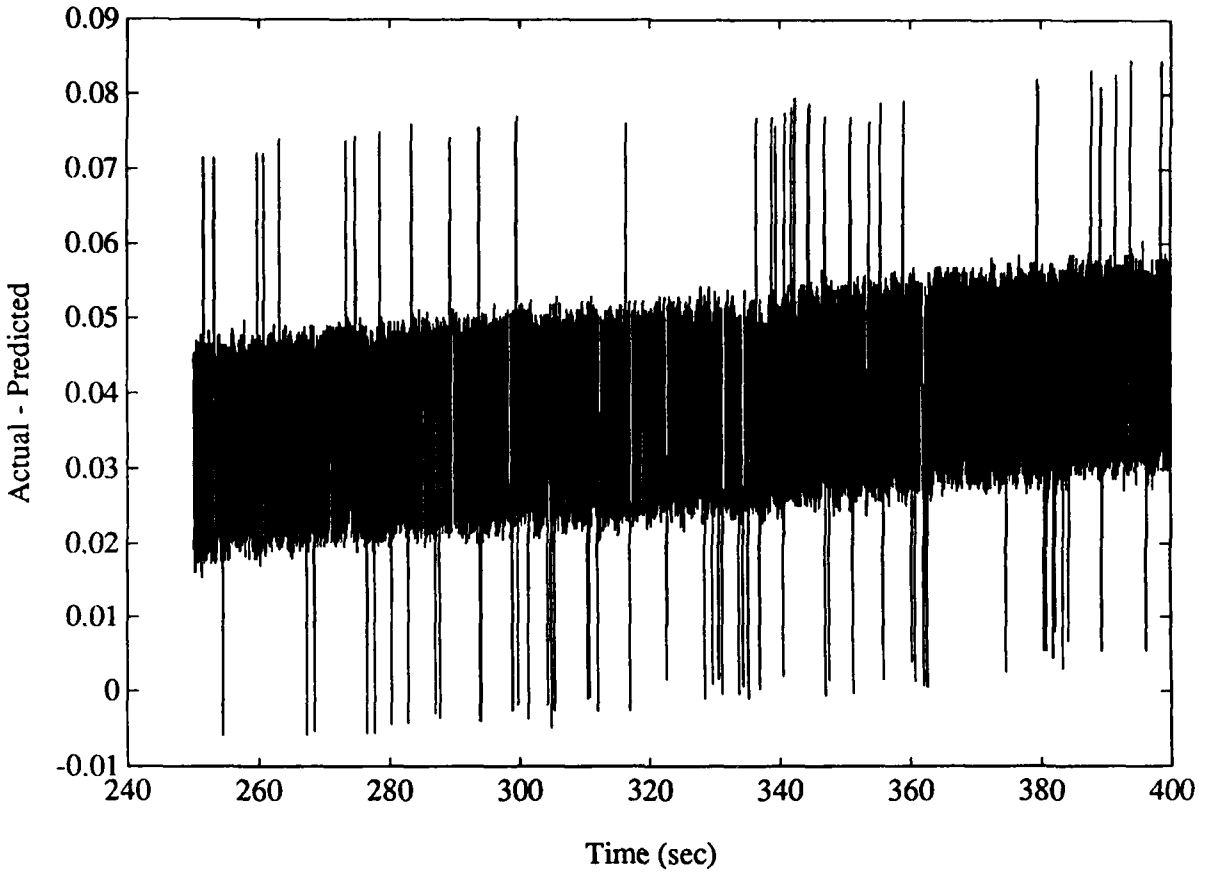
0.09
0.08
0.07
0.06
0.05
0.04
0.03
0.02
0.01
0
-0.01
Actual - Predicted
240
260
280
300
320
340
360
380
400
Time (sec)

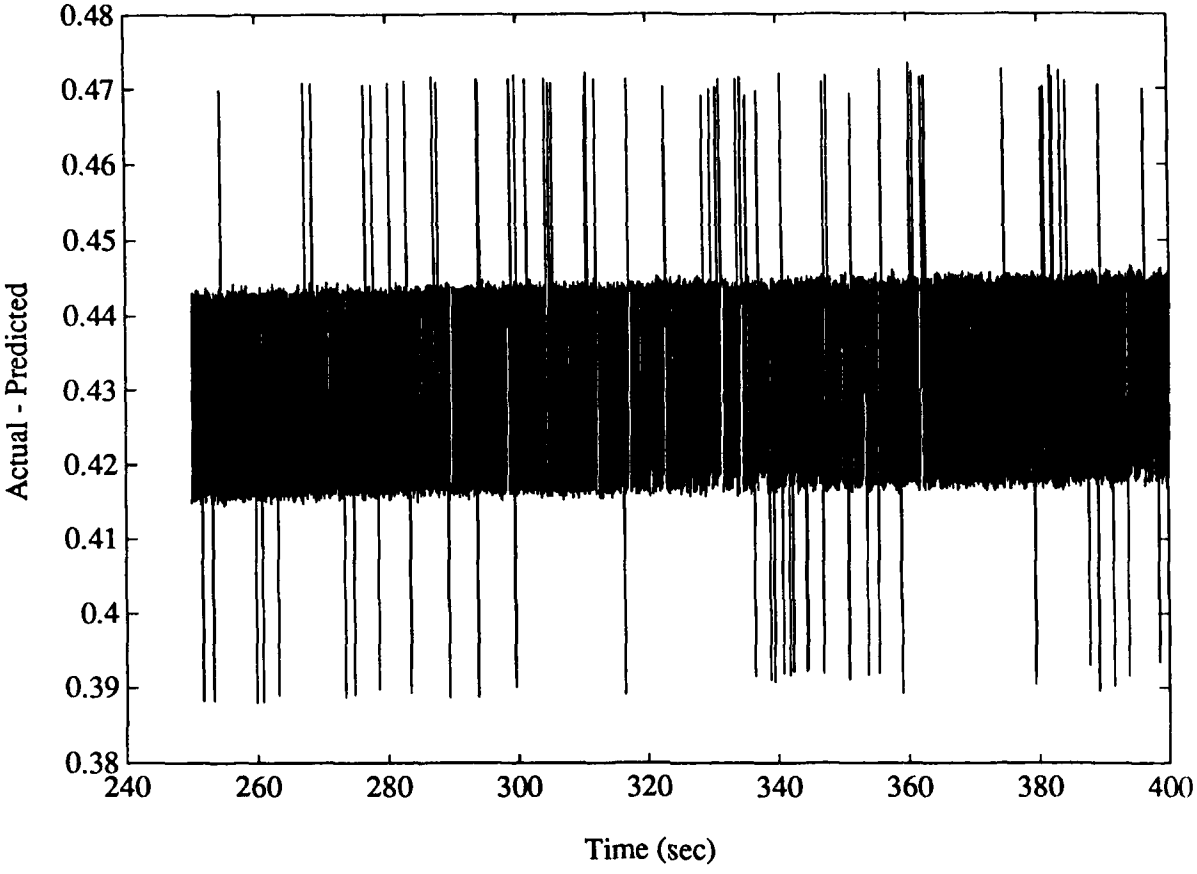
0.48
0.47
0.46
0.45
0.44
0.43
0.42
0.41
0.4
0.39
0.38
Actual - Predicted
240
260
280
300
320
340
360
380
400
Time (sec)

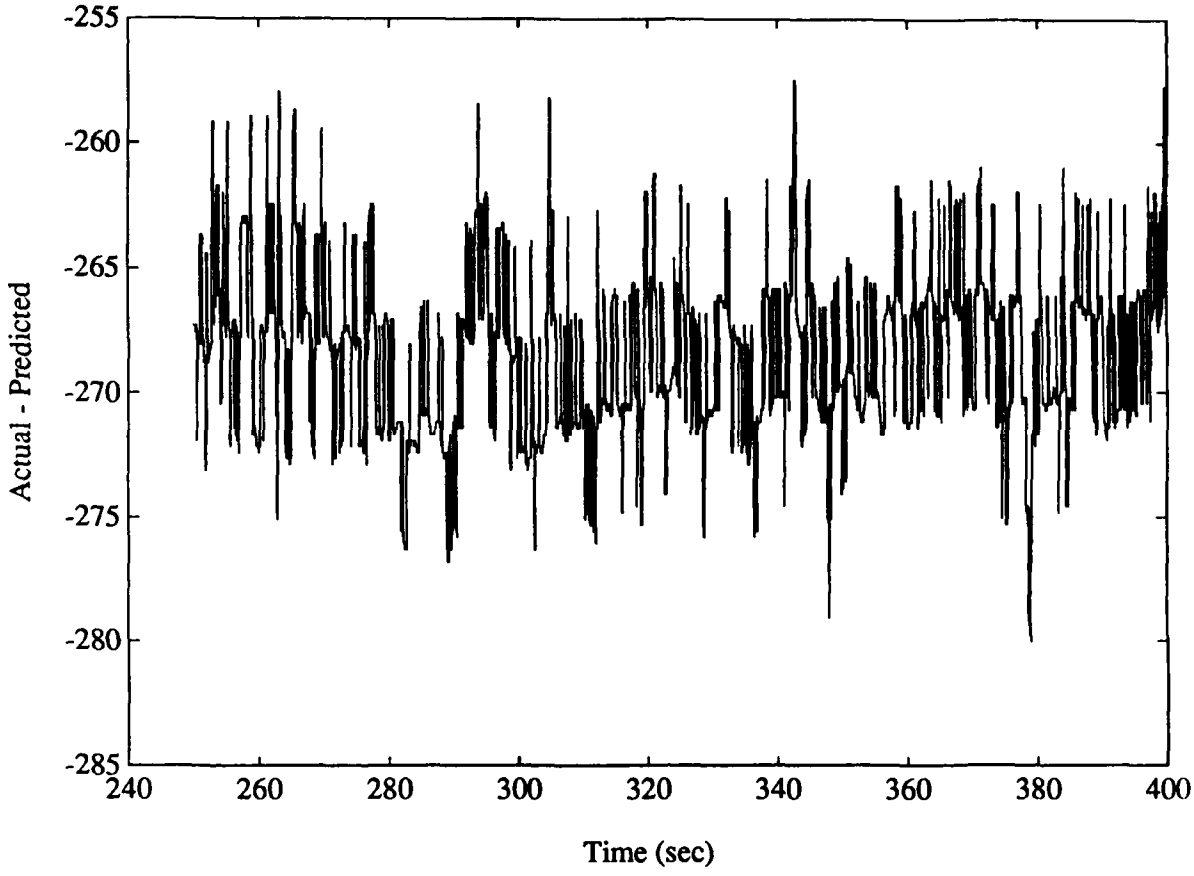
-255
-260
-265
-270
-275
-280
-285
Actual - Predicted
240
260
280
300
320
340
360
380
400
Time (sec)

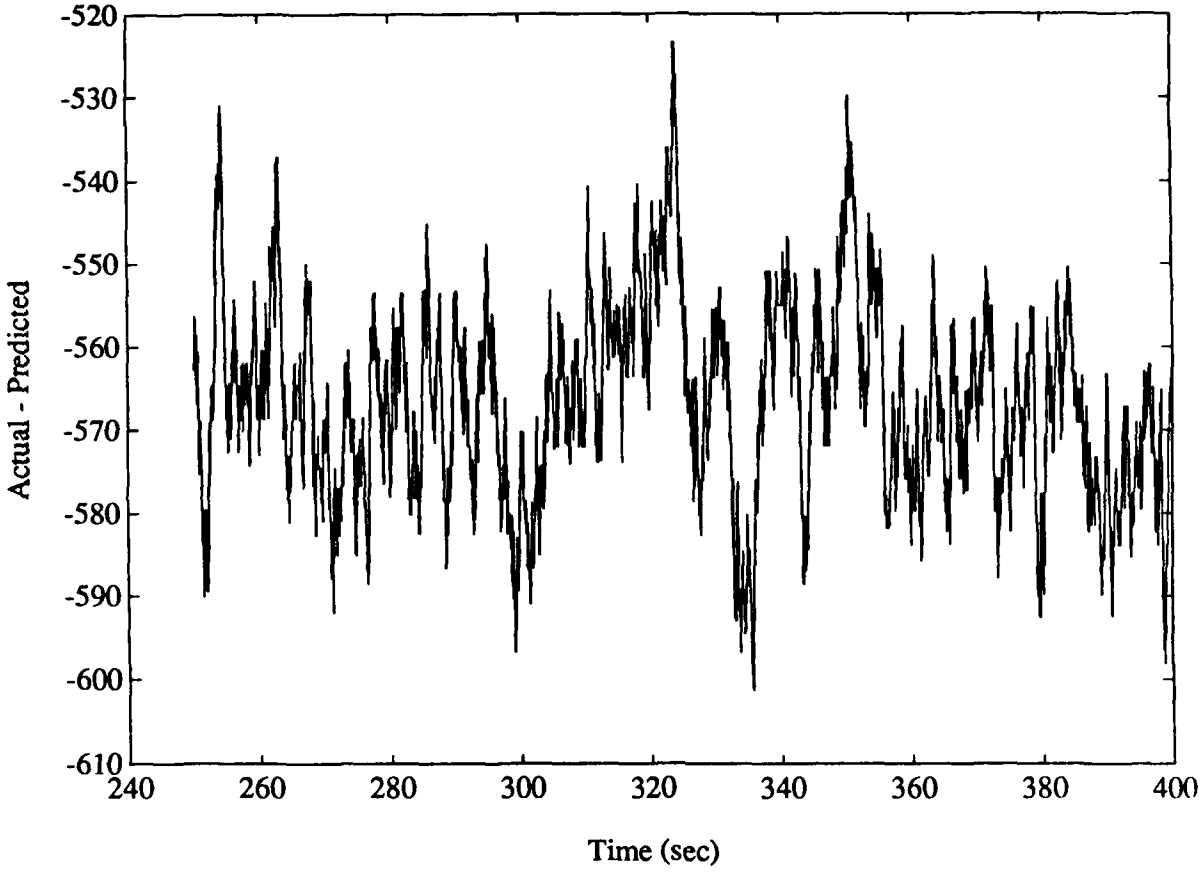
-520
-530
-540
-550
-560
-570
-580
-590
-600
-610
Actual - Predicted
240
260
280
300
320
340
360
380
400
Time (sec)

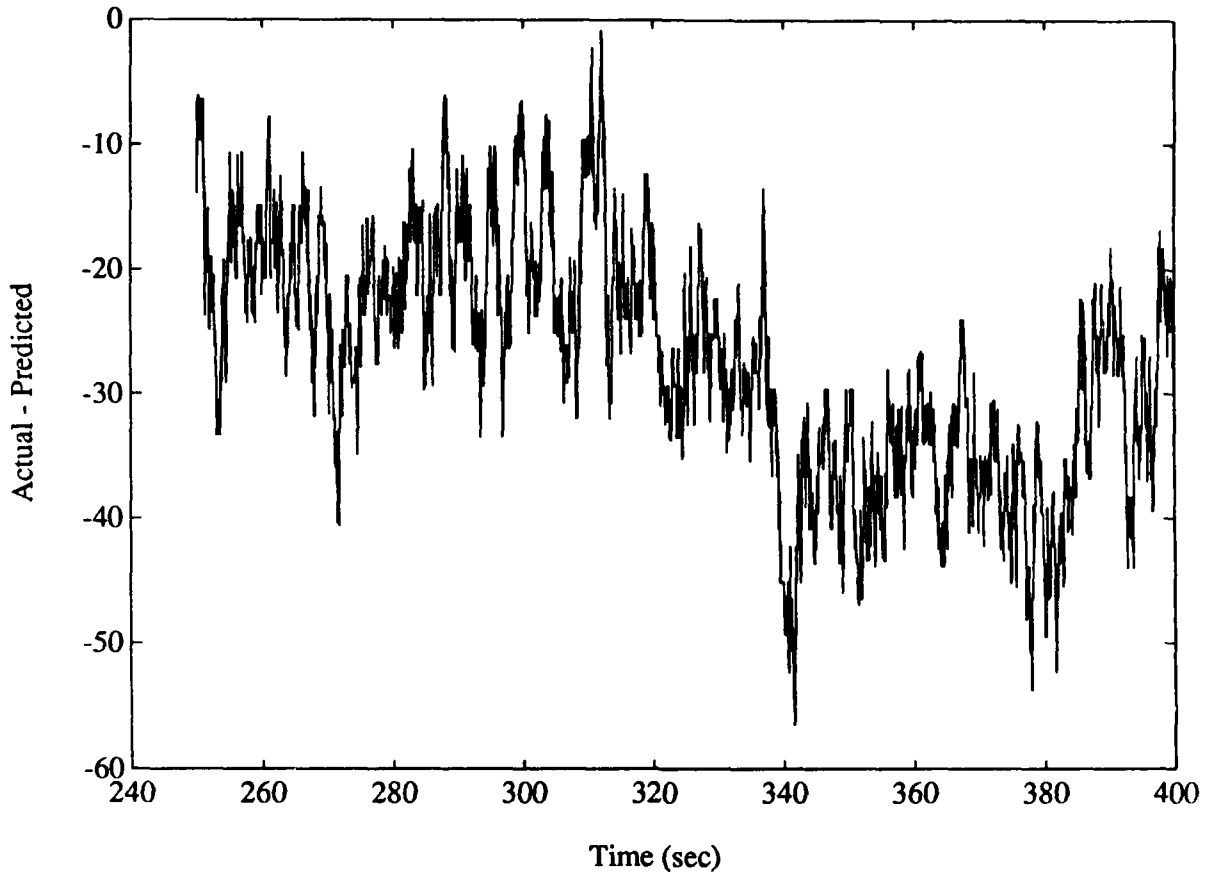
0
-10
-20
-30
-40
-50
-60
240
260
280
300
320
340
360
380
400
Actual - Predicted
Time (sec)

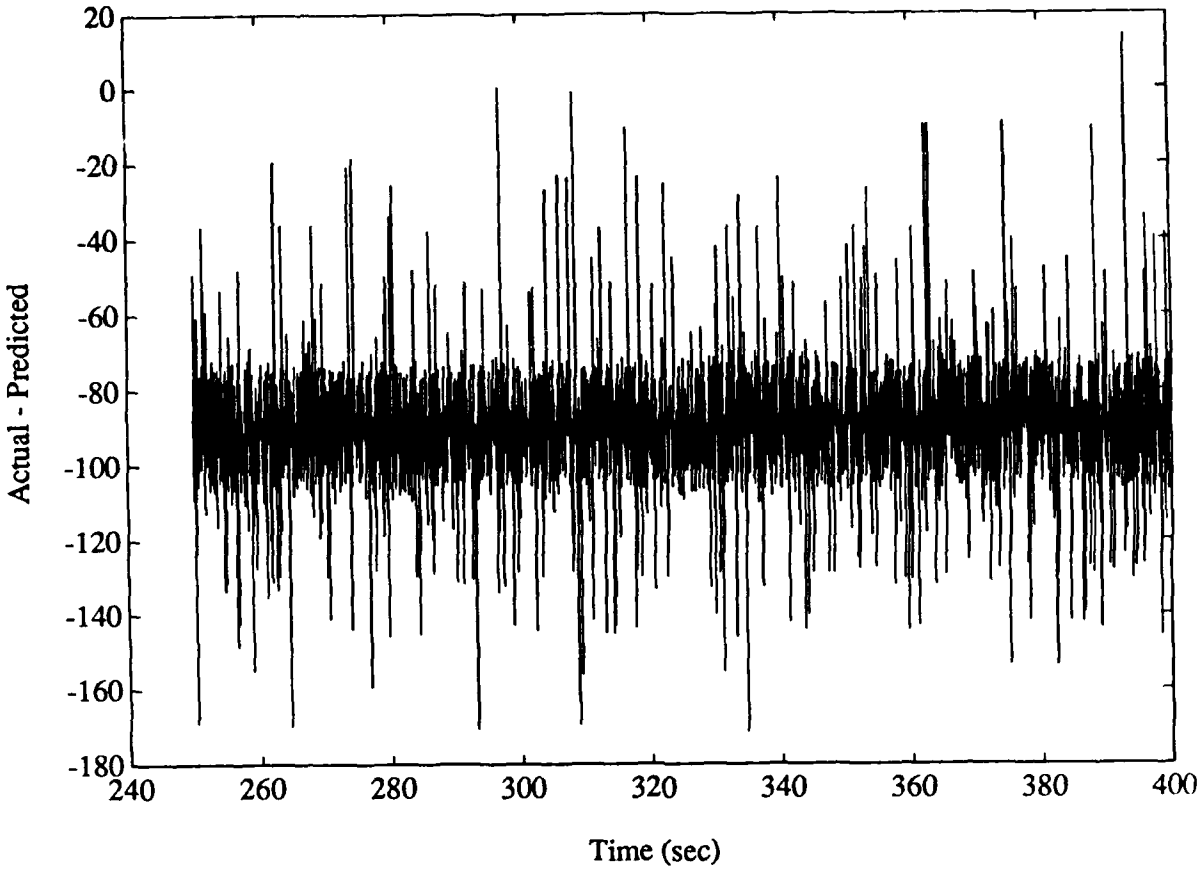
20
0
-20
-40
-60
-80
-100
-120
-140
-160
-180
Actual - Predicted
240
260
280
300
320
340
360
380
400
Time (sec)

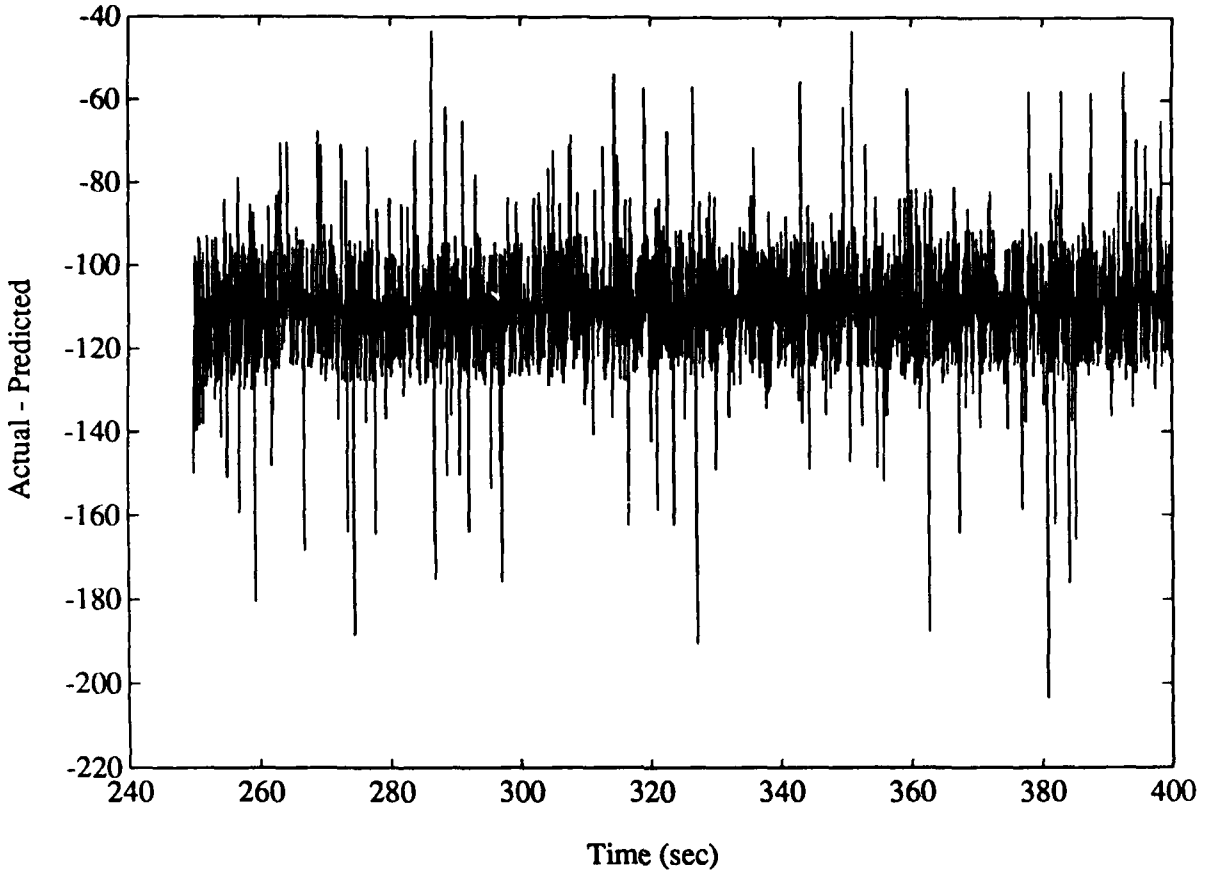
-40
-60
-80
-100
-120
-140
-160
-180
-200
-220
Actual - Predicted
240
260
280
300
320
340
360
380
400
Time (sec)

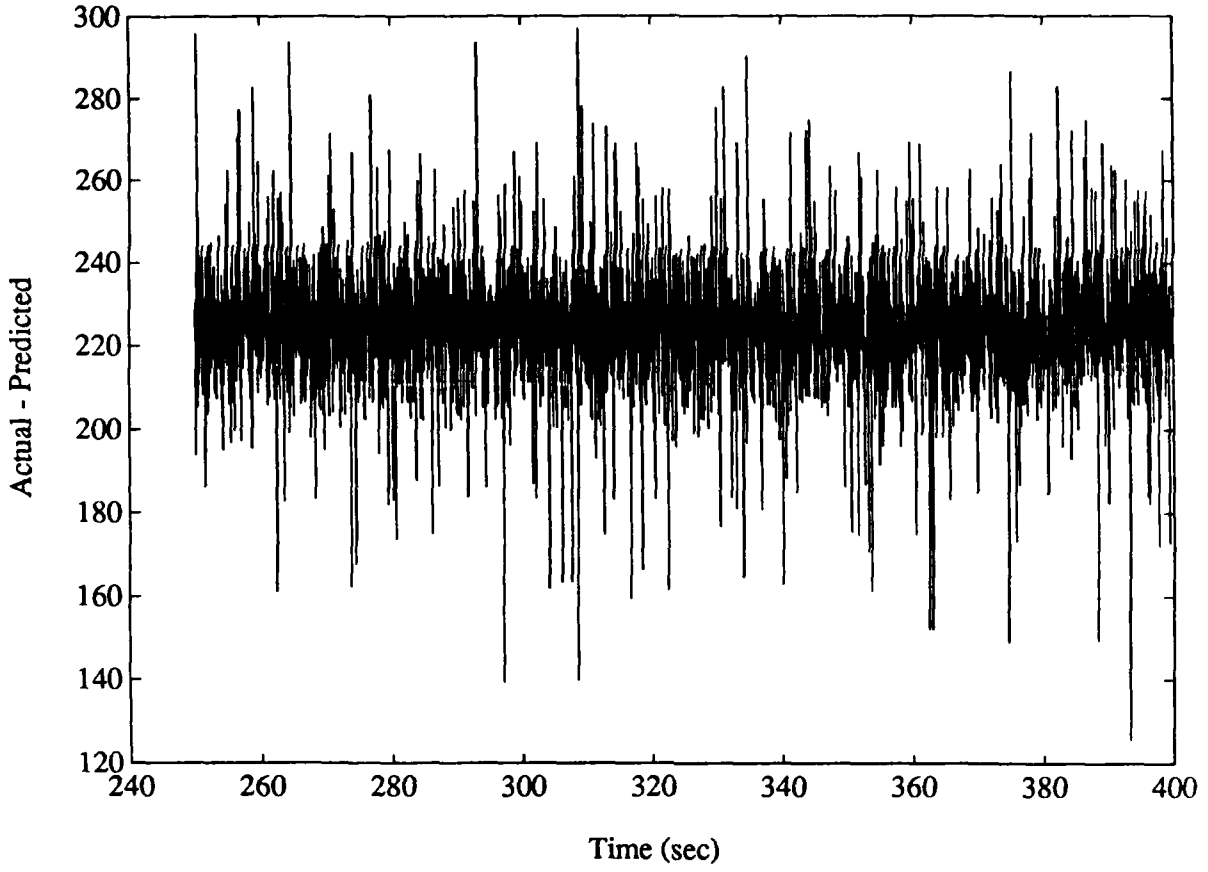
Actual - Predicted
300
280
260
240
220
200
180
160
140
120
240
260
280
300
320
340
360
380
400
Time (sec)

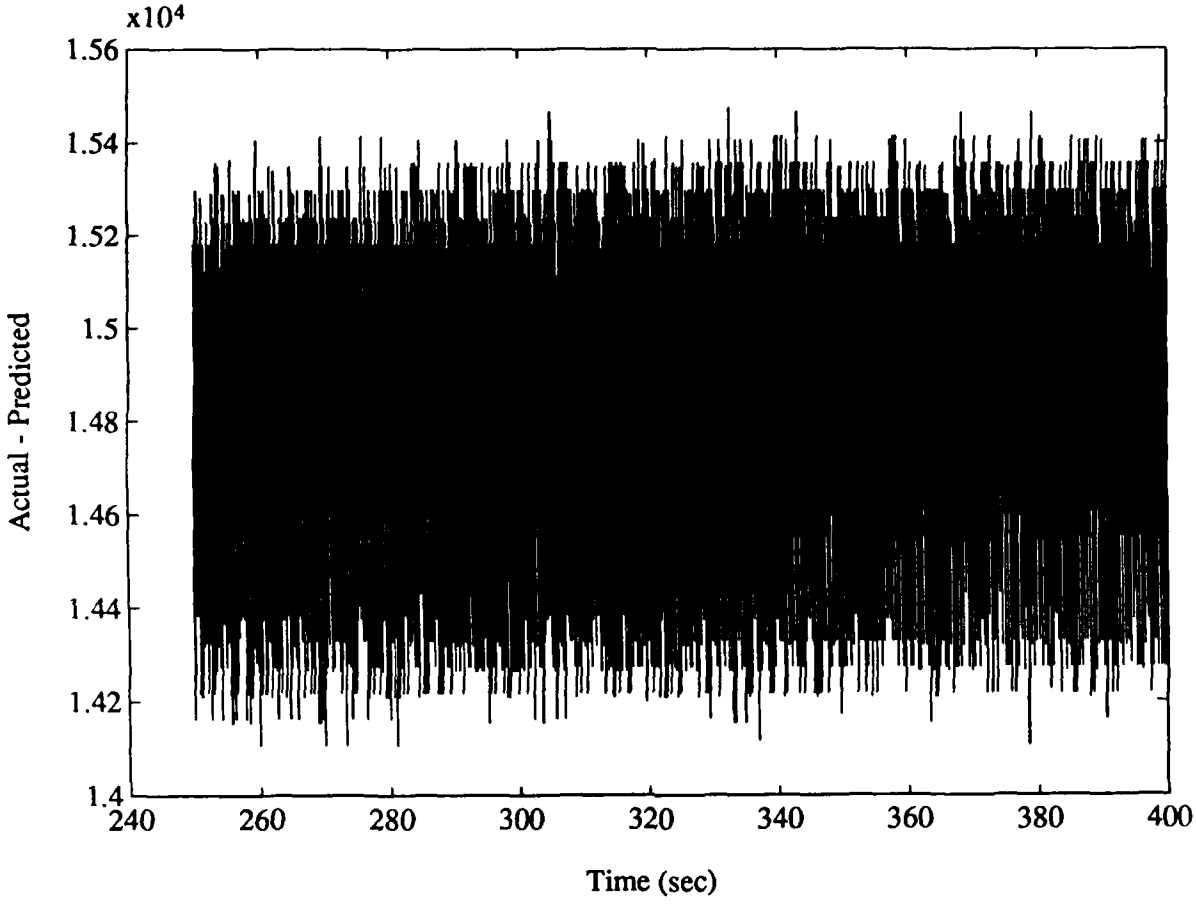
x10^4
1.56
1.54
1.52
1.5
1.48
1.46
1.44
1.42
1.4
Actual - Predicted
240
260
280
300
320
340
360
380
400
Time (sec)

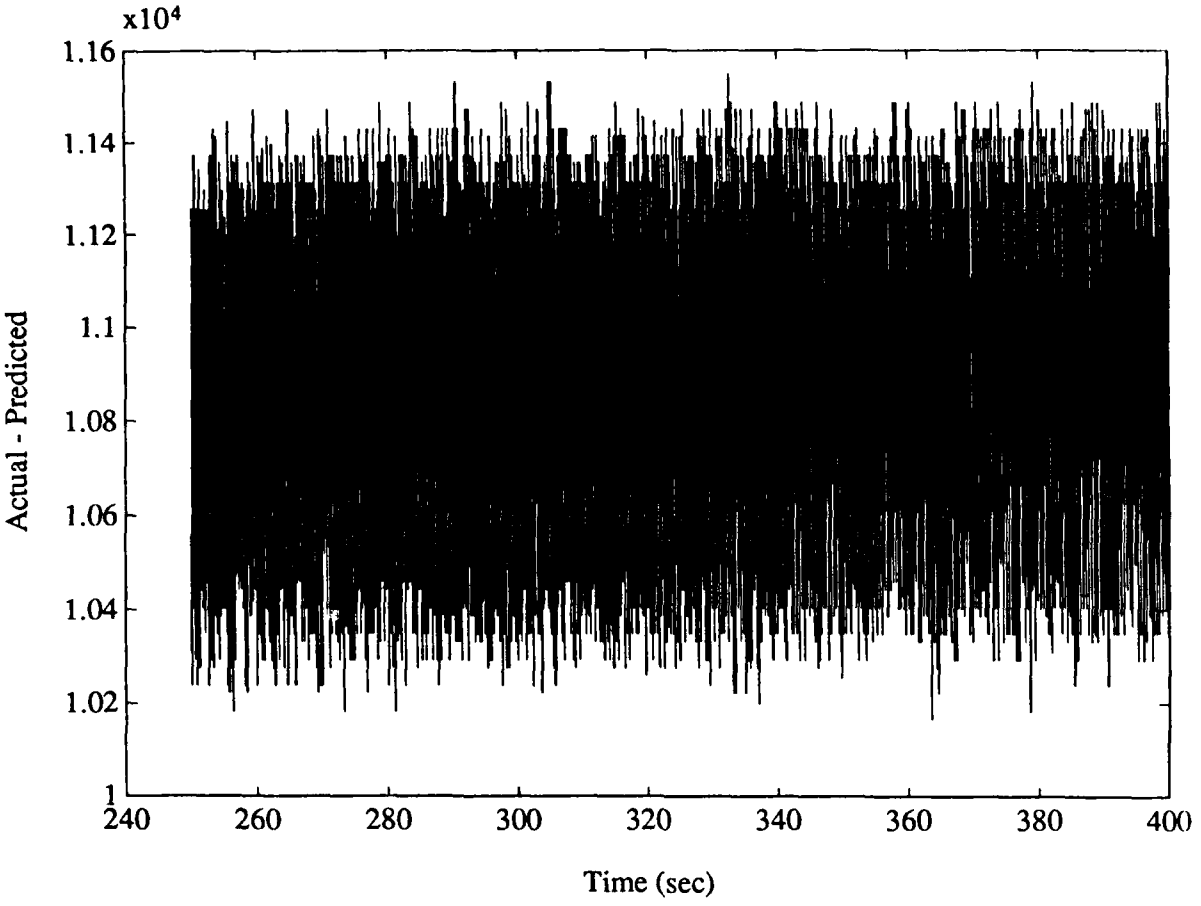
x10^4
1.16
1.14
1.12
1.1
1.08
1.06
1.04
1.02
1
Actual - Predicted
240
260
280
300
320
340
360
380
400
Time (sec)

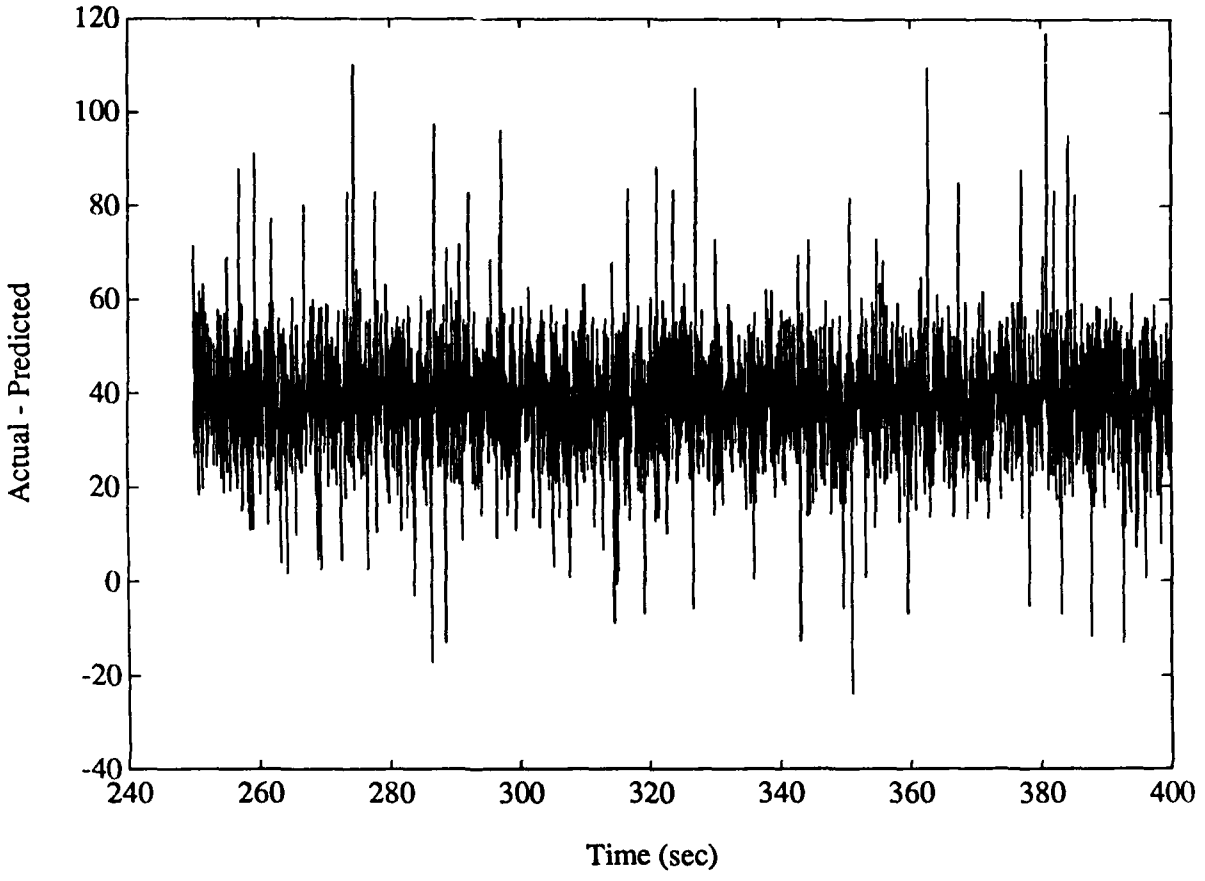
120
100
80
60
40
20
0
-20
-40
240
260
280
300
320
340
360
380
400
Actual - Predicted
Time (sec)

APPENDIX C: TWO SIGMA DATABASE DATA

GENCORP
AEROJET

Aerojet TechSystems

Huntsville Operations
700 Boulevard South Suite 306
Huntsville AL 35802-2176
(205) 883-0500

TO: ML Gage

11 April 1990

FROM: DM Matson

DISTRIBUTION: JH Berroteran, RL Bickford, DB Makel, Dept. 9842 file

SUBJECT: Two-sigma Variation of CADS Sensor Data as a Function of Engine Power Level

Enclosures:
(1) Typical Flight Data for Selected Parameters
(2) CADS Flight Data as a Function of Engine Power Level

The attached enclosures contain flight data taken from histo ical SSME sources. Enclosure 1 contains typical flight data for chamber pressure, Lox inlet pressure, and turbine discharge temperatures for fuel and ox pumps. These parameters are selected such that the CADS data in enclosure 2 can be intelligently correlated.

The main combustion chamber pressure was selected to indicate power level as a function of time for the flight of engine 0217. The nominal power drops from 104 percent to 65 percent between approximately thirty to seventy seconds from liftoff and then returns to 104 percent. It will be obvious later that the only truly meaningful data at maximum Q is represented by the 104 percent data base in enclosure 2.

LOX inlet pressure shows a maximum at about 80 seconds and a minimum at about 120 seconds after liftoff. These points represent maximum Q and SRB separation, respectively. In order to evaluate the flight data, NASA engineers elected to examine these two operational modes and composed two data baselines. The method used to identify these modes was to take data at the maximum fuel turbine and maximum ox turbine temperature conditions. Data showing this effect occurring at approximately 90 and 120 seconds after liftoff can be respectively seen in the last two sensor traces in enclosure 1.

The results of the two-sigma analysis are shown in enclosure 2.

If I can be of any further assistance, please call. For more information on this database, NASA engineer Mike Ise (pronounced "Easy") can be reached at (205)544-4946. He is most helpful but the demands on his time are high.

Douglas M. Matson
Materials/Test Specialist

ENCLOSURE 1 Typical Flight Data for Selected Parameters

MCC Pressure

LOX Inlet Pressure

HPFTT Discharge Temperature

HPOTT Discharge Temperature

All data taken from Engine S/N 2017

S 1

E41P1023D ME-1 ACC PRESSURE (AVG) PSIA

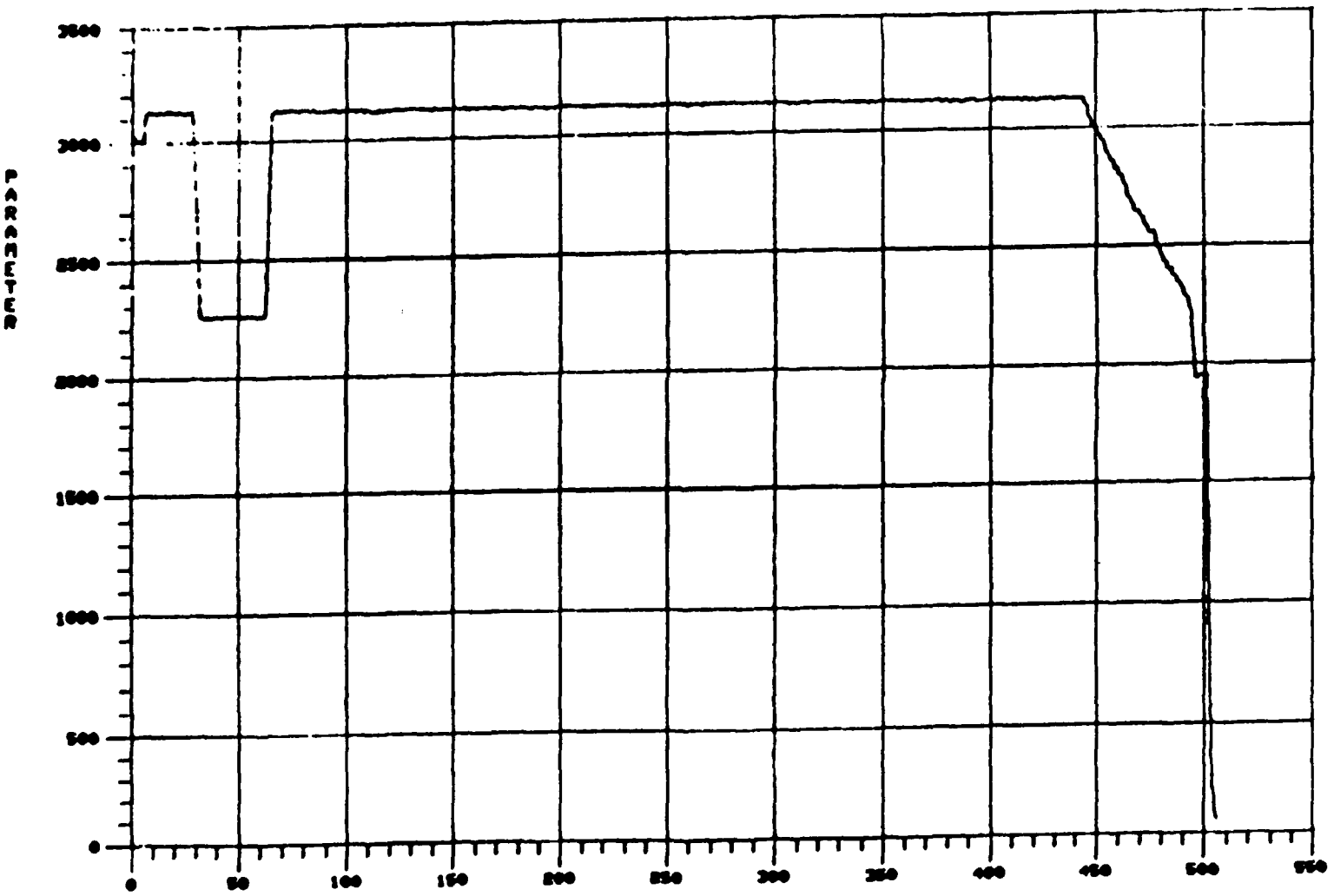

REFERENCE TIME: 83 169 11 32 59 0
ST97DB

TIME FROM LIFTOFF (T0) - SECS.

RSFC EP26
DATE: 01 APR 86
TIME: 16:07:03

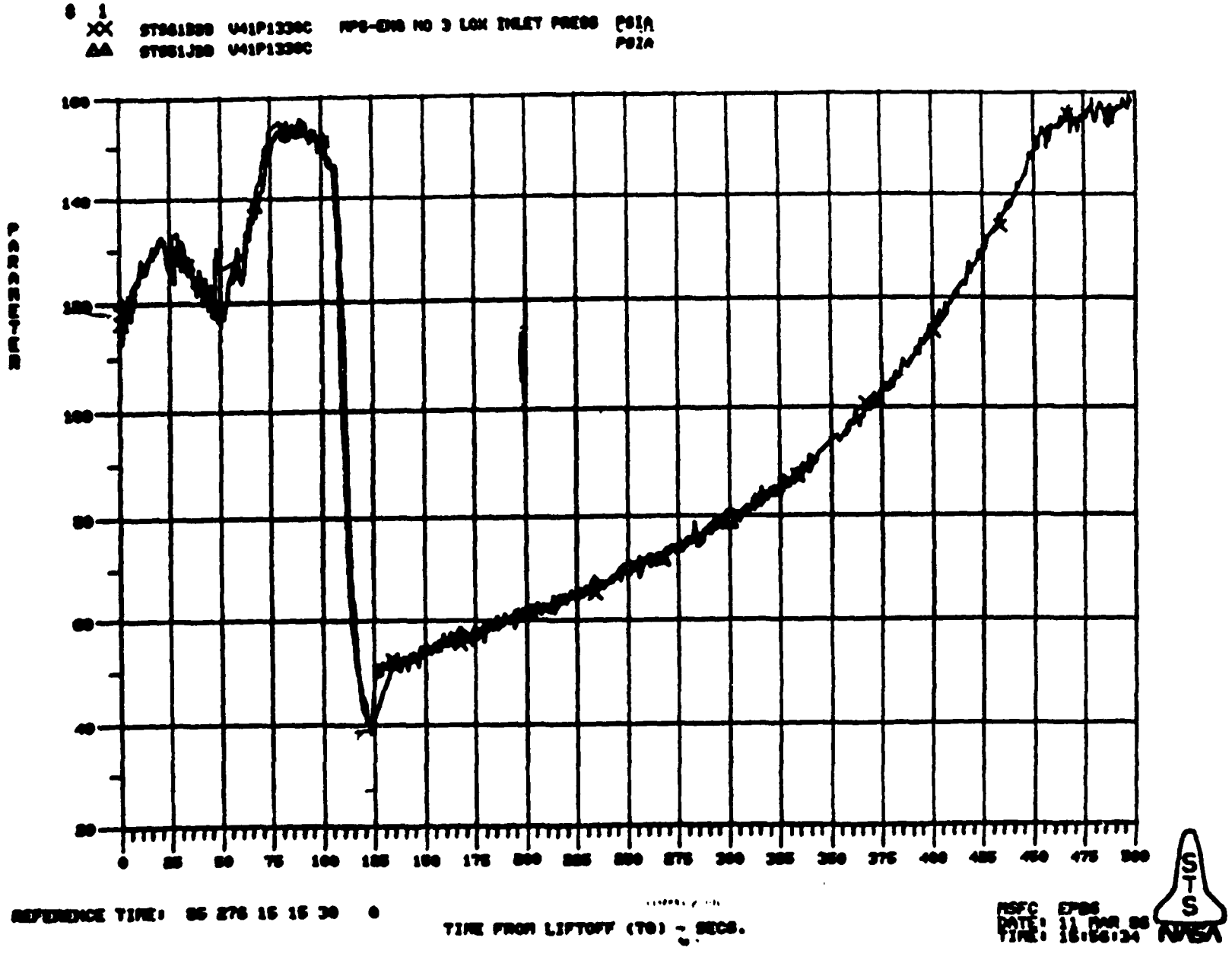
8 1
XX ST561B00 U41P1320C RPS-ENG NO 3 LOX INLET PRESS PSIA
ΔΔ ST561J00 U41P1320C PSIA
PERCENTAGE
100
140
120
100
80
60
40
20
0
25
50
75
100
125
150
175
200
225
250
275
300
325
350
375
400
425
450
475
500
REFERENCE TIME: 85 278 15 15 30 0
TIME FROM LIFTOFF (T0) - SECS.
MSFC ED86
DATE: 11 OCT 85
TIME: 16:06:24
STS
NASA

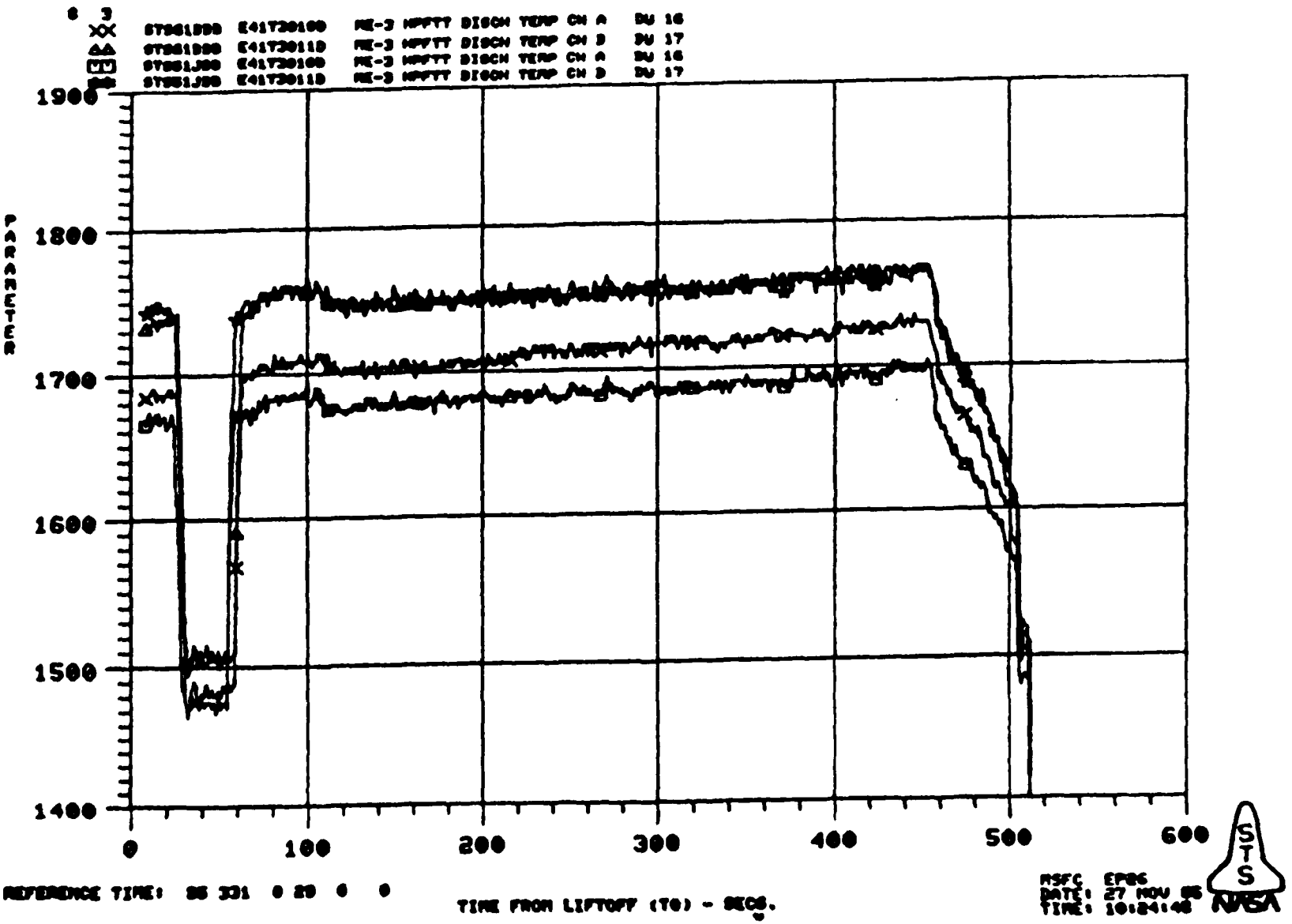
3
ST981D0B E41T20108 ME-3 MPTT DISCH TEMP CH A DU 16
ST981D0B E41T20118 ME-3 MPTT DISCH TEMP CH B DU 17
ST981J0B E41T20108 ME-3 MPTT DISCH TEMP CH A DU 16
ST981J0B E41T20118 ME-3 MPTT DISCH TEMP CH B DU 17
PARAMETER
1900
1800
1700
1600
1500
1400
0
100
200
300
400
500
600
REFERENCE TIME: 86 331 0 20 0 0
TIME FROM LIFTOFF (TO) - SECS.
MSFC EPBG
DATE: 27 NOV 86
TIME: 10:24:46
STS
NASA

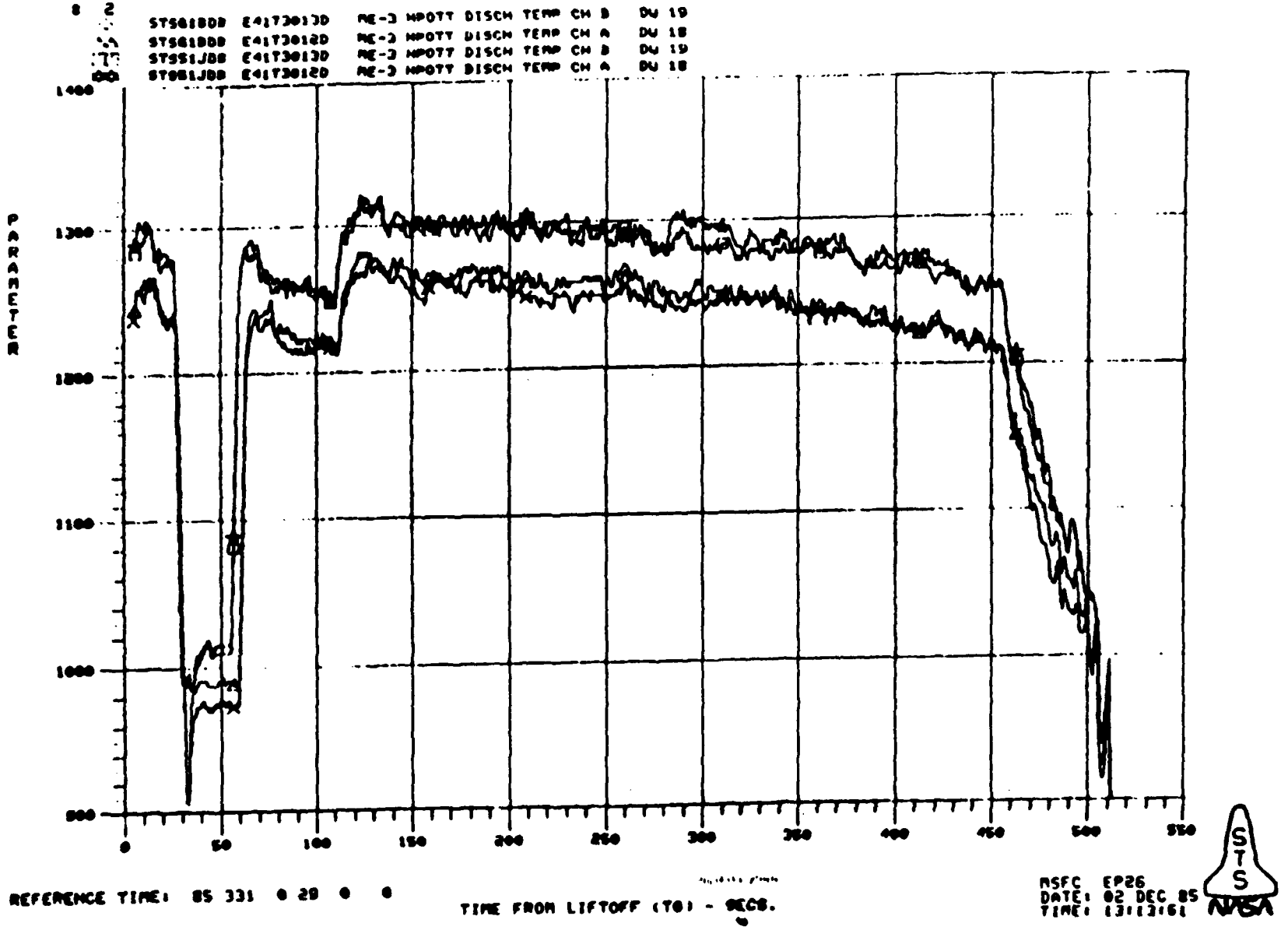
STS61BDB E41T30130 RE-3 MPOTT DISCH TEMP CH B DU 19
STS61BDB E41T30120 RE-3 MPOTT DISCH TEMP CH A DU 18
STS51JDB E41T30130 RE-3 MPOTT DISCH TEMP CH B DU 19
STS61JDB E41T30120 RE-3 MPOTT DISCH TEMP CH A DU 18
PARAMETER
1400
1300
1200
1100
1000
900
0
50
100
150
200
250
300
350
400
450
500
550
REFERENCE TIME: 85 331 0 29 0 0
TIME FROM LIFTOFF (T0) - SECS.
MSFC EP26
DATE: 02 DEC 85
TIME: 13:13:61
STS
NASA

ENCLOSURE 2 CADS Flight Data as a Function of Engine Power Level

Phase II Data Base (Issue Date 10-13-89)
Summary of CADS sensor data encompassing
approximately 150 flight firings

MAX FUEL TURBINE TEMPS		MCC PC	LPFP DS PR	LPFP DS T	LPFTP SPD	HPFP DS PR	MCC CLT DS PR	MCC CLT DS T
100% RPL DATABASE	AVERAGE	3006.25	224.80	42.62	15421.41	5878.55	4302.93	466.80
	+2 SIGMA	3008.87	250.65	43.57	16047.87	5950.62	4510.12	498.83
	-2 SIGMA	3003.63	198.95	41.67	14794.95	5806.49	4095.74	434.76
	SIGMA	1.31	12.92	0.48	313.23	36.03	103.60	16.02
104% RPL DATABASE	AVERAGE	3126.37	233.10	42.66	15846.23	6180.71	4500.39	462.05
	+2 SIGMA	3133.06	261.71	43.45	16519.77	6258.00	4707.52	495.88
	-2 SIGMA	3119.68	204.48	41.88	15172.69	6103.43	4293.25	428.23
	SIGMA	3.35	14.31	0.39	336.77	38.64	103.57	16.91
109% RPL DATABASE	AVERAGE	3276.84	245.49	42.99	16402.56	6573.26	4788.54	461.59
	+2 SIGMA	3279.16	274.37	43.78	17009.71	6646.77	4993.09	497.34
	-2 SIGMA	3274.51	216.61	42.21	15795.41	6499.74	4583.98	425.84
	SIGMA	1.16	14.44	0.39	303.57	36.76	102.28	17.87
65% RPL DATABASE	AVERAGE	1953.88	215.69	42.41	13413.71	3834.84	2840.63	451.65
	+2 SIGMA	1956.02	234.35	43.25	14032.45	3896.77	2964.76	489.22
	-2 SIGMA	1951.73	197.03	41.56	12794.97	3772.91	2716.51	414.09
	SIGMA	1.07	9.33	0.42	309.37	30.97	62.06	18.78
NOMINAL LOX VENT								
104% NOMINAL LOX VENT	AVERAGE	3126.48	234.54	42.60	15840.44	6177.77	4489.33	460.98
	+2 SIGMA	3128.82	262.18	43.37	16494.86	6252.99	4709.61	493.30
	-2 SIGMA	3124.14	206.90	41.83	15186.03	6102.56	4269.05	428.66
	SIGMA	1.17	13.82	0.38	327.21	37.61	110.14	16.16
MAX LOX TURBINE TEMPS								
100% RPL DATABASE	AVERAGE	3005.70	227.65	42.49	15389.50	5875.26	4287.90	465.11
	+2 SIGMA	3008.77	253.91	43.51	16015.85	5950.77	4510.80	494.81
	-2 SIGMA	3002.63	201.40	41.48	14763.15	5799.74	4065.01	435.41
	SIGMA	1.54	13.13	0.51	313.18	37.76	111.45	14.85
104% RPL DATABASE	AVERAGE	3126.53	236.24	42.52	15857.84	6184.19	4486.84	460.67
	+2 SIGMA	3129.03	263.99	43.23	16519.13	6259.80	4701.57	493.75
	-2 SIGMA	3124.03	208.49	41.81	15196.56	6108.58	4272.10	427.58
	SIGMA	1.25	13.88	0.35	330.64	37.80	107.37	16.54
109% RPL DATABASE	AVERAGE	3276.85	247.15	42.94	16403.19	6574.62	4783.54	460.64
	+2 SIGMA	3279.88	276.04	43.72	16998.65	6643.60	4991.06	495.46
	-2 SIGMA	3273.82	218.25	42.15	15807.73	6505.64	4576.01	425.82
	SIGMA	1.52	14.45	0.39	297.73	34.49	103.76	17.41
65% RPL DATABASE	AVERAGE	1954.26	216.06	42.39	13407.20	3833.77	2840.28	451.69
	+2 SIGMA	1956.61	234.71	43.24	14024.58	3894.29	2963.92	489.75
	-2 SIGMA	1951.92	197.41	41.54	12789.83	3773.25	2716.63	413.64
	SIGMA	1.17	9.33	0.42	308.69	30.26	61.82	19.03

HPFT T A	HPFT T B	FPB PC	HPFTP SPD	HPFTP CLT LNR PI	ACC FL INJ PR	LPOP DS PR	LPOTP SPD	HPOP DS PR
1662.71	1678.84	4891.53	34389.38	3329.44	3243.12	352.40	5033.97	3883.72
1781.54	1770.75	5036.27	34867.32	3437.76	3387.12	390.60	5142.16	3931.56
1543.89	1586.93	4746.78	33911.44	3221.11	3099.11	314.20	4925.78	3835.89
59.41	45.95	72.37	238.97	54.16	72.00	19.10	54.09	23.92
1706.98	1725.73	5148.52	35241.35	3456.42	3383.95	368.94	5149.13	4069.01
1824.12	1824.22	5285.52	35762.55	3547.70	3537.49	425.30	5260.55	4124.88
1589.85	1627.25	5011.53	34720.16	3365.14	3230.41	312.59	5037.72	4013.13
58.57	49.24	68.50	260.60	45.64	76.77	28.18	55.71	27.94
1725.00	1755.62	5464.25	36322.25	3644.97	3539.98	376.60	5288.86	4294.77
1835.69	1862.12	5610.33	36843.44	3760.15	3573.57	436.27	5413.30	4348.72
1614.32	1649.11	5318.17	35801.06	3529.79	3506.39	316.93	5164.42	4240.81
55.34	53.25	73.04	260.60	57.59	16.79	29.84	62.22	26.98
1499.97	1491.84	2922.49	26947.35	2129.16	2078.90	286.74	3894.36	2343.27
1585.56	1571.63	2975.39	27311.24	2194.41	2194.27	295.35	3965.20	2363.47
1414.39	1412.04	2869.59	26583.45	2063.92	1963.53	278.14	3823.53	2323.06
42.79	39.90	26.45	181.95	32.62	57.68	4.30	35.42	10.10
1691.98	1714.61	5172.23	35210.09	3449.76	3389.79	348.80	5165.78	4071.22
1806.66	1810.59	5306.09	35715.10	3530.19	3578.61	370.68	5267.74	4125.08
1577.29	1618.62	5038.38	34705.08	3369.32	3200.98	326.91	5063.83	4017.37
57.34	47.99	66.93	252.50	40.22	94.41	10.94	50.98	26.93
1647.74	1668.17	4912.18	34329.44	3322.32	3247.91	345.65	5044.72	3884.32
1765.03	1761.39	5041.44	34818.28	3418.32	3386.64	364.93	5161.39	3936.61
1530.46	1574.94	4782.93	33840.61	3226.33	3109.17	326.38	4928.05	3832.02
58.64	46.61	64.63	244.42	48.00	69.37	9.64	58.34	26.15
1678.49	1702.81	5176.62	35194.83	3453.29	3392.71	320.26	5180.86	4073.47
1788.08	1794.23	5299.92	35669.12	3541.39	3606.77	367.86	5278.31	4130.23
1568.91	1611.39	5053.32	34720.54	3365.19	3178.64	272.65	5083.40	4016.71
54.79	45.71	61.65	237.15	44.05	107.03	23.80	48.73	28.38
1704.35	1740.57	5476.98	36303.74	3643.14	3546.29	350.08	5307.05	4296.54
1816.21	1850.40	5613.20	36868.53	3757.60	3637.15	415.08	5438.32	4352.54
1592.49	1630.75	5340.75	35738.95	3528.68	3455.43	285.07	5175.77	4240.53
55.93	54.91	68.11	282.39	57.23	45.43	32.50	65.64	28.00
1495.16	1489.94	2923.45	26944.99	2129.42	2079.31	286.65	3894.46	2343.86
1577.64	1568.40	2974.97	27298.86	2194.97	2194.28	295.29	3963.09	2362.85
1412.67	1411.47	2871.92	26591.11	2063.87	1964.33	278.00	3825.84	2324.87
41.24	39.23	25.76	176.94	32.78	57.49	4.32	34.31	9.49

HPFP DS T	PFP BAL CAV P	HPFP CL T	HPFP DRN PR	HPFP DRN T	LPFT IN PR	FL PR INT PR	FL PR INT T	OPB PC	FPOV ACT POS
93.78	4554.84	305.53	9.91	313.97	4266.92	3224.81	452.61	4943.71	79.53
96.61	4681.50	386.96	21.64	465.68	4464.59	3353.85	483.95	5112.68	83.32
90.95	4428.18	224.09	-1.82	162.26	4069.25	3095.77	421.26	4774.75	75.73
1.41	63.33	40.72	5.87	75.85	98.84	64.52	15.67	84.48	1.90
95.78	4813.27	305.20	7.59	315.76	4467.87	3359.08	447.76	5209.10	81.55
98.60	4946.16	388.97	19.34	483.81	4660.03	3490.69	481.25	5288.21	85.72
92.95	4680.38	221.43	-4.16	147.71	4275.71	3227.47	414.26	5129.98	77.38
1.41	66.44	41.88	5.88	84.02	96.08	65.81	16.75	39.56	2.09
98.45	5159.94	305.04	6.62	316.81	4748.75	3545.09	447.04	5539.14	83.58
101.74	5339.44	375.41	17.62	481.57	4948.06	3672.87	481.64	5663.36	88.35
95.15	4980.43	234.66	-4.38	152.05	4549.44	3417.32	412.43	5414.91	78.81
1.65	89.75	35.19	5.50	82.38	99.66	63.89	17.30	62.11	2.39
77.34	3018.65	269.07	1.79	257.42	2817.73	2077.14	437.20	2832.26	68.41
79.99	3105.69	335.90	2.21	404.43	2942.81	2151.21	473.96	2863.86	70.02
74.69	2931.61	202.24	1.38	110.41	2692.64	2003.06	400.44	2800.66	66.80
1.32	43.52	33.42	0.21	73.51	62.54	37.04	18.38	15.80	0.81
95.36	4811.24	298.64	7.60	308.90	4461.54	3341.81	446.86	5220.03	81.07
101.89	4949.27	381.31	19.35	468.76	4659.58	3471.78	478.02	5294.04	85.04
88.83	4673.20	215.96	-4.14	149.04	4263.50	3211.85	415.69	5146.01	77.10
3.26	69.02	41.34	5.87	79.93	99.02	64.98	15.58	37.01	1.98
93.42	4552.41	297.11	9.91	309.59	4258.24	3201.24	450.79	4940.22	79.09
96.07	4683.50	359.44	21.65	462.15	4462.81	3348.48	479.35	5106.34	82.89
90.77	4421.33	234.78	-1.84	157.03	4053.68	3054.00	422.22	4774.09	75.28
1.33	65.54	31.17	5.87	76.28	102.28	73.62	14.28	83.06	1.90
95.44	4814.55	298.46	7.49	309.60	4461.92	3306.35	446.36	5239.00	80.40
98.08	4947.98	371.66	19.18	471.26	4657.08	3427.36	478.47	5316.31	84.12
92.80	4681.12	225.26	-4.20	147.93	4266.75	3185.33	414.26	5161.70	76.68
1.32	66.71	36.60	5.84	80.83	97.58	60.51	16.05	38.65	1.86
98.26	5161.15	302.37	6.63	316.12	4747.81	3532.65	445.99	5558.14	82.78
101.31	5336.42	377.00	17.63	480.63	4947.22	3679.46	479.59	5685.86	87.56
95.22	4985.88	227.73	-4.37	151.60	4548.40	3385.85	412.39	5430.41	77.99
1.52	87.63	37.32	5.50	82.26	99.70	73.40	16.80	63.86	2.39
77.29	3017.12	270.53	1.80	258.26	2816.74	2075.81	437.16	2832.32	68.38
79.92	3105.32	341.64	2.21	403.88	2942.25	2149.02	474.08	2863.28	69.97
74.67	2928.93	199.42	1.39	112.64	2691.23	2002.61	400.23	2801.37	66.79
1.31	44.10	35.56	0.21	72.81	62.75	36.60	18.46	15.48	0.79

HPFP SPD	LPFP SPD	HPOP BCAV PR A	HPOP BCAV PR B	MCC OX INJ T	MCC OX INJ PR	POGO PRCHG PR	HX DS PR	HX INT PR
34397.21	15443.46	2905.02	2751.07	195.75	3537.01	1201.56	3662.82	3637.87
34858.12	16063.63	3128.52	3036.75	198.52	3571.21	1405.11	4058.66	4037.21
33936.30	14823.29	2681.52	2465.40	192.99	3502.81	998.01	3266.99	3238.53
230.46	310.09	111.75	142.84	1.38	17.10	101.77	197.92	199.67
35242.46	15869.53	3036.05	2898.79	197.11	3698.06	1220.44	3713.29	3684.10
35706.42	16543.07	3257.23	3158.59	201.89	3736.20	1446.83	4214.48	4207.94
34778.50	15196.00	2814.87	2638.99	192.34	3659.92	994.05	3212.10	3160.25
231.98	336.77	110.59	129.90	2.39	19.07	113.20	250.60	261.92
36320.08	16430.25	3135.73	3076.07	199.91	3898.34	1302.40	3931.32	3900.56
36802.89	17030.54	3412.63	3380.17	203.23	3948.32	1517.34	4467.04	4452.36
35837.28	15829.97	2858.84	2771.96	196.59	3848.36	1087.45	3395.60	3348.76
241.40	300.14	138.45	152.05	1.66	24.99	107.47	267.86	275.90
26967.76	13443.02	1852.54	1624.43	181.57	2179.31	716.58	2088.69	2064.64
27316.12	14037.76	1940.77	1738.46	184.72	2201.96	826.71	2331.39	2320.81
26619.39	12848.29	1764.32	1510.40	178.42	2156.66	606.46	1845.99	1808.47
174.18	297.37	44.11	57.02	1.57	11.33	55.06	121.35	128.08
35222.48	15866.39	3022.63	2888.58	197.42	3697.21	1197.18	3660.29	3633.65
35687.28	16519.00	3245.28	3121.71	200.40	3736.52	1428.13	4179.79	4172.80
34757.68	15213.78	2799.98	2655.45	194.45	3657.91	966.24	3140.79	3094.51
232.40	326.31	111.32	116.57	1.49	19.65	115.47	259.75	269.57
34359.22	15416.86	2902.40	2743.55	195.73	3535.89	1145.56	3524.45	3479.39
34783.52	16042.50	3127.25	3033.67	198.43	3571.87	1414.41	4005.57	3983.22
33934.93	14791.22	2677.54	2453.44	193.02	3499.90	876.70	3043.33	2975.55
212.15	312.82	112.43	145.06	1.35	17.99	134.43	240.56	251.92
35210.69	15884.18	3003.49	2865.95	197.37	3697.61	1150.20	3519.76	3475.30
35653.30	16541.16	3228.68	3126.58	209.56	3735.59	1375.98	3956.81	3928.75
34768.08	15227.20	2778.30	2605.32	185.17	3659.63	924.42	3082.70	3021.84
221.30	328.49	112.60	130.31	6.10	18.99	112.89	218.53	226.73
36306.02	16434.16	3118.93	3061.30	200.51	3899.27	1274.68	3852.10	3818.47
36768.07	17023.75	3402.06	3373.75	203.86	3946.80	1503.59	4402.83	4394.97
35843.97	15844.57	2835.80	2748.85	197.17	3851.75	1045.76	3301.36	3241.97
231.02	294.80	141.57	156.22	1.67	23.76	114.46	275.37	288.25
26959.28	13435.82	1852.90	1624.36	181.54	2179.22	716.45	2085.74	2062.28
27301.77	14029.75	1941.42	1738.02	184.66	2201.61	822.51	2323.50	2313.22
26616.79	12841.89	1764.38	1510.70	178.42	2156.83	610.38	1847.97	1811.34
171.25	296.96	44.26	56.83	1.56	11.20	53.03	118.88	125.47

HX INT T	OPOV ACT POS	LPOP SPD	HPOP SPD
831.85	64.74	5039.07	27376.68
901.19	67.26	5126.17	28163.23
762.51	62.21	4951.98	26590.13
34.67	1.26	43.55	393.28
860.72	66.82	5149.35	28154.18
935.58	70.04	5258.25	29028.69
785.86	63.59	5040.45	27279.67
37.43	1.61	54.45	437.25
904.42	71.17	5294.08	29278.15
979.09	75.06	5409.91	30287.81
829.75	67.28	5178.25	28268.48
37.34	1.95	57.91	504.83
686.04	54.06	3895.57	19539.05
752.73	55.46	3963.45	19926.59
619.35	52.66	3827.69	19151.51
33.34	0.70	33.94	193.77
867.66	67.14	5165.48	28258.89
934.34	70.31	5259.36	29019.53
800.98	63.98	5071.60	27498.25
33.34	1.58	46.94	380.32
837.28	64.65	5043.48	27414.84
912.83	67.09	5126.81	28202.54
761.72	62.21	4960.14	26627.14
37.78	1.22	41.67	393.85
894.14	67.74	5181.51	28489.18
964.76	71.18	5272.33	29133.58
823.51	64.30	5090.70	27844.77
35.31	1.72	45.41	322.20
929.38	71.90	5313.48	29509.15
1006.58	75.60	5432.24	30513.66
852.19	68.20	5194.72	28504.64
38.60	1.85	59.38	502.26
690.75	54.06	3895.94	19540.37
755.06	55.51	3963.22	19901.62
626.44	52.61	3828.66	19179.13
32.16	0.73	33.64	180.62

Appendix D : PATTERN MATCHING SOFTWARE

Commercially Available Pattern Matching
and
Neural Network Software

Package Name	Product Description	Publisher
1. NeuroSym Neurocomputing Library	Library of neural networks programmed in C language; requires C compiler; source code provided; 12 architectures included.	NeuroSym Corporation P. O. Box 980683 Houston, TX 77098-0683 (713) 523-5777
2. Brain Maker V 2.3 Brain Maker Professional V 2.0	Stand-alone neural net development tool; Some C source code provided with Professional V 2.0; 8 architectures included.	California Scientific Software 10141 Evening Star Dr., #6 Grass Valley, CA 95945 (916) 477-7481
3. NeuroShell	Stand-alone neural net development tool; Source code provided with run time option; 2 architectures available.	Ward Systems Group, Inc. 245 West Patrick Street Frederick, MD 21701
4. Professional II Plus	Stand-alone neural net development tool; 31 architectures supported.	Neural Ware, Inc. Penn Center West, Bldg. IV, Suite Pittsburg, PA 15276 (412) 787-8222
5. Explore Net 3000	Stand-alone neural net development tool; requires AT with Microsoft Windows. 21 architectures included; no source code available.	Hecht-Nielsen Neurocomputers 5501 Oberlin Drive San Diego, CA 92121 (619) 546-8877
6. pLOGIC	Stand-alone statistical pattern-recognition software; requires 336-based PC with math coprocessor, plus 2 megabytes extended memory; source code available, but not included.	pLOGIC Knowledge Systems, Inc. 23133 Hawthorne Blvd., 3rd Floor Torrance, CA 90505 (213) 378-3760
7. NDS 1000 Version 1.2	Stand-alone neural network pattern recognition tool; uses 1 proprietary architecture; versions available for PC and Sun Workstations; source code not available. Can be imbedded in hardware.	Nestor, Inc. One Richmond Square Providence, RI 02906
8. MacBrain	Stand-alone neural net development tool; requries MacIntosh Plus or better; 12 architectures and some source code (C and Pascal) included.	Neurix 327 A Street, 6th Fl. Boston, MA 02102 (617) 577-1202

Report Documentation Page

1. Report No.	2. Government Accession No.	3. Recipient's Catalog No.
CR 187124		

4. Title and Subtitle

Sensor Data Validation and Reconstruction
Phase 1: System Architecture Study

5. Report Date

June 1991

6. Performing Organization Code

8. Performing Organization Report No.

7. Author(s)

D.K. Makel, W.H. Flaspohler, T.W. Pickmore

10. Work Unit No.

9. Performing Organization Name and Address

Aerojet Propulsion Division
P. O. Box 13222
Sacramento, California 95813-6000

11. Contract or Grant No. NAS 3-25883

NAS 3-25883

13. Type of Report and Period Covered

Task 3 Summary Report
May 1990 - Feb 1991

12. Sponsoring Agency Name and Address

National Aeronautics and Space Administration
Lewis Research Center
21000 Brookpark Road
Cleveland, Ohio 44135

14. Sponsoring Agency Code

15. Supplementary Notes

This final report describes the work performed under Task Order 3 of the Development of Life Prediction Capabilities contract.

The NASA technical monitor was Claudia Meyer.

16. Abstract

The sensor validation and data reconstruction task (1) reviewed relevant literature and selected applicable validation and reconstruction techniques for further study, (2) analyzed the selected techniques and emphasized those which could be used for both validation and reconstruction, (3) analyzed SSME hot fire test data to determine statistical and physical relationships between various parameters, (4) developed statistical and empirical correlations between parameters to perform validation and reconstruction tasks, using a computer aided engineering (CAE) package, (5) conceptually designed an expert system based knowledge fusion tool, which allows the user to relate diverse types of information when validating sensor data. The host hardware for the system is intended to be a Sun SPARCstation, but could be any RISC workstation with a UNIX operating system and a windowing/graphics system such as Motif or Dataviews. The information fusion tool is intended to be developed using NEXPERT Object expert system shell, and the C programming language.

17. Key Words (Suggested by Author(s))	18. Distribution Statement
Sensor Validation, Data Reconstruction, Space Shuttle Main Engine, Rocket Engine Diagnostics, Expert Systems, Bayesian Belief Networks	Unclassified - Unlimited

19. Security Classif. (of this report)	20. Security Classif. (of this page)	21. No. of pages	22. Price
Unclassified	Unclassified	327	

NASA FORM 1626 OCT 86